The Astrophysical Journal Supplement Series, 260:26 (145pp), 2022 June https://doi.org/10.3847/1538-4365/ac5044

Generalized Fluid Models of the Braginskii Type

P. Hunana[1,2], T. Passot[3], E. Khomenko[1,2], D. Martínez-Gómez[1,2], M. Collados[1,2], A. Tenerani[4], G. P. Zank[5,6], Y. Maneva[7], M. L. Goldstein[8], and G. M. Webb[5]
[1] Instituto de Astrofísica de Canarias (IAC), La Laguna, Tenerife, E-38205, Spain; peter.hunana@gmail.com
[2] Universidad de La Laguna, La Laguna, Tenerife, E-38206, Spain
[3] Université Côte d'Azur, Observatoire de la Côte d'Azur, CNRS, Laboratoire Lagrange, Bd de l'Observatoire, CS 34229, F-06304 Nice cedex 4, France
[4] Department of Physics, University of Texas, Austin, TX 78712, USA
[5] Center for Space Plasma and Aeronomic Research (CSPAR), University of Alabama, Huntsville, AL 35805, USA
[6] Department of Space Science, University of Alabama, Huntsville, AL 35899, USA
[7] Royal Observatory of Belgium, B-1180 Brussels, Belgium
[8] Space Science Institute, Boulder, CO 80301, USA
Received 2021 October 18; revised 2022 January 27; accepted 2022 January 29; published 2022 June 17

Abstract

Several generalizations of the well-known fluid model of Braginskii (1965) are considered. We use the Landau collisional operator and the moment method of Grad. We focus on the 21-moment model that is analogous to the Braginskii model, and we also consider a 22-moment model. Both models are formulated for general multispecies plasmas with arbitrary masses and temperatures, where all of the fluid moments are described by their evolution equations. The 21-moment model contains two "heat flux vectors" (third- and fifth-order moments) and two "viscosity tensors" (second- and fourth-order moments). The Braginskii model is then obtained as a particular case of a one ion–electron plasma with similar temperatures, with decoupled heat fluxes and viscosity tensors expressed in a quasistatic approximation. We provide all of the numerical values of the Braginskii model in a fully analytic form (together with the fourth- and fifth-order moments). For multispecies plasmas, the model makes the calculation of the transport coefficients straightforward. Formulation in fluid moments (instead of Hermite moments) is also suitable for implementation into existing numerical codes. It is emphasized that it is the quasistatic approximation that makes some Braginskii coefficients divergent in a weakly collisional regime. Importantly, we show that the heat fluxes and viscosity tensors are coupled even in the linear approximation, and that the fully contracted (scalar) perturbations of the fourth-order moment, which are accounted for in the 22-moment model, modify the energy exchange rates. We also provide several appendices, which can be useful as a guide for deriving the Braginskii model with the moment method of Grad.

Unified Astronomy Thesaurus concepts: Collision processes (2065); Plasma physics (2089); Space plasmas (1544)

1. Introduction

The fluid model of Braginskii (1958, 1965) represents a cornerstone of plasma transport theory, and it is used in many different areas, from solar physics to laboratory plasmas. The Braginskii model and its generalizations can be derived through two major classical routes: (1) Chapman–Enskog expansions (Chapman & Cowling 1939) and (2) the moment method of Grad (1949a, 1949b, 1958). There also exists a more modern route, with the projection operator (Krommes 2018a, 2018b). Both classical routes were originally developed for gases, where the full Boltzmann collisional operator has to be used. As was shown by Landau (1936, 1937), for charged particles interacting through Coulomb collisions, the Boltzmann operator can be partially simplified, and this collisional operator is known as the Landau operator. It is now well established that for Coulomb collisions both the Landau and Boltzmann operators yield the same results, if in the Boltzmann operator one introduces integration cutoffs that remove the divergences in the same way as the Coulomb logarithm does. With the Landau operator, the Boltzmann equation is then typically called the Landau equation. By introducing Rosenbluth potentials, the Landau operator can be rewritten into a general Fokker–Planck form, and the name Fokker–Planck equation is often used as well. Nevertheless, many authors use the Boltzmann operator during calculations even when Coulomb collisions are considered, because the simplification is not exceedingly large. Braginskii used the Landau operator. Of course, both routes, through both Chapman–Enskog expansions and the moment method of Grad, have subvariations as to how the methods are implemented that have been developed over the years. For the Chapman–Enskog method, where the distribution function is expanded in Laguerre–Sonine polynomials, see, for example, Braginskii (1958), Hinton (1983), Helander & Sigmar (2002), and Kunz (2021).

Here we use the moment method of Grad, which consists of expanding the distribution function in tensorial Hermite polynomials. Concerning only viscosity tensors and heat fluxes (and neglecting fully contracted scalar perturbations and higher-order tensorial "anisotropies," as Balescu (1988) calls them), the method of Grad consists of approximating the distribution

function as a series

$$f_a = f_a^{(0)}(1 + \chi_a); \qquad \chi_a = \sum_{n=1}^{N}[h_{ij}^{(2n)}H_{ij}^{(2n)} + h_i^{(2n+1)}H_i^{(2n+1)}], \tag{1}$$

where $f_a^{(0)}$ is Maxwellian, "a" is the species index, the indices i and j run from 1 to 3, H are Hermite polynomials, and h are Hermite moments. Matrices $h_{ij}^{(2n)}$ are traceless and can be viewed as viscosity tensors (stress tensors), and vectors $h_i^{(2n+1)}$ can be viewed as heat fluxes. The series is cut at some chosen N, and this distribution function is then used in the Landau (or Boltzmann) equation, which is integrated to obtain a corresponding fluid model. The usual quasistatic approximation does not have to be applied, and one obtains evolution equations for all of the considered moments. For example, prescribing a strict Maxwellian with perturbation $\chi_a = 0$ (or, equivalently, $N = 0$) represents the 5-moment model, with evolution equations for density, fluid velocity, and scalar pressure (temperature), where stress tensors and heat fluxes are zero. Prescribing $N = 1$ represents the 13-moment model, which contains an evolution equation for one traceless viscosity tensor (five independent components) and an evolution equation for one heat flux vector (three independent components). This model thus contains the main ingredients of the model of Braginskii, i.e., the usual viscosity tensor and the usual heat flux vector are present. However, prescribing a quasistatic approximation yields, for example, the coefficient of the parallel electron heat conductivity (for a one-ion electron plasma with ion charge $Z_i = 1$) with a value of 1.34 instead of the Braginskii value of 3.16, meaning the model is not sufficiently precise. Prescribing $N = 2$ represents a 21-moment model, and this model can be viewed as containing evolution equations for two viscosity tensors and two heat flux vectors. It can be shown that expressing the viscosity tensors and heat fluxes in a quasistatic approximation yields a model that is equivalent to Braginskii (1965). In fact, as pointed out by Balescu (1988), for example, the Hermite polynomials are directly related to the Laguerre–Sonine polynomials (see Equation (192)), and thus the Chapman–Enskog method and the moment method of Grad have to yield equivalent results at the end. In general, if both heat fluxes and viscosities are accounted for, an N-Laguerre model therefore represents a $(5 + 8N)$-moment model. For a summary of the various possible models, see Section 8.4 with Tables 1 and 2.

Of course, the model of Braginskii can be generalized in many different ways. Naturally, one might focus on the case of the one-ion electron plasma considered by Braginskii, and increase the order of N to study the convergence of transport coefficients with higher-order Laguerre (Hermite) schemes. Several studies of this kind have been done in the past (some being numerically imprecise, some considering only unmagnetized plasmas, and some only having an ion charge of $Z_i = 1$). For example, before Braginskii, Landshoff (1949, 1951) calculated several transport coefficients with models from $N = 1$ to $N = 4$. Kaneko (1960) improved the numerical accuracy of Landshoff and also considered $N = 5$. Kaneko & Taguchi (1978) and Kaneko & Yamao (1980) performed large calculations up to $N = 49$. Perhaps the most comprehensive study to date was done by Ji & Held (2013), who studied the convergence of all of the transport coefficients up to $N = 160$. Other useful references can be found in Epperlein & Haines (1986). These last two studies emphasize that while the transport coefficients parallel to the magnetic field (or for unmagnetized plasma) converge rapidly for $N \geqslant 2$, this is not the case for some of the perpendicular transport coefficients. For clarity, in the famous work of Spitzer & Härm (1953), and the previous work of Cohen et al. (1950), where only unmagnetized plasma was considered and viscosity tensors were neglected, the perturbation χ_a, which satisfies the Landau equation, was found numerically, and the model thus technically corresponds to $N = \infty$. Their work was criticized (even though a bit unfairly) in the monograph of Balescu (1988, Part 1, p. 266), who calculated all of the usual transport coefficients with the moment method of Grad for the $N = 2$ and $N = 3$ cases (i.e., the 21-moment model and the 29-moment model). Note that the 3-Laguerre calculations of Balescu (1988) were shown to be incorrect by Ji & Held (2013), who were able to trace the problem to his analytic collisional matrices (they have also corrected the coefficients in the collisional matrices of Braginskii 1958, which were fortunately not used in his $N = 2$ calculation). That there is a problem with the $N = 3$ transport coefficients of Balescu (1988) can be also seen by a comparison with Kaneko (1960), for example. Here we focus on the 2-Laguerre approximation used by Braginskii (1965), i.e., the 21-moment model, with the goal of extracting more physical information from that scheme.

For the 5-moment model and the 13-moment model, the method of Grad was explored in great detail by Burgers (1969) and Schunk (1975, 1977, and references therein). The Boltzmann operator was used and several interaction potentials were considered, such as collisions between neutral particles (hard-sphere interaction), between charges (Coulomb interaction), or an induced dipole interaction when an ion polarizes a colliding neutral (so-called Maxwell molecule interaction). These models have two important properties that the Braginskii model does not have: (1) because the formulation uses evolution equations for stress tensors and heat fluxes, rather than quasistatic approximation, these models do not become divergent if a regime of low collisionality is encountered; and (2) the formulation is a general multifluid description with arbitrary masses m_a, m_b and temperatures T_a, T_b. Note that the review paper of Braginskii (1965) also contains Section 7, about multicomponent plasmas, which is often implicitly cited in the solar literature; but this section should be viewed as heuristic from a perspective that no heat fluxes or stress tensors were calculated. In plasma physics, the work of Braginskii (1958, 1965) is celebrated for his results for a one ion–electron plasma. Here we use the Landau operator and consider only Coulomb collisions. Nevertheless, we will employ the 21-moment model, and we thus improve the precision of the 13-moment model of Burgers (1969)–Schunk (1977) for this interaction potential, so that the precision matches Braginskii. We will use the restriction that the relative drift velocity between two colliding species must be small in comparison to their thermal speeds. The same restriction applies for the Braginskii model, for the Burgers–Schunk 13-moment model (the exception is Maxwell molecule interaction), and for higher-order schemes. For Coulomb collisions and hard-sphere collisions, only the simplest

5-moment model has been fully calculated analytically without this restriction (Tanenbaum 1967; Burgers 1969; Schunk 1977), yielding the runaway effect.

Several multifluid descriptions with the level of precision of Braginskii have been considered in the past: see, for example, Hinton (1983), Zhdanov (2002; originally published in 1982), Ji & Held (2006; who actually consider general N), and Simakov & Molvig (2014, 2016a, 2016b); or, for the case of neoclassical theory (toroidal geometry applicable to tokamaks), see Hirshman & Sigmar (1977, 1981). Our model seems to be very close to the model of Zhdanov (2002), Chapter 8.1, who indeed uses the method of Grad and calculates the 21-moment model with it. We did not verify full equivalence because of his puzzling notation. Even if equivalence is eventually shown for the case of small temperature differences between ions, we consider a more general case where the temperatures of all the species are arbitrary. Our clear formulation with fluid moments (instead of Hermite moments) might also be easier to implement into existing numerical codes. Arbitrary temperatures were also considered by Ji & Held (2006), but we did not verify equivalence with their model either. We only verified equivalence with their model for the special case of a one ion–electron plasma with small temperature differences of Braginskii, by using the collisional matrices from Ji & Held (2013).

Additionally, for all of the considered moments, we provide the left-hand sides of our evolution equations in a fully nonlinear form, which is important for direct numerical simulations, and which are not typically given. An important difference then arises even at the linear level, because calculations are typically performed with decoupled viscosity tensors and heat fluxes, meaning that the two viscosity tensors interact only with each other, and the two heat fluxes interact only with each other. We consider coupling between heat fluxes and stress tensors, where (even at the linear level in a quasistatic approximation) a heat flux enters a stress tensor and a stress tensor enters a heat flux. Such couplings are often considered in the collisionless regime: see, e.g., Macmahon (1965), Mikhailovskii & Smolyakov (1985), Goswami et al. (2005), Ramos (2005), Passot et al. (2012), and Hunana et al. (2019a, 2019b), where the effect is important for the perpendicular fast mode, for example, or for the growth rate of the firehose instability (see, e.g., Figure 10 in Hunana et al. 2019b). The coupling might also be important in the highly collisional regime if sufficiently high frequencies (or short wavelengths) are considered. The coupling was neglected by Braginskii (1958, 1965), Spitzer & Härm (1953), and Spitzer (1962); and, as an example, we consider an unmagnetized one ion–electron plasma in detail, and we provide stress tensors and heat fluxes where this coupling is taken into account.

The coupling between viscosity tensors and heat fluxes then inevitably leads to the next step, replacing Equation (1) with

$$f_a = f_a^{(0)}(1+\chi_a); \qquad \chi_a = \sum_{n=1}^{N}[h_{ij}^{(2n)}H_{ij}^{(2n)} + h_i^{(2n+1)}H_i^{(2n+1)} + h^{(2n)}H^{(2n)}], \tag{2}$$

where the scalar hermite moments $h^{(2n)}$ can be viewed as fully contracted (scalar) perturbations of fluid moments. The lowest-order moment $h^{(2)}=0$ and all of the higher-order ones are generally nonzero. Thus, prescribing $N=1$ still yields the 13-moment model, but prescribing $N=2$ now yields the 22-moment model. This model is a natural extension of the Braginskii model, because it takes into account the fully contracted perturbations $\widetilde{X}_a^{(4)} = m_a\int|\boldsymbol{c}_a|^4(f_a - f_a^{(0)})d^3v$ of the fourth-order fluid moment. Accounting for the scalar perturbations according to (2), for $N\geqslant 1$ an N-Laguerre model then represents a $(4+9N)$-moment model. Another possibility for writing Equation (2) is to separate the matrices $\sum_{n=1}^{N} h_{ij}^{(2n)}H_{ij}^{(2n)}$, and to write the sum for the vectors and scalars from $n=0$, with an imposed requirement that $h^{(0)}=0$, $h^{(2)}=0$, and $h_i^{(1)}=0$ (where the first one is nontrivial). This is the choice of Balescu (1988, p. 174), for example, in his Equations (3.11) and (3.16).

Finally, the main purpose of this work is to make the moment method of Grad and the exciting work of Braginskii more understandable, as reflected in our relatively lengthy appendix.

The entire paper is separated into eight sections and 14 appendices. The main paper summarizes the obtained results, while the appendices provide the detailed calculations.

In Section 2, we formulate the entire 21-moment model. We start with a formulation valid for a general collisional operator $C(f_a)$, where both the left-hand sides and the collisional right-hand sides of the evolution equations are given in a fully nonlinear form. We then provide the collisional contributions for arbitrary masses and temperatures calculated with the Landau operator. The collisional contributions are calculated in the usual semilinear approximation, where the relative drifts between species are small in comparison to their thermal speeds (i.e., the runaway effect is not considered), and the product of f_af_b is approximated as $f_af_b = f_a^{(0)}f_b^{(0)}(1+\chi_a+\chi_b)$, where the "cross" contributions $\chi_a\chi_b$ are neglected. We then provide a simplified model where the differences in the temperatures between species are small. For clarity, we also reduce our model to the 13-moment model, and we provide a formulation that is more compact than the one given by Burgers (1969)–Schunk (1977) (because we only consider Coulomb collisions). We then simplify the evolution equations of our 21-moment model into a semilinear approximation where viscosity tensors and heat fluxes are decoupled, and these are used in Sections 3 and 4.

In Section 3, we compare our model to Braginskii (1965) by considering a one ion–electron plasma with similar temperatures, i.e., where the temperature differences between species are small with respect to their mean values. We provide all of the transport coefficients in a fully analytic form, and we verify the entire Table II of Braginskii (1965; two of his coefficients are not precise). Parallel electron coefficients (or, equivalently, for an unmagnetized plasma) can also be found in Simakov & Molvig (2014). We also provide analytic results for the viscosity of the fourth-order fluid moment and the heat flux of the fifth-order fluid moment, which are not typically given.

In Section 4, we use the idea of Hinton (1983), Zhdanov (2002), and Simakov & Molvig (2014), for example, that because of the smallness of the electron/ion mass ratios, the *electron* coefficients of Braginskii can be straightforwardly generalized to multiple ion

species, by introducing an effective ion charge and effective ion velocity. All of the electron analytic coefficients that are given in Section 3 are thus generalized to multi-ion species with a simple transformation.

In Section 5, we discuss the coupling between viscosity tensors and heat fluxes. We provide evolution equations in the semilinear approximation, where this coupling is retained, and we introduce a technique for splitting the moments into their first and second orders.

In Section 6, we consider an example of an unmagnetized one ion–electron plasma and explicitly calculate the coupling of stress tensors and heat fluxes. All of the results are given in a fully analytic form, as well as with numerical values for the ion charge $Z_i = 1$.

In Section 7, we first formulate the fully nonlinear 22-moment model for a general collisional operator. We then provide the multifluid collisional contributions calculated with the Landau operator in the semilinear approximation, and we show that the perturbations $\widetilde{X}^{(4)}$ modify the energy exchange rates. We also provide quasistatic solutions for a one ion–electron plasma, and we show that the perturbations $\widetilde{X}^{(4)}$ have their own heat conductivities.

In Section 8, we discuss various topics. (1) We discuss energy conservation. (2) We clarify that from a multifluid perspective, the Braginskii choice of ion collisional time τ_i should be interpreted as $\tau_i = \tau_{ii}$, and not as $\tau_i = \sqrt{2}\,\tau_{ii}$. (3) To clarify the higher-order schemes, and to double-check our evolution equations, we calculate the fluid hierarchy for a general N, with an unspecified collisional operator. (4) We discuss irreducible and reducible Hermite polynomials and show that both yield the same results. (5) We provide fully nonlinear Rosenbluth potentials for the 22-moment model, which might be useful in further studies of the runaway effect with this scheme. (6) We discuss Hermite closures and their relation to fluid closures, which are required to close the fluid hierarchy. We also correct our previous erroneous interpretation that Landau fluid closures are necessary to go beyond the fourth-order moment. (7) We discuss the inclusion of gravity. (8) We use our multifluid formulation to double-check the precision of the m_e/m_i expansions. We consider unmagnetized proton–electron plasma and calculate the transport coefficients exactly, without using the smallness of m_e/m_i. (9) We discuss the limitations of our approach. (10) We provide conclusions, with examples of where our model might be useful.

Appendix A introduces the general concept of tensorial fluid moments and provides an evolution equation for an nth-order fluid moment $\bar{\bar{\boldsymbol{X}}}_a^{(n)}$ in the presence of a general (unspecified) collisional operator, Equation (A12). This evolution equation also remains valid in the presence of gravity; see the discussion in Section 8.7.

Appendix B introduces the tensorial Hermite polynomials of Grad (1949a, 1949b, 1958) and discusses in detail the construction of the perturbations around the Maxwellian distribution function, i.e., Equations (1) and (2), which are summarized in Tables 1 and 2. The construction of Hermite closures is addressed as well.

Appendix C derives the evolution equations for the 22-moment model (for an unspecified collisional operator) by applying contractions at the evolution equations from Appendix A and by using the decompositions of moments and Hermite closures from Appendix B.

Appendix D uses a different technique and, instead of applying contractions at the equations of Appendix A, a simplified fluid hierarchy of a general nth-order is obtained directly, which only consists of evolution equations for scalars, vectors, and matrices. The evaluation of these equations for a specific "n" recovers the 22-moment equations of Appendix C.

Appendix E introduces the BGK (relaxation-type) collisional operator of Bhatnagar et al. (1954) and Gross & Krook (1956), which greatly clarifies the analytic forms of the Braginskii viscosity tensors and heat fluxes. The viscosities and heat conductivities of both models are directly compared in Figures 3–5. The nonlinear solution for the viscosity tensor (with respect to a general direction of the magnetic field $\hat{\boldsymbol{b}}$) is addressed in Appendix E.4, and Appendix E.6 clarifies the ambipolar diffusion between two ion species.

Appendix F introduces a general (unspecified) Fokker–Planck collisional operator with its dynamical friction vector $\boldsymbol{A}_{ab}$ and diffusion tensor $\bar{\bar{\boldsymbol{D}}}_{ab}$. General relations for the collisional integrals (of nth order) are provided, which can be used once the $\boldsymbol{A}_{ab}$ and $\bar{\bar{\boldsymbol{D}}}_{ab}$ are specified.

Appendix G introduces the Landau collisional operator, where the $\boldsymbol{A}_{ab}$ and $\bar{\bar{\boldsymbol{D}}}_{ab}$ are expressed in the usual form through the Rosenbluth potentials. The 5-moment model (strict Maxwellians) is then considered, and the usual collisional momentum exchange rates $\boldsymbol{R}_{ab}$ and energy exchange rates Q_{ab}, with the assumption of small drifts between species, are derived in detail in Appendices G.1 and G.2. Both contributions are then recalculated with unrestricted drifts in Appendix G.3, where instead of the Rosenbluth potentials, the "center-of-mass" transformation typically used with the Boltzmann collisional operator has to be used, because the collisional integrals seem to be too complicated to calculate directly. This is further discussed in Appendix G.4.

Appendix H considers the 8-moment model, where the simplest heat flux is present, and the multifluid model of Burgers (1969)–Schunk (1977) is calculated in detail. For a direct comparison with Braginskii, a one ion–electron plasma is then considered, and quasistatic heat fluxes, together with the resulting momentum exchange rates, are obtained as well. It is shown that in the limit of a strong magnetic field, the perpendicular and cross conductivities $\kappa_\perp$ and $\kappa_\times$ match the Braginskii model exactly (for both the ion and electron species), and only the parallel conductivities $\kappa_\parallel$ are different.

Appendix I compares the parallel heat fluxes and momentum exchange rates of Braginskii (1965) with the models of Burgers (1969)–Schunk (1977), Killie et al. (2004), Landshoff (1949, 1951), and Spitzer & Härm (1953); see Tables 8–12. Useful conversion relations for the results of Kaneko (1960) and Balescu (1988) are provided as well. The notation of Spitzer & Härm (1953) is clarified in Appendix I.1, and it is shown that their model, as well as the model of Killie et al. (2004), break the Onsager symmetry.

Appendix J calculates in detail the 10-moment multifluid model of Burgers (1969)–Schunk (1977), where the simplest viscosity tensor is present. It is shown that in the limit of a strong magnetic field, the perpendicular viscosities and gyroviscosities

η_1, η_2, η_3, η_4 match the Braginskii model exactly (for both the ion and electron species), and only the parallel viscosities η_0 are different.

Appendix K calculates in detail the momentum exchange rates and collisional contributions for the heat fluxes in our 21- and 22-moment multifluid models. The calculations are shown for the 11-moment model, where only the heat fluxes are present (and viscosities and scalar perturbation are absent), because in the semilinear approximation the calculations can be split. Similarly, the collisional contributions for viscosity tensors are calculated in Appendix L, and the contributions for the scalar perturbation of the fourth-order moment are calculated in Appendix M.

Appendix N uses our 21-moment model and calculates the heat conductivities and viscosities for two examples of an unmagnetized plasma consisting of two ion species (collisions with electrons are neglected). The first example (Appendix N.1) is a plasma consisting of protons and alpha particles (fully ionized Helium), typical in astrophysical applications. The second example (Appendix N.3) is a deuterium–tritium plasma used in plasma fusion.

2. Multifluid Generalization of Braginskii (21-moment Model)

Our model is formulated with heat flux vectors

$$\boldsymbol{X}_a^{(3)} = m_a \int \boldsymbol{c}_a |\boldsymbol{c}_a|^2 f_a \, d^3v = 2\boldsymbol{q}_a; \qquad \boldsymbol{X}_a^{(5)} = m_a \int \boldsymbol{c}_a |\boldsymbol{c}_a|^4 f_a \, d^3v, \tag{3}$$

and traceless viscosity tensors

$$\bar{\bar{\boldsymbol{\Pi}}}_a^{(2)} = m_a \int \left(\boldsymbol{c}_a \boldsymbol{c}_a - \frac{\bar{\bar{\boldsymbol{I}}}}{3} |\boldsymbol{c}_a|^2 \right) f_a \, d^3v; \quad \bar{\bar{\boldsymbol{\Pi}}}_a^{(4)} = m_a \int \left(\boldsymbol{c}_a \boldsymbol{c}_a - \frac{\bar{\bar{\boldsymbol{I}}}}{3} |\boldsymbol{c}_a|^2 \right) |\boldsymbol{c}_a|^2 f_a \, d^3v, \tag{4}$$

where the fluctuating velocity $\boldsymbol{c}_a = \boldsymbol{v} - \boldsymbol{u}_a$ and "a" is the species index. We are using free wording because $\boldsymbol{X}_a^{(5)}$ is not really a heat flux and $\bar{\bar{\boldsymbol{\Pi}}}_a^{(4)}$ is not really a viscosity tensor. Also, we use the wording "viscosity tensor" and "stress tensor" interchangeably throughout the entire text. The species indices are moved freely up and down. We also define the usual rate-of-strain tensor $\bar{\bar{\boldsymbol{W}}}_a = (\nabla \boldsymbol{u}_a)^S - (2/3)\bar{\bar{\boldsymbol{I}}} \nabla \cdot \boldsymbol{u}_a$, symmetric operator $A_{ij}^S = A_{ij} + A_{ji}$, and gravitational acceleration $\boldsymbol{G}$. All other definitions are addressed in Appendix A. We note that the definition of the heat flux in Equation (1.21) of Braginskii (1965) contains two well-known misprints, with prime symbols missing on his fluctuating velocities $\boldsymbol{v}'$. The heat flux is defined correctly in Braginskii (1958).

We first present a formulation with a general (unspecified) collisional operator $C(f_a)$. We define the (tensorial) collisional contributions

$$\begin{aligned}
&\boldsymbol{R}_a = m_a \int \boldsymbol{v} C(f_a) d^3v; \qquad Q_a = \frac{m_a}{2} \int |\boldsymbol{c}_a|^2 C(f_a) d^3v; \\
&\bar{\bar{\boldsymbol{Q}}}_a^{(2)} = m_a \int \boldsymbol{c}_a \boldsymbol{c}_a C(f_a) d^3v; \qquad \bar{\bar{\boldsymbol{Q}}}_a^{(3)} = m_a \int \boldsymbol{c}_a \boldsymbol{c}_a \boldsymbol{c}_a C(f_a) d^3v; \\
&\bar{\bar{\boldsymbol{Q}}}_a^{(4)} = m_a \int \boldsymbol{c}_a \boldsymbol{c}_a \boldsymbol{c}_a \boldsymbol{c}_a C(f_a) d^3v; \qquad \bar{\bar{\boldsymbol{Q}}}_a^{(5)} = m_a \int \boldsymbol{c}_a \boldsymbol{c}_a \boldsymbol{c}_a \boldsymbol{c}_a \boldsymbol{c}_a C(f_a) d^3v,
\end{aligned} \tag{5}$$

where $\boldsymbol{R}_a$ are the usual momentum exchange rates and Q_a are the usual energy exchange rates. Then, it can be shown that the integration of the Boltzmann equation yields the following nonlinear 21-moment model (see the details in Appendix C), where the basic evolution equations read

$$\frac{d_a}{dt} n_a + n_a \nabla \cdot \boldsymbol{u}_a = 0; \tag{6}$$

$$\frac{d_a}{dt} \boldsymbol{u}_a + \frac{1}{\rho_a} \nabla \cdot \bar{\bar{\boldsymbol{p}}}_a - \boldsymbol{G} - \frac{eZ_a}{m_a} \left(\boldsymbol{E} + \frac{1}{c} \boldsymbol{u}_a \times \boldsymbol{B} \right) = \frac{\boldsymbol{R}_a}{\rho_a}; \tag{7}$$

$$\frac{d_a}{dt} p_a + \frac{5}{3} p_a \nabla \cdot \boldsymbol{u}_a + \frac{2}{3} \nabla \cdot \boldsymbol{q}_a + \frac{2}{3} \bar{\bar{\boldsymbol{\Pi}}}_a^{(2)} : (\nabla \boldsymbol{u}_a) = \frac{2}{3} Q_a, \tag{8}$$

and are accompanied by evolution equations for the stress tensors and heat flux vectors:

$$\frac{d_a \bar{\bar{\Pi}}_a^{(2)}}{dt} + \bar{\bar{\Pi}}_a^{(2)} \nabla \cdot \boldsymbol{u}_a + \Omega_a (\hat{\boldsymbol{b}} \times \bar{\bar{\Pi}}_a^{(2)})^S + (\bar{\bar{\Pi}}_a^{(2)} \cdot \nabla \boldsymbol{u}_a)^S - \frac{2}{3} \bar{\bar{I}} (\bar{\bar{\Pi}}_a^{(2)} : \nabla \boldsymbol{u}_a) + \frac{2}{5} \left[(\nabla \boldsymbol{q}_a)^S - \frac{2}{3} \bar{\bar{I}} \nabla \cdot \boldsymbol{q}_a \right] + p_a \bar{\bar{W}}_a = \bar{\bar{Q}}_a^{(2)\prime} \equiv \bar{\bar{Q}}_a^{(2)} - \frac{\bar{\bar{I}}}{3} \mathrm{Tr} \bar{\bar{Q}}_a^{(2)}; \tag{9}$$

$$\frac{d_a \boldsymbol{q}_a}{dt} + \frac{7}{5} \boldsymbol{q}_a \nabla \cdot \boldsymbol{u}_a + \frac{7}{5} \boldsymbol{q}_a \cdot \nabla \boldsymbol{u}_a + \frac{2}{5} (\nabla \boldsymbol{u}_a) \cdot \boldsymbol{q}_a + \Omega_a \hat{\boldsymbol{b}} \times \boldsymbol{q}_a + \frac{5}{2} p_a \nabla \left(\frac{p_a}{\rho_a} \right) + \frac{1}{2} \nabla \cdot \bar{\bar{\Pi}}_a^{(4)} - \frac{5}{2} \frac{p_a}{\rho_a} \nabla \cdot \bar{\bar{\Pi}}_a^{(2)} - \frac{1}{\rho_a} (\nabla \cdot \bar{\bar{p}}_a) \cdot \bar{\bar{\Pi}}_a^{(2)} = \boldsymbol{Q}_a^{(3)\prime} \equiv \frac{1}{2} \mathrm{Tr} \bar{\bar{Q}}_a^{(3)} - \frac{5}{2} \frac{p_a}{\rho_a} \boldsymbol{R}_a - \frac{1}{\rho_a} \boldsymbol{R}_a \cdot \bar{\bar{\Pi}}_a^{(2)}; \tag{10}$$

$$\frac{d_a}{dt} \bar{\bar{\Pi}}_a^{(4)} + \frac{1}{5} \left[(\nabla \boldsymbol{X}_a^{(5)})^S - \frac{2}{3} \bar{\bar{I}} (\nabla \cdot \boldsymbol{X}_a^{(5)}) \right] + \frac{9}{7} (\nabla \cdot \boldsymbol{u}_a) \bar{\bar{\Pi}}_a^{(4)} + \frac{9}{7} (\bar{\bar{\Pi}}_a^{(4)} \cdot \nabla \boldsymbol{u}_a)^S + \frac{2}{7} ((\nabla \boldsymbol{u}_a) \cdot \bar{\bar{\Pi}}_a^{(4)})^S - \frac{22}{21} \bar{\bar{I}} (\bar{\bar{\Pi}}_a^{(4)} : \nabla \boldsymbol{u}_a) + \Omega_a (\hat{\boldsymbol{b}} \times \bar{\bar{\Pi}}_a^{(4)})^S + 7 \frac{p_a^2}{\rho_a} \bar{\bar{W}}_a - \frac{14}{5 \rho_a} \left[((\nabla \cdot \bar{\bar{p}}_a) \boldsymbol{q}_a)^S - \frac{2}{3} \bar{\bar{I}} (\nabla \cdot \bar{\bar{p}}_a) \cdot \boldsymbol{q}_a \right] = \bar{\bar{Q}}_a^{(4)\prime} \equiv \mathrm{Tr} \bar{\bar{Q}}_a^{(4)} - \frac{\bar{\bar{I}}}{3} \mathrm{Tr} \mathrm{Tr} \bar{\bar{Q}}_a^{(4)} - \frac{14}{5 \rho_a} \left[(\boldsymbol{R}_a \boldsymbol{q}_a)^S - \frac{2}{3} \bar{\bar{I}} (\boldsymbol{R}_a \cdot \boldsymbol{q}_a) \right]; \tag{11}$$

$$\frac{d_a}{dt} \boldsymbol{X}_a^{(5)} + \nabla \cdot \bar{\bar{\Pi}}_a^{(6)} + \frac{9}{5} \boldsymbol{X}_a^{(5)} (\nabla \cdot \boldsymbol{u}_a) + \frac{9}{5} \boldsymbol{X}_a^{(5)} \cdot \nabla \boldsymbol{u}_a + \frac{4}{5} (\nabla \boldsymbol{u}_a) \cdot \boldsymbol{X}_a^{(5)} + \Omega_a \hat{\boldsymbol{b}} \times \boldsymbol{X}_a^{(5)} + 70 \frac{p_a^2}{\rho_a} \nabla \left(\frac{p_a}{\rho_a} \right) - 35 \frac{p_a^2}{\rho_a^2} \nabla \cdot \bar{\bar{\Pi}}_a^{(2)} - \frac{4}{\rho_a} (\nabla \cdot \bar{\bar{p}}_a) \cdot \bar{\bar{\Pi}}_a^{(4)} = \boldsymbol{Q}_a^{(5)\prime} \equiv \mathrm{Tr} \mathrm{Tr} \bar{\bar{Q}}_a^{(5)} - 35 \frac{p_a^2}{\rho_a^2} \boldsymbol{R}_a - \frac{4}{\rho_a} \boldsymbol{R}_a \cdot \bar{\bar{\Pi}}_a^{(4)}. \tag{12}$$

The last equation is closed with a fluid closure (derived from a Hermite closure):

$$\bar{\bar{\Pi}}_a^{(6)} = m_a \int \left(\boldsymbol{c}_a \boldsymbol{c}_a - \frac{\bar{\bar{I}}}{3} |\boldsymbol{c}_a|^2 \right) |\boldsymbol{c}_a|^4 f_a \, d^3 v = 18 \frac{p_a}{\rho_a} \bar{\bar{\Pi}}_a^{(4)} - 63 \frac{p_a^2}{\rho_a^2} \bar{\bar{\Pi}}_a^{(2)}. \tag{13}$$

The system above thus represents a generalized model of Braginskii (1965), where the evolution equations for all of the moments are fully nonlinear and valid for a general collisional operator $C(f_a)$. It is a 21-moment model (1 density, 3 velocity, and 1 scalar pressure; 3 for each heat flux vector and 5 for each viscosity tensor).

2.1. Collisional Contributions (Arbitrary Masses and Temperatures)

We use the Landau collisional operator. All of the collisional contributions are evaluated in a semilinear approximation, with an assumption that the differences in the drift velocities $\boldsymbol{u}_b - \boldsymbol{u}_a$ are small with respect to thermal velocities. All of the nonlinear quantities, such as $\boldsymbol{q}_a \cdot (\boldsymbol{u}_b - \boldsymbol{u}_a)$, including $|\boldsymbol{u}_b - \boldsymbol{u}_a|^2$, are thus neglected in the multifluid description, which is consistent with models of Burgers (1969) and Schunk (1977). For energy conservation and a particular case of a one ion–electron plasma, see Section 8.1. The wording "semilinear" just means that expressions containing pressures and densities, such as $(p_a/\rho_a)\boldsymbol{q}_a$, are retained and not fully linearized with their mean pressure/density values. However, for example, the last terms of the collisional contributions in Equations (10)–(12) proportional to $\boldsymbol{R}_a \boldsymbol{q}_a$, $\boldsymbol{R}_a \cdot \bar{\bar{\Pi}}_a^{(2)}$, and $\boldsymbol{R}_a \cdot \bar{\bar{\Pi}}_a^{(4)}$ are neglected in the semilinear approximation.

We introduce the usual reduced mass and reduced temperature

$$\mu_{ab} = \frac{m_a m_b}{m_a + m_b}; \qquad T_{ab} = \frac{m_a T_b + m_b T_a}{m_a + m_b}, \tag{14}$$

together with the collisional frequency (178). The momentum exchange rates are given by

$$\boldsymbol{R}_a = \sum_{b \neq a} \nu_{ab} \left\{ \rho_a (\boldsymbol{u}_b - \boldsymbol{u}_a) + \frac{\mu_{ab}}{T_{ab}} \left[V_{ab(1)} \boldsymbol{q}_a - V_{ab(2)} \frac{\rho_a}{\rho_b} \boldsymbol{q}_b \right] - \frac{3}{56} \left(\frac{\mu_{ab}}{T_{ab}} \right)^2 \left[\boldsymbol{X}_a^{(5)} - \frac{\rho_a}{\rho_b} \boldsymbol{X}_b^{(5)} \right] \right\}, \tag{15}$$

with coefficients that include both masses and temperatures, but which we simply call "mass-ratio coefficients":

$$V_{ab(1)} = \frac{(21/10) T_a m_b + (3/5) T_b m_a}{T_a m_b + T_b m_a}; \qquad V_{ab(2)} = \frac{(3/5) T_a m_b + (21/10) T_b m_a}{T_a m_b + T_b m_a}. \tag{16}$$

These and the other mass-ratio coefficients given below come from the Landau collisional operator introduced in Appendices F and G, where one uses perturbed distribution functions of the 21-moment model; see Section 8.4 and Appendix B, with the calculations of the collisional integrals in Appendices K and L. The energy exchange rates are given by

$$Q_a = \sum_{b\neq a} 3\rho_a \nu_{ab} \frac{T_b - T_a}{m_a + m_b}, \tag{17}$$

where $|\boldsymbol{u}_b - \boldsymbol{u}_a|^2$ are neglected, as discussed above. The heat flux exchange rates are given by

$$\begin{aligned}\boldsymbol{Q}_a^{(3)\prime} &= -[2\nu_{aa} + \sum_{b\neq a}\nu_{ab}\hat{D}_{ab(1)}]\boldsymbol{q}_a + \sum_{b\neq a}\nu_{ab}\hat{D}_{ab(2)}\frac{\rho_a}{\rho_b}\boldsymbol{q}_b \\ &\quad + \left[\frac{3}{70}\nu_{aa} + \sum_{b\neq a}\nu_{ab}\hat{E}_{ab(1)}\right]\frac{\rho_a}{p_a}\boldsymbol{X}_a^{(5)} - \sum_{b\neq a}\nu_{ab}\hat{E}_{ab(2)}\frac{\rho_b}{p_b}\frac{\rho_a}{\rho_b}\boldsymbol{X}_b^{(5)} \\ &\quad - p_a\sum_{b\neq a}\nu_{ab}(\boldsymbol{u}_b - \boldsymbol{u}_a)\hat{U}_{ab(1)},\end{aligned} \tag{18}$$

with mass-ratio coefficients

$$\begin{aligned}\hat{U}_{ab(1)} &= \frac{3m_b(3T_a m_a + T_a m_b - 2T_b m_a)}{2(T_a m_b + T_b m_a)(m_a + m_b)}; \\ \hat{D}_{ab(1)} &= \{75T_a^3 m_a m_b^3 + 95T_a^3 m_b^4 + 174T_a^2 T_b m_a m_b^3 + 300T_a T_b^2 m_a^3 m_b + 498T_a T_b^2 m_a^2 m_b^2 + 60T_b^3 m_a^4 \\ &\quad + 104T_b^3 m_a^3 m_b\}[20(T_a m_b + T_b m_a)^3(m_a + m_b)]^{-1}; \\ \hat{D}_{ab(2)} &= \frac{9T_a m_b^2(10T_a^2 m_a m_b + 6T_a^2 m_b^2 + 45T_a T_b m_a^2 + 27T_a T_b m_a m_b - 14T_b^2 m_a^2)}{20(T_a m_b + T_b m_a)^3(m_a + m_b)}; \\ \hat{E}_{ab(1)} &= \frac{3T_a m_b(19T_a^2 m_a m_b^2 + 23T_a^2 m_b^3 - 2T_a T_b m_a^2 m_b + 36T_a T_b m_a m_b^2 + 84T_b^2 m_a^3 + 118T_b^2 m_a^2 m_b)}{560(T_a m_b + T_b m_a)^3(m_a + m_b)}; \\ \hat{E}_{ab(2)} &= \frac{9T_a T_b m_a m_b^2(7T_a m_a + 5T_a m_b - 2T_b m_a)}{112(T_a m_b + T_b m_a)^3(m_a + m_b)}.\end{aligned} \tag{19}$$

The fifth-order-moment exchange rates are given by

$$\begin{aligned}\boldsymbol{Q}_a^{(5)\prime} &= -\left[\frac{76}{5}\nu_{aa} + \sum_{b\neq a}\nu_{ab}\hat{F}_{ab(1)}\right]\frac{p_a}{\rho_a}\boldsymbol{q}_a + \sum_{b\neq a}\nu_{ab}\hat{F}_{ab(2)}\frac{p_a}{\rho_a}\frac{\rho_a}{\rho_b}\boldsymbol{q}_b \\ &\quad - \left[\frac{3}{35}\nu_{aa} + \sum_{b\neq a}\nu_{ab}\hat{G}_{ab(1)}\right]\boldsymbol{X}_a^{(5)} - \sum_{b\neq a}\nu_{ab}\hat{G}_{ab(2)}\frac{p_a}{p_b}\boldsymbol{X}_b^{(5)} \\ &\quad - \frac{p_a^2}{\rho_a}\sum_{b\neq a}\nu_{ab}(\boldsymbol{u}_b - \boldsymbol{u}_a)\hat{U}_{ab(2)},\end{aligned} \tag{20}$$

with mass-ratio coefficients

$$\begin{aligned}\hat{U}_{ab(2)} &= \frac{3m_b(17T_a^2 m_a m_b + 9T_a^2 m_b^2 + 42T_a T_b m_a^2 + 6T_a T_b m_a m_b - 28T_b^2 m_a^2)}{(T_a m_b + T_b m_a)^2(m_a + m_b)}; \\ \hat{F}_{ab(1)} &= \{855T_a^5 m_a m_b^4 + 759T_a^5 m_b^5 + 2340T_a^4 T_b m_a^2 m_b^3 + 1972T_a^4 T_b m_a m_b^4 + 2640T_a^3 T_b^2 m_a^3 m_b^2 \\ &\quad + 2332T_a^3 T_b^2 m_a^2 m_b^3 + 5880T_a^2 T_b^3 m_a^4 m_b + 3324T_a^2 T_b^3 m_a^3 m_b^2 - 3080T_a T_b^4 m_a^4 m_b - 560T_b^5 m_a^5\} \\ &\quad \times [10(T_a m_b + T_b m_a)^4(m_a + m_b)T_a]^{-1}; \\ \hat{F}_{ab(2)} &= 3T_a m_b^2\{70T_a^3 m_a m_b^2 + 102T_a^3 m_b^3 + 385T_a^2 T_b m_a^2 m_b + 561T_a^2 T_b m_a m_b^2 + 1890T_a T_b^2 m_a^3 \\ &\quad + 1446T_a T_b^2 m_a^2 m_b - 588T_b^3 m_a^3\}[10(T_a m_b + T_b m_a)^4(m_a + m_b)]^{-1}; \\ \hat{G}_{ab(1)} &= -\{565T_a^4 m_a m_b^4 + 533T_a^4 m_b^5 + 1270T_a^3 T_b m_a^2 m_b^3 + 1190T_a^3 T_b m_a m_b^4 + 1020T_a^2 T_b^2 m_a^3 m_b^2 \\ &\quad + 1152T_a^2 T_b^2 m_a^2 m_b^3 + 3640T_a T_b^3 m_a^4 m_b + 1916T_a T_b^3 m_a^3 m_b^2 - 1400T_b^4 m_a^5 - 3304T_b^4 m_a^4 m_b\} \\ &\quad \times [280(T_a m_b + T_b m_a)^4(m_a + m_b)]^{-1}; \\ \hat{G}_{ab(2)} &= -\frac{3T_a T_b m_a m_b^2(3T_a^2 m_a m_b - 5T_a^2 m_b^2 - 42T_a T_b m_a^2 - 38T_a T_b m_a m_b + 12T_b^2 m_a^2)}{8(T_a m_b + T_b m_a)^4(m_a + m_b)}.\end{aligned} \tag{21}$$

The exchange rates for the usual stress tensor are given by

$$\bar{\bar{\boldsymbol{Q}}}_a^{(2)\,\prime} = -\frac{21}{10}\nu_{aa}\bar{\bar{\boldsymbol{\Pi}}}_a^{(2)} + \frac{9}{70}\nu_{aa}\frac{\rho_a}{p_a}\bar{\bar{\boldsymbol{\Pi}}}_a^{(4)} + \sum_{b\neq a}\frac{\rho_a\nu_{ab}}{m_a+m_b}\left[-\hat{K}_{ab(1)}\frac{1}{n_a}\bar{\bar{\boldsymbol{\Pi}}}_a^{(2)} + \hat{K}_{ab(2)}\frac{1}{n_b}\bar{\bar{\boldsymbol{\Pi}}}_b^{(2)} + L_{ab(1)}\frac{\rho_a}{n_a p_a}\bar{\bar{\boldsymbol{\Pi}}}_a^{(4)} - L_{ab(2)}\frac{\rho_b}{n_b p_b}\bar{\bar{\boldsymbol{\Pi}}}_b^{(4)}\right], \tag{22}$$

with mass-ratio coefficients

$$\begin{aligned}
\hat{K}_{ab(1)} &= \frac{10T_a^2 m_a m_b^2 + 15T_a^2 m_b^3 + 35T_a T_b m_a^2 m_b + 42T_a T_b m_a m_b^2 + 10T_b^2 m_a^3 + 12T_b^2 m_a^2 m_b}{5(T_a m_b + T_b m_a)^2 m_a};\\
\hat{K}_{ab(2)} &= \frac{6T_a^2 m_a m_b + 4T_a^2 m_b^2 + 21T_a T_b m_a^2 + 14T_a T_b m_a m_b - 5T_b^2 m_a^2}{5(T_a m_b + T_b m_a)^2};\\
L_{ab(1)} &= \frac{3T_a m_b(2T_a m_a m_b + 3T_a m_b^2 + 7T_b m_a^2 + 8T_b m_a m_b)}{35(T_a m_b + T_b m_a)^2 m_a};\\
L_{ab(2)} &= \frac{3m_a T_b(5T_a m_a + 4T_a m_b - T_b m_a)}{35(T_a m_b + T_b m_a)^2}.
\end{aligned} \tag{23}$$

Finally, the fourth-order stress tensor exchange rates are given by

$$\bar{\bar{\boldsymbol{Q}}}_a^{(4)\,\prime} = -\frac{53}{20}\nu_{aa}\frac{p_a}{\rho_a}\bar{\bar{\boldsymbol{\Pi}}}_a^{(2)} - \frac{79}{140}\nu_{aa}\bar{\bar{\boldsymbol{\Pi}}}_a^{(4)} + \sum_{b\neq a}\nu_{ab}\left[-\hat{M}_{ab(1)}\frac{p_a}{\rho_a}\bar{\bar{\boldsymbol{\Pi}}}_a^{(2)} + \hat{M}_{ab(2)}\frac{p_a^2}{\rho_a p_b}\bar{\bar{\boldsymbol{\Pi}}}_b^{(2)} - N_{ab(1)}\bar{\bar{\boldsymbol{\Pi}}}_a^{(4)} - N_{ab(2)}\frac{p_a^2\rho_b}{p_b^2\rho_a}\bar{\bar{\boldsymbol{\Pi}}}_b^{(4)}\right], \tag{24}$$

with mass-ratio coefficients

$$\begin{aligned}
\hat{M}_{ab(1)} &= \{48T_a^4 m_a m_b^3 + 36T_a^4 m_b^4 + 216T_a^3 T_b m_a^2 m_b^2 + 107T_a^3 T_b m_a m_b^3 + 378T_a^2 T_b^2 m_a^3 m_b\\
&\quad + 36T_a^2 T_b^2 m_a^2 m_b^2 - 315T_a T_b^3 m_a^3 m_b - 70T_b^4 m_a^4\}[5(T_a m_b + T_b m_a)^3 T_a(m_b + m_a)]^{-1};\\
\hat{M}_{ab(2)} &= -\{T_b m_a(18T_a^3 m_a m_b^2 - 4T_a^3 m_b^3 + 81T_a^2 T_b m_a^2 m_b - 18T_a^2 T_b m_a m_b^2 - 147T_a T_b^2 m_a^3\\
&\quad - 189T_a T_b^2 m_a^2 m_b + 35T_b^3 m_a^3)\}[5(T_a m_b + T_b m_a)^3 T_a(m_b + m_a)]^{-1};\\
N_{ab(1)} &= -\{16T_a^3 m_a m_b^3 + 12T_a^3 m_b^4 + 72T_a^2 T_b m_a^2 m_b^2 + 21T_a^2 T_b m_a m_b^3 + 126T_a T_b^2 m_a^3 m_b\\
&\quad - 54T_a T_b^2 m_a^2 m_b^2 - 140T_b^3 m_a^4 - 273T_b^3 m_a^3 m_b\}[35(T_a m_b + T_b m_a)^3(m_b + m_a)]^{-1};\\
N_{ab(2)} &= -\frac{3T_b^2 m_a^2(35T_a^2 m_a m_b + 12T_a^2 m_b^2 - 35T_a T_b m_a^2 - 51T_a T_b m_a m_b + 7T_b^2 m_a^2)}{35(T_a m_b + T_b m_a)^3 T_a(m_b + m_a)}.
\end{aligned} \tag{25}$$

The entire system is now fully specified, and it represents a multifluid generalization of the model of Braginskii (1965). Coupled with Maxwell's equations, it can be used in multifluid numerical simulations. Importantly, when the collisional frequencies become small, the right-hand sides of the evolution equations just become small and no coefficients become divergent, which is in contrast to the model of Braginskii, where the quasistatic approximation is used for the stress tensors and heat fluxes. For a detailed discussion of the limitations of our model in a regime of low collisionality, see Section 8.9. The model of Braginskii is obtained as a particular case of a one ion–electron plasma with similar temperatures, in a quasistatic and quasilinear approximation for the viscosity tensors and heat fluxes, where, additionally, the coupling between the viscosity tensors and heat fluxes is neglected.

2.2. Collisional Contributions for Small Temperature Differences

In many instances, it might be satisfactory to consider a situation where the temperature differences between species are small. The mass-ratio coefficients (16) then become

$$V_{ab(1)} = \frac{(21/10)m_b + (3/5)m_a}{m_b + m_a}; \qquad V_{ab(2)} = \frac{(3/5)m_b + (21/10)m_a}{m_b + m_a}, \tag{26}$$

the mass-ratio coefficients (19) simplify into

$$\hat{D}_{ab(1)} = \frac{3m_a^3 + (86/5)m_a^2 m_b + (77/10)m_a m_b^2 + (19/4)m_b^3}{(m_a + m_b)^3};$$
$$\hat{D}_{ab(2)} = \frac{(279/20)m_a m_b^2 + (27/10)m_b^3}{(m_a + m_b)^3};$$
$$\hat{E}_{ab(1)} = \frac{(9/20)m_a^2 m_b + (6/35)m_a m_b^2 + (69/560)m_b^3}{(m_a + m_b)^3};$$
$$\hat{E}_{ab(2)} = \frac{(45/112)m_a m_b^2}{(m_a + m_b)^3}; \qquad \hat{U}_{ab(1)} = \frac{3}{2}\frac{m_b}{(m_a + m_b)}, \tag{27}$$

the mass-ratio coefficients (21) become

$$\hat{F}_{ab(1)} = \frac{(-56)m_a^4 + 336m_a^3 m_b + (1302/5)m_a^2 m_b^2 + (1034/5)m_a m_b^3 + (759/10)m_b^4}{(m_a + m_b)^4};$$
$$\hat{F}_{ab(2)} = \frac{(1953/5)m_a^2 m_b^2 + (1587/10)m_a m_b^3 + (153/5)m_b^4}{(m_a + m_b)^4};$$
$$\hat{G}_{ab(1)} = \frac{5m_a^4 - (31/5)m_a^3 m_b - (30/7)m_a^2 m_b^2 - (611/140)m_a m_b^3 - (533/280)m_b^4}{(m_a + m_b)^4};$$
$$\hat{G}_{ab(2)} = \frac{(45/4)m_a^2 m_b^2 + (15/8)m_a m_b^3}{(m_a + m_b)^4}; \qquad \hat{U}_{ab(2)} = \frac{42m_a m_b + 27m_b^2}{(m_a + m_b)^2}, \tag{28}$$

the mass-ratio coefficients (23) become

$$\hat{K}_{ab(1)} = \frac{10m_a^2 + 37m_a m_b + 15m_b^2}{5m_a(m_b + m_a)}; \qquad \hat{K}_{ab(2)} = \frac{4(4m_a + m_b)}{5(m_b + m_a)};$$
$$L_{ab(1)} = \frac{3(7m_a + 3m_b)m_b}{35m_a(m_b + m_a)}; \qquad L_{ab(2)} = \frac{12m_a}{35(m_a + m_b)}, \tag{29}$$

and the mass-ratio coefficients (25) simplify into

$$\hat{M}_{ab(1)} = -\frac{70m_a^3 - 133m_a^2 m_b - 119m_a m_b^2 - 36m_b^3}{5(m_b + m_a)^3}; \qquad \hat{M}_{ab(2)} = \frac{4m_a(28m_a^2 - m_a m_b + m_b^2)}{5(m_b + m_a)^3};$$
$$N_{ab(1)} = \frac{140m_a^3 + 7m_a^2 m_b - 25m_a m_b^2 - 12m_b^3}{35(m_b + m_a)^3}; \qquad N_{ab(2)} = \frac{12m_a^2(7m_a - 3m_b)}{35(m_b + m_a)^3}. \tag{30}$$

2.3. Reduction to the 13-moment Model

As a partial double-check of our calculations, neglecting the evolution Equations (11)–(12) for $\bar{\bar{\mathbf{\Pi}}}_a^{(4)}$ and $\boldsymbol{X}_a^{(5)}$, and, in the evolution Equations (9)–(10) for $\bar{\bar{\mathbf{\Pi}}}_a^{(2)}$ and $\boldsymbol{q}_a$, prescribing the closures (which are derived from Hermite closures)

$$\boldsymbol{X}_a^{(5)} = 28\frac{p_a}{\rho_a}\boldsymbol{q}_a; \qquad \bar{\bar{\mathbf{\Pi}}}_a^{(4)} = 7\frac{p_a}{\rho_a}\bar{\bar{\mathbf{\Pi}}}_a^{(2)}, \tag{31}$$

our 21-moment model simplifies into the 13-moment model, given by the collisional contributions

$$\boldsymbol{R}_a = \sum_{b\neq a}\nu_{ab}\left[\rho_a(\boldsymbol{u}_b - \boldsymbol{u}_a) + \frac{3}{5}\frac{\mu_{ab}}{T_{ab}}\left(\boldsymbol{q}_a - \frac{\rho_a}{\rho_b}\boldsymbol{q}_b\right)\right];$$
$$\boldsymbol{Q}_a^{(3)\prime} = -\frac{4}{5}\nu_{aa}\boldsymbol{q}_a + \sum_{b\neq a}\nu_{ab}\left[-\hat{D}_{ab(1)}^{*}\boldsymbol{q}_a + \hat{D}_{ab(2)}^{*}\frac{\rho_a}{\rho_b}\boldsymbol{q}_b - p_a(\boldsymbol{u}_b - \boldsymbol{u}_a)\hat{U}_{ab(1)}\right];$$
$$\bar{\bar{\boldsymbol{Q}}}_a^{(2)\prime} = -\frac{6}{5}\nu_{aa}\bar{\bar{\mathbf{\Pi}}}_a^{(2)} + \sum_{b\neq a}\frac{\rho_a\nu_{ab}}{m_a + m_b}\left[-\hat{K}_{ab(1)}^{*}\frac{1}{n_a}\bar{\bar{\mathbf{\Pi}}}_a^{(2)} + \hat{K}_{ab(2)}^{*}\frac{1}{n_b}\bar{\bar{\mathbf{\Pi}}}_b^{(2)}\right], \tag{32}$$

with the mass-ratio coefficients

$$\hat{D}^*_{ab(1)} = \frac{9T_a^2 m_a m_b^2 + 13T_a^2 m_b^3 - 6T_a T_b m_a^2 m_b + 20T_a T_b m_a m_b^2 + 30T_b^2 m_a^3 + 52T_b^2 m_a^2 m_b}{10(m_a + m_b)(T_a m_b + T_b m_a)^2};$$
$$\hat{D}^*_{ab(2)} = \frac{9T_a m_b^2 (5T_a m_a + 3T_a m_b - 2T_b m_a)}{10(m_a + m_b)(T_a m_b + T_b m_a)^2};$$
$$\hat{K}^*_{ab(1)} = \frac{2(2T_a m_a m_b + 3T_a m_b^2 + 5T_b m_a^2 + 6T_b m_a m_b)}{5m_a(T_a m_b + T_b m_a)}; \qquad \hat{K}^*_{ab(2)} = \frac{2(3T_a m_a + 2T_a m_b - T_b m_a)}{5(T_a m_b + T_b m_a)}, \tag{33}$$

where $\hat{U}_{ab(1)}$ is unchanged from the 21-moment model. It can be shown that for Coulomb collisions, this model is equivalent to Equations (44)–(49) of Schunk (1977), first calculated by Burgers (1969). For small temperature differences, the mass-ratio coefficients become

$$\hat{D}^*_{ab(1)} = \frac{30m_a^2 + 16m_a m_b + 13m_b^2}{10(m_a + m_b)^2}; \qquad \hat{D}^*_{ab(2)} = \frac{27m_b^2}{10(m_a + m_b)^2};$$
$$\hat{K}^*_{ab(1)} = \frac{2m_a + (6/5)m_b}{m_a}; \qquad \hat{K}^*_{ab(2)} = \frac{4}{5}; \qquad \hat{U}_{ab(1)} = \frac{3}{2}\frac{m_b}{(m_a + m_b)}. \tag{34}$$

Our new 21-moment model can thus be viewed as a generalization of the multifluid description of Burgers (1969) and Schunk (1977), where the heat fluxes and stress tensors are described more accurately, and with the same level of precision as in Braginskii (1965). Nevertheless, we only use the Landau collisional operator applicable for Coulomb collisions, whereas Burgers–Schunk use the more general Boltzmann collisional operator and account for several different interaction potentials.

2.4. Semilinear Approximation (Decoupled Stress Tensors and Heat Fluxes)

Here we consider the 21-moment model with evolution Equations (9)–(12) in the semilinear approximation, where additionally viscosity tensors and heat fluxes are decoupled. It will be shown later that the contributions introduced by the coupling are smaller by a factor of $1/\nu_{aa}$. Within the semilinear approximation, we also assume that there are no large-scale gradients of considered fluid moments. For example, the decoupling removes the last terms on the left-hand sides of Equations (10), (11), and (12) proportional to $(\nabla p_a)\boldsymbol{q}_a$, $(\nabla p_a)\cdot\bar{\bar{\boldsymbol{\Pi}}}_a^{(2)}$ and $(\nabla p_a)\cdot\bar{\bar{\boldsymbol{\Pi}}}_a^{(4)}$. We also neglect these terms within the semilinear approximation when the coupling is considered (see Sections 5 and 6). In the presence of large-scale gradients in pressure/temperature, these terms might become significant, together with many other terms that are neglected in the semilinear approximation. The evolution equations for the heat flux vectors simplify into

$$\frac{d_a}{dt}\boldsymbol{q}_a + \Omega_a\hat{\boldsymbol{b}}\times\boldsymbol{q}_a + \frac{5}{2}p_a\nabla\left(\frac{p_a}{\rho_a}\right) = \boldsymbol{Q}_a^{(3)\prime}; \tag{35}$$

$$\frac{d_a}{dt}\boldsymbol{X}_a^{(5)} + \Omega_a\hat{\boldsymbol{b}}\times\boldsymbol{X}_a^{(5)} + 70\frac{p_a^2}{\rho_a}\nabla\left(\frac{p_a}{\rho_a}\right) = \boldsymbol{Q}_a^{(5)\prime}, \tag{36}$$

and the evolution equations for the viscosity tensors become

$$\frac{d_a}{dt}\bar{\bar{\boldsymbol{\Pi}}}_a^{(2)} + \Omega_a(\hat{\boldsymbol{b}}\times\bar{\bar{\boldsymbol{\Pi}}}_a^{(2)})^S + p_a\bar{\bar{\boldsymbol{W}}}_a = \bar{\bar{\boldsymbol{Q}}}_a^{(2)\prime}; \tag{37}$$

$$\frac{d_a}{dt}\bar{\bar{\boldsymbol{\Pi}}}_a^{(4)} + \Omega_a(\hat{\boldsymbol{b}}\times\bar{\bar{\boldsymbol{\Pi}}}_a^{(4)})^S + 7\frac{p_a^2}{\rho_a}\bar{\bar{\boldsymbol{W}}}_a = \bar{\bar{\boldsymbol{Q}}}_a^{(4)\prime}. \tag{38}$$

The above system will be used to recover the transport coefficients of Braginskii (1965). In some instances, it might actually be advantageous to suppress the nonlinearities in numerical simulations, and to perform multifluid simulations with the system (35)–(38) instead of the system (9)–(12).

3. One Ion–Electron Plasma

3.1. Ion Heat Flux $\boldsymbol{q}_{\rm a}$ of Braginskii (Self-collisions)

Here we consider a one ion–electron plasma of similar temperatures, which is the choice of Braginskii (1965). For the ion heat flux, Braginskii neglects ion–electron collisions. Considering only self-collisions, the evolution equations for ion heat fluxes read

$$\frac{d_a}{dt}\boldsymbol{q}_a + \Omega_a\hat{\boldsymbol{b}}\times\boldsymbol{q}_a + \frac{5}{2}p_a\nabla\left(\frac{p_a}{\rho_a}\right) = -\frac{4}{5}\nu_{aa}\boldsymbol{q}_a + \frac{3}{70}\nu_{aa}\left(\frac{\rho_a}{p_a}\boldsymbol{X}_a^{(5)} - 28\boldsymbol{q}_a\right); \tag{39}$$

$$\frac{d_a}{dt}\boldsymbol{X}_a^{(5)} + \Omega_a\hat{\boldsymbol{b}}\times\boldsymbol{X}_a^{(5)} + 70\frac{p_a^2}{\rho_a}\nabla\left(\frac{p_a}{\rho_a}\right) = -\frac{88}{5}\nu_{aa}\frac{p_a}{\rho_a}\boldsymbol{q}_a - \frac{3}{35}\nu_{aa}\left(\boldsymbol{X}_a^{(5)} - 28\frac{p_a}{\rho_a}\boldsymbol{q}_a\right). \tag{40}$$

Neglecting the evolution Equation (40), and prescribing closure (31), which neglects the second term on the right-hand side of (39), yields the ion heat flux model of Burgers–Schunk, with the well-known $-4/5$ constant. However, now the equations read:

$$\begin{aligned}
&\frac{d_a}{dt}\boldsymbol{q}_a + \Omega_a\hat{\boldsymbol{b}}\times\boldsymbol{q}_a + \frac{5}{2}p_a\nabla\left(\frac{p_a}{\rho_a}\right) = -2\nu_{aa}\boldsymbol{q}_a + \frac{3}{70}\nu_{aa}\frac{\rho_a}{p_a}\boldsymbol{X}_a^{(5)};\\
&\frac{d_a}{dt}\boldsymbol{X}_a^{(5)} + \Omega_a\hat{\boldsymbol{b}}\times\boldsymbol{X}_a^{(5)} + 70\frac{p_a^2}{\rho_a}\nabla\left(\frac{p_a}{\rho_a}\right) = -\frac{76}{5}\nu_{aa}\frac{p_a}{\rho_a}\boldsymbol{q}_a - \frac{3}{35}\nu_{aa}\boldsymbol{X}_a^{(5)}.
\end{aligned} \tag{41}$$

Prescribing the quasistatic approximation (by canceling the d_a/dt) yields an analytic solution (see, for example, the general vector Equation (E23) with solution (E24))

$$\boldsymbol{q}_a = -\kappa_\parallel^a\nabla_\parallel T_a - \kappa_\perp^a\nabla_\perp T_a + \kappa_\times^a\hat{\boldsymbol{b}}\times\nabla T_a, \tag{42}$$

and thermal conductivities

$$\begin{aligned}
\kappa_\parallel^a &= \frac{125}{32}\frac{p_a}{\nu_{aa}m_a};\\
\kappa_\perp^a &= \frac{p_a}{\nu_{aa}m_a}\frac{2x^2 + (648/245)}{x^4 + (3313/1225)x^2 + (20736/30625)};\\
\kappa_\times^a &= \frac{p_a}{\nu_{aa}m_a}\frac{(5/2)x^3 + (2277/490)x}{x^4 + (3313/1225)x^2 + (20736/30625)},
\end{aligned} \tag{43}$$

where $x = \Omega_a/\nu_{aa}$. Alternatively, by using numerical values,

$$\begin{aligned}
\kappa_\parallel^a &= 3.906\frac{p_a}{\nu_{aa}m_a};\\
\kappa_\perp^a &= \frac{p_a}{\nu_{aa}m_a}\frac{2x^2 + 2.645}{x^4 + 2.704x^2 + 0.6771};\\
\kappa_\times^a &= \frac{p_a}{\nu_{aa}m_a}\frac{(5/2)x^3 + 4.647x}{x^4 + 2.704x^2 + 0.6771},
\end{aligned} \tag{44}$$

which recovers the ion heat flux of Braginskii (1965), his Equation (4.40). We use the Braginskii notation with vectors $\nabla_\parallel = \hat{\boldsymbol{b}}\hat{\boldsymbol{b}}\cdot\nabla$ and $\nabla_\perp = \bar{\bar{\boldsymbol{I}}}_\perp\cdot\nabla = -\hat{\boldsymbol{b}}\times\hat{\boldsymbol{b}}\times\nabla$.

3.2. Ion Heat Flux $\boldsymbol{X}_a^{(5)}$ (Self-collisions)

The solution for the vector $\boldsymbol{X}_a^{(5)}$ has a similar form:

$$\boldsymbol{X}_a^{(5)} = \frac{p_a}{\rho_a}[-\kappa_\parallel^{a(5)}\nabla_\parallel T_a - \kappa_\perp^{a(5)}\nabla_\perp T_a + \kappa_\times^{a(5)}\hat{\boldsymbol{b}}\times\nabla T_a], \tag{45}$$

with "thermal conductivities"

$$\kappa_{\parallel}^{a(5)} = \underbrace{\frac{2975}{24}}_{123.96} \frac{p_a}{\nu_{aa} m_a};$$
$$\kappa_{\perp}^{a(5)} = \frac{p_a}{\nu_{aa} m_a} \frac{44x^2 + (14688/175)}{x^4 + (3313/1225)x^2 + (20736/30625)};$$
$$\kappa_{\times}^{a(5)} = \frac{p_a}{\nu_{aa} m_a} \frac{70x^3 + (1086/7)x}{x^4 + (3313/1225)x^2 + (20736/30625)}. \tag{46}$$

3.3. Electron Heat Flux $\boldsymbol{q}_{\rm e}$ of Braginskii

Considering a one ion–electron plasma with similar temperatures, and keeping only the dominant term in an m_e/m_i expansion, the mass-ratio coefficients (26), (27), and (28) simplify into

$$V_{ei(1)} = \frac{21}{10}; \quad V_{ei(2)} = \frac{3}{5};$$
$$\hat{D}_{ei(1)} = \frac{19}{4}; \quad \hat{D}_{ei(2)} = \frac{27}{10}; \quad \hat{E}_{ei(1)} = \frac{69}{560}; \quad \hat{E}_{ei(2)} = \frac{45}{112}\frac{m_e}{m_i}; \quad \hat{U}_{ei(1)} = \frac{3}{2}$$
$$\hat{F}_{ei(1)} = \frac{759}{10}; \quad \hat{F}_{ei(2)} = \frac{153}{5}; \quad \hat{G}_{ei(1)} = -\frac{533}{280}; \quad \hat{G}_{ei(2)} = \frac{15}{8}\frac{m_e}{m_i}; \quad \hat{U}_{ei(2)} = 27, \tag{47}$$

and the collisional exchange rates become

$$\boldsymbol{R}_e = -\rho_e \nu_{ei} \delta \boldsymbol{u} + \frac{21}{10}\frac{\rho_e}{p_e}\nu_{ei}\boldsymbol{q}_e - \frac{3}{56}\frac{\rho_e^2}{p_e^2}\nu_{ei}\boldsymbol{X}_e^{(5)}; \tag{48}$$

$$\boldsymbol{Q}_e^{(3)\,\prime} = +\frac{3}{2}p_e\nu_{ei}\delta\boldsymbol{u} - \left[2\nu_{ee} + \frac{19}{4}\nu_{ei}\right]\boldsymbol{q}_e + \left[\frac{3}{70}\nu_{ee} + \frac{69}{560}\nu_{ei}\right]\frac{\rho_e}{p_e}\boldsymbol{X}_e^{(5)}; \tag{49}$$

$$\boldsymbol{Q}_e^{(5)\,\prime} = +27\frac{p_e^2}{\rho_e}\nu_{ei}\delta\boldsymbol{u} - \left[\frac{76}{5}\nu_{ee} + \frac{759}{10}\nu_{ei}\right]\frac{p_e}{\rho_e}\boldsymbol{q}_e - \left[\frac{3}{35}\nu_{ee} - \frac{533}{280}\nu_{ei}\right]\boldsymbol{X}_e^{(5)}, \tag{50}$$

where $\delta\boldsymbol{u} = \boldsymbol{u}_e - \boldsymbol{u}_i$, and enter the right-hand sides of the electron momentum equation and the evolution equations for the electron heat flux vectors

$$\frac{d_e}{dt}\boldsymbol{q}_e + \Omega_e\hat{\boldsymbol{b}} \times \boldsymbol{q}_e + \frac{5}{2}p_e\nabla\left(\frac{p_e}{\rho_e}\right) = \boldsymbol{Q}_e^{(3)\,\prime};$$
$$\frac{d_e}{dt}\boldsymbol{X}_e^{(5)} + \Omega_e\hat{\boldsymbol{b}} \times \boldsymbol{X}_e^{(5)} + 70\frac{p_e^2}{\rho_e}\nabla\left(\frac{p_e}{\rho_e}\right) = \boldsymbol{Q}_e^{(5)\,\prime}. \tag{51}$$

In Braginskii (1965), the results are expressed through the collisional frequency ν_{ei}, and conversion with $\nu_{ee} = \nu_{ei}/(Z_i\sqrt{2})$ yields

$$\boldsymbol{Q}_e^{(3)\,\prime} = +\frac{3}{2}p_e\nu_{ei}\delta\boldsymbol{u} - \left[\frac{\sqrt{2}}{Z_i} + \frac{19}{4}\right]\nu_{ei}\boldsymbol{q}_e + \left[\frac{3}{70\sqrt{2}Z_i} + \frac{69}{560}\right]\nu_{ei}\frac{\rho_e}{p_e}\boldsymbol{X}_e^{(5)};$$
$$\boldsymbol{Q}_e^{(5)\,\prime} = +27\frac{p_e^2}{\rho_e}\nu_{ei}\delta\boldsymbol{u} - \left[\frac{76}{5\sqrt{2}Z_i} + \frac{759}{10}\right]\nu_{ei}\frac{p_e}{\rho_e}\boldsymbol{q}_e - \left[\frac{3}{35\sqrt{2}Z_i} - \frac{533}{280}\right]\nu_{ei}\boldsymbol{X}_e^{(5)}. \tag{52}$$

In a quasistatic approximation, the solution of (51), (52) recovers the famous electron heat flux of Braginskii (1965), together with vector $\boldsymbol{X}_e^{(5)}$ (which is of course not given by Braginskii). Substituting these results into the momentum exchange rates (48) recovers the $\boldsymbol{R}_e$ of Braginskii.

We use the same notation as Braginskii (1965) with $x = \Omega_e/\nu_{ei}$, except (as is the norm in more recent papers) our Ω_e is formulated as a general Ω_a and is thus negative, whereas in Braginskii Ω_e is defined as positive. This yields a simple change of signs in front of the "cross" ($\times$) terms with respect to Braginskii. In a quasistatic approximation, the electron heat flux is split into a thermal part and a frictional part $\boldsymbol{q}_e = \boldsymbol{q}_e^T + \boldsymbol{q}_e^u$, where

$$\boldsymbol{q}_e^T = -\kappa_{\parallel}^e\nabla_{\parallel}T_e - \kappa_{\perp}^e\nabla_{\perp}T_e + \kappa_{\times}^e\hat{\boldsymbol{b}} \times \nabla T_e;$$
$$\boldsymbol{q}_e^u = \beta_0 p_e\delta\boldsymbol{u}_{\parallel} + p_e\delta\boldsymbol{u}_{\perp}\frac{\beta_1' x^2 + \beta_0'}{\triangle} - p_e\hat{\boldsymbol{b}} \times \delta\boldsymbol{u}\frac{\beta_1'' x^3 + \beta_0'' x}{\triangle}, \tag{53}$$

and the heat conductivities are given by

$$\kappa_{\parallel}^{e} = \frac{p_e}{m_e \nu_{ei}} \gamma_0; \qquad \kappa_{\perp}^{e} = \frac{p_e}{m_e \nu_{ei}} \frac{\gamma_1' x^2 + \gamma_0'}{\triangle}; \qquad \kappa_{\times}^{e} = \frac{p_e}{m_e \nu_{ei}} \frac{\gamma_1'' x^3 + \gamma_0'' x}{\triangle}. \tag{54}$$

The momentum exchange rates are also split into a thermal part and a frictional part $\boldsymbol{R}_e = \boldsymbol{R}_e^T + \boldsymbol{R}_e^u$ (thermal force and friction force), according to

$$\begin{aligned} \boldsymbol{R}_e^u &= -\alpha_0 \rho_e \nu_{ei} \delta \boldsymbol{u}_{\parallel} - \rho_e \nu_{ei} \delta \boldsymbol{u}_{\perp} \left(1 - \frac{\alpha_1' x^2 + \alpha_0'}{\triangle}\right) - \rho_e \nu_{ei} \hat{\boldsymbol{b}} \times \delta \boldsymbol{u} \frac{\alpha_1'' x^3 + \alpha_0'' x}{\triangle}; \\ \boldsymbol{R}_e^T &= -\beta_0 n_e \nabla_{\parallel} T_e - n_e \nabla_{\perp} T_e \frac{\beta_1' x^2 + \beta_0'}{\triangle} + n_e \hat{\boldsymbol{b}} \times \nabla T_e \frac{\beta_1'' x^3 + \beta_0'' x}{\triangle}. \end{aligned} \tag{55}$$

Instead of the numerical Table II on p. 25 of Braginskii (1965), we provide all of the coefficients in a fully analytic form for a general ion charge Z_i, which are given by

$$\alpha_0 = \frac{4(16Z_i^2 + 61Z_i\sqrt{2} + 72)}{217Z_i^2 + 604Z_i\sqrt{2} + 288}; \qquad \beta_0 = \frac{30Z_i(11Z_i + 15\sqrt{2})}{217Z_i^2 + 604Z_i\sqrt{2} + 288};$$
$$\gamma_0 = \frac{25Z_i(433Z_i + 180\sqrt{2})}{4(217Z_i^2 + 604Z_i\sqrt{2} + 288)}; \tag{56}$$

$$\triangle = x^4 + \delta_1 x^2 + \delta_0;$$
$$\delta_0 = \left(\frac{217Z_i^2 + 604Z_i\sqrt{2} + 288}{700Z_i^2}\right)^2;$$
$$\delta_1 = \frac{586601Z_i^2 + 330152Z_i\sqrt{2} + 106016}{78400Z_i^2}; \tag{57}$$

$$\alpha_1' = \frac{9(40337Z_i + 10996\sqrt{2})}{78400Z_i};$$
$$\alpha_0' = \frac{9(217Z_i^2 + 604Z_i\sqrt{2} + 288)(17Z_i + 40\sqrt{2})}{490000Z_i^3};$$
$$\alpha_1'' = \frac{477}{280}; \qquad \alpha_0'' = \frac{9(64Z_i^2 + 151Z_i\sqrt{2} + 253)}{6125Z_i^2}; \tag{58}$$

$$\beta_1' = \frac{3(709Z_i + 172\sqrt{2})}{560Z_i};$$
$$\beta_0' = \frac{3(217Z_i^2 + 604Z_i\sqrt{2} + 288)(11Z_i + 15\sqrt{2})}{49000Z_i^3};$$
$$\beta_1'' = \frac{3}{2}; \qquad \beta_0'' = \frac{3(5729Z_i^2 + 6711Z_i\sqrt{2} + 4728)}{19600Z_i^2}; \tag{59}$$

$$\gamma_1' = \frac{13Z_i + 4\sqrt{2}}{4Z_i};$$
$$\gamma_0' = \frac{(217Z_i^2 + 604Z_i\sqrt{2} + 288)(433Z_i + 180\sqrt{2})}{78400Z_i^3};$$
$$\gamma_1'' = \frac{5}{2}; \qquad \gamma_0'' = \frac{320797Z_i^2 + 202248Z_i\sqrt{2} + 72864}{31360Z_i^2}. \tag{60}$$

The numerical values for $Z_i = 1$ are given in the first column of Table II of Braginskii (1965), and the parallel coefficients are $\alpha_0 = 0.5129$, $\beta_0 = 0.7110$, and $\gamma_0 = 3.1616$, for example, matching his values exactly. We checked the entire Table II of Braginskii, and his table is very precise, except for two values. For the α_0 coefficient, the values for $Z_i = 2$, 3 should be changed according to $0.4408 \rightarrow 0.4309$, $0.3965 \rightarrow 0.3954$. The rest of his table is calculated very accurately, with a handful of irrelevant last digit rounding changes (such as $3.7703 \rightarrow 3.7702$ in δ_0 ($Z_i = 1$) and $0.2400 \rightarrow 0.2399$ in α_0'' ($Z_i = 3$); and for the $Z_i = 4$ charge, $0.3752 \rightarrow 0.3751$ in α_0, $9.055 \rightarrow 9.056$ in δ_0, and $0.4478 \rightarrow 0.4477$ in β_0', etc.).

Analytic results (56) for parallel coefficients α_0, β_0, and γ_0 were also obtained by Simakov & Molvig (2014); see also Section 4. To triple-check our other results, we recalculated our approach with the analytic collisional matrices of Ji & Held (2013), see their Equations (28a)–(28f), together with (40)–(44) and other formulas, which yielded the same analytic expressions. Unfortunately, the analytic results of Balescu (1988) are written in a such a complicated form (see his p. 236, with the collisional matrices on p. 198 and

the required conversion Equation (5.7.13) on p. 270) that we were only able to verify an analytic match with his parallel coefficients. The formulation of Balescu (1988) is so different from Braginskii that Balescu himself (p. 275) only claims a match of below 1% for the 21-moment model, without further analyzing possible discrepancies.

3.4. Electron Heat Flux $\boldsymbol{X}_e^{(5)}$

Similar to the usual electron heat flux $\boldsymbol{q}_e$, a quasistatic solution for the heat flux vector $\boldsymbol{X}_e^{(5)}$ has to be split into a thermal part and a frictional part, according to

$$\boldsymbol{X}_e^{(5)T} = \frac{p_e}{\rho_e}[-\kappa_\parallel^{e(5)}\nabla_\parallel T_e - \kappa_\perp^{e(5)}\nabla_\perp T_e + \kappa_\times^{e(5)}\hat{\boldsymbol{b}}\times\nabla T_e];$$
$$\boldsymbol{X}_e^{(5)u} = \frac{p_e^2}{\rho_e}\left[\beta_0^{(5)}\delta\boldsymbol{u}_\parallel + \frac{\beta_1^{(5)\prime}x^2 + \beta_0^{(5)\prime}}{\triangle}\delta\boldsymbol{u}_\perp - \frac{\beta_1^{(5)\prime\prime}x^3 + \beta_0^{(5)\prime\prime}x}{\triangle}\hat{\boldsymbol{b}}\times\delta\boldsymbol{u}\right], \tag{61}$$

with the thermal conductivities

$$\kappa_\parallel^{e(5)} = \frac{p_e}{m_e\nu_{ei}}\gamma_0^{(5)}; \qquad \kappa_\perp^{e(5)} = \frac{p_e}{m_e\nu_{ei}}\frac{\gamma_1^{(5)\prime}x^2 + \gamma_0^{(5)\prime}}{\triangle}; \qquad \kappa_\times^{e(5)} = \frac{p_e}{m_e\nu_{ei}}\frac{\gamma_1^{(5)\prime\prime}x^3 + \gamma_0^{(5)\prime\prime}x}{\triangle}. \tag{62}$$

The analytic coefficients are given by

$$\beta_0^{(5)} = \frac{840Z_i(13\sqrt{2} + 12Z_i)}{217Z_i^2 + 604Z_i\sqrt{2} + 288};$$
$$\beta_1^{(5)\prime} = \frac{3(5829Z_i + 1172\sqrt{2})}{280Z_i};$$
$$\beta_0^{(5)\prime} = \frac{3(217Z_i^2 + 604Z_i\sqrt{2} + 288)(12Z_i + 13\sqrt{2})}{1750Z_i^3};$$
$$\beta_1^{(5)\prime\prime} = 27; \qquad \beta_0^{(5)\prime\prime} = \frac{3(7611Z_i^2 + 8429Z_i\sqrt{2} + 5000)}{700Z_i^2}, \tag{63}$$

and

$$\gamma_0^{(5)} = \frac{175Z_i(204\sqrt{2} + 571Z_i)}{217Z_i^2 + 604Z_i\sqrt{2} + 288};$$
$$\gamma_1^{(5)\prime} = \frac{113Z_i + 44\sqrt{2}}{2Z_i};$$
$$\gamma_0^{(5)\prime} = \frac{(217Z_i^2 + 604Z_i\sqrt{2} + 288)(571Z_i + 204\sqrt{2})}{2800Z_i^3};$$
$$\gamma_1^{(5)\prime\prime} = 70; \qquad \gamma_0^{(5)\prime\prime} = \frac{430783Z_i^2 + 261672Z_i\sqrt{2} + 86880}{1120Z_i^2}, \tag{64}$$

with $\triangle$ unchanged and given by (57). These results were substituted into the momentum exchange rates $\boldsymbol{R}_e$, Equation (48), to obtain the final expression for the friction force and the thermal force. The useful relations are

$$\alpha_0 = 1 - \frac{21}{10}\beta_0 + \frac{3}{56}\beta_0^{(5)}; \qquad \alpha_1' = \frac{21}{10}\beta_1' - \frac{3}{56}\beta_1^{(5)\prime};$$
$$\alpha_0' = \frac{21}{10}\beta_0' - \frac{3}{56}\beta_0^{(5)\prime}; \qquad \alpha_1'' = \frac{21}{10}\beta_1'' - \frac{3}{56}\beta_1^{(5)\prime\prime}; \qquad \alpha_0'' = \frac{21}{10}\beta_0'' - \frac{3}{56}\beta_0^{(5)\prime\prime};$$
$$\beta_0 = \frac{21}{10}\gamma_0 - \frac{3}{56}\gamma_0^{(5)}; \qquad \beta_1' = \frac{21}{10}\gamma_1' - \frac{3}{56}\gamma_1^{(5)\prime};$$
$$\beta_0' = \frac{21}{10}\gamma_0' - \frac{3}{56}\gamma_0^{(5)\prime}; \qquad \beta_1'' = \frac{21}{10}\gamma_1'' - \frac{3}{56}\gamma_1^{(5)\prime\prime}; \qquad \beta_0'' = \frac{21}{10}\gamma_0'' - \frac{3}{56}\gamma_0^{(5)\prime\prime}. \tag{65}$$

For $Z_i = 1$, the transport coefficients (63), (64) have numerical values

$$\beta_0^{(5)} = 18.778; \qquad \beta_1^{(5)\prime} = 80.212; \qquad \beta_0^{(5)\prime} = 70.797; \qquad \beta_1^{(5)\prime\prime} = 27; \qquad \beta_0^{(5)\prime\prime} = 105.135;$$
$$\gamma_0^{(5)} = 110.664; \qquad \gamma_1^{(5)\prime} = 87.613; \qquad \gamma_0^{(5)\prime} = 417.221; \qquad \gamma_1^{(5)\prime\prime} = 70; \qquad \gamma_0^{(5)\prime\prime} = 792.610. \tag{66}$$

3.5. Ion Viscosity $\bar{\bar{\mathbf{\Pi}}}_a^{(2)}$ of Braginskii (Self-collisions)

Considering self-collisions, the evolution equations for the ion viscosity tensors read

$$\frac{d_a}{dt}\bar{\bar{\mathbf{\Pi}}}_a^{(2)} + \Omega_a(\hat{\boldsymbol{b}} \times \bar{\bar{\mathbf{\Pi}}}_a^{(2)})^S + p_a\bar{\bar{\boldsymbol{W}}}_a = -\frac{6}{5}\nu_{aa}\bar{\bar{\mathbf{\Pi}}}_a^{(2)} + \frac{9}{70}\nu_{aa}\left(\frac{\rho_a}{p_a}\bar{\bar{\mathbf{\Pi}}}_a^{(4)} - 7\bar{\bar{\mathbf{\Pi}}}_a^{(2)}\right); \tag{67}$$

$$\frac{d_a}{dt}\bar{\bar{\mathbf{\Pi}}}_a^{(4)} + \Omega_a(\hat{\boldsymbol{b}} \times \bar{\bar{\mathbf{\Pi}}}_a^{(4)})^S + 7\frac{p_a^2}{\rho_a}\bar{\bar{\boldsymbol{W}}}_a = -\frac{33}{5}\nu_{aa}\frac{p_a}{\rho_a}\bar{\bar{\mathbf{\Pi}}}_a^{(2)} - \frac{79}{140}\nu_{aa}\left(\bar{\bar{\mathbf{\Pi}}}_a^{(4)} - 7\frac{p_a}{\rho_a}\bar{\bar{\mathbf{\Pi}}}_a^{(2)}\right). \tag{68}$$

Neglecting (68), and prescribing closure (31), which neglects the second term on the right-hand side of (67), yields the ion viscosity model of Burgers–Schunk, with the well-known $-6/5$ constant. However, now the equations read

$$\begin{aligned}
&\frac{d_a}{dt}\bar{\bar{\mathbf{\Pi}}}_a^{(2)} + \Omega_a(\hat{\boldsymbol{b}} \times \bar{\bar{\mathbf{\Pi}}}_a^{(2)})^S + p_a\bar{\bar{\boldsymbol{W}}}_a = -\frac{21}{10}\nu_{aa}\bar{\bar{\mathbf{\Pi}}}_a^{(2)} + \frac{9}{70}\nu_{aa}\frac{\rho_a}{p_a}\bar{\bar{\mathbf{\Pi}}}_a^{(4)};\\
&\frac{d_a}{dt}\bar{\bar{\mathbf{\Pi}}}_a^{(4)} + \Omega_a(\hat{\boldsymbol{b}} \times \bar{\bar{\mathbf{\Pi}}}_a^{(4)})^S + 7\frac{p_a^2}{\rho_a}\bar{\bar{\boldsymbol{W}}}_a = -\frac{53}{20}\nu_{aa}\frac{p_a}{\rho_a}\bar{\bar{\mathbf{\Pi}}}_a^{(2)} - \frac{79}{140}\nu_{aa}\bar{\bar{\mathbf{\Pi}}}_a^{(4)}.
\end{aligned} \tag{69}$$

In a quasistatic approximation, the solution of (69) yields $\bar{\bar{\mathbf{\Pi}}}_a^{(2)}$ in the following form (see, for example, Appendix E.4):

$$\bar{\bar{\mathbf{\Pi}}}_a^{(2)} = -\eta_0^a\bar{\bar{\boldsymbol{W}}}_0 - \eta_1^a\bar{\bar{\boldsymbol{W}}}_1 - \eta_2^a\bar{\bar{\boldsymbol{W}}}_2 + \eta_3^a\bar{\bar{\boldsymbol{W}}}_3 + \eta_4^a\bar{\bar{\boldsymbol{W}}}_4; \tag{70}$$

$$\begin{aligned}
&\bar{\bar{\boldsymbol{W}}}_0 = \frac{3}{2}(\bar{\bar{\boldsymbol{W}}}_a\colon \hat{\boldsymbol{b}}\hat{\boldsymbol{b}})\left(\hat{\boldsymbol{b}}\hat{\boldsymbol{b}} - \frac{\bar{\bar{\boldsymbol{I}}}}{3}\right);\\
&\bar{\bar{\boldsymbol{W}}}_1 = \bar{\bar{\boldsymbol{I}}}_\perp \cdot \bar{\bar{\boldsymbol{W}}}_a \cdot \bar{\bar{\boldsymbol{I}}}_\perp + \frac{1}{2}(\bar{\bar{\boldsymbol{W}}}_a\colon \hat{\boldsymbol{b}}\hat{\boldsymbol{b}})\bar{\bar{\boldsymbol{I}}}_\perp;\\
&\bar{\bar{\boldsymbol{W}}}_2 = (\bar{\bar{\boldsymbol{I}}}_\perp \cdot \bar{\bar{\boldsymbol{W}}}_a \cdot \hat{\boldsymbol{b}}\hat{\boldsymbol{b}})^S;\\
&\bar{\bar{\boldsymbol{W}}}_3 = \frac{1}{2}(\hat{\boldsymbol{b}} \times \bar{\bar{\boldsymbol{W}}}_a \cdot \bar{\bar{\boldsymbol{I}}}_\perp)^S;\\
&\bar{\bar{\boldsymbol{W}}}_4 = (\hat{\boldsymbol{b}} \times \bar{\bar{\boldsymbol{W}}}_a \cdot \hat{\boldsymbol{b}}\hat{\boldsymbol{b}})^S,
\end{aligned} \tag{71}$$

which is equivalent to Equations (4.41) and (4.42) of Braginskii (1965), after one prescribes in his $\bar{\bar{\boldsymbol{W}}}_0$ that the matrix $\bar{\bar{\boldsymbol{W}}}_a$ is traceless. Alternatively, with respect to $\hat{\boldsymbol{b}} = (0, 0, 1)$ (a straight magnetic field applied in the z-direction),

$$\begin{aligned}
&\Pi_{xx}^{a(2)} = -\frac{\eta_0^a}{2}(W_{xx}^a + W_{yy}^a) - \frac{\eta_1^a}{2}(W_{xx}^a - W_{yy}^a) - \eta_3^a W_{xy}^a;\\
&\Pi_{xy}^{a(2)} = \frac{\eta_3^a}{2}(W_{xx}^a - W_{yy}^a) - \eta_1^a W_{xy}^a;\\
&\Pi_{xz}^{a(2)} = -\eta_4^a W_{yz}^a - \eta_2^a W_{xz}^a;\\
&\Pi_{yy}^{a(2)} = -\frac{\eta_0^a}{2}(W_{xx}^a + W_{yy}^a) + \frac{\eta_1^a}{2}(W_{xx}^a - W_{yy}^a) + \eta_3^a W_{xy}^a;\\
&\Pi_{yz}^{a(2)} = \eta_4^a W_{xz}^a - \eta_2^a W_{yz}^a;\\
&\Pi_{zz}^{a(2)} = -\eta_0^a W_{zz}^a,
\end{aligned} \tag{72}$$

which is Equation (2.21) of Braginskii (1965). The ion viscosities are

$$\begin{aligned}
&\eta_0^a = \frac{1025}{1068}\frac{p_a}{\nu_{aa}};\\
&\eta_2^a = \frac{p_a}{\nu_{aa}}\frac{(6/5)x^2 + (10947/4900)}{x^4 + (79321/19600)x^2 + (71289/30625)};\\
&\eta_4^a = \frac{p_a}{\nu_{aa}}\frac{x^3 + (46561/19600)x}{x^4 + (79321/19600)x^2 + (71289/30625)},
\end{aligned} \tag{73}$$

where $x = \Omega_a/\nu_{aa}$ and $\eta_1^a(x) = \eta_2^a(2x)$; $\eta_3^a(x) = \eta_4^a(2x)$. (The solution is easily obtained for the parallel "zz" direction with $\Omega_a = 0$, and for perpendicular directions, for example, by choosing coupled "xz" and "yz" directions, and solving four equations in four

unknowns.) Alternatively, using numerical values,

$$\eta_0^a = 0.960\frac{p_a}{\nu_{aa}};$$
$$\eta_2^a = \frac{p_a}{\nu_{aa}}\frac{(6/5)x^2 + 2.234}{x^4 + 4.047x^2 + 2.328};$$
$$\eta_4^a = \frac{p_a}{\nu_{aa}}\frac{x^3 + 2.376x}{x^4 + 4.047x^2 + 2.328}, \tag{74}$$

recovering the ion viscosities of Braginskii (1965), his Equation (4.44). The numerical values in Braginskii are evaluated precisely, with the sole exception of one value in the denominator, where his rounded 4.03 should be replaced by 4.05.

3.6. Ion Viscosity $\bar{\bar{\mathbf{\Pi}}}_a^{(4)}$ (Self-collisions)

The ion viscosity tensor $\bar{\bar{\mathbf{\Pi}}}_a^{(4)}$ is given by

$$\bar{\bar{\mathbf{\Pi}}}_a^{(4)} = \frac{p_a}{\rho_a}[-\eta_0^{a(4)}\bar{\bar{\mathbf{W}}}_0 - \eta_1^{a(4)}\bar{\bar{\mathbf{W}}}_1 - \eta_2^{a(4)}\bar{\bar{\mathbf{W}}}_2 + \eta_3^{a(4)}\bar{\bar{\mathbf{W}}}_3 + \eta_4^{a(4)}\bar{\bar{\mathbf{W}}}_4], \tag{75}$$

with the matrices $\bar{\bar{\mathbf{W}}}_0 - \bar{\bar{\mathbf{W}}}_4$ (71) unchanged, and the viscosities

$$\eta_0^{a(4)} = \frac{8435}{1068}\frac{p_a}{\nu_{aa}};$$
$$\eta_2^{a(4)} = \frac{p_a}{\nu_{aa}}\frac{(33/5)x^2 + (64347/3500)}{x^4 + (79321/19600)x^2 + (71289/30625)};$$
$$\eta_4^{a(4)} = \frac{p_a}{\nu_{aa}}\frac{7x^3 + (59989/2800)x}{x^4 + (79321/19600)x^2 + (71289/30625)}, \tag{76}$$

where $\eta_1^{a(4)}(x) = \eta_2^{a(4)}(2x)$, $\eta_3^{a(4)}(x) = \eta_4^{a(4)}(2x)$ holds, or with numerical values,

$$\eta_0^{a(4)} = 7.898\frac{p_a}{\nu_{aa}};$$
$$\eta_2^{a(4)} = \frac{p_a}{\nu_{aa}}\frac{6.600x^2 + 18.385}{x^4 + 4.047x^2 + 2.328};$$
$$\eta_4^{a(4)} = \frac{p_a}{\nu_{aa}}\frac{7x^3 + 21.425x}{x^4 + 4.047x^2 + 2.328}. \tag{77}$$

3.7. Electron Viscosity $\bar{\bar{\mathbf{\Pi}}}_e^{(2)}$ of Braginskii

For a one ion–electron plasma with similar temperatures, the mass-ratio coefficients (29), (30) simplify into

$$\hat{K}_{ei(1)} = 3\frac{m_i}{m_e}; \qquad \hat{K}_{ei(2)} = \frac{4}{5}; \qquad L_{ei(1)} = \frac{9}{35}\frac{m_i}{m_e}; \qquad L_{ei(2)} = \frac{12}{35}\frac{m_e}{m_i};$$
$$\hat{M}_{ei(1)} = \frac{36}{5}; \qquad \hat{M}_{ei(2)} = \frac{4}{5}\frac{m_e}{m_i}; \qquad N_{ei(1)} = -\frac{12}{35}; \qquad N_{ei(2)} = -\frac{36}{35}\frac{m_e^2}{m_i^2}, \tag{78}$$

and the collisional exchange rates for the viscosity tensors become

$$\bar{\bar{\mathbf{Q}}}_e^{(2)\prime} = -\left(\frac{21}{10}\nu_{ee} + 3\nu_{ei}\right)\bar{\bar{\mathbf{\Pi}}}_e^{(2)} + \left(\frac{9}{70}\nu_{ee} + \frac{9}{35}\nu_{ei}\right)\frac{\rho_e}{p_e}\bar{\bar{\mathbf{\Pi}}}_e^{(4)};$$
$$\bar{\bar{\mathbf{Q}}}_e^{(4)\prime} = -\left(\frac{53}{20}\nu_{ee} + \frac{36}{5}\nu_{ei}\right)\frac{p_e}{\rho_e}\bar{\bar{\mathbf{\Pi}}}_e^{(2)} + \left(-\frac{79}{140}\nu_{ee} + \frac{12}{35}\nu_{ei}\right)\bar{\bar{\mathbf{\Pi}}}_e^{(4)}. \tag{79}$$

Converting everything to ν_{ei} with $\nu_{ee} = \nu_{ei}/(Z_i\sqrt{2})$ yields

$$\bar{\bar{\mathbf{Q}}}_e^{(2)\prime} = -\left(\frac{21}{10Z_i\sqrt{2}} + 3\right)\nu_{ei}\bar{\bar{\mathbf{\Pi}}}_e^{(2)} + \left(\frac{9}{70Z_i\sqrt{2}} + \frac{9}{35}\right)\nu_{ei}\frac{\rho_e}{p_e}\bar{\bar{\mathbf{\Pi}}}_e^{(4)};$$
$$\bar{\bar{\mathbf{Q}}}_e^{(4)\prime} = -\left(\frac{53}{20Z_i\sqrt{2}} + \frac{36}{5}\right)\nu_{ei}\frac{p_e}{\rho_e}\bar{\bar{\mathbf{\Pi}}}_e^{(2)} + \left(-\frac{79}{140Z_i\sqrt{2}} + \frac{12}{35}\right)\nu_{ei}\bar{\bar{\mathbf{\Pi}}}_e^{(4)}, \tag{80}$$

and these contributions enter the right-hand sides of the evolution equations

$$\frac{d_e}{dt}\bar{\bar{\mathbf{\Pi}}}_e^{(2)} + \Omega_e(\hat{\boldsymbol{b}} \times \bar{\bar{\mathbf{\Pi}}}_e^{(2)})^S + p_e \bar{\bar{\boldsymbol{W}}}_e = \bar{\bar{\boldsymbol{Q}}}_e^{(2)\,\prime};$$
$$\frac{d_e}{dt}\bar{\bar{\mathbf{\Pi}}}_e^{(4)} + \Omega_e(\hat{\boldsymbol{b}} \times \bar{\bar{\mathbf{\Pi}}}_e^{(4)})^S + 7\frac{p_e^2}{\rho_e}\bar{\bar{\boldsymbol{W}}}_e = \bar{\bar{\boldsymbol{Q}}}_e^{(4)\,\prime}. \tag{81}$$

In a quasistatic approximation, the solution of (80), (81) yields the electron viscosity tensor $\bar{\bar{\mathbf{\Pi}}}_e^{(2)}$ in the form (70), (71), with the electron viscosities

$$\eta_0^e = \frac{p_e}{\nu_{ei}}\frac{5Z_i(408Z_i + 205\sqrt{2})}{6(192Z_i^2 + 301Z_i\sqrt{2} + 178)};$$
$$\eta_2^e = \frac{p_e}{\nu_{ei}}\left[\frac{3\sqrt{2} + 6Z_i}{5Z_i}x^2 + \frac{3(192Z_i^2 + 301Z_i\sqrt{2} + 178)(408Z_i + 205\sqrt{2})}{196000Z_i^3}\right]\Big/ \triangle;$$
$$\eta_4^e = \frac{p_e}{\nu_{ei}}x\left[x^2 + \frac{119520Z_i^2 + 101784\sqrt{2}Z_i + 46561}{39200Z_i^2}\right]\Big/ \triangle;$$
$$\triangle = x^4 + \frac{212256Z_i^2 + 176376\sqrt{2}Z_i + 79321}{39200Z_i^2}x^2 + \left(\frac{3(192Z_i^2 + 301Z_i\sqrt{2} + 178)}{700Z^2}\right)^2, \tag{82}$$

where $x = \Omega_e/\nu_{ei}$ and the relations $\eta_1^e(x) = \eta_2^e(2x)$, $\eta_3^e(x) = \eta_4^e(2x)$. For the particular case of $Z_i = 1$, these electron viscosities become

$$\eta_0^e = \frac{p_e}{\nu_{ei}}\frac{2040 + 1025\sqrt{2}}{2220 + 1806\sqrt{2}};$$
$$\eta_2^e = \frac{p_e}{\nu_{ei}}\left[\frac{3\sqrt{2} + 6}{5}x^2 + \frac{297987}{98000}\sqrt{2} + \frac{82311}{19600}\right]\Big/ \triangle;$$
$$\eta_4^e = \frac{p_e}{\nu_{ei}}x\left[x^2 + \frac{12723}{4900}\sqrt{2} + \frac{166081}{39200}\right]\Big/ \triangle;$$
$$\triangle = x^4 + \left(\frac{22047}{4900}\sqrt{2} + \frac{291577}{39200}\right)x^2 + \left(\frac{1431459}{245000} + \frac{14319}{3500}\sqrt{2}\right), \tag{83}$$

or with numerical values,

$$\eta_0^e = 0.73094\frac{p_e}{\nu_{ei}};$$
$$\eta_2^e = \frac{p_e}{\nu_{ei}}(2.049x^2 + 8.500)/\triangle;$$
$$\eta_4^e = \frac{p_e}{\nu_{ei}}x(x^2 + 7.909)/\triangle;$$
$$\triangle = x^4 + 13.801x^2 + 11.628, \tag{84}$$

recovering the electron viscosity of Braginskii (1965), his Equation (4.45). It appears that the Braginskii parallel viscosity value of 0.733 is slightly imprecise, and should be 0.731 instead. The analytic result for parallel viscosity η_0^e agrees with Simakov & Molvig (2014), and the value 0.73094 agrees with Ji & Held (2013); see the inset of their Figure 3 (curiously, in a more precise 3-Laguerre approximation, the coefficient changes to 0.733). Note that for $x \to 0$, viscosity $\eta_2^e \to \eta_0^e$. As discussed previously, our Ω_e is negative and in Braginskii it is positive, yielding an opposite sign in front of η_4^e. Braginskii offers electron viscosities only for $Z_i = 1$. The analytic result (82) is useful for quickly calculating the electron viscosities for any Z_i. Ji & Held (2013, 2015) also provide useful fitting formulas.

3.8. Electron Viscosity $\bar{\bar{\mathbf{\Pi}}}_e^{(4)}$

The solution for the electron viscosity tensor $\bar{\bar{\mathbf{\Pi}}}_e^{(4)}$ has the form (75) with the viscosities

$$\eta_0^{e(4)} = \frac{p_e}{\nu_{ei}} \frac{35Z_i(552Z_i + 241\sqrt{2})}{6(192Z_i^2 + 301Z_i\sqrt{2} + 178)};$$
$$\eta_2^{e(4)} = \frac{p_e}{\nu_{ei}}\left[\frac{33\sqrt{2} + 48Z_i}{10Z_i}x^2 + \frac{3(192Z_i^2 + 301Z_i\sqrt{2} + 178)(552Z_i + 241\sqrt{2})}{28000Z_i^3}\right]\Big/ \triangle\,;$$
$$\eta_4^{e(4)} = \frac{p_e}{\nu_{ei}}x\left[7x^2 + \frac{173088Z_i^2 + 142032Z_i\sqrt{2} + 59989}{5600Z_i^2}\right]\Big/ \triangle\,, \tag{85}$$

where the denominator $\triangle$ is equivalent to (82). For the particular case of $Z_i = 1$, these electron viscosities become

$$\eta_0^{e(4)} = \frac{p_e}{\nu_{ei}} \frac{35(241\sqrt{2} + 552)}{6(301\sqrt{2} + 370)};$$
$$\eta_2^{e(4)} = \frac{p_e}{\nu_{ei}}\left[\frac{33\sqrt{2} + 48}{10}x^2 + \frac{382983}{14000}\sqrt{2} + \frac{523983}{14000}\right]\Big/ \triangle\,;$$
$$\eta_4^{e(4)} = \frac{p_e}{\nu_{ei}}x\left[7x^2 + \frac{8877}{350}\sqrt{2} + \frac{233077}{5600}\right]\Big/ \triangle\,, \tag{86}$$

with $\triangle$ equal to (83), and with numerical values,

$$\eta_0^{e(4)} = 6.546\frac{p_e}{\nu_{ei}};$$
$$\eta_2^{e(4)} = \frac{p_e}{\nu_{ei}}(9.467x^2 + 76.114)\Big/ \triangle\,;$$
$$\eta_4^{e(4)} = \frac{p_e}{\nu_{ei}}x(7x^2 + 77.489)\Big/ \triangle\,;$$
$$\triangle = x^4 + 13.801x^2 + 11.628. \tag{87}$$

4. Generalized Electron Coefficients for Multispecies Plasmas

Here we use the idea of Simakov & Molvig (2014), and before that Zhdanov (2002; originally published in 1982) and Hinton (1983), for example, who pointed out that because of the smallness of the mass ratios m_e/m_i, the electron coefficients of Braginskii (1965) can be straightforwardly generalized for multispecies plasmas. Simakov & Molvig (2014) considered unmagnetized plasmas and provide analytic parallel coefficients α_0, β_0, and γ_0, together with the parallel electron viscosity η_0^e. Here we show that the same construction applies when a magnetic field is present, and that all of the electron coefficients provided in the previous section can be easily generalized in the same way. One starts by considering the general multispecies description with the collisional contributions given in Section 2.2. Because of the smallness of m_e/m_i, the mass-ratio coefficients for each ion species simplify into (47). One introduces an effective ion charge together with an effective ion velocity:

$$Z_{\rm eff} = \frac{\sum_i \nu_{ei}}{\sqrt{2}\,\nu_{ee}} = \frac{\sum_i n_i Z_i^2}{n_e}; \qquad \langle \boldsymbol{u}_i\rangle_{\rm eff} = \frac{\sum_i \nu_{ei}\boldsymbol{u}_i}{\sum_i \nu_{ei}}, \tag{88}$$

and it is straightforward to show that the collisional contributions for a one ion–electron plasma (48), (52) are then replaced by

$$\boldsymbol{R}_e = -\rho_e(\sum_i \nu_{ei})(\boldsymbol{u}_e - \langle \boldsymbol{u}_i\rangle_{\rm eff}) + \frac{21}{10}\frac{\rho_e}{p_e}(\sum_i \nu_{ei})\boldsymbol{q}_e - \frac{3}{56}\frac{\rho_e^2}{p_e^2}(\sum_i \nu_{ei})\boldsymbol{X}_e^{(5)}; \tag{89}$$

$$\boldsymbol{Q}_e^{(3)\,\prime} = +\frac{3}{2}p_e(\sum_i \nu_{ei})(\boldsymbol{u}_e - \langle \boldsymbol{u}_i\rangle_{\rm eff}) - \left[\frac{\sqrt{2}}{Z_{\rm eff}} + \frac{19}{4}\right](\sum_i \nu_{ei})\boldsymbol{q}_e + \left[\frac{3}{70\sqrt{2}Z_{\rm eff}} + \frac{69}{560}\right](\sum_i \nu_{ei})\frac{\rho_e}{p_e}\boldsymbol{X}_e^{(5)}; \tag{90}$$

$$\boldsymbol{Q}_e^{(5)\,\prime} = +27\frac{p_e^2}{\rho_e}(\sum_i \nu_{ei})(\boldsymbol{u}_e - \langle \boldsymbol{u}_i\rangle_{\rm eff}) - \left[\frac{76}{5\sqrt{2}Z_{\rm eff}} + \frac{759}{10}\right](\sum_i \nu_{ei})\frac{p_e}{\rho_e}\boldsymbol{q}_e - \left[\frac{3}{35\sqrt{2}Z_{\rm eff}} - \frac{533}{280}\right](\sum_i \nu_{ei})\boldsymbol{X}_e^{(5)}. \tag{91}$$

The contributions (90), (91) enter the right-hand sides of the electron evolution Equations (51). The system is completely the same as for the one ion–electron plasma, if in (48), (52) the following replacement is applied:

$$Z_i \to Z_{\rm eff}; \qquad \nu_{ei} \to \sum_i \nu_{ei}; \qquad \delta\boldsymbol{u} = \boldsymbol{u}_e - \boldsymbol{u}_i \to \boldsymbol{u}_e - \langle \boldsymbol{u}_i\rangle_{\rm eff}. \tag{92}$$

If the evolution equations can be obtained with the transformation (92), then of course their solutions can be obtained with the same transformation as well. The same transformation applies for the viscous evolution Equations (80), (81) and their solutions. As an example, the generalized (thermal) electron heat of Braginskii (1965) for multispecies plasmas reads

$$\boldsymbol{q}_e^T = -\kappa_\parallel^e \nabla_\parallel T_e - \kappa_\perp^e \nabla_\perp T_e + \kappa_\times^e \hat{\boldsymbol{b}} \times \nabla T_e; \tag{93}$$

$$\kappa_\parallel^e = \frac{p_e}{m_e(\sum_i \nu_{ei})}\gamma_0; \qquad \kappa_\perp^e = \frac{p_e}{m_e(\sum_i \nu_{ei})}\frac{\gamma_1' x^2 + \gamma_0'}{\triangle}; \qquad \kappa_\times^e = \frac{p_e}{m_e(\sum_i \nu_{ei})}\frac{\gamma_1'' x^3 + \gamma_0'' x}{\triangle}; \tag{94}$$

$$\gamma_0 = \frac{25Z_{\rm eff}(433Z_{\rm eff} + 180\sqrt{2})}{4(217Z_{\rm eff}^2 + 604Z_{\rm eff}\sqrt{2} + 288)}; \qquad \gamma_1' = \frac{13Z_{\rm eff} + 4\sqrt{2}}{4Z_{\rm eff}}; \qquad \gamma_1'' = \frac{5}{2};$$

$$\gamma_0' = \frac{(217Z_{\rm eff}^2 + 604Z_{\rm eff}\sqrt{2} + 288)(433Z_{\rm eff} + 180\sqrt{2})}{78400Z_{\rm eff}^3}; \qquad \gamma_0'' = \frac{320797Z_{\rm eff}^2 + 202248Z_{\rm eff}\sqrt{2} + 72864}{31360Z_{\rm eff}^2};$$

$$\triangle = x^4 + \delta_1 x^2 + \delta_0; \qquad \delta_0 = \left(\frac{217Z_{\rm eff}^2 + 604Z_{\rm eff}\sqrt{2} + 288}{700Z_{\rm eff}^2}\right)^2;$$

$$\delta_1 = \frac{586601Z_{\rm eff}^2 + 330152Z_{\rm eff}\sqrt{2} + 106016}{78400Z_{\rm eff}^2}, \tag{95}$$

where $x = \Omega_e/(\sum_i \nu_{ei})$. With recipe (92), one obtains generalized solutions for the frictional electron heat flux $\boldsymbol{q}_e^u$, together with solutions for $\boldsymbol{X}_e^{(5)}$ and the viscosity tensors $\bar{\bar{\boldsymbol{\Pi}}}_e^{(2)}$, $\bar{\bar{\boldsymbol{\Pi}}}_e^{(4)}$, which are not repeated here.

From the electron momentum equation, the electric field then becomes

$$\boldsymbol{E} = -\frac{1}{c}\boldsymbol{u}_e \times \boldsymbol{B} - \frac{1}{en_e}\nabla\cdot\bar{\bar{\boldsymbol{p}}}_e + \frac{m_e}{e}\boldsymbol{G} + (\sum_i \nu_{ei})\left[+\frac{m_e}{e}(\langle \boldsymbol{u}_i\rangle_{\rm eff} - \boldsymbol{u}_e) + \frac{21}{10}\frac{m_e}{ep_e}\boldsymbol{q}_e - \frac{3}{56}\frac{\rho_e^2}{en_e p_e^2}\boldsymbol{X}_e^{(5)}\right] - \frac{m_e}{e}\frac{d_e\boldsymbol{u}_e}{dt}, \tag{96}$$

and the expressions for the heat fluxes $\boldsymbol{q}_e$ and $\boldsymbol{X}_e^{(5)}$ enter the electric field.

5. Generalization with Coupling of Stress Tensors and Heat Fluxes

Here we consider the coupling between viscosity tensors and heat fluxes. Using the semilinear approximation, and retaining the coupling, the 21-moment model (9)–(12) simplifies into

$$\frac{d_a}{dt}\bar{\bar{\boldsymbol{\Pi}}}_a^{(2)} + \Omega_a(\hat{\boldsymbol{b}} \times \bar{\bar{\boldsymbol{\Pi}}}_a^{(2)})^S + p_a\bar{\bar{\boldsymbol{W}}}_a + \frac{2}{5}\left((\nabla\boldsymbol{q}_a)^S - \frac{2}{3}\bar{\bar{\boldsymbol{I}}}\nabla\cdot\boldsymbol{q}_a\right) = \bar{\bar{\boldsymbol{Q}}}_a^{(2)\prime} = \bar{\bar{\boldsymbol{Q}}}_a^{(2)} - \frac{\bar{\bar{\boldsymbol{I}}}}{3}{\rm Tr}\,\bar{\bar{\boldsymbol{Q}}}_a^{(2)}; \tag{97}$$

$$\frac{d_a}{dt}\boldsymbol{q}_a + \Omega_a\hat{\boldsymbol{b}} \times \boldsymbol{q}_a + \frac{5}{2}p_a\nabla\left(\frac{p_a}{\rho_a}\right) + \frac{1}{2}\nabla\cdot\bar{\bar{\boldsymbol{\Pi}}}_a^{(4)} - \frac{5}{2}\frac{p_a}{\rho_a}\nabla\cdot\bar{\bar{\boldsymbol{\Pi}}}_a^{(2)} = \boldsymbol{Q}_a^{(3)\prime} = \frac{1}{2}{\rm Tr}\,\bar{\bar{\boldsymbol{Q}}}_a^{(3)} - \frac{5}{2}\frac{p_a}{\rho_a}\boldsymbol{R}_a; \tag{98}$$

$$\frac{d_a}{dt}\bar{\bar{\boldsymbol{\Pi}}}_a^{(4)} + \Omega_a(\hat{\boldsymbol{b}} \times \bar{\bar{\boldsymbol{\Pi}}}_a^{(4)})^S + 7\frac{p_a^2}{\rho_a}\bar{\bar{\boldsymbol{W}}}_a + \frac{1}{5}\left[(\nabla\boldsymbol{X}_a^{(5)})^S - \frac{2}{3}\bar{\bar{\boldsymbol{I}}}(\nabla\cdot\boldsymbol{X}_a^{(5)})\right] = \bar{\bar{\boldsymbol{Q}}}_a^{(4)\prime} = {\rm Tr}\,\bar{\bar{\boldsymbol{Q}}}_a^{(4)} - \frac{\bar{\bar{\boldsymbol{I}}}}{3}{\rm Tr}{\rm Tr}\bar{\bar{\boldsymbol{Q}}}_a^{(4)}; \tag{99}$$

$$\frac{d_a}{dt}\boldsymbol{X}_a^{(5)} + \Omega_a\hat{\boldsymbol{b}} \times \boldsymbol{X}_a^{(5)} + 70\frac{p_a^2}{\rho_a}\nabla\left(\frac{p_a}{\rho_a}\right) + 18\frac{p_a}{\rho_a}\nabla\cdot\bar{\bar{\boldsymbol{\Pi}}}_a^{(4)} - 98\frac{p_a^2}{\rho_a^2}\nabla\cdot\bar{\bar{\boldsymbol{\Pi}}}_a^{(2)} = \boldsymbol{Q}_a^{(5)\prime} = {\rm Tr}{\rm Tr}\bar{\bar{\boldsymbol{Q}}}_a^{(5)} - 35\frac{p_a^2}{\rho_a^2}\boldsymbol{R}_a. \tag{100}$$

Terms such as $(\nabla p_a)\boldsymbol{q}_a$ are neglected, and large-scale gradients are assumed to be small (see Section 2.4). The right-hand sides were given in Sections 2.1 and 2.2, and those for one ion–electron plasmas in Section 3. The system now represents a generalization of Braginskii (1965), where heat fluxes and stress tensors are coupled. For the highest level of precision, one should solve dispersion relations directly with the above system, where all of the heat fluxes and stress tensors are *independent* variables. At the lowest level

of precision, one prescribes the quasistatic approximation and cancels the time derivatives d/dt. Nevertheless, for sufficiently low frequencies there exists a "middle-route" procedure, known from the algebra of collisionless models, by decomposing each moment into its first and second orders:

$$\boldsymbol{q}_a = \boldsymbol{q}_a^{(1)} + \boldsymbol{q}_a^{(2)}; \qquad \boldsymbol{X}_a^{(5)} = \boldsymbol{X}_a^{(5,1)} + \boldsymbol{X}_a^{(5,2)};$$
$$\bar{\bar{\boldsymbol{\Pi}}}_a^{(2)} = \bar{\bar{\boldsymbol{\Pi}}}_a^{(2,1)} + \bar{\bar{\boldsymbol{\Pi}}}_a^{(2,2)}; \qquad \bar{\bar{\boldsymbol{\Pi}}}_a^{(4)} = \bar{\bar{\boldsymbol{\Pi}}}_a^{(4,1)} + \bar{\bar{\boldsymbol{\Pi}}}_a^{(4,2)}, \tag{101}$$

and by neglecting the time derivative of the second-order moments. One can consider

$$\frac{d_a}{dt}\bar{\bar{\boldsymbol{\Pi}}}_a^{(2,1)} + \Omega_a(\hat{\boldsymbol{b}} \times \bar{\bar{\boldsymbol{\Pi}}}_a^{(2)})^S + p_a \bar{\bar{\boldsymbol{W}}}_a + \frac{2}{5}\left((\nabla \boldsymbol{q}_a^{(1)})^S - \frac{2}{3}\bar{\bar{\boldsymbol{I}}}\nabla\cdot\boldsymbol{q}_a^{(1)}\right) = \bar{\bar{\boldsymbol{Q}}}_a^{(2)\,\prime}; \tag{102}$$

$$\frac{d_a}{dt}\bar{\bar{\boldsymbol{\Pi}}}_a^{(4,1)} + \Omega_a(\hat{\boldsymbol{b}} \times \bar{\bar{\boldsymbol{\Pi}}}_a^{(4)})^S + 7\frac{p_a^2}{\rho_a}\bar{\bar{\boldsymbol{W}}}_a + \frac{1}{5}\left[(\nabla \boldsymbol{X}_a^{(5,1)})^S - \frac{2}{3}\bar{\bar{\boldsymbol{I}}}(\nabla\cdot\boldsymbol{X}_a^{(5,1)})\right] = \bar{\bar{\boldsymbol{Q}}}_a^{(4)\,\prime}; \tag{103}$$

$$\frac{d_a}{dt}\boldsymbol{q}_a^{(1)} + \Omega_a\hat{\boldsymbol{b}} \times \boldsymbol{q}_a + \frac{5}{2}p_a\nabla\left(\frac{p_a}{\rho_a}\right) + \frac{1}{2}\nabla\cdot\bar{\bar{\boldsymbol{\Pi}}}_a^{(4,1)} - \frac{5}{2}\frac{p_a}{\rho_a}\nabla\cdot\bar{\bar{\boldsymbol{\Pi}}}_a^{(2,1)} = \boldsymbol{Q}_a^{(3)\,\prime}; \tag{104}$$

$$\frac{d_a}{dt}\boldsymbol{X}_a^{(5,1)} + \Omega_a\hat{\boldsymbol{b}} \times \boldsymbol{X}_a^{(5)} + 70\frac{p_a^2}{\rho_a}\nabla\left(\frac{p_a}{\rho_a}\right) + 18\frac{p_a}{\rho_a}\nabla\cdot\bar{\bar{\boldsymbol{\Pi}}}_a^{(4,1)} - 98\frac{p_a^2}{\rho_a^2}\nabla\cdot\bar{\bar{\boldsymbol{\Pi}}}_a^{(2,1)} = \boldsymbol{Q}_a^{(5)\,\prime}, \tag{105}$$

where the collisional contributions on the right-hand sides contain the full moments $\bar{\bar{\boldsymbol{\Pi}}}_a^{(2)}$, $\bar{\bar{\boldsymbol{\Pi}}}_a^{(4)}$, $\boldsymbol{q}_a$, and $\boldsymbol{X}_a^{(5)}$. In the collisionless regime, a similar procedure was used by Macmahon (1965), Mikhailovskii & Smolyakov (1985), Goswami et al. (2005), Ramos (2005), and Passot et al. (2012), for example, and it is well known that retaining the time derivatives d/dt is crucial for recovering the dispersion relation of the perpendicular fast mode with respect to kinetic theory (its wavenumber dependence in the long-wavelength limit). It is straightforward to further increase the precision by retaining full $\boldsymbol{q}_a$ and $\boldsymbol{X}_a^{(5)}$ in the last terms of (102) and (103), for example, or by retaining full $\bar{\bar{\boldsymbol{\Pi}}}_a^{(2)}$ and $\bar{\bar{\boldsymbol{\Pi}}}_a^{(4)}$ in the last terms of (104) and (105) (which we do not show). The procedure and its application is described in detail in Hunana et al. (2019b; see Sections 5.8 and 5.9), and the coupling of stress tensors and heat fluxes is also crucial for the firehose instability (see Figures 7 and 10 there; see also figures with simpler models in Hunana & Zank 2017).

6. Coupling for Unmagnetized One Ion–Electron Plasma

We further focus on the particular case of a one ion–electron plasma with similar temperatures. It is of course possible to algebraically solve the entire system (102)–(105) with a magnetic field present, which will be presented elsewhere. Here, for clarity and to demonstrate our point, we find it sufficient to focus on an unmagnetized plasma. Equivalently, we thus only consider solutions for parallel moments along the magnetic field, similar to the heat flux model of Spitzer & Härm (1953). For the heat flux Equations (102), (103), it is beneficial to introduce the matrices

$$\bar{\bar{\boldsymbol{Y}}}_a^{(3,1)} = (\nabla \boldsymbol{q}_a^{(1)})^S - \frac{2}{3}\bar{\bar{\boldsymbol{I}}}\nabla\cdot\boldsymbol{q}_a^{(1)}; \qquad \bar{\bar{\boldsymbol{Y}}}_a^{(5,1)} = (\nabla \boldsymbol{X}_a^{(5,1)})^S - \frac{2}{3}\bar{\bar{\boldsymbol{I}}}\nabla\cdot\boldsymbol{X}_a^{(5,1)}, \tag{106}$$

which are symmetric and traceless, analogous to the matrix $\bar{\bar{\boldsymbol{W}}}_a$.

6.1. Ion Species (Self-collisions)

For the ion species, the viscosity tensors have the following form:

$$\bar{\bar{\boldsymbol{\Pi}}}_a^{(2,1)} = -\frac{1025}{1068}\frac{p_a}{\nu_{aa}}\bar{\bar{\boldsymbol{W}}}_a;$$
$$\bar{\bar{\boldsymbol{\Pi}}}_a^{(2,2)} = -\frac{1}{\nu_{aa}}\left[\frac{79}{534}\bar{\bar{\boldsymbol{Y}}}_a^{(3,1)} + \frac{3}{178}\frac{\rho_a}{p_a}\bar{\bar{\boldsymbol{Y}}}_a^{(5,1)} + \frac{395}{1068}\frac{\partial\bar{\bar{\boldsymbol{\Pi}}}_a^{(2,1)}}{\partial t} + \frac{15}{178}\frac{\rho_a}{p_a}\frac{\partial\bar{\bar{\boldsymbol{\Pi}}}_a^{(4,1)}}{\partial t}\right];$$
$$\bar{\bar{\boldsymbol{\Pi}}}_a^{(4,1)} = -\frac{8435}{1068}\frac{p_a^2}{\rho_a\nu_{aa}}\bar{\bar{\boldsymbol{W}}}_a;$$
$$\bar{\bar{\boldsymbol{\Pi}}}_a^{(4,2)} = +\frac{1}{\nu_{aa}}\left[+\frac{371}{534}\frac{p_a}{\rho_a}\bar{\bar{\boldsymbol{Y}}}_a^{(3,1)} - \frac{49}{178}\bar{\bar{\boldsymbol{Y}}}_a^{(5,1)} + \frac{1855}{1068}\frac{p_a}{\rho_a}\frac{\partial\bar{\bar{\boldsymbol{\Pi}}}_a^{(2,1)}}{\partial t} - \frac{245}{178}\frac{\partial\bar{\bar{\boldsymbol{\Pi}}}_a^{(4,1)}}{\partial t}\right], \tag{107}$$

and the heat fluxes become

$$\boldsymbol{q}_a^{(1)} = -\frac{125}{32}\frac{p_a}{m_a\nu_{aa}}\nabla T_a;$$
$$\boldsymbol{q}_a^{(2)} = +\frac{1}{\nu_{aa}}\left[+\frac{515}{96}\frac{p_a}{\rho_a}\nabla\cdot\bar{\bar{\boldsymbol{\Pi}}}_a^{(2,1)} - \frac{95}{96}\nabla\cdot\bar{\bar{\boldsymbol{\Pi}}}_a^{(4,1)} - \frac{5}{48}\frac{\partial\boldsymbol{q}_a^{(1)}}{\partial t} - \frac{5}{96}\frac{\rho_a}{p_a}\frac{\partial\boldsymbol{X}_a^{(5,1)}}{\partial t}\right];$$
$$\boldsymbol{X}_a^{(5,1)} = -\frac{2975}{24}\frac{p_a^2}{\rho_a m_a\nu_{aa}}\nabla T_a;$$
$$\boldsymbol{X}_a^{(5,2)} = +\frac{1}{\nu_{aa}}\left[+\frac{p_a^2}{\rho_a^2}\frac{13825}{72}\nabla\cdot\bar{\bar{\boldsymbol{\Pi}}}_a^{(2,1)} - \frac{2485}{72}\frac{p_a}{\rho_a}\nabla\cdot\bar{\bar{\boldsymbol{\Pi}}}_a^{(4,1)} + \frac{665}{36}\frac{p_a}{\rho_a}\frac{\partial\boldsymbol{q}_a^{(1)}}{\partial t} - \frac{175}{72}\frac{\partial\boldsymbol{X}_a^{(5,1)}}{\partial t}\right]. \tag{108}$$

The model is fully specified and closed, and can be used in the given form. Nevertheless, it is possible to further apply the semilinear approximation, in which case the viscosity corrections simplify into

$$\bar{\bar{\boldsymbol{\Pi}}}_a^{(2,2)} = +\underbrace{\frac{45575}{17088}}_{2.6671}\frac{p_a}{m_a\nu_{aa}^2}\left[2\nabla\nabla T_a - \frac{2}{3}\bar{\bar{\boldsymbol{I}}}\nabla^2 T_a\right] + \underbrace{\frac{1164025}{1140624}}_{1.0205}\frac{p_a}{\nu_{aa}^2}\frac{\partial\bar{\bar{\boldsymbol{W}}}_a}{\partial t};$$
$$\bar{\bar{\boldsymbol{\Pi}}}_a^{(4,2)} = +\underbrace{\frac{536725}{17088}}_{31.4095}\frac{p_a^2}{\rho_a m_a\nu_{aa}^2}\left[2\nabla\nabla T_a - \frac{2}{3}\bar{\bar{\boldsymbol{I}}}\nabla^2 T_a\right] + \underbrace{\frac{10498075}{1140624}}_{9.2038}\frac{p_a^2}{\rho_a\nu_{aa}^2}\frac{\partial\bar{\bar{\boldsymbol{W}}}_a}{\partial t}, \tag{109}$$

and the heat flux corrections become

$$\boldsymbol{q}_a^{(2)} = +\underbrace{\frac{45575}{17088}}_{2.6671}\frac{p_a^2}{\rho_a\nu_{aa}^2}\nabla\cdot\bar{\bar{\boldsymbol{W}}}_a + \underbrace{\frac{31625}{4608}}_{6.8631}\frac{p_a}{m_a\nu_{aa}^2}\frac{\partial\nabla T_a}{\partial t};$$
$$\boldsymbol{X}_a^{(5,2)} = +\underbrace{\frac{1131725}{12816}}_{88.3056}\frac{p_a^3}{\rho_a^2\nu_{aa}^2}\nabla\cdot\bar{\bar{\boldsymbol{W}}}_a + \underbrace{\frac{791875}{3456}}_{229.1305}\frac{p_a^2}{\rho_a m_a\nu_{aa}^2}\frac{\partial\nabla T_a}{\partial t}. \tag{110}$$

6.2. Electron Species

For the electron species, it is useful to introduce the denominator

$$D_1 = 192Z_i^2 + 301\sqrt{2}Z_i + 178, \tag{111}$$

and the solutions for the stress tensors are:

$$\bar{\bar{\boldsymbol{\Pi}}}_e^{(2,1)} = -\frac{5Z_i(205\sqrt{2} + 408Z_i)}{6D_1}\frac{p_e}{\nu_{ei}}\bar{\bar{\boldsymbol{W}}}_e;$$
$$\bar{\bar{\boldsymbol{\Pi}}}_e^{(2,2)} = -\frac{1}{D_1\nu_{ei}}\left[\frac{Z_i}{3}(79\sqrt{2} - 96Z_i)\bar{\bar{\boldsymbol{Y}}}_e^{(3,1)} + 3Z_i(\sqrt{2} + 4Z_i)\frac{\rho_e}{p_e}\bar{\bar{\boldsymbol{Y}}}_e^{(5,1)}\right.$$
$$\left. + \frac{5}{6}Z_i(79\sqrt{2} - 96Z_i)\frac{\partial\bar{\bar{\boldsymbol{\Pi}}}_e^{(2,1)}}{\partial t} + 15Z_i(\sqrt{2} + 4Z_i)\frac{\rho_e}{p_e}\frac{\partial\bar{\bar{\boldsymbol{\Pi}}}_e^{(4,1)}}{\partial t}\right];$$
$$\bar{\bar{\boldsymbol{\Pi}}}_e^{(4,1)} = -\frac{35Z_i(241\sqrt{2} + 552Z_i)}{6D_1}\frac{p_e^2}{\rho_e\nu_{ei}}\bar{\bar{\boldsymbol{W}}}_e;$$
$$\bar{\bar{\boldsymbol{\Pi}}}_e^{(4,2)} = +\frac{1}{D_1\nu_{ei}}\left[\frac{7}{3}Z_i(53\sqrt{2} + 288Z_i)\frac{p_e}{\rho_e}\bar{\bar{\boldsymbol{Y}}}_e^{(3,1)} - 7Z_i(7\sqrt{2} + 20Z_i)\bar{\bar{\boldsymbol{Y}}}_e^{(5,1)}\right.$$
$$\left. + \frac{35}{6}Z_i(53\sqrt{2} + 288Z_i)\frac{p_e}{\rho_e}\frac{\partial\bar{\bar{\boldsymbol{\Pi}}}_e^{(2,1)}}{\partial t} - 35Z_i(7\sqrt{2} + 20Z_i)\frac{\partial\bar{\bar{\boldsymbol{\Pi}}}_e^{(4,1)}}{\partial t}\right], \tag{112}$$

with the matrices $\bar{\bar{\boldsymbol{Y}}}_e$ defined by (106). For the heat fluxes, it is useful to define the denominator

$$D_2 = 217Z_i^2 + 604Z_i\sqrt{2} + 288, \tag{113}$$

together with $\delta\boldsymbol{u} = \boldsymbol{u}_e - \boldsymbol{u}_i$, and the results read

$$\begin{aligned}
\boldsymbol{q}_e^{(1)} &= -\frac{25Z_i(180\sqrt{2} + 433Z_i)}{4D_2}\frac{p_e}{m_e\nu_{ei}}\nabla T_e + \frac{30Z_i(15\sqrt{2} + 11Z_i)}{D_2}p_e\delta\boldsymbol{u};\\
\boldsymbol{q}_e^{(2)} &= +\frac{1}{D_2\nu_{ei}}\left[\frac{5}{4}Z_i(1236\sqrt{2} + 4097Z_i)\frac{p_e}{\rho_e}\nabla\cdot\bar{\bar{\boldsymbol{\Pi}}}_e^{(2,1)} - \frac{5}{4}Z_i(228\sqrt{2} + 709Z_i)\nabla\cdot\bar{\bar{\boldsymbol{\Pi}}}_e^{(4,1)}\right.\\
&\quad\left. - \frac{5}{2}Z_i(12\sqrt{2} - 533Z_i)\frac{\partial\boldsymbol{q}_e^{(1)}}{\partial t} - \frac{15}{4}Z_i(4\sqrt{2} + 23Z_i)\frac{\rho_e}{p_e}\frac{\partial\boldsymbol{X}_e^{(5,1)}}{\partial t}\right];\\
\boldsymbol{X}_e^{(5,1)} &= -\frac{175Z_i(204\sqrt{2} + 571Z_i)}{D_2}\frac{p_e^2}{\rho_e m_e\nu_{ei}}\nabla T_e + \frac{840Z_i(13\sqrt{2} + 12Z_i)}{D_2}\frac{p_e^2}{\rho_e}\delta\boldsymbol{u};\\
\boldsymbol{X}_e^{(5,2)} &= \frac{1}{D_2\nu_{ei}}\left[+175Z_i(316\sqrt{2} + 1103Z_i)\frac{p_e^2}{\rho_e^2}\nabla\cdot\bar{\bar{\boldsymbol{\Pi}}}_e^{(2,1)} - 35Z_i(284\sqrt{2} + 951Z_i)\frac{p_e}{\rho_e}\nabla\cdot\bar{\bar{\boldsymbol{\Pi}}}_e^{(4,1)}\right.\\
&\quad\left. +70Z_i(76\sqrt{2} + 759Z_i)\frac{p_e}{\rho_e}\frac{\partial\boldsymbol{q}_e^{(1)}}{\partial t} - 175Z_i(4\sqrt{2} + 19Z_i)\frac{\partial\boldsymbol{X}_e^{(5,1)}}{\partial t}\right].
\end{aligned} \tag{114}$$

The system is now fully specified and can be used in this form. For the particular case of $Z_i = 1$, the numerical values become

$$\begin{aligned}
\bar{\bar{\boldsymbol{\Pi}}}_e^{(2,1)} &= -0.7309\frac{p_e}{\nu_{ei}}\bar{\bar{\boldsymbol{W}}}_e;\\
\bar{\bar{\boldsymbol{\Pi}}}_e^{(2,2)} &= -\frac{1}{\nu_{ei}}\left[0.006587\bar{\bar{\boldsymbol{Y}}}_e^{(3,1)} + 0.02041\frac{\rho_e}{p_e}\bar{\bar{\boldsymbol{Y}}}_e^{(5,1)} + 0.01647\frac{\partial\bar{\bar{\boldsymbol{\Pi}}}_e^{(2,1)}}{\partial t} + 0.1021\frac{\rho_e}{p_e}\frac{\partial\bar{\bar{\boldsymbol{\Pi}}}_e^{(4,1)}}{\partial t}\right];\\
\bar{\bar{\boldsymbol{\Pi}}}_e^{(4,1)} &= -6.5455\frac{p_e^2}{\rho_e\nu_{ei}}\bar{\bar{\boldsymbol{W}}}_e;\\
\bar{\bar{\boldsymbol{\Pi}}}_e^{(4,2)} &= +\frac{1}{\nu_{ei}}\left[1.0644\frac{p_e}{\rho_e}\bar{\bar{\boldsymbol{Y}}}_e^{(3,1)} - 0.2630\bar{\bar{\boldsymbol{Y}}}_e^{(5,1)} + 2.6609\frac{p_e}{\rho_e}\frac{\partial\bar{\bar{\boldsymbol{\Pi}}}_e^{(2,1)}}{\partial t} - 1.3152\frac{\partial\bar{\bar{\boldsymbol{\Pi}}}_e^{(4,1)}}{\partial t}\right];
\end{aligned} \tag{115}$$

$$\begin{aligned}
\boldsymbol{q}_e^{(1)} &= -3.1616\frac{p_e}{m_e\nu_{ei}}\nabla T_e + 0.7110p_e\delta\boldsymbol{u};\\
\boldsymbol{q}_e^{(2)} &= +\frac{1}{\nu_{ei}}\left[5.3754\frac{p_e}{\rho_e}\nabla\cdot\bar{\bar{\boldsymbol{\Pi}}}_e^{(2,1)} - 0.9486\nabla\cdot\bar{\bar{\boldsymbol{\Pi}}}_e^{(4,1)} + 0.9492\frac{\partial\boldsymbol{q}_e^{(1)}}{\partial t} - 0.07906\frac{\rho_e}{p_e}\frac{\partial\boldsymbol{X}_e^{(5,1)}}{\partial t}\right];\\
\boldsymbol{X}_e^{(5,1)} &= -110.664\frac{p_e^2}{\rho_e m_e\nu_{ei}}\nabla T_e + 18.7783\frac{p_e^2}{\rho_e}\delta\boldsymbol{u};\\
\boldsymbol{X}_e^{(5,2)} &= \frac{1}{\nu_{ei}}\left[199.554\frac{p_e^2}{\rho_e^2}\nabla\cdot\bar{\bar{\boldsymbol{\Pi}}}_e^{(2,1)} - 34.831\frac{p_e}{\rho_e}\nabla\cdot\bar{\bar{\boldsymbol{\Pi}}}_e^{(4,1)} + 44.625\frac{p_e}{\rho_e}\frac{\partial\boldsymbol{q}_e^{(1)}}{\partial t} - 3.1747\frac{\partial\boldsymbol{X}_e^{(5,1)}}{\partial t}\right].
\end{aligned} \tag{116}$$

By further applying the quasilinear approximation, the corrections to the electron viscosities become

$$\bar{\bar{\mathbf{\Pi}}}_e^{(2,2)} = +\frac{25Z_i^2(119520Z_i^2 + 101784Z_i\sqrt{2} + 46561)}{18D_1^2}\frac{p_e}{\nu_{ei}^2}\frac{\partial\bar{\bar{\boldsymbol{W}}}_e}{\partial t} - \frac{10Z_i^2(11040Z_i^2 + 15557Z_i\sqrt{2} + 8922)}{D_2D_1}\frac{p_e}{\nu_{ei}}\left[(\nabla\delta\boldsymbol{u})^S - \frac{2}{3}\bar{\bar{\boldsymbol{I}}}\nabla\cdot\delta\boldsymbol{u}\right] + \frac{25Z_i^2(534000Z_i^2 + 366451Z_i\sqrt{2} + 131256)}{12D_2D_1}\frac{p_e}{\nu_{ei}^2 m_e}\left[2\nabla\nabla T_e - \frac{2}{3}\bar{\bar{\boldsymbol{I}}}\nabla^2 T_e\right]; \tag{117}$$

$$\bar{\bar{\mathbf{\Pi}}}_e^{(4,2)} = +\frac{175Z_i^2(173088Z_i^2 + 142032Z_i\sqrt{2} + 59989)}{18D_1^2}\frac{p_e^2}{\nu_{ei}^2\rho_e}\frac{\partial\bar{\bar{\boldsymbol{W}}}_e}{\partial t} - \frac{70Z_i^2(16992Z_i^2 + 23993Z_i\sqrt{2} + 13698)}{D_2D_1}\frac{p_e^2}{\nu_{ei}\rho_e}\left[(\nabla\delta\boldsymbol{u})^S - \frac{2}{3}\bar{\bar{\boldsymbol{I}}}\nabla\cdot\delta\boldsymbol{u}\right] + \frac{175Z_i^2(834576Z_i^2 + 603679Z_i\sqrt{2} + 220824)}{12D_2D_1}\frac{p_e^2}{\nu_{ei}^2 m_e\rho_e}\left[2\nabla\nabla T_e - \frac{2}{3}\bar{\bar{\boldsymbol{I}}}\nabla^2 T_e\right]; \tag{118}$$

together with the corrections for the heat fluxes:

$$\boldsymbol{q}_e^{(2)} = \frac{25Z_i^2(534000Z_i^2 + 366451Z_i\sqrt{2} + 131256)}{12D_1D_2}\frac{p_e^2}{\rho_e\nu_{ei}^2}\nabla\cdot\bar{\bar{\boldsymbol{W}}}_e - \frac{75Z_i^2(5729Z_i^2 + 6711Z_i\sqrt{2} + 4728)}{D_2^2}\frac{p_e}{\nu_{ei}}\frac{\partial\delta\boldsymbol{u}}{\partial t} + \frac{125Z_i^2(320797Z_i^2 + 202248Z_i\sqrt{2} + 72864)}{8D_2^2}\frac{p_e}{\nu_{ei}^2 m_e}\frac{\partial\nabla T_e}{\partial t};$$

$$\boldsymbol{X}_e^{(5,2)} = \frac{175Z_i^2(712272Z_i^2 + 463249Z_i\sqrt{2} + 155208)}{3D_1D_2}\frac{p_e^3}{\rho_e^2\nu_{ei}^2}\nabla\cdot\bar{\bar{\boldsymbol{W}}}_e - \frac{2100Z_i^2(7611Z_i^2 + 8429Z_i\sqrt{2} + 5000)}{D_2^2}\frac{p_e^2}{\nu_{ei}\rho_e}\frac{\partial\delta\boldsymbol{u}}{\partial t} + \frac{875Z_i^2(430783Z_i^2 + 261672Z_i\sqrt{2} + 86880)}{2D_2^2}\frac{p_e^2}{\nu_{ei}^2\rho_e m_e}\frac{\partial\nabla T_e}{\partial t}. \tag{119}$$

For the ion charge $Z_i = 1$, the numerical values read

$$\bar{\bar{\mathbf{\Pi}}}_e^{(2,2)} = +0.6801\frac{p_e}{\nu_{ei}^2}\frac{\partial\bar{\bar{\boldsymbol{W}}}_e}{\partial t} - 0.3880\frac{p_e}{\nu_{ei}}\left[(\nabla\delta\boldsymbol{u})^S - \frac{2}{3}\bar{\bar{\boldsymbol{I}}}\nabla\cdot\delta\boldsymbol{u}\right] + 2.2799\frac{p_e}{\nu_{ei}^2 m_e}\left[2\nabla\nabla T_e - \frac{2}{3}\bar{\bar{\boldsymbol{I}}}\nabla^2 T_e\right]; \tag{120}$$

$$\bar{\bar{\mathbf{\Pi}}}_e^{(4,2)} = +6.6638\frac{p_e^2}{\nu_{ei}^2\rho_e}\frac{\partial\bar{\bar{\boldsymbol{W}}}_e}{\partial t} - 4.1827\frac{p_e^2}{\nu_{ei}\rho_e}\left[(\nabla\delta\boldsymbol{u})^S - \frac{2}{3}\bar{\bar{\boldsymbol{I}}}\nabla\cdot\delta\boldsymbol{u}\right] + 25.7440\frac{p_e^2}{\nu_{ei}^2 m_e\rho_e}\left[2\nabla\nabla T_e - \frac{2}{3}\bar{\bar{\boldsymbol{I}}}\nabla^2 T_e\right]; \tag{121}$$

together with

$$\boldsymbol{q}_e^{(2)} = 2.2799\frac{p_e^2}{\rho_e\nu_{ei}^2}\nabla\cdot\bar{\bar{\boldsymbol{W}}}_e - 0.8098\frac{p_e}{\nu_{ei}}\frac{\partial\delta\boldsymbol{u}}{\partial t} + 5.7487\frac{p_e}{\nu_{ei}^2 m_e}\frac{\partial\nabla T_e}{\partial t};$$

$$\boldsymbol{X}_e^{(5,2)} = 82.1278\frac{p_e^3}{\rho_e^2\nu_{ei}^2}\nabla\cdot\bar{\bar{\boldsymbol{W}}}_e - 27.8859\frac{p_e^2}{\nu_{ei}\rho_e}\frac{\partial\delta\boldsymbol{u}}{\partial t} + 210.2318\frac{p_e^2}{\nu_{ei}^2\rho_e m_e}\frac{\partial\nabla T_e}{\partial t}. \tag{122}$$

The rate-of-strain tensor $\bar{\bar{\boldsymbol{W}}}_e$ obviously enters the electron heat fluxes, even in a quasistatic approximation.

6.3. Momentum Exchange Rates

The collisional momentum exchange rates $\boldsymbol{R}_e = -\boldsymbol{R}_i$, given by (48), can also be split into first- and second-order $\boldsymbol{R}_e = \boldsymbol{R}_e^{(1)} + \boldsymbol{R}_e^{(2)}$, according to

$$\boldsymbol{R}_e^{(1)} = -\rho_e \nu_{ei} \delta \boldsymbol{u} + \frac{21}{10}\frac{\rho_e}{p_e}\nu_{ei}\boldsymbol{q}_e^{(1)} - \frac{3}{56}\frac{\rho_e^2}{p_e^2}\nu_{ei}\boldsymbol{X}_e^{(5,1)};$$
$$\boldsymbol{R}_e^{(2)} = +\frac{21}{10}\frac{\rho_e}{p_e}\nu_{ei}\boldsymbol{q}_e^{(2)} - \frac{3}{56}\frac{\rho_e^2}{p_e^2}\nu_{ei}\boldsymbol{X}_e^{(5,2)}. \tag{123}$$

Then by using results given in the previous section,

$$\boldsymbol{R}_e^{(1)} = -\nu_{ei}\rho_e \frac{(D_2 - 153Z_i^2 - 360Z_i\sqrt{2})}{D_2}\delta\boldsymbol{u} - \frac{30Z_i(15\sqrt{2} + 11Z_i)}{D_2} n_e \nabla T_e;$$
$$\boldsymbol{R}_e^{(2)} = +\frac{6Z_i(47\sqrt{2} + 69Z_i)}{D_2}\nabla\cdot\bar{\bar{\boldsymbol{\Pi}}}_e^{(2,1)} - \frac{6Z_i(11\sqrt{2} + 13Z_i)}{D_2}\frac{\rho_e}{p_e}\nabla\cdot\bar{\bar{\boldsymbol{\Pi}}}_e^{(4,1)}$$
$$-\frac{12Z_i(29\sqrt{2} + 4Z_i)}{D_2}\frac{\rho_e}{p_e}\frac{\partial\boldsymbol{q}_e^{(1)}}{\partial t} + \frac{3Z_i(2\sqrt{2} - Z_i)}{D_2}\frac{\rho_e^2}{p_e^2}\frac{\partial\boldsymbol{X}_e^{(5,1)}}{\partial t}, \tag{124}$$

or for a particular case of $Z_i = 1$,

$$\boldsymbol{R}_e^{(2)} = +0.5980\nabla\cdot\bar{\bar{\boldsymbol{\Pi}}}_e^{(2,1)} - 0.1261\frac{\rho_e}{p_e}\nabla\cdot\bar{\bar{\boldsymbol{\Pi}}}_e^{(4,1)}$$
$$-0.3974\frac{\rho_e}{p_e}\frac{\partial\boldsymbol{q}_e^{(1)}}{\partial t} + 0.004036\frac{\rho_e^2}{p_e^2}\frac{\partial\boldsymbol{X}_e^{(5,1)}}{\partial t}. \tag{125}$$

Finally, at a semilinear level,

$$\boldsymbol{R}_e^{(2)} = \frac{10Z_i^2(11040Z_i^2 + 15557Z_i\sqrt{2} + 8922)}{D_1 D_2}\frac{p_e}{\nu_{ei}}\nabla\cdot\bar{\bar{\boldsymbol{W}}}_e$$
$$-\frac{720Z_i^2(64Z_i^2 + 151Z_i\sqrt{2} + 253)}{D_2^2}\rho_e\frac{\partial(\delta\boldsymbol{u})}{\partial t}$$
$$+\frac{75Z_i^2(5729Z_i^2 + 6711Z_i\sqrt{2} + 4728)}{D_2^2}\frac{n_e}{\nu_{ei}}\frac{\partial\nabla T_e}{\partial t}, \tag{126}$$

and for $Z_i = 1$, the full momentum exchange rates become

$$\boldsymbol{R}_e = -0.5129\nu_{ei}\rho_e\delta\boldsymbol{u} - 0.7110 n_e\nabla T_e + 0.3880\frac{p_e}{\nu_{ei}}\nabla\cdot\bar{\bar{\boldsymbol{W}}}_e - 0.2068\rho_e\frac{\partial(\delta\boldsymbol{u})}{\partial t} + 0.8098\frac{n_e}{\nu_{ei}}\frac{\partial\nabla T_e}{\partial t}, \tag{127}$$

where $\delta\boldsymbol{u} = \boldsymbol{u}_e - \boldsymbol{u}_i$. Only the first two terms of (127) were considered by Braginskii (1965) and Spitzer & Härm (1953; with this latter having slightly different proportionality constants—see Appendix I). A further generalization, by keeping the full $\bar{\bar{\boldsymbol{\Pi}}}_a^{(2)}$ and $\bar{\bar{\boldsymbol{\Pi}}}_a^{(4)}$ viscosity tensors in the last terms of (104) and (105), brings another three terms to $\boldsymbol{R}_e$ (not shown). Naturally, in a highly collisional regime ($\nu_{ei} \gg \omega$), all of the additional terms are small in comparison to the first two terms of (127). Nevertheless, at higher frequencies (shorter-length scales), these additional contributions might become significant. Interestingly, the rate-of-strain tensor $\bar{\bar{\boldsymbol{W}}}_e$ enters the momentum exchange rates (even at the linear level), with the contribution $\nabla\cdot\bar{\bar{\boldsymbol{W}}}_e = \nabla^2\boldsymbol{u}_e + (1/3)\nabla(\nabla\cdot\boldsymbol{u}_e)$. Note that some terms are proportional to $1/\nu_{ei}$ and become unbounded (divergent) in a regime of low collisionality, which is a consequence of the expansion procedure (i.e., a quasistatic approximation). The evolution Equations (97)–(100) are of course well defined in the regime of low collisionality.

7. Multifluid 22-moment Model

Here we consider a natural generalization of the 21-moment model, by accounting for a fully contracted perturbation of the fourth-order fluid moment $X_{ijkl}^{a(4)} = m_a \int c_i^a c_j^a c_k^a c_l^a f_a d^3v$. The fully contracted (scalar) moment is decomposed into its Maxwellian core and

a perturbation $\widetilde{X}_a^{(4)}$ (denoted with tilde), according to

$$X_a^{(4)} = m_a \int |\boldsymbol{c}_a|^4 f_a \, d^3v = 15\frac{p_a^2}{\rho_a} + \widetilde{X}_a^{(4)}, \tag{128}$$

meaning a definition of $\widetilde{X}_a^{(4)} = m_a \int |\boldsymbol{c}_a|^4 (f_a - f_a^{(0)}) d^3v$, where $f_a^{(0)}$ is Maxwellian. The scalar perturbation $\widetilde{X}_a^{(4)}$ enters the decomposition of the fourth-order moment

$$\begin{aligned} X_{ijkl}^{a(4)} = &\frac{1}{15}\left(15\frac{p_a^2}{\rho_a} + \widetilde{X}_a^{(4)}\right)(\delta_{ij}\delta_{kl} + \delta_{ik}\delta_{jl} + \delta_{il}\delta_{jk}) \\ &+ \frac{1}{7}[\Pi_{ij}^{a(4)}\delta_{kl} + \Pi_{ik}^{a(4)}\delta_{jl} + \Pi_{il}^{a(4)}\delta_{jk} + \Pi_{jk}^{a(4)}\delta_{il} + \Pi_{jl}^{a(4)}\delta_{ik} + \Pi_{kl}^{a(4)}\delta_{ij}] + \sigma_{ijkl}^{a(4)\,\prime}, \end{aligned} \tag{129}$$

where we neglect the traceless tensor $\sigma_{ijkl}^{a(4)\,\prime}$, so the entire model now represents the 22-moment model. The fully nonlinear model is given by the evolution Equations (6)–(9), which are unchanged, together with

$$\begin{aligned} &\frac{d_a \boldsymbol{q}_a}{dt} + \frac{7}{5}\boldsymbol{q}_a \nabla \cdot \boldsymbol{u}_a + \frac{7}{5}\boldsymbol{q}_a \cdot \nabla \boldsymbol{u}_a + \frac{2}{5}(\nabla \boldsymbol{u}_a) \cdot \boldsymbol{q}_a + \Omega_a \hat{\boldsymbol{b}} \times \boldsymbol{q}_a + \frac{5}{2}p_a \nabla\left(\frac{p_a}{\rho_a}\right) \\ &\quad + \frac{1}{6}\nabla \widetilde{X}_a^{(4)} + \frac{1}{2}\nabla \cdot \bar{\bar{\boldsymbol{\Pi}}}_a^{(4)} - \frac{5}{2}\frac{p_a}{\rho_a}\nabla \cdot \bar{\bar{\boldsymbol{\Pi}}}_a^{(2)} - \frac{1}{\rho_a}(\nabla \cdot \bar{\bar{\boldsymbol{p}}}_a) \cdot \bar{\bar{\boldsymbol{\Pi}}}_a^{(2)} \\ &\quad = \boldsymbol{Q}_a^{(3)\,\prime} \equiv \frac{1}{2}\mathrm{Tr}\,\bar{\bar{\boldsymbol{Q}}}_a^{(3)} - \frac{5}{2}\frac{p_a}{\rho_a}\boldsymbol{R}_a - \frac{1}{\rho_a}\boldsymbol{R}_a \cdot \bar{\bar{\boldsymbol{\Pi}}}_a^{(2)}; \end{aligned} \tag{130}$$

$$\begin{aligned} &\frac{d_a}{dt}\bar{\bar{\boldsymbol{\Pi}}}_a^{(4)} + \frac{1}{5}\left[(\nabla \boldsymbol{X}_a^{(5)})^S - \frac{2}{3}\bar{\bar{\boldsymbol{I}}}(\nabla \cdot \boldsymbol{X}_a^{(5)})\right] + \frac{9}{7}(\nabla \cdot \boldsymbol{u}_a)\bar{\bar{\boldsymbol{\Pi}}}_a^{(4)} + \frac{9}{7}(\bar{\bar{\boldsymbol{\Pi}}}_a^{(4)} \cdot \nabla \boldsymbol{u}_a)^S \\ &\quad + \frac{2}{7}((\nabla \boldsymbol{u}_a) \cdot \bar{\bar{\boldsymbol{\Pi}}}_a^{(4)})^S - \frac{22}{21}\bar{\bar{\boldsymbol{I}}}(\bar{\bar{\boldsymbol{\Pi}}}_a^{(4)} : \nabla \boldsymbol{u}_a) - \frac{14}{5\rho_a}\left[((\nabla \cdot \bar{\bar{\boldsymbol{p}}}_a)\boldsymbol{q}_a)^S - \frac{2}{3}\bar{\bar{\boldsymbol{I}}}(\nabla \cdot \bar{\bar{\boldsymbol{p}}}_a) \cdot \boldsymbol{q}_a\right] \\ &\quad + \Omega_a(\hat{\boldsymbol{b}} \times \bar{\bar{\boldsymbol{\Pi}}}_a^{(4)})^S + \frac{7}{15}\left(15\frac{p_a^2}{\rho_a} + \widetilde{X}_a^{(4)}\right)\bar{\bar{\boldsymbol{W}}}_a \\ &= \bar{\bar{\boldsymbol{Q}}}_a^{(4)\,\prime} \equiv \mathrm{Tr}\,\bar{\bar{\boldsymbol{Q}}}_a^{(4)} - \frac{\bar{\bar{\boldsymbol{I}}}}{3}\mathrm{Tr}\mathrm{Tr}\bar{\bar{\boldsymbol{Q}}}_a^{(4)} - \frac{14}{5\rho_a}\left[(\boldsymbol{R}_a \boldsymbol{q}_a)^S - \frac{2}{3}\bar{\bar{\boldsymbol{I}}}(\boldsymbol{R}_a \cdot \boldsymbol{q}_a)\right]; \end{aligned} \tag{131}$$

$$\begin{aligned} &\frac{d_a}{dt}\widetilde{X}_a^{(4)} + \nabla \cdot \boldsymbol{X}_a^{(5)} - 20\frac{p_a}{\rho_a}\nabla \cdot \boldsymbol{q}_a + \frac{7}{3}\widetilde{X}_a^{(4)}(\nabla \cdot \boldsymbol{u}_a) + 4\left(\bar{\bar{\boldsymbol{\Pi}}}_a^{(4)} - 5\frac{p_a}{\rho_a}\bar{\bar{\boldsymbol{\Pi}}}_a^{(2)}\right) : \nabla \boldsymbol{u}_a \\ &\quad - \frac{8}{\rho_a}(\nabla \cdot \bar{\bar{\boldsymbol{p}}}_a) \cdot \boldsymbol{q}_a = \widetilde{Q}_a^{(4)\,\prime} \equiv \mathrm{Tr}\mathrm{Tr}\bar{\bar{\boldsymbol{Q}}}_a^{(4)} - 20\frac{p_a}{\rho_a}Q_a - \frac{8}{\rho_a}\boldsymbol{R}_a \cdot \boldsymbol{q}_a; \end{aligned} \tag{132}$$

$$\begin{aligned} &\frac{d_a}{dt}\boldsymbol{X}_a^{(5)} + \frac{1}{3}\nabla \widetilde{X}_a^{(6)} + \nabla \cdot \bar{\bar{\boldsymbol{\Pi}}}_a^{(6)} + \frac{9}{5}\boldsymbol{X}_a^{(5)}(\nabla \cdot \boldsymbol{u}_a) + \frac{9}{5}\boldsymbol{X}_a^{(5)} \cdot \nabla \boldsymbol{u}_a + \frac{4}{5}(\nabla \boldsymbol{u}_a) \cdot \boldsymbol{X}_a^{(5)} + \Omega_a \hat{\boldsymbol{b}} \times \boldsymbol{X}_a^{(5)} \\ &\quad + 70\frac{p_a^2}{\rho_a}\nabla\left(\frac{p_a}{\rho_a}\right) - 35\frac{p_a^2}{\rho_a^2}\nabla \cdot \bar{\bar{\boldsymbol{\Pi}}}_a^{(2)} - \frac{7}{3\rho_a}(\nabla \cdot \bar{\bar{\boldsymbol{p}}}^a)\widetilde{X}_a^{(4)} - \frac{4}{\rho_a}(\nabla \cdot \bar{\bar{\boldsymbol{p}}}^a) \cdot \bar{\bar{\boldsymbol{\Pi}}}_a^{(4)} \\ &= \boldsymbol{Q}_a^{(5)\,\prime} \equiv \boldsymbol{Q}_a^{(5)} - 35\frac{p_a^2}{\rho_a^2}\boldsymbol{R}_a - \frac{7}{3\rho_a}\boldsymbol{R}_a \widetilde{X}_a^{(4)} - \frac{4}{\rho_a}\boldsymbol{R}_a \cdot \bar{\bar{\boldsymbol{\Pi}}}_a^{(4)}. \end{aligned} \tag{133}$$

The last Equation (133) is closed with closure (13) for the stress tensor $\bar{\bar{\boldsymbol{\Pi}}}_a^{(6)}$, together with a closure for the scalar perturbation (derived from a Hermite closure)

$$\widetilde{X}_a^{(6)} = m_a \int |\boldsymbol{c}_a|^6 (f_a - f_a^{(0)}) d^3v = 21\frac{p_a}{\rho_a}\widetilde{X}_a^{(4)}. \tag{134}$$

In the semilinear approximations, the 22-moment model reads

$$\frac{d_a}{dt}\bar{\bar{\boldsymbol{\Pi}}}_a^{(2)} + \Omega_a(\hat{\boldsymbol{b}} \times \bar{\bar{\boldsymbol{\Pi}}}_a^{(2)})^S + p_a \bar{\bar{\boldsymbol{W}}}_a + \frac{2}{5}\left((\nabla \boldsymbol{q}_a)^S - \frac{2}{3}\bar{\bar{\boldsymbol{I}}}\nabla\cdot\boldsymbol{q}_a\right) = \bar{\bar{\boldsymbol{Q}}}_a^{(2)\,\prime}; \tag{135}$$

$$\frac{d_a}{dt}\boldsymbol{q}_a + \Omega_a\hat{\boldsymbol{b}}\times\boldsymbol{q}_a + \frac{5}{2}p_a\nabla\left(\frac{p_a}{\rho_a}\right) + \frac{1}{2}\nabla\cdot\bar{\bar{\boldsymbol{\Pi}}}_a^{(4)} - \frac{5}{2}\frac{p_a}{\rho_a}\nabla\cdot\bar{\bar{\boldsymbol{\Pi}}}_a^{(2)} + \frac{1}{6}\nabla\widetilde{X}_a^{(4)} = \boldsymbol{Q}_a^{(3)\,\prime}; \tag{136}$$

$$\frac{d_a}{dt}\bar{\bar{\boldsymbol{\Pi}}}_a^{(4)} + \Omega_a(\hat{\boldsymbol{b}}\times\bar{\bar{\boldsymbol{\Pi}}}_a^{(4)})^S + 7\frac{p_a^2}{\rho_a}\bar{\bar{\boldsymbol{W}}}_a + \frac{1}{5}\left[(\nabla\boldsymbol{X}_a^{(5)})^S - \frac{2}{3}\bar{\bar{\boldsymbol{I}}}(\nabla\cdot\boldsymbol{X}_a^{(5)})\right] = \bar{\bar{\boldsymbol{Q}}}_a^{(4)\,\prime}; \tag{137}$$

$$\frac{d_a}{dt}\widetilde{X}_a^{(4)} + \nabla\cdot\boldsymbol{X}_a^{(5)} - 20\frac{p_a}{\rho_a}\nabla\cdot\boldsymbol{q}_a = \widetilde{Q}_a^{(4)\,\prime} = \mathrm{Tr}\mathrm{Tr}\bar{\bar{\boldsymbol{Q}}}_a^{(4)} - 20\frac{p_a}{\rho_a}Q_a; \tag{138}$$

$$\frac{d_a}{dt}\boldsymbol{X}_a^{(5)} + \Omega_a\hat{\boldsymbol{b}}\times\boldsymbol{X}_a^{(5)} + 70\frac{p_a^2}{\rho_a}\nabla\left(\frac{p_a}{\rho_a}\right) + 18\frac{p_a}{\rho_a}\nabla\cdot\bar{\bar{\boldsymbol{\Pi}}}_a^{(4)} - 98\frac{p_a^2}{\rho_a^2}\nabla\cdot\bar{\bar{\boldsymbol{\Pi}}}_a^{(2)} + 7\frac{p_a}{\rho_a}\nabla\widetilde{X}_a^{(4)} = \boldsymbol{Q}_a^{(5)\,\prime}. \tag{139}$$

As discussed in Section 2.4, in the semilinear approximation, we are neglecting terms such as $(\nabla p_a)\boldsymbol{q}_a$, which might become significant in the presence of large-scale gradients, together with the other terms that are neglected. In comparison to the 21-moment model given by (97)–(100), the evolution Equations (135) and (137) for stress tensors $\bar{\bar{\boldsymbol{\Pi}}}_a^{(2)}$ and $\bar{\bar{\boldsymbol{\Pi}}}_a^{(4)}$ remain unchanged. Importantly, the collisional contributions $\boldsymbol{R}_a$, $\bar{\bar{\boldsymbol{Q}}}_a^{(2)\,\prime}$, $\boldsymbol{Q}_a^{(3)\,\prime}$, $\bar{\bar{\boldsymbol{Q}}}_a^{(4)\,\prime}$, and $\boldsymbol{Q}_a^{(5)\,\prime}$, given in Section 2.1, remain unchanged as well. The only differences are: (1) the scalar perturbations $\widetilde{X}_a^{(4)}$ now enter the left-hand sides of the evolution Equations (136) and (139) for heat fluxes $\boldsymbol{q}_a$ and $\boldsymbol{X}_a^{(5)}$; (2) a new evolution Equation (138) for scalar $\widetilde{X}_a^{(4)}$ is present, with collisional contributions $\widetilde{Q}_a^{(4)\,\prime}$ that need to be specified; and (3) the energy exchange rates Q_a entering the scalar pressure Equation (8) are modified, and given below.

7.1. Collisional Contributions (Arbitrary Temperatures)

The energy exchange rates entering Equation (8) are now given by

$$Q_a = \sum_{b\neq a} Q_{ab} = \sum_{b\neq a}\frac{\rho_a\nu_{ab}}{(m_a+m_b)}\left\{3(T_b - T_a) + \hat{P}_{ab(1)}\frac{\rho_a}{n_a p_a}\widetilde{X}_a^{(4)} - \hat{P}_{ab(2)}\frac{\rho_b}{n_b p_b}\widetilde{X}_b^{(4)}\right\}, \tag{140}$$

with the mass-ratio coefficients

$$\hat{P}_{ab(1)} = \frac{3T_a m_b(5T_b m_b + 4T_b m_a - T_a m_b)}{40(T_a m_b + T_b m_a)^2}; \qquad \hat{P}_{ab(2)} = \frac{3T_b m_a(5T_a m_a + 4T_a m_b - T_b m_a)}{40(T_a m_b + T_b m_a)^2}. \tag{141}$$

Interestingly, the scalar perturbations $\widetilde{X}_a^{(4)}$ thus enter the energy exchange rates. For self-collisions, all of the contributions naturally disappear. As also discussed later, in Section 8.1, for multifluid models the conservation of energy $Q_{ab} + Q_{ba} = (\boldsymbol{u}_b - \boldsymbol{u}_a)\cdot\boldsymbol{R}_{ab}$ is only satisfied approximately, because in the semilinear approximation the differences in the drifts $\boldsymbol{u}_b - \boldsymbol{u}_a$ are assumed to be small, meaning $Q_{ab} + Q_{ba} = 0$ holds. To satisfy the energy conservation exactly, the collisional integrals would have to be calculated nonlinearly, with unrestricted drifts (i.e., with the runaway effect). Nevertheless, for a plasma consisting of only two species (such as a one ion–electron plasma), the conservation of energy can be imposed by hand, by calculating Q_{ab} according to (140), (141), and prescribing $Q_{ba} = -Q_{ab} + (\boldsymbol{u}_b - \boldsymbol{u}_a)\cdot\boldsymbol{R}_{ab}$.

The collisional exchange rates entering evolution Equation (138) are given by

$$\widetilde{Q}_a^{(4)\,\prime} = -\frac{4}{5}\nu_{aa}\widetilde{X}_a^{(4)} + \sum_{b\neq a}\nu_{ab}\left\{-\frac{p_a^2}{\rho_a}\frac{(T_b - T_a)}{T_a}\hat{S}_{ab(0)} - \widetilde{X}_a^{(4)}\hat{S}_{ab(1)} + \frac{p_a^2\rho_b}{p_b^2\rho_a}\widetilde{X}_b^{(4)}\hat{S}_{ab(2)}\right\}, \tag{142}$$

with the mass-ratio coefficients

$$\hat{S}_{ab(0)} = \frac{36T_a m_a m_b}{(T_a m_b + T_b m_a)(m_b + m_a)};$$
$$\hat{S}_{ab(1)} = -\{m_a(17T_a^3 m_b^3 - 36T_a^2 T_b m_a m_b^2 - 69T_a^2 T_b m_b^3 + 12T_a T_b^2 m_a^2 m_b - 48T_a T_b^2 m_a m_b^2 - 40T_b^3 m_a^3 - 84T_b^3 m_a^2 m_b)\}[10(T_a m_b + T_b m_a)^3(m_b + m_a)]^{-1};$$
$$\hat{S}_{ab(2)} = \frac{3T_b^2 m_a^2 m_b(7T_a m_a + 4T_a m_b - 3T_b m_a)}{2(T_a m_b + T_b m_a)^3(m_b + m_a)}, \tag{143}$$

where the self-collisional contributions are represented by the first term of (142).

7.1.1. Small Temperature Differences

For small temperature differences, the mass-ratio coefficients become

$$\hat{P}_{ab(1)} = \frac{3m_b}{10(m_b + m_a)}; \qquad \hat{P}_{ab(2)} = \frac{3m_a}{10(m_b + m_a)};$$
$$\hat{S}_{ab(0)} = \frac{36m_a m_b}{(m_b + m_a)^2}; \qquad \hat{S}_{ab(1)} = \frac{2m_a(10m_a^2 + 8m_a m_b + 13m_b^2)}{5(m_b + m_a)^3}; \qquad \hat{S}_{ab(2)} = \frac{6m_a^2 m_b}{(m_b + m_a)^3}, \tag{144}$$

and, for example, for self-collisions $\hat{S}_{aa(1)} = 31/20$ and $\hat{S}_{aa(2)} = 3/4$. We further consider a one ion–electron plasma.

7.2. Ion Species (Self-collisions)

In a quasistatic approximation, the solution of Equation (138) becomes

$$\widetilde{X}_a^{(4)} = -\frac{5}{4\nu_{aa}}\left[\nabla \cdot \boldsymbol{X}_a^{(5)} - 20\frac{p_a}{\rho_a}\nabla \cdot \boldsymbol{q}_a\right]. \tag{145}$$

The quasistatic solution is thus completely determined by the heat fluxes $\boldsymbol{q}_a$ and $\boldsymbol{X}_a^{(5)}$, and for a magnetized plasma it has the following form:

$$\widetilde{X}_a^{(4)} = -\frac{5}{4\nu_{aa}}\left\{\nabla \cdot \left[\frac{p_a}{\rho_a}(-\kappa_\parallel^{a(5)}\nabla_\parallel T_a - \kappa_\perp^{a(5)}\nabla_\perp T_a + \kappa_\times^{a(5)}\hat{\boldsymbol{b}} \times \nabla T_a)\right] - 20\frac{p_a}{\rho_a}\nabla \cdot (-\kappa_\parallel^a \nabla_\parallel T_a - \kappa_\perp^a \nabla_\perp T_a + \kappa_\times^a \hat{\boldsymbol{b}} \times \nabla T_a)\right\}, \tag{146}$$

where the thermal conductivities are given by (43), (46).

It feels natural to define the thermal conductivities (of the moment $\widetilde{X}_a^{(4)}$):

$$\kappa_\parallel^{a(4)} = \frac{5}{4}(\kappa_\parallel^{a(5)} - 20\kappa_\parallel^a); \qquad \kappa_\perp^{a(4)} = \frac{5}{4}(\kappa_\perp^{a(5)} - 20\kappa_\perp^a); \qquad \kappa_\times^{a(4)} = \frac{5}{4}(\kappa_\times^{a(5)} - 20\kappa_\times^a), \tag{147}$$

and result (146) then transforms into

$$\widetilde{X}_a^{(4)} = -\frac{p_a}{\nu_{aa}\rho_a}\nabla \cdot [-\kappa_\parallel^{a(4)}\nabla_\parallel T_a - \kappa_\perp^{a(4)}\nabla_\perp T_a + \kappa_\times^{a(4)}\hat{\boldsymbol{b}} \times \nabla T_a] - \frac{5}{4\nu_{aa}}(-\kappa_\parallel^{a(5)}\nabla_\parallel T_a - \kappa_\perp^{a(5)}\nabla_\perp T_a + \kappa_\times^{a(5)}\hat{\boldsymbol{b}} \times \nabla T_a) \cdot \nabla\left(\frac{p_a}{\rho_a}\right), \tag{148}$$

with the thermal conductivities

$$\kappa_\parallel^{a(4)} = \frac{1375}{24}\frac{p_a}{\nu_{aa} m_a};$$
$$\kappa_\perp^{a(4)} = \frac{p_a}{\nu_{aa} m_a}\frac{5x^2 + (9504/245)}{x^4 + (3313/1225)x^2 + (20736/30625)};$$
$$\kappa_\times^{a(4)} = \frac{p_a}{\nu_{aa} m_a}\frac{25x^3 + (3810/49)x}{x^4 + (3313/1225)x^2 + (20736/30625)}. \tag{149}$$

The second term of (148) is strictly nonlinear, and may be neglected for simplicity. The solution for $\widetilde{X}_a^{(4)}$ can thus be written as a divergence of a heat flux vector defined by the expression in the square brackets of (148). We have used Braginskii notation with vectors $\nabla_\parallel = \hat{\boldsymbol{b}}\hat{\boldsymbol{b}} \cdot \nabla$ and $\nabla_\perp = \bar{\bar{\boldsymbol{I}}}_\perp \cdot \nabla = -\hat{\boldsymbol{b}} \times \hat{\boldsymbol{b}} \times \nabla$.

The resulting (148) can be further simplified in the semilinear approximation, where one may use $\nabla \cdot (\hat{\boldsymbol{b}} \times \nabla T_a) = 0$, and so

$$\widetilde{X}_a^{(4)} = + \frac{p_a}{\nu_{aa}\rho_a}[\kappa_\parallel^{a(4)}\nabla_\parallel^2 T_a + \kappa_\perp^{a(4)}\nabla_\perp^2 T_a], \tag{150}$$

with scalars $\nabla_\parallel^2 = \hat{\boldsymbol{b}}\hat{\boldsymbol{b}}\colon \nabla\nabla$ and $\nabla_\perp^2 = \nabla^2 - \nabla_\parallel^2$, and, for zero magnetic field,

$$\widetilde{X}_a^{(4)} = + \underbrace{\frac{1375}{24}}_{57.292}\frac{p_a^2}{\nu_{aa}^2\rho_a m_a}\nabla^2 T_a. \tag{151}$$

Note that the result is proportional to $1/\nu_{aa}^2$, and thus small in a highly collisional regime.

7.3. Electron Species (One Ion–Electron Plasma)

Here we consider a one ion–electron plasma with small temperature differences. Similar to Braginskii, an exact energy conservation can be imposed by hand, according to

$$Q_{ie} = \frac{\rho_i\nu_{ie}}{m_i}\left[3(T_e - T_i) + \frac{3}{10}m_e\left(\frac{\widetilde{X}_i^{(4)}}{p_i} - \frac{\widetilde{X}_e^{(4)}}{p_e}\right)\right]; \qquad Q_{ei} = -Q_{ie} - (\boldsymbol{u}_e - \boldsymbol{u}_i)\cdot\boldsymbol{R}_{ei}. \tag{152}$$

The electron coefficients (144) become $\hat{S}_{ei(1)} = (26/5)(m_e/m_i)$ and $\hat{S}_{ei(2)} = 6(m_e/m_i)^2$, and the collisional contributions (142) have a simple form:

$$\widetilde{Q}_e^{(4)\prime} = -\frac{4}{5}\nu_{ee}\widetilde{X}_e^{(4)}, \tag{153}$$

determined solely by the electron–electron collisions. A quasistatic solution of Equation (138) then becomes

$$\widetilde{X}_e^{(4)} = -\frac{5\sqrt{2}Z_i}{4\nu_{ei}}\left[\nabla\cdot\boldsymbol{X}_e^{(5)} - 20\frac{p_e}{\rho_e}\nabla\cdot\boldsymbol{q}_e\right], \tag{154}$$

where we have used $\nu_{ee} = \nu_{ei}/(Z_i\sqrt{2})$. The electron heat fluxes are given by (53) and (61), and are of course determined by both electron–electron and electron–ion collisions. The full solution thus consists of the thermal and frictional parts $\widetilde{X}_e^{(4)} = \widetilde{X}_e^{(4)T} + \widetilde{X}_e^{(4)u}$, where

$$\begin{aligned}\widetilde{X}_e^{(4)T} = &-\frac{5\sqrt{2}Z_i}{4\nu_{ei}}\left\{\nabla\cdot\left[\frac{p_e}{\rho_e}(-\kappa_\parallel^{e(5)}\nabla_\parallel T_e - \kappa_\perp^{e(5)}\nabla_\perp T_e + \kappa_\times^{e(5)}\hat{\boldsymbol{b}}\times\nabla T_e)\right]\right.\\ &\left.- 20\frac{p_e}{\rho_e}\nabla\cdot(-\kappa_\parallel^e\nabla_\parallel T_e - \kappa_\perp^e\nabla_\perp T_e + \kappa_\times^e\hat{\boldsymbol{b}}\times\nabla T_e)\right\};\end{aligned} \tag{155}$$

$$\begin{aligned}\widetilde{X}_e^{(4)u} = &-\frac{5Z_i\sqrt{2}}{4\nu_{ei}}\left\{\nabla\cdot\left[\frac{p_e^2}{\rho_e}\left(\beta_0^{(5)}\delta\boldsymbol{u}_\parallel + \frac{\beta_1^{(5)\prime}x^2 + \beta_0^{(5)\prime}}{\triangle}\delta\boldsymbol{u}_\perp - \frac{\beta_1^{(5)\prime\prime}x^3 + \beta_0^{(5)\prime\prime}x}{\triangle}\hat{\boldsymbol{b}}\times\delta\boldsymbol{u}\right)\right]\right.\\ &\left.- 20\frac{p_e}{\rho_e}\nabla\cdot\left(\beta_0 p_e\delta\boldsymbol{u}_\parallel + p_e\delta\boldsymbol{u}_\perp\frac{\beta_1' x^2 + \beta_0'}{\triangle} - p_e\hat{\boldsymbol{b}}\times\delta\boldsymbol{u}\frac{\beta_1'' x^3 + \beta_0'' x}{\triangle}\right)\right\},\end{aligned} \tag{156}$$

with $\delta\boldsymbol{u} = \boldsymbol{u}_e - \boldsymbol{u}_i$. It is again natural to define the electron thermal conductivities (of the moment $\widetilde{X}_e^{(4)}$):

$$\kappa_\parallel^{e(4)} = \frac{5\sqrt{2}Z_i}{4}(\kappa_\parallel^{e(5)} - 20\kappa_\parallel^e); \qquad \kappa_\perp^{e(4)} = \frac{5\sqrt{2}Z_i}{4}(\kappa_\perp^{e(5)} - 20\kappa_\perp^e); \qquad \kappa_\times^{e(4)} = \frac{5\sqrt{2}Z_i}{4}(\kappa_\times^{e(5)} - 20\kappa_\times^e), \tag{157}$$

together with the transport coefficients

$$\beta_0^{(4)} = \frac{5\sqrt{2}Z_i}{4}(\beta_0^{(5)} - 20\beta_0); \qquad \beta_1^{(4)\prime} = \frac{5\sqrt{2}Z_i}{4}(\beta_1^{(5)\prime} - 20\beta_1'); \qquad \beta_0^{(4)\prime} = \frac{5\sqrt{2}Z_i}{4}(\beta_0^{(5)\prime} - 20\beta_0');$$
$$\beta_1^{(4)\prime\prime} = \frac{5\sqrt{2}Z_i}{4}(\beta_1^{(5)\prime\prime} - 20\beta_1''); \qquad \beta_0^{(4)\prime\prime} = \frac{5\sqrt{2}Z_i}{4}(\beta_0^{(5)\prime\prime} - 20\beta_0''); \tag{158}$$

$$\gamma_0^{(4)} = \frac{5\sqrt{2}Z_i}{4}(\gamma_0^{(5)} - 20\gamma_0); \qquad \gamma_1^{(4)\prime} = \frac{5\sqrt{2}Z_i}{4}(\gamma_1^{(5)\prime} - 20\gamma_1'); \qquad \gamma_0^{(4)\prime} = \frac{5\sqrt{2}Z_i}{4}(\gamma_0^{(5)\prime} - 20\gamma_0');$$
$$\gamma_1^{(4)\prime\prime} = \frac{5\sqrt{2}Z_i}{4}(\gamma_1^{(5)\prime\prime} - 20\gamma_1''); \qquad \gamma_0^{(4)\prime\prime} = \frac{5\sqrt{2}Z_i}{4}(\gamma_0^{(5)\prime\prime} - 20\gamma_0''). \tag{159}$$

The thermal and frictional parts then become

$$\widetilde{X}_e^{(4)T} = -\frac{p_e}{\nu_{ei}\rho_e}\nabla\cdot(-\kappa_\parallel^{e(4)}\nabla_\parallel T_e - \kappa_\perp^{e(4)}\nabla_\perp T_e + \kappa_\times^{e(4)}\hat{\boldsymbol{b}}\times\nabla T_e)$$
$$- \frac{5\sqrt{2}Z_i}{4\nu_{ei}}(-\kappa_\parallel^{e(5)}\nabla_\parallel T_e - \kappa_\perp^{e(5)}\nabla_\perp T_e + \kappa_\times^{e(5)}\hat{\boldsymbol{b}}\times\nabla T_e)\cdot\nabla\left(\frac{p_e}{\rho_e}\right); \tag{160}$$

$$\widetilde{X}_e^{(4)u} = -\frac{p_e}{\nu_{ei}\rho_e}\nabla\cdot\left(\beta_0^{(4)}p_e\delta\boldsymbol{u}_\parallel + \frac{\beta_1^{(4)\prime}x^2 + \beta_0^{(4)\prime}}{\triangle}p_e\delta\boldsymbol{u}_\perp - \frac{\beta_1^{(4)\prime\prime}x^3 + \beta_0^{(4)\prime\prime}x}{\triangle}p_e\hat{\boldsymbol{b}}\times\delta\boldsymbol{u}\right)$$
$$- \frac{5\sqrt{2}Z_i}{4\nu_{ei}}\nabla\cdot\left(\beta_0^{(5)}p_e\delta\boldsymbol{u}_\parallel + \frac{\beta_1^{(5)\prime}x^2 + \beta_0^{(5)\prime}}{\triangle}p_e\delta\boldsymbol{u}_\perp - \frac{\beta_1^{(5)\prime\prime}x^3 + \beta_0^{(5)\prime\prime}x}{\triangle}p_e\hat{\boldsymbol{b}}\times\delta\boldsymbol{u}\right)\cdot\nabla\left(\frac{p_e}{\rho_e}\right), \tag{161}$$

where the second terms of (160) and (161) are purely nonlinear and may be neglected for simplicity. The thermal conductivities are

$$\kappa_\parallel^{e(4)} = \frac{p_e}{m_e\nu_{ei}}\gamma_0^{(4)}; \qquad \kappa_\perp^{e(4)} = \frac{p_e}{m_e\nu_{ei}}\frac{\gamma_1^{(4)\prime}x^2 + \gamma_0^{(4)\prime}}{\triangle}; \qquad \kappa_\times^{e(4)} = \frac{p_e}{m_e\nu_{ei}}\frac{\gamma_1^{(4)\prime\prime}x^3 + \gamma_0^{(4)\prime\prime}x}{\triangle}, \tag{162}$$

and the transport coefficients become

$$\beta_0^{(4)} = \frac{150Z_i^2\sqrt{2}(16\sqrt{2} + 29Z_i)}{217Z_i^2 + 604Z_i\sqrt{2} + 288}; \qquad \beta_1^{(4)\prime} = -\frac{3\sqrt{2}(548\sqrt{2} + 1261Z_i)}{224};$$
$$\beta_0^{(4)\prime} = \frac{3\sqrt{2}(217Z_i^2 + 604Z_i\sqrt{2} + 288)(16\sqrt{2} + 29Z_i)}{9800Z_i^2};$$
$$\beta_1^{(4)\prime\prime} = -\frac{15Z_i\sqrt{2}}{4}; \qquad \beta_0^{(4)\prime\prime} = \frac{3\sqrt{2}(3079Z_i^2 + 3181Z_i\sqrt{2} + 1420)}{490Z_i}; \tag{163}$$

$$\gamma_0^{(4)} = \frac{250Z_i^2\sqrt{2}(66\sqrt{2} + 229Z_i)}{217Z_i^2 + 604Z_i\sqrt{2} + 288}; \qquad \gamma_1^{(4)\prime} = \frac{5\sqrt{2}(4\sqrt{2} - 17Z_i)}{8};$$
$$\gamma_0^{(4)\prime} = \frac{\sqrt{2}(217Z_i^2 + 604Z_i\sqrt{2} + 288)(66\sqrt{2} + 229Z_i)}{1960Z_i^2};$$
$$\gamma_1^{(4)\prime\prime} = 25Z_i\sqrt{2}; \qquad \gamma_0^{(4)\prime\prime} = \frac{\sqrt{2}(176437Z_i^2 + 102558Z_i\sqrt{2} + 30480)}{784Z_i}; \tag{164}$$

$$\triangle = x^4 + \delta_1 x^2 + \delta_0;$$
$$\delta_0 = \left(\frac{217Z_i^2 + 604Z_i\sqrt{2} + 288}{700Z_i^2}\right)^2; \qquad \delta_1 = \frac{586601Z_i^2 + 330152Z_i\sqrt{2} + 106016}{78400Z_i^2}, \tag{165}$$

and with numerical values for $Z_i = 1$,

$$\beta_0^{(4)} = 8.0576; \quad \beta_1^{(4)\prime} = -38.5624; \quad \beta_0^{(4)\prime} = 30.3787; \quad \beta_1^{(4)\prime\prime} = -5.3033; \quad \beta_0^{(4)\prime\prime} = 77.9054;$$
$$\gamma_0^{(4)} = 83.8471; \quad \gamma_1^{(4)\prime} = -10.0260; \quad \gamma_0^{(4)\prime} = 316.1179; \quad \gamma_1^{(4)\prime\prime} = 35.3553; \quad \gamma_0^{(4)\prime\prime} = 634.8735;$$
$$\delta_0 = 3.7702; \quad \delta_1 = 14.7898. \tag{166}$$

At the semilinear level, the solution becomes

$$\widetilde{X}_e^{(4)T} = + \frac{p_e}{\nu_{ei}\rho_e}[\kappa_{\parallel}^{e(4)}\nabla_{\parallel}^2 T_e + \kappa_{\perp}^{e(4)}\nabla_{\perp}^2 T_e]; \tag{167}$$

$$\widetilde{X}_e^{(4)u} = - \frac{p_e^2}{\nu_{ei}\rho_e}\left[\beta_0^{(4)}\nabla\cdot\delta\boldsymbol{u}_{\parallel} + \frac{\beta_1^{(4)\prime}x^2 + \beta_0^{(4)\prime}}{\triangle}\nabla\cdot\delta\boldsymbol{u}_{\perp} - \frac{\beta_1^{(4)\prime\prime}x^3 + \beta_0^{(4)\prime\prime}x}{\triangle}\nabla\cdot(\hat{\boldsymbol{b}}\times\delta\boldsymbol{u})\right], \tag{168}$$

and for zero magnetic field,

$$\widetilde{X}_e^{(4)} = \gamma_0^{(4)}\frac{p_e^2}{\nu_{ei}^2\rho_e m_e}\nabla^2 T_e - \beta_0^{(4)}\frac{p_e^2}{\nu_{ei}\rho_e}\nabla\cdot\delta\boldsymbol{u}. \tag{169}$$

8. Discussion and Conclusions

Here we discuss various topics that we find to be of importance.

8.1. Energy Conservation

The collisional integrals were calculated in a semilinear approximation, where all quantities such as $\boldsymbol{q}_a\cdot(\boldsymbol{u}_b-\boldsymbol{u}_a)$ or $|\boldsymbol{u}_b-\boldsymbol{u}_a|^2$ were neglected and considered small. This approach is typically used for calculations with Landau or Boltzmann collisional operators, and is used in the models of Burgers (1969) and Schunk (1977), for example. Importantly, an exact energy conservation $Q_{ab}+Q_{ba}=(\boldsymbol{u}_b-\boldsymbol{u}_a)\cdot\boldsymbol{R}_{ab}$ cannot be achieved, because the collisional integrals would have to be calculated nonlinearly. An exact conservation of energy can be achieved only in two particular cases, the first being a one ion–electron plasma (or a two-species plasma) where the conservation of energy can be imposed by hand, according to

$$Q_{ie} = 3n_e\nu_{ei}(T_e - T_i)\frac{m_e}{m_i}; \qquad Q_{ei} = -Q_{ie} - (\boldsymbol{u}_e - \boldsymbol{u}_i)\cdot\boldsymbol{R}_{ei}, \tag{170}$$

which is the choice of Braginskii (1965); see his Equation (2.18). Such a construction cannot be done in general for multispecies plasmas, and the conservation of energy is thus satisfied only approximately.

The second particular case involves neglecting all heat fluxes and stress tensors, and considering only a 5-moment model with perturbation $\chi_a=0$. In this specific example of collisions between strict Maxwellians, multifluid calculations can be done for unrestricted drifts (see Burgers 1969; Schunk 1977; and our Appendix G.3), yielding

$$\boldsymbol{R}_{ab} = \rho_a\nu_{ab}(\boldsymbol{u}_b - \boldsymbol{u}_a)\Phi_{ab}; \tag{171}$$

$$Q_{ab} = \rho_a\nu_{ab}\left[3\frac{T_b - T_a}{m_a + m_b}\Psi_{ab} + \frac{m_b}{m_a + m_b}|\boldsymbol{u}_b - \boldsymbol{u}_a|^2\Phi_{ab}\right], \tag{172}$$

where one defines the functions

$$\Psi_{ab} = e^{-\epsilon^2}; \qquad \Phi_{ab} = \left(\frac{3}{4}\sqrt{\pi}\frac{\mathrm{erf}(\epsilon)}{\epsilon^3} - \frac{3}{2}\frac{e^{-\epsilon^2}}{\epsilon^2}\right); \qquad \epsilon = \frac{|\boldsymbol{u}_b - \boldsymbol{u}_a|}{\sqrt{v_{\mathrm{tha}}^2 + v_{\mathrm{thb}}^2}}, \tag{173}$$

the thermal velocities $v_{\mathrm{tha}}^2 = 2T_a/m_a$, and the collisional frequencies (178). Because $\rho_a\nu_{ab}=\rho_b\nu_{ba}$ holds, both momentum and energy are conserved. The collisional exchange rates (171), (172) represent the "runaway" effect, and the function Φ_{ab} is directly related to the Chandrasekhar function; for further details, see Appendix G.3 and Figure 6.

For a particular case, when the differences in the drift velocities $|\boldsymbol{u}_b-\boldsymbol{u}_a|$ become much smaller than the thermal velocities, so that $\epsilon\ll 1$, functions $\Phi_{ab}\to 1$ and $\Psi_{ab}\to 1$ and $\boldsymbol{R}_{ab}=\rho_a\nu_{ab}(\boldsymbol{u}_b-\boldsymbol{u}_a)$. To correctly account for the small $|\boldsymbol{u}_b-\boldsymbol{u}_a|^2$ contributions in Q_{ab}, while keeping the differences in temperatures unrestricted, is achieved by $\Psi_{ab}=1-\epsilon^2$, yielding the following equivalent forms:

$$Q_{ab} = \rho_a\nu_{ab}\left[3\frac{T_b - T_a}{m_a + m_b}\left(1 - \frac{|\boldsymbol{u}_b - \boldsymbol{u}_a|^2}{\frac{2T_a}{m_a} + \frac{2T_b}{m_b}}\right) + \frac{m_b}{m_b + m_a}|\boldsymbol{u}_b - \boldsymbol{u}_a|^2\right]; \tag{174}$$

$$Q_{ab} = \rho_a\nu_{ab}\left[3\frac{T_b - T_a}{m_a + m_b} + \frac{3}{2}\left(\frac{T_a m_b}{T_a m_b + T_b m_a} - \frac{1}{3}\frac{m_b}{m_b + m_a}\right)|\boldsymbol{u}_b - \boldsymbol{u}_a|^2\right]; \tag{175}$$

and see also (G32). Energy is still conserved. When, additionally, the differences in temperatures are small as well (with respect to their mean temperature), the frictional part simplifies into

$$Q_{ab} = \rho_a \nu_{ab}\left[3\frac{T_b - T_a}{m_a + m_b} + \frac{m_b}{m_a + m_b}|\boldsymbol{u}_b - \boldsymbol{u}_a|^2\right]. \tag{176}$$

One can of course neglect the runaway effect from the beginning, and account for small $|\boldsymbol{u}_b - \boldsymbol{u}_a|^2$ contributions either through the center-of-mass velocity transformation, as is done in the appendix of Braginskii (1965), for example, or by using the Rosenbluth potentials; see Appendices G.1, G.2.

Note that, considering the 22-moment model, the fully contracted scalar perturbations $\widetilde{X}^{(4)}$ modify the energy conservation, according to

$$Q_{ab} = \frac{\rho_a \nu_{ab}}{(m_a + m_b)}\left[3(T_b - T_a) + \hat{P}_{ab(1)}\frac{\rho_a}{n_a p_a}\widetilde{X}_a^{(4)} - \hat{P}_{ab(2)}\frac{\rho_b}{n_b p_b}\widetilde{X}_b^{(4)}\right];$$
$$\hat{P}_{ab(1)} = \frac{3T_a m_b(5T_b m_b + 4T_b m_a - T_a m_b)}{40(T_a m_b + T_b m_a)^2}; \qquad \hat{P}_{ab(2)} = \frac{3T_b m_a(5T_a m_a + 4T_a m_b - T_b m_a)}{40(T_a m_b + T_b m_a)^2}, \tag{177}$$

and for only two species one can again impose an exact energy conservation by hand; see, e.g., (152).

8.2. Collisional Frequencies for Ion–Electron Plasma

The Landau collisional operator yields the following collisional frequencies (see, for example, Hinton 1983 or our Appendix G.1):

$$\nu_{ab} = \tau_{ab}^{-1} = \frac{16}{3}\sqrt{\pi}\frac{n_b e^4 Z_a^2 Z_b^2 \ln\Lambda}{m_a^2(v_{\rm tha}^2 + v_{\rm thb}^2)^{3/2}}\left(1 + \frac{m_a}{m_b}\right), \tag{178}$$

where $v_{\rm tha}^2 = 2T_a/m_a$, and $\rho_a\nu_{ab} = \rho_b\nu_{ba}$ holds. Equivalently, in the form of Burgers (1969) and Schunk (1977),

$$\nu_{ab} = \frac{16}{3}\sqrt{\pi}\left(\frac{\mu_{ab}}{2T_{ab}}\right)^{3/2}\frac{m_b n_b}{m_a + m_b}\frac{e^4 Z_a^2 Z_b^2 \ln\Lambda}{\mu_{ab}^2}, \tag{179}$$

where the reduced mass μ_{ab} and reduced temperature T_{ab} are defined in (14). For a particular case of self-collisions,

$$\nu_{aa} = \frac{4}{3}\sqrt{\pi}\frac{n_a e^4 Z_a^4 \ln\Lambda}{T_a^{3/2}\sqrt{m_a}}. \tag{180}$$

For a particular case of $T_a = T_b = T$,

$$\nu_{ab} = \frac{4}{3}\sqrt{2\pi}\frac{n_b e^4 Z_a^2 Z_b^2 \ln\Lambda}{T^{3/2}}\frac{\sqrt{\mu_{ab}}}{m_a}, \tag{181}$$

which identifies with Equation (7.6) of Braginskii (1965; after one uses $\nu_{ab} = n_b\mu_{ab}\alpha_{ab}'/m_a$). For a particular case of a one ion–electron plasma, the collisional frequencies simplify into

$$\nu_{ii} = \frac{4}{3}\sqrt{\pi}\frac{n_i e^4 Z_i^4 \ln\Lambda}{T_i^{3/2}\sqrt{m_i}}; \qquad \nu_{ie} = \frac{4}{3}\sqrt{2\pi}\frac{n_e e^4 Z_i^2 \ln\Lambda}{T_e^{3/2}\sqrt{m_i}}\sqrt{\frac{m_e}{m_i}};$$
$$\nu_{ee} = \frac{4}{3}\sqrt{\pi}\frac{n_e e^4 \ln\Lambda}{T_e^{3/2}\sqrt{m_e}}; \qquad \nu_{ei} = \frac{4}{3}\sqrt{2\pi}\frac{n_i e^4 Z_i^2 \ln\Lambda}{T_e^{3/2}\sqrt{m_e}}, \tag{182}$$

where one assumes $T_i/m_i \ll T_e/m_e$, so the ions cannot be extremely hot. Obviously, $\nu_{ii} \gg \nu_{ie}$ (by a factor of $\sqrt{m_i/m_e}$ for equal temperatures and $Z_i = 1$), but $\nu_{ee} \sim \nu_{ei}$, with the exact relation $\nu_{ei} = Z_i\sqrt{2}\nu_{ee}$ after one uses $n_e = Z_i n_i$. The relation $\rho_i\nu_{ie} = \rho_e\nu_{ei}$ holds exactly in (182). Note the important difference that while ν_{ei} contains a factor of $\sqrt{2}$, ν_{ii} does not. Thus, comparing the Braginskii (1965) expressions (2.5i) and (2.5e) with the (182) definitions, Braginskii clearly uses

$$\tau_i = \tau_{ii}; \qquad \tau_e = \tau_{ei}, \tag{183}$$

which also agrees with his definition (7.6), equivalent to our (181).

However, very often when considering ion–electron plasma, a different definition of ν_{ab} is used, without the reduced mass, in the following form:

$$m_a \ll m_b: \qquad \nu_{ab} = \tau_{ab}^{-1} = \frac{16}{3}\sqrt{\pi}\frac{n_b e^4 Z_a^2 Z_b^2 \ln\Lambda}{m_a^2 v_{\rm tha}^3} = \frac{4}{3}\sqrt{2\pi}\frac{n_b e^4 Z_a^2 Z_b^2 \ln\Lambda}{T_a^{3/2}\sqrt{m_a}}, \tag{184}$$

which, for example, agrees with the appendix of Helander & Sigmar (2002, p. 277; after using cgs units $\epsilon_0 \to 1/(4\pi)$). We have added the $m_a \ll m_b$ designation, even though it is not present in Helander & Sigmar (2002), because obviously it is the only way of obtaining (184) from the general (178). Importantly, $\rho_a \nu_{ab} \neq \rho_b \nu_{ba}$, and if one were to use (184) to calculate ν_{ie}, the result would be erroneous. Instead, the ν_{ie} must be calculated from ν_{ei}, so that the momentum is conserved. Technically, (184) should not be used for self-collisions either. Nevertheless, using (184) yields the following collisional frequencies:

$$\nu_{ii} = \frac{4}{3}\sqrt{2\pi}\,\frac{n_i e^4 Z_i^4 \ln\Lambda}{T_i^{3/2}\sqrt{m_i}}; \qquad \nu_{ie} = \frac{m_e n_e}{m_i n_i}\nu_{ei} = \frac{4}{3}\sqrt{2\pi}\,\frac{n_e e^4 Z_i^2 \ln\Lambda}{T_e^{3/2}\sqrt{m_i}}\sqrt{\frac{m_e}{m_i}};$$
$$\nu_{ee} = \frac{4}{3}\sqrt{2\pi}\,\frac{n_e e^4 \ln\Lambda}{T_e^{3/2}\sqrt{m_e}}; \qquad \nu_{ei} = \frac{4}{3}\sqrt{2\pi}\,\frac{n_i e^4 Z_i^2 \ln\Lambda}{T_e^{3/2}\sqrt{m_e}}. \tag{185}$$

Now ν_{ii} contains a factor of $\sqrt{2}$, leading to an interpretation that Braginskii uses:

$$\tau_i = \sqrt{2}\,\tau_{ii}; \qquad \tau_e = \tau_{ei}. \tag{186}$$

Also, for $Z_i = 1$, the relation $\nu_{ee} = \nu_{ei}$ now holds. These definitions of the collisional frequencies are used in the majority of the modern plasma literature, where one argues that it seems unnatural to introduce asymmetry between ν_{ii} and ν_{ei} (see, e.g., Part 1 of Balescu 1988, p.192, p.274). Obviously, for multispecies plasmas, collisional frequencies (178) have to be used, and we thus find it much more natural to use the original Braginskii (1965) definitions (182), (183) for an ion–electron plasma also. Of course, for the Landau operator, both approaches yield the same results, because the collisional integrals are properly calculated. However, a difference arises for the phenomenological operators such as the BGK or the Dougherty (Lenard–Bernstein) operators, where one needs to add $\nu_{ee} + \nu_{ei}$, for example. Calculating this addition according to (185) would be incorrect, and one has to use (182) instead. A comparison of the Braginskii viscosities and heat conductivities with the BGK operator can be found in Appendix E.3.

8.3. Fluid Hierarchy

Even though we do not calculate the collisional integrals for general nth order moments, we find it useful to discuss the fluid hierarchy and formulate it for a general collisional operator $C(f_a)$. One defines heat flux vectors, stress tensors, and fully contracted moments according to

$$\boldsymbol{X}_a^{(2n+1)} = m_a \int \boldsymbol{c}_a |\boldsymbol{c}_a|^{2n} f_a\, d^3v;$$
$$\bar{\bar{\boldsymbol{\Pi}}}_a^{(2n)} = m_a \int \left(\boldsymbol{c}_a\boldsymbol{c}_a - \frac{\bar{\bar{\boldsymbol{I}}}}{3}|\boldsymbol{c}_a|^2\right)|\boldsymbol{c}_a|^{2n-2} f_a\, d^3v;$$
$$X_a^{(2n)} = m_a \int |\boldsymbol{c}_a|^{2n} f_a\, d^3v = (2n+1)!!\,\frac{p_a^n}{\rho_a^{n-1}} + \widetilde{X}_a^{(2n)}, \tag{187}$$

together with the collisional contributions

$$\vec{\mathcal{Q}}_a^{(2n+1)} = m_a \int |\boldsymbol{c}_a|^{2n} \boldsymbol{c}_a C(f_a)\, d^3v;$$
$$\bar{\bar{\mathcal{Q}}}_a^{(2n)} = m_a \int |\boldsymbol{c}_a|^{2n-2} \boldsymbol{c}_a\boldsymbol{c}_a C(f_a)\, d^3v;$$
$$Q_a^{(2n)} = m_a \int |\boldsymbol{c}_a|^{2n} C(f_a)\, d^3v; \qquad Q_a = \frac{m_a}{2}\int |\boldsymbol{c}_a|^2 C(f_a)\, d^3v, \tag{188}$$

where, to prevent incompatibility with the previous notation, we use $\mathcal{Q}$ (mathcal Q) instead of $\boldsymbol{Q}$ for vectors and matrices. The new notation fixes the problem that, for example, $\boldsymbol{Q}_a^{(3)\,\prime}$ was used for the right-hand side of the evolution equation of the heat flux $\boldsymbol{q}_a$, and not for $\boldsymbol{X}_a^{(3)}$. It also clarifies that in the vector notation, the matrix $\bar{\bar{\mathcal{Q}}}_a^{(2n)} = \mathrm{TrTr}\ \ldots\ \mathrm{Tr}\,\bar{\bar{\boldsymbol{Q}}}_a^{(2n)}$. Note that $Q_a^{(2)} = 2Q_a$, $X_a^{(2)} = 3p_a$, $\widetilde{X}_a^{(2)} = 0$, $\boldsymbol{X}_a^{(3)} = 2\boldsymbol{q}_a$, and $\boldsymbol{X}_a^{(1)} = 0$.

Fully nonlinear evolution equations are given in Appendix D; see (D13)–(D15). In the semilinear approximation, these simplify into evolution equations for vectors valid for $n \geqslant 1$:

$$\frac{d_a}{dt}\boldsymbol{X}_a^{(2n+1)} + \frac{1}{3}\nabla\widetilde{X}_a^{(2n+2)} + \nabla\cdot\bar{\bar{\boldsymbol{\Pi}}}_a^{(2n+2)} - \frac{(2n+3)!!}{3}\frac{p_a^n}{\rho_a^n}\nabla\cdot\bar{\bar{\boldsymbol{\Pi}}}_a^{(2)} + \Omega_a\hat{\boldsymbol{b}}\times\boldsymbol{X}_a^{(2n+1)}$$
$$+ (2n+3)!!\,\frac{(n)}{3}\frac{p_a^n}{\rho_a^{n-1}}\nabla\left(\frac{p_a}{\rho_a}\right) = \vec{\mathcal{Q}}_a^{(2n+1)\,\prime} = \vec{\mathcal{Q}}_a^{(2n+1)} - \frac{(2n+3)!!}{3}\frac{p_a^n}{\rho_a^n}\boldsymbol{R}_a, \tag{189}$$

stress tensors valid for $n \geqslant 1$:

$$\frac{d_a}{dt}\bar{\bar{\boldsymbol{\Pi}}}_a^{(2n)} + \frac{1}{5}\left[(\nabla \boldsymbol{X}_a^{(2n+1)})^S - \frac{2}{3}\bar{\bar{\boldsymbol{I}}}\nabla\cdot\boldsymbol{X}_a^{(2n+1)}\right] + \Omega_a(\hat{\boldsymbol{b}}\times\bar{\bar{\boldsymbol{\Pi}}}_a^{(2n)})^S + \frac{(2n+3)!!}{15}\frac{p_a^n}{\rho_a^{n-1}}\bar{\bar{\boldsymbol{W}}}_a = \bar{\bar{\boldsymbol{\mathcal{Q}}}}_a^{(2n)\prime} = \bar{\bar{\boldsymbol{\mathcal{Q}}}}_a^{(2n)} - \frac{\bar{\bar{\boldsymbol{I}}}}{3}Q_a^{(2n)}, \tag{190}$$

and scalar perturbations valid for $n \geqslant 2$:

$$\frac{d_a}{dt}\widetilde{X}_a^{(2n)} + \nabla\cdot\boldsymbol{X}_a^{(2n+1)} - (2n+1)!!\,\frac{(2n)}{3}\left(\frac{p_a}{\rho_a}\right)^{n-1}\nabla\cdot\boldsymbol{q}_a = \widetilde{Q}_a^{(2n)\prime} = Q_a^{(2n)} - (2n+1)!!\,\frac{(2n)}{3}\left(\frac{p_a}{\rho_a}\right)^{n-1}Q_a, \tag{191}$$

where (n) without a species index should not be confused with the number density. Equation (191) is also valid for $n = 1$, but it is identically zero. In comparison to the previous notation, $\vec{\boldsymbol{\mathcal{Q}}}_a^{(3)\prime} = 2\boldsymbol{Q}_a^{(3)\prime}$, $\vec{\boldsymbol{\mathcal{Q}}}_a^{(5)\prime} = \boldsymbol{Q}_a^{(5)\prime}$, $\bar{\bar{\boldsymbol{\mathcal{Q}}}}_a^{(2)\prime} = \bar{\bar{\boldsymbol{Q}}}_a^{(2)\prime}$, and $\bar{\bar{\boldsymbol{\mathcal{Q}}}}_a^{(4)\prime} = \bar{\bar{\boldsymbol{Q}}}_a^{(4)\prime}$.

8.4. Reducible and Irreducible Hermite Polynomials

The *irreducible* Hermite polynomials $H(\tilde{\boldsymbol{c}})$ (notation without tilde) are usually defined through Laguerre–Sonine polynomials $L(\tilde{\boldsymbol{c}})$ (see, for example, Equation (G1.4.4) on p. 326 of Balescu 1988):

$$H^{(2n)}(\tilde{c}) = L_n^{(1/2)}\left(\frac{\tilde{c}^2}{2}\right); \qquad H_i^{(2n+1)}(\tilde{\boldsymbol{c}}) = \sqrt{\frac{3}{2}}\,\tilde{c}_i L_n^{(3/2)}\left(\frac{\tilde{c}^2}{2}\right);$$
$$H_{ij}^{(2n)}(\tilde{\boldsymbol{c}}) = \sqrt{\frac{15}{8}}\,(\tilde{c}_i\tilde{c}_j - \frac{\tilde{c}^2}{3}\delta_{ij})L_{n-1}^{(5/2)}\left(\frac{\tilde{c}^2}{2}\right), \tag{192}$$

where we use tilde for the normalized fluctuating velocity $\tilde{\boldsymbol{c}} = \sqrt{m_a/T_a}\boldsymbol{c}_a$, with the species indices dropped. In our calculations, we find it more natural to use the *reducible* Hermite polynomials $\tilde{H}(\tilde{\boldsymbol{c}})$ (notation with tilde) of Grad, defined according to

$$\tilde{H}^{(m)}_{r_1r_2\ldots r_m}(\tilde{\boldsymbol{c}}) = (-1)^m e^{\frac{\tilde{c}^2}{2}}\frac{\partial}{\partial\tilde{c}_{r_1}}\frac{\partial}{\partial\tilde{c}_{r_2}}\cdots\frac{\partial}{\partial\tilde{c}_{r_m}}e^{-\frac{\tilde{c}^2}{2}}. \tag{193}$$

Applying a sufficient number of contractions then yields definitions of fully contracted scalars, vectors, and matrices:

$$\tilde{H}^{(2n)} = \tilde{H}^{(2n)}_{r_1r_1\ldots r_nr_n}; \qquad \tilde{H}_i^{(2n+1)} = \tilde{H}^{(2n+1)}_{ir_1r_1\ldots r_nr_n}; \qquad \tilde{H}_{ij}^{(2n)} = \tilde{H}^{(2n)}_{ijr_1r_1\ldots r_{n-1}r_{n-1}}, \tag{194}$$

together with conveniently defined traceless matrices (notation with hat):

$$\hat{H}_{ij}^{(2n)} = \tilde{H}_{ij}^{(2n)} - \frac{1}{3}\delta_{ij}\tilde{H}^{(2n)}. \tag{195}$$

The relation between the irreducible and reducible Hermite polynomials can then be shown to be

$$H^{(2n)} = \left(\frac{1}{2^n n!(2n+1)!!}\right)^{1/2}\tilde{H}^{(2n)}; \qquad H_i^{(2n+1)} = \left(\frac{3}{2^n n!(2n+3)!!}\right)^{1/2}\tilde{H}_i^{(2n+1)};$$
$$H_{ij}^{(2n)} = \left(\frac{15}{2^n(n-1)!(2n+3)!!}\right)^{1/2}\hat{H}_{ij}^{(2n)}, \tag{196}$$

with both approaches using essentially the same polynomials, the only difference being the location of the normalization factors. The reducible Hermite polynomials are used to define the Hermite moments

$$\tilde{h}^{(2n)} = \frac{1}{n_a}\int f_a\tilde{H}^{(2n)}d^3c; \qquad \tilde{h}_i^{(2n+1)} = \frac{1}{n_a}\int f_a\tilde{H}_i^{(2n+1)}d^3c; \qquad \hat{h}_{ij}^{(2n)} = \frac{1}{n_a}\int f_a\hat{H}_{ij}^{(2n)}d^3c, \tag{197}$$

and analogously for the irreducible ones. Note that the scalar $\tilde{h}^{(2)} = 0$, and we thus often use $\hat{h}_{ij}^{(2)} = \tilde{h}_{ij}^{(2)} = (1/n_a)\int f_a\tilde{H}_{ij}^{(2)}d^3c$. Finally, by using orthogonality relations, one obtains the perturbation χ_a of the distribution function $f_a = f_a^{(0)}(1+\chi_a)$ around the

Table 1
Summary of the Various Models with the Perturbation χ_a Given in Reducible Hermite Moments

Model Name	Corresponding Perturbation of $f_a = f_a^{(0)}(1+\chi_a)$ in Hermite Moments
5-moment	$\chi_a = 0$
8-moment	$\chi_a = \frac{1}{10}\tilde{h}_i^{(3)}\tilde{H}_i^{(3)}$
10-moment	$\chi_a = \frac{1}{2}\tilde{h}_{ij}^{(2)}\tilde{H}_{ij}^{(2)}$
13-moment	$\chi_a = \frac{1}{2}\tilde{h}_{ij}^{(2)}\tilde{H}_{ij}^{(2)} + \frac{1}{10}\tilde{h}_i^{(3)}\tilde{H}_i^{(3)}$
20-moment	$\chi_a = \frac{1}{2}\tilde{h}_{ij}^{(2)}\tilde{H}_{ij}^{(2)} + \frac{1}{6}\tilde{h}_{ijk}^{(3)}\tilde{H}_{ijk}^{(3)}$
21-moment	$\chi_a = \frac{1}{2}\tilde{h}_{ij}^{(2)}\tilde{H}_{ij}^{(2)} + \frac{1}{10}\tilde{h}_i^{(3)}\tilde{H}_i^{(3)} + \frac{1}{28}\hat{h}_{ij}^{(4)}\tilde{H}_{ij}^{(4)} + \frac{1}{280}\tilde{h}_i^{(5)}\tilde{H}_i^{(5)}$
22-moment	$\chi_a = \frac{1}{2}\tilde{h}_{ij}^{(2)}\tilde{H}_{ij}^{(2)} + \frac{1}{10}\tilde{h}_i^{(3)}\tilde{H}_i^{(3)} + \frac{1}{28}\hat{h}_{ij}^{(4)}\tilde{H}_{ij}^{(4)} + \frac{1}{120}\tilde{h}^{(4)}\tilde{H}^{(4)} + \frac{1}{280}\tilde{h}_i^{(5)}\tilde{H}_i^{(5)}$
9-moment	$\chi_a = \frac{1}{10}\tilde{h}_i^{(3)}\tilde{H}_i^{(3)} + \frac{1}{120}\tilde{h}^{(4)}\tilde{H}^{(4)}$
11-moment	$\chi_a = \frac{1}{10}\tilde{h}_i^{(3)}\tilde{H}_i^{(3)} + \frac{1}{280}\tilde{h}_i^{(5)}\tilde{H}_i^{(5)}$
12- moment	$\chi_a = \frac{1}{10}\tilde{h}_i^{(3)}\tilde{H}_i^{(3)} + \frac{1}{120}\tilde{h}^{(4)}\tilde{H}^{(4)} + \frac{1}{280}\tilde{h}_i^{(5)}\tilde{H}_i^{(5)}$
15-moment	$\chi_a = \frac{1}{2}\tilde{h}_{ij}^{(2)}\tilde{H}_{ij}^{(2)} + \frac{1}{28}\hat{h}_{ij}^{(4)}\tilde{H}_{ij}^{(4)}$
16-moment	$\chi_a = \frac{1}{2}\tilde{h}_{ij}^{(2)}\tilde{H}_{ij}^{(2)} + \frac{1}{28}\hat{h}_{ij}^{(4)}\tilde{H}_{ij}^{(4)} + \frac{1}{120}\tilde{h}^{(4)}\tilde{H}^{(4)}$

Note. Species indices "a" are dropped. The upper half of the table contains "major" models, and the lower half contains other possibilities. Note that the 16-moment model should not be confused with the anisotropic (bi-Maxwellian-based) 16-moment model described in Section 8.9.

Maxwellian $f_a^{(0)}$, in the following form:

$$\chi_a = \sum_{n=1}^{N}\left[\frac{15}{2^n(n-1)!(2n+3)!!}\hat{h}_{ij}^{(2n)}\hat{H}_{ij}^{(2n)} + \frac{1}{2^n n!(2n+1)!!}\tilde{h}^{(2n)}\tilde{H}^{(2n)} + \frac{3}{2^n n!(2n+3)!!}\tilde{h}_i^{(2n+1)}\tilde{H}_i^{(2n+1)}\right]; \tag{198}$$

$$\chi_a = \sum_{n=1}^{N}[h_{ij}^{(2n)}H_{ij}^{(2n)} + h^{(2n)}H^{(2n)} + h_i^{(2n+1)}H_i^{(2n+1)}], \tag{199}$$

and the two approaches are equivalent. Alternatively, because $\hat{h}_{ij}^{(2n)}$ are traceless, it is possible to use $\hat{h}_{ij}^{(2n)}\hat{H}_{ij}^{(2n)} = \hat{h}_{ij}^{(2n)}\tilde{H}_{ij}^{(2n)}$. Note that $2^n n!(2n+1)!!=(2n+1)!$. The 13-moment model of Burgers–Schunk is obtained by $N=1$. Prescribing $N=2$ yields the 22-moment model

$$\chi_a = \frac{1}{2}\hat{h}_{ij}^{(2)}\hat{H}_{ij}^{(2)} + \frac{1}{10}\tilde{h}_i^{(3)}\tilde{H}_i^{(3)} + \frac{1}{28}\hat{h}_{ij}^{(4)}\hat{H}_{ij}^{(4)} + \frac{1}{120}\tilde{h}^{(4)}\tilde{H}^{(4)} + \frac{1}{280}\tilde{h}_i^{(5)}\tilde{H}_i^{(5)}, \tag{200}$$

with Hermite polynomials

$$\tilde{H}_i^{(3)} = \tilde{c}_i(\tilde{c}^2 - 5); \qquad \tilde{H}_i^{(5)} = \tilde{c}_i(\tilde{c}^4 - 14\tilde{c}^2 + 35);$$
$$\hat{H}_{ij}^{(2)} = \left(\tilde{c}_i\tilde{c}_j - \frac{\delta_{ij}}{3}\tilde{c}^2\right); \qquad \hat{H}_{ij}^{(4)} = \left(\tilde{c}_i\tilde{c}_j - \frac{\delta_{ij}}{3}\tilde{c}^2\right)(\tilde{c}^2 - 7); \qquad \tilde{H}^{(4)} = \tilde{c}^4 - 10\tilde{c}^2 + 15, \tag{201}$$

and neglecting $\tilde{h}^{(4)} = 0$ (meaning $\widetilde{X}^{(4)} = 0$) yields the 21-moment model.

The transformation from Hermite to fluid moments is done according to

$$\tilde{\boldsymbol{h}}_a^{(3)} = \frac{2}{p_a}\sqrt{\frac{m_a}{T_a}}\boldsymbol{q}_a; \qquad \tilde{\boldsymbol{h}}_a^{(5)} = \frac{1}{p_a}\sqrt{\frac{m_a}{T_a}}\left(\frac{m_a}{T_a}\boldsymbol{X}_a^{(5)} - 28\boldsymbol{q}_a\right);$$
$$\hat{\tilde{\boldsymbol{h}}}_a^{(2)} = \tilde{\hat{\boldsymbol{h}}}_a^{(2)} = \frac{1}{p_a}\bar{\boldsymbol{\Pi}}_a^{(2)}; \qquad \hat{\tilde{\boldsymbol{h}}}_a^{(4)} = \frac{\rho_a}{p_a^2}\bar{\boldsymbol{\Pi}}_a^{(4)} - \frac{7}{p_a}\bar{\boldsymbol{\Pi}}_a^{(2)}; \qquad \tilde{h}_a^{(4)} = \frac{\rho_a}{p_a^2}\widetilde{X}_a^{(4)}. \tag{202}$$

Various models are summarized in Tables 1 and 2. In Table 1, the perturbation χ_a is given in reducible Hermite moments, and in Table 2 the perturbation is given in fluid moments.

Table 2
Summary of the Various Models with the Perturbation χ_a Given in Fluid Moments

Model Name	Corresponding Perturbation of $f_a = f_a^{(0)}(1+\chi_a)$ in Fluid Moments
5-moment	$\chi_a = 0$
8-moment	$\chi_a = -\frac{m_a}{p_a T_a}(\boldsymbol{q}_a \cdot \boldsymbol{c}_a)\left(1 - \frac{m_a}{5T_a}c_a^2\right)$
10-moment	$\chi_a = \frac{m_a}{2p_a T_a}(\bar{\bar{\boldsymbol{\Pi}}}_a^{(2)} : \boldsymbol{c}_a\boldsymbol{c}_a)$
13-moment	$\chi_a = \frac{m_a}{2p_a T_a}(\bar{\bar{\boldsymbol{\Pi}}}_a^{(2)} : \boldsymbol{c}_a\boldsymbol{c}_a) - \frac{m_a}{p_a T_a}(\boldsymbol{q}_a \cdot \boldsymbol{c}_a)\left(1 - \frac{m_a}{5T_a}c_a^2\right)$
20-moment	$\chi_a = \frac{m_a}{2p_a T_a}(\bar{\bar{\boldsymbol{\Pi}}}_a^{(2)} : \boldsymbol{c}_a\boldsymbol{c}_a) + \frac{m_a^2}{6p_a T_a^2}(\boldsymbol{c}_a \cdot \bar{\bar{\boldsymbol{q}}}_a : \boldsymbol{c}_a\boldsymbol{c}_a) - \frac{m_a}{p_a T_a}(\boldsymbol{q}_a \cdot \boldsymbol{c}_a)$
21-moment	$\chi_a = \frac{1}{2p_a}(\bar{\bar{\boldsymbol{\Pi}}}_a^{(2)} : \tilde{\boldsymbol{c}}_a\tilde{\boldsymbol{c}}_a) + \frac{1}{28}\left[\frac{\rho_a}{p_a^2}(\bar{\bar{\boldsymbol{\Pi}}}_a^{(4)} : \tilde{\boldsymbol{c}}_a\tilde{\boldsymbol{c}}_a) - \frac{7}{p_a}(\bar{\bar{\boldsymbol{\Pi}}}_a^{(2)} : \tilde{\boldsymbol{c}}_a\tilde{\boldsymbol{c}}_a)\right](\tilde{c}_a^2 - 7)$
	$+\frac{1}{5p_a}\sqrt{\frac{m_a}{T_a}}(\boldsymbol{q}_a \cdot \tilde{\boldsymbol{c}}_a)(\tilde{c}_a^2 - 5)$
	$+\frac{1}{280p_a}\sqrt{\frac{m_a}{T_a}}\left[\frac{\rho_a}{p_a}(\boldsymbol{X}_a^{(5)} \cdot \tilde{\boldsymbol{c}}_a) - 28(\boldsymbol{q}_a \cdot \tilde{\boldsymbol{c}}_a)\right](\tilde{c}_a^4 - 14\tilde{c}_a^2 + 35)$
22-moment	$\chi_a = \frac{1}{2p_a}(\bar{\bar{\boldsymbol{\Pi}}}_a^{(2)} : \tilde{\boldsymbol{c}}_a\tilde{\boldsymbol{c}}_a) + \frac{1}{28}\left[\frac{\rho_a}{p_a^2}(\bar{\bar{\boldsymbol{\Pi}}}_a^{(4)} : \tilde{\boldsymbol{c}}_a\tilde{\boldsymbol{c}}_a) - \frac{7}{p_a}(\bar{\bar{\boldsymbol{\Pi}}}_a^{(2)} : \tilde{\boldsymbol{c}}_a\tilde{\boldsymbol{c}}_a)\right](\tilde{c}_a^2 - 7)$
	$+\frac{1}{5p_a}\sqrt{\frac{m_a}{T_a}}(\boldsymbol{q}_a \cdot \tilde{\boldsymbol{c}}_a)(\tilde{c}_a^2 - 5)$
	$+\frac{1}{280p_a}\sqrt{\frac{m_a}{T_a}}\left[\frac{\rho_a}{p_a}(\boldsymbol{X}_a^{(5)} \cdot \tilde{\boldsymbol{c}}_a) - 28(\boldsymbol{q}_a \cdot \tilde{\boldsymbol{c}}_a)\right](\tilde{c}_a^4 - 14\tilde{c}_a^2 + 35)$
	$+\frac{1}{120}\frac{\rho_a}{p_a^2}\tilde{X}_a^{(4)}(\tilde{c}_a^4 - 10\tilde{c}^2 + 15)$

Note. The results for the 21- and 22-moment models are written with normalized $\tilde{\boldsymbol{c}}_a = \sqrt{m_a/T_a}\boldsymbol{c}_a$.

8.5. Rosenbluth Potentials (22-moment Model)

Here we summarize the Rosenbluth potentials, defined according to

$$H_b(\boldsymbol{v}) = \int \frac{f_b(\boldsymbol{v}')}{|\boldsymbol{v}' - \boldsymbol{v}|}d^3v'; \qquad G_b(\boldsymbol{v}) = \int |\boldsymbol{v}' - \boldsymbol{v}| f_b(\boldsymbol{v}')d^3v', \tag{203}$$

where the first potential should not be confused with the irreducible Hermite polynomials. For the 22-moment model, the fully nonlinear results read

$$\begin{aligned} H_b(\boldsymbol{v}) = n_b\sqrt{\frac{m_b}{T_b}}\Bigg\{&\frac{1}{\tilde{y}}\operatorname{erf}\left(\frac{\tilde{y}}{\sqrt{2}}\right) - \sqrt{\frac{2}{\pi}}\frac{e^{-\tilde{y}^2/2}}{10}\left(\tilde{\boldsymbol{y}} \cdot \tilde{\boldsymbol{h}}_b^{(3)} + (\tilde{y}^2 - 5)\frac{\tilde{\boldsymbol{y}} \cdot \tilde{\boldsymbol{h}}_b^{(5)}}{28}\right) \\ &+\frac{1}{2}(\hat{\bar{\bar{\boldsymbol{h}}}}_b^{(2)} : \tilde{\boldsymbol{y}}\tilde{\boldsymbol{y}})\left[\frac{3}{\tilde{y}^5}\operatorname{erf}\left(\frac{\tilde{y}}{\sqrt{2}}\right) - \sqrt{\frac{2}{\pi}}\left(\frac{1}{\tilde{y}^2} + \frac{3}{\tilde{y}^4}\right)e^{-\tilde{y}^2/2}\right] \\ &-\frac{1}{28}(\hat{\bar{\bar{\boldsymbol{h}}}}_b^{(4)} : \tilde{\boldsymbol{y}}\tilde{\boldsymbol{y}})\sqrt{\frac{2}{\pi}}e^{-\tilde{y}^2/2} + \frac{1}{120}\tilde{h}_b^{(4)}(3 - \tilde{y}^2)\sqrt{\frac{2}{\pi}}e^{-\tilde{y}^2/2}\Bigg\}; \end{aligned} \tag{204}$$

$$\begin{aligned} G_b(\boldsymbol{v}) = n_b\sqrt{\frac{T_b}{m_b}}\Bigg\{&\sqrt{\frac{2}{\pi}}e^{-\tilde{y}^2/2} + \left(\tilde{y} + \frac{1}{\tilde{y}}\right)\operatorname{erf}\left(\frac{\tilde{y}}{\sqrt{2}}\right) \\ &+\left(\frac{\operatorname{erf}(\tilde{y}/\sqrt{2})}{5\tilde{y}^3} - \sqrt{\frac{2}{\pi}}\frac{e^{-\tilde{y}^2/2}}{5\tilde{y}^2}\right)\tilde{\boldsymbol{y}} \cdot \tilde{\boldsymbol{h}}_b^{(3)} - \sqrt{\frac{2}{\pi}}\frac{e^{-\tilde{y}^2/2}}{140}\tilde{\boldsymbol{y}} \cdot \tilde{\boldsymbol{h}}_b^{(5)} \\ &-\frac{1}{2}(\hat{\bar{\bar{\boldsymbol{h}}}}_b^{(2)} : \tilde{\boldsymbol{y}}\tilde{\boldsymbol{y}})\left[\frac{3}{\tilde{y}^4}\sqrt{\frac{2}{\pi}}e^{-\tilde{y}^2/2} + \left(\frac{1}{\tilde{y}^3} - \frac{3}{\tilde{y}^5}\right)\operatorname{erf}\left(\frac{\tilde{y}}{\sqrt{2}}\right)\right] \\ &-\frac{1}{14}(\hat{\bar{\bar{\boldsymbol{h}}}}_b^{(4)} : \tilde{\boldsymbol{y}}\tilde{\boldsymbol{y}})\left[\sqrt{\frac{2}{\pi}}\left(\frac{1}{\tilde{y}^2} + \frac{3}{\tilde{y}^4}\right)e^{-\tilde{y}^2/2} - \frac{3}{\tilde{y}^5}\operatorname{erf}\left(\frac{\tilde{y}}{\sqrt{2}}\right)\right] - \frac{1}{60}\tilde{h}_b^{(4)}\sqrt{\frac{2}{\pi}}e^{-\tilde{y}^2/2}\Bigg\}, \end{aligned} \tag{205}$$

where we use the variable

$$\tilde{\boldsymbol{y}} = \sqrt{\frac{m_b}{T_b}}(\boldsymbol{v} - \boldsymbol{u}_b). \tag{206}$$

Table 3
Summary of (MHD) Hermite Closures, Together with Corresponding Fluid Closures

Hermite Closures	Fluid Closures
$\tilde{h}_i^{(3)} = 0$	$X_i^{(3)} = 0$
$\tilde{h}^{(4)} = 0$	$\widetilde{X}^{(4)} = 0$
$\tilde{h}_i^{(5)} = 0$	$X_i^{(5)} = 14\frac{p}{\rho}X_i^{(3)}$
$\tilde{h}^{(6)} = 0$	$\widetilde{X}^{(6)} = 21\frac{p}{\rho}\widetilde{X}^{(4)}$
$\tilde{h}_i^{(7)} = 0$	$X_i^{(7)} = 27\frac{p}{\rho}X_i^{(5)} - 189\frac{p^2}{\rho^2}X_i^{(3)}$
$\tilde{h}^{(8)} = 0$	$\widetilde{X}^{(8)} = 36\frac{p}{\rho}\widetilde{X}^{(6)} - 378\frac{p^2}{\rho^2}\widetilde{X}^{(4)}$
$\tilde{h}_i^{(9)} = 0$	$X_i^{(9)} = 44\frac{p}{\rho}X_i^{(7)} - 594\frac{p^2}{\rho^2}X_i^{(5)} + 2772\frac{p^3}{\rho^3}X_i^{(3)}$

Note. Species indices "a" are dropped. The usual heat flux $q_i = X_i^{(3)}/2$. Note that beyond the fourth-order moment, both classes start to differ. It can be shown that erroneously prescribing closures at the last retained moment, such as $X_i^{(5)} = 0$ or $\widetilde{X}^{(6)} = 0$, leads to unphysical instabilities (unless one prescribes $X_i^{(3)}$ or $\widetilde{X}^{(4)} = 0$ as well), which is later demonstrated in Appendix B.8, Table 5. A general form for the closures corresponding to $\tilde{h}_i^{(2n+1)} = 0$ and $\tilde{h}^{(2n)} = 0$ is given by (208). An analogous table can be constructed for CGL parallel closures; see Appendix B.9, Table 6.

These Rosenbluth potentials are used to calculate the dynamical friction vector $\boldsymbol{A}_{ab}$ and the diffusion tensor $\bar{\bar{\boldsymbol{D}}}_{ab}$, which then form the Landau collisional operator, according to

$$\boldsymbol{A}_{ab}(\boldsymbol{v}) = 2\frac{c_{ab}}{m_a^2}\left(1 + \frac{m_a}{m_b}\right)\frac{\partial H_b(\boldsymbol{v})}{\partial \boldsymbol{v}}; \qquad \bar{\bar{\boldsymbol{D}}}_{ab}(\boldsymbol{v}) = 2\frac{c_{ab}}{m_a^2}\frac{\partial^2 G_b(\boldsymbol{v})}{\partial \boldsymbol{v}\partial \boldsymbol{v}}; \qquad c_{ab} = 2\pi e^4 Z_a^2 Z_b^2 \ln\Lambda;$$
$$C_{ab}(f_a, f_b) = -\frac{\partial}{\partial \boldsymbol{v}} \cdot \left[\boldsymbol{A}_{ab} f_a - \frac{1}{2}\frac{\partial}{\partial \boldsymbol{v}} \cdot (\bar{\bar{\boldsymbol{D}}}_{ab} f_a)\right]. \tag{207}$$

The dynamical friction vectors and diffusion tensors can be found in the appendix; see Equations (K15)–(K16), (L13)–(L14), and (M4)–(M5). For clarity, we split the calculations into heat fluxes (Appendix K), viscosities (Appendix L), and scalar perturbations (Appendix M). These results are fully nonlinear and could potentially be useful for constructing more sophisticated models that could capture collisional effects beyond the semilinear approximation, or perhaps for exploring the runaway effect numerically. All of the equations can be transformed from Hermite moments to fluid moments by (202).

8.6. Hermite Closures

The general hierarchy of evolution Equations (189)–(191) needs to be closed with appropriate closures at the last retained fluid moment. The correct form of a fluid closure is obtained in the Hermite space, by cutting the perturbation χ_a given by (198) at an appropriate N. For example, the 22-moment model is obtained with Hermite closures $\tilde{h}_a^{(6)} = 0$ and $\tilde{h}_{ij}^{a(6)} = 0$, which translate into fluid closures (134) and (13).

It is useful to summarize the closures for higher-order moments, with the details given in Appendix B. It can be shown that for vectors and scalars, the fluid closures derived from the Hermite closures read

$$\boldsymbol{X}_a^{(2n+1)} = \sum_{m=1}^{n-1}(-1)^{m+n+1}\left(\frac{p_a}{\rho_a}\right)^{n-m}\frac{n!}{m!(n-m)!}\frac{(2n+3)!!}{(2m+3)!!}\boldsymbol{X}_a^{(2m+1)};$$
$$\widetilde{X}_a^{(2n)} = \sum_{m=2}^{n-1}(-1)^{m+n+1}\left(\frac{p_a}{\rho_a}\right)^{n-m}\frac{n!}{m!(n-m)!}\frac{(2n+1)!!}{(2m+1)!!}\widetilde{X}_a^{(2m)}, \tag{208}$$

together the with closures for stress-tensors

$$\bar{\bar{\boldsymbol{\Pi}}}_a^{(2n)} = \sum_{m=0}^{n-2}(-1)^{m+n}\left(\frac{p_a}{\rho_a}\right)^{n-m-1}\frac{(n-1)!}{m!(n-m-1)!}\frac{(2n+3)!!}{(2m+5)!!}\bar{\bar{\boldsymbol{\Pi}}}_a^{(2m+2)}, \tag{209}$$

where the result is zero if the upper summation index is less than the lower summation index, yielding closures $\boldsymbol{X}_a^{(3)} = 0$, $\widetilde{X}_a^{(4)} = 0$, and $\bar{\bar{\boldsymbol{\Pi}}}_a^{(2)} = 0$. The closures are summarized in Tables 3 and 4.

Here we need to address one incorrect interpretation that we used in some of our previous papers. In the last paragraph of Hunana et al. (2018), and also in Hunana et al. (2019a, 2019b), it is claimed that Landau fluid closures are necessary to go beyond the fourth-order moment in the fluid hierarchy. This interpretation was obtained in the Chew, Goldberger, and Low (Chew et al. 1956; CGL)

Table 4

Similar to Table 3, but for Hermite Closures $\hat{h}_{ij}^{(2n)} = 0$

Hermite Closures	Fluid Closures
$\hat{h}_{ij}^{(2)} = 0$	$\Pi_{ij}^{(2)} = 0$
$\hat{h}_{ij}^{(4)} = 0$	$\Pi_{ij}^{(4)} = 7\frac{p}{\rho}\Pi_{ij}^{(2)}$
$\hat{h}_{ij}^{(6)} = 0$	$\Pi_{ij}^{(6)} = 18\frac{p}{\rho}\Pi_{ij}^{(4)} - 63\frac{p^2}{\rho^2}\Pi_{ij}^{(2)}$
$\hat{h}_{ij}^{(8)} = 0$	$\Pi_{ij}^{(8)} = 33\frac{p}{\rho}\Pi_{ij}^{(6)} - 297\frac{p^2}{\rho^2}\Pi_{ij}^{(4)} + 693\frac{p^3}{\rho^3}\Pi_{ij}^{(2)}$

Note. A general form for the closures corresponding to $\hat{h}_{ij}^{(2n)} = 0$ is given by (209).

framework for parallel moments by considering the closures at the last retained moment, $\widetilde{X}_a^{(2n)} = 0$ and $\boldsymbol{X}_{\|a}^{(2n+1)} = 0$. It was shown (see the detailed proof in Section 12.2 in Hunana et al. 2019b) that beyond the fourth-order moment, all fluid models become unstable if these closures are used. The proof is constructed correctly. What is incorrect is the interpretation that the proof implies—that Landau fluid closures are required to overcome this issue. The much simpler Hermite closures overcome this difficulty as well.

In other words, beyond the fourth-order moment it is not possible to cut the fluid hierarchy by simply neglecting the next order moment with closures such as $\boldsymbol{X}_a^{(5)} = 0$ or $\widetilde{X}_a^{(6)} = 0$, and such closures should be viewed as erroneous. For the CGL model, the closures have different coefficients than for the MHD model, because the moments are defined differently (a brief summary is given in Appendix B.9, Table 6). The CGL closures will be addressed in detail in a separate publication.

Importantly, the problem also disappears when one decouples the fluid hierarchy. For example, higher-order Laguerre (Hermite) schemes that are typically used to obtain more precise transport coefficients for $\boldsymbol{q}_a$ and $\bar{\bar{\boldsymbol{\Pi}}}_a^{(2)}$ neglect all of the scalar perturbations $\widetilde{X}_a^{(4)} = \cdots = \widetilde{X}_a^{(2n)} = 0$, together with neglecting the coupling between heat fluxes and stress tensors. In our formulation, this yields the system

$$\frac{d_a}{dt}\boldsymbol{X}_a^{(2n+1)} + \Omega_a\hat{\boldsymbol{b}} \times \boldsymbol{X}_a^{(2n+1)} + (2n+3)!!\,\frac{(n)}{3}\frac{p_a^n}{\rho_a^{n-1}}\nabla\left(\frac{p_a}{\rho_a}\right) = \vec{\boldsymbol{Q}}_a^{(2n+1)} - \frac{(2n+3)!!}{3}\frac{p_a^n}{\rho_a^n}\boldsymbol{R}_a; \tag{210}$$

$$\frac{d_a}{dt}\bar{\bar{\boldsymbol{\Pi}}}_a^{(2n)} + \Omega_a(\hat{\boldsymbol{b}} \times \bar{\bar{\boldsymbol{\Pi}}}_a^{(2n)})^S + \frac{(2n+3)!!}{15}\frac{p_a^n}{\rho_a^{n-1}}\bar{\bar{\boldsymbol{W}}}_a = \bar{\bar{\boldsymbol{Q}}}_a^{(2n)} - \frac{\bar{\bar{\boldsymbol{I}}}}{3}Q_a^{(2n)}. \tag{211}$$

The closures (208), (209) are not required, because the equations are decoupled. We did not calculate the collisional contributions for higher-order moments, but in the semilinear approximation Equations (210)–(211) remain decoupled and represent two independent hierarchies. An essential feature of the Landau (or the Boltzmann) collisional operator is that the operator couples all of the heat fluxes together, and it also couples all of the stress tensors together. Thus, going higher and higher in the fluid hierarchy does not create new contributions in a quasistatic approximation, but yields increasingly precise transport coefficients for $\boldsymbol{q}_a$ and $\bar{\bar{\boldsymbol{\Pi}}}_a^{(2)}$. Also, because the momentum exchange rates $\boldsymbol{R}_a$ contain contributions from all of the heat fluxes $\boldsymbol{X}_a^{(3)} \ldots \boldsymbol{X}_a^{(2n+1)}$, they become increasingly precise as well. System (210)–(211) nicely clarifies how higher-order schemes can be viewed. Reinstating the coupling between heat fluxes and viscosity tensors introduces additional contributions, but does not change the transport coefficients of the decoupled system. A brief comparison of the various models is presented in Appendix I.

8.7. Inclusion of Gravity

We have not explicitly considered the force of gravity in our calculations in the appendix; nevertheless, its inclusion is trivial. With the gravitational acceleration $\boldsymbol{G}$ included, the Boltzmann equation reads

$$\frac{\partial f_a}{\partial t} + \boldsymbol{v}\cdot\nabla f_a + \left[\boldsymbol{G} + \frac{eZ_a}{m_a}\left(\boldsymbol{E} + \frac{1}{c}\boldsymbol{v}\times\boldsymbol{B}\right)\right]\cdot\nabla_v f_a = C(f_a). \tag{212}$$

We use big $\boldsymbol{G}$ instead of small $\boldsymbol{g}$ to clearly distinguish it from the heat flux $\boldsymbol{q}$. Gravity does not enter the collisional operator, and collisional integrals with the right-hand side are not affected. Gravity enters the left-hand side, and when the Boltzmann equation is integrated gravity of course enters the fluid hierarchy of moments. With the two exceptions of the density equation and the pressure tensor equation, gravity enters the evolution equations for all other moments, analogously as the electric field does. An explicit

collisionless equation for a general nth-order moment with the electric field present is Equation (12.13) of Hunana et al. (2019b), for example. Because no Maxwell equations are used in deriving the fluid hierarchy, the presence of gravity can be accounted for by simply replacing

$$\frac{eZ_a}{m_a}\boldsymbol{E} \rightarrow \boldsymbol{G} + \frac{eZ_a}{m_a}\boldsymbol{E}. \tag{213}$$

Furthermore, such a hierarchy is not very useful, because the evolution equation for an nth-order moment is coupled with "n" momentum equations. Subtracting these momentum equations yields the final Equation (12.16) in Hunana et al. (2019b), where the electric field is not present, meaning that gravity is not present either. In other words, the collisionless Equation (12.16) of Hunana et al., as well as our new collisional Equation (A12), remain valid in the presence of gravitational force. The inclusion of gravity in the entire model is thus achieved trivially, by adding $-\boldsymbol{G}$ into the left-hand side of the momentum Equation (7) (which we have done), and no additional calculations are required. In the main text, the only other equation that contains gravity is the electric field Equation (96).

8.8. Precision of m_e/m_i Expansions (Unmagnetized Proton–Electron Plasma)

The multifluid formulation is also an excellent tool for double-checking the precision of m_e/m_i expansions. It is again possible to consider a one ion–electron plasma, but this time to calculate the transport coefficients precisely, without any expansions in the smallness of m_e/m_i. As an example, we consider an unmagnetized proton–electron plasma ($Z_p = 1$, $m_p/m_e = 1836.15267$) with similar temperatures $T_e = T_p = T_{ep}$. Charge neutrality implies $n_e = n_p$, and so $p_e = p_p$. We maintain $\nabla T_e \neq \nabla T_p$, however, because the gradients can be different. We first calculate the heat fluxes. For clarity, we are solving four coupled evolution equations, which are explicitly given in Appendix N; see Equations (N1)–(N4).

A precise calculation should not use simplified collisional times (182) where expansions in m_e/m_i have been made, but exact collisional times (178) with numerical values $\nu_{ee} = 0.707299\nu_{ep}$ and $\nu_{pp} = 0.0165063\nu_{ep}$ (we take $\ln\Lambda$ to be constant). The quasistatic approximation then yields the heat fluxes

$$\begin{aligned}
\boldsymbol{q}_e &= [-3.159370\nabla T_e + 8.301 \times 10^{-6}\nabla T_p]\frac{p_e}{m_e\nu_{ep}} + 0.711046 p_e\delta\boldsymbol{u};\\
\boldsymbol{X}_e^{(5)} &= [-110.5793\nabla T_e + 1.376 \times 10^{-3}\nabla T_p]\frac{p_e^2}{\rho_e m_e\nu_{ep}} + 18.78249\frac{p_e^2}{\rho_e}\delta\boldsymbol{u};\\
\boldsymbol{q}_p &= [-3.302411\nabla T_p + 0.2516 \times 10^{-3}\nabla T_e]\frac{p_p}{m_p\nu_{pp}} + 0.206535 \times 10^{-4} p_p\delta\boldsymbol{u};\\
\boldsymbol{X}_p^{(5)} &= [-103.3984\nabla T_p + 0.7863 \times 10^{-2}\nabla T_e]\frac{p_p^2}{\rho_p m_p\nu_{pp}} + 0.646475 \times 10^{-3}\frac{p_p^2}{\rho_p}\delta\boldsymbol{u},
\end{aligned} \tag{214}$$

where $\delta\boldsymbol{u} = (\boldsymbol{u}_e - \boldsymbol{u}_p)$. For the electron heat flux $\boldsymbol{q}_e$, note the difference of the thermal conductivity 3.1594 from the Braginskii value 3.1616. The difference is caused by calculating the mass-ratio coefficients (27), (28) exactly, without m_e/m_p expansions, as well as by using slightly different ratios of frequencies (a less-precise calculation, neglecting proton–proton collisions by $\nu_{pp} = 0$ and using simplified $\nu_{ee} = \nu_{ep}/\sqrt{2}$ yields 3.1600).

For the proton heat flux $\boldsymbol{q}_p$, the relatively large difference between the thermal conductivity 3.302 and the Braginskii self-collisional value $125/32 = 3.906$ is caused by the proton–electron collisions. This is similarly the case for the $\boldsymbol{X}_p^{(5)}$, where the self-collisional value is $2975/24 = 123.96$. Calculating the coupled system exactly has a nice advantage, since one can calculate the momentum exchange rates in two different ways:

$$\begin{aligned}
\boldsymbol{R}_e &= \nu_{ep}\left\{-\rho_e\delta\boldsymbol{u} + \frac{\mu_{ep}}{T_{ep}}\left[V_{ep(1)}\boldsymbol{q}_e - V_{ep(2)}\frac{\rho_e}{\rho_p}\boldsymbol{q}_p\right] - \frac{3}{56}\left(\frac{\mu_{ep}}{T_{ep}}\right)^2\left[\boldsymbol{X}_e^{(5)} - \frac{\rho_e}{\rho_p}\boldsymbol{X}_p^{(5)}\right]\right\};\\
\boldsymbol{R}_p &= \nu_{pe}\left\{+\rho_p\delta\boldsymbol{u} + \frac{\mu_{ep}}{T_{ep}}\left[V_{pe(1)}\boldsymbol{q}_p - V_{pe(2)}\frac{\rho_p}{\rho_e}\boldsymbol{q}_e\right] - \frac{3}{56}\left(\frac{\mu_{ep}}{T_{ep}}\right)^2\left[\boldsymbol{X}_p^{(5)} - \frac{\rho_p}{\rho_e}\boldsymbol{X}_e^{(5)}\right]\right\},
\end{aligned} \tag{215}$$

and both options yield the same result:

$$\boldsymbol{R}_e = -\boldsymbol{R}_p = -0.711046 n_e\nabla T_e - 0.2065 \times 10^{-4} n_e\nabla T_p - 0.513306\rho_e\nu_{ep}\delta\boldsymbol{u}. \tag{216}$$

The viscosities of the proton–electron plasma are (for clarity, we are solving four equations in four unknowns, explicitly given by (N5)–(N8))

$$\bar{\bar{\mathbf{\Pi}}}_e^{(2)} = [-0.730622\bar{\bar{\mathbf{W}}}_e - 0.2800 \times 10^{-2}\bar{\bar{\mathbf{W}}}_p]\frac{p_e}{\nu_{ei}};$$
$$\bar{\bar{\mathbf{\Pi}}}_e^{(4)} = [-6.542519\bar{\bar{\mathbf{W}}}_e + 3.1509 \times 10^{-2}\bar{\bar{\mathbf{W}}}_p]\frac{p_e^2}{\rho_e\nu_{ei}};$$
$$\bar{\bar{\mathbf{\Pi}}}_p^{(2)} = [-0.892105\bar{\bar{\mathbf{W}}}_p - 0.4621 \times 10^{-4}\bar{\bar{\mathbf{W}}}_e]\frac{p_p}{\nu_{pp}};$$
$$\bar{\bar{\mathbf{\Pi}}}_p^{(4)} = [-7.250870\bar{\bar{\mathbf{W}}}_p - 0.3759 \times 10^{-3}\bar{\bar{\mathbf{W}}}_e]\frac{p_p^2}{\rho_p\nu_{pp}}, \tag{217}$$

and for proton species, the relatively large differences from self-collisional values $1025/1068 = 0.960$ and $8435/1068 = 7.898$ are again caused by proton–electron collisions. In Appendix N, we consider other examples of coupling between the two species, and we calculate the heat fluxes and viscosities for protons and alpha particles (fully ionized Helium), and for the deuterium–tritium plasma used in plasma fusion.

8.9. Limitations of Our Approach

It is important to clarify the limitations of our model. In the highly collisional regime, our limitations are the same as for the model of Braginskii (1965). For example, we describe only Coulomb collisions and we do not take into account ionization, recombination, or radiative transfer. Additionally, our approach shows that the coupling of stress tensors and heat fluxes should ideally be investigated with the 22-moment model. Even though this model is fully formulated in Section 7, including its collisional contributions calculated with the Landau operator, we have not used this model to further explore the resulting coupling.

8.9.1. Weakly Collisional Regime: Expansions around Bi-Maxwellians

The situation becomes more complicated in the weakly collisional regime where there might not be enough collisions to keep the distribution function sufficiently close to the equilibrium Maxwellian $f_a^{(0)}$. The distribution function might evolve to such an extent that the core assumptions in the entire derivation break down, i.e., Equation (1) loses its validity. A better approach then is to consider expansions similar to Equation (1), but around a bi-Maxwellian $f_a^{(0)}$ (see e.g., Oraevskii et al. 1968; Chodura & Pohl 1971; Demars & Schunk 1979; Barakat & Schunk 1982, and references therein), which can handle much larger departures from the highly collisional Maxwellian distribution. In order to point out the differences and difficulties associated with this approach, it is of interest to briefly describe how the expansions around an anisotropic bi-Maxwellian would look. The simplest anisotropic model is known as the CGL, after the pioneering work of Chew, Goldberger, and Low (Chew et al. 1956). The differences with our current approach start with the decomposition of the pressure tensor p_{ij}^a defined in (A2), and the decomposition reads

$$\text{isotropic:} \qquad \bar{\bar{\boldsymbol{p}}}_a = p_a\bar{\bar{\boldsymbol{I}}} + \bar{\bar{\mathbf{\Pi}}}_a^{(2)}; \tag{218}$$

$$\begin{aligned}\text{anisotropic:} \qquad \bar{\bar{\boldsymbol{p}}}_a &= p_{\parallel a}\hat{\boldsymbol{b}}\hat{\boldsymbol{b}} + p_{\perp a}(\bar{\bar{\boldsymbol{I}}} - \hat{\boldsymbol{b}}\hat{\boldsymbol{b}}) + \bar{\bar{\mathbf{\Pi}}}_a^{(2)\mathrm{CGL}} \\ &= p_a\bar{\bar{\boldsymbol{I}}} + (p_{\parallel a} - p_{\perp a})\left(\hat{\boldsymbol{b}}\hat{\boldsymbol{b}} - \frac{\bar{\bar{\boldsymbol{I}}}}{3}\right) + \bar{\bar{\mathbf{\Pi}}}_a^{(2)\mathrm{CGL}},\end{aligned} \tag{219}$$

with scalar pressures

$$p_{\parallel a} = \bar{\bar{\boldsymbol{p}}}_a : \hat{\boldsymbol{b}}\hat{\boldsymbol{b}} = m_a\int c_{\parallel a}^2 f_a\, d^3v; \qquad p_{\perp a} = \bar{\bar{\boldsymbol{p}}}_a : \bar{\bar{\boldsymbol{I}}}_\perp/2 = \frac{m_a}{2}\int |\boldsymbol{c}_{\perp a}|^2 f_a\, d^3v. \tag{220}$$

Directly from the above definitions, the stress tensors satisfy

$$\mathrm{Tr}\,\bar{\bar{\mathbf{\Pi}}}_a^{(2)} = \mathrm{Tr}\,\bar{\bar{\mathbf{\Pi}}}_a^{(2)\mathrm{CGL}} = 0; \qquad \bar{\bar{\mathbf{\Pi}}}_a^{(2)} : \hat{\boldsymbol{b}}\hat{\boldsymbol{b}} \neq 0; \qquad \bar{\bar{\mathbf{\Pi}}}_a^{(2)\mathrm{CGL}} : \hat{\boldsymbol{b}}\hat{\boldsymbol{b}} = 0, \tag{221}$$

and while $\bar{\bar{\mathbf{\Pi}}}_a^{(2)}$ has five independent components, $\bar{\bar{\mathbf{\Pi}}}_a^{(2)\mathrm{CGL}}$ has only four.

The decomposition of the heat flux tensor q_{ijk}^a defined by Equation (A2) is slightly more complicated. In an arbitrary collisional regime, one needs to define two heat flux vectors:

$$\boldsymbol{S}_a^{\parallel} = \bar{\bar{\boldsymbol{q}}}_a : \hat{\boldsymbol{b}}\hat{\boldsymbol{b}} = m_a\int c_{\parallel a}^2 \boldsymbol{c}_a f_a\, d^3v; \qquad \boldsymbol{S}_a^{\perp} = \bar{\bar{\boldsymbol{q}}}_a : \bar{\bar{\boldsymbol{I}}}_\perp/2 = \frac{m_a}{2}\int |\boldsymbol{c}_{\perp a}|^2 \boldsymbol{c}_a f_a\, d^3v. \tag{222}$$

These heat flux vectors are further split by projecting them along the $\hat{\boldsymbol{b}}$, which defines the *gyrotropic* (scalar) heat fluxes $q_{\|a}$ and $q_{\perp a}$, and the perpendicular projection defines the *nongyrotropic heat flux vectors* $\boldsymbol{S}_{\perp a}^{\|}$ and $\boldsymbol{S}_{\perp a}^{\perp}$, according to

$$q_{\|a} = \hat{\boldsymbol{b}} \cdot \boldsymbol{S}_a^{\|} = m_a \int c_{\|a}^2 c_{\|a} f_a \, d^3v; \qquad q_{\perp a} = \hat{\boldsymbol{b}} \cdot \boldsymbol{S}_a^{\perp} = \frac{m_a}{2} \int |\boldsymbol{c}_{\perp a}|^2 c_{\|a} f_a \, d^3v;$$
$$\boldsymbol{S}_{\perp a}^{\|} = \bar{\bar{\boldsymbol{I}}}_{\perp} \cdot \boldsymbol{S}_a^{\|} = m_a \int c_{\|a}^2 \boldsymbol{c}_{\perp a} f_a \, d^3v; \qquad \boldsymbol{S}_{\perp a}^{\perp} = \bar{\bar{\boldsymbol{I}}}_{\perp} \cdot \boldsymbol{S}_a^{\perp} = \frac{m_a}{2} \int |\boldsymbol{c}_{\perp a}|^2 \boldsymbol{c}_{\perp a} f_a \, d^3v. \tag{223}$$

The following relations then hold $\boldsymbol{S}_a^{\|} = q_{\|a}\hat{\boldsymbol{b}} + \boldsymbol{S}_{\perp a}^{\|}$ and $\boldsymbol{S}_a^{\perp} = q_{\perp a}\hat{\boldsymbol{b}} + \boldsymbol{S}_{\perp a}^{\perp}$, together with $\hat{\boldsymbol{b}} \cdot \boldsymbol{S}_{\perp a}^{\|} = 0$ and $\hat{\boldsymbol{b}} \cdot \boldsymbol{S}_{\perp a}^{\perp} = 0$. The two different decompositions of the entire heat flux tensor then read

$$\text{isotropic:} \qquad \bar{\bar{\boldsymbol{q}}}_a = \frac{2}{5}[\boldsymbol{q}_a \bar{\bar{\boldsymbol{I}}}]^S + \bar{\bar{\boldsymbol{\sigma}}}_a'; \tag{224}$$

$$\text{anisotropic:} \qquad \bar{\bar{\boldsymbol{q}}}_a = q_{\|a}\hat{\boldsymbol{b}}\hat{\boldsymbol{b}}\hat{\boldsymbol{b}} + q_{\perp a}[\hat{\boldsymbol{b}}\bar{\bar{\boldsymbol{I}}}_{\perp}]^S + [\boldsymbol{S}_{\perp a}^{\|}\hat{\boldsymbol{b}}\hat{\boldsymbol{b}}]^S + \frac{1}{2}[\boldsymbol{S}_{\perp a}^{\perp}\bar{\bar{\boldsymbol{I}}}_{\perp}]^S + \bar{\bar{\boldsymbol{\sigma}}}_a;$$
$$= q_{\perp a}[\hat{\boldsymbol{b}}\bar{\bar{\boldsymbol{I}}}]^S + (q_{\|a} - 3q_{\perp a})\hat{\boldsymbol{b}}\hat{\boldsymbol{b}}\hat{\boldsymbol{b}} + \frac{1}{2}[\boldsymbol{S}_{\perp a}^{\perp}\bar{\bar{\boldsymbol{I}}}]^S + \left[\left(\boldsymbol{S}_{\perp a}^{\|} - \frac{\boldsymbol{S}_{\perp a}^{\perp}}{2}\right)\hat{\boldsymbol{b}}\hat{\boldsymbol{b}}\right]^S + \bar{\bar{\boldsymbol{\sigma}}}_a, \tag{225}$$

where both $\bar{\bar{\boldsymbol{\sigma}}}_a'$ and $\bar{\bar{\boldsymbol{\sigma}}}_a$ are traceless. Neglecting these traceless contributions, the isotropic approach accounts for three (out of 10) scalar components of $\bar{\bar{\boldsymbol{q}}}_a$, and represents a 13-moment model (one density, three velocity, one scalar pressure, five stress tensor, and three heat flux $\boldsymbol{q}_a$ components). The anisotropic approach accounts for six scalar components of $\bar{\bar{\boldsymbol{q}}}_a$ and represents a 16-moment model, described by 16 scalar evolution Equations. (One density, three velocity, two scalar pressures, four stress tensor components, and three for each heat flux vector $\boldsymbol{S}_a^{\|}$ and $\boldsymbol{S}_a^{\perp}$.) Unfortunately, such a complicated decomposition of the heat flux is necessary in an arbitrary collisional regime, and we only used decomposition (224). For clarity, the direct relation with the usual heat flux vector $\boldsymbol{q}_a$ reads

$$\boldsymbol{q}_a = \frac{1}{2}\boldsymbol{S}_a^{\|} + \boldsymbol{S}_a^{\perp} = \left(\frac{1}{2}q_{\|a} + q_{\perp a}\right)\hat{\boldsymbol{b}} + \frac{1}{2}\boldsymbol{S}_{\perp a}^{\|} + \boldsymbol{S}_{\perp a}^{\perp}. \tag{226}$$

Note that both $q_{\|a}$ and $q_{\perp a}$ denote components along the $\hat{\boldsymbol{b}}$. The highly collisional limit is achieved by $q_{\|a} = 3q_{\perp a}$ and $\boldsymbol{S}_{\perp a}^{\|} = \boldsymbol{S}_{\perp a}^{\perp}/2$, in which case $\boldsymbol{q}_a = (5/2)q_{\perp a}\hat{\boldsymbol{b}} + (5/4)\boldsymbol{S}_{\perp a}^{\perp}$ or, equivalently, $\boldsymbol{q}_a = (5/6)q_{\|a}\hat{\boldsymbol{b}} + (5/2)\boldsymbol{S}_{\perp a}^{\|}$. We use the same notation as, for example, the collisionless papers by Passot & Sulem (2007), Sulem & Passot (2015), and Hunana et al. (2019a, 2019b).

These anisotropic decompositions must be retained in an arbitrary collisional regime. However, calculations with the Landau (Boltzmann) collisional operators then become very complicated. Notably, Chodura & Pohl (1971), Demars & Schunk (1979), and Barakat & Schunk (1982) used the anisotropic 16-moment model, as described above, and calculated the collisional contributions for several interaction potentials. Judging from the papers above, maintaining the precision of our current model (where the fourth- and fifth-order moments are considered), and extending it to an anisotropic (bi-Maxwellian) regime, seems to be so complicated that it might not be worth the effort. Curiously, in a simplified spherically symmetric radial geometry, Cuperman et al. (1980, 1981) and Cuperman & Dryer (1985) considered what seems like a mixture of anisotropic and isotropic moments, with anisotropic temperatures, an isotropic heat flux vector, and the parallel (anisotropic) perturbation of the fourth-order moment (which we call $\tilde{r}_{\|\|a}$).

8.9.2. Landau Fluid Closures for the Collisionless Case

In contrast to the free-streaming formula of Hollweg (1974, 1976), in plasma physics the collisionless heat flux is typically associated with the phenomenon of Landau damping. For example, the collisionless linear kinetic theory expanded around a bi-Maxwellian with mean *zero drifts* in gyrotropic limit yields in Fourier space a perturbation of the distribution function $f_a = f_a^{(0)}(1 + \chi_a)$ in the following form:

$$\chi_a = \frac{B_{\|}^{(1)}}{B_0}\frac{m_a}{2T_{\perp a}^{(0)}}\left[v_{\perp}^2 + \frac{T_{\perp a}^{(0)}}{T_{\|a}^{(0)}}\frac{k_{\|}v_{\|}v_{\perp}^2}{(\omega - k_{\|}v_{\|})}\right] + \Phi\frac{eZ_a}{T_{\|a}^{(0)}}\frac{k_{\|}v_{\|}}{(\omega - k_{\|}v_{\|})}, \tag{227}$$

with the electrostatic potential $\Phi = iE_{\|}^{(1)}/k_{\|}$. Integrating (227) then yields a parallel collisionless heat flux,

$$q_{\|a}^{(1)} = -v_{\mathrm{th}\|\mathrm{a}} n_a^{(0)} T_{\|a}^{(0)} \mathrm{sign}(\mathrm{k}_{\|})(\zeta_a + 2\zeta_a^3 R(\zeta_a) - 3\zeta_a R(\zeta_a))\left[\frac{B_{\|}^{(1)}}{B_0}\frac{T_{\perp a}^{(0)}}{T_{\|a}^{(0)}} + \Phi\frac{eZ_a}{T_{\|a}^{(0)}}\right], \tag{228}$$

with variable $\zeta_a = \omega/(|k_{\|}|v_{\mathrm{th}\|\mathrm{a}})$, parallel thermal speed $v_{\mathrm{th}\|\mathrm{a}} = \sqrt{2T_{\|a}/m_a}$, plasma response function $R(\zeta_a) = 1 + \zeta_a Z(\zeta_a)$, and plasma dispersion function $Z(\zeta_a) = i\sqrt{\pi}\exp(-\zeta_a^2)[1 + \mathrm{erf}(i\zeta_a)]$. Such a kinetic answer can be expressed in fluid variables by searching for

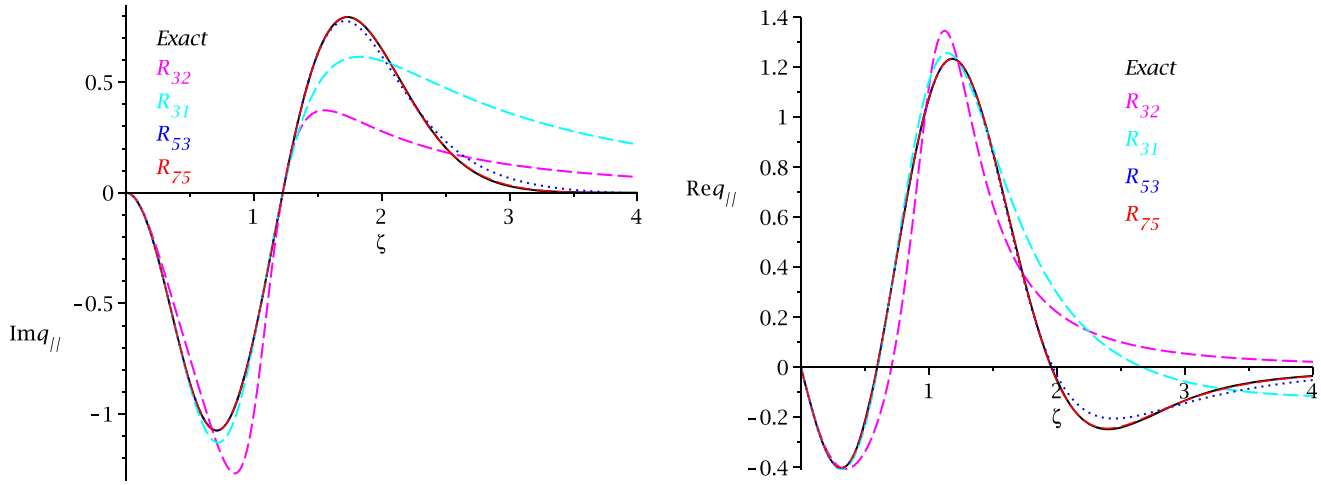

Figure 1. Comparison of normalized collisionless heat fluxes $\hat{q}_{\|a} = \zeta_a + (2\zeta_a^3 - 3\zeta_a)R(\zeta_a)$ in a weakly damped regime with real-valued ζ_a. Left: the imaginary part of $\hat{q}_{\|a}$. Right: the real part of $\hat{q}_{\|a}$. The colors are described in the text. Our Braginskii-type models do not contain these collisionless heat fluxes.

Landau fluid closures, by, for example, replacing the $R(\zeta_a)$ with its three-pole Padé approximants:

$$R_{3,2}(\zeta_a) = \frac{1 - i\frac{\sqrt{\pi}}{2}\zeta_a}{1 - i\frac{3\sqrt{\pi}}{2}\zeta_a - 2\zeta_a^2 + i\sqrt{\pi}\zeta_a^3}; \qquad R_{3,1}(\zeta_a) = \frac{1 - i\frac{(4-\pi)}{\sqrt{\pi}}\zeta_a}{1 - i\frac{4}{\sqrt{\pi}}\zeta_a - 2\zeta_a^2 + 2i\frac{(4-\pi)}{\sqrt{\pi}}\zeta_a^3}. \tag{229}$$

The use of Padé approximants allows one to express (228) through lower-order moments and eliminate the explicit dependence on ζ_a, yielding collisionless heat fluxes in Fourier space:

$$R_{3,2}(\zeta_a): \qquad q_{\|a}^{(1)} = -\, i\frac{2}{\sqrt{\pi}} n_a^{(0)} v_{\mathrm{th}\|\mathrm{a}} \mathrm{sign}(\mathrm{k}_\|) T_{\|a}^{(1)}; \tag{230}$$

$$R_{3,1}(\zeta_a): \qquad q_{\|a}^{(1)} = \frac{3\pi - 8}{4 - \pi} p_{\|a}^{(0)} u_{\|a}^{(1)} - i\frac{\sqrt{\pi}}{4 - \pi} n_a^{(0)} v_{\mathrm{th}\|\mathrm{a}} \mathrm{sign}(\mathrm{k}_\|) T_{\|a}^{(1)}, \tag{231}$$

where $T_{\|a}^{(1)}$ is the perturbed temperature and $u_{\|a}^{(1)}$ is the perturbed fluid velocity (a mean value of $u_{\|a}^{(0)} = 0$ is assumed). The heat flux closure (230) was obtained by Hammett & Perkins (1990) and Snyder et al. (1997), and closure (231) is Equation (2) in Hunana et al. (2018; or Equation (3.211) in Hunana et al. 2019a). In real space, these collisionless heat fluxes become

$$R_{3,2}(\zeta_a): \qquad q_{\|a}(z) = -\frac{2}{\pi^{3/2}} n_a^{(0)} v_{\mathrm{th}\|\mathrm{a}} \mathrm{V.P.} \int_0^\infty \frac{T_{\|a}^{(1)}(z + z') - T_{\|a}^{(1)}(z - z')}{z'} dz'; \tag{232}$$

$$R_{3,1}(\zeta_a): \qquad q_{\|a}(z) = \frac{3\pi - 8}{4 - \pi} p_{\|a}^{(0)} u_{\|a}^{(1)} - \frac{n_a^{(0)} v_{\mathrm{th}\|\mathrm{a}}}{\sqrt{\pi}(4 - \pi)} \mathrm{V.P.} \int_0^\infty \frac{T_{\|a}^{(1)}(z + z') - T_{\|a}^{(1)}(z - z')}{z'} dz', \tag{233}$$

where the nonlocality presents itself as an integral over the entire magnetic field line, where the temperatures everywhere along that field line matter in order to determine the heat flux at a specific spatial point. Note that the thermal part of (233) is almost two times larger than (232). The Cauchy principal value can be replaced by $\lim_{\epsilon \to +0} \int_\epsilon^\infty$. This approach thus indeed allows one to have expressions for collisionless heat fluxes in a quasistatic approximation. However, as is well known, these expressions are not very precise with respect to kinetic theory. For example, the precision can easily be compared by plotting the normalized heat fluxes $\hat{q}_{\|a} = \zeta_a + 2\zeta_a^3 R(\zeta_a) - 3\zeta_a R(\zeta_a)$, which are shown in Figure 1. A weakly damped regime with a real-valued ζ_a is considered. The left-hand panel shows the imaginary part of $\hat{q}_{\|a}$, and the right-hand panel shows the real part of $\hat{q}_{\|a}$. The exact kinetic heat flux is shown by the solid black line, the heat flux $R_{3,2}$ is shown by the dashed magenta line, and the heat flux $R_{3,1}$ is shown by the dashed cyan line. For comparison, higher-order fluid models with approximants $R_{5,3}$ (the dotted blue line) and $R_{7,5}$ (the dashed red line) are shown as well (see Equations (A11) and (A38) in Hunana et al. 2019a). The $R_{5,3}$ model represents a dynamic closure at the fourth-order moment, and the $R_{7,5}$ model represents a dynamic closure at the sixth-order moment, given by Equations (5) and (8) of Hunana et al. (2018). The heat fluxes in these higher-order models are thus described by their usual evolution equations; nevertheless, their precision can be compared with the same technique. Which quasistatic heat flux is a better choice depends on the value of ζ_a, because the $R_{3,1}$ has a higher power series precision (for small ζ_a) and the $R_{3,2}$ has a higher asymptotic series precision (for large ζ_a). Regimes $\zeta_a \ll 1$ can be viewed as isothermal, and regimes $\zeta_a \gg 1$ can be viewed as adiabatic. In the left-hand panel of Figure 1, the $R_{3,1}$ is more precise up to roughly $\zeta_a = 2.3$, and in the right-hand panel up to $\zeta_a = 1.6$. For larger ζ_a values than shown, the $R_{3,1}$ heat flux converges much more slowly to the correct zero values than the $R_{3,2}$, especially for the real part.

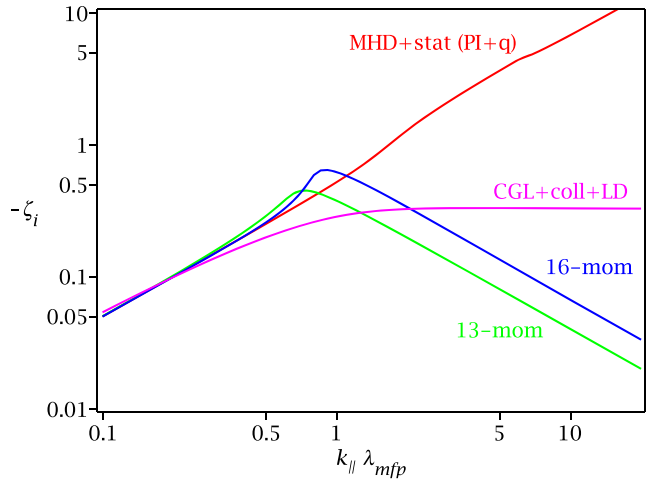

Figure 2. Normalized damping rate $\zeta_i = \omega_i/(|k_\parallel| v_{\mathrm{th}\parallel})$ for a parallel propagating ion sound wave as a function of $k_\parallel \lambda_{\mathrm{mfp}}$, where λ_{mfp} is a mean-free path. Red line: Braginskii-type (isotropic) 13-moment model with quasistatic stress tensor and heat flux. Green line: Braginskii-type 13-moment model with evolution equations for the stress tensor and heat flux. Blue line: bi-Maxwellian 16-moment model with evolution equations for parallel and perpendicular pressures and (gyrotropic) heat fluxes. Magenta line: Landau fluid model with the quasistatic heat fluxes of Snyder et al. (1997).

The major obstacle to precision for the quasistatic heat fluxes of the Landau fluid models actually comes from the perpendicular heat flux $q_{\perp a}$ (which is along the $\hat{\boldsymbol{b}}$), because only a closure of Snyder et al. (1997) with a crude Padé approximant $R_1(\zeta_a) = 1/(1 - i\sqrt{\pi}\zeta_a)$ is available. As a consequence, for large ζ_a values, the quasistatic heat flux $q_{\perp a}$ fails to disappear and instead converges to a constant value. To recover the adiabatic behavior for $q_{\perp a}$, one has to abandon the idea of quasistatic $q_{\perp a}$ and consider its evolution equation, with a closure at the fourth-order moment. There is a vast amount of literature about Landau fluids with various approaches; see, e.g., Hammett & Perkins (1990), Hammett et al. (1992), Snyder et al. (1997), Snyder & Hammett (2001), Goswami et al. (2005), Passot & Sulem (2007), Passot et al. (2012), Sulem & Passot (2015), Joseph & Dimits (2016), Hunana et al. (2018), Ji & Joseph (2018), Chen et al. (2019), Wang et al. (2019), and references therein, where some authors also include collisional effects. For a simple introductory guide to collisionless Landau fluids, see Hunana et al. (2019a). As a side note, Landau fluid closures are not constructed with any specific mode in mind (as incorrectly criticized by Scudder 2021, for example). The closures are constructed universally for all of the modes, so that numerical simulations can be performed; see e.g., Perrone et al. (2018). Interestingly, as discussed by Meyrand et al. (2019), from a nonlinear perspective, the effect of Landau damping might be canceled out by the effect of plasma echo. From a linear perspective, the presence of drifts also modifies the Landau damping, because the variable ζ_a that enters the plasma response function $R(\zeta_a)$ then contains the drift velocity $u_{\parallel a}$. For sufficiently large drifts, the sound mode can be generated by the current-driven ion-acoustic instability; see, e.g., Gurnett & Bhattacharjee (2005, p. 368), or Fitzpatrick (2015, p. 258); and for a three-component plasma, which allows the net current to be zero by the ion–ion (or the electron–ion and electron–electron) acoustic instability, see Gary (1993, pp. 44–55).

8.9.3. Ion Sound Wave Damping in Homogeneous Media: Comparison of Various Models

To further clarify our limitations, it is useful to explore the linear properties of the waves propagating along the ambient magnetic field (assumed to be straight and aligned with the z-coordinate) in a homogeneous medium, in regimes that range from highly collisional to weakly collisional ones. In particular, let us consider the damping of a monochromatic ion sound wave of parallel wavenumber $k_\parallel$ in a proton–electron plasma where the electrons are assumed to be cold. The latter assumption is not physically appropriate, because kinetic theory is not well-defined for cold electrons (see, e.g., the discussion in Hunana et al. 2019a, p. 73), but it allows one to simplify the presentation with the goal of describing the general behavior, not providing precise values of the damping rates. Four different models are compared in Figure 2, all using the heuristic BGK collisional operator, which leads to much simpler calculations for models with a distribution function expanded around a bi-Maxwellian. The x-axis shows $k_\parallel \lambda_{\mathrm{mfp}}$, where $\lambda_{\mathrm{mfp}} = v_{\mathrm{th}\parallel}/\nu$ is the ion mean-free path and ν is the collisional frequency, so that $k_\parallel \lambda_{\mathrm{mfp}} \ll 1$ represents a highly collisional regime and $k_\parallel \lambda_{\mathrm{mfp}} \gg 1$ represents a weakly collisional regime. The y-axis shows a damping rate as an imaginary part of $\zeta = \omega/(|k_\parallel| v_{\mathrm{th}\parallel})$. The usual isotropic 13-moment model (the green line) and the anisotropic 16-moment model (the blue line), with all of the moments described by their time-dependent (dynamical) evolution equations, were discussed after Equation (225). For the parallel sound mode at the linear level considered here, the 13-moment model is reduced to evolution equations for ρ, u_z, p, Π_{zz}, and q_z (we consider the case where Π_{zz} and q_z are coupled) and the 16-moment model reduces to evolution equations for ρ, u_z, $p_\parallel$, $p_\perp$, $q_\parallel$, and $q_\perp$ (we consider the mean equal pressures $p_\parallel^{(0)} = p_\perp^{(0)}$). Figure 2 shows that these two models behave in a similar way: both reach a maximum damping rate around $k_\parallel \lambda_{\mathrm{mfp}} \sim 0.5 - 1$, and converge toward a zero damping rate in the collisionless regime (with only a small shift in $k_\parallel \lambda_{\mathrm{mfp}}$ between them). In contrast, the red line, corresponding to the 13-moment model with the Π_{zz} and q_z taken in the quasistatic approximation, shows that the damping rate does not reach a maximum and instead continues to increase in a weakly collisional regime, while around $k_\parallel \lambda_{\mathrm{mfp}} \sim 6.3$ the sound mode stops existing (it becomes nonpropagating, with zero real frequency). This is consequence of the quasistatic approximation for the stress tensor $\Pi_{zz} \sim 1/\nu$, which in the collisionless regime becomes unbounded (the parallel heat flux $q_z \sim 1/\nu$ becomes unbounded as well, but this simply reflects an isothermal behavior with no damping present). While a vanishing

damping is preferred against a quantity that blows up in a weakly collisional regime, all three models are technically incorrect, because the Landau damping provides a significant contribution to the damping rate as the plasma becomes weakly collisional. To illustrate the importance of the Landau damping, the magenta line displays the damping rate obtained with a Landau fluid model that contains the evolution equations for ρ, u_z, $p_\parallel$, and $p_\perp$, but where the quasistatic $q_\parallel$ and $q_\perp$ are given by the collisionally modified 3+1 closures of Snyder et al. (1997), i.e., their Equations (48)–(49), which for the isotropic mean temperatures $T^{(0)}_{\parallel a} = T^{(0)}_{\perp a}$ considered here are equivalent to (our thermal speed contains a factor of 2, which is not the case in that paper)

$$q^{(1)}_{\parallel a} = -\frac{\frac{4}{3\pi-8}n^{(0)}_a v^2_{\mathrm{th}\parallel \mathrm{a}}}{\bar{\nu}_a + \frac{2\sqrt{\pi}}{3\pi-8}v_{\mathrm{th}\parallel \mathrm{a}}|k_\parallel|} ik_\parallel T^{(1)}_{\parallel a}; \qquad q^{(1)}_{\perp a} = -\frac{\frac{1}{2}n^{(0)}_a v^2_{\mathrm{th}\parallel \mathrm{a}}}{\bar{\nu}_a + \frac{\sqrt{\pi}}{2}v_{\mathrm{th}\parallel \mathrm{a}}|k_\parallel|} ik_\parallel T^{(1)}_{\perp a}, \tag{234}$$

where, in general, $\bar{\nu}_a = \sum_b \nu_{ab}$. Technically, closures (234) are only applicable to a weakly collisional regime, because $q_{\parallel a} \neq 3q_{\perp a}$ in the highly collisional limit. In spite of this, and the additional difficulty associated with the cold electron limit considered here, an interesting point is that the behavior of the damping rate is very close to the predictions of the three other models in the highly collisional regime, while the damping rate converges to a constant value in the collisionless case. This is in fact analogous to the case of the damping of a pure sound wave in rarefied media, which was considered by Stubbe (1994) and Stubbe & Sukhorukov (1999). In the former paper, the result of an experiment by Meyer & Sessler (1957; measuring the damping length of a sound wave of a given frequency ω, emitted at one end of a domain filled with a rarefied neutral gas) is compared with various theoretical models. The results are very similar to those presented here, and show in particular that the damping is dominated by a nonlocal effect analogous to Landau damping when $2\nu/\omega$ decreases below unity (see Figures 6 and 7 of Stubbe 1994). This simple result for the damping of an ion sound wave shows that, in a homogeneous medium, a Braginskii-type model provides reasonable predictions, as long as the typical wavelength is larger than the mean-free path, or, equivalently, when its frequency stays below the collision frequency. More sophisticated models are needed in the weakly collisional case, which should retain new contributions originating from a Landau fluid closure.

8.9.4. Large Gradients and Large Drifts

It is now of interest to consider inhomogeneous situations, where other applicability conditions apply for the Braginskii-type models. In high-energy-density laser-produced plasmas, there are often situations that are relevant for inertial confinement fusion experiments, where the typical electron mean-free path becomes of the order of the typical scale of the electron temperature gradients, or even larger. In this case, the usual Braginskii formulas, used for the Nernst effect (see, e.g., Lancia et al. 2014), for example, become invalid and have to be replaced by nonlocal expressions. In this context, an explicit nonlocal formula was proposed by Luciani et al. (1983) for the electron thermal heat flux due to steep temperature gradients, offering an improvement (in the one-dimensional case) to the Spitzer & Härm (1953) heat flux, where one required proportionality constant is obtained by a fitting from Fokker–Planck simulations. A further extension to three dimensions was proposed by Schurtz et al. (2000), but it is to be noted that this approach is not appropriate in the very weakly collisional case, as, for example, in the Solar corona, when the density has significantly decreased.

Additional complications arise in a regime of weak collisionality. In space physics, the collisionless heat flux is typically associated with the free-streaming formula of Hollweg (1974, 1976):

$$\boldsymbol{q}^{\mathrm{Hollweg}}_e = \frac{3}{2}p_e \boldsymbol{u}_{\mathrm{sw}}\alpha, \tag{235}$$

where one multiplies the thermal energy of one electron $(3/2)T_e$ (we take $k_b = 1$ throughout the entire paper) with the number density n_e and the solar wind speed $\boldsymbol{u}_{\mathrm{sw}}$. The free "bugger factor" α, as Hollweg (1974) calls it, is dependent on a given form of an electron distribution function, where the tail had departed and run away. Note that the parallel *frictional* heat fluxes (i.e., due to *small* differences in the drifts $\delta\boldsymbol{u}$) of Spitzer & Härm (1953) and Braginskii (1965) are also independent of collisional frequencies, even though they are derived from collisions, and up to the numerical values have the same form as (235). As a side note, in the numerical model of Spitzer & Härm (1953), the frictional heat flux is technically incorrect, because it does not satisfy the Onsager symmetry—see our Tables 11 and 9—which was already criticized by Balescu (1988, p. 268). Of course, in our usual fluid formalism, a tail of a distribution function cannot suddenly depart. Even though our model contains evolution equations for the perturbation of the fourth-order moment (i.e., a "reduced kurtosis" that describes whether a distribution is tail-heavy or tail-light) and also for the fifth-order moment (sometimes called a hyperskewness), our distribution functions still have to remain sufficiently close to Maxwellian. For the isotropic 5-moment model (i.e., strict Maxwellians), the runaway effect is just represented through the collisional contributions $\boldsymbol{R}_{ab}$ and Q_{ab}, which decrease to zero for large drifts (see Equations (171)–(173) derived in Appendix G.3; see also Dreicer 1959; Tanenbaum 1967; Burgers 1969; Schunk 1977; Balescu 1988). We note that for sufficiently large drifts between species, various instabilities can develop with a subsequent development of turbulence, which should restrict the runaway effect long before relativistic effects. Importantly, it is unclear how the heat flux collisional contributions $\boldsymbol{Q}^{(3)\,\prime}_{ab}$ (and higher) would look for unrestricted drifts, because the collisional integrals seem exceedingly complicated. Even if calculated, only the drifts between species would be allowed to be unrestricted, and the distribution of each species would have to be restricted to remain close to Maxwellian. For the simplest CGL plasmas (i.e., considering colliding strict bi-Maxwellians with no stress tensors or heat fluxes), the corresponding collisional integrals were numerically evaluated for selected cases by Barakat & Schunk (1981). For a further particular case of

unrestricted drifts only *along* the magnetic field and Coulomb collisions, Hellinger & Trávníček (2009) obtained exact analytic forms for the collisional integrals (for $p_{\parallel}$ and $p_{\perp}$), which are expressed through double hypergeometric functions, however. Judging from the two papers above, the proper extension of our model to an anisotropic regime with unrestricted drifts seems to be overly complicated. Another approach for the heat flux modeling was presented by Canullo et al. (1996).

8.9.5. Comments on the Positivity of the Perturbed Distribution Function

An additional complication arises in a low-collisionality regime in the presence of sufficiently strong large-scale gradients. The perturbations of the distribution function considered in Equation (1) might become so large that the corresponding model might become invalid. The distribution function around which to expand is indeed not well defined in this case. Strictly speaking, in a weakly collisional (or a collisionless) regime, one should abandon the construction of fluid models derived from the Boltzmann equation, and perform kinetic simulations by directly evolving the Boltzmann equation. Perhaps the best example is a radially expanding flow, such as the solar corona with emerging solar wind, where the spherical expansion creates strong large-scale gradients and simultaneously drives the system toward a collisionless regime. It seems that in this extreme case it might indeed be possible (but not with certainty) that the underlying distribution function could even become negative, $f_a < 0$, which is of course unphysical. We anticipate that our 21- and 22-moment models might fail in this particular situation, even if the evolution equations are retained, but, as discussed below, we were unfortunately not able to reach a clear conclusion and further research is needed to clearly establish the areas of validity.

The $f_a < 0$ has been criticized, for example, by Scudder (2021) and Cranmer & Schiff (2021), and references therein, on an example of an 8-moment model in a quasistatic approximation. It is in fact questionable if the $f_a < 0$ can be shown in a quasistatic approximation. It is necessary to distinguish between two different cases, depending whether large-scale gradients are present or absent during the transition into the low-collisionality regime. In the homogeneous case, the situation is clear, because one needs to describe the presence of waves with frequencies ω, and neglecting the time derivative d/dt in the evolution equations automatically imposes the requirement $\omega \ll \nu$, i.e., the collisional frequencies ν must remain sufficiently large. In this case, it is erroneous to simply take the quasistatic heat flux $\boldsymbol{q}_a \sim 1/\nu$, evaluate it for some arbitrarily small ν, and claim that $f_a < 0$. Instead, it is necessary to retain the evolution equations with $d\boldsymbol{q}_a/dt$; see, e.g., (41), (51) or the coupled system (135)–(139), which preclude one from reaching the direct interpretation that $f_a < 0$ (unless one calculates the eigenvector and shows otherwise). The negativity of the distribution function may not take place and, as a consequence, the procedure seems inadequate for disproving the moment method of Grad in a homogeneous low-collisionality regime. The situation is much less clear when large-scale gradients are present, as in the example of solar wind expansion. In that case, it is possible to argue that keeping the evolution equations and solving an initial value problem might only help temporarily, because the system eventually has to converge to some stationary solution, which might show that $f_a < 0$. Such a possibility seems to be implied by the simple one-dimensional radially expanding quasistatic models (see, e.g., Cranmer & Schiff 2021, and references therein). However, the quasistatic approximation can be questioned in this case as well, but from a different perspective. Introducing a heat flux or a stress tensor is analogous to introducing a new degree of freedom into a system, and if this new degree of freedom is not restricted in any way, it might of course yield an unphysical system. In plasma physics, degrees of freedom are usually restricted by associated instabilities that develop, which cannot be revealed in a quasistatic approximation (even if an instability is nonpropagating). Useful examples are the anisotropic CGL and 16-moment models described above. Using a quasistatic approximation, one might erroneously conclude that the temperature anisotropy can grow without bounds in these models, whereas considering evolution equations reveals the firehose and mirror instabilities, which can restrict the anisotropy. A similar situation might be applicable here, where sufficiently large drifts (and possibly large heat fluxes and stress tensors) might cause various instabilities and also the development of turbulence, but further clarifications are needed as to whether our fluid models contain some of these instabilities, especially considering that our collisional contributions are valid only when the differences in the drifts between species are much smaller than their thermal velocities. In this regard, it is not clear if it is appropriate to neglect the Alfvénic fluctuations in the radially expanding models. Finally, it is also not clear if it is physically meaningful to show $f_a < 0$ by skipping the stress tensor in the expansions of Grad (which is a second-order moment before the third-order heat flux moment), because its contributions to a total f_a might be significant. For a sufficient proof that the f_a can become negative, it might be necessary to consider at least the 13-moment model, where both the stress tensors and heat fluxes are retained.

8.10. Conclusions

We have discussed various generalizations of the 21-moment model of Braginskii (1958, 1965). (1) We have presented a multifluid formulation for arbitrary masses m_a and m_b and arbitrary temperatures T_a and T_b. (2) All of the fluid moments are described by their evolution equations, whose left-hand sides are given in a fully nonlinear form. (3) Formulation with evolution equations has the important consequence that the model does not become divergent (unbounded) if a regime of low collisionality is encountered. (4) For a one ion–electron plasma, we have provided all of the Braginskii transport coefficients in a fully analytic form for a general ion charge Z_i (and arbitrary strength of magnetic field). (5) We have also provided fully analytic higher-order transport coefficients (for $\bar{\bar{\boldsymbol{\Pi}}}^{(4)}$ and $\boldsymbol{X}^{(5)}$), which are not typically given. (6) All of the electron coefficients were further generalized to multi-ion plasmas. (7) We have considered coupling between viscosity tensors and heat fluxes, where a heat flux enters a viscosity tensor and a viscosity tensor enters a heat flux. As a consequence, we have introduced new higher-order physical effects, even for the simplest case of the unmagnetized one ion–electron plasma of Spitzer & Härm (1953). For example, the electron rate of strain tensor $\bar{\bar{\boldsymbol{W}}}_e$ enters the electron heat fluxes even linearly, and thus it subsequently enters the momentum exchange rates linearly; see Equation (127). (8) We have formulated the 22-moment model, which is a natural extension of the 21-moment model, where one takes into account fully

contracted scalar perturbations $\widetilde{X}_a^{(4)}$ entering the decomposition of the fourth-order moment $X_{ijkl}^{a(4)}$; see Equation (129). The collisional contributions for this model with arbitrary masses and temperatures are given in Section 7.1, and supplement those given in Section 2.1 for the 21-moment model. Interestingly, the scalar perturbations $\widetilde{X}_a^{(4)}$ modify the energy exchange rates; see Equations (140) or (177). In the quasistatic approximation, the scalar perturbations $\widetilde{X}_a^{(4)}$ can be written as the divergence of heat flux vectors with their own heat conductivities; see, for example, the solutions for a one ion–electron plasma with the ion heat conductivities (149) and the electron heat conductivities (162). These corrections remain small in the highly collisional regime, but might become significant at small wavelengths and/or at large frequencies.

Our model can be useful for direct numerical simulations, as well as for the quick calculation of the transport coefficients in a quasistatic approximation. We provide three examples for coupling between two species. Thermal conductivities and viscosities for unmagnetized proton–electron plasma (without m_e/m_p expansions) were presented in Section 8.8, and two examples for protons–alpha particles and deuterium–tritium were moved to Appendix N. Our model can also be useful from an observational perspective. For example, the parallel thermal heat flux $\boldsymbol{q}_e$ of Braginskii (1965) and Spitzer & Härm (1953; they only differ by 3.16 versus 3.20 factors, rounded as 3.2) is sometimes analyzed in observational studies; see, e.g., Salem et al. (2003), Bale et al. (2013), Halekas et al. (2021), and Verscharen et al. (2019, p. 61). It is also measured in (exospheric) kinetic numerical simulations (Landi et al. 2014). Our model suggests that it would be beneficial to analyze both parallel heat fluxes, which for $Z_i = 1$ read

$$\boldsymbol{q}_e = \frac{\boldsymbol{X}_e^{(3)}}{2} = -\,3.2\frac{p_e}{m_e\nu_{ei}}\nabla T_e; \qquad \boldsymbol{X}_e^{(5)} = -\,110.7\frac{p_e^2}{\rho_e m_e \nu_{ei}}\nabla T_e, \tag{236}$$

and which can be analyzed with the same techniques. For long parallel mean-free paths (in the low collisionality regime), both heat fluxes naturally have to become nonlocal and independent of the mean-free path. Our limitations are described in Section 8.9, and the "flattening/saturation" of the heat fluxes due to the runaway effect and Landau damping is not captured in our model. Our model is aimed at the highly collisional regime, and in the low-collisionality regime our heat fluxes are just described by their evolution equations, where the collisional right-hand sides are small. Nevertheless, it would be interesting to see if in observational studies or kinetic simulations the $\boldsymbol{X}_e^{(5)}$ could be described by a free-streaming formula similar to the one of Hollweg (1974, 1976), in a form $\boldsymbol{X}_e^{(5)} = (3/2)(p_e^2/\rho_e)\boldsymbol{u}_{\rm sw}\alpha_5$, where the "bugger factor" α_5 has to be determined from a given form of a distribution function, or if such a concept does not apply for $\boldsymbol{X}_e^{(5)}$. As a side note, concerning collisionless heat fluxes for plasmas where spherical expansion and large drifts are not present and Landau damping dominates, our model actually implies that a correct interpretation should not be that the Landau damping diminishes/saturates the heat flux in a low-collisionality regime. The correct interpretation is that the Landau damping creates the collisionless heat flux. Collisionless Landau fluid closures for quasistatic parallel scalar $X_{\parallel}^{(5)}$ can be found in Hunana et al. (2019a, p. 84). In addition to (236), it might be also useful to analyze the scalar perturbation, which for $Z_i = 1$ reads

$$\widetilde{X}_e^{(4)} = +\,83.8\frac{p_e^2}{\nu_{ei}^2\rho_e m_e}\nabla^2 T_e. \tag{237}$$

Our multifluid model might also be useful for the modeling of the enrichment of minor ion abundances in stellar atmospheres, because of the very precise thermal force (thermal diffusion). Let us summarize the thermal force description in three major models: the model of Burgers (1969)–Schunk (1977), the model of Killie et al. (2004), and our model. Of course, all three models are formulated as general multifluid models, but for the simplicity of the discussion let us simplify and compare only the thermal forces given by

$$\text{Burgers–Schunk:} \qquad \boldsymbol{R}_e^T = +\,\frac{3}{5}\frac{\rho_e}{p_e}\nu_{ei}\boldsymbol{q}_e; \tag{238}$$

$$\text{Killie et al.:} \qquad \boldsymbol{R}_e^T = +\,\frac{6}{35}\frac{\rho_e}{p_e}\nu_{ei}\boldsymbol{q}_e; \tag{239}$$

$$\text{present paper:} \qquad \boldsymbol{R}_e^T = +\,\frac{21}{10}\frac{\rho_e}{p_e}\nu_{ei}\boldsymbol{q}_e - \frac{3}{56}\frac{\rho_e^2}{p_e^2}\nu_{ei}\boldsymbol{X}_e^{(5)}. \tag{240}$$

Note that the viscosity tensors are not required to describe the thermal force, and focusing only on the heat fluxes, instead of the 13-moment model of Burgers–Schunk, one can consider only the 8-moment model. Similarly, instead of our 21- and 22-moment models, one can consider only the 11-moment model. In general, the parallel thermal heat flux is given by $\boldsymbol{q}_e = -\,\gamma_0 p_e/(m_e\nu_{ei})\nabla T_e$ and the resulting parallel thermal force by $\boldsymbol{R}_e^T = -\,\beta_0 n_e \nabla T_e$, with coefficients γ_0 and β_0. From the work of Spitzer & Härm (1953), for $Z_i = 1$, the correct coefficient of thermal conductivity is $\gamma_0 = 3.203$ and the correct coefficient of thermal force is $\beta_0 = 0.703$. The model of Burgers–Schunk (238) has thermal conductivity $\gamma_0 = 1.34$, and with that value it describes the thermal force actually quite accurately, yielding $\beta_0 = 0.804$ (for other Z_i values, see the comparison in Table 9 in Appendix I). However, a problem arises if one

uses the correct value of thermal conductivity $\gamma_0 = 3.2$ in expression (238), which overestimates the thermal force. Killie et al. (2004) developed a different 8-moment model, where the expansion is done differently than in Equation (1), with the goal of improving the heat flux and the thermal force of Burgers–Schunk. The model is described in Appendix I.2. For $Z_i = 1$, its heat flux value is $\gamma_0 = 3.92$, which greatly improves the model of Burgers–Schunk, and for that value it also improves the thermal force, yielding $\beta_0 = 0.672$. Additionally, one can now use the correct $\gamma_0 = 3.2$ value in expression (239) and the thermal force will be roughly correct (and $7/2$ times smaller than Burgers–Schunk). However, as we point out in Appendix I (see Table 11), the model of Killie et al. (2004) breaks the Onsager symmetry between the frictional heat flux and the thermal force. The numerical model of Spitzer & Härm (1953) also does not satisfy the Onsager symmetry, and its frictional heat flux is technically incorrect, even though in this case the discrepancies are small. Our model satisfies the Onsager symmetry, and it has thermal conductivity $\gamma_0 = 3.1616$ and thermal force $\beta_0 = 0.711$ (the same as Braginskii). In summary, our multifluid model has a very precise thermal force (240), with a precision equal to Braginskii (1965), and we thus offer an improvement to the multifluid models of Burgers (1969)–Schunk (1977) and Killie et al. (2004).

This work was supported by the European Research Council in the frame of the Consolidating Grant ERC-2017-CoG771310-PI2FA, "Partial Ionisation: Two-Fluid Approach," led by Elena Khomenko. Anna Tenerani acknowledges the support of the NASA Heliophysics Supporting Research Grant #80NSSC18K1211. We acknowledge the support of the NSF EPSCoR RII-Track-1 Cooperative Agreement No. OIA-1655280, "Connecting the Plasma Universe to Plasma Technology in Alabama," led by Gary P. Zank. Gary M. Webb was funded in part by NASA grant 80NSSC19K0075. The manuscript can be also found at http://arxiv.org/abs/2201.11561.

Appendix A
General Evolution Equations

We consider the Boltzmann equation (in cgs units)

$$\frac{\partial f_a}{\partial t} + \boldsymbol{v} \cdot \nabla f_a + \frac{eZ_a}{m_a}\left(\boldsymbol{E} + \frac{1}{c}\boldsymbol{v} \times \boldsymbol{B}\right) \cdot \nabla_v f_a = C(f_a), \tag{A1}$$

where "a" is a species index and $C(f_a) = \sum_b C_{ab}(f_a, f_b)$ is the Landau collisional operator, so Equation (A1) is called the Landau equation. One defines the usual number density $n_a = \int f_a d^3v$, density $\rho_a = m_a n_a$, fluid velocity $\boldsymbol{u}_a = (1/n_a)\int \boldsymbol{v} f_a d^3v$, and fluctuating velocity $\boldsymbol{c}_a = \boldsymbol{v} - \boldsymbol{u}_a$, and further defines the pressure tensor $\bar{\bar{\boldsymbol{p}}}_a$, heat flux tensor $\bar{\bar{\boldsymbol{q}}}_a$, fourth-order moment $\bar{\bar{\boldsymbol{r}}}_a$, and fifth-order and sixth-order moments $\bar{\bar{\boldsymbol{X}}}_a^{(5)}$, $\bar{\bar{\boldsymbol{X}}}_a^{(6)}$, respectively, according to

$$\bar{\bar{\boldsymbol{p}}}_a = m_a \int \boldsymbol{c}_a \boldsymbol{c}_a f_a \, d^3v; \qquad \bar{\bar{\boldsymbol{q}}}_a = m_a \int \boldsymbol{c}_a \boldsymbol{c}_a \boldsymbol{c}_a f_a \, d^3v; \qquad \bar{\bar{\boldsymbol{r}}}_a = m_a \int \boldsymbol{c}_a \boldsymbol{c}_a \boldsymbol{c}_a \boldsymbol{c}_a f_a \, d^3v; \tag{A2}$$

$$\bar{\bar{\boldsymbol{X}}}_a^{(5)} = m_a \int \boldsymbol{c}_a \boldsymbol{c}_a \boldsymbol{c}_a \boldsymbol{c}_a \boldsymbol{c}_a f_a \, d^3v; \qquad \bar{\bar{\boldsymbol{X}}}_a^{(6)} = m_a \int \boldsymbol{c}_a \boldsymbol{c}_a \boldsymbol{c}_a \boldsymbol{c}_a \boldsymbol{c}_a \boldsymbol{c}_a f_a \, d^3v. \tag{A3}$$

The writing of the tensor product $\otimes$ is suppressed everywhere and $\boldsymbol{c}_a\boldsymbol{c}_a = \boldsymbol{c}_a \otimes \boldsymbol{c}_a$. For complicated fluid models, the species index "a" often blurs the clarity of the tensor algebra, and thus in the vector notation (A2) we emphasize tensors of second rank and above with the double overbar symbol. Sometimes we move the index "a" freely up and down (which here does not represent any mathematical operation), and in the index notation the index "a" is often dropped completely, so, for example, $p_{ij}^a = m_a \int c_i^a c_j^a f_a \, d^3v$ and $p_{ij} = m\int c_i c_j f d^3v$ are equivalent. The Einstein summation convention does not apply for the species index "a", and summations over other particle species are written down explicitly. The divergence is defined through the first index $(\nabla \cdot \bar{\bar{\boldsymbol{p}}}_a)_j = \partial_i p_{ij}^a$.

Here we do not consider ionization and recombination processes, and the Landau collisional operator conserves the number of particles $\int C(f_a) d^3v = 0$ for each species. One defines a unit vector in the direction of the magnetic field $\hat{\boldsymbol{b}} = \boldsymbol{B}/|\boldsymbol{B}|$, cyclotron frequency $\Omega_a = eZ_a|\boldsymbol{B}|/(m_a c)$, and convective derivative $d_a/dt = \partial/\partial t + \boldsymbol{u}_a \cdot \nabla$. It is also useful to define a symmetric operator $'S'$, which acts on a matrix as $A_{ij}^S = A_{ij} + A_{ji}$ and on a tensor of the third rank as $A_{ijk}^S = A_{ijk} + A_{jki} + A_{kij}$, i.e., it cycles around all indices. We often use operator trace Tr and unit matrix $\bar{\bar{\boldsymbol{I}}}$, where $\mathrm{Tr}\bar{\bar{\boldsymbol{A}}} = \bar{\bar{\boldsymbol{I}}} : \bar{\bar{\boldsymbol{A}}}$, and operator ":" represents double contraction. We also use $\bar{\bar{\boldsymbol{I}}}_\perp = \bar{\bar{\boldsymbol{I}}} - \hat{\boldsymbol{b}}\hat{\boldsymbol{b}}$.

To derive the model of Braginskii (1965) with the moment method of Grad, it is necessary to consider the evolution equation for the fifth-order moment $\bar{\bar{\boldsymbol{X}}}_a^{(5)}$ and perform a closure at $\bar{\bar{\boldsymbol{X}}}_a^{(6)}$. Integrating (A1) over velocity space yields the the following hierarchy of

evolution equations:

$$\frac{\partial n_a}{\partial t} + \nabla \cdot (n_a \boldsymbol{u}_a) = 0; \tag{A4}$$

$$\frac{\partial \boldsymbol{u}_a}{\partial t} + \boldsymbol{u}_a \cdot \nabla \boldsymbol{u}_a + \frac{1}{\rho_a} \nabla \cdot \bar{\bar{\boldsymbol{p}}}_a - \frac{eZ_a}{m_a}\left(\boldsymbol{E} + \frac{1}{c}\boldsymbol{u}_a \times \boldsymbol{B}\right) = \frac{\boldsymbol{R}_a}{\rho_a}; \tag{A5}$$

$$\frac{\partial \bar{\bar{\boldsymbol{p}}}_a}{\partial t} + \nabla \cdot (\bar{\bar{\boldsymbol{q}}}_a + \boldsymbol{u}_a \bar{\bar{\boldsymbol{p}}}_a) + [\bar{\bar{\boldsymbol{p}}}_a \cdot \nabla \boldsymbol{u}_a + \Omega_a \hat{\boldsymbol{b}} \times \bar{\bar{\boldsymbol{p}}}_a]^S = \bar{\bar{\boldsymbol{Q}}}_a^{(2)}; \tag{A6}$$

$$\frac{\partial \bar{\bar{\boldsymbol{q}}}_a}{\partial t} + \nabla \cdot (\bar{\bar{\boldsymbol{r}}}_a + \boldsymbol{u}_a \bar{\bar{\boldsymbol{q}}}_a) + \left[\bar{\bar{\boldsymbol{q}}}_a \cdot \nabla \boldsymbol{u}_a + \Omega_a \hat{\boldsymbol{b}} \times \bar{\bar{\boldsymbol{q}}}_a - \frac{1}{\rho_a}(\nabla \cdot \bar{\bar{\boldsymbol{p}}}_a)\bar{\bar{\boldsymbol{p}}}_a\right]^S = \bar{\bar{\boldsymbol{Q}}}_a^{(3)} - \frac{1}{\rho_a}[\boldsymbol{R}_a \bar{\bar{\boldsymbol{p}}}_a]^S; \tag{A7}$$

$$\frac{\partial}{\partial t}\bar{\bar{\boldsymbol{r}}}_a + \nabla \cdot (\bar{\bar{\boldsymbol{X}}}_a^{(5)} + \boldsymbol{u}_a \bar{\bar{\boldsymbol{r}}}_a) + \left[\bar{\bar{\boldsymbol{r}}}_a \cdot \nabla \boldsymbol{u}_a + \Omega_a \hat{\boldsymbol{b}} \times \bar{\bar{\boldsymbol{r}}}_a - \frac{1}{\rho_a}(\nabla \cdot \bar{\bar{\boldsymbol{p}}}_a)\bar{\bar{\boldsymbol{q}}}_a\right]^S = \bar{\bar{\boldsymbol{Q}}}_a^{(4)} - \frac{1}{\rho_a}[\boldsymbol{R}_a \bar{\bar{\boldsymbol{q}}}_a]^S; \tag{A8}$$

$$\frac{\partial}{\partial t}\bar{\bar{\boldsymbol{X}}}_a^{(5)} + \nabla \cdot (\bar{\bar{\boldsymbol{X}}}_a^{(6)} + \boldsymbol{u}_a \bar{\bar{\boldsymbol{X}}}_a^{(5)}) + \left[\bar{\bar{\boldsymbol{X}}}_a^{(5)} \cdot \nabla \boldsymbol{u}_a + \Omega_a \hat{\boldsymbol{b}} \times \bar{\bar{\boldsymbol{X}}}_a^{(5)} - \frac{1}{\rho_a}(\nabla \cdot \bar{\bar{\boldsymbol{p}}}_a)\bar{\bar{\boldsymbol{r}}}_a\right]^S = \bar{\bar{\boldsymbol{Q}}}_a^{(5)} - \frac{1}{\rho_a}[\boldsymbol{R}_a \bar{\bar{\boldsymbol{r}}}_a]^S, \tag{A9}$$

where the collisional contributions on the right-hand sides are given by (5). It is also possible to define a general nth-order moment $\bar{\bar{\boldsymbol{X}}}_a^{(n)}$ and collisional contributions $\bar{\bar{\boldsymbol{Q}}}_a^{(n)}$:

$$X^{(n)}_{r_1 r_2 \ldots r_n} = m \int c_{r_1} c_{r_2} \ldots c_{r_n} f d^3 v; \qquad Q^{(n)}_{r_1 r_2 \ldots r_n} = m \int c_{r_1} c_{r_2} \ldots c_{r_n} C(f) d^3 v, \tag{A10}$$

together with a symmetric operator "S" that cycles around all of its indices:

$$[X^{(n)}]^S_{r_1 r_2 r_3 \ldots r_n} = X^{(n)}_{r_1 r_2 r_3 \ldots r_n} + X^{(n)}_{r_2 r_3 \ldots r_n r_1} + X^{(n)}_{r_3 \ldots r_n r_1 r_2} + \cdots \cdots + X^{(n)}_{r_n r_1 r_2 r_3 \ldots r_{n-1}}, \tag{A11}$$

(so that it contains "n" terms) and derive the following evolution equation for $\bar{\bar{\boldsymbol{X}}}_a^{(n)}$:

$$\frac{\partial}{\partial t}\bar{\bar{\boldsymbol{X}}}_a^{(n)} + \nabla \cdot (\bar{\bar{\boldsymbol{X}}}_a^{(n+1)} + \boldsymbol{u}_a \bar{\bar{\boldsymbol{X}}}_a^{(n)}) + \left[\bar{\bar{\boldsymbol{X}}}_a^{(n)} \cdot \nabla \boldsymbol{u}_a + \Omega_a \hat{\boldsymbol{b}} \times \bar{\bar{\boldsymbol{X}}}_a^{(n)} - \frac{1}{\rho_a}(\nabla \cdot \bar{\bar{\boldsymbol{p}}}_a)\bar{\bar{\boldsymbol{X}}}_a^{(n-1)}\right]^S$$
$$= \bar{\bar{\boldsymbol{Q}}}_a^{(n)} - \frac{1}{\rho_a}[\boldsymbol{R}_a \bar{\bar{\boldsymbol{X}}}_a^{(n-1)}]^S, \tag{A12}$$

valid for $n \geqslant 2$. The left-hand side of (A12) is equal to the collisionless Equation (12.16) of Hunana et al. (2019b). Evolution Equations (A6)–(A9) can then easily be obtained by the evaluation of (A12). Note that definition (A10) yields $\bar{\bar{\boldsymbol{X}}}^{(2)} = \bar{\bar{\boldsymbol{p}}}$, $\bar{\bar{\boldsymbol{X}}}^{(3)} = \bar{\bar{\boldsymbol{q}}}$, and $\bar{\bar{\boldsymbol{X}}}^{(4)} = \bar{\bar{\boldsymbol{r}}}$, but $\bar{\bar{\boldsymbol{X}}}^{(1)} = 0$.

As has already been pointed out by Grad (1949a, 1949b), who developed the moment approach considering rarefied gases, because fluid moments are symmetric in all of their indices, a general nth-order moment $\bar{\bar{\boldsymbol{X}}}^{(n)}$ contains $\binom{n+2}{n} = (n+1)(n+2)/2$ distinct (scalar) components. So the density has 1, the velocity has 3, the pressure tensor has 6, the heat flux tensor has 10, $\bar{\bar{\boldsymbol{X}}}^{(4)}$ has 15, and $\bar{\bar{\boldsymbol{X}}}^{(5)}$ has 21 scalar components. The system (A4)–(A9) thus represents a 56-moment model.

Appendix B
Tensorial Hermite Decomposition

In the famous work of Grad (1949a, 1949b, 1958), the so-called *tensorial* Hermite decomposition is used, which is a generalization of the one-dimensional version. The one-dimensional Hermite polynomials of order "m" are defined as

$$H^{(m)}(x) = (-1)^m e^{\frac{x^2}{2}} \frac{d^m}{dx^m} e^{-\frac{x^2}{2}}, \tag{B1}$$

and evaluated step by step as $H^{(0)} = 1$, $H^{(1)} = x$, $H^{(2)} = x^2 - 1$, $H^{(3)} = x^3 - 3x$, $H^{(4)} = x^4 - 6x^2 + 3$, and $H^{(5)} = x^5 - 10x^3 + 15x$. So polynomials of even order contain only even powers of x and polynomials of odd order contain only odd powers of x. These polynomials are orthogonal to each other by

$$\frac{1}{\sqrt{2\pi}} \int_{-\infty}^{\infty} H^{(n)}(x) H^{(m)}(x) e^{-\frac{x^2}{2}} dx = n! \delta_{nm}. \tag{B2}$$

Note that the "weight" $\exp(-x^2/2)$ was used by Grad instead of the quantum-mechanical $\exp(-x^2)$. Of course, it is important to use the correct weights with both classes of Hermite polynomials. Curiously, if the weight is accidentally mismatched (i.e., by using $\exp(-x^2)$ in our (B2) or $\exp(-x^2/2)$ in the quantum version), in addition to naturally wrong numerical constants, the even–even and odd–odd couples of polynomials are not orthogonal any more! The generalization to tensors for the isotropic Maxwellian distribution

reads

$$\tilde{H}^{(m)}_{r_1,r_2\ldots r_m}(\tilde{\boldsymbol{c}}) = (-1)^m e^{\frac{\tilde{c}^2}{2}} \frac{\partial}{\partial \tilde{c}_{r_1}} \frac{\partial}{\partial \tilde{c}_{r_2}} \cdots \frac{\partial}{\partial \tilde{c}_{r_m}} e^{-\frac{\tilde{c}^2}{2}}. \tag{B3}$$

We use the same notation as Balescu (1988), where *reducible* Hermite polynomials are denoted with tilde, and *irreducible* polynomials have no tilde. We have added tilde on normalized $\tilde{\boldsymbol{c}}$ to make transitioning to usual fluid moments straightforward. Then explicit evaluation step by step gives

$$\begin{aligned}
&\tilde{H}^{(0)}(\tilde{\boldsymbol{c}}) = 1;\\
&\tilde{H}^{(1)}_i(\tilde{\boldsymbol{c}}) = \tilde{c}_i;\\
&\tilde{H}^{(2)}_{ij}(\tilde{\boldsymbol{c}}) = \tilde{c}_i\tilde{c}_j - \delta_{ij};\\
&\tilde{H}^{(3)}_{ijk}(\tilde{\boldsymbol{c}}) = \tilde{c}_i\tilde{c}_j\tilde{c}_k - (\delta_{ij}\tilde{c}_k + \delta_{jk}\tilde{c}_i + \delta_{ik}\tilde{c}_j);\\
&\tilde{H}^{(4)}_{ijkl}(\tilde{\boldsymbol{c}}) = \tilde{c}_i\tilde{c}_j\tilde{c}_k\tilde{c}_l - (\delta_{ij}\tilde{c}_k\tilde{c}_l + \delta_{jk}\tilde{c}_l\tilde{c}_i + \delta_{kl}\tilde{c}_i\tilde{c}_j + \delta_{li}\tilde{c}_j\tilde{c}_k + \delta_{ik}\tilde{c}_j\tilde{c}_l + \delta_{jl}\tilde{c}_i\tilde{c}_k)\\
&\qquad + \delta_{ij}\delta_{kl} + \delta_{ik}\delta_{jl} + \delta_{il}\delta_{jk},
\end{aligned} \tag{B4}$$

and quickly starts to grow:

$$\begin{aligned}
\tilde{H}^{(5)}_{ijklm}(\tilde{\boldsymbol{c}}) = {}& \tilde{c}_i\tilde{c}_j\tilde{c}_k\tilde{c}_l\tilde{c}_m - (\delta_{ij}\tilde{c}_k\tilde{c}_l\tilde{c}_m + \delta_{jk}\tilde{c}_l\tilde{c}_i\tilde{c}_m + \delta_{kl}\tilde{c}_i\tilde{c}_j\tilde{c}_m + \delta_{li}\tilde{c}_j\tilde{c}_k\tilde{c}_m + \delta_{ik}\tilde{c}_j\tilde{c}_l\tilde{c}_m\\
&+\delta_{jl}\tilde{c}_i\tilde{c}_k\tilde{c}_m + \delta_{im}\tilde{c}_j\tilde{c}_k\tilde{c}_l + \delta_{jm}\tilde{c}_i\tilde{c}_k\tilde{c}_l + \delta_{km}\tilde{c}_i\tilde{c}_j\tilde{c}_l + \delta_{lm}\tilde{c}_i\tilde{c}_j\tilde{c}_k)\\
&+\delta_{ij}\delta_{kl}\tilde{c}_m + \delta_{ik}\delta_{jl}\tilde{c}_m + \delta_{il}\delta_{jk}\tilde{c}_m + \delta_{ij}\delta_{km}\tilde{c}_l + \delta_{ij}\delta_{lm}\tilde{c}_k\\
&+\delta_{jk}\delta_{lm}\tilde{c}_i + \delta_{jk}\delta_{im}\tilde{c}_l + \delta_{kl}\delta_{im}\tilde{c}_j + \delta_{kl}\delta_{jm}\tilde{c}_i + \delta_{li}\delta_{jm}\tilde{c}_k\\
&+\delta_{li}\delta_{km}\tilde{c}_j + \delta_{ik}\delta_{jm}\tilde{c}_l + \delta_{ik}\delta_{lm}\tilde{c}_j + \delta_{jl}\delta_{im}\tilde{c}_k + \delta_{jl}\delta_{km}\tilde{c}_i.
\end{aligned} \tag{B5}$$

The choice of Grad with $\exp(-x^2/2)$ has a great benefit, because no numerical constants are present in the entire hierarchy of Hermite polynomials, which is not the case for the weight $\exp(-x^2)$. Here, numerical factors appear only after one applies contractions (traces) at the above expressions. Similar to the one-dimensional case, polynomials of even order contain only terms with even numbers of velocities $\tilde{c}$, and polynomials of odd order contain only terms with odd numbers of $\tilde{c}$.

For a Maxwellian distribution, the normalized velocity is

$$\tilde{\boldsymbol{c}} = \sqrt{\frac{m_a}{T_a}}(\boldsymbol{v} - \boldsymbol{u}_a) = \sqrt{\frac{m_a}{T_a}}\boldsymbol{c}, \tag{B6}$$

where, for simplicity, we suppress the writing of species index "a" for velocity $\boldsymbol{c}$ in the expressions that follow, and for many other variables as well (the Hermite decomposition is done independently for each species, and the species variable "a" just makes the expressions more blurry). It is possible to work in both normalized and physical units. The entire distribution function can be written as

$$f_a = f_a^{(0)}(1 + \chi_a) = n_a\left(\frac{m_a}{T_a}\right)^{3/2}\phi^{(0)}(1 + \chi_a); \qquad \phi^{(0)} = \frac{e^{-\frac{\tilde{c}^2}{2}}}{(2\pi)^{3/2}}, \tag{B7}$$

where χ_a represents the wanted perturbation. One can go quickly between the physical and normalized units by

$$\int f_a(\boldsymbol{c})d^3c = n_a\int\phi^{(0)}(1 + \chi_a(\tilde{\boldsymbol{c}}))d^3\tilde{c}. \tag{B8}$$

The tensorial polynomials are again orthogonal to each other, where, by using "weight" $\phi^{(0)}$:

$$\begin{aligned}
&\int \phi^{(0)}\tilde{H}^{(0)}\tilde{H}^{(0)}d^3\tilde{c} = 1;\\
&\int \phi^{(0)}\tilde{H}^{(1)}_i\tilde{H}^{(1)}_j d^3\tilde{c} = \delta_{ij};\\
&\int \phi^{(0)}\tilde{H}^{(2)}_{ij}\tilde{H}^{(2)}_{kl} d^3\tilde{c} = \delta_{ik}\delta_{jl} + \delta_{il}\delta_{jk};\\
&\int \phi^{(0)}\tilde{H}^{(3)}_{r_1r_2r_3}\tilde{H}^{(3)}_{s_1s_2s_3}d^3\tilde{c} = \delta_{r_1s_1}\delta_{r_2s_2}\delta_{r_3s_3} + \delta_{r_1s_1}\delta_{r_2s_3}\delta_{r_3s_2} + \delta_{r_1s_2}\delta_{r_2s_1}\delta_{r_3s_3}\\
&\qquad +\delta_{r_1s_2}\delta_{r_2s_3}\delta_{r_3s_1} + \delta_{r_1s_3}\delta_{r_2s_1}\delta_{r_3s_2} + \delta_{r_1s_3}\delta_{r_2s_2}\delta_{r_3s_1},
\end{aligned} \tag{B9}$$

and the expressions quickly become long:

$$\begin{aligned}\int \phi^{(0)}\tilde{H}^{(4)}_{r_1r_2r_3r_4}\tilde{H}^{(4)}_{s_1s_2s_3s_4}d^3\tilde{c} = &+\delta_{r_1s_1}\delta_{r_2s_2}\delta_{r_3s_3}\delta_{r_4s_4} + \delta_{r_1s_1}\delta_{r_2s_2}\delta_{r_3s_4}\delta_{r_4s_3} + \delta_{r_1s_1}\delta_{r_2s_3}\delta_{r_3s_2}\delta_{r_4s_4}\\ &+\delta_{r_1s_1}\delta_{r_2s_3}\delta_{r_3s_4}\delta_{r_4s_2} + \delta_{r_1s_1}\delta_{r_2s_4}\delta_{r_3s_2}\delta_{r_4s_3} + \delta_{r_1s_1}\delta_{r_2s_4}\delta_{r_3s_3}\delta_{r_4s_2}\\ &+\delta_{r_1s_2}\delta_{r_2s_1}\delta_{r_3s_3}\delta_{r_4s_4} + \delta_{r_1s_2}\delta_{r_2s_1}\delta_{r_3s_4}\delta_{r_4s_3} + \delta_{r_1s_2}\delta_{r_2s_3}\delta_{r_3s_1}\delta_{r_4s_4}\\ &+\delta_{r_1s_2}\delta_{r_2s_3}\delta_{r_3s_4}\delta_{r_4s_1} + \delta_{r_1s_2}\delta_{r_2s_4}\delta_{r_3s_1}\delta_{r_4s_3} + \delta_{r_1s_2}\delta_{r_2s_4}\delta_{r_3s_3}\delta_{r_4s_1}\\ &+\delta_{r_1s_3}\delta_{r_2s_1}\delta_{r_3s_2}\delta_{r_4s_4} + \delta_{r_1s_3}\delta_{r_2s_1}\delta_{r_3s_4}\delta_{r_4s_2} + \delta_{r_1s_3}\delta_{r_2s_2}\delta_{r_3s_1}\delta_{r_4s_4}\\ &+\delta_{r_1s_3}\delta_{r_2s_2}\delta_{r_3s_4}\delta_{r_4s_1} + \delta_{r_1s_3}\delta_{r_2s_4}\delta_{r_3s_1}\delta_{r_4s_2} + \delta_{r_1s_3}\delta_{r_2s_4}\delta_{r_3s_2}\delta_{r_4s_1}\\ &+\delta_{r_1s_4}\delta_{r_2s_1}\delta_{r_3s_2}\delta_{r_4s_3} + \delta_{r_1s_4}\delta_{r_2s_1}\delta_{r_3s_3}\delta_{r_4s_2} + \delta_{r_1s_4}\delta_{r_2s_2}\delta_{r_3s_1}\delta_{r_4s_3}\\ &+\delta_{r_1s_4}\delta_{r_2s_2}\delta_{r_3s_3}\delta_{r_4s_1} + \delta_{r_1s_4}\delta_{r_2s_3}\delta_{r_3s_1}\delta_{r_4s_2} + \delta_{r_1s_4}\delta_{r_2s_3}\delta_{r_3s_2}\delta_{r_4s_1}.\end{aligned} \tag{B10}$$

The general orthogonality can be written by introducing the multi-indices $\boldsymbol{r} = r_1 \ldots r_n$ and $\boldsymbol{s} = s_1 \ldots s_m$:

$$\int \phi^{(0)}\tilde{H}^{(n)}_{\boldsymbol{r}}\tilde{H}^{(m)}_{\boldsymbol{s}}d^3\tilde{c} = \delta_{mn}\boldsymbol{\delta}^{(n)}_{\boldsymbol{rs}}, \tag{B11}$$

where the new symbol $\boldsymbol{\delta}^{(n)}_{\boldsymbol{rs}}$ is equal to one, if the indices $r_1 \ldots r_n$ are a permutation of $s_1 \ldots s_n$, but otherwise is zero. In other words, for $n = m$, the right-hand side contains $n!$ terms, where each of these terms has the form $\delta_{r_1s_1}\delta_{r_2s_2} \ldots \delta_{r_ns_n}$, and to calculate the other terms it is necessary to keep the r-indices fixed, and do all the possible permutations with s-indices (or vice versa). A particular case of (B11) reads

$$m \neq 0: \qquad \int \phi^{(0)}\tilde{H}^{(m)}_{\boldsymbol{s}}d^3\tilde{c} = 0, \tag{B12}$$

i.e., the integral over a single Hermite polynomial with weight $\phi^{(0)}$ is zero.

The goal of the Hermite expansion is to find the perturbation of the distribution function χ_a in (B7). For the most general decomposition, one can chose to express the perturbation χ_a as a sum of Hermite polynomials:

$$\begin{aligned}\chi_a &= \sum_{m=1}^{\infty} A^{(m)}_{r_1r_2\ldots r_m}\tilde{H}^{(m)}_{r_1r_2\ldots r_m}\\ &= A^{(1)}_{r_1}\tilde{H}^{(1)}_{r_1} + A^{(2)}_{r_1r_2}\tilde{H}^{(2)}_{r_1r_2} + A^{(3)}_{r_1r_2r_3}\tilde{H}^{(3)}_{r_1r_2r_3} + A^{(4)}_{r_1r_2r_3r_4}\tilde{H}^{(4)}_{r_1r_2r_3r_4} + \cdots,\end{aligned} \tag{B13}$$

where the coefficients $A^{(m)}_{r_1r_2\ldots r_m}$ need to be found. Note that full contractions over all indices are present and the result is a scalar. Multiplying (B13) by weight $\phi^{(0)}$ and polynomial $\tilde{H}^{(n)}_{s_1s_2\ldots s_n}$, and integrating over $d^3\tilde{c}$ by using orthogonality (B11), then yields

$$\int \chi_a\phi^{(0)}\tilde{H}^{(n)}_{\boldsymbol{s}}d^3\tilde{c} = A^{(n)}_{\boldsymbol{r}}\delta^{(n)}_{\boldsymbol{rs}} = n!A^{(n)}_{\boldsymbol{s}}, \tag{B14}$$

where the last equality holds because coefficient $A^{(n)}_{\boldsymbol{s}}$ is a fluid variable and symmetric in all of its indices. The coefficients $A^{(n)}_{\boldsymbol{s}}$ are thus found according to

$$A^{(n)}_{\boldsymbol{s}} = \frac{1}{n!}\int \chi_a\phi^{(0)}\tilde{H}^{(n)}_{\boldsymbol{s}}(\tilde{\boldsymbol{c}})d^3\tilde{c} = \frac{1}{n!}\int (1+\chi_a)\phi^{(0)}\tilde{H}^{(n)}_{\boldsymbol{s}}(\tilde{\boldsymbol{c}})d^3\tilde{c} = \frac{1}{n!}\underbrace{[\tfrac{1}{n_a}\int f_a\tilde{H}^{(n)}_{\boldsymbol{s}}(\tilde{\boldsymbol{c}})d^3c]}_{\tilde{h}^{(n)}_{\boldsymbol{s}}}, \tag{B15}$$

where we have used the orthogonality relation (B12) and changed the integration variable to d^3c with (B8). The quantities in the brackets of (B15) are called *Hermite moments* $\tilde{h}^{(n)}_{\boldsymbol{s}}$. The entire Hermite expansion then can be summarized into two easy steps.

(1) Calculate the Hermite moments:

$$\tilde{h}^{a(m)}_{r_1r_2\ldots r_m} = \frac{1}{n_a}\int f_a\tilde{H}^{a(m)}_{r_1r_2\ldots r_m}(\tilde{\boldsymbol{c}})d^3c, \tag{B16}$$

(2) the final perturbation is:

$$\chi_a = \sum_{m=1}^{\infty}\frac{1}{m!}\tilde{h}^{a(m)}_{r_1r_2\ldots r_m}\tilde{H}^{a(m)}_{r_1r_2\ldots r_m}(\tilde{\boldsymbol{c}}). \tag{B17}$$

It is useful to omit writing the species indices "a" on both $\tilde{h}$ and $\tilde{H}$, as well as on the fluid moments, so we will keep the species index only for n_a, m_a, T_a, and p_a. The final perturbations will be written in a full form.

By using definitions of general fluid moments, one straightforwardly calculates the Hermite moments:

$$\tilde{h}_i^{(1)} = \frac{1}{n_a}\int f_a \tilde{H}_i^{(1)} d^3c = 0;$$
$$\tilde{h}_{ij}^{(2)} = \frac{1}{n_a}\int f_a \tilde{H}_{ij}^{(2)} d^3c = \frac{1}{p_a}\Pi_{ij}^{(2)};$$
$$\tilde{h}_{ijk}^{(3)} = \frac{1}{n_a}\int f_a \tilde{H}_{ijk}^{(3)} d^3c = \frac{1}{p_a}\sqrt{\frac{m_a}{T_a}}\, q_{ijk}, \tag{B18}$$

together with

$$\begin{aligned}\tilde{h}_{ijkl}^{(4)} &= \frac{1}{n_a}\int f_a \tilde{H}_{ijkl}^{(4)}(\boldsymbol{c}) d^3c = \frac{\rho_a}{p_a^2} r_{ijkl} + \delta_{ij}\delta_{kl} + \delta_{ik}\delta_{jl} + \delta_{il}\delta_{jk} \\ &\quad -\frac{1}{p_a}(\delta_{ij}p_{kl} + \delta_{jk}p_{li} + \delta_{kl}p_{ij} + \delta_{li}p_{jk} + \delta_{ik}p_{jl} + \delta_{jl}p_{ik}) \\ &= \frac{\rho_a}{p_a^2} r_{ijkl} - (\delta_{ij}\delta_{kl} + \delta_{ik}\delta_{jl} + \delta_{il}\delta_{jk}) \\ &\quad -\frac{1}{p_a}(\delta_{ij}\Pi_{kl}^{(2)} + \delta_{jk}\Pi_{li}^{(2)} + \delta_{kl}\Pi_{ij}^{(2)} + \delta_{li}\Pi_{jk}^{(2)} + \delta_{ik}\Pi_{jl}^{(2)} + \delta_{jl}\Pi_{ik}^{(2)}),\end{aligned} \tag{B19}$$

and

$$\begin{aligned}\tilde{h}_{ijklm}^{(5)} &= \frac{1}{n_a}\int f_a \tilde{H}_{ijklm}^{(5)}(\boldsymbol{c}) d^3c = \frac{\rho_a^{3/2}}{p_a^{5/2}} X_{ijklm}^{(5)} - \frac{\rho_a^{1/2}}{p_a^{3/2}}(\delta_{ij}q_{klm} + \delta_{jk}q_{lim} + \delta_{kl}q_{ijm} + \delta_{li}q_{jkm} \\ &\quad +\delta_{ik}q_{jlm} + \delta_{jl}q_{ikm} + \delta_{im}q_{jkl} + \delta_{jm}q_{ikl} + \delta_{km}q_{ijl} + \delta_{lm}q_{ijk}).\end{aligned} \tag{B20}$$

B.1. Usual Perturbations of Grad

B.1.1. 20-moment Model

Using the definition of the perturbation (B17) and cutting the hierarchy at

$$\chi_a = \tilde{h}_i^{(1)}\tilde{H}_i^{(1)} + \frac{1}{2}\tilde{h}_{ij}^{(2)}\tilde{H}_{ij}^{(2)} + \frac{1}{6}\tilde{h}_{ijk}^{(3)}\tilde{H}_{ijk}^{(3)}, \tag{B21}$$

yields the 20-moment perturbation of Grad:

$$\text{20-moment:} \qquad \chi_a = \frac{m_a}{2p_aT_a}(\bar{\bar{\boldsymbol{\Pi}}}_a^{(2)}\colon \boldsymbol{c}_a\boldsymbol{c}_a) + \frac{m_a^2}{6p_aT_a^2}(\boldsymbol{c}_a\cdot\bar{\bar{\boldsymbol{q}}}_a\colon \boldsymbol{c}_a\boldsymbol{c}_a) - \frac{m_a}{p_aT_a}(\boldsymbol{q}_a\cdot\boldsymbol{c}_a), \tag{B22}$$

where one defines vector $\boldsymbol{q}_a = (1/2)\mathrm{Tr}\,\bar{\bar{\boldsymbol{q}}}_a$.

B.1.2. 13-moment Model

To quickly obtain the simplified 13-moment model of Grad, one can use $\bar{\bar{\boldsymbol{q}}} = (2/5)(\boldsymbol{q}\bar{\bar{\boldsymbol{I}}})^S + \boldsymbol{\sigma}'$ with $\boldsymbol{\sigma}'$ neglected (the validity of this equation is shown below), and calculating $\boldsymbol{c}\cdot\bar{\bar{\boldsymbol{q}}}\colon \boldsymbol{c}\boldsymbol{c} = (6/5)(\boldsymbol{q}\cdot\boldsymbol{c})c^2$ yields the 13-moment model:

$$\text{13-moment:} \qquad \chi_a = \frac{m_a}{2p_aT_a}(\bar{\bar{\boldsymbol{\Pi}}}_a^{(2)}\colon \boldsymbol{c}_a\boldsymbol{c}_a) - \frac{m_a}{p_aT_a}(\boldsymbol{q}_a\cdot\boldsymbol{c}_a)\left(1 - \frac{m_a}{5T_a}c_a^2\right). \tag{B23}$$

Rederiving the heat flux contribution of the 13-moment model from scratch can be done by using a contracted Hermite polynomial:

$$\tilde{H}_i^{(3)} \equiv \delta_{jk}\tilde{H}_{ijk}^{(3)} = \tilde{c}_i(\tilde{c}^2 - 5). \tag{B24}$$

However, one needs to be careful about the normalization constant, because applying the contractions $\delta_{r_1r_2}$ and $\delta_{s_1s_2}$ on (B9) yields

$$\int \phi^{(0)}\tilde{H}_i^{(3)}\tilde{H}_j^{(3)} d^3\tilde{c} = 10\delta_{ij}, \tag{B25}$$

which can be also verified by direct calculation. (Note that it is important to apply the contractions on (B9) as stated above, and not accidentally as $\delta_{r_1s_1}\delta_{r_2s_2}$, which would yield an erroneous coefficient 20, as the contraction must satisfy definition (B24)). Then, one

calculates the Hermite moment:

$$\tilde{h}_i^{(3)} = \frac{1}{n_a}\int f_a \tilde{H}_i^{(3)} d^3c = \frac{2}{p_a}\sqrt{\frac{m_a}{T_a}}\,\vec{q}_i, \tag{B26}$$

(which is equal to $\tilde{h}_{ikk}^{(3)}$) and the heat flux perturbation becomes

$$\text{8-moment:} \qquad \chi_a = \frac{1}{10}\tilde{h}_i^{(3)}\tilde{H}_i^{(3)} = -\frac{m_a}{p_a T_a}(\boldsymbol{q}_a\cdot\boldsymbol{c}_a)\left(1-\frac{m_a}{5T_a}c_a^2\right), \tag{B27}$$

recovering (B23).

B.1.3. Double-checking the Fluid Moments

Using the 8-moment perturbation (B27) (or the perturbation of the 13-moment model (B23)), it is possible to calculate the heat flux moment, for example, by switching to normalized units and using the integral (B89), which is valid for any vector $\boldsymbol{q}$, yielding

$$\begin{aligned}\text{13-moment:} \qquad q_{ijk} &= m_a\int c_i c_j c_k f_a^{(0)}(1+\chi_a)d^3c = -\int \tilde{c}_i\tilde{c}_j\tilde{c}_k(\boldsymbol{q}\cdot\tilde{\boldsymbol{c}})\left(1-\frac{\tilde{c}^2}{5}\right)\phi^{(0)}d^3\tilde{c}\\ &= \frac{2}{5}[\bar{\bar{\boldsymbol{I}}}\boldsymbol{q}]^S_{ijk}.\end{aligned} \tag{B28}$$

In contrast, using the 20-moment perturbation (B22) and integral (B91) yields the identity $\bar{\bar{\boldsymbol{q}}} = \bar{\bar{\boldsymbol{q}}}$, as it should. Thus, the full heat flux tensor can be decomposed as

$$\bar{\bar{\boldsymbol{q}}} = \frac{2}{5}[\bar{\bar{\boldsymbol{I}}}\boldsymbol{q}]^S + \boldsymbol{\sigma}', \tag{B29}$$

where $\boldsymbol{\sigma}'$ represents the highest-order irreducible part of the heat flux tensor, and by applying a trace at (B29) it can be verified that $\boldsymbol{\sigma}'$ is traceless. The calculation of the fourth-order moment $\bar{\bar{\boldsymbol{r}}}$ yields (with either the 10-, 13-, or 20-moment model)

$$\begin{aligned} r_{ijkl} &= m_a\int c_i c_j c_k c_l f_a^{(0)}(1+\chi_a)d^3c\\ &= \frac{p_a^2}{\rho_a}\int \tilde{c}_i\tilde{c}_j\tilde{c}_k\tilde{c}_l\phi^{(0)}d^3\tilde{c} + \frac{p_a}{2\rho_a}\int \tilde{c}_i\tilde{c}_j\tilde{c}_k\tilde{c}_l\tilde{\boldsymbol{c}}\tilde{\boldsymbol{c}}:\bar{\bar{\boldsymbol{\Pi}}}^{(2)}\phi^{(0)}d^3\tilde{c}\\ &= \frac{p_a^2}{\rho_a}[\delta_{ij}\delta_{kl}+\delta_{ik}\delta_{jl}+\delta_{jk}\delta_{il}] + \frac{p_a}{\rho_a}[\delta_{ij}\Pi_{kl}^{(2)}+\delta_{ik}\Pi_{jl}^{(2)}+\delta_{il}\Pi_{jk}^{(2)}+\delta_{jk}\Pi_{il}^{(2)}+\delta_{jl}\Pi_{ik}^{(2)}+\delta_{kl}\Pi_{ij}^{(2)}],\end{aligned} \tag{B30}$$

where one can use the integrals (B84), (B100). Applying a trace at (B30) yields

$$\mathrm{Tr}\bar{\bar{\boldsymbol{r}}} = 5\frac{p_a^2}{\rho_a}\bar{\bar{\boldsymbol{I}}} + 7\frac{p_a}{\rho_a}\bar{\bar{\boldsymbol{\Pi}}}^{(2)}; \qquad \mathrm{TrTr}\bar{\bar{\boldsymbol{r}}} = 15\frac{p_a^2}{\rho_a}. \tag{B31}$$

If one does not want to use our provided integrals from Appendix B.6 (or wants to verify them), all of the needed integrals can be calculated by using the powerful orthogonality theorem. As an example,

$$\int \tilde{c}_i\tilde{c}_j\tilde{c}_k\tilde{H}_{lmn}^{(3)}\phi^{(0)}d^3\tilde{c} = \int \tilde{H}_{ijk}^{(3)}\tilde{H}_{lmn}^{(3)}\phi^{(0)}d^3\tilde{c} + \int(\delta_{ij}\tilde{c}_k+\delta_{jk}\tilde{c}_i+\delta_{ik}\tilde{c}_j)\tilde{H}_{lmn}^{(3)}\phi^{(0)}d^3\tilde{c}, \tag{B32}$$

where the first term is calculated with the orthogonality (B9), and the second term is zero (because all of the resulting terms can be rewritten as $\tilde{H}_i^{(1)}\tilde{H}_{lmn}^{(3)}$, which yields zero after integration; see also integral (B83)).

In some calculations, one actually does not need to work with the complicated right-hand side of (B9), because once the integral is calculated, the result is going to be applied on $\tilde{h}_{s_1s_2s_3}^{(3)}$, which is a fluid variable and symmetric in all of its indices. Let us demonstrate it by using the 20-moment heat flux perturbation

$$\chi_a = \frac{1}{6}\tilde{h}_{s_1s_2s_3}^{(3)}\tilde{H}_{s_1s_2s_3}^{(3)}(\tilde{\boldsymbol{c}}), \tag{B33}$$

and calculating the heat flux moment again, this time with the Hermite variables:

$$\begin{aligned} q_{r_1r_2r_3} &= m_a \int c_{r_1}c_{r_2}c_{r_3}f_a^{(0)}(1+\chi_a)d^3c \\ &= \frac{p_a}{6}\sqrt{\frac{T_a}{m_a}}\,\tilde{h}^{(3)}_{s_1s_2s_3}\int \tilde{c}_{r_1}\tilde{c}_{r_2}\tilde{c}_{r_3}\tilde{H}^{(3)}_{s_1s_2s_3}\phi^{(0)}d^3\tilde{c} \\ &= \frac{p_a}{6}\sqrt{\frac{T_a}{m_a}}\,\tilde{h}^{(3)}_{s_1s_2s_3}\int \tilde{H}^{(3)}_{r_1r_2r_3}\tilde{H}^{(3)}_{s_1s_2s_3}\phi^{(0)}d^3\tilde{c} \\ &= \frac{p_a}{6}\sqrt{\frac{T_a}{m_a}}\,\tilde{h}^{(3)}_{s_1s_2s_3}\boldsymbol{\delta}^{(3)}_{(r_1r_2r_3)(s_1s_2s_3)} \\ &= p_a\sqrt{\frac{T_a}{m_a}}\,\tilde{h}^{(3)}_{r_1r_2r_3}. \end{aligned} \tag{B34}$$

In the derivation, we did not use the complicated right-hand side of (B9), we only used $\tilde{h}^{(n)}_{\boldsymbol{r}}\boldsymbol{\delta}^{(n)}_{\boldsymbol{rs}} = n!\tilde{h}^{(n)}_{\boldsymbol{s}}$, and the factor of 3! canceled out as well.

Similarly, using the same perturbation (B33), one can derive the fifth-order fluid moment $\bar{\bar{\boldsymbol{X}}}^{(5)}$, by using the Hermite polynomial $\tilde{H}^{(5)}_{ijklm}$, Equation (B5), according to

$$\begin{aligned} X^{(5)}_{r_1r_2r_3r_4r_5} &= m_a \int c_{r_1}c_{r_2}c_{r_3}c_{r_4}c_{r_5}f_a^{(0)}(1+\chi_a)d^3c \\ &= \frac{p_a}{6}\left(\frac{T_a}{m_a}\right)^{3/2}\tilde{h}^{(3)}_{s_1s_2s_3}\int \tilde{c}_{r_1}\tilde{c}_{r_2}\tilde{c}_{r_3}\tilde{c}_{r_4}\tilde{c}_{r_5}\tilde{H}^{(3)}_{s_1s_2s_3}\phi^{(0)}d^3\tilde{c} \\ &= \frac{p_a}{6}\left(\frac{T_a}{m_a}\right)^{3/2}\tilde{h}^{(3)}_{s_1s_2s_3}\int [\delta_{r_1r_2}\tilde{c}_{r_3}\tilde{c}_{r_4}\tilde{c}_{r_5} + \delta_{r_2r_3}\tilde{c}_{r_4}\tilde{c}_{r_1}\tilde{c}_{r_5} + \delta_{r_3r_4}\tilde{c}_{r_1}\tilde{c}_{r_2}\tilde{c}_{r_5} \\ &\quad +\delta_{r_4r_1}\tilde{c}_{r_2}\tilde{c}_{r_3}\tilde{c}_{r_5} + \delta_{r_1r_3}\tilde{c}_{r_2}\tilde{c}_{r_4}\tilde{c}_{r_5} + \delta_{r_2r_4}\tilde{c}_{r_1}\tilde{c}_{r_3}\tilde{c}_{r_5} + \delta_{r_1r_5}\tilde{c}_{r_2}\tilde{c}_{r_3}\tilde{c}_{r_4} \\ &\quad +\delta_{r_2r_5}\tilde{c}_{r_1}\tilde{c}_{r_3}\tilde{c}_{r_4} + \delta_{r_3r_5}\tilde{c}_{r_1}\tilde{c}_{r_2}\tilde{c}_{r_4} + \delta_{r_4r_5}\tilde{c}_{r_1}\tilde{c}_{r_2}\tilde{c}_{r_3}]\tilde{H}^{(3)}_{s_1s_2s_3}\phi^{(0)}d^3\tilde{c} \\ &= p_a\left(\frac{T_a}{m_a}\right)^{3/2}[\delta_{r_1r_2}\tilde{h}^{(3)}_{r_3r_4r_5} + \delta_{r_2r_3}\tilde{h}^{(3)}_{r_4r_1r_5} + \delta_{r_3r_4}\tilde{h}^{(3)}_{r_1r_2r_5} \\ &\quad +\delta_{r_4r_1}\tilde{h}^{(3)}_{r_2r_3r_5} + \delta_{r_1r_3}\tilde{h}^{(3)}_{r_2r_4r_5} + \delta_{r_2r_4}\tilde{h}^{(3)}_{r_1r_3r_5} + \delta_{r_1r_5}\tilde{h}^{(3)}_{r_2r_3r_4} \\ &\quad +\delta_{r_2r_5}\tilde{h}^{(3)}_{r_1r_3r_4} + \delta_{r_3r_5}\tilde{h}^{(3)}_{r_1r_2r_4} + \delta_{r_4r_5}\tilde{h}^{(3)}_{r_1r_2r_3}]. \end{aligned} \tag{B35}$$

Or this can be rewritten with the heat fluxes according to (B18) and using the usual indices:

$$\begin{aligned} X^{(5)}_{ijklm} &= \frac{p_a}{\rho_a}[\delta_{ij}q_{klm} + \delta_{jk}q_{lim} + \delta_{kl}q_{ijm} + \delta_{li}q_{jkm} + \delta_{ik}q_{jlm} \\ &\quad +\delta_{jl}q_{ikm} + \delta_{im}q_{jkl} + \delta_{jm}q_{ikl} + \delta_{km}q_{ijl} + \delta_{lm}q_{ijk}], \end{aligned} \tag{B36}$$

and by using the heat flux decomposition (B29) with $\boldsymbol{\sigma}'$ neglected:

$$\begin{aligned} X^{(5)}_{ijklm} &= \frac{4}{5}\frac{p_a}{\rho_a}[q_i(\delta_{jk}\delta_{lm} + \delta_{kl}\delta_{jm} + \delta_{jl}\delta_{km}) + q_j(\delta_{kl}\delta_{im} + \delta_{il}\delta_{km} + \delta_{ik}\delta_{lm}) \\ &\quad +q_k(\delta_{ij}\delta_{lm} + \delta_{il}\delta_{jm} + \delta_{jl}\delta_{im}) + q_l(\delta_{ij}\delta_{km} + \delta_{jk}\delta_{im} + \delta_{ik}\delta_{jm}) \\ &\quad +q_m(\delta_{ij}\delta_{kl} + \delta_{jk}\delta_{il} + \delta_{ik}\delta_{jl})]. \end{aligned} \tag{B37}$$

Applying the contractions at (B36) yields

$$\begin{aligned} [\mathrm{Tr}\,\bar{\bar{\boldsymbol{X}}}^{(5)}]_{ijk} &= \frac{p_a}{\rho_a}[2(\bar{\bar{\boldsymbol{I}}}\boldsymbol{q})^S + 9\bar{\bar{\boldsymbol{q}}}]_{ijk} = \frac{28}{5}\frac{p_a}{\rho_a}(\bar{\bar{\boldsymbol{I}}}\boldsymbol{q})^S_{ijk} + 9\frac{p_a}{\rho_a}\sigma_{ijk}{}'; \\ \boldsymbol{X}^{(5)} &= \mathrm{Tr}\mathrm{Tr}\bar{\bar{\boldsymbol{X}}}^{(5)} = 28\frac{p_a}{\rho_a}\boldsymbol{q}. \end{aligned} \tag{B38}$$

B.2. Higher-order Perturbations (Full $\bar{\bar{\boldsymbol{X}}}^{(4)}$ and $\bar{\bar{\boldsymbol{X}}}^{(5)}$ Moments)

By using the technique described above, it is possible to use the following higher-order perturbation:

$$\chi_a = \frac{1}{2!}\tilde{h}^{(2)}_{s_1s_2}\tilde{H}^{(2)}_{s_1s_2} + \frac{1}{3!}\tilde{h}^{(3)}_{s_1s_2s_3}\tilde{H}^{(3)}_{s_1s_2s_3} + \frac{1}{4!}\tilde{h}^{(4)}_{s_1s_2s_3s_4}\tilde{H}^{(4)}_{s_1s_2s_3s_4} + \frac{1}{5!}\tilde{h}^{(5)}_{s_1s_2s_3s_4s_5}\tilde{H}^{(5)}_{s_1s_2s_3s_4s_5}, \tag{B39}$$

and directly calculate the fluid moments (we use $\bar{\bar{\boldsymbol{X}}}^{(4)}$ instead of $\bar{\bar{\boldsymbol{r}}}$ from now on):

$$\begin{aligned}[\bar{\bar{\boldsymbol{X}}}^{(4)}]_{r_1r_2r_3r_4} = \frac{p_a^2}{\rho_a}[&\tilde{h}^{(4)}_{r_1r_2r_3r_4} + \delta_{r_1r_2}\tilde{h}^{(2)}_{r_3r_4} + \delta_{r_2r_3}\tilde{h}^{(2)}_{r_1r_4} + \delta_{r_3r_4}\tilde{h}^{(2)}_{r_1r_2}\\ &+\delta_{r_1r_4}\tilde{h}^{(2)}_{r_2r_3} + \delta_{r_1r_3}\tilde{h}^{(2)}_{r_2r_4} + \delta_{r_2r_4}\tilde{h}^{(2)}_{r_1r_3}\\ &+\delta_{r_1r_2}\delta_{r_3r_4} + \delta_{r_1r_3}\delta_{r_2r_4} + \delta_{r_2r_3}\delta_{r_1r_4}],\end{aligned} \tag{B40}$$

and

$$\begin{aligned}[\bar{\bar{\boldsymbol{X}}}^{(5)}]_{r_1r_2r_3r_4r_5} = p_a\left(\frac{T_a}{m_a}\right)^{3/2}[&\tilde{h}^{(5)}_{r_1r_2r_3r_4r_5} + \delta_{r_1r_2}\tilde{h}^{(3)}_{r_3r_4r_5} + \delta_{r_2r_3}\tilde{h}^{(3)}_{r_4r_1r_5} + \delta_{r_3r_4}\tilde{h}^{(3)}_{r_1r_2r_5}\\ &+\delta_{r_4r_1}\tilde{h}^{(3)}_{r_2r_3r_5} + \delta_{r_1r_3}\tilde{h}^{(3)}_{r_2r_4r_5} + \delta_{r_2r_4}\tilde{h}^{(3)}_{r_1r_3r_5} + \delta_{r_1r_5}\tilde{h}^{(3)}_{r_2r_3r_4}\\ &+\delta_{r_2r_5}\tilde{h}^{(3)}_{r_1r_3r_4} + \delta_{r_3r_5}\tilde{h}^{(3)}_{r_1r_2r_4} + \delta_{r_4r_5}\tilde{h}^{(3)}_{r_1r_2r_3}].\end{aligned} \tag{B41}$$

Both results contain new contributions, represented by the $\tilde{h}^{(4)}_{r_1r_2r_3r_4}$ and $\tilde{h}^{(5)}_{r_1r_2r_3r_4r_5}$.

It is useful to introduce notation where, by applying a contraction at a tensor, the contracted indices will be suppressed, so, for example, $\tilde{h}^{(3)}_i \equiv \tilde{h}^{(3)}_{ikk}$, or $X^{(4)}_{ij} \equiv X^{(4)}_{ijkk}$ and $X^{(4)} \equiv X^{(4)}_{iikk}$. We define all of the contractions without any additional factors, with the sole exception of the heat flux vector $\boldsymbol{q}$, where the additional factor of $1/2$ is present, to match its usual definition. To emphasize this difference, in the index notation we thus keep an arrow on the components of the heat flux vector $\boldsymbol{q}_i$, to clearly distinguish it from the contracted tensor $\boldsymbol{q}_{ijk}$.

Applying the contractions at (B40), (B41) then yields

$$\begin{aligned}
X^{(4)}_{ij} &= \frac{p_a^2}{\rho_a}[\tilde{h}^{(4)}_{ij} + 7\tilde{h}^{(2)}_{ij} + 5\delta_{ij}];\\
X^{(4)} &= \frac{p_a^2}{\rho_a}[\tilde{h}^{(4)} + 15];\\
X^{(5)}_{ijk} &= \frac{p_a^2}{\rho_a}\sqrt{\frac{T_a}{m_a}}[\tilde{h}^{(5)}_{ijk} + \delta_{ij}\tilde{h}^{(3)}_k + \delta_{jk}\tilde{h}^{(3)}_i + \delta_{ik}\tilde{h}^{(3)}_j + 9\tilde{h}^{(3)}_{ijk}];\\
X^{(5)}_i &= \frac{p_a^2}{\rho_a}\sqrt{\frac{T_a}{m_a}}[\tilde{h}^{(5)}_i + 14\tilde{h}^{(3)}_i],
\end{aligned} \tag{B42}$$

and applying the contractions at the Hermite moments (B18)–(B20) yields

$$\begin{aligned}
\tilde{h}^{(2)}_{ij} &= \frac{1}{p_a}\Pi^{(2)}_{ij}; \qquad \tilde{h}^{(3)}_i = \frac{2}{p_a}\sqrt{\frac{m_a}{T_a}}\vec{q}_i;\\
\tilde{h}^{(4)}_{ij} &= \frac{\rho_a}{p_a^2}X^{(4)}_{ij} - 5\delta_{ij} - \frac{7}{p_a}\Pi^{(2)}_{ij};\\
\tilde{h}^{(4)} &= \frac{\rho_a}{p_a^2}X^{(4)} - 15;\\
\tilde{h}^{(5)}_{ijk} &= \frac{1}{p_a}\sqrt{\frac{m_a}{T_a}}\left[\frac{\rho_a}{p_a}X^{(5)}_{ijk} - (2\delta_{ij}\vec{q}_k + 2\delta_{jk}\vec{q}_i + 2\delta_{ik}\vec{q}_j + 9q_{ijk})\right];\\
\tilde{h}^{(5)}_i &= \frac{1}{p_a}\sqrt{\frac{m_a}{T_a}}\left(\frac{\rho_a}{p_a}X^{(5)}_i - 28\vec{q}_i\right).
\end{aligned} \tag{B43}$$

B.2.1. Viscosity $\Pi_{ij}^{(4)}$ of the Fourth-order Moment $X_{ij}^{(4)}$

The usual viscosity tensor is defined as a traceless matrix:

$$\Pi_{ij}^{(2)} = m_a \int \left(c_i c_j - \frac{1}{3}\delta_{ij} c^2 \right) f_a \, d^3c. \tag{B44}$$

Similarly, it is beneficial to introduce a traceless viscosity tensor of the fourth-order fluid moment:

$$\Pi_{ij}^{(4)} = m_a \int \left(c_i c_j - \frac{1}{3}\delta_{ij} c^2 \right) c^2 f_a \, d^3c. \tag{B45}$$

In other words, the moment $X_{ij}^{(4)}$ is decomposed as

$$X_{ij}^{(4)} = \frac{\delta_{ij}}{3} X^{(4)} + \Pi_{ij}^{(4)}, \tag{B46}$$

where the fully contracted $X^{(4)} = m_a \int c^4 f_a d^3c$. Scalar $X^{(4)}$ is further decomposed to its "core" Maxwellian part, and the additional perturbation $\widetilde{X}^{(4)}$ (with wide tilde), according to

$$X^{(4)} = 15 \frac{p_a^2}{\rho_a} + \widetilde{X}^{(4)}, \tag{B47}$$

and the corresponding Hermite moments thus become

$$\begin{aligned} \tilde{h}_{ij}^{(4)} &= \frac{\rho_a}{p_a^2} \frac{\delta_{ij}}{3} \widetilde{X}^{(4)} + \frac{\rho_a}{p_a^2} \Pi_{ij}^{(4)} - \frac{7}{p_a} \Pi_{ij}^{(2)}; \\ \tilde{h}^{(4)} &= \frac{\rho_a}{p_a^2} \widetilde{X}^{(4)}. \end{aligned} \tag{B48}$$

It is important to emphasize that depending on the choice of perturbation χ_a, in general $\widetilde{X}^{(4)}$ is nonzero. However, this perturbation is not required to derive the model of Braginskii (1965), and Balescu (1988), for example, prescribes irreducible $h^{(4)} = 0$. In the next section, we will consider simplified perturbations and derive the above results in a more direct manner; nevertheless, the more general case (B39) is a very useful guide in demonstrating that it is possible to consider perturbations with nonzero $h^{(4)}$.

Finally, because the reducible matrix $\tilde{h}_{ij}^{(4)}$ is not traceless in general (unless one prescribes the Hermite closure $\tilde{h}^{(4)} = 0$, which makes it traceless by definition), it is useful to introduce traceless

$$\hat{h}_{ij}^{(4)} = \tilde{h}_{ij}^{(4)} - \frac{\delta_{ij}}{3} \tilde{h}^{(4)} = \frac{\rho_a}{p_a^2} \Pi_{ij}^{(4)} - \frac{7}{p_a} \Pi_{ij}^{(2)}, \tag{B49}$$

where we use hat instead of tilde.

B.2.2. Simplified Perturbations (21-moment Model)

Instead of working with very complicated perturbations (B39), it was shown by Balescu (1988) that to obtain the model of Braginskii (1965), it is sufficient to work with simplified

$$\chi_a = h_{ij}^{(2)} H_{ij}^{(2)} + h_i^{(3)} H_i^{(3)} + h_{ij}^{(4)} H_{ij}^{(4)} + h_i^{(5)} H_i^{(5)}. \tag{B50}$$

The perturbation (B50) is written with *irreducible* Hermite polynomials (notation without tilde), as discussed in the next section. This perturbation represents the 21-moment model, and recovers both the stress tensor and the heat flux of Braginskii. However, the connection between irreducible and reducible Hermite polynomials can be very blurry at first, and we continue with *reducible* Hermite polynomials.

Applying the contractions at the hierarchy of the reducible polynomials (B5) yields

$$\begin{aligned} \tilde{H}_i^{(3)} &= \tilde{c}_i(\tilde{c}^2 - 5); \qquad & \tilde{H}_i^{(5)} &= \tilde{c}_i(\tilde{c}^4 - 14\tilde{c}^2 + 35); \\ \tilde{H}_{ij}^{(2)} &= \tilde{c}_i \tilde{c}_j - \delta_{ij}; \qquad & \tilde{H}_{ij}^{(4)} &= \tilde{c}_i \tilde{c}_j (\tilde{c}^2 - 7) - \delta_{ij}(\tilde{c}^2 - 5). \end{aligned} \tag{B51}$$

By using these polynomials, the Hermite moments then calculate

$$\begin{aligned} \tilde{h}_i^{(3)} &= \frac{2}{p_a} \sqrt{\frac{m_a}{T_a}} \vec{q}_i; \qquad & \tilde{h}_i^{(5)} &= \frac{1}{p_a} \sqrt{\frac{m_a}{T_a}} \left(\frac{\rho_a}{p_a} X_i^{(5)} - 28 \vec{q}_i \right); \\ \tilde{h}_{ij}^{(2)} &= \frac{1}{p_a} \Pi_{ij}^{(2)}; \qquad & \hat{h}_{ij}^{(4)} &= \frac{\rho_a}{p_a^2} \Pi_{ij}^{(4)} - \frac{7}{p_a} \Pi_{ij}^{(2)}, \end{aligned}$$

of course recovering previous results. The reducible Hermite polynomials satisfy the following orthogonality relations:

$$\int \tilde{H}_i^{(3)}\tilde{H}_j^{(3)}\phi^{(0)}d^3\tilde{c} = 10\delta_{ij}; \qquad \int \tilde{H}_i^{(5)}\tilde{H}_j^{(5)}\phi^{(0)}d^3\tilde{c} = 280\delta_{ij};$$
$$\int \tilde{H}_{ij}^{(2)}\tilde{H}_{kl}^{(2)}\phi^{(0)}d^3\tilde{c} = \delta_{ik}\delta_{jl} + \delta_{il}\delta_{jk};$$
$$\int \tilde{H}_{ij}^{(4)}\tilde{H}_{kl}^{(4)}\phi^{(0)}d^3\tilde{c} = 14(\delta_{ik}\delta_{jl} + \delta_{il}\delta_{jk}) + 4\delta_{ij}\delta_{kl}, \tag{B52}$$

and because the Hermite moments $\tilde{h}_{kl}^{(2)}$, $\hat{h}_{kl}^{(4)}$ are symmetric and traceless,

$$\tilde{h}_{kl}^{(2)}\int \tilde{H}_{ij}^{(2)}\tilde{H}_{kl}^{(2)}\phi^{(0)}d^3\tilde{c} = 2\tilde{h}_{ij}^{(2)}; \qquad \hat{h}_{kl}^{(4)}\int \tilde{H}_{ij}^{(4)}\tilde{H}_{kl}^{(4)}\phi^{(0)}d^3\tilde{c} = 28\hat{h}_{ij}^{(4)}. \tag{B53}$$

Thus, a perturbation that can be directly derived from the hierarchy of the reducible Hermite polynomials (with no reference to irreducible Hermite polynomials or Laguerre–Sonine polynomials) reads

$$\chi_a = \frac{1}{2}\tilde{h}_{ij}^{(2)}\tilde{H}_{ij}^{(2)} + \frac{1}{10}\tilde{h}_i^{(3)}\tilde{H}_i^{(3)} + \frac{1}{28}\hat{h}_{ij}^{(4)}\tilde{H}_{ij}^{(4)} + \frac{1}{280}\tilde{h}_i^{(5)}\tilde{H}_i^{(5)}, \tag{B54}$$

where each term is calculated as

$$\frac{1}{10}\tilde{h}_i^{(3)}\tilde{H}_i^{(3)} = \frac{1}{5p_a}\sqrt{\frac{m_a}{T_a}}(\boldsymbol{q}_a\cdot\tilde{\boldsymbol{c}}_a)(\tilde{c}_a^2 - 5);$$
$$\frac{1}{280}\tilde{h}_i^{(5)}\tilde{H}_i^{(5)} = \frac{1}{280p_a}\sqrt{\frac{m_a}{T_a}}\left[\frac{\rho_a}{p_a}(\boldsymbol{X}^{a(5)}\cdot\tilde{\boldsymbol{c}}_a) - 28(\boldsymbol{q}_a\cdot\tilde{\boldsymbol{c}}_a)\right](\tilde{c}_a^4 - 14\tilde{c}_a^2 + 35);$$
$$\frac{1}{2}\tilde{h}_{ij}^{(2)}\tilde{H}_{ij}^{(2)} = \frac{1}{2p_a}(\bar{\bar{\boldsymbol{\Pi}}}_a^{(2)}:\tilde{\boldsymbol{c}}_a\tilde{\boldsymbol{c}}_a);$$
$$\frac{1}{28}\hat{h}_{ij}^{(4)}\tilde{H}_{ij}^{(4)} = \frac{1}{28}\left[\frac{\rho_a}{p_a^2}(\bar{\bar{\boldsymbol{\Pi}}}_a^{(4)}:\tilde{\boldsymbol{c}}_a\tilde{\boldsymbol{c}}_a) - \frac{7}{p_a}(\bar{\bar{\boldsymbol{\Pi}}}_a^{(2)}:\tilde{\boldsymbol{c}}_a\tilde{\boldsymbol{c}}_a)\right](\tilde{c}_a^2 - 7), \tag{B55}$$

with normalized velocity $\tilde{\boldsymbol{c}}_a = \sqrt{m_a/T_a}\boldsymbol{c}_a$. Bellow, we show that the perturbation (B54), (B55) is equivalent to the perturbation of Balescu (B50), obtained with irreducible polynomials. The final perturbation of the 21-moment model that recovers Braginskii (1965) thus reads

$$\chi_a = \frac{1}{2p_a}(\bar{\bar{\boldsymbol{\Pi}}}_a^{(2)}:\tilde{\boldsymbol{c}}_a\tilde{\boldsymbol{c}}_a) + \frac{1}{28}\left[\frac{\rho_a}{p_a^2}(\bar{\bar{\boldsymbol{\Pi}}}_a^{(4)}:\tilde{\boldsymbol{c}}_a\tilde{\boldsymbol{c}}_a) - \frac{7}{p_a}(\bar{\bar{\boldsymbol{\Pi}}}_a^{(2)}:\tilde{\boldsymbol{c}}_a\tilde{\boldsymbol{c}}_a)\right](\tilde{c}_a^2 - 7)$$
$$+\frac{1}{5p_a}\sqrt{\frac{m_a}{T_a}}(\boldsymbol{q}_a\cdot\tilde{\boldsymbol{c}}_a)(\tilde{c}_a^2 - 5) + \frac{1}{280p_a}\sqrt{\frac{m_a}{T_a}}\left[\frac{\rho_a}{p_a}(\boldsymbol{X}^{a(5)}\cdot\tilde{\boldsymbol{c}}_a) - 28(\boldsymbol{q}_a\cdot\tilde{\boldsymbol{c}}_a)\right](\tilde{c}_a^4 - 14\tilde{c}_a^2 + 35). \tag{B56}$$

Finally, because $\hat{h}_{ij}^{(4)}$ is traceless, its double contraction with $\tilde{H}_{ij}^{(4)}$ makes the part of this polynomial proportional to δ_{ij} redundant in the final perturbation. It is possible to define another traceless polynomial (with hat instead of tilde):

$$\hat{H}_{ij}^{(4)} = \tilde{H}_{ij}^{(4)} - \frac{\delta_{ij}}{3}\tilde{H}^{(4)} = \left(\tilde{c}_i\tilde{c}_j - \frac{\delta_{ij}}{3}\tilde{c}^2\right)(\tilde{c}^2 - 7), \tag{B57}$$

and replace the following term in the perturbation (B54):

$$\hat{h}_{ij}^{(4)}\tilde{H}_{ij}^{(4)} = \hat{h}_{ij}^{(4)}\hat{H}_{ij}^{(4)}, \tag{B58}$$

where the part of (B57) proportional to δ_{ij} is still suppressed in the final perturbation. However, the traceless definition (B57) now makes it possible to directly define the traceless Hermite moment $\hat{h}_{ij}^{(4)}$ as an integral over $\hat{H}_{ij}^{(4)}$:

$$\hat{h}_{ij}^{(4)} = \frac{1}{n_a}\int f_a\hat{H}_{ij}^{(4)}d^3c. \tag{B59}$$

This is the main motivation behind irreducible Hermite polynomials, as is further clarified below.

B.3. Irreducible Hermite Polynomials

In the work of Balescu (1988), the *irreducible* Hermite polynomials are defined through Laguerre–Sonine polynomials, according to (see Equation (G1.4.4) on p. 326 of Balescu)

$$H^{(2n)}(\tilde{c}) = L_n^{1/2}\left(\frac{\tilde{c}^2}{2}\right);$$
$$H_i^{(2n+1)}(\tilde{\boldsymbol{c}}) = \sqrt{\frac{3}{2}}\tilde{c}_i L_n^{3/2}\left(\frac{\tilde{c}^2}{2}\right);$$
$$H_{ij}^{(2n)}(\tilde{\boldsymbol{c}}) = \sqrt{\frac{15}{8}}\,(\tilde{c}_i\tilde{c}_j - \frac{\tilde{c}^2}{3}\delta_{ij})L_{n-1}^{5/2}\left(\frac{\tilde{c}^2}{2}\right). \tag{B60}$$

To recover the Braginskii (1965) model, one only needs (see Table 4.1 on p. 327 of Balescu)

$$H_i^{(3)} = \frac{1}{\sqrt{10}}\tilde{c}_i(\tilde{c}^2 - 5); \qquad H_i^{(5)} = \frac{1}{2\sqrt{70}}\tilde{c}_i(\tilde{c}^4 - 14\tilde{c}^2 + 35);$$
$$H_{ij}^{(2)} = \frac{1}{\sqrt{2}}\left(\tilde{c}_i\tilde{c}_j - \frac{1}{3}\tilde{c}^2\delta_{ij}\right); \qquad H_{ij}^{(4)} = \frac{1}{2\sqrt{7}}(\tilde{c}_i\tilde{c}_j - \frac{1}{3}\tilde{c}^2\delta_{ij})(\tilde{c}^2 - 7), \tag{B61}$$

yielding Hermite moments

$$h_i^{(3)} = \sqrt{\frac{2}{5}}\frac{1}{p_a}\sqrt{\frac{m_a}{T_a}}\vec{q}_i; \qquad h_i^{(5)} = \frac{1}{2\sqrt{70}\,p_a}\sqrt{\frac{m_a}{T_a}}\left[\frac{\rho_a}{p_a}X_i^{(5)} - 28\vec{q}_i\right];$$
$$h_{ij}^{(2)} = \frac{1}{\sqrt{2}\,p_a}\Pi_{ij}^{(2)}; \qquad h_{ij}^{(4)} = \frac{1}{2\sqrt{7}\,p_a}\left[\frac{\rho_a}{p_a}\Pi_{ij}^{(4)} - 7\Pi_{ij}^{(2)}\right]. \tag{B62}$$

Furthermore, the orthogonal relations are

$$\int \phi^{(0)}H_i^{(2n+1)}H_j^{(2n+1)}d^3c = \delta_{ij}; \qquad h_{kl}^{(2n)}\int \phi^{(0)}H_{ij}^{(2n)}H_{kl}^{(2n)}d^3c = h_{ij}^{(2n)}, \tag{B63}$$

yielding perturbation (B50), which then recovers perturbation (B54), (B55) obtained with reducible polynomials. Both approaches are therefore equivalent, which is further addressed in Appendix B.7.

B.3.1. Higher-order Tensorial "Anisotropies"

It is useful to clarify what contributions are obtained by using the irreducible Hermite polynomials:

$$H_{ijk}^{(3)}(\tilde{\boldsymbol{c}}) = \tilde{c}_i\tilde{c}_j\tilde{c}_k - \frac{1}{5}\tilde{c}^2(\delta_{ij}\tilde{c}_k + \delta_{jk}\tilde{c}_i + \delta_{ik}\tilde{c}_j);$$
$$H_{ijkl}^{(4)}(\tilde{\boldsymbol{c}}) = \tilde{c}_i\tilde{c}_j\tilde{c}_k\tilde{c}_l - \frac{1}{7}\tilde{c}^2(\delta_{ij}\tilde{c}_k\tilde{c}_l + \delta_{jk}\tilde{c}_l\tilde{c}_i + \delta_{kl}\tilde{c}_i\tilde{c}_j + \delta_{li}\tilde{c}_j\tilde{c}_k + \delta_{ik}\tilde{c}_j\tilde{c}_l + \delta_{jl}\tilde{c}_i\tilde{c}_k)$$
$$+ \frac{1}{35}\tilde{c}^4(\delta_{ij}\delta_{kl} + \delta_{ik}\delta_{jl} + \delta_{il}\delta_{jk}), \tag{B64}$$

which Balescu (1988) calls "anisotropies" (even though they are valid as a perturbation for isotropic Maxwellians). Importantly, applying a trace on (B64) yields zero. The corresponding Hermite moments calculate

$$h_{ijk}^{(3)} = \frac{1}{p_a}\sqrt{\frac{m_a}{T_a}}\left[\bar{\bar{\boldsymbol{q}}} - \frac{2}{5}(\bar{\bar{\boldsymbol{I}}}\boldsymbol{q})^S\right]_{ijk} = \frac{1}{p_a}\sqrt{\frac{m_a}{T_a}}\,\sigma'_{ijk}; \qquad h_{ijkl}^{(4)} = \frac{\rho_a}{p_a^2}\sigma_{ijkl}^{(4)\prime}, \tag{B65}$$

and directly yield the highest-order irreducible parts.

B.4. Decomposition of $X_{ijkl}^{(4)}$

We continue with the *reducible* Hermite polynomials. To decompose the full fourth-order fluid moment $X_{ijkl}^{(4)}$, it is necessary to consider the following perturbation (i.e., the 16-moment model):

$$\chi_a = \frac{1}{2}\tilde{h}_{ij}^{(2)}\tilde{H}_{ij}^{(2)} + \frac{1}{28}\hat{h}_{ij}^{(4)}\tilde{H}_{ij}^{(4)} + \frac{1}{120}\tilde{h}^{(4)}\tilde{H}^{(4)}, \tag{B66}$$

and, by using this perturbation, to calculate $X_{ijkl}^{(4)}$. In comparison to the previous perturbation of the 21-moment model, the last term with Hermite polynomial $\tilde{H}^{(4)}$ is new. It is derived with orthogonality relation $\int \phi^{(0)}H^{(4)}H^{(4)}d^3\tilde{c} = 120$. We will need the following

integrals. Applying the contraction $\delta_{r_3 r_4}$ at the orthogonality relation (B10) yields

$$\begin{aligned}\int \tilde{H}^{(4)}_{r_1 r_2}\tilde{c}_{s_1}\tilde{c}_{s_2}\tilde{c}_{s_3}\tilde{c}_{s_4}\phi^{(0)}d^3\tilde{c} &= \int \tilde{H}^{(4)}_{r_1 r_2}\tilde{H}^{(4)}_{s_1 s_2 s_3 s_4}\phi^{(0)}d^3\tilde{c}\\ &= +\,2\delta_{r_1 s_1}\delta_{r_2 s_2}\delta_{s_3 s_4} + 2\delta_{r_1 s_1}\delta_{r_2 s_3}\delta_{s_2 s_4} + 2\delta_{r_1 s_1}\delta_{r_2 s_4}\delta_{s_2 s_3}\\ &+2\delta_{r_1 s_2}\delta_{r_2 s_1}\delta_{s_3 s_4} + 2\delta_{r_1 s_2}\delta_{r_2 s_3}\delta_{s_1 s_4} + 2\delta_{r_1 s_2}\delta_{r_2 s_4}\delta_{s_1 s_3}\\ &+2\delta_{r_1 s_3}\delta_{r_2 s_1}\delta_{s_2 s_4} + 2\delta_{r_1 s_3}\delta_{r_2 s_2}\delta_{s_1 s_4} + 2\delta_{r_1 s_3}\delta_{r_2 s_4}\delta_{s_1 s_2}\\ &+2\delta_{r_1 s_4}\delta_{r_2 s_1}\delta_{s_2 s_3} + 2\delta_{r_1 s_4}\delta_{r_2 s_2}\delta_{s_1 s_3} + 2\delta_{r_1 s_4}\delta_{r_2 s_3}\delta_{s_1 s_2},\end{aligned} \tag{B67}$$

and, further, applying traceless $\hat{h}^{(4)}_{r_1 r_2}$ at (B67) leads to

$$\begin{aligned}&\hat{h}^{(4)}_{r_1 r_2}\int \tilde{H}^{(4)}_{r_1 r_2}\tilde{c}_{s_1}\tilde{c}_{s_2}\tilde{c}_{s_3}\tilde{c}_{s_4}\phi^{(0)}d^3\tilde{c}\\ &=4[\hat{h}^{(4)}_{s_1 s_2}\delta_{s_3 s_4} + \hat{h}^{(4)}_{s_1 s_3}\delta_{s_2 s_4} + \hat{h}^{(4)}_{s_1 s_4}\delta_{s_2 s_3} + \hat{h}^{(4)}_{s_2 s_3}\delta_{s_1 s_4} + \hat{h}^{(4)}_{s_2 s_4}\delta_{s_1 s_3} + \hat{h}^{(4)}_{s_3 s_4}\delta_{s_1 s_2}].\end{aligned} \tag{B68}$$

Applying the contraction $\delta_{r_1 r_2}$ at (B67) and multiplying by $\tilde{h}^{(4)}$ yields

$$\tilde{h}^{(4)}\int \tilde{H}^{(4)}\tilde{c}_{s_1}\tilde{c}_{s_2}\tilde{c}_{s_3}\tilde{c}_{s_4}\phi^{(0)}d^3\tilde{c} = 8\tilde{h}^{(4)}[\delta_{s_1 s_2}\delta_{s_3 s_4} + \delta_{s_1 s_3}\delta_{s_2 s_4} + \delta_{s_1 s_4}\delta_{s_2 s_3}]. \tag{B69}$$

Similarly,

$$\begin{aligned}&\tilde{h}^{(2)}_{r_1 r_2}\int \tilde{H}^{(2)}_{r_1 r_2}\tilde{c}_{s_1}\tilde{c}_{s_2}\tilde{c}_{s_3}\tilde{c}_{s_4}\phi^{(0)}d^3\tilde{c}\\ &= 2[\tilde{h}^{(2)}_{s_1 s_2}\delta_{s_3 s_4} + \tilde{h}^{(2)}_{s_1 s_3}\delta_{s_2 s_4} + \tilde{h}^{(2)}_{s_1 s_4}\delta_{s_2 s_3} + \tilde{h}^{(2)}_{s_2 s_3}\delta_{s_1 s_4} + \tilde{h}^{(2)}_{s_2 s_4}\delta_{s_1 s_3} + \tilde{h}^{(2)}_{s_3 s_4}\delta_{s_1 s_2}].\end{aligned} \tag{B70}$$

The results (B68), (B69), (B70) allow us to calculate the $X^{(4)}_{ijkl}$ moment, which becomes

$$\begin{aligned}X^{(4)}_{ijkl} &= m_a\int f^{(0)}_a\left[1 + \frac{1}{2}\tilde{h}^{(2)}_{r_1 r_2}\tilde{H}^{(2)}_{r_1 r_2} + \frac{1}{28}\hat{h}^{(4)}_{r_1 r_2}\tilde{H}^{(4)}_{r_1 r_2} + \frac{1}{120}\tilde{h}^{(4)}\tilde{H}^{(4)}\right]c_i c_j c_k c_l d^3c\\ &= +\frac{1}{15}\frac{p_a^2}{\rho_a}(15 + \tilde{h}^{(4)})(\delta_{ij}\delta_{kl} + \delta_{ik}\delta_{jl} + \delta_{jk}\delta_{il})\\ &\quad +\frac{1}{7}\frac{p_a^2}{\rho_a}[(\hat{h}^{(4)}_{ij} + 7\tilde{h}^{(2)}_{ij})\delta_{kl} + (\hat{h}^{(4)}_{ik} + 7\tilde{h}^{(2)}_{ik})\delta_{jl} + (\hat{h}^{(4)}_{il} + 7\tilde{h}^{(2)}_{il})\delta_{jk}\\ &\quad +(\hat{h}^{(4)}_{jk} + 7\tilde{h}^{(2)}_{jk})\delta_{il} + (\hat{h}^{(4)}_{jl} + 7\tilde{h}^{(2)}_{jl})\delta_{ik} + (\hat{h}^{(4)}_{kl} + 7\tilde{h}^{(2)}_{kl})\delta_{ij}].\end{aligned} \tag{B71}$$

Form (B71) nicely shows how various parts of perturbation (B66) contribute to the decomposition, including the new $\tilde{h}^{(4)}$. Prescribing the Hermite closures $\hat{h}^{(4)}_{ij} = 0$, $\tilde{h}^{(4)} = 0$ recovers decomposition (B30) used in the Burgers–Schunk model. Finally, rewritten with the fluid moments

$$\Pi^{(4)}_{ij} = \frac{p_a^2}{\rho_a}(\hat{h}^{(4)}_{ij} + 7\tilde{h}^{(2)}_{ij}); \qquad \widetilde{X}^{(4)} = \frac{p_a^2}{\rho_a}\tilde{h}^{(4)}; \qquad X^{(4)} = 15\frac{p_a^2}{\rho_a} + \widetilde{X}^{(4)}, \tag{B72}$$

and representing all of the other terms that were not obtained from (B66) by traceless $\sigma^{(4)\prime}_{ijkl}$ (which represents the highest-order irreducible part of $X^{(4)}_{ijkl}$), the decomposition becomes

$$\begin{aligned}X^{(4)}_{ijkl} &= \frac{1}{15}X^{(4)}(\delta_{ij}\delta_{kl} + \delta_{ik}\delta_{jl} + \delta_{il}\delta_{jk})\\ &\quad +\frac{1}{7}[\Pi^{(4)}_{ij}\delta_{kl} + \Pi^{(4)}_{ik}\delta_{jl} + \Pi^{(4)}_{il}\delta_{jk} + \Pi^{(4)}_{jk}\delta_{il} + \Pi^{(4)}_{jl}\delta_{ik} + \Pi^{(4)}_{kl}\delta_{ij}] + \sigma^{(4)\prime}_{ijkl},\end{aligned} \tag{B73}$$

or equivalently,

$$\begin{aligned}X^{(4)}_{ijkl} &= -\frac{1}{35}X^{(4)}(\delta_{ij}\delta_{kl} + \delta_{ik}\delta_{jl} + \delta_{il}\delta_{jk})\\ &\quad +\frac{1}{7}[X^{(4)}_{ij}\delta_{kl} + X^{(4)}_{ik}\delta_{jl} + X^{(4)}_{il}\delta_{jk} + X^{(4)}_{jk}\delta_{il} + X^{(4)}_{jl}\delta_{ik} + X^{(4)}_{kl}\delta_{ij}] + \sigma^{(4)\prime}_{ijkl}.\end{aligned} \tag{B74}$$

Decomposition (B73) is equivalent to Equation (30.22) of Grad (1958). Essentially, any tensorial moment can be decomposed by subtracting all of the possible contractions of that moment. Note that simply prescribing the closure $\Pi^{(4)}_{ij} = 0$ in (B73) would be erroneous, unless one also prescribes $\Pi^{(2)}_{ij} = 0$ as well. The correct simplification of (B73) is obtained by prescribing the Hermite closure $\hat{h}^{(4)}_{ij} = 0$, meaning by prescribing the fluid closure $\Pi^{(4)}_{ij} = 7(p_a/\rho_a)\Pi^{(2)}_{ij}$. Additionally, one can also prescribe the Hermite

closure $\tilde{h}^{(4)} = 0$, which is equivalent to the fluid closure $\widetilde{X}^{(4)} = 0$.

B.5. Decomposition of $X^{(5)}_{ijklm}$

We only use the simplified perturbation

$$\chi_a = \frac{1}{10}\tilde{h}_i^{(3)}\tilde{H}_i^{(3)} + \frac{1}{280}\tilde{h}_i^{(5)}\tilde{H}_i^{(5)}. \tag{B75}$$

By using this perturbation, it is possible to calculate the fifth-order fluid moment:

$$\begin{aligned} X^{(5)}_{s_1s_2s_3s_4s_5} = \frac{1}{35}\frac{p_a^{5/2}}{\rho_a^{3/2}}[&(\tilde{h}^{(5)}_{s_1} + 14\tilde{h}^{(3)}_{s_1})(\delta_{s_2s_3}\delta_{s_4s_5} + \delta_{s_2s_4}\delta_{s_3s_5} + \delta_{s_2s_5}\delta_{s_3s_4}) \\ &+(\tilde{h}^{(5)}_{s_2} + 14\tilde{h}^{(3)}_{s_2})(\delta_{s_1s_3}\delta_{s_4s_5} + \delta_{s_1s_4}\delta_{s_3s_5} + \delta_{s_1s_5}\delta_{s_3s_4}) \\ &+(\tilde{h}^{(5)}_{s_3} + 14\tilde{h}^{(3)}_{s_3})(\delta_{s_1s_2}\delta_{s_4s_5} + \delta_{s_1s_4}\delta_{s_2s_5} + \delta_{s_1s_5}\delta_{s_2s_4}) \\ &+(\tilde{h}^{(5)}_{s_4} + 14\tilde{h}^{(3)}_{s_4})(\delta_{s_1s_2}\delta_{s_3s_5} + \delta_{s_1s_3}\delta_{s_2s_5} + \delta_{s_1s_5}\delta_{s_2s_3}) \\ &+(\tilde{h}^{(5)}_{s_5} + 14\tilde{h}^{(3)}_{s_5})(\delta_{s_1s_2}\delta_{s_3s_4} + \delta_{s_1s_3}\delta_{s_2s_4} + \delta_{s_1s_4}\delta_{s_2s_3})]. \end{aligned} \tag{B76}$$

Because we consider the simplified perturbation (B75), we do not consider full decomposition with $\sigma^{(5)\,\prime}$. Prescribing the Hermite closure $\tilde{h}_i^{(5)} = 0$ yields the previously obtained decomposition (B37). Finally, by switching from Hermite to fluid moments,

$$\tilde{h}_i^{(3)} = 2\frac{\rho_a^{1/2}}{p_a^{3/2}}\vec{q}_i; \qquad \tilde{h}_i^{(5)} = \frac{\rho_a^{1/2}}{p_a^{3/2}}\left(\frac{\rho_a}{p_a}X_i^{(5)} - 28\vec{q}_i\right); \qquad \tilde{h}_i^{(5)} + 14\tilde{h}_i^{(3)} = \frac{\rho_a^{3/2}}{p_a^{5/2}}X_i^{(5)}, \tag{B77}$$

the decomposition becomes

$$\begin{aligned} X^{(5)}_{s_1s_2s_3s_4s_5} = \frac{1}{35}[&X^{(5)}_{s_1}(\delta_{s_2s_3}\delta_{s_4s_5} + \delta_{s_2s_4}\delta_{s_3s_5} + \delta_{s_2s_5}\delta_{s_3s_4}) \\ &+X^{(5)}_{s_2}(\delta_{s_1s_3}\delta_{s_4s_5} + \delta_{s_1s_4}\delta_{s_3s_5} + \delta_{s_1s_5}\delta_{s_3s_4}) \\ &+X^{(5)}_{s_3}(\delta_{s_1s_2}\delta_{s_4s_5} + \delta_{s_1s_4}\delta_{s_2s_5} + \delta_{s_1s_5}\delta_{s_2s_4}) \\ &+X^{(5)}_{s_4}(\delta_{s_1s_2}\delta_{s_3s_5} + \delta_{s_1s_3}\delta_{s_2s_5} + \delta_{s_1s_5}\delta_{s_2s_3}) \\ &+X^{(5)}_{s_5}(\delta_{s_1s_2}\delta_{s_3s_4} + \delta_{s_1s_3}\delta_{s_2s_4} + \delta_{s_1s_4}\delta_{s_2s_3})]. \end{aligned} \tag{B78}$$

As a double-check, applying contraction $\delta_{s_4s_5}$ at the last expression yields

$$X^{(5)}_{s_1s_2s_3} = \frac{1}{5}[X^{(5)}_{s_1}\delta_{s_2s_3} + X^{(5)}_{s_2}\delta_{s_1s_3} + X^{(5)}_{s_3}\delta_{s_1s_2}], \tag{B79}$$

and applying another contraction yields an identity. Note that it is not possible to perform the closure $\boldsymbol{X}^{(5)} = 0$, as such a closure would be erroneous (unless $\boldsymbol{q} = 0$ is prescribed as well). Instead, one needs to perform the closure at the Hermite moment $\tilde{h}_i^{(5)} = 0$, or, in other words, the correct closure is $\boldsymbol{X}^{(5)} = 28(p_a/\rho_a)\boldsymbol{q}$.

B.6. Table of Useful Integrals

The Hermite polynomials allow one to build the hierarchy of the following integrals. One introduces the weight

$$\phi^{(0)} = \frac{e^{-\tilde{c}^2/2}}{(2\pi)^{3/2}}, \tag{B80}$$

and for any odd "*m*," the following integral holds:

$$m = \text{odd}: \qquad \int \tilde{c}_{r_1}\tilde{c}_{r_2}\tilde{c}_{r_3}\ \ldots\ \tilde{c}_{r_m}\phi^{(0)}d^3\tilde{c} = 0. \tag{B81}$$

The validity of (B81) can be shown by using "common-sense" symmetries and Gaussian integration, or by rewriting the integral with pairs of Hermite polynomials, one of even order and one of odd order, $\tilde{H}^{(r_m+1)/2}\tilde{H}^{(r_m-1)/2}$ (where the result of the integration is zero), and a hierarchy of lower-order integrals that will also be odd–even pairs, yielding zero.

A particular case of the orthogonality theorem is that for any $m \neq 0$, an integral over any single Hermite polynomial with weight $\phi^{(0)}$ is zero:

$$m \neq 0: \qquad \int \tilde{H}^{(m)}_{r_1 r_2 r_3 \ldots r_m} \phi^{(0)} d^3\tilde{c} = 0. \tag{B82}$$

The two rules (B81), (B82) allow one to calculate the integrals for any even "m" number of velocities $\tilde{\boldsymbol{c}}$, such as $\tilde{\boldsymbol{c}}\tilde{\boldsymbol{c}}\tilde{\boldsymbol{c}}\tilde{\boldsymbol{c}}\tilde{\boldsymbol{c}}\tilde{\boldsymbol{c}}$, which would otherwise be very difficult to do just by using "common-sense" symmetries and Gaussian integration. Actually, for "m" being even, quicker than using (B82) is rewriting the integrals into $\tilde{H}^{(m/2)}\tilde{H}^{(m/2)}$ and using the orthogonality relations (B9). A very useful integral also reads

$$m < n: \qquad \int \tilde{c}_{r_1} \ldots \tilde{c}_{r_m} H^{(n)}_{s_1 \ldots s_n} \phi^{(0)} d^3\tilde{c} = 0, \tag{B83}$$

the validity of which is easily shown by rewriting $\tilde{c}_{r_1} \ldots \tilde{c}_{r_m}$ with $H^{(m)}_{r_1 \ldots r_m}$ (where the result of the integration is zero) and a hierarchy of lower-order Hermite polynomials where the result of the integration is also zero.

It is possible to build the following table when "m" is even:

$$\begin{aligned} \int \phi^{(0)} d^3\tilde{c} &= 1; \\ \int \tilde{c}_i \tilde{c}_j \phi^{(0)} d^3\tilde{c} &= \delta_{ij}; \\ \int \tilde{c}_i \tilde{c}_j \tilde{c}_k \tilde{c}_l \phi^{(0)} d^3\tilde{c} &= \delta_{ij}\delta_{kl} + \delta_{ik}\delta_{jl} + \delta_{jk}\delta_{il}; \end{aligned} \tag{B84}$$

$$\begin{aligned} \int \tilde{c}_{r_1}\tilde{c}_{r_2}\tilde{c}_{r_3}\tilde{c}_{s_1}\tilde{c}_{s_2}\tilde{c}_{s_3}\phi^{(0)} d^3\tilde{c} = {} & \delta_{r_1 s_1}(\delta_{r_2 s_2}\delta_{r_3 s_3} + \delta_{r_2 s_3}\delta_{r_3 s_2}) \\ & + \delta_{r_1 s_2}(\delta_{r_2 s_1}\delta_{r_3 s_3} + \delta_{r_2 s_3}\delta_{r_3 s_1}) + \delta_{r_1 s_3}(\delta_{r_2 s_1}\delta_{r_3 s_2} + \delta_{r_2 s_2}\delta_{r_3 s_1}) \\ & + \delta_{r_1 r_2}(\delta_{s_1 s_2}\delta_{r_3 s_3} + \delta_{s_2 s_3}\delta_{r_3 s_1} + \delta_{s_3 s_1}\delta_{r_3 s_2}) \\ & + \delta_{r_1 r_3}(\delta_{s_1 s_2}\delta_{r_2 s_3} + \delta_{s_2 s_3}\delta_{r_2 s_1} + \delta_{s_3 s_1}\delta_{r_2 s_2}) \\ & + \delta_{r_2 r_3}(\delta_{s_1 s_2}\delta_{r_1 s_3} + \delta_{s_2 s_3}\delta_{r_1 s_1} + \delta_{s_3 s_1}\delta_{r_1 s_2}). \end{aligned} \tag{B85}$$

These integrals can be used to obtain other useful integrals, for example, those that are valid for any (three-dimensional) vector $\boldsymbol{q}$:

$$\int \tilde{c}_i \tilde{c}_j \tilde{c}_k (\tilde{\boldsymbol{c}} \cdot \boldsymbol{q}) \phi^{(0)} d^3\tilde{c} = \delta_{ij}\vec{q}_k + \delta_{jk}\vec{q}_i + \delta_{ki}\vec{q}_j = [\bar{\bar{\boldsymbol{I}}}\boldsymbol{q}]^S_{ijk}; \tag{B86}$$

$$\begin{aligned} \int \tilde{c}_{r_1}\tilde{c}_{r_2}\tilde{c}_{r_3}\tilde{c}_{s_1}\tilde{c}_{s_2}(\tilde{\boldsymbol{c}} \cdot \boldsymbol{q})\phi^{(0)} d^3\tilde{c} = {} & \delta_{r_1 s_1}(\delta_{r_2 s_2}\vec{q}_{r_3} + \vec{q}_{r_2}\delta_{r_3 s_2}) \\ & + \delta_{r_1 s_2}(\delta_{r_2 s_1}\vec{q}_{r_3} + \vec{q}_{r_2}\delta_{r_3 s_1}) + \vec{q}_{r_1}(\delta_{r_2 s_1}\delta_{r_3 s_2} + \delta_{r_2 s_2}\delta_{r_3 s_1}) \\ & + \delta_{r_1 r_2}(\delta_{s_1 s_2}\vec{q}_{r_3} + \vec{q}_{s_2}\delta_{r_3 s_1} + \vec{q}_{s_1}\delta_{r_3 s_2}) \\ & + \delta_{r_1 r_3}(\delta_{s_1 s_2}\vec{q}_{r_2} + \vec{q}_{s_2}\delta_{r_2 s_1} + \vec{q}_{s_1}\delta_{r_2 s_2}) \\ & + \delta_{r_2 r_3}(\delta_{s_1 s_2}\vec{q}_{r_1} + \vec{q}_{s_2}\delta_{r_1 s_1} + \vec{q}_{s_1}\delta_{r_1 s_2}). \end{aligned} \tag{B87}$$

and by further contractions,

$$\int \tilde{c}_i \tilde{c}_j \tilde{c}_k \tilde{c}^2 (\tilde{\boldsymbol{c}} \cdot \boldsymbol{q}) \phi^{(0)} d^3\tilde{c} = 7(\delta_{ij}\vec{q}_k + \delta_{jk}\vec{q}_i + \delta_{ki}\vec{q}_j) = 7[\bar{\bar{\boldsymbol{I}}}\boldsymbol{q}]^S_{ijk}; \tag{B88}$$

$$\int \tilde{c}_i \tilde{c}_j \tilde{c}_k \left(1 - \frac{\tilde{c}^2}{5}\right)(\tilde{\boldsymbol{c}} \cdot \boldsymbol{q}) \phi^{(0)} d^3\tilde{c} = -\frac{2}{5}[\bar{\bar{\boldsymbol{I}}}\boldsymbol{q}]^S_{ijk}. \tag{B89}$$

As a quick double-check of the above results, by performing the further contractions

$$\int \tilde{c}_i \tilde{c}^2 (\tilde{\boldsymbol{c}} \cdot \boldsymbol{q}) \phi^{(0)} d^3\tilde{c} = 5\vec{q}_i; \qquad \int \tilde{c}_i \tilde{c}^4 (\tilde{\boldsymbol{c}} \cdot \boldsymbol{q}) \phi^{(0)} d^3\tilde{c} = 35\vec{q}_i, \tag{B90}$$

which is easy to verify directly.

Similarly, for a triple contraction with any fully symmetric third-rank tensor $\bar{\bar{\bar{\boldsymbol{q}}}}$:

$$\int \tilde{c}_i \tilde{c}_j \tilde{c}_k (\tilde{\boldsymbol{c}}\tilde{\boldsymbol{c}} : \bar{\bar{\bar{\boldsymbol{q}}}} \cdot \tilde{\boldsymbol{c}}) \phi^{(0)} d^3\tilde{c} = 6(q_{ijk} + \vec{q}_i \delta_{jk} + \vec{q}_j \delta_{ik} + \vec{q}_k \delta_{ij}); \tag{B91}$$

$$\int \tilde{c}_i \tilde{c}^2 (\tilde{\boldsymbol{c}}\tilde{\boldsymbol{c}} : \bar{\bar{\bar{\boldsymbol{q}}}} \cdot \tilde{\boldsymbol{c}}) \phi^{(0)} d^3\tilde{c} = 42\vec{q}_i, \tag{B92}$$

where one defines vector $\boldsymbol{q} = (1/2)\mathrm{Tr}\,\bar{\bar{\boldsymbol{q}}}$. Finally, for any (3×3) matrix $\bar{\bar{\boldsymbol{A}}}$:

$$\int \tilde{c}_i\tilde{c}_j(\tilde{\boldsymbol{c}}\tilde{\boldsymbol{c}}\colon \bar{\bar{\boldsymbol{A}}})\phi^{(0)}d^3\tilde{c} = A_{ij} + A_{ji} + (\mathrm{Tr}\bar{\bar{\boldsymbol{A}}})\delta_{ij}; \tag{B93}$$

$$\begin{aligned}\int \tilde{c}_{r_1}\tilde{c}_{r_2}\tilde{c}_{r_3}\tilde{c}_{s_1}(\tilde{\boldsymbol{c}}\tilde{\boldsymbol{c}}\colon \bar{\bar{\boldsymbol{A}}})\phi^{(0)}d^3\tilde{c} &= \delta_{r_1s_1}(A_{r_2r_3} + A_{r_3r_2})\\ &+\delta_{r_2s_1}(A_{r_1r_3} + A_{r_3r_1}) + \delta_{r_3s_1}(A_{r_1r_2} + A_{r_2r_1})\\ &+\delta_{r_1r_2}(A_{r_3s_1} + A_{s_1r_3} + (\mathrm{Tr}\bar{\bar{\boldsymbol{A}}})\delta_{r_3s_1})\\ &+\delta_{r_1r_3}(A_{r_2s_1} + A_{s_1r_2} + (\mathrm{Tr}\bar{\bar{\boldsymbol{A}}})\delta_{r_2s_1})\\ &+\delta_{r_2r_3}(A_{r_1s_1} + A_{s_1r_1} + (\mathrm{Tr}\bar{\bar{\boldsymbol{A}}})\delta_{r_1s_1}),\end{aligned} \tag{B94}$$

and by further contractions,

$$\int \tilde{c}^2(\tilde{\boldsymbol{c}}\tilde{\boldsymbol{c}}\colon \bar{\bar{\boldsymbol{A}}})\phi^{(0)}d^3\tilde{c} = 5\,\mathrm{Tr}\bar{\bar{\boldsymbol{A}}}; \tag{B95}$$

$$\int \tilde{c}_i\tilde{c}_j\tilde{c}^2(\tilde{\boldsymbol{c}}\tilde{\boldsymbol{c}}\colon \bar{\bar{\boldsymbol{A}}})\phi^{(0)}d^3\tilde{c} = 7(A_{ij} + A_{ji} + (\mathrm{Tr}\bar{\bar{\boldsymbol{A}}})\delta_{ij}); \tag{B96}$$

$$\int \tilde{c}^4(\tilde{\boldsymbol{c}}\tilde{\boldsymbol{c}}\colon \bar{\bar{\boldsymbol{A}}})\phi^{(0)}d^3\tilde{c} = 35\,\mathrm{Tr}\bar{\bar{\boldsymbol{A}}}, \tag{B97}$$

and so for symmetric traceless matrix $\bar{\bar{\boldsymbol{\Pi}}}$:

$$\int \tilde{c}_i\tilde{c}_j(\tilde{\boldsymbol{c}}\tilde{\boldsymbol{c}}\colon \bar{\bar{\boldsymbol{\Pi}}})\phi^{(0)}d^3\tilde{c} = 2\Pi_{ij}; \tag{B98}$$

$$\int \tilde{c}_i\tilde{c}_j\tilde{c}^2(\tilde{\boldsymbol{c}}\tilde{\boldsymbol{c}}\colon \bar{\bar{\boldsymbol{\Pi}}})\phi^{(0)}d^3\tilde{c} = 14\Pi_{ij}; \tag{B99}$$

$$\begin{aligned}&\int \tilde{c}_i\tilde{c}_j\tilde{c}_k\tilde{c}_l(\tilde{\boldsymbol{c}}\tilde{\boldsymbol{c}}\colon \bar{\bar{\boldsymbol{\Pi}}})\phi^{(0)}d^3\tilde{c}\\ &\quad=2(\delta_{ij}\Pi_{kl} + \delta_{ik}\Pi_{jl} + \delta_{il}\Pi_{jk} + \delta_{jk}\Pi_{il} + \delta_{jl}\Pi_{ik} + \delta_{kl}\Pi_{ij}).\end{aligned} \tag{B100}$$

A curious reader might find the following integrals useful:

$$\begin{aligned}&\int \tilde{c}_i\tilde{c}_j\tilde{c}_k\tilde{c}_l\tilde{c}^2\phi^{(0)}d^3\tilde{c} = 7[\delta_{ij}\delta_{kl} + \delta_{ik}\delta_{jl} + \delta_{il}\delta_{jk}];\\ &\int \tilde{c}_i\tilde{c}_j\tilde{c}_k\tilde{c}_l(\tilde{c}^2 - 7)\phi^{(0)}d^3\tilde{c} = 0;\\ &\int \tilde{c}_i\tilde{c}_j(\tilde{c}^2 - 5)\phi^{(0)}d^3\tilde{c} = 0;\\ &\int (\tilde{c}^2 - 3)\phi^{(0)}d^3\tilde{c} = 0.\end{aligned} \tag{B101}$$

B.7. General n*th-order Perturbation*

The hierarchy of the simplified *reducible* Hermite polynomials (with tilde) can be calculated directly from (B3) as

$$\begin{aligned}&\tilde{H}_i^{(1)} = \tilde{c}_i;\\ &\tilde{H}_{ij}^{(2)} = \tilde{c}_i\tilde{c}_j - \delta_{ij};\\ &\tilde{H}_i^{(3)} = \tilde{c}_i(\tilde{c}^2 - 5);\\ &\tilde{H}_{ij}^{(4)} = \tilde{c}_i\tilde{c}_j(\tilde{c}^2 - 7) - \delta_{ij}(\tilde{c}^2 - 5);\\ &\tilde{H}_i^{(5)} = \tilde{c}_i(\tilde{c}^4 - 14\tilde{c}^2 + 35);\\ &\tilde{H}_{ij}^{(6)} = \tilde{c}_i\tilde{c}_j(\tilde{c}^4 - 18\tilde{c}^2 + 63) - \delta_{ij}(\tilde{c}^4 - 14\tilde{c}^2 + 35);\\ &\tilde{H}_i^{(7)} = \tilde{c}_i(\tilde{c}^6 - 27\tilde{c}^4 + 189\tilde{c}^2 - 315);\\ &\tilde{H}_{ij}^{(8)} = \tilde{c}_i\tilde{c}_j(\tilde{c}^6 - 33\tilde{c}^4 + 297\tilde{c}^2 - 693) - \delta_{ij}(\tilde{c}^6 - 27\tilde{c}^4 + 189\tilde{c}^2 - 315);\\ &\tilde{H}_i^{(9)} = \tilde{c}_i(\tilde{c}^8 - 44\tilde{c}^6 + 594\tilde{c}^4 - 2772\tilde{c}^2 + 3465),\end{aligned} \tag{B102}$$

and the fully contracted ones for the even orders are

$$\begin{aligned}
\tilde{H}^{(2)} &= \tilde{c}^2 - 3;\\
\tilde{H}^{(4)} &= \tilde{c}^4 - 10\tilde{c}^2 + 15;\\
\tilde{H}^{(6)} &= \tilde{c}^6 - 21\tilde{c}^4 + 105\tilde{c}^2 - 105;\\
\tilde{H}^{(8)} &= \tilde{c}^8 - 36\tilde{c}^6 + 378\tilde{c}^4 - 1260\tilde{c}^2 + 945.
\end{aligned} \tag{B103}$$

The even order polynomials $\tilde{H}_{ij}^{(2n)}$ can be rewritten into

$$\begin{aligned}
\tilde{H}_{ij}^{(2)} &= \left(\tilde{c}_i\tilde{c}_j - \frac{\delta_{ij}}{3}\tilde{c}^2\right) + \frac{\delta_{ij}}{3}\tilde{H}^{(2)};\\
\tilde{H}_{ij}^{(4)} &= \left(\tilde{c}_i\tilde{c}_j - \frac{\delta_{ij}}{3}\tilde{c}^2\right)(\tilde{c}^2 - 7) + \frac{\delta_{ij}}{3}\tilde{H}^{(4)};\\
\tilde{H}_{ij}^{(6)} &= \left(\tilde{c}_i\tilde{c}_j - \frac{\delta_{ij}}{3}\tilde{c}^2\right)(\tilde{c}^4 - 18\tilde{c}^2 + 63) + \frac{\delta_{ij}}{3}\tilde{H}^{(6)};\\
\tilde{H}_{ij}^{(8)} &= \left(\tilde{c}_i\tilde{c}_j - \frac{\delta_{ij}}{3}\tilde{c}^2\right)(\tilde{c}^6 - 33\tilde{c}^4 + 297\tilde{c}^2 - 693) + \frac{\delta_{ij}}{3}\tilde{H}^{(8)}.
\end{aligned} \tag{B104}$$

The orthogonality relations can be calculated as

$$\begin{aligned}
&\int \phi^{(0)}\tilde{H}_i^{(1)}\tilde{H}_j^{(1)}d^3\tilde{c} = \delta_{ij}; \qquad \int \phi^{(0)}\tilde{H}^{(2)}\tilde{H}^{(2)}d^3\tilde{c} = 6;\\
&\int \phi^{(0)}\tilde{H}_i^{(3)}\tilde{H}_j^{(3)}d^3\tilde{c} = 10\delta_{ij}; \qquad \int \phi^{(0)}\tilde{H}^{(4)}\tilde{H}^{(4)}d^3\tilde{c} = 120;\\
&\int \phi^{(0)}\tilde{H}_i^{(5)}\tilde{H}_j^{(5)}d^3\tilde{c} = 280\delta_{ij}; \qquad \int \phi^{(0)}\tilde{H}^{(6)}\tilde{H}^{(6)}d^3\tilde{c} = 5040;\\
&\int \phi^{(0)}\tilde{H}_i^{(7)}\tilde{H}_j^{(7)}d^3\tilde{c} = 15120\delta_{ij}; \qquad \int \phi^{(0)}\tilde{H}^{(8)}\tilde{H}^{(8)}d^3\tilde{c} = 362880;\\
&\int \phi^{(0)}\tilde{H}_i^{(9)}\tilde{H}_j^{(9)}d^3\tilde{c} = 1330560\delta_{ij},
\end{aligned} \tag{B105}$$

together with

$$\begin{aligned}
&\hat{h}_{kl}^{(2)}\int \phi^{(0)}\tilde{H}_{ij}^{(2)}\tilde{H}_{kl}^{(2)}d^3\tilde{c} = 2\tilde{h}_{ij}^{(2)}; \qquad \hat{h}_{kl}^{(4)}\int \phi^{(0)}\tilde{H}_{ij}^{(4)}\tilde{H}_{kl}^{(4)}d^3\tilde{c} = 28\hat{h}_{ij}^{(4)};\\
&\hat{h}_{kl}^{(6)}\int \phi^{(0)}\tilde{H}_{ij}^{(6)}\tilde{H}_{kl}^{(6)}d^3\tilde{c} = 1008\hat{h}_{ij}^{(6)}; \qquad \hat{h}_{kl}^{(8)}\int \phi^{(0)}\tilde{H}_{ij}^{(8)}\tilde{H}_{kl}^{(8)}d^3\tilde{c} = 66528\hat{h}_{ij}^{(8)},
\end{aligned} \tag{B106}$$

where we used traceless Hermite moments (with hat):

$$\hat{h}_{ij}^{(2n)} = \tilde{h}_{ij}^{(2n)} - \frac{1}{3}\delta_{ij}\tilde{h}^{(2n)}, \tag{B107}$$

with $\tilde{h}^{(2)} = 0$ (so that $\hat{h}_{ij}^{(2)} = \tilde{h}_{ij}^{(2)}$). The perturbation of the distribution function then becomes

$$\begin{aligned}
\chi_a = &\frac{1}{2}\tilde{h}_{ij}^{(2)}\tilde{H}_{ij}^{(2)} + \frac{1}{10}\tilde{h}_i^{(3)}\tilde{H}_i^{(3)} + \frac{1}{28}\hat{h}_{ij}^{(4)}\tilde{H}_{ij}^{(4)} + \frac{1}{120}\tilde{h}^{(4)}\tilde{H}^{(4)} + \frac{1}{280}\tilde{h}_i^{(5)}\tilde{H}_i^{(5)}\\
&+\frac{1}{1008}\hat{h}_{ij}^{(6)}\tilde{H}_{ij}^{(6)} + \frac{1}{5040}\tilde{h}^{(6)}\tilde{H}^{(6)} + \frac{1}{15120}\tilde{h}_i^{(7)}\tilde{H}_i^{(7)}\\
&+\frac{1}{66528}\hat{h}_{ij}^{(8)}\tilde{H}_{ij}^{(8)} + \frac{1}{362880}\tilde{h}^{(8)}\tilde{H}^{(8)} + \frac{1}{1330560}\tilde{h}_i^{(9)}\tilde{H}_i^{(9)} + \cdots .
\end{aligned} \tag{B108}$$

The corresponding perturbation with the irreducible polynomials reads

$$\begin{aligned}
\chi_a = &h_{ij}^{(2)}H_{ij}^{(2)} + h_i^{(3)}H_i^{(3)} + h_{ij}^{(4)}H_{ij}^{(4)} + h^{(4)}H^{(4)} + h_i^{(5)}H_i^{(5)}\\
&+ h_{ij}^{(6)}H_{ij}^{(6)} + h^{(6)}H^{(6)} + h_i^{(7)}H_i^{(7)} + h_{ij}^{(8)}H_{ij}^{(8)} + h^{(8)}H^{(8)} + h_i^{(9)}H_i^{(9)} + \cdots ,
\end{aligned} \tag{B109}$$

i.e., no normalization constants are explicitly present. Now one can clearly see the motivation behind the definition of irreducible polynomials of Balescu (1988), where the direct relation between irreducible (no tilde) and reducible (tilde) Hermite polynomials can

be shown to be

$$H^{(2n)} = \left(\frac{1}{2^n n!(2n+1)!!}\right)^{1/2} \tilde{H}^{(2n)};$$
$$H_i^{(2n+1)} = \left(\frac{3}{2^n n!(2n+3)!!}\right)^{1/2} \tilde{H}_i^{(2n+1)};$$
$$H_{ij}^{(2n)} = \left(\frac{15}{2^n (n-1)!(2n+3)!!}\right)^{1/2} \left(\tilde{H}_{ij}^{(2n)} - \frac{1}{3}\delta_{ij}\tilde{H}^{(2n)}\right). \tag{B110}$$

Up to the normalization constants (which can be viewed as coming from the orthogonality relations), the scalar and vector polynomials are equivalent to each other. The only difference is for the matrices $H_{ij}^{(2n)}$, where the irreducible polynomials are defined as traceless. Multiplying (B110) by f_a/n_a and integrating over d^3c yields analogous relations for the Hermite moments:

$$h^{(2n)} = \left(\frac{1}{2^n n!(2n+1)!!}\right)^{1/2} \tilde{h}^{(2n)};$$
$$h_i^{(2n+1)} = \left(\frac{3}{2^n n!(2n+3)!!}\right)^{1/2} \tilde{h}_i^{(2n+1)};$$
$$h_{ij}^{(2n)} = \left(\frac{15}{2^n (n-1)!(2n+3)!!}\right)^{1/2} \underbrace{(\tilde{h}_{ij}^{(2n)} - \frac{1}{3}\delta_{ij}\tilde{h}^{(2n)})}_{\hat{h}_{ij}^{(2n)}}. \tag{B111}$$

Importantly, because $\hat{h}_{ij}^{(2n)}$ is traceless, multiplying (B110) and (B111) yields

$$h_{ij}^{(2n)} H_{ij}^{(2n)} = \frac{15}{2^n (n-1)!(2n+3)!!}\, \hat{h}_{ij}^{(2n)} \tilde{H}_{ij}^{(2n)}. \tag{B112}$$

The two approaches, with reducible and irreducible polynomials, thus yield the same result, with the only difference being the location of the normalization constants. Furthermore, it feels natural to define traceless polynomials (with hat instead of tilde):

$$\hat{H}_{ij}^{(2n)} = \tilde{H}_{ij}^{(2n)} - \frac{1}{3}\delta_{ij}\tilde{H}^{(2n)}, \tag{B113}$$

and on the right-hand side of (B112) replace

$$\hat{h}_{ij}^{(2n)} \tilde{H}_{ij}^{(2n)} = \hat{h}_{ij}^{(2n)} \hat{H}_{ij}^{(2n)}, \tag{B114}$$

which holds because $\hat{h}_{ij}^{(2n)}$ is traceless. The main advantage of introducing the polynomials $\hat{H}_{ij}^{(2n)}$ is that, instead of calculating $\hat{h}_{ij}^{(2n)}$ from its definition (B107), one can directly define

$$\hat{h}_{ij}^{(2n)} = \frac{1}{n_a}\int f_a \hat{H}_{ij}^{(2n)} d^3c. \tag{B115}$$

Then the two approaches are indeed equivalent, because the same polynomials are used, with the location of the normalization constants being an ad hoc choice.

From the Appendix of Balescu (1988), one can guess and then verify the following generalizations for the reducible polynomials:

$$\tilde{H}^{(2n)} = \sum_{m=0}^{n} (-1)^{m+n} \frac{n!}{m!(n-m)!} \frac{(2n+1)!!}{(2m+1)!!} \tilde{c}^{2m}; \tag{B116}$$

$$\tilde{H}_i^{(2n+1)} = \tilde{c}_i \sum_{m=0}^{n} (-1)^{m+n} \frac{n!}{m!(n-m)!} \frac{(2n+3)!!}{(2m+3)!!} \tilde{c}^{2m}; \tag{B117}$$

$$\begin{aligned}\tilde{H}_{ij}^{(2n)} &= \tilde{c}_i\tilde{c}_j \left(\sum_{m=0}^{n-1} (-1)^{m+n-1} \frac{(n-1)!}{m!(n-m-1)!} \frac{(2n+3)!!}{(2m+5)!!} \tilde{c}^{2m}\right) - \delta_{ij} \frac{\tilde{H}_k^{(2n-1)}}{\tilde{c}_k} \\ &= \left(\tilde{c}_i\tilde{c}_j - \frac{\delta_{ij}}{3}\tilde{c}^2\right)\left(\sum_{m=0}^{n-1} (-1)^{m+n-1} \frac{(n-1)!}{m!(n-m-1)!} \frac{(2n+3)!!}{(2m+5)!!} \tilde{c}^{2m}\right) + \frac{\delta_{ij}}{3}\tilde{H}^{(2n)};\end{aligned} \tag{B118}$$

$$\hat{H}_{ij}^{(2n)} = \left(\tilde{c}_i\tilde{c}_j - \frac{\delta_{ij}}{3}\tilde{c}^2\right)\left(\sum_{m=0}^{n-1} (-1)^{m+n-1} \frac{(n-1)!}{m!(n-m-1)!} \frac{(2n+3)!!}{(2m+5)!!} \tilde{c}^{2m}\right). \tag{B119}$$

Applying a trace at (B118) yields (B116). Similarly, the orthogonal relations are

$$\int \phi^{(0)} \tilde{H}^{(2n)} \tilde{H}^{(2m)} d^3\tilde{c} = 2^n n!(2n+1)!!\ \delta_{nm}; \tag{B120}$$

$$\int \phi^{(0)} \tilde{H}_i^{(2n+1)} \tilde{H}_j^{(2m+1)} d^3\tilde{c} = \frac{2^n n!(2n+3)!!}{3}\ \delta_{ij}\delta_{nm}; \tag{B121}$$

$$\int \phi^{(0)} \tilde{H}_{ij}^{(2n)} \tilde{H}_{kl}^{(2m)} d^3\tilde{c} = \frac{2^{n-1}(n-1)!(2n+1)!!}{15}[(2n+3)(\delta_{ik}\delta_{jl}+\delta_{il}\delta_{jk})+2(n-1)\delta_{ij}\delta_{kl}]\delta_{nm}; \tag{B122}$$

$$\int \phi^{(0)} \hat{H}_{ij}^{(2n)} \hat{H}_{kl}^{(2m)} d^3\tilde{c} = \frac{2^{n-1}(n-1)!(2n+3)!!}{15}\left[\delta_{ik}\delta_{jl}+\delta_{il}\delta_{jk}-\frac{2}{3}\delta_{ij}\delta_{kl}\right]\delta_{nm}, \tag{B123}$$

and applying $\delta_{ij}\delta_{kl}$ on (B122) recovers (B120). Note that the orders of the Hermite moments "m" and "n" are one-dimensional and $\delta_{nn}=1$. In contrast, for the indices, $\delta_{ii}=3$ applies. Also note that $n!=n!!(n-1)!!$ and $2^n n!=(2n)!!$, implying $2^n n!(2n+1)!!=(2n+1)!$. Applying traceless $\hat{h}_{kl}^{(2n)}$ on (B122) or (B123) yields the orthogonal relation

$$\begin{aligned}\hat{h}_{kl}^{(2n)} \int \phi^{(0)} \hat{H}_{ij}^{(2n)} \hat{H}_{kl}^{(2n)} d^3\tilde{c} &= \hat{h}_{kl}^{(2n)} \int \phi^{(0)} \tilde{H}_{ij}^{(2n)} \tilde{H}_{kl}^{(2n)} d^3\tilde{c} \\ &= \frac{2^n(n-1)!(2n+3)!!}{15}\hat{h}_{ij}^{(2n)}.\end{aligned} \tag{B124}$$

Finally, the general perturbation then can be written as

$$\begin{aligned}\chi_a = \sum_{n=1}^{\infty}\Bigg[&\frac{15}{2^n(n-1)!(2n+3)!!}\hat{h}_{ij}^{(2n)}\hat{H}_{ij}^{(2n)} + \frac{1}{2^n n!(2n+1)!!}\tilde{h}^{(2n)}\tilde{H}^{(2n)} \\ &+\frac{3}{2^n n!(2n+3)!!}\tilde{h}_i^{(2n+1)}\tilde{H}_i^{(2n+1)}\Bigg],\end{aligned} \tag{B125}$$

where for the first term $\tilde{h}^{(2)}=0$ (and so $\hat{h}_{ij}^{(2)}=\tilde{h}_{ij}^{(2)}$). Alternatively, $\hat{h}_{ij}^{(2n)}\hat{H}_{ij}^{(2n)}=\hat{h}_{ij}^{(2n)}\tilde{H}_{ij}^{(2n)}$. The perturbation (B125) is equivalent to a perturbation with irreducible polynomials:

$$\chi_a = \sum_{n=1}^{\infty}[h_{ij}^{(2n)}H_{ij}^{(2n)} + h^{(2n)}H^{(2n)} + h_i^{(2n+1)}H_i^{(2n+1)}], \tag{B126}$$

where again $h^{(2)}=0$.

B.8. Hierarchy of MHD Hermite Closures

Let us use the third-order moment $X_i^{(3)}=2q_i$ instead of the heat flux, so that no additional factors are present (also note that $X^{(2)}=3p$). The even order moments are decomposed according to

$$X_{ij}^{(2n)} = \frac{\delta_{ij}}{3}X^{(2n)} + \Pi_{ij}^{(2n)}, \tag{B127}$$

where the scalar part $X^{(2n)}$ is further decomposed into its Maxwellian "core" and perturbation $\widetilde{X}^{(2n)}$ (with wide tilde), as

$$X^{(2n)} = (2n+1)!!\,\frac{p^n}{\rho^{n-1}} + \widetilde{X}^{(2n)}, \tag{B128}$$

so, for example,

$$X^{(4)} = 15\frac{p^2}{\rho} + \widetilde{X}^{(4)}; \qquad X^{(6)} = 105\frac{p^3}{\rho^2} + \widetilde{X}^{(6)}; \qquad X^{(8)} = 945\frac{p^4}{\rho^3} + \widetilde{X}^{(8)}. \tag{B129}$$

Then, by using the Hermite polynomials (B102)–(B104), one calculates the hierarchy of the Hermite moments:

$$\begin{aligned}
\tilde{h}_i^{(3)} &= \frac{\rho^{1/2}}{p^{3/2}} X_i^{(3)}; \qquad \tilde{h}^{(4)} = \frac{\rho}{p}\widetilde{X}^{(4)};\\
\tilde{h}_i^{(5)} &= \frac{\rho^{1/2}}{p^{3/2}}\left[\frac{\rho}{p}X_i^{(5)} - 14X_i^{(3)}\right]; \qquad \tilde{h}^{(6)} = \frac{\rho}{p^2}\left[\frac{\rho}{p}\widetilde{X}^{(6)} - 21\widetilde{X}^{(4)}\right];\\
\tilde{h}_i^{(7)} &= \frac{\rho^{1/2}}{p^{3/2}}\left[\frac{\rho^2}{p^2}X_i^{(7)} - 27\frac{\rho}{p}X_i^{(5)} + 189X_i^{(3)}\right];\\
\tilde{h}^{(8)} &= \frac{\rho}{p^2}\left[\frac{\rho^2}{p^2}\widetilde{X}^{(8)} - 36\frac{\rho}{p}\widetilde{X}^{(6)} + 378\widetilde{X}^{(4)}\right];\\
\tilde{h}_i^{(9)} &= \frac{\rho^{1/2}}{p^{3/2}}\left[\frac{\rho^3}{p^3}X_i^{(9)} - 44\frac{\rho^2}{p^2}X_i^{(7)} + 594\frac{\rho}{p}X_i^{(5)} - 2772X_i^{(3)}\right],
\end{aligned} \tag{B130}$$

together with

$$\begin{aligned}
\hat{h}_{ij}^{(4)} &= \frac{1}{p}\left[\frac{\rho}{p}\Pi_{ij}^{(4)} - 7\Pi_{ij}^{(2)}\right];\\
\hat{h}_{ij}^{(6)} &= \frac{1}{p}\left[\frac{\rho^2}{p^2}\Pi_{ij}^{(6)} - 18\frac{\rho}{p}\Pi_{ij}^{(4)} + 63\Pi_{ij}^{(2)}\right];\\
\hat{h}_{ij}^{(8)} &= \frac{1}{p}\left[\frac{\rho^3}{p^3}\Pi_{ij}^{(8)} - 33\frac{\rho^2}{p^2}\Pi_{ij}^{(6)} + 297\frac{\rho}{p}\Pi_{ij}^{(4)} - 693\Pi_{ij}^{(2)}\right].
\end{aligned} \tag{B131}$$

Prescribing the last retained Hermite moment to be zero then yields the corresponding fluid closures that are summarized in Section 8.6, Tables 3 and 4.

B.8.1. Propagation along the B*-field (Ion-acoustic Mode)*

For a propagation parallel to the mean magnetic field that is applied in the z-direction, linearized equations without collisions read

$$\begin{aligned}
&\frac{\partial \rho}{\partial t} + \rho_0 \partial_z u_z = 0; \qquad \frac{\partial u_z}{\partial t} + \frac{1}{\rho_0}\partial_z p = 0;\\
&\frac{\partial p}{\partial t} + \frac{5}{3}p_0\partial_z u_z + \frac{2}{3}\partial_z q_z = 0;\\
&\frac{\partial q_z}{\partial t} + \frac{1}{6}\partial_z X^{(4)} - \frac{5}{2}\frac{p_0}{\rho_0}\partial_z p = 0;\\
&\frac{\partial X^{(4)}}{\partial t} + \partial_z X_z^{(5)} + \frac{7}{3}X_0^{(4)}\partial_z u_z = 0;\\
&\frac{\partial X_z^{(5)}}{\partial t} + \frac{1}{3}\partial_z X^{(6)} - \frac{7}{3}\frac{X_0^{(4)}}{\rho_0}\partial_z p = 0,
\end{aligned} \tag{B132}$$

where all of the variables are scalars. We are neglecting collisions and viscosities, to make direct comparison with the CGL model in the next section. The even order moments are decomposed into a Maxwellian "core" and tilde perturbations with (B129), so that their mean values are $X_0^{(4)} = 15p_0^2/\rho_0$ and $X_0^{(6)} = 105p_0^3/\rho_0^2$. These moments are thus linearized according to

$$X^{(4)} \overset{\text{lin.}}{=} X_0^{(4)}\left(2\frac{p}{p_0} - \frac{\rho}{\rho_0}\right) + \widetilde{X}^{(4)}; \qquad X^{(6)} \overset{\text{lin.}}{=} X_0^{(6)}\left(3\frac{p}{p_0} - 2\frac{\rho}{\rho_0}\right) + \widetilde{X}^{(6)}, \tag{B133}$$

Table 5
Summary of the Hermite Closures and Corresponding Dispersion Relations for the Parallel Propagating Ion-acoustic Mode (Electrons Are Cold), Where $\zeta = \omega/(|k_\parallel| v_{\rm th})$

Closure	Dispersion Relation	Solution $\pm\zeta =$
$\tilde{h}_z^{(3)} = 0$	$\zeta^2 - 5/6 = 0$	0.913
$\tilde{h}^{(4)} = 0$	$\zeta^4 - (5/3)\zeta^2 + (5/12) = 0$	0.553; 1.166
$\tilde{h}_z^{(5)} = 0$	$\zeta^4 - (7/3)\zeta^2 + (35/36) = 0$	0.737; 1.338
$\tilde{h}^{(6)} = 0$	$\zeta^6 - (7/2)\zeta^4 + (35/12)\zeta^2 - (35/72) = 0$	0.471; 0.966; 1.531
$X_z^{(5)} = 0$	$\zeta^4 - (35/36) = 0$	0.99; 0.99 i
$\widetilde{X}^{(6)} = 0$	$\zeta^6 - (35/12)\zeta^2 + (35/36) = 0$	0.59; 1.23; 1.36 i

Note. With the Hermite closures (the upper half of the table), no spurious instabilities are present. Unphysical instabilities appear if one prescribes erroneous fluid closures at the last retained moment $X_z^{(5)} = 0$ or $\widetilde{X}^{(6)} = 0$ (the lower half of the table). However, if one prescribes at the same time, $\widetilde{X}^{(6)} = 0$ and $\widetilde{X}^{(4)} = 0$, the system is again well defined, with a dispersion relation equivalent to the closure $\tilde{h}^{(4)} = 0$.

and the last three equations of (B132) then become

$$\frac{\partial q_z}{\partial t} + \frac{1}{6}\partial_z \widetilde{X}^{(4)} + \frac{5}{2}\frac{p_0}{\rho_0}\left(\partial_z p - \frac{p_0}{\rho_0}\partial_z \rho\right) = 0;$$
$$\frac{\partial \widetilde{X}^{(4)}}{\partial t} + \partial_z X_z^{(5)} - 20\frac{p_0}{\rho_0}\partial_z q_z = 0;$$
$$\frac{\partial X_z^{(5)}}{\partial t} + \frac{1}{3}\partial_z \widetilde{X}^{(6)} + 70\frac{p_0^2}{\rho_0^2}\left(\partial_z p - \frac{p_0}{\rho_0}\partial_z \rho\right) = 0. \tag{B134}$$

Prescribing a closure at the last retained moment yields the dispersion relations in the variable $\zeta = \omega/(|k_\parallel| v_{\rm th})$ that are summarized in Table 5.

The example clearly demonstrates that Landau fluid closures are actually *not* required to go beyond the fourth-order moment, which contradicts a claim in the last paragraph of Hunana et al. (2018) and also claims in various parts of Hunana et al. (2019a, 2019b; see, e.g., Section 12.2 in Part 1). Obviously, the closures $X_z^{(5)} = 0$ or $\widetilde{X}^{(6)} = 0$ are not allowed by the fluid hierarchy (unless $q_z = 0$ or $\widetilde{X}^{(4)} = 0$ as well). Instead, for moments of order $n \geqslant 5$, one needs to construct "classical" closures at the Hermite moments. Nevertheless, all of the Landau fluid closures reported in the above papers are constructed correctly.

Out of curiosity, prescribing closures with a free parameter "a" as $X_z^{(5)} = 28a(p_0/\rho_0)q_z$ or $\widetilde{X}^{(6)} = 21a(p_0/\rho_0)\widetilde{X}^{(4)}$ yields the following dispersion relations:

$$\zeta^4 - \frac{7a}{3}\zeta^2 + \frac{35a}{18} - \frac{35}{36} = 0; \tag{B135}$$

$$\zeta^6 - \frac{7a}{2}\zeta^4 + \left(\frac{35a}{6} - \frac{35}{12}\right)\zeta^2 - \frac{35a}{24} + \frac{35}{36} = 0. \tag{B136}$$

The $X_z^{(5)}$ closure with dispersion relation (B135) yields an instability for $a < 1/2$, and the $\widetilde{X}^{(6)}$ closure with (B136) yields an instability for $a < 2/3$. There are therefore a lot of closures that do not create these unphysical instabilities.

Finally, the situation is saved by completely decoupling the odd and even moments, prescribing $\widetilde{X}^{(6)} = \widetilde{X}^{(4)} = 0$, for example, so that Equations (B134) are replaced by

$$\frac{\partial q_z}{\partial t} + \frac{5}{2}\frac{p_0}{\rho_0}\left(\partial_z p - \frac{p_0}{\rho_0}\partial_z \rho\right) = 0;$$
$$\frac{\partial X_z^{(5)}}{\partial t} + 70\frac{p_0^2}{\rho_0^2}\left(\partial_z p - \frac{p_0}{\rho_0}\partial_z \rho\right) = 0. \tag{B137}$$

The dispersion relation of this model is equivalent to the closure $\tilde{h}^{(4)} = 0$.

B.9. Hierarchy of CGL (Parallel) Hermite Closures

The hierarchy of one-dimensional Hermite polynomials calculates (with weight $\exp(-\tilde{c}^2/2)$)

$$\begin{aligned}
H^{(1)} &= \tilde{c};\\
H^{(2)} &= \tilde{c}^2 - 1;\\
H^{(3)} &= \tilde{c}(\tilde{c}^2 - 3);\\
H^{(4)} &= \tilde{c}^4 - 6\tilde{c}^2 + 3;\\
H^{(5)} &= \tilde{c}(\tilde{c}^4 - 10\tilde{c}^2 + 15);\\
H^{(6)} &= \tilde{c}^6 - 15\tilde{c}^4 + 45\tilde{c}^2 - 15;\\
H^{(7)} &= \tilde{c}(\tilde{c}^6 - 21\tilde{c}^4 + 105\tilde{c}^2 - 105);\\
H^{(8)} &= \tilde{c}^8 - 28\tilde{c}^6 + 210\tilde{c}^4 - 420\tilde{c}^2 + 105;\\
H^{(9)} &= \tilde{c}(\tilde{c}^8 - 36\tilde{c}^6 + 378\tilde{c}^4 - 1260\tilde{c}^2 + 945),
\end{aligned} \tag{B138}$$

further yielding the following hierarchy of Hermite moments:

$$\begin{aligned}
&h^{(1)} = 0; \qquad h^{(2)} = 0;\\
&h^{(3)} = \frac{\rho^{1/2}}{p^{3/2}} X^{(3)}; \qquad h^{(4)} = \frac{\rho}{p^2}\widetilde{X}^{(4)};\\
&h^{(5)} = \frac{\rho^{1/2}}{p^{3/2}}\left(\frac{\rho}{p}X^{(5)} - 10X^{(3)}\right); \qquad h^{(6)} = \frac{\rho}{p^2}\left(\frac{\rho}{p}\widetilde{X}^{(6)} - 15\widetilde{X}^{(4)}\right);\\
&h^{(7)} = \frac{\rho^{1/2}}{p^{3/2}}\left(\frac{\rho^2}{p^2}X^{(7)} - 21\frac{\rho}{p}X^{(5)} + 105X^{(3)}\right);\\
&h^{(8)} = \frac{\rho}{p^2}\left(\frac{\rho^2}{p^2}\widetilde{X}^{(8)} - 28\frac{\rho}{p}\widetilde{X}^{(6)} + 210\widetilde{X}^{(4)}\right);\\
&h^{(9)} = \frac{\rho^{1/2}}{p^{3/2}}\left(\frac{\rho^3}{p^3}X^{(9)} - 36\frac{\rho^2}{p^2}X^{(7)} + 378\frac{\rho}{p}X^{(5)} - 1260X^{(3)}\right),
\end{aligned} \tag{B139}$$

where the even moments were separated into

$$\begin{aligned}
&X^{(4)} = 3\frac{p^2}{\rho} + \widetilde{X}^{(4)}; \qquad X^{(6)} = 15\frac{p^3}{\rho^2} + \widetilde{X}^{(6)}; \qquad X^{(8)} = 105\frac{p^4}{\rho^3} + \widetilde{X}^{(8)};\\
&X^{(2n)} = (2n-1)!!\,\frac{p^n}{\rho^{n-1}} + \widetilde{X}^{(2n)}.
\end{aligned} \tag{B140}$$

This yields the hierarchy of Hermite closures summarized in Table 6. Note the difference between (B140) and the isotropic (MHD) decomposition (B128) (in the three-dimensional CGL geometry, one typically uses the notation $X^{(4)} = r_{\|\|}$).

Hermite polynomials (B138) can be written in a general form:

$$\begin{aligned}
H^{(2n+1)} &= \sum_{m=0}^{n}(-1)^{n-m}\frac{(2n+1)!}{2^{n-m}(2m+1)!(n-m)!}\tilde{c}^{2m+1};\\
H^{(2n)} &= \sum_{m=0}^{n}(-1)^{n-m}\frac{(2n)!}{2^{n-m}(2m)!(n-m)!}\tilde{c}^{2m}.
\end{aligned} \tag{B141}$$

Then it can be shown that prescribing the Hermite closure $h^{(2n+1)} = 0$ or $h^{(2n)} = 0$ is equivalent to prescribing the fluid closure

$$\begin{aligned}
X^{(2n+1)} &= \sum_{m=1}^{n-1}(-1)^{n-m+1}\frac{(2n+1)!}{2^{n-m}(2m+1)!(n-m)!}\left(\frac{p}{\rho}\right)^{n-m}X^{(2m+1)};\\
\widetilde{X}^{(2n)} &= \sum_{m=2}^{n-1}(-1)^{n-m+1}\frac{(2n)!}{2^{n-m}(2m)!(n-m)!}\left(\frac{p}{\rho}\right)^{n-m}\widetilde{X}^{(2m)}.
\end{aligned} \tag{B142}$$

By using Equations (12.49)–(12.54) from Hunana et al. (2019b), we calculate the corresponding dispersion relations, which are summarized in Table 7.

Table 6
Summary of Hermite Closures for Parallel CGL Moments, Together with Corresponding Fluid Closures

Hermite Closures	Fluid Closures
$h^{(3)}=0$	$X^{(3)}=0$
$h^{(4)}=0$	$\widetilde{X}^{(4)}=0$
$h^{(5)}=0$	$X^{(5)}=10\frac{p}{\rho}X^{(3)}$
$h^{(6)}=0$	$\widetilde{X}^{(6)}=15\frac{p}{\rho}\widetilde{X}^{(4)}$
$h^{(7)}=0$	$X^{(7)}=21\frac{p}{\rho}X^{(5)}-105\frac{p^2}{\rho^2}X^{(3)}$
$h^{(8)}=0$	$\widetilde{X}^{(8)}=28\frac{p}{\rho}\widetilde{X}^{(6)}-210\frac{p^2}{\rho^2}\widetilde{X}^{(4)}$
$h^{(9)}=0$	$X^{(9)}=36\frac{p}{\rho}X^{(7)}-378\frac{p^2}{\rho^2}X^{(5)}+1260\frac{p^3}{\rho^3}X^{(3)}$

Note. The usual parallel heat flux $q_{\parallel}=X^{(3)}$. Note that beyond the fourth-order moment, both classes start to differ. A general form corresponding to $h^{(2n+1)}=0$ and $h^{(2n)}=0$ is given by (B142).

Table 7
Summary of Hermite Closures and Corresponding Dispersion Relations for the Parallel Propagating Ion-acoustic Mode (Electrons Are Cold), Where $\zeta=\omega/(|k_{\parallel}|v_{\rm th})$

Closure	Dispersion Relation	Solution $\pm\zeta=$
$h^{(3)}=0$	$\zeta^2-3/2=0$	1.225
$h^{(4)}=0$	$\zeta^4-3\zeta^2+3/4=0$	0.525; 1.651
$h^{(5)}=0$	$\zeta^4-5\zeta^2+15/4=0$	0.959; 2.020
$h^{(6)}=0$	$\zeta^6-(15/2)\zeta^4+(45/4)\zeta^2-15/8=0$	0.436; 1.336; 2.351
$h^{(7)}=0$	$\zeta^6-(21/2)\zeta^4+(105/4)\zeta^2-105/8=0$	0.816; 1.674; 2.652
$h^{(8)}=0$	$\zeta^8-14\zeta^6+(105/2)\zeta^4-(105/2)\zeta^2+105/16=0$	0.381; 1.157; 1.982; 2.931
$h^{(9)}=0$	$\zeta^8-18\zeta^6+(189/2)\zeta^4-(315/2)\zeta^2+945/16=0$	0.724; 1.469; 2.267; 3.191

Note. No spurious instabilities are present. Spurious instabilities occur if one prescribes the closures $\widetilde{X}^{(2n)}=0$ or $X^{(2n+1)}=0$ at the last retained moment.

Curiously, from Hunana et al. (2019a), the not "well-behaved" Padé approximants of the plasma dispersion function $R(\zeta)$ that contain no Landau damping read

$$R_{4,5}(\zeta)=\frac{1-(2/3)\zeta^2}{1-4\zeta^2+(4/3)\zeta^4};$$
$$R_{6,9}(\zeta)=\frac{1-(8/5)\zeta^2+(4/15)\zeta^4}{1-6\zeta^2+4\zeta^4-(8/15)\zeta^6};$$
$$R_{8,13}(\zeta)=\frac{1-(94/35)\zeta^2+(20/21)\zeta^4-(8/105)\zeta^6}{1-8\zeta^2+8\zeta^4-(32/15)\zeta^6+(16/105)\zeta^8}. \tag{B143}$$

Comparing (B143) with Table 7, one comes to the nonobvious observation that the denominators of the above approximants are equal to the dispersion relations obtained with the Hermite closures $h^{(4)}=0$, $h^{(6)}=0$, and $h^{(8)}=0$. This observation is analogous to the Landau fluid closures when electrons are cold; see Equation (3.358) of Hunana et al. (2019a). Thus, it is expected that for proton–electron plasma with finite temperatures (and with electron inertia retained), these three dispersion relations will be equivalent to

$$\frac{T_{\parallel e}^{(0)}}{T_{\parallel p}^{(0)}}R_{n,n'}(\zeta_p)+R_{n,n'}(\zeta_e)=0, \tag{B144}$$

which we did not verify.

Appendix C
Evolution Equations for the 22-moment Model

Here we use evolution Equations (A4)–(A9), and by applying the contractions at these equations we obtain the 22-moment model in detail. The pressure tensor is decomposed as $p_{ij}^a=p_a\delta_{ij}+\Pi_{ij}^{a(2)}$, where the scalar pressure $p_a=p_{ii}^a/3$. Instead of considering the full moments $X_{ijk}^{(3)}$, $X_{ijkl}^{(4)}$, $X_{ijklm}^{(5)}$, and $X_{ijklmn}^{(6)}$, one only considers the contracted vectors and matrices

$$X_i^{a(3)}=X_{ijj}^{a(3)};\qquad X_{ij}^{a(4)}=X_{ijkk}^{a(4)};\qquad X_i^{a(5)}=X_{ijjkk}^{a(5)};\qquad X_{ij}^{a(6)}=X_{ijkkll}^{a(6)}. \tag{C1}$$

The even order moments are decomposed by separating the traceless viscosity tensors $\Pi_{ij}^{(2n)}$:

$$X_{ij}^{a(4)} = \frac{\delta_{ij}}{3} X^{a(4)} + \Pi_{ij}^{a(4)}; \qquad X_{ij}^{a(6)} = \frac{\delta_{ij}}{3} X^{a(6)} + \Pi_{ij}^{a(6)}, \tag{C2}$$

where the fully contracted (scalars) $X^{a(4)} = X_{iijj}^{a(4)}$, $X^{a(6)} = X_{iijjkk}^{a(6)}$. The scalars are further decomposed into their "Maxwellian core" and a perturbation around this core (which is denoted by wide tilde):

$$X_a^{(4)} = \mathrm{Tr}\mathrm{Tr}\bar{\bar{\boldsymbol{r}}}_a = 15\frac{p_a^2}{\rho_a} + \widetilde{\mathrm{X}}_a^{(4)}; \qquad \mathrm{X}_a^{(6)} = \mathrm{Tr}\mathrm{Tr}\mathrm{Tr}\bar{\bar{\boldsymbol{X}}}_a^{(6)} = 105\frac{p_a^3}{\rho_a^2} + \widetilde{\mathrm{X}}_a^{(6)}. \tag{C3}$$

As in Braginskii (1965), we use notation with the Boltzmann constant $k_{\mathrm{B}} = 1$, and the temperature is defined as $T_a = p_a/n_a$. Note that $m_a/T_a = \rho_a/p_a$.

C.1. Decomposition of Moments

The heat flux tensor q_{ijk} and moments $X_{ijkl}^{(4)}$, $X_{ijklm}^{(5)}$ are decomposed according to (see Appendix B)

$$q_{ijk}^a = \frac{2}{5}[\bar{\bar{\boldsymbol{I}}}\boldsymbol{q}^a]_{ijk}^S; \tag{C4}$$

$$\begin{aligned} X_{ijkl}^{a(4)} = &\frac{1}{15}\left(15\frac{p_a^2}{\rho_a} + \widetilde{X}^{a(4)}\right)(\delta_{ij}\delta_{kl} + \delta_{ik}\delta_{jl} + \delta_{il}\delta_{jk}) \\ &+\frac{1}{7}[\Pi_{ij}^{a(4)}\delta_{kl} + \Pi_{ik}^{a(4)}\delta_{jl} + \Pi_{il}^{a(4)}\delta_{jk} + \Pi_{jk}^{a(4)}\delta_{il} + \Pi_{jl}^{a(4)}\delta_{ik} + \Pi_{kl}^{a(4)}\delta_{ij}]; \end{aligned} \tag{C5}$$

$$\begin{aligned} X_{s_1s_2s_3s_4s_5}^{a(5)} = &\frac{1}{35}[X_{s_1}^{a(5)}(\delta_{s_2s_3}\delta_{s_4s_5} + \delta_{s_2s_4}\delta_{s_3s_5} + \delta_{s_2s_5}\delta_{s_3s_4}) \\ &+X_{s_2}^{a(5)}(\delta_{s_1s_3}\delta_{s_4s_5} + \delta_{s_1s_4}\delta_{s_3s_5} + \delta_{s_1s_5}\delta_{s_3s_4}) \\ &+X_{s_3}^{a(5)}(\delta_{s_1s_2}\delta_{s_4s_5} + \delta_{s_1s_4}\delta_{s_2s_5} + \delta_{s_1s_5}\delta_{s_2s_4}) \\ &+X_{s_4}^{a(5)}(\delta_{s_1s_2}\delta_{s_3s_5} + \delta_{s_1s_3}\delta_{s_2s_5} + \delta_{s_1s_5}\delta_{s_2s_3}) \\ &+X_{s_5}^{a(5)}(\delta_{s_1s_2}\delta_{s_3s_4} + \delta_{s_1s_3}\delta_{s_2s_4} + \delta_{s_1s_4}\delta_{s_2s_3})], \end{aligned} \tag{C6}$$

where the highest-order irreducible parts of moments (C4)–(C6), denoted as $\sigma_{ijk}^{(3)'}$, $\sigma_{ijkl}^{(4)'}$, and $\sigma_{ijklm}^{(5)'}$, are neglected (which provides the reduction from the 56-moment model to the 22-moment model).

C.2. Evolution Equation for the Scalar Pressure $\mathrm{p_a}$

By using the decomposition $\bar{\bar{\boldsymbol{p}}}_a = p_a\bar{\bar{\boldsymbol{I}}} + \bar{\bar{\boldsymbol{\Pi}}}_a^{(2)}$, the evolution equation for the scalar pressure p_a is obtained by applying $(1/3)\mathrm{Tr}$ on the pressure tensor Equation (A6), yielding

$$\frac{\partial p_a}{\partial t} + \boldsymbol{u}_a \cdot \nabla p_a + \frac{5}{3}p_a\nabla\cdot\boldsymbol{u}_a + \frac{2}{3}\nabla\cdot\boldsymbol{q}_a + \frac{2}{3}\bar{\bar{\boldsymbol{\Pi}}}_a^{(2)}:(\nabla\boldsymbol{u}_a) = \frac{1}{3}\mathrm{Tr}\,\bar{\bar{\boldsymbol{Q}}}_a^{(2)} = \frac{2}{3}Q_a. \tag{C7}$$

Alternatively, using temperature $T_a = p_a/n_a$ yields the following equation:

$$\frac{3}{2}n_a\frac{d_aT_a}{dt} + p_a\nabla\cdot\boldsymbol{u}_a + \nabla\cdot\boldsymbol{q}_a + \bar{\bar{\boldsymbol{\Pi}}}_a^{(2)}:(\nabla\boldsymbol{u}_a) = \frac{1}{2}\mathrm{Tr}\,\bar{\bar{\boldsymbol{Q}}}_a^{(2)} = Q_a, \tag{C8}$$

which identifies with Equation (2.3) of Braginskii (1965). The collisional energy exchange rates

$$Q_a = \frac{m_a}{2}\int|\boldsymbol{c}_a|^2C(f_a)d^3v. \tag{C9}$$

C.3. Evolution Equation for the Viscosity Tensor $\bar{\bar{\mathbf{\Pi}}}_a^{(2)}$

The evolution equation for the usual viscosity tensor is obtained by subtracting $\bar{\bar{\boldsymbol{I}}}$ times (C7) from (A6), yielding

$$\frac{d_a\bar{\bar{\mathbf{\Pi}}}_a^{(2)}}{dt} + \bar{\bar{\mathbf{\Pi}}}_a^{(2)}\nabla\cdot\boldsymbol{u}_a + \Omega_a(\hat{\boldsymbol{b}}\times\bar{\bar{\mathbf{\Pi}}}_a^{(2)})^S + (\bar{\bar{\mathbf{\Pi}}}_a^{(2)}\cdot\nabla\boldsymbol{u}_a)^S - \frac{2}{3}\bar{\bar{\boldsymbol{I}}}(\bar{\bar{\mathbf{\Pi}}}_a^{(2)}:\nabla\boldsymbol{u}_a) + \nabla\cdot\bar{\bar{\boldsymbol{q}}}_a - \frac{2}{3}\bar{\bar{\boldsymbol{I}}}\nabla\cdot\boldsymbol{q}_a$$
$$+p_a\left[(\nabla\boldsymbol{u}_a)^S - \frac{2}{3}\bar{\bar{\boldsymbol{I}}}\nabla\cdot\boldsymbol{u}_a\right] = \bar{\bar{\boldsymbol{Q}}}_a^{(2)} - \frac{\bar{\bar{\boldsymbol{I}}}}{3}\mathrm{Tr}\,\bar{\bar{\boldsymbol{Q}}}_a^{(2)}. \tag{C10}$$

It is possible to define the well-known rate-of-strain tensor:

$$\bar{\bar{\boldsymbol{W}}}_a = (\nabla\boldsymbol{u}_a)^S - \frac{2}{3}\bar{\bar{\boldsymbol{I}}}\nabla\cdot\boldsymbol{u}_a. \tag{C11}$$

Equation (C10) is exact. Using the heat flux decomposition (C4) yields $\nabla\cdot\bar{\bar{\boldsymbol{q}}}_a = (2/5)((\nabla\boldsymbol{q}_a)^S + \bar{\bar{\boldsymbol{I}}}\nabla\cdot\boldsymbol{q}_a)$, and so Equation (C10) becomes

$$\frac{d_a\bar{\bar{\mathbf{\Pi}}}_a^{(2)}}{dt} + \bar{\bar{\mathbf{\Pi}}}_a^{(2)}\nabla\cdot\boldsymbol{u}_a + \Omega_a(\hat{\boldsymbol{b}}\times\bar{\bar{\mathbf{\Pi}}}_a^{(2)})^S + (\bar{\bar{\mathbf{\Pi}}}_a^{(2)}\cdot\nabla\boldsymbol{u}_a)^S - \frac{2}{3}\bar{\bar{\boldsymbol{I}}}(\bar{\bar{\mathbf{\Pi}}}_a^{(2)}:\nabla\boldsymbol{u}_a) + \frac{2}{5}\left[(\nabla\boldsymbol{q}_a)^S - \frac{2}{3}\bar{\bar{\boldsymbol{I}}}\nabla\cdot\boldsymbol{q}_a\right]$$
$$+p_a\bar{\bar{\boldsymbol{W}}}_a = \bar{\bar{\boldsymbol{Q}}}_a^{(2)\prime} \equiv \bar{\bar{\boldsymbol{Q}}}_a^{(2)} - \frac{\bar{\bar{\boldsymbol{I}}}}{3}\mathrm{Tr}\,\bar{\bar{\boldsymbol{Q}}}_a^{(2)}, \tag{C12}$$

which, for example, identifies with Equations (39)–(40) of Schunk (1977). It is possible to define

$$\bar{\bar{\boldsymbol{W}}}_a^q = \frac{2}{5}\left[(\nabla\boldsymbol{q}_a)^S - \frac{2}{3}\bar{\bar{\boldsymbol{I}}}\nabla\cdot\boldsymbol{q}_a\right], \tag{C13}$$

where we use a heat flux superscript "q" to differentiate it from (C11). As a double check, applying a trace on (C12) shows that both sides are zero.

C.4. Evolution Equation for the Heat Flux Vector $\boldsymbol{q}_a$

The evolution equation for $\boldsymbol{q}_a$ is obtained by applying $(1/2)\mathrm{Tr}$ on (A7), yielding

$$\frac{d_a\boldsymbol{q}_a}{dt} + \boldsymbol{q}_a\nabla\cdot\boldsymbol{u}_a + \boldsymbol{q}_a\cdot\nabla\boldsymbol{u}_a + \bar{\bar{\boldsymbol{q}}}_a:\nabla\boldsymbol{u}_a + \Omega_a\hat{\boldsymbol{b}}\times\boldsymbol{q}_a + \frac{1}{2}\mathrm{Tr}\,\nabla\cdot\bar{\bar{\boldsymbol{r}}}_a - \frac{1}{\rho_a}\left[\frac{3}{2}p_a\nabla\cdot\bar{\bar{\boldsymbol{p}}}_a + (\nabla\cdot\bar{\bar{\boldsymbol{p}}}_a)\cdot\bar{\bar{\boldsymbol{p}}}_a\right]$$
$$=\frac{1}{2}\mathrm{Tr}\left[\bar{\bar{\boldsymbol{Q}}}_a^{(3)} - \frac{p_a}{\rho_a}(\boldsymbol{R}_a\bar{\bar{\boldsymbol{I}}})^S\right] - \frac{1}{\rho_a}\boldsymbol{R}_a\cdot\bar{\bar{\mathbf{\Pi}}}_a^{(2)}, \tag{C14}$$

where $\mathrm{Tr}(\boldsymbol{R}_a\bar{\bar{\boldsymbol{I}}})^S = 5\boldsymbol{R}_a$. This equation is exact. Using the heat flux decomposition (C4) yields

$$\bar{\bar{\boldsymbol{q}}}_a:\nabla\boldsymbol{u}_a = (2/5)[\boldsymbol{q}_a\cdot\nabla\boldsymbol{u}_a + (\nabla\boldsymbol{u}_a)\cdot\boldsymbol{q}_a + \boldsymbol{q}_a\nabla\cdot\boldsymbol{u}_a], \tag{C15}$$

and applying a trace at decomposition (C5) yields

$$\mathrm{Tr}\,\bar{\bar{\boldsymbol{r}}}_a = 5\frac{p_a^2}{\rho_a}\bar{\bar{\boldsymbol{I}}} + \frac{\bar{\bar{\boldsymbol{I}}}}{3}\widetilde{X}_a^{(4)} + \bar{\bar{\mathbf{\Pi}}}_a^{(4)}, \tag{C16}$$

which is of course equivalent to decomposition (C2), (C3). Note that the closure $\mathrm{Tr}\,\bar{\bar{\boldsymbol{r}}}_a = 5\frac{p_a^2}{\rho_a}\bar{\bar{\boldsymbol{I}}}$ can be viewed as an isotropic analogy of the anisotropic bi-Maxwellian "normal" closure $r_{\|\|a} = \frac{3p_{\|a}^2}{\rho}$, $r_{\|\perp a} = \frac{p_{\|a}p_{\perp a}}{\rho_a}$, $r_{\perp\perp a} = \frac{2p_{\perp a}^2}{\rho_a}$, with $p_{\|a} = p_{\perp a} = p_a$, because the following general identity holds for any gyrotropic distribution function: $\mathrm{Tr}\,\bar{\bar{\boldsymbol{r}}}_a^{\mathrm{g}} = r_{\|\|a}\hat{\boldsymbol{b}}\hat{\boldsymbol{b}} + r_{\|\perp a}(\bar{\bar{\boldsymbol{I}}} + \hat{\boldsymbol{b}}\hat{\boldsymbol{b}}) + 2r_{\perp\perp a}(\bar{\bar{\boldsymbol{I}}} - \hat{\boldsymbol{b}}\hat{\boldsymbol{b}})$. Then one calculates

$$\frac{1}{2}\mathrm{Tr}\,\nabla\cdot\bar{\bar{\boldsymbol{r}}}_a = \frac{5}{2}\nabla\left(\frac{p_a^2}{\rho_a}\right) + \frac{1}{6}\nabla\widetilde{X}_a^{(4)} + \frac{1}{2}\nabla\cdot\bar{\bar{\mathbf{\Pi}}}_a^{(4)}, \tag{C17}$$

together with

$$\frac{1}{2}\mathrm{Tr}\,\nabla\cdot\bar{\bar{\boldsymbol{r}}}_a - \frac{1}{\rho_a}\left[\frac{3}{2}p_a\nabla\cdot\bar{\bar{\boldsymbol{p}}}_a + (\nabla\cdot\bar{\bar{\boldsymbol{p}}}_a)\cdot\bar{\bar{\boldsymbol{p}}}_a\right] = \frac{5}{2}p_a\nabla\left(\frac{p_a}{\rho_a}\right) + \frac{1}{6}\nabla\widetilde{X}_a^{(4)} + \frac{1}{2}\nabla\cdot\bar{\bar{\mathbf{\Pi}}}_a^{(4)}$$
$$-\frac{5}{2}\frac{p_a}{\rho_a}\nabla\cdot\bar{\bar{\mathbf{\Pi}}}_a^{(2)} - \frac{1}{\rho_a}(\nabla\cdot\bar{\bar{\boldsymbol{p}}}_a)\cdot\bar{\bar{\mathbf{\Pi}}}_a^{(2)}, \tag{C18}$$

and evolution Equation (C14) becomes

$$\frac{d_a \boldsymbol{q}_a}{dt} + \frac{7}{5}\boldsymbol{q}_a \nabla \cdot \boldsymbol{u}_a + \frac{7}{5}\boldsymbol{q}_a \cdot \nabla \boldsymbol{u}_a + \frac{2}{5}(\nabla \boldsymbol{u}_a) \cdot \boldsymbol{q}_a + \Omega_a \hat{\boldsymbol{b}} \times \boldsymbol{q}_a + \frac{5}{2} p_a \nabla \left(\frac{p_a}{\rho_a} \right)$$
$$+ \frac{1}{6}\nabla \widetilde{X}_a^{(4)} + \frac{1}{2}\nabla \cdot \bar{\bar{\boldsymbol{\Pi}}}_a^{(4)} - \frac{5}{2}\frac{p_a}{\rho_a}\nabla \cdot \bar{\bar{\boldsymbol{\Pi}}}_a^{(2)} - \frac{1}{\rho_a}(\nabla \cdot \bar{\bar{\boldsymbol{p}}}_a) \cdot \bar{\bar{\boldsymbol{\Pi}}}_a^{(2)}$$
$$= \boldsymbol{Q}_a^{(3)\prime} \equiv \frac{1}{2}\mathrm{Tr}\,\bar{\bar{\boldsymbol{Q}}}_a^{(3)} - \frac{5}{2}\frac{p_a}{\rho_a}\boldsymbol{R}_a - \frac{1}{\rho_a}\boldsymbol{R}_a \cdot \bar{\bar{\boldsymbol{\Pi}}}_a^{(2)}. \tag{C19}$$

As a double check, reducing the 22-moment model into the 13-moment model with the closures $\widetilde{X}_a^{(4)} = 0$ and $\bar{\bar{\boldsymbol{\Pi}}}_a^{(4)} = 7(p_a/\rho_a)\bar{\bar{\boldsymbol{\Pi}}}_a^{(2)}$ yields

$$\frac{1}{2}\nabla \cdot \bar{\bar{\boldsymbol{\Pi}}}_a^{(4)} - \frac{5}{2}\frac{p_a}{\rho_a}\nabla \cdot \bar{\bar{\boldsymbol{\Pi}}}_a^{(2)} \xrightarrow{13-\mathrm{m}} \frac{p_a}{\rho_a}\nabla \cdot \bar{\bar{\boldsymbol{\Pi}}}_a^{(2)} + \frac{7}{2}\bar{\bar{\boldsymbol{\Pi}}}_a^{(2)} \cdot \nabla \left(\frac{p_a}{\rho_a} \right), \tag{C20}$$

then evolution Equation (C19) recovers Equations (39)–(40) of Schunk (1977).

C.5. Evolution Equation for the Viscosity Tensor $\bar{\bar{\boldsymbol{\Pi}}}_a^{(4)}$

The nonlinear evolution equation for the fourth-order moment $r_{ijkl}^a = X_{ijkl}^{a(4)}$ is given by (A8). First, we need to obtain the evolution equation for the matrix $(\mathrm{Tr}\,\bar{\bar{\boldsymbol{r}}}^a)_{ij} = \mathrm{X}_{ij}^{a(4)}$, which is further decomposed into (C2) and (C3). Applying a trace at (A8) yields

$$\frac{d_a}{dt}\mathrm{Tr}\,\bar{\bar{\boldsymbol{r}}}_a + \nabla \cdot (\mathrm{Tr}\,\bar{\bar{\boldsymbol{X}}}_a^{(5)}) + (\nabla \cdot \boldsymbol{u}_a)\mathrm{Tr}\,\bar{\bar{\boldsymbol{r}}}_a + 2\bar{\bar{\boldsymbol{r}}}_a : \nabla \boldsymbol{u}_a$$
$$+ \left[(\mathrm{Tr}\,\bar{\bar{\boldsymbol{r}}}_a) \cdot \nabla \boldsymbol{u}_a + \Omega_a \hat{\boldsymbol{b}} \times (\mathrm{Tr}\,\bar{\bar{\boldsymbol{r}}}_a) - \frac{2}{\rho_a}(\nabla \cdot \bar{\bar{\boldsymbol{p}}}_a)\boldsymbol{q}_a \right]^S - \frac{2}{\rho_a}(\nabla \cdot \bar{\bar{\boldsymbol{p}}}_a) \cdot \bar{\bar{\boldsymbol{q}}}_a$$
$$= \mathrm{Tr}\,\bar{\bar{\boldsymbol{Q}}}_a^{(4)} - \frac{2}{\rho_a}[(\boldsymbol{R}_a \boldsymbol{q}_a)^S + \boldsymbol{R}_a \cdot \bar{\bar{\boldsymbol{q}}}_a]. \tag{C21}$$

As a quick double check, Equation (C21) appears equivalent to Equation (3.4.35) of Balescu (1988, p. 154; after accounting for the different normalization constants of 1/2 and adding a missing "s" index to his fourth-order moment S_{rsnm}). Applying another trace at (C21) yields

$$\frac{d_a}{dt}X_a^{(4)} + \nabla \cdot \boldsymbol{X}_a^{(5)} + (\nabla \cdot \boldsymbol{u}_a)X_a^{(4)} + 4(\mathrm{Tr}\,\bar{\bar{\boldsymbol{r}}}_a) : \nabla \boldsymbol{u}_a - \frac{8}{\rho_a}(\nabla \cdot \bar{\bar{\boldsymbol{p}}}_a) \cdot \boldsymbol{q}_a$$
$$= \mathrm{Tr}\mathrm{Tr}\bar{\bar{\boldsymbol{Q}}}_a^{(4)} - \frac{8}{\rho_a}\boldsymbol{R}_a \cdot \boldsymbol{q}_a. \tag{C22}$$

To obtain the evolution equation for the matrix $\Pi_{ij}^{a(4)}$, we need to subtract $(\bar{\bar{\boldsymbol{I}}}/3)$ times (C22) from (C21). For example, we need to calculate

$$X_{ijk}^{a(5)} = \frac{1}{5}(X_i^{a(5)}\delta_{jk} + X_j^{a(5)}\delta_{ik} + X_k^{a(5)}\delta_{ij});$$
$$\partial_k X_{kij}^{a(5)} = \frac{1}{5}(\partial_j X_i^{a(5)} + \partial_i X_j^{a(5)} + \delta_{ij}\partial_k X_k^{a(5)});$$
$$(\partial_k X_{kij}^{a(5)}) - \frac{\delta_{ij}}{3}\partial_k X_k^{a(5)} = \frac{1}{5}\left(\partial_j X_i^{a(5)} + \partial_i X_j^{a(5)} - \frac{2}{3}\delta_{ij}\partial_k X_k^{a(5)} \right), \tag{C23}$$

together with

$$\begin{aligned}
\bar{\bar{r}}_a\colon \nabla \boldsymbol{u}_a &= \frac{1}{15} X_a^{(4)} ((\nabla \boldsymbol{u}_a)^S + \bar{\bar{\boldsymbol{I}}} (\nabla \cdot \boldsymbol{u}_a)) \\
&\quad + \frac{1}{7} [\bar{\bar{\boldsymbol{\Pi}}}_a^{(4)} (\nabla \cdot \boldsymbol{u}_a) + \bar{\bar{\boldsymbol{I}}} (\bar{\bar{\boldsymbol{\Pi}}}_a^{(4)} \colon \nabla \boldsymbol{u}_a) + (\bar{\bar{\boldsymbol{\Pi}}}_a^{(4)} \cdot \nabla \boldsymbol{u}_a)^S + ((\nabla \boldsymbol{u}_a) \cdot \bar{\bar{\boldsymbol{\Pi}}}_a^{(4)})^S]; \\
\mathrm{Tr}\, \bar{\bar{r}}_a\colon \nabla \boldsymbol{u}_a &= \frac{1}{3} X_a^{(4)} (\nabla \cdot \boldsymbol{u}_a) + \bar{\bar{\boldsymbol{\Pi}}}_a^{(4)} \colon \nabla \boldsymbol{u}_a; \\
2\bar{\bar{r}}_a\colon \nabla \boldsymbol{u}_a - \frac{\bar{\bar{\boldsymbol{I}}}}{3} 4\, \mathrm{Tr}\, \bar{\bar{r}}_a\colon \nabla \boldsymbol{u}_a &= \frac{2}{15} X_a^{(4)} \left((\nabla \boldsymbol{u}_a)^S - \frac{7}{3} \bar{\bar{\boldsymbol{I}}} (\nabla \cdot \boldsymbol{u}_a) \right) - \frac{22}{21} \bar{\bar{\boldsymbol{I}}} (\bar{\bar{\boldsymbol{\Pi}}}_a^{(4)} \colon \nabla \boldsymbol{u}_a) \\
&\quad + \frac{2}{7} [\bar{\bar{\boldsymbol{\Pi}}}_a^{(4)} (\nabla \cdot \boldsymbol{u}_a) + (\bar{\bar{\boldsymbol{\Pi}}}_a^{(4)} \cdot \nabla \boldsymbol{u}_a)^S + ((\nabla \boldsymbol{u}_a) \cdot \bar{\bar{\boldsymbol{\Pi}}}_a^{(4)})^S],
\end{aligned} \tag{C24}$$

and the useful identities are

$$\begin{aligned}
[(\mathrm{Tr}\, \bar{\bar{r}}_a) \cdot \nabla \boldsymbol{u}_a]^S &= \frac{1}{3} X_a^{(4)} (\nabla \boldsymbol{u}_a)^S + [\bar{\bar{\boldsymbol{\Pi}}}_a^{(4)} \cdot \nabla \boldsymbol{u}]^S; \\
[\hat{\boldsymbol{b}} \times (\mathrm{Tr}\, \bar{\bar{r}}_a)]^S &= [\hat{\boldsymbol{b}} \times \bar{\bar{\boldsymbol{\Pi}}}_a^{(4)}]^S.
\end{aligned} \tag{C25}$$

The heat flux contributions calculate

$$(\nabla \cdot \bar{\bar{\boldsymbol{p}}}_a) \cdot \bar{\bar{\boldsymbol{q}}}_a = \frac{2}{5} [((\nabla \cdot \bar{\bar{\boldsymbol{p}}}_a) \boldsymbol{q}_a)^S + \bar{\bar{\boldsymbol{I}}} (\nabla \cdot \bar{\bar{\boldsymbol{p}}}_a) \cdot \boldsymbol{q}_a],$$

so the heat fluxes are added as

$$\begin{aligned}
&- 2((\nabla \cdot \bar{\bar{\boldsymbol{p}}}_a) \boldsymbol{q}_a)^S - 2(\nabla \cdot \bar{\bar{\boldsymbol{p}}}_a) \cdot \bar{\bar{\boldsymbol{q}}}_a + \bar{\bar{\boldsymbol{I}}} \frac{8}{3} (\nabla \cdot \bar{\bar{\boldsymbol{p}}}_a) \cdot \boldsymbol{q}_a \\
&= - \frac{14}{5} \left[((\nabla \cdot \bar{\bar{\boldsymbol{p}}}_a) \boldsymbol{q}_a)^S - \frac{2}{3} \bar{\bar{\boldsymbol{I}}} (\nabla \cdot \bar{\bar{\boldsymbol{p}}}_a) \cdot \boldsymbol{q}_a \right].
\end{aligned} \tag{C26}$$

The fully nonlinear evolution equation for the matrix $\bar{\bar{\boldsymbol{\Pi}}}_a^{(4)}$ thus reads

$$\begin{aligned}
&\frac{d_a}{dt} \bar{\bar{\boldsymbol{\Pi}}}_a^{(4)} + \frac{1}{5} \left[(\nabla \boldsymbol{X}_a^{(5)})^S - \frac{2}{3} \bar{\bar{\boldsymbol{I}}} (\nabla \cdot \boldsymbol{X}_a^{(5)}) \right] + \frac{9}{7} (\nabla \cdot \boldsymbol{u}_a) \bar{\bar{\boldsymbol{\Pi}}}_a^{(4)} + \frac{9}{7} (\bar{\bar{\boldsymbol{\Pi}}}_a^{(4)} \cdot \nabla \boldsymbol{u}_a)^S \\
&\quad + \frac{2}{7} ((\nabla \boldsymbol{u}_a) \cdot \bar{\bar{\boldsymbol{\Pi}}}_a^{(4)})^S - \frac{22}{21} \bar{\bar{\boldsymbol{I}}} (\bar{\bar{\boldsymbol{\Pi}}}_a^{(4)} \colon \nabla \boldsymbol{u}_a) - \frac{14}{5\rho_a} \left[((\nabla \cdot \bar{\bar{\boldsymbol{p}}}_a) \boldsymbol{q}_a)^S - \frac{2}{3} \bar{\bar{\boldsymbol{I}}} (\nabla \cdot \bar{\bar{\boldsymbol{p}}}_a) \cdot \boldsymbol{q}_a \right] \\
&\quad + \Omega_a (\hat{\boldsymbol{b}} \times \bar{\bar{\boldsymbol{\Pi}}}_a^{(4)})^S + \frac{7}{15} \left(15 \frac{p_a^2}{\rho_a} + \widetilde{X}_a^{(4)} \right) \left[(\nabla \boldsymbol{u}_a)^S - \frac{2}{3} \bar{\bar{\boldsymbol{I}}} (\nabla \cdot \boldsymbol{u}_a) \right] \\
&= \bar{\bar{\boldsymbol{Q}}}_a^{(4)\,\prime} \equiv \mathrm{Tr}\, \bar{\bar{\boldsymbol{Q}}}_a^{(4)} - \frac{\bar{\bar{\boldsymbol{I}}}}{3} \mathrm{Tr}\mathrm{Tr} \bar{\bar{\boldsymbol{Q}}}_a^{(4)} - \frac{14}{5\rho_a} \left[(\boldsymbol{R}_a \boldsymbol{q}_a)^S - \frac{2}{3} \bar{\bar{\boldsymbol{I}}} (\boldsymbol{R}_a \cdot \boldsymbol{q}_a) \right].
\end{aligned} \tag{C27}$$

At the semilinear level (while keeping the d/dt), evolution Equation (C27) simplifies into

$$\begin{aligned}
&\frac{d_a}{dt} \bar{\bar{\boldsymbol{\Pi}}}_a^{(4)} + \frac{1}{5} \left[(\nabla \boldsymbol{X}_a^{(5)})^S - \frac{2}{3} \bar{\bar{\boldsymbol{I}}} (\nabla \cdot \boldsymbol{X}_a^{(5)}) \right] + \Omega_a (\hat{\boldsymbol{b}} \times \bar{\bar{\boldsymbol{\Pi}}}_a^{(4)})^S \\
&\quad + 7 \frac{p_a^2}{\rho_a} \left[(\nabla \boldsymbol{u}_a)^S - \frac{2}{3} \bar{\bar{\boldsymbol{I}}} (\nabla \cdot \boldsymbol{u}_a) \right] = \bar{\bar{\boldsymbol{Q}}}_a^{(4)\,\prime} = \mathrm{Tr}\, \bar{\bar{\boldsymbol{Q}}}_a^{(4)} - \frac{\bar{\bar{\boldsymbol{I}}}}{3} \mathrm{Tr}\mathrm{Tr} \bar{\bar{\boldsymbol{Q}}}_a^{(4)}.
\end{aligned} \tag{C28}$$

Finally, neglecting the coupling between heat fluxes and viscosities (which is the choice of Braginskii), the simplest evolution equation reads

$$\frac{d_a}{dt} \bar{\bar{\boldsymbol{\Pi}}}_a^{(4)} + \Omega_a (\hat{\boldsymbol{b}} \times \bar{\bar{\boldsymbol{\Pi}}}_a^{(4)})^S + 7 \frac{p_a^2}{\rho_a} \bar{\bar{\boldsymbol{W}}}_a = \bar{\bar{\boldsymbol{Q}}}_a^{(4)\,\prime}, \tag{C29}$$

where $\bar{\bar{\boldsymbol{W}}}_a = (\nabla \boldsymbol{u}_a)^S - (2/3) \bar{\bar{\boldsymbol{I}}} (\nabla \cdot \boldsymbol{u}_a)$ is the usual rate-of-strain tensor.

C.6. Evolution Equation for the Perturbation $\widetilde{X}_a^{(4)}$

The fully nonlinear evolution Equation (C22) for $X_a^{(4)}$ reads

$$\frac{d_a}{dt}X_a^{(4)} + \nabla\cdot\boldsymbol{X}_a^{(5)} + \frac{7}{3}X_a^{(4)}(\nabla\cdot\boldsymbol{u}_a) + 4\bar{\bar{\boldsymbol{\Pi}}}_a^{(4)}\colon\nabla\boldsymbol{u}_a - \frac{8}{\rho_a}(\nabla\cdot\bar{\bar{\boldsymbol{p}}}_a)\cdot\boldsymbol{q}_a$$
$$= \mathrm{TrTr}\bar{\bar{\boldsymbol{Q}}}_a^{(4)} - \frac{8}{\rho_a}\boldsymbol{R}_a\cdot\boldsymbol{q}_a. \tag{C30}$$

Then, by using $X_a^{(4)} = 15(p_a^2/\rho_a) + \widetilde{X}_a^{(4)}$ with

$$\frac{d_a}{dt}\left(\frac{p_a^2}{\rho_a}\right) = \frac{p_a}{\rho_a}\left[-\frac{7}{3}p_a\nabla\cdot\boldsymbol{u}_a - \frac{4}{3}\nabla\cdot\boldsymbol{q}_a - \frac{4}{3}\bar{\bar{\boldsymbol{\Pi}}}_a^{(2)}\colon\nabla\boldsymbol{u}_a + \frac{4}{3}Q_a\right], \tag{C31}$$

one obtains the fully nonlinear evolution equation for $\widetilde{X}_a^{(4)}$:

$$\frac{d_a}{dt}\widetilde{X}_a^{(4)} + \nabla\cdot\boldsymbol{X}_a^{(5)} - 20\frac{p_a}{\rho_a}\nabla\cdot\boldsymbol{q}_a + \frac{7}{3}\widetilde{X}_a^{(4)}(\nabla\cdot\boldsymbol{u}_a) + 4\left(\bar{\bar{\boldsymbol{\Pi}}}_a^{(4)} - 5\frac{p_a}{\rho_a}\bar{\bar{\boldsymbol{\Pi}}}_a^{(2)}\right)\colon\nabla\boldsymbol{u}_a$$
$$- \frac{8}{\rho_a}(\nabla\cdot\bar{\bar{\boldsymbol{p}}}_a)\cdot\boldsymbol{q}_a = \widetilde{Q}_a^{(4)\,\prime} \equiv \mathrm{TrTr}\bar{\bar{\boldsymbol{Q}}}_a^{(4)} - 20\frac{p_a}{\rho_a}Q_a - \frac{8}{\rho_a}\boldsymbol{R}_a\cdot\boldsymbol{q}_a, \tag{C32}$$

and, at the semilinear level,

$$\frac{d_a}{dt}\widetilde{X}_a^{(4)} + \nabla\cdot\boldsymbol{X}_a^{(5)} - 20\frac{p_a}{\rho_a}\nabla\cdot\boldsymbol{q}_a = \widetilde{Q}_a^{(4)\,\prime} = \mathrm{TrTr}\bar{\bar{\boldsymbol{Q}}}_a^{(4)} - 20\frac{p_a}{\rho_a}Q_a. \tag{C33}$$

The collisional contributions can be found in Section 7.1; see Equation (142).

C.7. Evolution Equation for the Heat Flux Vector $\boldsymbol{X}_a^{(5)}$

Applying a trace twice at (A9) yields

$$\frac{\partial}{\partial t}\mathrm{TrTr}\bar{\bar{\boldsymbol{X}}}^{a(5)} + \nabla\cdot(\mathrm{TrTr}\bar{\bar{\boldsymbol{X}}}^{a(6)}) + \nabla\cdot(\boldsymbol{u}^a\mathrm{TrTr}\bar{\bar{\boldsymbol{X}}}^{a(5)}) + (\mathrm{TrTr}\bar{\bar{\boldsymbol{X}}}^{a(5)}\cdot\nabla)\boldsymbol{u}^a$$
$$+ 4(\mathrm{Tr}\,\bar{\bar{\boldsymbol{X}}}^{a(5)})\colon\nabla\boldsymbol{u}^a + \Omega_a\hat{\boldsymbol{b}}\times(\mathrm{TrTr}\bar{\bar{\boldsymbol{X}}}^{a(5)}) - \frac{1}{\rho_a}[(\nabla\cdot\bar{\bar{\boldsymbol{p}}}^a)\mathrm{TrTr}\bar{\bar{\boldsymbol{X}}}^{a(4)} + 4(\nabla\cdot\bar{\bar{\boldsymbol{p}}}^a)\cdot\mathrm{Tr}\,\bar{\bar{\boldsymbol{X}}}^{a(4)}]$$
$$= \mathrm{TrTr}\bar{\bar{\boldsymbol{Q}}}^{a(5)} - \frac{1}{\rho_a}[\boldsymbol{R}^a\mathrm{TrTr}\bar{\bar{\boldsymbol{X}}}^{a(4)} + 4\boldsymbol{R}^a\cdot\mathrm{Tr}\,\bar{\bar{\boldsymbol{X}}}^{a(4)}]. \tag{C34}$$

By using the definitions of the vectors $\boldsymbol{X}^{(5)} = \mathrm{TrTr}\bar{\bar{\boldsymbol{X}}}^{(5)}$, $\boldsymbol{Q}^{(5)} = \mathrm{TrTr}\bar{\bar{\boldsymbol{Q}}}^{(5)}$, and

$$X_{ijk}^{(5)} = \frac{1}{5}[X_i^{(5)}\delta_{jk} + X_j^{(5)}\delta_{ik} + X_k^{(5)}\delta_{ij}];$$
$$X_{ijk}^{(5)}\partial_j u_k = \frac{1}{5}[X_i^{(5)}\nabla\cdot\boldsymbol{u}_a + X_j^{(5)}\partial_j u_i^a + X_k^{(5)}\partial_i u_k^a], \tag{C35}$$

together with the decompositions (C2) and (C3), the fully nonlinear evolution equation becomes

$$\frac{d_a}{dt}\boldsymbol{X}_a^{(5)} + \frac{1}{3}\nabla\widetilde{X}_a^{(6)} + \nabla\cdot\bar{\bar{\boldsymbol{\Pi}}}_a^{(6)} + \frac{9}{5}\boldsymbol{X}_a^{(5)}(\nabla\cdot\boldsymbol{u}_a) + \frac{9}{5}\boldsymbol{X}_a^{(5)}\cdot\nabla\boldsymbol{u}_a + \frac{4}{5}(\nabla\boldsymbol{u}_a)\cdot\boldsymbol{X}_a^{(5)} + \Omega_a\hat{\boldsymbol{b}}\times\boldsymbol{X}_a^{(5)}$$
$$+70\frac{p_a^2}{\rho_a}\nabla\left(\frac{p_a}{\rho_a}\right) - 35\frac{p_a^2}{\rho_a^2}\nabla\cdot\bar{\bar{\boldsymbol{\Pi}}}_a^{(2)} - \frac{7}{3\rho_a}(\nabla\cdot\bar{\bar{\boldsymbol{p}}}^a)\widetilde{X}_a^{(4)} - \frac{4}{\rho_a}(\nabla\cdot\bar{\bar{\boldsymbol{p}}}^a)\cdot\bar{\bar{\boldsymbol{\Pi}}}_a^{(4)}$$
$$= \boldsymbol{Q}_a^{(5)\,\prime} \equiv \boldsymbol{Q}_a^{(5)} - 35\frac{p_a^2}{\rho_a^2}\boldsymbol{R}_a - \frac{7}{3\rho_a}\boldsymbol{R}_a\widetilde{X}_a^{(4)} - \frac{4}{\rho_a}\boldsymbol{R}_a\cdot\bar{\bar{\boldsymbol{\Pi}}}_a^{(4)}. \tag{C36}$$

Because we do not go higher in the hierarchy, the model is closed with the closures (see Equations (B130) and (B131) or Section 8.6 with Tables 3 and 4)

$$\widetilde{X}_a^{(6)} = 21\frac{p_a}{\rho_a}\widetilde{X}_a^{(4)}; \qquad \bar{\bar{\mathbf{\Pi}}}_a^{(6)} = 18\frac{p_a}{\rho_a}\bar{\bar{\mathbf{\Pi}}}_a^{(4)} - 63\frac{p_a^2}{\rho_a^2}\bar{\bar{\mathbf{\Pi}}}_a^{(2)}. \tag{C37}$$

At a semilinear level, Equation (C36) becomes

$$\frac{d_a}{dt}\boldsymbol{X}_a^{(5)} + 7\frac{p_a}{\rho_a}\nabla\widetilde{X}_a^{(4)} + 18\frac{p_a}{\rho_a}\nabla\cdot\bar{\bar{\mathbf{\Pi}}}_a^{(4)} - 98\frac{p_a^2}{\rho_a^2}\nabla\cdot\bar{\bar{\mathbf{\Pi}}}_a^{(2)} + \Omega_a\hat{\boldsymbol{b}}\times\boldsymbol{X}_a^{(5)} + 70\frac{p_a^2}{\rho_a}\nabla\left(\frac{p_a}{\rho_a}\right) = \boldsymbol{Q}_a^{(5)\,\prime} = \boldsymbol{Q}_a^{(5)} - 35\frac{p_a^2}{\rho_a^2}\boldsymbol{R}_a. \tag{C38}$$

Appendix D
Simplified General Fluid Hierarchy

Previously, we introduced a full fluid hierarchy in Section A, which contains n-dimensional moments $X_{ijk\ldots n}^{(n)}$. By applying contractions at these moments in Appendix C, we derived evolution equations for the 22-moment model. Instead of doing that, it is of course possible to obtain evolution equations for contracted moments directly from the Boltzmann equation. This simplified hierarchy is formulated with heat fluxes (vectors) and stress tensors (matrices)

$$\boldsymbol{X}_a^{(2n+1)} = m_a\int\boldsymbol{c}_a|\boldsymbol{c}_a|^{2n}f_a\,d^3v; \qquad \bar{\bar{\mathbf{\Pi}}}_a^{(2n)} = m_a\int\left(\boldsymbol{c}_a\boldsymbol{c}_a - \frac{\bar{\bar{\boldsymbol{I}}}}{3}|\boldsymbol{c}_a|^2\right)|\boldsymbol{c}_a|^{2n-2}f_a\,d^3v, \tag{D1}$$

together with fully contracted scalars, which are decomposed into a Maxwellian core and perturbation (notation with tilde)

$$X_a^{(2n)} = m_a\int|\boldsymbol{c}_a|^{2n}f_a\,d^3v = (2n+1)!!\,\frac{p_a^n}{\rho_a^{n-1}} + \widetilde{X}_a^{(2n)}, \tag{D2}$$

meaning a definition of $\widetilde{X}_a^{(2n)} = m_a\int|\boldsymbol{c}_a|^{2n}(f_a - f_a^{(0)})d^3v$, where $f_a^{(0)}$ is Maxwellian. In another words, one considers the matrices

$$X_{ij}^{a(2n)} = m_a\int|\boldsymbol{c}_a|^{2n-2}c_i^a c_j^a f_a\,d^3v = \frac{\delta_{ij}}{3}X^{a(2n)} + \Pi_{ij}^{a(2n)}, \tag{D3}$$

which are decomposed into fully contracted scalars and stress tensors. Note that $\boldsymbol{X}_a^{(1)} = 0$ and $\widetilde{X}_a^{(2)} = 0$.

Unfortunately, the traditional definition of the heat flux vector $\boldsymbol{q}_a = (1/2)\mathrm{Tr}\,\bar{\bar{\boldsymbol{q}}}_a$, which contains a factor of $1/2$, goes against the general ideology that no additional factors are introduced by contractions. Also, we have previously reserved vector $\boldsymbol{Q}_a^{(3)\,\prime}$ for the right-hand side of the heat flux $\boldsymbol{q}_a$ evolution equation, and not for $\boldsymbol{X}_a^{(3)}$. Obviously, our previous notation is not ideal for generalization to nth-order moments. To circumvent all of the problems with the previous definitions, we define new collisional contributions for the heat fluxes and stress tensors with $\mathcal{Q}$ (mathcal of Q), as the vectors and matrices

$$\mathcal{Q}_i^{a(2n+1)} = m_a\int|\boldsymbol{c}_a|^{2n}c_i^a C(f_a)d^3v;$$
$$\mathcal{Q}_{ij}^{a(2n)} = m_a\int|\boldsymbol{c}_a|^{2n-2}c_i^a c_j^a C(f_a)d^3v; \tag{D4}$$

together with the fully contracted

$$Q_a^{(2n)} = m_a\int|\boldsymbol{c}_a|^{2n}C(f_a)d^3v; \qquad Q_a = \frac{m_a}{2}\int|\boldsymbol{c}_a|^2C(f_a)d^3v. \tag{D5}$$

The energy exchange rates Q_a contain the traditional factor of $1/2$, and $Q_a^{(2)} = 2Q_a$. The momentum exchange rates $\boldsymbol{R}_a = m_a\int\boldsymbol{v}C(f_a)d^3v$. In the vector notation, matrix $\bar{\bar{\boldsymbol{\mathcal{Q}}}}^{a(2n)} = \mathrm{TrTr}\ldots\mathrm{Tr}\,\bar{\bar{\boldsymbol{Q}}}^{a(2n)}$.

Then, the direct integration of the Boltzmann equation and the subtraction of the momentum equations yields the evolution equations for the scalars

$$\frac{\partial}{\partial t}X^{a(2n)} + \partial_k(u_k^a X^{a(2n)}) + \partial_k X_k^{a(2n+1)} + (2n)X_{ik}^{a(2n)}\partial_k u_i^a - \frac{(2n)}{\rho_a}(\nabla\cdot\bar{\bar{\boldsymbol{p}}}^a)_k X_k^{a(2n-1)} = Q^{a(2n)} - \frac{(2n)}{\rho_a}R_k^a X_k^{a(2n-1)}, \tag{D6}$$

where (n) without a species index should not be confused with the number density, the evolution equations for the vectors

$$\begin{aligned}&\frac{\partial}{\partial t}X_i^{a(2n+1)} + \partial_k(u_k^a X_i^{a(2n+1)}) + \partial_k X_{ki}^{a(2n+2)} + X_k^{a(2n+1)}\partial_k u_i^a + (2n)X_{ijk}^{a(2n+1)}\partial_k u_j^a\\ &\quad -\frac{(2n)}{\rho_a}(\nabla\cdot\bar{\bar{\boldsymbol{p}}}^a)_k X_{ki}^{a(2n)} - \frac{1}{\rho_a}(\nabla\cdot\bar{\bar{\boldsymbol{p}}}^a)_i X^{a(2n)} + \Omega_a(\hat{\boldsymbol{b}}\times\boldsymbol{X}^{a(2n+1)})_i\\ &\quad = \mathcal{Q}_i^{a(2n+1)} - \frac{1}{\rho_a}R_i^a X^{a(2n)} - \frac{(2n)}{\rho_a}R_k^a X_{ki}^{a(2n)},\end{aligned} \tag{D7}$$

and the matrices

$$\begin{aligned}&\frac{\partial}{\partial t}X_{ij}^{a(2n)} + \partial_k(u_k^a X_{ij}^{a(2n)}) + \partial_k X_{kij}^{a(2n+1)} + (2n-2)X_{ijkl}^{a(2n)}(\partial_k u_l^a)\\ &\quad + \left[X_{ik}^{a(2n)}\partial_k u_j^a + \Omega_a(\hat{\boldsymbol{b}}\times\bar{\bar{\boldsymbol{X}}}^{a(2n)})_{ij} - \frac{1}{\rho_a}(\nabla\cdot\bar{\bar{\boldsymbol{p}}}^a)_i X_j^{a(2n-1)}\right]^S - \frac{(2n-2)}{\rho_a}(\nabla\cdot\bar{\bar{\boldsymbol{p}}}^a)_k X_{kij}^{a(2n-1)}\\ &\quad = \mathcal{Q}_{ij}^{a(2n)} - \frac{1}{\rho_a}[R_i^a X_j^{a(2n-1)}]^S - \frac{(2n-2)}{\rho_a}R_k^a X_{kij}^{a(2n-1)},\end{aligned} \tag{D8}$$

which are valid for $n \geqslant 1$. For example, evaluating (D6) for $n = 1$ yields the evolution equation for the scalar pressure p_a. Applying a trace at (D8) recovers (D6).

The matrices $X_{ij}^{a(2n)}$ are then decomposed according to (D3), where the stress tensors $\Pi_{ij}^{a(2n)}$ are traceless, and higher-order tensors are decomposed according to (where the tensors σ are neglected, which is the core of the hierarchy simplification)

$$X_{ijk}^{a(2n+1)} = \frac{1}{5}[X_i^{a(2n+1)}\delta_{jk} + X_j^{a(2n+1)}\delta_{ik} + X_k^{a(2n+1)}\delta_{ij}]; \tag{D9}$$

$$\begin{aligned}X_{ijkl}^{a(2n)} &= \frac{1}{15}X^{a(2n)}(\delta_{ij}\delta_{kl} + \delta_{ik}\delta_{jl} + \delta_{il}\delta_{jk})\\ &\quad + \frac{1}{7}[\Pi_{ij}^{a(2n)}\delta_{kl} + \Pi_{ik}^{a(2n)}\delta_{jl} + \Pi_{il}^{a(2n)}\delta_{jk} + \Pi_{jk}^{a(2n)}\delta_{il} + \Pi_{jl}^{a(2n)}\delta_{ik} + \Pi_{kl}^{a(2n)}\delta_{ij}].\end{aligned} \tag{D10}$$

Applying a trace at (D9) yields the identity, and applying a trace at (D10) yields the decomposition (D3). The evolution equations for the fully contracted moments (scalars) then become

$$\frac{d_a}{dt}X_a^{(2n)} + \nabla\cdot\boldsymbol{X}_a^{(2n+1)} + \frac{(2n+3)}{3}X_a^{(2n)}\nabla\cdot\boldsymbol{u}_a + (2n)\bar{\bar{\boldsymbol{\Pi}}}_a^{(2n)}:\nabla\boldsymbol{u}_a - \frac{(2n)}{\rho_a}(\nabla\cdot\bar{\bar{\boldsymbol{p}}}_a)\cdot\boldsymbol{X}_a^{(2n-1)} = Q_a^{(2n)} - \frac{(2n)}{\rho_a}\boldsymbol{R}_a\cdot\boldsymbol{X}_a^{(2n-1)}, \tag{D11}$$

for the heat fluxes (vectors)

$$\begin{aligned}&\frac{d_a}{dt}\boldsymbol{X}_a^{(2n+1)} + \frac{(2n+5)}{5}[\boldsymbol{X}_a^{(2n+1)}\nabla\cdot\boldsymbol{u}_a + \boldsymbol{X}_a^{(2n+1)}\cdot\nabla\boldsymbol{u}_a] + \frac{(2n)}{5}(\nabla\boldsymbol{u}_a)\cdot\boldsymbol{X}_a^{(2n+1)}\\ &\quad + \frac{1}{3}\nabla X_a^{(2n+2)} + \nabla\cdot\bar{\bar{\boldsymbol{\Pi}}}_a^{(2n+2)} - \frac{(2n+3)}{3\rho_a}(\nabla\cdot\bar{\bar{\boldsymbol{p}}}_a)X_a^{(2n)} - \frac{(2n)}{\rho_a}(\nabla\cdot\bar{\bar{\boldsymbol{p}}}_a)\cdot\bar{\bar{\boldsymbol{\Pi}}}_a^{(2n)}\\ &\quad + \Omega_a\hat{\boldsymbol{b}}\times\boldsymbol{X}_a^{(2n+1)} = \vec{\boldsymbol{\mathcal{Q}}}_a^{(2n+1)} - \frac{(2n+3)}{3\rho_a}\boldsymbol{R}_a X_a^{(2n)} - \frac{(2n)}{\rho_a}\boldsymbol{R}_a\cdot\bar{\bar{\boldsymbol{\Pi}}}_a^{(2n)},\end{aligned} \tag{D12}$$

and for the stress tensors (matrices)

$$\begin{aligned}
&\frac{d_a}{dt}\bar{\bar{\boldsymbol{\Pi}}}_a^{(2n)} + \frac{1}{5}\left[(\nabla \boldsymbol{X}_a^{(2n+1)})^S - \frac{2}{3}\bar{\bar{\boldsymbol{I}}}\nabla\cdot\boldsymbol{X}_a^{(2n+1)}\right] + \frac{(2n+5)}{7}\bar{\bar{\boldsymbol{\Pi}}}_a^{(2n)}(\nabla\cdot\boldsymbol{u}_a)\\
&\quad + \left[\frac{(2n+5)}{7}(\bar{\bar{\boldsymbol{\Pi}}}_a^{(2n)}\cdot\nabla\boldsymbol{u}_a)^S + \frac{(2n-2)}{7}((\nabla\boldsymbol{u}_a)\cdot\bar{\bar{\boldsymbol{\Pi}}}_a^{(2n)})^S - \frac{2(4n+3)}{21}\bar{\bar{\boldsymbol{I}}}(\bar{\bar{\boldsymbol{\Pi}}}_a^{(2n)}:\nabla\boldsymbol{u}_a)\right]\\
&\quad - \frac{(2n+3)}{5\rho_a}\left[((\nabla\cdot\bar{\bar{\boldsymbol{p}}}_a)\boldsymbol{X}_a^{(2n-1)})^S - \frac{2}{3}\bar{\bar{\boldsymbol{I}}}(\nabla\cdot\bar{\bar{\boldsymbol{p}}}_a)\cdot\boldsymbol{X}_a^{(2n-1)}\right]\\
&\quad + \Omega_a(\hat{\boldsymbol{b}}\times\bar{\bar{\boldsymbol{\Pi}}}_a^{(2n)})^S + \frac{(2n+3)}{15}X_a^{(2n)}\bar{\bar{\boldsymbol{W}}}_a\\
&= \bar{\bar{\boldsymbol{\mathcal{Q}}}}_a^{(2n)\prime} \equiv \bar{\bar{\boldsymbol{\mathcal{Q}}}}_a^{(2n)} - \frac{\bar{\bar{\boldsymbol{I}}}}{3}Q_a^{(2n)} - \frac{(2n+3)}{5\rho_a}\left[(\boldsymbol{R}_a\boldsymbol{X}_a^{(2n-1)})^S - \frac{2}{3}\bar{\bar{\boldsymbol{I}}}\boldsymbol{R}_a\cdot\boldsymbol{X}_a^{(2n-1)}\right].
\end{aligned} \tag{D13}$$

By applying a trace at Equation (D13), it can be verified that it is traceless.

The fully contracted scalar variables are then decomposed into a Maxwellian core and perturbation (with tilde) according to (D2), yielding the evolution equation for scalars

$$\begin{aligned}
&\frac{d_a}{dt}\widetilde{X}_a^{(2n)} + \nabla\cdot\boldsymbol{X}_a^{(2n+1)} + \frac{(2n+3)}{3}\widetilde{X}_a^{(2n)}\nabla\cdot\boldsymbol{u}_a + (2n)\bar{\bar{\boldsymbol{\Pi}}}_a^{(2n)}:\nabla\boldsymbol{u}_a\\
&\quad -(2n+1)!!\,\frac{(2n)}{3}\left(\frac{p_a}{\rho_a}\right)^{n-1}[\nabla\cdot\boldsymbol{q}_a + \bar{\bar{\boldsymbol{\Pi}}}_a^{(2)}:\nabla\boldsymbol{u}_a] - \frac{(2n)}{\rho_a}(\nabla\cdot\bar{\bar{\boldsymbol{p}}}_a)\cdot\boldsymbol{X}_a^{(2n-1)}\\
&= \widetilde{Q}_a^{(2n)\prime} \equiv Q_a^{(2n)} - (2n+1)!!\,\frac{(2n)}{3}\left(\frac{p_a}{\rho_a}\right)^{n-1}Q_a - \frac{(2n)}{\rho_a}\boldsymbol{R}_a\cdot\boldsymbol{X}_a^{(2n-1)},
\end{aligned} \tag{D14}$$

and for heat fluxes

$$\begin{aligned}
&\frac{d_a}{dt}\boldsymbol{X}_a^{(2n+1)} + \frac{(2n+5)}{5}[\boldsymbol{X}_a^{(2n+1)}\nabla\cdot\boldsymbol{u}_a + \boldsymbol{X}_a^{(2n+1)}\cdot\nabla\boldsymbol{u}_a] + \frac{(2n)}{5}(\nabla\boldsymbol{u}_a)\cdot\boldsymbol{X}_a^{(2n+1)}\\
&\quad + \frac{1}{3}\nabla\widetilde{X}_a^{(2n+2)} + \nabla\cdot\bar{\bar{\boldsymbol{\Pi}}}_a^{(2n+2)} - \frac{(2n+3)}{3\rho_a}(\nabla\cdot\bar{\bar{\boldsymbol{p}}}_a)\widetilde{X}_a^{(2n)} - \frac{(2n)}{\rho_a}(\nabla\cdot\bar{\bar{\boldsymbol{p}}}_a)\cdot\bar{\bar{\boldsymbol{\Pi}}}_a^{(2n)}\\
&\quad + (2n+3)!!\,\frac{(n)}{3}\frac{p_a^n}{\rho_a^{n-1}}\nabla\left(\frac{p_a}{\rho_a}\right) - \frac{(2n+3)!!}{3}\frac{p_a^n}{\rho_a^n}\nabla\cdot\bar{\bar{\boldsymbol{\Pi}}}_a^{(2)} + \Omega_a\hat{\boldsymbol{b}}\times\boldsymbol{X}_a^{(2n+1)}\\
&= \vec{\boldsymbol{\mathcal{Q}}}_a^{(2n+1)\prime} \equiv \vec{\boldsymbol{\mathcal{Q}}}_a^{(2n+1)} - \frac{(2n+3)}{3\rho_a}\boldsymbol{R}_a\widetilde{X}_a^{(2n)} - \frac{(2n+3)!!}{3}\frac{p_a^n}{\rho_a^n}\boldsymbol{R}_a - \frac{(2n)}{\rho_a}\boldsymbol{R}_a\cdot\bar{\bar{\boldsymbol{\Pi}}}_a^{(2n)}.
\end{aligned} \tag{D15}$$

The evolution equation for the stress tensors (D13) contains only one trivial term with $X_a^{(2n)}$, where

$$\frac{(2n+3)}{15}X_a^{(2n)}\bar{\bar{\boldsymbol{W}}}_a = \frac{(2n+3)!!}{15}\frac{p_a^n}{\rho_a^{n-1}}\bar{\bar{\boldsymbol{W}}}_a + \frac{(2n+3)}{15}\widetilde{X}_a^{(2n)}\bar{\bar{\boldsymbol{W}}}_a,$$

and we do not rewrite the full equation. Equations (D13)–(D15) are valid for $n \geqslant 1$, where for $n = 1$ (D14) reduces to zero, so this equation is meaningful only for $n \geqslant 2$. In the semilinear approximation, the hierarchy simplifies into (189)–(191).

Appendix E
BGK Collisional Operator

Before the calculations with the Landau collisional operator, it is beneficial to first become familiar with the heuristic relaxation-type operator known as BGK, after Bhatnagar–Gross–Krook (Bhatnagar et al. 1954; Gross & Krook 1956), written in the following form:

$$C(f_a) = \sum_b C_{ab}(f_a) = -\sum_b \nu_{ab}(f_a - f_{ab}^{(0)}). \tag{E1}$$

The Maxwellian $f_{ab}^{(0)}$ has two indices and is defined as

$$f_{ab}^{(0)} = n_a\left(\frac{m_a}{2\pi T_a}\right)^{3/2}\exp\left(-\frac{m_a|\boldsymbol{v}-\boldsymbol{u}_b|^2}{2T_a}\right). \tag{E2}$$

Note that only the velocity $\boldsymbol{u}_b$ has the index "b" and that the temperature, mass, and density have the index "a." Accounting for different temperatures is possible by considering the generalized BGK operators of Haack et al. (2017). The simple BGK operator yields momentum and energy exchange rates

$$\boldsymbol{R}_{ab} = \rho_a \nu_{ab}(\boldsymbol{u}_b - \boldsymbol{u}_a); \qquad Q_{ab} = \frac{1}{2}\rho_a \nu_{ab}|\boldsymbol{u}_b - \boldsymbol{u}_a|^2, \tag{E3}$$

where both the momentum and energy are conserved (note that for heuristic operators it is advisable to directly calculate both $\boldsymbol{R}_{ab}$ and $\boldsymbol{R}_{ba}$ together with Q_{ab} and Q_{ba} to verify that they are well-defined). This BGK operator also satisfies the Boltzmann H-theorem, which for multispecies plasmas has the general form

$$\int C_{ab}(f_a)\ln f_a\, d^3v + \int C_{ba}(f_b)\ln f_b\, d^3v \leqslant 0, \tag{E4}$$

where the equality is true only if f_a and f_b are Maxwellians. For the BGK operator, each part of the H-theorem (E4) is satisfied independently. It can be shown that $\int (f_a - f_{ab}^{(0)})\ln f_{ab}^{(0)}\, d^3v = 0$, and subtracting this integral from the first term of (E4) yields

$$\begin{aligned}\int C_{ab}(f_a)\ln f_a\, d^3v &= \nu_{ab}\int (f_{ab}^{(0)} - f_a)\ln f_a\, d^3v - \underbrace{\nu_{ab}\int (f_{ab}^{(0)} - f_a)\ln f_{ab}^{(0)}\, d^3v}_{0} \\ &= \nu_{ab}\int (f_{ab}^{(0)} - f_a)\ln\left(\frac{f_a}{f_{ab}^{(0)}}\right) d^3v \leqslant 0,\end{aligned} \tag{E5}$$

where in the last step one uses that for any real numbers $a > 0$ and $b > 0$, the following identity holds: $(a - b)\ln(b/a) \leqslant 0$ (the identity is easily verified, because for $a > b$ the first term is positive and the logarithm is negative, and for $a < b$ the first term is negative and the logarithm is positive; the identity is equal to zero only if $a = b$).

The BGK collisional contributions calculate

$$\bar{\bar{\boldsymbol{Q}}}_{ab}^{(2)} = m_a \int \boldsymbol{c}_a\boldsymbol{c}_a C_{ab}(f_a)d^3v = -\nu_{ab}\bar{\bar{\boldsymbol{\Pi}}}_a^{(2)} + \nu_{ab}\rho_a\delta\boldsymbol{u}\delta\boldsymbol{u}; \tag{E6}$$

$$\bar{\bar{\boldsymbol{Q}}}_{ab}^{(3)} = m_a \int \boldsymbol{c}_a\boldsymbol{c}_a\boldsymbol{c}_a C_{ab}(f_a)d^3v = -\nu_{ab}\bar{\bar{\boldsymbol{q}}}_a + \nu_{ab}p_a[\delta\boldsymbol{u}\bar{\bar{\boldsymbol{I}}}]^S + \nu_{ab}\rho_a\delta\boldsymbol{u}\delta\boldsymbol{u}\delta\boldsymbol{u}, \tag{E7}$$

where $\delta\boldsymbol{u} = \boldsymbol{u}_b - \boldsymbol{u}_a$.

E.1. Viscosity Tensor $\bar{\bar{\boldsymbol{\Pi}}}_a^{(2)}$

The collisional contributions that enter the right-hand side of evolution Equation (C12) are

$$\bar{\bar{\boldsymbol{Q}}}_a^{(2)\prime} \equiv \bar{\bar{\boldsymbol{Q}}}_a^{(2)} - \frac{\bar{\bar{\boldsymbol{I}}}}{3}\mathrm{Tr}\,\bar{\bar{\boldsymbol{Q}}}_a^{(2)} = -\bar{\nu}_a\bar{\bar{\boldsymbol{\Pi}}}_a^{(2)} - \bar{\bar{\boldsymbol{W}}}_a^{\mathrm{frict}}, \tag{E8}$$

where we define

$$\bar{\nu}_a = \sum_b \nu_{ab}; \tag{E9}$$

$$\bar{\bar{\boldsymbol{W}}}_a^{\mathrm{frict}} = -\rho_a\sum_b \nu_{ab}\left(\delta\boldsymbol{u}\delta\boldsymbol{u} - \frac{\bar{\bar{\boldsymbol{I}}}}{3}|\delta\boldsymbol{u}|^2\right), \tag{E10}$$

and where the superscript "frict" means the frictional contributions due to $\delta\boldsymbol{u}$. The frictional contributions are only nonlinear, but we keep them to show that it is possible to take them into account. Using the quasistatic approximation, evolution Equation (C12) can be simplified into

$$(\hat{\boldsymbol{b}} \times \bar{\bar{\boldsymbol{\Pi}}}_a^{(2)})^S + \frac{\bar{\nu}_a}{\Omega_a}\bar{\bar{\boldsymbol{\Pi}}}_a^{(2)} = -\frac{1}{\Omega_a}(p_a\bar{\bar{\boldsymbol{W}}}_a + \bar{\bar{\boldsymbol{W}}}_a^q + \bar{\bar{\boldsymbol{W}}}_a^{\mathrm{frict}}), \tag{E11}$$

where the matrices $\bar{\bar{\boldsymbol{W}}}_a$ and $\bar{\bar{\boldsymbol{W}}}_a^q$ are given by (C11), (C13). Equation (E11) can be directly solved. Nevertheless, the stress tensor of Braginskii does not contain heat flux contributions or frictional contributions. To understand the solution of Braginskii more clearly, let us first solve the above equation only with the matrix $\bar{\bar{\boldsymbol{W}}}_a$.

The simplest quasistatic $\bar{\bar{\boldsymbol{\Pi}}}_a^{(2)}$ is thus obtained by solving

$$(\hat{\boldsymbol{b}} \times \bar{\bar{\boldsymbol{\Pi}}}_a^{(2)})^S + \frac{\bar{\nu}_a}{\Omega_a}\bar{\bar{\boldsymbol{\Pi}}}_a^{(2)} = -\frac{p_a}{\Omega_a}\bar{\bar{\boldsymbol{W}}}_a. \tag{E12}$$

For any traceless and symmetric matrix $\bar{\bar{\boldsymbol{W}}}_a$, the solution of (E12) reads (see the details in Appendix E.4)

$$\begin{aligned}
\bar{\bar{\boldsymbol{\Pi}}}_a^{(2)} &= -\eta_0^a \bar{\bar{\boldsymbol{W}}}_0 - \eta_1^a \bar{\bar{\boldsymbol{W}}}_1 - \eta_2^a \bar{\bar{\boldsymbol{W}}}_2 + \eta_3^a \bar{\bar{\boldsymbol{W}}}_3 + \eta_4^a \bar{\bar{\boldsymbol{W}}}_4;\\
\bar{\bar{\boldsymbol{W}}}_0 &= \frac{3}{2}(\bar{\bar{\boldsymbol{W}}}_a : \hat{\boldsymbol{b}}\hat{\boldsymbol{b}})\left(\hat{\boldsymbol{b}}\hat{\boldsymbol{b}} - \frac{\bar{\bar{\boldsymbol{I}}}}{3}\right);\\
\bar{\bar{\boldsymbol{W}}}_1 &= \bar{\bar{\boldsymbol{I}}}_\perp \cdot \bar{\bar{\boldsymbol{W}}}_a \cdot \bar{\bar{\boldsymbol{I}}}_\perp + \frac{1}{2}(\bar{\bar{\boldsymbol{W}}}_a : \hat{\boldsymbol{b}}\hat{\boldsymbol{b}})\bar{\bar{\boldsymbol{I}}}_\perp;\\
\bar{\bar{\boldsymbol{W}}}_2 &= (\bar{\bar{\boldsymbol{I}}}_\perp \cdot \bar{\bar{\boldsymbol{W}}}_a \cdot \hat{\boldsymbol{b}}\hat{\boldsymbol{b}})^S;\\
\bar{\bar{\boldsymbol{W}}}_3 &= \frac{1}{2}(\hat{\boldsymbol{b}} \times \bar{\bar{\boldsymbol{W}}}_a \cdot \bar{\bar{\boldsymbol{I}}}_\perp)^S;\\
\bar{\bar{\boldsymbol{W}}}_4 &= (\hat{\boldsymbol{b}} \times \bar{\bar{\boldsymbol{W}}}_a \cdot \hat{\boldsymbol{b}}\hat{\boldsymbol{b}})^S,
\end{aligned} \tag{E13}$$

with BGK viscosity coefficients

$$\eta_0^a = \frac{p_a}{\bar{\nu}_a}; \quad \eta_1^a = \frac{p_a \bar{\nu}_a}{4\Omega_a^2 + \bar{\nu}_a^2}; \quad \eta_2^a = \frac{p_a \bar{\nu}_a}{\Omega_a^2 + \bar{\nu}_a^2}; \quad \eta_3^a = \frac{2p_a \Omega_a}{4\Omega_a^2 + \bar{\nu}_a^2}; \quad \eta_4^a = \frac{p_a \Omega_a}{\Omega_a^2 + \bar{\nu}_a^2}. \tag{E14}$$

The coefficient η_0 is called the parallel viscosity, η_1, η_2 are perpendicular viscosities, and η_3, η_4 are gyroviscosities. Importantly, the BGK solution (E13) is identical to the form of the Braginskii (1965) viscosity tensor, his Equations (4.41)–(4.42), only his viscosities are different. A comparison is presented in the next section. All four matrices $\bar{\bar{\boldsymbol{W}}}_0, \ldots \bar{\bar{\boldsymbol{W}}}_4$ are traceless and $\bar{\bar{\boldsymbol{W}}}_0 + \bar{\bar{\boldsymbol{W}}}_1 + \bar{\bar{\boldsymbol{W}}}_2 = \bar{\bar{\boldsymbol{W}}}_a$.

When the magnetic field is zero, so that $\Omega_a = 0$ and $\eta_0^a = \eta_1^a = \eta_2^a$, the stress tensor (E13) simplifies into $\bar{\bar{\boldsymbol{\Pi}}}_a^{(2)} = -\eta_0^a \bar{\bar{\boldsymbol{W}}}_a$ and contributes to the momentum equations in a familiar form:

$$\boldsymbol{B} = 0: \qquad \nabla \cdot \bar{\bar{\boldsymbol{\Pi}}}_a^{(2)} = -\nabla \cdot (\eta_0^a \bar{\bar{\boldsymbol{W}}}_a) = -\eta_0^a\left(\nabla^2 \boldsymbol{u}_a + \frac{1}{3}\nabla(\nabla \cdot \boldsymbol{u}_a)\right) - (\nabla \eta_0^a) \cdot \bar{\bar{\boldsymbol{W}}}_a, \tag{E15}$$

analogously to the viscosity of the Navier–Stokes equations (the last term can be neglected if η_0^a is spatially independent).

If the mean magnetic field is sufficiently strong that its curvature can be neglected, (E13) can be evaluated with respect to $\hat{\boldsymbol{b}}_0 = (0, 0, 1)$, yielding

$$\begin{aligned}
\Pi_{xx}^{(2)a} &= -\frac{\eta_0^a}{2}(W_{xx}^a + W_{yy}^a) - \frac{\eta_1^a}{2}(W_{xx}^a - W_{yy}^a) - \eta_3^a W_{xy}^a;\\
\Pi_{xy}^{(2)a} &= \frac{\eta_3^a}{2}(W_{xx}^a - W_{yy}^a) - \eta_1^a W_{xy}^a;\\
\Pi_{xz}^{(2)a} &= -\eta_4^a W_{yz}^a - \eta_2^a W_{xz}^a;\\
\Pi_{yy}^{(2)a} &= -\frac{\eta_0^a}{2}(W_{xx}^a + W_{yy}^a) + \frac{\eta_1^a}{2}(W_{xx}^a - W_{yy}^a) + \eta_3^a W_{xy}^a;\\
\Pi_{yz}^{(2)a} &= \eta_4^a W_{xz}^a - \eta_2^a W_{yz}^a;\\
\Pi_{zz}^{(2)a} &= -\eta_0^a W_{zz}^a,
\end{aligned} \tag{E16}$$

which is Equation (2.21) of Braginskii (1965). As a double check, adding $\Pi_{xx}^{(2)a} + \Pi_{yy}^{(2)a} + \Pi_{zz}^{(2)a} = -\eta_0^a(W_{xx}^a + W_{yy}^a + W_{zz}^a) = 0$, so the stress tensor is indeed traceless (even though all of the diagonal components are nonzero). For strong magnetic field $\Omega_a \gg \bar{\nu}_a$, the viscosities (E14) simplify into

$$\eta_0^a = \frac{p_a}{\bar{\nu}_a}; \quad \eta_1^a = \frac{1}{4}\frac{p_a \bar{\nu}_a}{\Omega_a^2}; \quad \eta_2^a = 4\eta_1^a; \quad \eta_3^a = \frac{p_a}{2\Omega_a}; \quad \eta_4^a = 2\eta_3^a. \tag{E17}$$

Considering only self-collisions, the BGK viscosity coefficients (E14) were first recovered by Kaufman (1960), even though he does not write them explicitly, and one needs to get them by rearranging his Equations (12)–(15) into form (E16). The same results for $\eta_0 - \eta_3$ can also be found in Helander & Sigmar (2002, p. 86), for example; see also Zank (2014, p. 164), although the η_4 coefficient is erroneously related to $\eta_3 = 2\eta_4$, which is a valid relation only in the limit when $x = \Omega_a/\bar{\nu}_a$ is small (i.e., a weak magnetic field). The correct relations are $\eta_3^a(x) = \eta_4^a(2x)$ and $\eta_1^a(x) = \eta_2^a(2x)$, which are valid for both the BGK and Braginskii solutions.

Now one can consider more general (E11), with the heat flux contributions $\bar{\bar{\boldsymbol{W}}}_a^q$ and the frictional contributions $\bar{\bar{\boldsymbol{W}}}_a^{\text{frict}}$. The solution of (E11) is analogous to (E13), because all of the matrices on the right-hand side are traceless and symmetric. However, it is useful to rewrite the solution in a different form by defining the new matrix

$$\widetilde{\bar{\bar{\boldsymbol{W}}}}_a = (\nabla \boldsymbol{u}_a)^S + \frac{2}{5p_a}(\nabla \boldsymbol{q}_a)^S, \tag{E18}$$

and the stress tensor then reads

$$\begin{aligned}
\bar{\bar{\boldsymbol{\Pi}}}_a^{(2)} &= -\eta_0^a \bar{\bar{\boldsymbol{W}}}_0 - \eta_1^a \bar{\bar{\boldsymbol{W}}}_1 - \eta_2^a \bar{\bar{\boldsymbol{W}}}_2 + \eta_3^a \bar{\bar{\boldsymbol{W}}}_3 + \eta_4^a \bar{\bar{\boldsymbol{W}}}_4;\\
\bar{\bar{\boldsymbol{W}}}_0 &= \left[\frac{3}{2}(\widetilde{\bar{\bar{\boldsymbol{W}}}}_a\colon \hat{\boldsymbol{b}}\hat{\boldsymbol{b}}) - \nabla\cdot\boldsymbol{u}_a - \frac{2}{5p_a}\nabla\cdot\boldsymbol{q}_a\right]\left(\hat{\boldsymbol{b}}\hat{\boldsymbol{b}} - \frac{\bar{\bar{\boldsymbol{I}}}}{3}\right)\\
&\quad -\frac{3}{2}\frac{\rho_a}{p_a}\left[\sum_b \nu_{ab}\left(\delta u_{\parallel}^2 - \frac{1}{3}|\delta\boldsymbol{u}|^2\right)\right]\left(\hat{\boldsymbol{b}}\hat{\boldsymbol{b}} - \frac{\bar{\bar{\boldsymbol{I}}}}{3}\right);\\
\bar{\bar{\boldsymbol{W}}}_1 &= \bar{\bar{\boldsymbol{I}}}_\perp\cdot\widetilde{\bar{\bar{\boldsymbol{W}}}}_a\cdot\bar{\bar{\boldsymbol{I}}}_\perp + \left[\frac{1}{2}(\widetilde{\bar{\bar{\boldsymbol{W}}}}_a\colon \hat{\boldsymbol{b}}\hat{\boldsymbol{b}}) - \nabla\cdot\boldsymbol{u}_a - \frac{2}{5p_a}\nabla\cdot\boldsymbol{q}_a\right]\bar{\bar{\boldsymbol{I}}}_\perp\\
&\quad -\frac{\rho_a}{p_a}\sum_b \nu_{ab}\left(\delta\boldsymbol{u}_\perp\delta\boldsymbol{u}_\perp - \frac{\bar{\bar{\boldsymbol{I}}}_\perp}{2}|\delta\boldsymbol{u}_\perp|^2\right);\\
\bar{\bar{\boldsymbol{W}}}_2 &= (\bar{\bar{\boldsymbol{I}}}_\perp\cdot\widetilde{\bar{\bar{\boldsymbol{W}}}}_a\cdot\hat{\boldsymbol{b}}\hat{\boldsymbol{b}})^S - \frac{\rho_a}{p_a}\sum_b \nu_{ab}[\delta u_{\parallel}\hat{\boldsymbol{b}}\delta\boldsymbol{u}_\perp]^S;\\
\bar{\bar{\boldsymbol{W}}}_3 &= \frac{1}{2}(\hat{\boldsymbol{b}}\times\widetilde{\bar{\bar{\boldsymbol{W}}}}_a\cdot\bar{\bar{\boldsymbol{I}}}_\perp)^S - \frac{\rho_a}{2p_a}\sum_b \nu_{ab}[(\hat{\boldsymbol{b}}\times\delta\boldsymbol{u})\delta\boldsymbol{u}_\perp]^S;\\
\bar{\bar{\boldsymbol{W}}}_4 &= (\hat{\boldsymbol{b}}\times\widetilde{\bar{\bar{\boldsymbol{W}}}}_a\cdot\hat{\boldsymbol{b}}\hat{\boldsymbol{b}})^S - \frac{\rho_a}{p_a}\sum_b \nu_{ab}[(\hat{\boldsymbol{b}}\times\delta\boldsymbol{u})\delta u_{\parallel}\hat{\boldsymbol{b}}]^S,
\end{aligned} \tag{E19}$$

with viscosities (E14). Prescribing $\boldsymbol{q}_a = 0$ and $\delta\boldsymbol{u} = 0$ of course recovers (E13).

E.2. Heat Flux Vector $\boldsymbol{q}_a$

We consider the 13-moment model, where evolution Equation (C19) becomes

$$\begin{aligned}
&\frac{d_a\boldsymbol{q}_a}{dt} + \frac{7}{5}\boldsymbol{q}_a\nabla\cdot\boldsymbol{u}_a + \frac{7}{5}\boldsymbol{q}_a\cdot\nabla\boldsymbol{u}_a + \frac{2}{5}(\nabla\boldsymbol{u}_a)\cdot\boldsymbol{q}_a + \Omega_a\hat{\boldsymbol{b}}\times\boldsymbol{q}_a + \frac{5}{2}p_a\nabla\left(\frac{p_a}{\rho_a}\right)\\
&\quad + \frac{p_a}{\rho_a}\nabla\cdot\bar{\bar{\boldsymbol{\Pi}}}_a^{(2)} + \frac{7}{2}\bar{\bar{\boldsymbol{\Pi}}}_a^{(2)}\cdot\nabla\left(\frac{p_a}{\rho_a}\right) - \frac{1}{\rho_a}(\nabla\cdot\bar{\bar{\boldsymbol{p}}}_a)\cdot\bar{\bar{\boldsymbol{\Pi}}}_a^{(2)},\\
&= \boldsymbol{Q}_a^{(3)\,\prime} \equiv \frac{1}{2}\mathrm{Tr}\,\bar{\bar{\boldsymbol{Q}}}_a^{(3)} - \frac{5}{2}\frac{p_a}{\rho_a}\boldsymbol{R}_a - \frac{1}{\rho_a}\boldsymbol{R}_a\cdot\bar{\bar{\boldsymbol{\Pi}}}_a^{(2)},
\end{aligned} \tag{E20}$$

and the BGK collisional contributions calculate

$$\frac{1}{2}\mathrm{Tr}\,\bar{\bar{\boldsymbol{Q}}}_{ab}^{(3)} - \frac{5}{2}\frac{p_a}{\rho_a}\boldsymbol{R}_{ab} = -\nu_{ab}\boldsymbol{q}_a + \frac{\nu_{ab}}{2}\rho_a\delta\boldsymbol{u}|\delta\boldsymbol{u}|^2. \tag{E21}$$

In a quasistatic approximation, (E20) can be simplified into

$$\begin{aligned}
\hat{\boldsymbol{b}}\times\boldsymbol{q}_a + \frac{\bar{\nu}_a}{\Omega_a}\boldsymbol{q}_a = -\frac{1}{\Omega_a}\Bigg[&\frac{5}{2}p_a\nabla\left(\frac{p_a}{\rho_a}\right) + \frac{p_a}{\rho_a}\nabla\cdot\bar{\bar{\boldsymbol{\Pi}}}_a^{(2)} + \frac{7}{2}\bar{\bar{\boldsymbol{\Pi}}}_a^{(2)}\cdot\nabla\left(\frac{p_a}{\rho_a}\right) - \frac{1}{\rho_a}(\nabla\cdot\bar{\bar{\boldsymbol{p}}}_a)\cdot\bar{\bar{\boldsymbol{\Pi}}}_a^{(2)}\\
&+ \frac{1}{\rho_a}\boldsymbol{R}_a\cdot\bar{\bar{\boldsymbol{\Pi}}}_a^{(2)} - \sum_b\frac{\nu_{ab}}{2}\rho_a\delta\boldsymbol{u}|\delta\boldsymbol{u}|^2\Bigg].
\end{aligned} \tag{E22}$$

A general vector equation (where $\boldsymbol{a}$ is an unspecified vector, unrelated to the species index)

$$\hat{\boldsymbol{b}}\times\boldsymbol{q}_a + \frac{\bar{\nu}_a}{\Omega_a}\boldsymbol{q}_a = -\frac{\boldsymbol{a}}{\Omega_a}, \tag{E23}$$

has the following exact solution (splitting the equation into parallel and perpendicular parts $\boldsymbol{q}_a = \boldsymbol{q}_{\parallel a} + \boldsymbol{q}_{\perp a}$ and $\boldsymbol{a} = \boldsymbol{a}_\parallel + \boldsymbol{a}_\perp$ with $\hat{\boldsymbol{b}}\times\boldsymbol{q}_{\parallel a} = 0$; applying $\hat{\boldsymbol{b}}\times$ on the perpendicular part; using $\hat{\boldsymbol{b}}\times(\hat{\boldsymbol{b}}\times\boldsymbol{q}_{\perp_a}) = -\boldsymbol{q}_{\perp a}$; and solving the two coupled perpendicular equations by eliminating $\hat{\boldsymbol{b}}\times\boldsymbol{q}_{\perp a}$):

$$\boldsymbol{q}_a = -\frac{1}{\bar{\nu}_a}(\boldsymbol{a}\cdot\hat{\boldsymbol{b}})\hat{\boldsymbol{b}} + \frac{\Omega_a}{\Omega_a^2 + \bar{\nu}_a^2}\hat{\boldsymbol{b}}\times\boldsymbol{a} - \frac{\bar{\nu}_a}{\Omega_a^2 + \bar{\nu}_a^2}\boldsymbol{a}_\perp. \tag{E24}$$

Note that $\hat{\boldsymbol{b}}\times\boldsymbol{a} = \hat{\boldsymbol{b}}\times\boldsymbol{a}_\perp$. Result (E24) represents the solution of Equation (E22). For zero magnetic field, $\boldsymbol{q}_a = -\boldsymbol{a}/\bar{\nu}_a$. The BGK frictional contributions due to $\delta\boldsymbol{u}$ are only nonlinear; in contrast, the electron heat flux of Braginskii contains frictional $\delta\boldsymbol{u}$

contributions that are linear. At the semilinear level, (E22) simplifies into

$$\hat{\boldsymbol{b}} \times \boldsymbol{q}_a + \frac{\bar{\nu}_a}{\Omega_a}\boldsymbol{q}_a = -\frac{1}{\Omega_a}\left[\frac{5}{2}p_a\nabla\left(\frac{p_a}{\rho_a}\right) + \frac{p_a}{\rho_a}\nabla\cdot\bar{\bar{\boldsymbol{\Pi}}}_a^{(2)}\right], \tag{E25}$$

with a solution again given by (E24). The BGK operator can therefore account for linear (!) contributions of the stress tensor $\bar{\bar{\boldsymbol{\Pi}}}_a^{(2)}$ that enters the heat flux $\boldsymbol{q}_a$, similar to the previous result for (E19), where the heat $\boldsymbol{q}_a$ flux entered the stress tensor $\bar{\bar{\boldsymbol{\Pi}}}_a^{(2)}$. Such a coupling is typically neglected with the Landau collisional operator.

The simplest BGK heat flux is a solution of the equation

$$\hat{\boldsymbol{b}} \times \boldsymbol{q}_a + \frac{\bar{\nu}_a}{\Omega_a}\boldsymbol{q}_a = -\frac{5}{2}\frac{p_a}{\Omega_a m_a}\nabla T_a, \tag{E26}$$

and the solution reads:

$$\boldsymbol{q}_a = -\kappa_\parallel^a\nabla_\parallel T_a - \kappa_\perp^a\nabla_\perp T_a + \kappa_\times^a\hat{\boldsymbol{b}}\times\nabla T_a, \tag{E27}$$

with thermal conductivities

$$\kappa_\parallel^a = \frac{5}{2}\frac{p_a}{\bar{\nu}_a m_a}; \qquad \kappa_\perp^a = \frac{5}{2}\frac{p_a}{m_a}\frac{\bar{\nu}_a}{(\Omega_a^2+\bar{\nu}_a^2)}; \qquad \kappa_\times^a = \frac{5}{2}\frac{p_a}{m_a}\frac{\Omega_a}{(\Omega_a^2+\bar{\nu}_a^2)}. \tag{E28}$$

We use the Braginskii notation with vector $\nabla_\parallel = \hat{\boldsymbol{b}}\hat{\boldsymbol{b}}\cdot\nabla$. If the magnetic field is zero, so that $\Omega_a = 0$ and $\kappa_\parallel^a = \kappa_\perp^a$, the solution simplifies into $\boldsymbol{q}_a = -\kappa_\parallel^a\nabla T_a$.

E.3. BGK versus Braginskii Comparison

Here we compare the BGK viscosities and heat conductivities with those of Braginskii (1965) for a one ion–electron plasma with ion charge $Z_i = 1$. The BGK viscosities (E14) contain $\bar{\nu}_a = \sum_b \nu_{ab}$, and in general should be added according to

$$\bar{\nu}_i = \nu_{ii} + \nu_{ie} = \nu_{ii}\left(1 + \frac{\sqrt{2}}{Z_i}\sqrt{\frac{m_e}{m_i}}\left(\frac{T_i}{T_e}\right)^{3/2}\right);$$
$$\bar{\nu}_e = \nu_{ee} + \nu_{ei} = \nu_{ei}\left(1 + \frac{1}{Z_i\sqrt{2}}\right). \tag{E29}$$

However, for the ion species, Braginskii neglects ion–electron collisions, and thus $\bar{\nu}_i = \nu_{ii}$ and $\bar{\nu}_e = 1.707\nu_{ei}$; see Section 8.2. Using Braginskii's notation with one-index $\nu_i = \nu_{ii}$ and $\nu_e = \nu_{ei}$ then implies

$$\bar{\nu}_a = \alpha_a\nu_a; \quad \text{where} \quad \alpha_i = 1; \quad \alpha_e = 1.707, \tag{E30}$$

and introducing the quantity $x = \Omega_a/\nu_a$, the BGK viscosities (E14) then become

$$\eta_0^a = \frac{p_a}{\alpha_a\nu_a}; \quad \eta_1^a = \frac{p_a}{\nu_a}\frac{\alpha_a}{4x^2+\alpha_a^2}; \quad \eta_2^a = \frac{p_a}{\nu_a}\frac{\alpha_a}{x^2+\alpha_a^2}; \quad \eta_3^a = \frac{p_a}{\nu_a}\frac{2x}{4x^2+\alpha_a^2}; \quad \eta_4^a = \frac{p_a}{\nu_a}\frac{x}{x^2+\alpha_a^2}. \tag{E31}$$

Note that $\eta_1^a(x) = \eta_2^a(2x)$ and $\eta_3^a(x) = \eta_4^a(2x)$. Similarly, the BGK heat conductivities (E28) become

$$\kappa_\parallel^a = \frac{5}{2\alpha_a}\frac{p_a}{\nu_a m_a}; \qquad \kappa_\perp^a = \frac{5}{2}\frac{p_a}{\nu_a m_a}\frac{\alpha_a}{(x^2+\alpha_a^2)}; \qquad \kappa_\times^a = \frac{5}{2}\frac{p_a}{\nu_a m_a}\frac{x}{(x^2+\alpha_a^2)}. \tag{E32}$$

The viscosities and heat conductivities for Braginskii are given in the main text. The ion viscosities are compared in Figure 3, the electron viscosities in Figure 4, and the heat conductivities in Figure 5. A small value of x represents a weak magnetic field and a large value of x represents a strong magnetic field.

E.4. Nonlinear Stress Tensor Decomposition

Here we want to consider the BGK equation for the stress tensor (E12),

$$(\hat{\boldsymbol{b}}\times\bar{\bar{\boldsymbol{\Pi}}})^S + \frac{\nu}{\Omega}\bar{\bar{\boldsymbol{\Pi}}} = -\frac{p}{\Omega}\bar{\bar{\boldsymbol{W}}}, \tag{E33}$$

and clarify the solution (E13). Species indices are dropped, and both $\bar{\bar{\boldsymbol{\Pi}}}$ and $\bar{\bar{\boldsymbol{W}}}$ are symmetric and traceless. First, we need to learn how to decompose any general matrix. It is useful for a moment to consider the undefined matrices $\bar{\bar{\boldsymbol{W}}}$ and $\bar{\bar{\boldsymbol{\Pi}}}$, which are not necessarily symmetric or traceless.

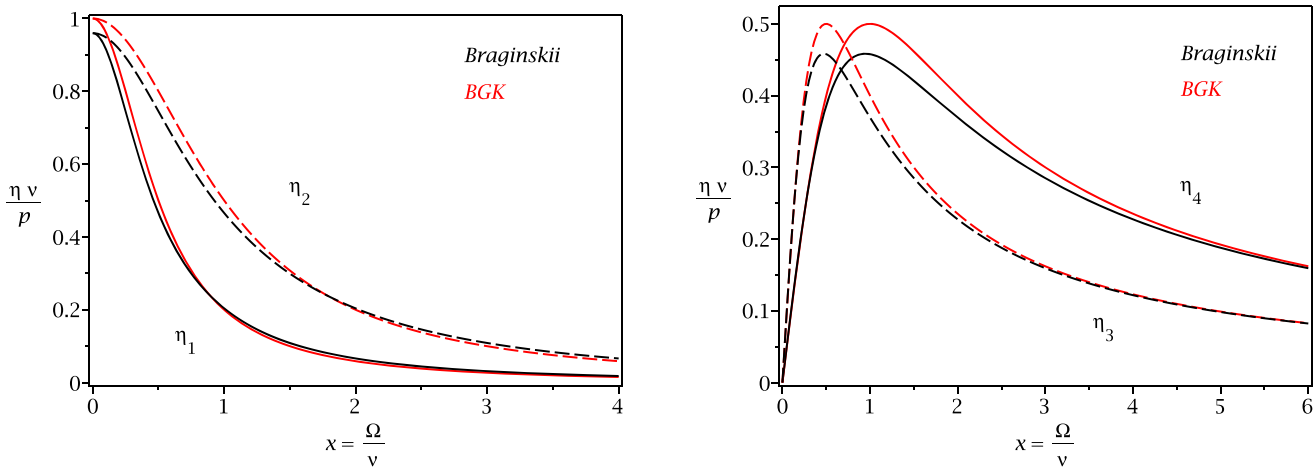

Figure 3. Ion viscosities of the BGK model (red) and of the Braginskii model (black), normalized as $\hat{\eta}^i = \eta^i \nu_{ii}/p_i$ vs. the ratio $x = \Omega_i/\nu_{ii}$. Left: perpendicular viscosities η_1^i, η_2^i. Right: gyroviscosities η_3^i, η_4^i. For large values of x, the BGK asymptotic profiles for $\hat{\eta}_3^i = 1/(2x)$ and $\hat{\eta}_4^i = 1/x$ become independent of collisional frequencies and match the asymptotic profiles of Braginskii exactly. The BGK asymptotic profiles for $\hat{\eta}_1^i = 1/(4x^2)$ and $\hat{\eta}_2^i = 1/x^2$ have the correct functional dependence, but differ from the Braginskii asymptotes by a proportionality constant. The BGK operator reproduces the ion viscosity of Braginskii with surprisingly good accuracy.

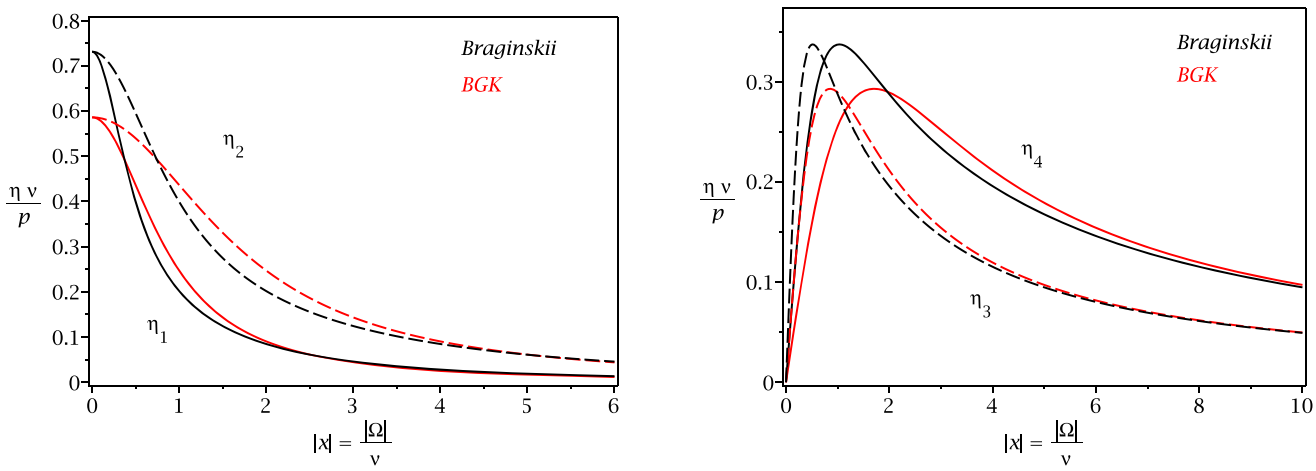

Figure 4. Electron viscosities, normalized as $\hat{\eta}^e = \eta^e \nu_{ei}/p_e$ vs. the ratio $|x| = |\Omega_e|/\nu_{ei}$. The results are less precise than for the ions in Figure 3, especially for small values of x; nevertheless, the same conclusions are obtained.

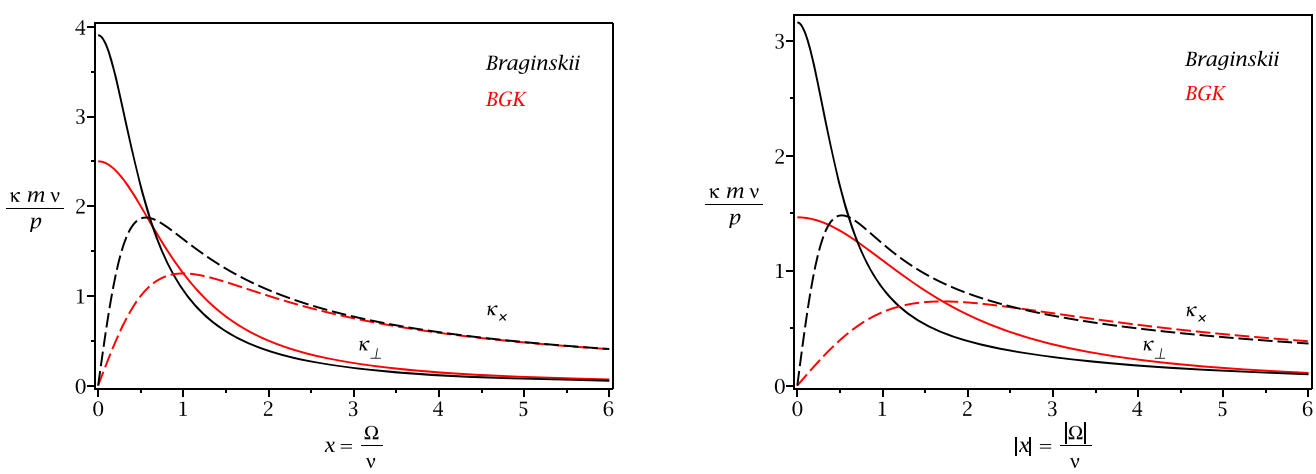

Figure 5. Heat conductivities $\kappa_\perp^a$ and $\kappa_\times^a$. Left: ion species, normalized as $\kappa^i m_i \nu_{ii}/p_i$. Right: electron species, normalized as $\kappa^e m_e \nu_{ei}/p_e$. For large values of x, the BGK asymptotic profiles $\kappa_\times^a$ (dashed lines) match the Braginskii results exactly, whereas for $\kappa_\perp^a$ (solid lines) the results differ by a proportionality constant.

E.4.1. Decomposition of a Matrix

We will work both in the reference frame of the magnetic field lines ($\hat{\boldsymbol{b}}_0 = (0, 0, 1)$), which nicely guide and clarify the calculations, and also in a laboratory reference frame with general $\hat{\boldsymbol{b}}$. In the reference frame of the magnetic field lines, one uses the matrices

$$\hat{\boldsymbol{b}}\hat{\boldsymbol{b}} = \begin{pmatrix} 0 & 0 & 0 \\ 0 & 0 & 0 \\ 0 & 0 & 1 \end{pmatrix}; \qquad \bar{\bar{\boldsymbol{I}}}_\perp = \bar{\bar{\boldsymbol{I}}} - \hat{\boldsymbol{b}}\hat{\boldsymbol{b}} = \begin{pmatrix} 1 & 0 & 0 \\ 0 & 1 & 0 \\ 0 & 0 & 0 \end{pmatrix}; \qquad \bar{\bar{\boldsymbol{I}}}^\times = \begin{pmatrix} 0 & -1 & 0 \\ +1 & 0 & 0 \\ 0 & 0 & 0 \end{pmatrix}, \tag{E34}$$

where the last matrix is defined as $\hat{\boldsymbol{b}} \times \bar{\bar{\boldsymbol{W}}} = (\bar{\bar{\boldsymbol{I}}}^\times) \cdot \bar{\bar{\boldsymbol{W}}}$. Then, one takes a general matrix $\bar{\bar{\boldsymbol{W}}}$, and starts multiplying it with the matrices $\hat{\boldsymbol{b}}\hat{\boldsymbol{b}}$ and $\bar{\bar{\boldsymbol{I}}}_\perp$ from the left and right, yielding a general decomposition:

$$\begin{aligned} \bar{\bar{\boldsymbol{W}}} &= \bar{\bar{\boldsymbol{W}}}_0{}' + \bar{\bar{\boldsymbol{W}}}_1{}' + \bar{\bar{\boldsymbol{W}}}_2; \\ \bar{\bar{\boldsymbol{W}}}_0{}' &= \hat{\boldsymbol{b}}\hat{\boldsymbol{b}} \cdot \bar{\bar{\boldsymbol{W}}} \cdot \hat{\boldsymbol{b}}\hat{\boldsymbol{b}} = (\bar{\bar{\boldsymbol{W}}}\colon \hat{\boldsymbol{b}}\hat{\boldsymbol{b}})\hat{\boldsymbol{b}}\hat{\boldsymbol{b}}; \\ \bar{\bar{\boldsymbol{W}}}_1{}' &= \bar{\bar{\boldsymbol{I}}}_\perp \cdot \bar{\bar{\boldsymbol{W}}} \cdot \bar{\bar{\boldsymbol{I}}}_\perp; \\ \bar{\bar{\boldsymbol{W}}}_2 &= \bar{\bar{\boldsymbol{I}}}_\perp \cdot \bar{\bar{\boldsymbol{W}}} \cdot \hat{\boldsymbol{b}}\hat{\boldsymbol{b}} + \hat{\boldsymbol{b}}\hat{\boldsymbol{b}} \cdot \bar{\bar{\boldsymbol{W}}} \cdot \bar{\bar{\boldsymbol{I}}}_\perp = (\bar{\bar{\boldsymbol{I}}}_\perp \cdot \bar{\bar{\boldsymbol{W}}} \cdot \hat{\boldsymbol{b}}\hat{\boldsymbol{b}})^S. \end{aligned} \tag{E35}$$

In the reference frame of the magnetic field lines,

$$\bar{\bar{\boldsymbol{W}}}_0{}' = \begin{pmatrix} 0 & 0 & 0 \\ 0 & 0 & 0 \\ 0 & 0 & W_{zz} \end{pmatrix}; \qquad \bar{\bar{\boldsymbol{W}}}_1{}' = \begin{pmatrix} W_{xx} & W_{xy} & 0 \\ W_{yx} & W_{yy} & 0 \\ 0 & 0 & 0 \end{pmatrix}; \qquad \bar{\bar{\boldsymbol{W}}}_2 = \begin{pmatrix} 0 & 0 & W_{xz} \\ 0 & 0 & W_{yz} \\ W_{zx} & W_{zy} & 0 \end{pmatrix}, \tag{E36}$$

and adding these matrices together obviously yields the full matrix $\bar{\bar{\boldsymbol{W}}}$. However, the decomposition (E35) also works in the laboratory reference frame with general $\hat{\boldsymbol{b}}$, as can be verified by adding the general matrices together. It is possible to consider an alternative decomposition, according to

$$\begin{aligned} \bar{\bar{\boldsymbol{W}}} &= \bar{\bar{\boldsymbol{W}}}_0 + \bar{\bar{\boldsymbol{W}}}_1 + \bar{\bar{\boldsymbol{W}}}_2; \\ \bar{\bar{\boldsymbol{W}}}_0 &= (\bar{\bar{\boldsymbol{W}}}\colon \hat{\boldsymbol{b}}\hat{\boldsymbol{b}})\hat{\boldsymbol{b}}\hat{\boldsymbol{b}} + \frac{1}{2}(\bar{\bar{\boldsymbol{W}}}\colon \bar{\bar{\boldsymbol{I}}}_\perp)\bar{\bar{\boldsymbol{I}}}_\perp; \\ \bar{\bar{\boldsymbol{W}}}_1 &= \bar{\bar{\boldsymbol{I}}}_\perp \cdot \bar{\bar{\boldsymbol{W}}} \cdot \bar{\bar{\boldsymbol{I}}}_\perp - \frac{1}{2}(\bar{\bar{\boldsymbol{W}}}\colon \bar{\bar{\boldsymbol{I}}}_\perp)\bar{\bar{\boldsymbol{I}}}_\perp; \\ \bar{\bar{\boldsymbol{W}}}_2 &= (\bar{\bar{\boldsymbol{I}}}_\perp \cdot \bar{\bar{\boldsymbol{W}}} \cdot \hat{\boldsymbol{b}}\hat{\boldsymbol{b}})^S, \end{aligned} \tag{E37}$$

where in the reference frame of the magnetic field lines,

$$\bar{\bar{\boldsymbol{W}}}_0 = \begin{pmatrix} \frac{1}{2}(W_{xx} + W_{yy}) & 0 & 0 \\ 0 & \frac{1}{2}(W_{xx} + W_{yy}) & 0 \\ 0 & 0 & W_{zz} \end{pmatrix}; \qquad \bar{\bar{\boldsymbol{W}}}_1 = \begin{pmatrix} \frac{1}{2}(W_{xx} - W_{yy}) & W_{xy} & 0 \\ W_{yx} & -\frac{1}{2}(W_{xx} - W_{yy}) & 0 \\ 0 & 0 & 0 \end{pmatrix}. \tag{E38}$$

The decomposition (E37) again works for general $\hat{\boldsymbol{b}}$, and in comparison to the previous decomposition $\bar{\bar{\boldsymbol{W}}}_0{}' + \bar{\bar{\boldsymbol{W}}}_1{}' = \bar{\bar{\boldsymbol{W}}}_0 + \bar{\bar{\boldsymbol{W}}}_1$. The advantage is that if $\bar{\bar{\boldsymbol{W}}}$ is traceless, then all three matrices are traceless. It is useful to rearrange (E37), by separating the trace of $\bar{\bar{\boldsymbol{W}}}$ with $(\bar{\bar{\boldsymbol{W}}}\colon \bar{\bar{\boldsymbol{I}}}_\perp)\bar{\bar{\boldsymbol{I}}}_\perp = (\bar{\bar{\boldsymbol{W}}}\colon \bar{\bar{\boldsymbol{I}}})\bar{\bar{\boldsymbol{I}}}_\perp - (\bar{\bar{\boldsymbol{W}}}\colon \hat{\boldsymbol{b}}\hat{\boldsymbol{b}})\bar{\bar{\boldsymbol{I}}}_\perp$, yielding the decomposition

$$\begin{aligned} \bar{\bar{\boldsymbol{W}}} &= \bar{\bar{\boldsymbol{W}}}_0 + \bar{\bar{\boldsymbol{W}}}_1 + \bar{\bar{\boldsymbol{W}}}_2; \\ \bar{\bar{\boldsymbol{W}}}_0 &= \frac{3}{2}(\bar{\bar{\boldsymbol{W}}}\colon \hat{\boldsymbol{b}}\hat{\boldsymbol{b}})\left(\hat{\boldsymbol{b}}\hat{\boldsymbol{b}} - \frac{\bar{\bar{\boldsymbol{I}}}}{3}\right) + \frac{1}{2}(\bar{\bar{\boldsymbol{W}}}\colon \bar{\bar{\boldsymbol{I}}})\bar{\bar{\boldsymbol{I}}}_\perp; \\ \bar{\bar{\boldsymbol{W}}}_1 &= \bar{\bar{\boldsymbol{I}}}_\perp \cdot \bar{\bar{\boldsymbol{W}}} \cdot \bar{\bar{\boldsymbol{I}}}_\perp + \frac{1}{2}(\bar{\bar{\boldsymbol{W}}}\colon \hat{\boldsymbol{b}}\hat{\boldsymbol{b}})\bar{\bar{\boldsymbol{I}}}_\perp - \frac{1}{2}(\bar{\bar{\boldsymbol{W}}}\colon \bar{\bar{\boldsymbol{I}}})\bar{\bar{\boldsymbol{I}}}_\perp; \\ \bar{\bar{\boldsymbol{W}}}_2 &= (\bar{\bar{\boldsymbol{I}}}_\perp \cdot \bar{\bar{\boldsymbol{W}}} \cdot \hat{\boldsymbol{b}}\hat{\boldsymbol{b}})^S. \end{aligned} \tag{E39}$$

The same decomposition is used for the stress tensor $\bar{\bar{\boldsymbol{\Pi}}}$:

$$\begin{aligned}
\bar{\bar{\boldsymbol{\Pi}}} &= \bar{\bar{\boldsymbol{\Pi}}}_0 + \bar{\bar{\boldsymbol{\Pi}}}_1 + \bar{\bar{\boldsymbol{\Pi}}}_2;\\
\bar{\bar{\boldsymbol{\Pi}}}_0 &= \frac{3}{2}(\bar{\bar{\boldsymbol{\Pi}}}\colon \hat{\boldsymbol{b}}\hat{\boldsymbol{b}})\left(\hat{\boldsymbol{b}}\hat{\boldsymbol{b}} - \frac{\bar{\bar{\boldsymbol{I}}}}{3}\right) + \frac{1}{2}(\bar{\bar{\boldsymbol{\Pi}}}\colon \bar{\bar{\boldsymbol{I}}})\bar{\bar{\boldsymbol{I}}}_\perp;\\
\bar{\bar{\boldsymbol{\Pi}}}_1 &= \bar{\bar{\boldsymbol{I}}}_\perp \cdot \bar{\bar{\boldsymbol{\Pi}}} \cdot \bar{\bar{\boldsymbol{I}}}_\perp + \frac{1}{2}(\bar{\bar{\boldsymbol{\Pi}}}\colon \hat{\boldsymbol{b}}\hat{\boldsymbol{b}})\bar{\bar{\boldsymbol{I}}}_\perp - \frac{1}{2}(\bar{\bar{\boldsymbol{\Pi}}}\colon \bar{\bar{\boldsymbol{I}}})\bar{\bar{\boldsymbol{I}}}_\perp;\\
\bar{\bar{\boldsymbol{\Pi}}}_2 &= (\bar{\bar{\boldsymbol{I}}}_\perp \cdot \bar{\bar{\boldsymbol{\Pi}}} \cdot \hat{\boldsymbol{b}}\hat{\boldsymbol{b}})^S.
\end{aligned} \tag{E40}$$

Let us solve for $\bar{\bar{\boldsymbol{\Pi}}}_0$. Applying $:\hat{\boldsymbol{b}}\hat{\boldsymbol{b}}$ and $:\bar{\bar{\boldsymbol{I}}}$ at Equation (E33) and using the identities

$$(\hat{\boldsymbol{b}} \times \bar{\bar{\boldsymbol{\Pi}}})^S\colon \hat{\boldsymbol{b}}\hat{\boldsymbol{b}} = 0; \qquad (\hat{\boldsymbol{b}} \times \bar{\bar{\boldsymbol{\Pi}}})^S\colon \bar{\bar{\boldsymbol{I}}} = 0, \tag{E41}$$

yields

$$\bar{\bar{\boldsymbol{\Pi}}}\colon \hat{\boldsymbol{b}}\hat{\boldsymbol{b}} = -\frac{p}{\nu}\bar{\bar{\boldsymbol{W}}}\colon \hat{\boldsymbol{b}}\hat{\boldsymbol{b}}; \qquad \bar{\bar{\boldsymbol{\Pi}}}\colon \bar{\bar{\boldsymbol{I}}} = -\frac{p}{\nu}\bar{\bar{\boldsymbol{W}}}\colon \bar{\bar{\boldsymbol{I}}}, \tag{E42}$$

and plugging these results into (E40) yields the final solution for the parallel stress tensor:

$$\bar{\bar{\boldsymbol{\Pi}}}_0 = -\frac{p}{\nu}\left[\frac{3}{2}(\bar{\bar{\boldsymbol{W}}}\colon \hat{\boldsymbol{b}}\hat{\boldsymbol{b}})\left(\hat{\boldsymbol{b}}\hat{\boldsymbol{b}} - \frac{\bar{\bar{\boldsymbol{I}}}}{3}\right) + \frac{1}{2}(\bar{\bar{\boldsymbol{W}}}\colon \bar{\bar{\boldsymbol{I}}})\bar{\bar{\boldsymbol{I}}}_\perp\right] = -\frac{p}{\nu}\bar{\bar{\boldsymbol{W}}}_0. \tag{E43}$$

The solution is valid for any general matrix $\bar{\bar{\boldsymbol{W}}}$ (not necessarily symmetric or traceless). If this result is compared with the expression (4.42) of Braginskii (1965), given below by (E46), one notices

$$\bar{\bar{\boldsymbol{W}}}_0^{\mathrm{BR}} = (E46) = \frac{3}{2}(\bar{\bar{\boldsymbol{W}}}\colon \hat{\boldsymbol{b}}\hat{\boldsymbol{b}})\left(\hat{\boldsymbol{b}}\hat{\boldsymbol{b}} - \frac{\bar{\bar{\boldsymbol{I}}}}{3}\right) + \frac{1}{2}(\bar{\bar{\boldsymbol{W}}}\colon \bar{\bar{\boldsymbol{I}}})\left(\frac{\bar{\bar{\boldsymbol{I}}}}{3} - \hat{\boldsymbol{b}}\hat{\boldsymbol{b}}\right) \neq \bar{\bar{\boldsymbol{W}}}_0, \tag{E44}$$

and his result is valid only if $\bar{\bar{\boldsymbol{W}}}$ is traceless (which it is). The reason why Braginskii left his result in form (E46), and did not simplify it with $\bar{\bar{\boldsymbol{W}}}\colon \bar{\bar{\boldsymbol{I}}} = 0$, is likely an alternative form (E47).

E.4.2. Symmetric and Traceless Matrices

We further consider only the symmetric and traceless matrices $\bar{\bar{\boldsymbol{W}}}$ and $\bar{\bar{\boldsymbol{\Pi}}}$, so all of the previous expressions are simplified with $\bar{\bar{\boldsymbol{W}}}\colon \bar{\bar{\boldsymbol{I}}} = 0$, $\bar{\bar{\boldsymbol{\Pi}}}\colon \bar{\bar{\boldsymbol{I}}} = 0$, and the BGK parallel stress tensor $\bar{\bar{\boldsymbol{\Pi}}}_0 = -(p/\nu)\bar{\bar{\boldsymbol{W}}}_0$. For clarity, it is useful to write several possible forms for

$$\bar{\bar{\boldsymbol{W}}}_0 = \frac{3}{2}(\bar{\bar{\boldsymbol{W}}}\colon \hat{\boldsymbol{b}}\hat{\boldsymbol{b}})\left(\hat{\boldsymbol{b}}\hat{\boldsymbol{b}} - \frac{\bar{\bar{\boldsymbol{I}}}}{3}\right); \tag{E45}$$

$$= \frac{3}{2}\left[\bar{\bar{\boldsymbol{W}}}\colon \left(\hat{\boldsymbol{b}}\hat{\boldsymbol{b}} - \frac{\bar{\bar{\boldsymbol{I}}}}{3}\right)\right]\left(\hat{\boldsymbol{b}}\hat{\boldsymbol{b}} - \frac{\bar{\bar{\boldsymbol{I}}}}{3}\right); \tag{E46}$$

$$= \frac{3}{2}\left[(\nabla \boldsymbol{u})^S\colon \left(\hat{\boldsymbol{b}}\hat{\boldsymbol{b}} - \frac{\bar{\bar{\boldsymbol{I}}}}{3}\right)\right]\left(\hat{\boldsymbol{b}}\hat{\boldsymbol{b}} - \frac{\bar{\bar{\boldsymbol{I}}}}{3}\right); \tag{E47}$$

$$= 3\left[(\nabla \boldsymbol{u})\colon \left(\hat{\boldsymbol{b}}\hat{\boldsymbol{b}} - \frac{\bar{\bar{\boldsymbol{I}}}}{3}\right)\right]\left(\hat{\boldsymbol{b}}\hat{\boldsymbol{b}} - \frac{\bar{\bar{\boldsymbol{I}}}}{3}\right); \tag{E48}$$

$$= 3\left[\hat{\boldsymbol{b}} \cdot (\nabla \boldsymbol{u}) \cdot \hat{\boldsymbol{b}} - \frac{1}{3}\nabla \cdot \boldsymbol{u}\right]\left(\hat{\boldsymbol{b}}\hat{\boldsymbol{b}} - \frac{\bar{\bar{\boldsymbol{I}}}}{3}\right). \tag{E49}$$

Braginskii uses (E46), Fitzpatrick (2015), for example, uses (E48), and we use (E45). In the reference frame of the magnetic field lines,

$$\bar{\bar{\boldsymbol{W}}}_0 = \frac{3}{2}W_{zz}\begin{pmatrix} -1/3, & 0, & 0\\ 0, & -1/3, & 0\\ 0, & 0, & +2/3\end{pmatrix}; \qquad \bar{\bar{\boldsymbol{\Pi}}}_0 = \frac{p}{\nu}W_{zz}\begin{pmatrix} 1/2, & 0, & 0\\ 0, & 1/2, & 0\\ 0, & 0, & -1\end{pmatrix}. \tag{E50}$$

To solve Equation (E33), it is beneficial to introduce two other matrices $\bar{\bar{W}}_3$, $\bar{\bar{W}}_4$, by decomposing

$$\begin{aligned}(\hat{\boldsymbol{b}} \times \bar{\bar{\boldsymbol{W}}})^S &= 2\bar{\bar{\boldsymbol{W}}}_3 + \bar{\bar{\boldsymbol{W}}}_4;\\ 2\bar{\bar{\boldsymbol{W}}}_3 &= (\hat{\boldsymbol{b}} \times \bar{\bar{\boldsymbol{W}}} \cdot \bar{\bar{\boldsymbol{I}}}_\perp)^S;\\ \bar{\bar{\boldsymbol{W}}}_4 &= (\hat{\boldsymbol{b}} \times \bar{\bar{\boldsymbol{W}}} \cdot \hat{\boldsymbol{b}}\hat{\boldsymbol{b}})^S,\end{aligned} \tag{E51}$$

where in the reference frame of the magnetic field lines,

$$2\bar{\bar{\boldsymbol{W}}}_3 = \begin{pmatrix} -2W_{xy} & W_{xx} - W_{yy} & 0\\ W_{xx} - W_{yy} & 2W_{xy} & 0\\ 0 & 0 & 0\end{pmatrix}; \qquad \bar{\bar{\boldsymbol{W}}}_4 = \begin{pmatrix} 0 & 0 & -W_{yz}\\ 0 & 0 & W_{xz}\\ -W_{yz} & W_{xz} & 0\end{pmatrix}. \tag{E52}$$

The decomposition (E51) is again valid for general $\hat{\boldsymbol{b}}$, which is easily verified using $\bar{\bar{\boldsymbol{I}}}_\perp + \hat{\boldsymbol{b}}\hat{\boldsymbol{b}} = \bar{\bar{\boldsymbol{I}}}$, and the stress tensor is decomposed in the same way:

$$\begin{aligned}(\hat{\boldsymbol{b}} \times \bar{\bar{\boldsymbol{\Pi}}})^S &= 2\bar{\bar{\boldsymbol{\Pi}}}_3 + \bar{\bar{\boldsymbol{\Pi}}}_4;\\ 2\bar{\bar{\boldsymbol{\Pi}}}_3 &= (\hat{\boldsymbol{b}} \times \bar{\bar{\boldsymbol{\Pi}}} \cdot \bar{\bar{\boldsymbol{I}}}_\perp)^S;\\ \bar{\bar{\boldsymbol{\Pi}}}_4 &= (\hat{\boldsymbol{b}} \times \bar{\bar{\boldsymbol{\Pi}}} \cdot \hat{\boldsymbol{b}}\hat{\boldsymbol{b}})^S.\end{aligned} \tag{E53}$$

Finally, applying $\hat{\boldsymbol{b}}\times$ at the matrices $\bar{\bar{\boldsymbol{W}}}_0 \ldots \bar{\bar{\boldsymbol{W}}}_4$ yields the following identities:

$$\begin{aligned}&(\hat{\boldsymbol{b}} \times \bar{\bar{\boldsymbol{W}}}_0)^S = 0; \qquad \hat{\boldsymbol{b}} \times \bar{\bar{\boldsymbol{W}}}_1 = \bar{\bar{\boldsymbol{W}}}_3; \qquad (\hat{\boldsymbol{b}} \times \bar{\bar{\boldsymbol{W}}}_2)^S = \bar{\bar{\boldsymbol{W}}}_4;\\ &\hat{\boldsymbol{b}} \times \bar{\bar{\boldsymbol{W}}}_3 = -\bar{\bar{\boldsymbol{W}}}_1; \qquad (\hat{\boldsymbol{b}} \times \bar{\bar{\boldsymbol{W}}}_4)^S = -\bar{\bar{\boldsymbol{W}}}_2,\end{aligned} \tag{E54}$$

which are easy to verify in a general reference frame with $\hat{\boldsymbol{b}}$. The same identities hold for the stress tensor

$$\begin{aligned}&(\hat{\boldsymbol{b}} \times \bar{\bar{\boldsymbol{\Pi}}}_0)^S = 0; \qquad \hat{\boldsymbol{b}} \times \bar{\bar{\boldsymbol{\Pi}}}_1 = \bar{\bar{\boldsymbol{\Pi}}}_3; \qquad (\hat{\boldsymbol{b}} \times \bar{\bar{\boldsymbol{\Pi}}}_2)^S = \bar{\bar{\boldsymbol{\Pi}}}_4;\\ &\hat{\boldsymbol{b}} \times \bar{\bar{\boldsymbol{\Pi}}}_3 = -\bar{\bar{\boldsymbol{\Pi}}}_1; \qquad (\hat{\boldsymbol{b}} \times \bar{\bar{\boldsymbol{\Pi}}}_4)^S = -\bar{\bar{\boldsymbol{\Pi}}}_2.\end{aligned} \tag{E55}$$

E.4.3. Final Solution

Now we are ready to solve Equation (E33), which is rewritten as

$$2\bar{\bar{\boldsymbol{\Pi}}}_3 + \bar{\bar{\boldsymbol{\Pi}}}_4 + \frac{\nu}{\Omega}(\bar{\bar{\boldsymbol{\Pi}}}_0 + \bar{\bar{\boldsymbol{\Pi}}}_1 + \bar{\bar{\boldsymbol{\Pi}}}_2) = -\frac{p}{\Omega}(\bar{\bar{\boldsymbol{W}}}_0 + \bar{\bar{\boldsymbol{W}}}_1 + \bar{\bar{\boldsymbol{W}}}_2). \tag{E56}$$

One solution, $\bar{\bar{\boldsymbol{\Pi}}}_0 = -(p/\nu)\bar{\bar{\boldsymbol{W}}}_0$, has already been obtained, and can be eliminated from (E56). For the rest of the equation, the most straightforward approach is to be guided by the reference frame of the magnetic field lines, which shows that the system (E56) can be directly split into two independent equations:

$$2\bar{\bar{\boldsymbol{\Pi}}}_3 + \frac{\nu}{\Omega}\bar{\bar{\boldsymbol{\Pi}}}_1 = -\frac{p}{\Omega}\bar{\bar{\boldsymbol{W}}}_1; \tag{E57}$$

$$\bar{\bar{\boldsymbol{\Pi}}}_4 + \frac{\nu}{\Omega}\bar{\bar{\boldsymbol{\Pi}}}_2 = -\frac{p}{\Omega}\bar{\bar{\boldsymbol{W}}}_2. \tag{E58}$$

In the general reference frame, the split can be achieved by applying $\bar{\bar{\boldsymbol{I}}}_\perp\cdot$ from left and right at (E56), for example, which, using identities $\bar{\bar{\boldsymbol{I}}}_\perp \cdot \bar{\bar{\boldsymbol{\Pi}}}_4 \cdot \bar{\bar{\boldsymbol{I}}}_\perp = 0$, $\bar{\bar{\boldsymbol{I}}}_\perp \cdot \bar{\bar{\boldsymbol{\Pi}}}_2 \cdot \bar{\bar{\boldsymbol{I}}}_\perp = 0$, and $\bar{\bar{\boldsymbol{I}}}_\perp \cdot \bar{\bar{\boldsymbol{W}}}_2 \cdot \bar{\bar{\boldsymbol{I}}}_\perp = 0$, yields (E57) and subsequently (E58). The split significantly simplifies the "inversion procedure."

Furthermore, applying $\hat{\boldsymbol{b}}\times$ at (E57), applying $\hat{\boldsymbol{b}}\times$ together with the symmetric operator at (E58), and using the identities (E54)–(E55) then gives

$$-2\bar{\bar{\boldsymbol{\Pi}}}_1 + \frac{\nu}{\Omega}\bar{\bar{\boldsymbol{\Pi}}}_3 = -\frac{p}{\Omega}\bar{\bar{\boldsymbol{W}}}_3; \tag{E59}$$

$$-\bar{\bar{\boldsymbol{\Pi}}}_2 + \frac{\nu}{\Omega}\bar{\bar{\boldsymbol{\Pi}}}_4 = -\frac{p}{\Omega}\bar{\bar{\boldsymbol{W}}}_4. \tag{E60}$$

Equations (E57), (E59) are coupled and can be treated as two equations in two unknowns, and similarly Equations (E58), (E60), finally yielding the solutions

$$\bar{\bar{\boldsymbol{\Pi}}}_1 = -\frac{p\nu}{4\Omega^2 + \nu^2}\bar{\bar{\boldsymbol{W}}}_1 + \frac{2p\Omega}{4\Omega^2 + \nu^2}\bar{\bar{\boldsymbol{W}}}_3; \tag{E61}$$

$$\bar{\bar{\boldsymbol{\Pi}}}_2 = -\frac{p\nu}{\Omega^2 + \nu^2}\bar{\bar{\boldsymbol{W}}}_2 + \frac{p\Omega}{\Omega^2 + \nu^2}\bar{\bar{\boldsymbol{W}}}_4. \tag{E62}$$

The entire solution for the stress tensor $\bar{\bar{\boldsymbol{\Pi}}} = \bar{\bar{\boldsymbol{\Pi}}}_0 + \bar{\bar{\boldsymbol{\Pi}}}_1 + \bar{\bar{\boldsymbol{\Pi}}}_2$ thus reads

$$\bar{\bar{\boldsymbol{\Pi}}} = -\frac{p}{\nu}\bar{\bar{\boldsymbol{W}}}_0 - \frac{p\nu}{4\Omega^2+\nu^2}\bar{\bar{\boldsymbol{W}}}_1 - \frac{p\nu}{\Omega^2+\nu^2}\bar{\bar{\boldsymbol{W}}}_2 + \frac{2p\Omega}{4\Omega^2+\nu^2}\bar{\bar{\boldsymbol{W}}}_3 + \frac{p\Omega}{\Omega^2+\nu^2}\bar{\bar{\boldsymbol{W}}}_4. \tag{E63}$$

E.5. BGK Operator and Electric Field

The BGK operator is also an excellent tool for clarifying various processes in fully ionized or partially ionized plasmas. Here we want to clarify the ohmic (magnetic) diffusion together with the ambipolar diffusion, both caused by the momentum exchange rates

$$\boldsymbol{R}_a = \sum_{b\neq a}\rho_a\nu_{ab}(\boldsymbol{u}_b - \boldsymbol{u}_a). \tag{E64}$$

From the BGK perspective, one does not need to worry about complicated Landau and Boltzmann operators, and simply "adopts" the correct collisional frequencies; see, for example, Appendix C of Schunk (1977). The momentum exchange rates (E64) are actually the correct answer if the relative drift velocities are small and one considers the 5-moment model (i.e., if the heat flux is neglected).

We restrict our focus to spatial scales much longer than the Debye length. The displacement current is neglected, the Gauss law $\nabla\cdot\boldsymbol{E} = 4\pi e\sum_a Z_a n_a$ is replaced by the charge neutrality, and no condition is placed on $\nabla\cdot\boldsymbol{E}$. The Maxwell equations then read

$$\sum_a Z_a n_a = 0; \qquad \boldsymbol{j} = \sum_a eZ_a n_a\boldsymbol{u}_a = \frac{c}{4\pi}\nabla\times\boldsymbol{B}; \tag{E65}$$

$$\frac{\partial\boldsymbol{B}}{\partial t} = -c\nabla\times\boldsymbol{E}; \qquad \nabla\cdot\boldsymbol{B} = 0. \tag{E66}$$

By focusing on the spatial and temporal scales of the ion and neutral species, we do not need to resolve the electron motion. In the electron momentum equation, the electron inertia represented by $d_e\boldsymbol{u}_e/dt$ is neglected (which does not mean that $m_e = 0$; relations $\rho_a\nu_{ab} = \rho_b\nu_{ba}$ still hold), and the electric field is expressed as

$$\boldsymbol{E} = -\frac{1}{c}\boldsymbol{u}_e\times\boldsymbol{B} - \frac{1}{en_e}\nabla\cdot\bar{\bar{\boldsymbol{p}}}_e + \frac{\boldsymbol{R}_e}{en_e}. \tag{E67}$$

The momentum equations for the ions then become

$$\rho_i\frac{d_i\boldsymbol{u}_i}{dt} + \nabla\cdot\bar{\bar{\boldsymbol{p}}}_i + \frac{Z_i n_i}{n_e}\nabla\cdot\bar{\bar{\boldsymbol{p}}}_e - \frac{eZ_i n_i}{c}(\boldsymbol{u}_i - \boldsymbol{u}_e)\times\boldsymbol{B} = \boldsymbol{R}_i + \frac{Z_i n_i}{n_e}\boldsymbol{R}_e. \tag{E68}$$

Also, by using (E65), the electron density n_e and electron velocity $\boldsymbol{u}_e$ are expressed as

$$n_e = \sum_i Z_i n_i; \qquad \boldsymbol{u}_e = \frac{1}{n_e}\sum_i Z_i n_i\boldsymbol{u}_i - \frac{\boldsymbol{j}}{en_e}; \qquad \boldsymbol{j} = \frac{c}{4\pi}\nabla\times\boldsymbol{B}, \tag{E69}$$

where the summations are over ion species. The electron density equation $\partial n_e/\partial t + \nabla\cdot(n_e\boldsymbol{u}_e) = 0$ becomes redundant, because multiplying all of the density equations for the charges (including electrons) by Z_a and summing them together yields a requirement $\nabla\cdot(\sum_a Z_a n_a\boldsymbol{u}_a) = 0$, which is automatically satisfied by $\nabla\cdot\boldsymbol{j} = 0$ in (E69). Expressions (E69) and (E67) can then be substituted to all of the other equations (which is easy to do numerically), and the occurrences of $\boldsymbol{E}$, $\boldsymbol{u}_e$, and n_e in the entire model are thus eliminated.

For a particular case of $\boldsymbol{R}_e$ given by (E64), the electric field (E67) then becomes

$$\begin{aligned}\boldsymbol{E} = &-\frac{1}{cn_e}\Big(\sum_i Z_i n_i\boldsymbol{u}_i\Big)\times\boldsymbol{B} + \frac{\boldsymbol{j}\times\boldsymbol{B}}{cen_e} - \frac{1}{en_e}\nabla\cdot\bar{\bar{\boldsymbol{p}}}_e + \frac{m_e}{e^2n_e}\boldsymbol{j}\sum_{a\neq e}\nu_{ea}\\ &+\frac{m_e}{e}\left[\Big(\sum_{a\neq e}\nu_{ea}\boldsymbol{u}_a\Big) - \frac{1}{n_e}\Big(\sum_{a\neq e}\nu_{ea}\Big)\Big(\sum_i Z_i n_i\boldsymbol{u}_i\Big)\right].\end{aligned} \tag{E70}$$

The summations over "a" include both ions and neutrals. The terms on the right-hand-side can be called the convective term, the Hall term, the electron pressure term, the ohmic term, and a mixed collisional term due to ion and neutral velocities, respectively. When (E70) is used in the induction equation, the ohmic term ($\sim\boldsymbol{j}$) becomes directly diffusive through the identity $\nabla\times(\eta_B\nabla\times\boldsymbol{B}) = -\eta_B\nabla^2\boldsymbol{B} + \nabla(\eta_B)\times(\nabla\times\boldsymbol{B})$, where one defines a coefficient of magnetic diffusion $\eta_B = (\sum_{a\neq e}\nu_{ea})m_e c^2/(4\pi e^2 n_e)$. In contrast, no other term in (E70) is directly diffusive in this sense. Nevertheless, the so-called ambipolar diffusion due to the differences in the velocities $\boldsymbol{u}_a$ between different species is still present implicitly, which can be shown by solving the dispersion relations. The explicit presence of ambipolar diffusion caused by $\sim -(\boldsymbol{j}\times\boldsymbol{B})\times\boldsymbol{B} = \boldsymbol{j}_\perp|\boldsymbol{B}|^2$ is revealed by the construction of a single-fluid model, formulated with respect to the center-of-mass velocity of all of the species. In general, ambipolar diffusion between two species with indices (a, b) exists if

$$\frac{Z_a}{m_a} \neq \frac{Z_b}{m_b}, \tag{E71}$$

which is demonstrated in Appendix E.6.

In partially ionized solar plasmas, one often focuses on a two-fluid model, formulated with center-of-mass velocities for the ion species $\langle \boldsymbol{u}_i \rangle = (\sum_i \rho_i \boldsymbol{u}_i)/\sum_i \rho_i$ and for the neutral species $\langle \boldsymbol{u}_n \rangle = (\sum_n \rho_n \boldsymbol{u}_n)/\sum_n \rho_n$. The velocities for each species are thus decomposed into $\boldsymbol{u}_i = \langle \boldsymbol{u}_i \rangle + \boldsymbol{w}_i$, $\boldsymbol{u}_n = \langle \boldsymbol{u}_n \rangle + \boldsymbol{w}_n$, where $\boldsymbol{w}_i$, $\boldsymbol{w}_n$ represent drifts; and because $\langle \boldsymbol{u}_i \rangle$, $\langle \boldsymbol{u}_n \rangle$ can be pulled out in front of the summations, the electric field (E70) transforms into

$$\begin{aligned}\boldsymbol{E} = &-\frac{1}{c}\langle \boldsymbol{u}_i \rangle \times \boldsymbol{B} - \frac{1}{cen_e}(\sum_i Z_i n_i \boldsymbol{w}_i) \times \boldsymbol{B} + \frac{\boldsymbol{j} \times \boldsymbol{B}}{cen_e} - \frac{1}{en_e}\nabla \cdot \bar{\bar{\boldsymbol{p}}}_e + \frac{m_e}{e^2 n_e}\boldsymbol{j}\sum_{a \neq e}\nu_{ea} \\ &+(\langle \boldsymbol{u}_n \rangle - \langle \boldsymbol{u}_i \rangle)\frac{m_e}{e}\sum_n \nu_{en} \\ &+\frac{m_e}{e}\left[(\sum_{a \neq e}\nu_{ea}\boldsymbol{w}_a) - \frac{1}{n_e}(\sum_{a \neq e}\nu_{ea})(\sum_i Z_i n_i \boldsymbol{w}_i)\right].\end{aligned} \tag{E72}$$

The electric field (E72) still represents a multifluid electric field, where one considers separate evolution equations for all of the drifts $\boldsymbol{w}_a$. To obtain a two-fluid electric field, these drifts have to be somehow eliminated, which is of course not straightforward to justify. In partially ionized solar plasmas, the usual justification is that (1) one takes into account only the first ionization degree, with all of the ions having $Z_i = 1$; (2) one prescribes that on average $\sum_i n_i \boldsymbol{w}_i = 0$ (which, for example, eliminates ambipolar diffusion between different ions), together with $\sum_n n_n \boldsymbol{w}_n = 0$; (3) all of the species have roughly the same temperature, which, using the collisional frequencies $\nu_{ei} = n_i f(T)/\sqrt{m_e}$, yields $\sum_i \nu_{ei}\boldsymbol{w}_i = 0$; and (4) all of the neutrals have roughly the same cross sections (radii r_n), which, using $\nu_{en} = n_n f(T) r_n^2/\sqrt{m_e}$, yields $\sum_n \nu_{en}\boldsymbol{w}_n = 0$. The two-fluid electric field thus reads

$$\begin{aligned}\boldsymbol{E} = &-\frac{1}{c}\langle \boldsymbol{u}_i \rangle \times \boldsymbol{B} + \frac{\boldsymbol{j} \times \boldsymbol{B}}{cen_e} - \frac{1}{en_e}\nabla \cdot \bar{\bar{\boldsymbol{p}}}_e + \frac{m_e}{e^2 n_e}\boldsymbol{j}\sum_{a \neq e}\nu_{ea} \\ &+(\langle \boldsymbol{u}_n \rangle - \langle \boldsymbol{u}_i \rangle)\frac{m_e}{e}\sum_n \nu_{en}.\end{aligned} \tag{E73}$$

The center-of-mass velocity for the ions $\langle \boldsymbol{u}_i \rangle$ can be freely replaced by the center-of-mass velocity for all the charges $\langle \boldsymbol{u}_c \rangle$ (which include electrons). Then, the electric field (E73) is almost identical to Equation (115) of Khomenko et al. (2014), except that the $\sum_n \nu_{en}$ in the last term of (E73) is replaced by $(\sum_n \nu_{en}) - (\sum_i \sum_n \nu_{in})$ in that paper. The difference arises from the alternative approach in that paper, where the electron inertia is not neglected from the beginning, but instead the electric field is derived by first summing momentum equations for all of the species together, and prescribing quasistatic current $\boldsymbol{j}$. Then, the subsequent expansion in the mass ratios retains the contributions from $\boldsymbol{R}_i$. Nevertheless, the missing contributions are small $\nu_{in} \ll \nu_{en}$, explaining the small difference between these two approaches.

For a particular case of only one ion species and one neutral species, so that $n_e = Z_i n_i$ and $\boldsymbol{u}_e = \boldsymbol{u}_i - \boldsymbol{j}/(en_e)$, the electric field (E70) simplifies into

$$\begin{aligned}\boldsymbol{E} = &-\frac{1}{c}\boldsymbol{u}_i \times \boldsymbol{B} + \frac{\boldsymbol{j} \times \boldsymbol{B}}{cen_e} - \frac{1}{en_e}\nabla \cdot \bar{\bar{\boldsymbol{p}}}_e + \frac{m_e}{e^2 n_e}\boldsymbol{j}(\nu_{ei} + \nu_{en}) \\ &+\frac{m_e}{e}\nu_{en}(\boldsymbol{u}_n - \boldsymbol{u}_i);\end{aligned} \tag{E74}$$

$$\begin{aligned}\frac{\partial \boldsymbol{B}}{\partial t} = &\nabla \times (\boldsymbol{u}_i \times \boldsymbol{B}) - \nabla \times \left(\frac{\boldsymbol{j}}{en_e} \times \boldsymbol{B}\right) + \frac{c}{e}\nabla \times \left(\frac{1}{n_e}\nabla \cdot \bar{\bar{\boldsymbol{p}}}_e\right) \\ &-\nabla \times (\eta_B \nabla \times \boldsymbol{B}) - \nabla \times \left[\frac{cm_e}{e}\nu_{en}(\boldsymbol{u}_n - \boldsymbol{u}_i)\right],\end{aligned} \tag{E75}$$

with the coefficient of magnetic diffusion $\eta_B = (\nu_{ei} + \nu_{en})m_e c^2/(4\pi e^2 n_e)$.

E.6. Ambipolar Diffusion of Two Ion Species

Here we consider a two-fluid model, consisting of two different ion species with species indices (i, j), so that the charge neutrality reads $n_e = Z_i n_i + Z_j n_j$. A particular case consisting of one ion and one neutral species can be obtained by prescribing $Z_j = 0$ and index $j = n$ (or $Z_i = 0$ and $i = n$). The momentum equations are

$$\rho_i \frac{d_i \boldsymbol{u}_i}{dt} + \nabla \cdot \bar{\bar{\boldsymbol{p}}}_i + \frac{Z_i n_i}{n_e}\nabla \cdot \bar{\bar{\boldsymbol{p}}}_e - \frac{eZ_i n_i}{c}\frac{Z_j n_j}{n_e}(\boldsymbol{u}_i - \boldsymbol{u}_j) \times \boldsymbol{B} - \frac{Z_i n_i}{cn_e}\boldsymbol{j} \times \boldsymbol{B} = \boldsymbol{R}_i + \frac{Z_i n_i}{n_e}\boldsymbol{R}_e; \tag{E76}$$

$$\rho_j \frac{d_j \boldsymbol{u}_j}{dt} + \nabla \cdot \bar{\bar{\boldsymbol{p}}}_j + \frac{Z_j n_j}{n_e}\nabla \cdot \bar{\bar{\boldsymbol{p}}}_e + \frac{eZ_i n_i}{c}\frac{Z_j n_j}{n_e}(\boldsymbol{u}_i - \boldsymbol{u}_j) \times \boldsymbol{B} - \frac{Z_j n_j}{cn_e}\boldsymbol{j} \times \boldsymbol{B} = \boldsymbol{R}_j + \frac{Z_j n_j}{n_e}\boldsymbol{R}_e, \tag{E77}$$

with the collisional right-hand sides being

$$\boldsymbol{R}_i + \frac{Z_i n_i}{n_e}\boldsymbol{R}_e = -(\boldsymbol{u}_i - \boldsymbol{u}_j)\left[\rho_i \nu_{ij} + \rho_e \nu_{ei}\left(\frac{Z_j n_j}{n_e}\right)^2 + \rho_e \nu_{ej}\left(\frac{Z_i n_i}{n_e}\right)^2\right] - \boldsymbol{j}\frac{m_e}{e n_e}(\nu_{ei} Z_j n_j - \nu_{ej} Z_i n_i);$$

$$\boldsymbol{R}_j + \frac{Z_j n_j}{n_e}\boldsymbol{R}_e = (\boldsymbol{u}_i - \boldsymbol{u}_j)\left[\rho_i \nu_{ij} + \rho_e \nu_{ei}\left(\frac{Z_j n_j}{n_e}\right)^2 + \rho_e \nu_{ej}\left(\frac{Z_i n_i}{n_e}\right)^2\right] + \boldsymbol{j}\frac{m_e}{e n_e}(\nu_{ei} Z_j n_j - \nu_{ej} Z_i n_i), \tag{E78}$$

and the electric field (which determines the induction equation) reading

$$\boldsymbol{E} = -\frac{1}{c n_e}(Z_i n_i \boldsymbol{u}_i + Z_j n_j \boldsymbol{u}_j) \times \boldsymbol{B} + \frac{\boldsymbol{j} \times \boldsymbol{B}}{c e n_e} - \frac{1}{e n_e}\nabla \cdot \bar{\bar{\boldsymbol{p}}}_e + \frac{m_e}{e^2 n_e}\boldsymbol{j}(\nu_{ei} + \nu_{ej}) + \frac{m_e}{e n_e}(\boldsymbol{u}_i - \boldsymbol{u}_j)(Z_j n_j \nu_{ei} - Z_i n_i \nu_{ej}). \tag{E79}$$

The ambipolar diffusion term $-\boldsymbol{j} \times \boldsymbol{B} \times \boldsymbol{B} = \boldsymbol{j}_\perp |\boldsymbol{B}|^2$ is not directly present in the electric field, and the only term that directly causes magnetic diffusion in the induction equation is the ohmic term ($\sim \boldsymbol{j}$). Nevertheless, the ambipolar diffusion is still present implicitly, which can be shown by solving the dispersion relations or by constructing a single-fluid model.

Using the same notation as Zaqarashvili et al. (2011), and introducing the center-of-mass velocity $\boldsymbol{V} = (\rho_i \boldsymbol{u}_i + \rho_j \boldsymbol{u}_j)/\rho$, where the total density $\rho = \rho_i + \rho_j$ and the difference in velocities $\boldsymbol{w} = \boldsymbol{u}_i - \boldsymbol{u}_j$, so that $\boldsymbol{u}_i = \boldsymbol{V} + (\rho_j/\rho)\boldsymbol{w}$, $\boldsymbol{u}_j = \boldsymbol{V} - (\rho_i/\rho)\boldsymbol{w}$, yields the momentum equations

$$\rho\frac{\partial \boldsymbol{V}}{\partial t} + \rho \boldsymbol{V} \cdot \nabla \boldsymbol{V} + \nabla \cdot (\bar{\bar{\boldsymbol{p}}}_i + \bar{\bar{\boldsymbol{p}}}_j + \bar{\bar{\boldsymbol{p}}}_e) - \frac{1}{c}\boldsymbol{j} \times \boldsymbol{B} + \nabla \cdot \left(\frac{\rho_i \rho_j}{\rho}\boldsymbol{w}\boldsymbol{w}\right) = 0; \tag{E80}$$

$$\frac{\partial \boldsymbol{w}}{\partial t} + \boldsymbol{w} \cdot \nabla \boldsymbol{V} + \boldsymbol{V} \cdot \nabla \boldsymbol{w} + \frac{\rho_j}{\rho}\boldsymbol{w} \cdot \nabla \boldsymbol{w} - \boldsymbol{w} \cdot \nabla\left(\frac{\rho_i}{\rho}\boldsymbol{w}\right) - \frac{e Z_i n_i Z_j n_j}{c n_e}\frac{\rho}{\rho_i \rho_j}\boldsymbol{w} \times \boldsymbol{B} + \frac{1}{\rho_i}\nabla \cdot \bar{\bar{\boldsymbol{p}}}_i - \frac{1}{\rho_j}\nabla \cdot \bar{\bar{\boldsymbol{p}}}_j + \frac{1}{n_e}\left(\frac{Z_i n_i}{\rho_i} - \frac{Z_j n_j}{\rho_j}\right)\left(\nabla \cdot \bar{\bar{\boldsymbol{p}}}_e - \frac{1}{c}\boldsymbol{j} \times \boldsymbol{B}\right)$$
$$= -\boldsymbol{w}\frac{\rho}{\rho_i \rho_j}\left[\rho_i \nu_{ij} + \rho_e \nu_{ei}\left(\frac{Z_j n_j}{n_e}\right)^2 + \rho_e \nu_{ej}\left(\frac{Z_i n_i}{n_e}\right)^2\right] - \boldsymbol{j}\frac{\rho}{\rho_i \rho_j}\frac{m_e}{e n_e}(\nu_{ei} Z_j n_j - \nu_{ej} Z_i n_i), \tag{E81}$$

with the electric field

$$\boldsymbol{E} = -\frac{1}{c}\boldsymbol{V} \times \boldsymbol{B} - \frac{1}{c n_e \rho}(Z_i n_i \rho_j - Z_j n_j \rho_i)\boldsymbol{w} \times \boldsymbol{B} + \frac{\boldsymbol{j} \times \boldsymbol{B}}{c e n_e} - \frac{1}{e n_e}\nabla \cdot \bar{\bar{\boldsymbol{p}}}_e + \frac{m_e}{e^2 n_e}\boldsymbol{j}(\nu_{ei} + \nu_{ej}) + \frac{m_e}{e n_e}\boldsymbol{w}(Z_j n_j \nu_{ei} - Z_i n_i \nu_{ej}). \tag{E82}$$

The system (E80)–(E82) is of course equivalent to (E76)–(E79). However, in a particular case when the collisions are very frequent, the right-hand side of (E81) becomes very large, and neglecting all of the "inertial" terms in the first line of (E81) with $\boldsymbol{w}$ allows one to obtain an explicit expression for the velocity difference

$$\boldsymbol{w} = \frac{1}{D}\left[-\boldsymbol{j}\frac{m_e}{e n_e}(\nu_{ei} Z_j n_j - \nu_{ej} Z_i n_i) - \frac{\rho_j}{\rho}\nabla \cdot \bar{\bar{\boldsymbol{p}}}_i + \frac{\rho_i}{\rho}\nabla \cdot \bar{\bar{\boldsymbol{p}}}_j - \frac{1}{\rho n_e}(Z_i n_i \rho_j - Z_j n_j \rho_i)\left(\nabla \cdot \bar{\bar{\boldsymbol{p}}}_e - \frac{1}{c}\boldsymbol{j} \times \boldsymbol{B}\right)\right], \tag{E83}$$

where we define the denominator

$$D = \left[\rho_i \nu_{ij} + \rho_e \nu_{ei}\left(\frac{Z_j n_j}{n_e}\right)^2 + \rho_e \nu_{ej}\left(\frac{Z_i n_i}{n_e}\right)^2\right]. \tag{E84}$$

For frequent collisions, only the first term in (E83) $\sim \boldsymbol{j}$ is finite, and all of the other terms are small. Nevertheless, the sought-after term is the last term in (E83) $\sim \boldsymbol{j} \times \boldsymbol{B}$, because when (E83) is used in (E82) it creates the ambipolar term $\sim -\boldsymbol{j} \times \boldsymbol{B} \times \boldsymbol{B}$. The single-

fluid electric field reads

$$\begin{aligned}\boldsymbol{E} = &-\frac{1}{c}\boldsymbol{V}\times\boldsymbol{B} + \boldsymbol{j}\frac{m_e}{e^2 n_e}\left[\nu_{ei}+\nu_{ej}-\frac{m_e}{n_e D}(\nu_{ei}Z_j n_j - \nu_{ej}Z_i n_i)^2\right]\\ &+\frac{\boldsymbol{j}\times\boldsymbol{B}}{cen_e}\left[1+\frac{2m_e}{n_e\rho D}(Z_i n_i\rho_j - Z_j n_j\rho_i)(\nu_{ei}Z_j n_j - \nu_{ej}Z_i n_i)\right]\\ &-\frac{\boldsymbol{j}\times\boldsymbol{B}\times\boldsymbol{B}}{c^2 n_e^2\rho^2 D}(Z_i n_i\rho_j - Z_j n_j\rho_i)^2\\ &-\frac{\nabla\cdot\bar{\bar{\boldsymbol{p}}}_e}{en_e}\left[1+\frac{m_e}{\rho n_e D}(Z_j n_j\nu_{ei} - Z_i n_i\nu_{ej})(Z_i n_i\rho_j - Z_j n_j\rho_i)\right]\\ &+\frac{m_e}{en_e\rho D}(Z_j n_j\nu_{ei} - Z_i n_i\nu_{ej})[-\rho_j\nabla\cdot\bar{\bar{\boldsymbol{p}}}_i + \rho_i\nabla\cdot\bar{\bar{\boldsymbol{p}}}_j]\\ &-\frac{1}{cn_e\rho^2 D}(Z_i n_i\rho_j - Z_j n_j\rho_i)\left[-\rho_j\nabla\cdot\bar{\bar{\boldsymbol{p}}}_i + \rho_i\nabla\cdot\bar{\bar{\boldsymbol{p}}}_j - \frac{1}{n_e}(Z_i n_i\rho_j - Z_j n_j\rho_i)\nabla\cdot\bar{\bar{\boldsymbol{p}}}_e\right]\times\boldsymbol{B}.\end{aligned} \tag{E85}$$

Importantly, the sign in front of the ambipolar term is negative, and because $-\boldsymbol{j}\times\boldsymbol{B}\times\boldsymbol{B} = +\boldsymbol{j}_\perp|\boldsymbol{B}|^2$, the term indeed creates diffusion in the induction equation. It is possible to define a coefficient of ambipolar diffusion:

$$\eta_{\rm A} = \frac{|\boldsymbol{B}|^2}{4\pi\rho}A = V_{\rm A}^2 A; \quad \text{where} \quad A = \frac{(Z_i n_i\rho_j - Z_j n_j\rho_i)^2}{n_e^2\rho D}, \tag{E86}$$

and $V_{\rm A}$ is the Alfvén speed. As a double check, prescribing zero charge for one of the species, the electric field (E85) identifies with Equation (A.10) of Zaqarashvili et al. (2011; for example, our denominator simplifies to $D = \alpha_{in} + \alpha_{en} = \alpha_n$). Also, $\eta_{\rm A} = |\boldsymbol{B}|^2\rho_n^2/(4\pi\rho^2(\rho_i\nu_{in} + \rho_e\nu_{en}))$ identifies with the usual coefficient of ambipolar diffusion; see, for example, Equation (20) in Khomenko & Collados (2012; after switching to cgs units with $\mu_0 \to 4\pi$). The ambipolar diffusion exists if

$$\frac{Z_i}{m_i} \neq \frac{Z_j}{m_j}. \tag{E87}$$

It is important to emphasize that the reduction to a single-fluid model was obtained by assuming that collisions are sufficiently frequent, and that the ambipolar diffusion (as well as other terms) now contains a denominator D, which can be simplified into $D = \rho_i\nu_{ij}$. So, when the collisional frequencies ν_{ij} become small, this leads to an artificial "explosion" of the ambipolar diffusion. This is nicely demonstrated in the figures of Zaqarashvili et al. (2011) plotted with respect to a wavenumber $\bar{k} \sim k/\nu$, where it is shown that for a single-fluid description, the ambipolar diffusion in a collisionless regime (when $\bar{k}$ becomes large) yields cutoff frequencies for waves. The mechanism is completely analogous to the "explosion" of the Braginskii stress tensor or the heat flux vector in a collisionless regime. In contrast, as they show in their two-fluid figures, no "explosion" of the ambipolar diffusion is present. The effect is further discussed in Zaqarashvili et al. (2012).

E.6.1. Damping of Alfvén Waves

For example, considering Alfvén waves at long wavelengths, and focusing only on the ambipolar diffusion (with the Hall-term, ohmic terms, and pressure terms neglected), the induction equation reads

$$\frac{\partial\boldsymbol{B}}{\partial t} = \nabla\times(\boldsymbol{V}\times\boldsymbol{B}) + \nabla\times[\eta_{\rm A}(\nabla\times\boldsymbol{B})_\perp], \tag{E88}$$

with the coefficient of ambipolar diffusion (E86). This yields the following dispersion relation for Alfvén waves:

$$\omega^2 + i\omega V_a^2 k_\parallel^2 A - V_{\rm A}^2 k_\parallel^2 = 0, \tag{E89}$$

with solutions

$$\omega = \pm V_{\rm A}|k_\parallel|\sqrt{1-\left(\frac{V_{\rm A}k_\parallel A}{2}\right)^2} - i\frac{V_{\rm A}^2 k_\parallel^2 A}{2}. \tag{E90}$$

Obviously, the Alfvén waves are damped, and for wavenumbers $k_\parallel \geqslant 2/(V_{\rm A}A)$ the real part of the frequency even becomes zero, so the wave stops existing (i.e., a cutoff wavenumber). For the particular case of one species being neutral, the quantity $A = \rho_n^2/(\rho\alpha_n)$, which can be approximated as $A = \rho_n^2/(\rho\alpha_{in}) = \zeta_n^2/(\zeta_i\nu_{in})$. Then, expressions (E89), (E90) identify with Equations (44)–(47) of Zaqarashvili et al. (2011); however, one needs to use their definition $\nu_{in} = \alpha_{in}/\rho$ instead of the more logical (and correct) $\nu_{in} = \alpha_{in}/\rho_i$.

Appendix F
General Fokker–Planck Collisional Operator

For Coulomb collisions, the Boltzmann collisional operator can be approximated by a general Fokker–Planck type of collisional operator,

$$C_{ab}(f_a, f_b) = -\nabla_v \cdot \left[\boldsymbol{A}_{ab} f_a - \frac{1}{2}\nabla_v \cdot (\bar{\bar{\boldsymbol{D}}}_{ab} f_a)\right], \tag{F1}$$

where the higher-order derivatives in velocity space are neglected, and where $\boldsymbol{A}$ is called a dynamical friction vector and $\bar{\bar{\boldsymbol{D}}}$ is called a diffusion tensor. In space physics and astrophysics, various approximations for $\boldsymbol{A}$ and $\bar{\bar{\boldsymbol{D}}}$ are used, and if a collisional operator has the form (F1), then Equation (A1) is summarily called the Fokker–Planck equation. Summation over all of the species (including self-collisions) then defines the full operator $C(f_a) = \sum_b C_{ab}(f_a, f_b)$, which can be also written as $C(f_a) = -\nabla_v \cdot [\boldsymbol{A}_a f_a - (1/2)\nabla_v \cdot (\bar{\bar{\boldsymbol{D}}}_a f_a)]$, where one defines $\boldsymbol{A}_a = \sum_b \boldsymbol{A}_{ab}$ and $\bar{\bar{\boldsymbol{D}}}_a = \sum_b \bar{\bar{\boldsymbol{D}}}_{ab}$. The Fokker–Planck operators work extremely well for any collisional process where collisions with a small scattering angle dominate, and where a lot of subsequent collisions gradually yield (in the sense of a random walk) a significant deviation from a particle's original velocity direction. This is exactly the case for the scattering by the electrostatic Coulomb force, where the Rutherford scattering cross section is proportional to $1/\sin^4(\chi/2)$ and heavily dominated by events with a small scattering angle χ.

For any tensor $\bar{\bar{\boldsymbol{X}}}$, a general Fokker–Planck operator can be integrated according to

$$\int \bar{\bar{\boldsymbol{X}}} C_{ab}(f_a, f_b) d^3v = \int f_a \boldsymbol{A}_{ab} \cdot \frac{\partial \bar{\bar{\boldsymbol{X}}}}{\partial \boldsymbol{v}} d^3v + \frac{1}{2}\int f_a \bar{\bar{\boldsymbol{D}}}_{ab} : \frac{\partial}{\partial \boldsymbol{v}} \frac{\partial \bar{\bar{\boldsymbol{X}}}}{\partial \boldsymbol{v}} d^3v, \tag{F2}$$

and, for clarity, explicitly in the index notation

$$\int \bar{\bar{\boldsymbol{X}}} C_{ab}(f_a, f_b) d^3v = \int f_a A_i^{ab} \frac{\partial \bar{\bar{\boldsymbol{X}}}}{\partial v_i} d^3v + \frac{1}{2}\int f_a D_{ij}^{ab} \frac{\partial}{\partial v_i}\frac{\partial \bar{\bar{\boldsymbol{X}}}}{\partial v_j} d^3v. \tag{F3}$$

The useful identities are

$$\frac{\partial |\boldsymbol{v}|}{\partial v_i} = \frac{v_i}{|\boldsymbol{v}|}; \quad \frac{\partial |\boldsymbol{c}|}{\partial v_i} = \frac{c_i}{|\boldsymbol{c}|}; \quad \frac{\partial |\boldsymbol{v}|^2}{\partial v_i} = 2v_i; \quad \frac{\partial |\boldsymbol{c}|^2}{\partial v_i} = 2c_i, \tag{F4}$$

and the tensorial collisional contributions defined in (5) can be calculated according to

$$\boldsymbol{R}_{ab} = m_a \int f_a \boldsymbol{A}_{ab} d^3v; \tag{F5}$$

$$Q_{ab} = m_a \int f_a \boldsymbol{A}_{ab} \cdot \boldsymbol{c}_a d^3v + \frac{m_a}{2}\int f_a \operatorname{Tr} \bar{\bar{\boldsymbol{D}}}_{ab} d^3v; \tag{F6}$$

$$\bar{\bar{\boldsymbol{Q}}}_{ab}^{(2)} = m_a \int f_a [\boldsymbol{A}_{ab}\boldsymbol{c}_a]^S d^3v + \frac{m_a}{2}\int f_a [\bar{\bar{\boldsymbol{D}}}_{ab}]^S d^3v; \tag{F7}$$

$$\bar{\bar{\boldsymbol{Q}}}_{ab}^{(3)} = m_a \int f_a [\boldsymbol{A}_{ab}\boldsymbol{c}_a\boldsymbol{c}_a]^S d^3v + \frac{m_a}{2}\int f_a [\bar{\bar{\boldsymbol{D}}}_{ab}^S \boldsymbol{c}_a]^S d^3v. \tag{F8}$$

If the diffusion tensor is symmetric, then $\bar{\bar{\boldsymbol{D}}}_{ab}^S = 2\bar{\bar{\boldsymbol{D}}}_{ab}$ (for clarity, the symmetric operator does not act on species indices, and in general $\bar{\bar{\boldsymbol{D}}}_{ab} \neq \bar{\bar{\boldsymbol{D}}}_{ba}$, similar to $\nu_{ab} \neq \nu_{ba}$, the symmetric operator acts as $(\bar{\bar{\boldsymbol{D}}}_{ij}^{ab})^S = \bar{\bar{\boldsymbol{D}}}_{ij}^{ab} + \bar{\bar{\boldsymbol{D}}}_{ji}^{ab}$). The fourth- and fifth-order collisional contributions are

$$(\bar{\bar{\boldsymbol{Q}}}_{ab}^{(4)})_{ijkl} = m_a \int f_a [\boldsymbol{A}_{ab}\boldsymbol{c}_a\boldsymbol{c}_a\boldsymbol{c}_a]_{ijkl}^S d^3v + \frac{m_a}{2}\int f_a [[\bar{\bar{\boldsymbol{D}}}_{ab}^S \boldsymbol{c}_a\boldsymbol{c}_a]_{ijkl}^S + (\bar{\bar{\boldsymbol{D}}}^{ab})_{ik}^S c_j^a c_l^a + (\bar{\bar{\boldsymbol{D}}}^{ab})_{jl}^S c_i^a c_k^a] d^3v; \tag{F9}$$

$$\begin{aligned}(\bar{\bar{\boldsymbol{Q}}}_{ab}^{(5)})_{ijklm} = {} & m_a \int f_a [\boldsymbol{A}_{ab}\boldsymbol{c}_a\boldsymbol{c}_a\boldsymbol{c}_a\boldsymbol{c}_a]_{ijklm}^S d^3v + \frac{m_a}{2}\int f_a [[\bar{\bar{\boldsymbol{D}}}_{ab}^S \boldsymbol{c}_a\boldsymbol{c}_a\boldsymbol{c}_a]_{ijklm}^S + (\bar{\bar{\boldsymbol{D}}}^{ab})_{ik}^S c_j^a c_l^a c_m^a \\ & + (\bar{\bar{\boldsymbol{D}}}^{ab})_{il}^S c_j^a c_k^a c_m^a + (\bar{\bar{\boldsymbol{D}}}^{ab})_{jl}^S c_i^a c_k^a c_m^a + (\bar{\bar{\boldsymbol{D}}}^{ab})_{jm}^S c_i^a c_k^a c_l^a + (\bar{\bar{\boldsymbol{D}}}^{ab})_{km}^S c_i^a c_j^a c_l^a] d^3v.\end{aligned} \tag{F10}$$

The first integral in (F9) proportional to $\boldsymbol{A}_{ab}$ contains four terms, and the second integral in (F9) proportional to $\bar{\bar{\boldsymbol{D}}}^{ab}$ contains 12 terms. Similarly, the first integral in (F10) contains five terms, and the second integral in (F10) contains 20 terms. The second integrals in (F9)–(F10) can be written simply by picking two indices for $\bar{\bar{\boldsymbol{D}}}^{ab}$ and giving the rest of the indices to $\boldsymbol{c}_a\boldsymbol{c}_a$ and $\boldsymbol{c}_a\boldsymbol{c}_a\boldsymbol{c}_a$. The generalization to the nth-order collisional contributions defined in (A10) is done naturally by introducing a set of indices $R = \{r_1 \ldots r_n\}$, together with an ordered set (s_1, s_2), and writing

$$\begin{aligned}(\bar{\bar{\boldsymbol{Q}}}_{ab}^{(n)})_{r_1 r_2 \ldots r_n} = {} & m_a \int f_a [A_{r_1}^{ab} c_{r_2}^a \ldots c_{r_n}^a]^S d^3v + \frac{m_a}{2}\int f_a [D_{s_1 s_2}^{ab} c_{s_3} \ldots c_{s_n}] d^3v; \\ & \text{where} \quad (s_1, s_2) \in R = \{r_1 \ldots r_n\}; \quad \text{and} \quad s_3 \ldots s_n \in R \backslash \{s_1, s_2\},\end{aligned} \tag{F11}$$

so that the first integral contains (n) terms, and the second integral contains $2\binom{n}{2} = n(n-1)$ terms. Alternatively, one can replace the ordered set (s_1, s_2) with a nonordered set $\{s_1, s_2\}$, and include the symmetric operator on $\bar{\bar{\boldsymbol{D}}}^{ab}$.

It is useful to write the collisional contributions for the contracted vectors, matrices, and scalars by assuming symmetric $\bar{\bar{\boldsymbol{D}}}^{ab}$. We use the definitions from Section 8.3 (see Equation (188)) that were also used in Appendix D; see Equations (D4) and (D5). This yields the collisional contributions for vectors:

$$\begin{aligned}\vec{\boldsymbol{\mathcal{Q}}}_{ab}^{(2n+1)} &= m_a \int [(2n)(\boldsymbol{A}^{ab}\cdot \boldsymbol{c}_a)\boldsymbol{c}_a|\boldsymbol{c}_a|^{2n-2} + \boldsymbol{A}^{ab}|\boldsymbol{c}_a|^{2n}]f_a\, d^3v \\ &+ m_a \int [(2n)(n-1)(\bar{\bar{\boldsymbol{D}}}^{ab}\colon \boldsymbol{c}_a\boldsymbol{c}_a)\boldsymbol{c}_a|\boldsymbol{c}_a|^{2n-4} + (n)(\mathrm{Tr}\,\bar{\bar{\boldsymbol{D}}}^{ab})\boldsymbol{c}_a|\boldsymbol{c}_a|^{2n-2} \\ &+ (2n)(\boldsymbol{c}_a\cdot\bar{\bar{\boldsymbol{D}}}^{ab})|\boldsymbol{c}_a|^{2n-2}]f_a\, d^3v;\end{aligned} \tag{F12}$$

for matrices:

$$\begin{aligned}\bar{\bar{\boldsymbol{\mathcal{Q}}}}_{ab}^{(2n)} &= m_a \int [(\boldsymbol{A}^{ab}\boldsymbol{c}_a)^S|\boldsymbol{c}_a|^{2n-2} + (2n-2)(\boldsymbol{A}^{ab}\cdot\boldsymbol{c}_a)\boldsymbol{c}_a\boldsymbol{c}_a|\boldsymbol{c}_a|^{2n-4}]f_a\, d^3v \\ &+ m_a \int [\bar{\bar{\boldsymbol{D}}}^{ab}|\boldsymbol{c}_a|^{2n-2} + (2n-2)(\bar{\bar{\boldsymbol{D}}}^{ab}\cdot\boldsymbol{c}_a\boldsymbol{c}_a)^S|\boldsymbol{c}_a|^{2n-4} \\ &+ (n-1)(\mathrm{Tr}\,\bar{\bar{\boldsymbol{D}}}^{ab})\boldsymbol{c}_a\boldsymbol{c}_a|\boldsymbol{c}_a|^{2n-4} + (n-1)(2n-4)(\bar{\bar{\boldsymbol{D}}}^{ab}\colon \boldsymbol{c}_a\boldsymbol{c}_a)\boldsymbol{c}_a\boldsymbol{c}_a|\boldsymbol{c}_a|^{2n-6}]f_a\, d^3v;\end{aligned} \tag{F13}$$

and for scalars:

$$\begin{aligned}Q_{ab}^{(2n)} &= m_a \int [(2n)(\boldsymbol{A}^{ab}\cdot\boldsymbol{c}_a)|\boldsymbol{c}_a|^{2n-2} + (n)(\mathrm{Tr}\,\bar{\bar{\boldsymbol{D}}}^{ab})|\boldsymbol{c}_a|^{2n-2} \\ &+ (2n)(n-1)(\bar{\bar{\boldsymbol{D}}}^{ab}\colon \boldsymbol{c}_a\boldsymbol{c}_a)|\boldsymbol{c}_a|^{2n-4}]f_a\, d^3v,\end{aligned} \tag{F14}$$

all valid for $n \geqslant 1$. Applying a trace at (F13) recovers (F14).

Appendix G
Landau Collisional Operator (5-moment Model)

For Coulomb collisions, a very accurate collisional operator was obtained by Landau (1936, 1937) in the following form (see, for example, Equation (1.2) in Braginskii 1958):

$$C_{ab}(f_a, f_b) = -\frac{2\pi e^4 Z_a^2 Z_b^2 \ln\Lambda}{m_a}\frac{\partial}{\partial \boldsymbol{v}}\cdot\int \bar{\bar{\boldsymbol{V}}}\cdot\left[\frac{f_a(\boldsymbol{v})}{m_b}\frac{\partial f_b(\boldsymbol{v}')}{\partial \boldsymbol{v}'} - \frac{f_b(\boldsymbol{v}')}{m_a}\frac{\partial f_a(\boldsymbol{v})}{\partial \boldsymbol{v}}\right]d^3v'; \tag{G1}$$

$$\bar{\bar{\boldsymbol{V}}} = \frac{\bar{\bar{\boldsymbol{I}}}}{|\boldsymbol{v}-\boldsymbol{v}'|} - \frac{(\boldsymbol{v}-\boldsymbol{v}')(\boldsymbol{v}-\boldsymbol{v}')}{|\boldsymbol{v}-\boldsymbol{v}'|^3}. \tag{G2}$$

With this collisional operator, Equation (A1) is known as the Landau equation. The Landau collisional operator is sometimes called the Landau collisional integral, because (G1) contains an integral over d^3v' (i.e., it is an integro-differential operator). The operator can be rewritten into the general Fokker–Planck form (F1) by introducing Rosenbluth potentials

$$H_b(\boldsymbol{v}) = \int \frac{f_b(\boldsymbol{v}')}{|\boldsymbol{v}-\boldsymbol{v}'|}d^3v'; \quad \text{and} \quad G_b(\boldsymbol{v}) = \int f_b(\boldsymbol{v}')|\boldsymbol{v}-\boldsymbol{v}'|d^3v', \tag{G3}$$

yielding (see, for example, Equations (7)–(8) of Hinton 1983)

$$\boldsymbol{A}_{ab} = 2\frac{c_{ab}}{m_a^2}\left(1+\frac{m_a}{m_b}\right)\frac{\partial H_b(\boldsymbol{v})}{\partial \boldsymbol{v}}; \qquad \bar{\bar{\boldsymbol{D}}}_{ab} = 2\frac{c_{ab}}{m_a^2}\frac{\partial^2 G_b(\boldsymbol{v})}{\partial \boldsymbol{v}\partial \boldsymbol{v}}; \qquad c_{ab} = 2\pi e^4 Z_a^2 Z_b^2 \ln\Lambda. \tag{G4}$$

The useful identities are

$$\frac{\partial}{\partial \boldsymbol{v}}\cdot\bar{\bar{\boldsymbol{V}}} = -2\frac{\boldsymbol{v}-\boldsymbol{v}'}{|\boldsymbol{v}-\boldsymbol{v}'|^3} = -\frac{\partial}{\partial \boldsymbol{v}'}\cdot\bar{\bar{\boldsymbol{V}}}; \qquad \frac{\partial^2}{\partial \boldsymbol{v}\partial \boldsymbol{v}}|\boldsymbol{v}-\boldsymbol{v}'| = \bar{\bar{\boldsymbol{V}}}, \tag{G5}$$

and it is easy to verify that (F1), (G4) recovers the Landau operator (G1) (after one uses the Gauss–Ostrogradsky divergence theorem in velocity d^3v', which makes the associated integral vanish). By using Laplacian $\nabla_v^2 = \nabla_v\cdot\nabla_v$, the following identity implies

$$\nabla_v^2\frac{1}{|\boldsymbol{v}-\boldsymbol{v}'|} = -4\pi\delta(\boldsymbol{v}-\boldsymbol{v}'); \quad \Rightarrow \quad \nabla_v^2 H_b(\boldsymbol{v}) = -4\pi f_b(\boldsymbol{v}). \tag{G6}$$

The Rosenbluth potential $H_b(\boldsymbol{v})$ is thus completely analogous to the electrostatic potential $\Phi(\boldsymbol{x})$ (with a Poisson equation $\nabla^2\Phi(\boldsymbol{x}) = -4\pi\rho_c(\boldsymbol{x})$, where $\rho_c(\boldsymbol{x})$ is the charge's spatial distribution), here just used in velocity space. Also, because of the identity $\nabla_v^2|\boldsymbol{v}-\boldsymbol{v}'| = 2/|\boldsymbol{v}-\boldsymbol{v}'|$, the Rosenbluth potentials are related by

$$H_b = \frac{1}{2}\nabla_v^2 G_b; \quad \Rightarrow \quad \boldsymbol{A}_{ab} = \frac{1}{2}\left(1+\frac{m_a}{m_b}\right)\frac{\partial}{\partial \boldsymbol{v}}\cdot\bar{\bar{\boldsymbol{D}}}_{ab}. \tag{G7}$$

However, the structure of the Rosenbluth potentials implies that the Landau operator is quite complicated. Indeed, the simplest example, when prescribing Maxwellian $f_b = n_b/(\pi^{3/2}v_{\rm thb}^3)\exp(-y^2)$ with the (vector) variable $\boldsymbol{y} = (\boldsymbol{v}-\boldsymbol{u}_b)/v_{\rm thb}$ and scalar $y = |\boldsymbol{y}|$, yields the Rosenbluth potentials

$$H_b(\boldsymbol{v}) = \frac{n_b}{v_{\rm thb}}\frac{\mathrm{erf(y)}}{y}; \tag{G8}$$

$$G_b(\boldsymbol{v}) = n_b v_{\rm thb}\left[\frac{1}{\sqrt{\pi}}e^{-y^2} + \left(\frac{1}{2y}+y\right)\mathrm{erf}(y)\right], \tag{G9}$$

where the error function $\mathrm{erf}(y) = (2/\sqrt{\pi})\int_0^y e^{-z^2}dz$ is present. These Rosenbluth potentials make the collisional contributions (F5), (F6) difficult to calculate.

For clarity on how the H_b is obtained, it is useful to introduce the (vector) variable $\boldsymbol{x} = (\boldsymbol{v}'-\boldsymbol{v})/v_{\rm thb}$ and the scalar $x = |\boldsymbol{x}|$, and change the integration into $d^3v' = v_{\rm thb}^3 d^3x$, so that

$$H_b(\boldsymbol{v}) = \frac{n_b}{\pi^{3/2}v_{\rm thb}^3}\int_{-\infty}^{\infty}\frac{e^{-\frac{|\boldsymbol{v}'-\boldsymbol{u}_b|^2}{v_{\rm thb}^2}}}{|\boldsymbol{v}'-\boldsymbol{v}|}d^3v' = \frac{n_b}{\pi^{3/2}v_{\rm thb}}\int_{-\infty}^{\infty}\frac{e^{-|\boldsymbol{x}+\boldsymbol{y}|^2}}{x}d^3x. \tag{G10}$$

In the last integral, the variable $\boldsymbol{y}$ is a constant (because $\boldsymbol{v}$ and $\boldsymbol{u}_b$ are constants). One introduces spherical coordinates in the $\boldsymbol{x}$-space with orthogonal unit vectors $\hat{\boldsymbol{e}}_1$, $\hat{\boldsymbol{e}}_2$, $\hat{\boldsymbol{e}}_3$, where the direction of vector $\boldsymbol{y}$ forms axis $\hat{\boldsymbol{e}}_3 = \boldsymbol{y}/y$, so that the vector

$$\boldsymbol{x} = x\sin\theta\cos\phi\hat{\boldsymbol{e}}_1 + x\sin\theta\sin\phi\hat{\boldsymbol{e}}_2 + x\cos\theta\hat{\boldsymbol{e}}_3. \tag{G11}$$

In this reference frame, $\boldsymbol{y} = (0,\ 0,\ y)$, and so $|\boldsymbol{x}+\boldsymbol{y}|^2 = x^2+y^2+2xy\cos\theta$. Then one can calculate the integral in spherical coordinates $d^3x = x^2\sin\theta dx d\theta d\phi$, yielding

$$\begin{aligned}\int_{-\infty}^{\infty}\frac{e^{-|\boldsymbol{x}+\boldsymbol{y}|^2}}{x}d^3x &= 2\pi\int_0^{\infty}\int_0^{\pi}xe^{-(x^2+y^2)}\sin\theta e^{-2xy\cos\theta}d\theta dx\\ &= 2\pi\int_0^{\infty}xe^{-(x^2+y^2)}\frac{1}{2xy}(e^{+2xy}-e^{-2xy})dx = \frac{\pi}{y}\int_0^{\infty}(e^{-(x-y)^2}-e^{-(x+y)^2})dx\\ &= \frac{\pi}{y}\left(\int_{-y}^{\infty}e^{-z^2}dz - \int_y^{\infty}e^{-z^2}dz\right) = \frac{\pi}{y}\int_{-y}^{y}e^{-z^2}dz = \frac{2\pi}{y}\int_0^y e^{-z^2}dz = \frac{\pi^{3/2}}{y}\mathrm{erf}(y),\end{aligned} \tag{G12}$$

recovering (G8). The result can be verified by calculating (G6). Similarly, the potential G_b can be obtained by calculating

$$\begin{aligned}\int_{-\infty}^{\infty}xe^{-|\boldsymbol{x}+\boldsymbol{y}|^2}d^3x &= \frac{\pi}{y}\int_0^{\infty}x^2(e^{-(x-y)^2}-e^{-(x+y)^2})dx = \frac{\pi}{y}\left(\int_{-y}^{\infty}(z+y)^2e^{-z^2}dz - \int_y^{\infty}(z-y)^2e^{-z^2}dz\right)\\ &= \frac{\pi}{y}\left(2\int_0^y z^2e^{-z^2}dz + 4y\int_y^{\infty}ze^{-z^2}dz + 2y^2\int_0^y e^{-z^2}dz\right) = \pi^{3/2}\left(y+\frac{1}{2y}\right)\mathrm{erf}(y) + \pi e^{-y^2},\end{aligned} \tag{G13}$$

recovering (G9), and which can be verified to satisfy (G7).

Note that because $\mathrm{erf}(0) = 0$, the error function can actually be defined as an indefinite integral:

$$\frac{2}{\sqrt{\pi}}\int e^{-x^2}dx = \mathrm{erf}(x); \qquad \frac{2}{\sqrt{\pi}}\int e^{-\frac{(x+a)^2}{b^2}}dx = \frac{\mathrm{erf}(x+a)}{b^2}.$$

The useful relations are $\mathrm{erf}(-x) = -\mathrm{erf}(x)$ and $\mathrm{erf}(\infty) = 1$. Then the calculations above can be done more elegantly, for example:

$$\int_0^{\infty}e^{-(x-y)^2}dx = \frac{\sqrt{\pi}}{2}\mathrm{erf}(x-y)\Big|_{x=0}^{x=\infty} = \frac{\sqrt{\pi}}{2}(1+\mathrm{erf}(y)).$$

G.1. Momentum Exchange Rates $\boldsymbol{R}_{\rm ab}$

To obtain the momentum exchange rates $\boldsymbol{R}_{ab}$, one needs to calculate

$$\boldsymbol{R}_{ab} = m_a \int f_a \boldsymbol{A}_{ab} d^3v = 2\frac{c_{ab}}{m_a}\left(1 + \frac{m_a}{m_b}\right)\int f_a \frac{\partial H_b}{\partial \boldsymbol{v}} d^3v;$$
$$= -2\frac{c_{ab}}{m_a}\left(1 + \frac{m_a}{m_b}\right)\int H_b \frac{\partial f_a}{\partial \boldsymbol{v}} d^3v. \tag{G14}$$

Prescribing Maxwellian $f_a = (n_a/(\pi^{3/2}v_{\rm tha}^3))\exp(-|\boldsymbol{v}-\boldsymbol{u}_a|^2/v_{\rm tha}^2)$ with general velocity $\boldsymbol{u}_a$ leads to the "runaway" effect addressed below in Appendix G.3. It is useful to first consider a simplified situation where the differences between the drift velocities $\boldsymbol{u}_a$ and $\boldsymbol{u}_b$ are small. The Maxwellian f_a is rewritten with the variable $\boldsymbol{y}$ and the variable $\boldsymbol{u} = (\boldsymbol{u}_b - \boldsymbol{u}_a)/v_{\rm tha}$, and expanded by assuming that $|\boldsymbol{u}| \ll 1$, so that

$$f_a = \frac{n_a}{\pi^{3/2}v_{\rm tha}^3} e^{-|\boldsymbol{y}\alpha+\boldsymbol{u}|^2} \simeq \frac{n_a}{\pi^{3/2}v_{\rm tha}^3} e^{-y^2\alpha^2}(1 - 2\alpha\boldsymbol{y}\cdot\boldsymbol{u}), \tag{G15}$$

where $\alpha = v_{\rm thb}/v_{\rm tha}$. Then the derivative

$$\frac{\partial f_a}{\partial \boldsymbol{v}} = -\frac{2n_a}{\pi^{3/2}v_{\rm tha}^4} e^{-y^2\alpha^2}[\boldsymbol{u} + \alpha\boldsymbol{y} - 2\alpha^2\boldsymbol{y}(\boldsymbol{y}\cdot\boldsymbol{u})], \tag{G16}$$

and one needs to calculate

$$\boldsymbol{R}_{ab} = \frac{4c_{ab}}{m_a}\left(1 + \frac{m_a}{m_b}\right)\frac{n_a n_b}{\pi^{3/2}v_{\rm tha}^4 v_{\rm thb}} \underbrace{\int_{-\infty}^{\infty} \frac{\mathrm{erf}(y)}{y} e^{-y^2\alpha^2}[\boldsymbol{u} + \alpha\boldsymbol{y} - 2\alpha^2\boldsymbol{y}(\boldsymbol{y}\cdot\boldsymbol{u})] d^3v}_{①+②+③}, \tag{G17}$$

where we split the integral into three parts. The integration over d^3v can be changed to $v_{\rm thb}^3 d^3y$. We will use

$$\int_0^\infty e^{-y^2\alpha^2} y\,\mathrm{erf}(y) dy = \frac{1}{2\alpha^2\sqrt{1+\alpha^2}};$$
$$\int_0^\infty e^{-y^2\alpha^2} y^3\,\mathrm{erf}(y) dy = \frac{3\alpha^2+2}{4\alpha^4(1+\alpha^2)^{3/2}}. \tag{G18}$$

The three integrals are then evaluated according to

$$① = \boldsymbol{u}\int_{-\infty}^{\infty} \frac{\mathrm{erf}(y)}{y} e^{-y^2\alpha^2} d^3v = \boldsymbol{u}v_{\rm thb}^3 4\pi \int_0^\infty y\,\mathrm{erf}(y) e^{-y^2\alpha^2} dy = \boldsymbol{u}v_{\rm thb}^3 \frac{2\pi}{\alpha^2\sqrt{1+\alpha^2}};$$
$$② = \alpha\int_{-\infty}^{\infty} \boldsymbol{y}\frac{\mathrm{erf}(y)}{y} e^{-y^2\alpha^2} d^3v = 0;$$
$$③ = -2\alpha^2\int_{-\infty}^{\infty} \boldsymbol{y}(\boldsymbol{y}\cdot\boldsymbol{u})\frac{\mathrm{erf}(y)}{y} e^{-y^2\alpha^2} d^3v = -\frac{2\alpha^2}{3}\boldsymbol{u}\int_{-\infty}^{\infty} y\,\mathrm{erf}(y) e^{-y^2\alpha^2} d^3v$$
$$= -\frac{8\pi}{3}\alpha^2 v_{\rm thb}^3 \boldsymbol{u}\int_0^\infty y^3\,\mathrm{erf}(y) e^{-y^2\alpha^2} dy = -\frac{8\pi}{3}\alpha^2 v_{\rm thb}^3 \boldsymbol{u}\frac{3\alpha^2+2}{4\alpha^4(1+\alpha^2)^{3/2}}, \tag{G19}$$

and so

$$① + ③ = \boldsymbol{u}v_{\rm thb}^3 \frac{2\pi}{3\alpha^2(1+\alpha^2)^{3/2}} = \boldsymbol{u}\frac{2\pi}{3}\frac{v_{\rm tha}^5 v_{\rm thb}}{(v_{\rm tha}^2 + v_{\rm thb}^2)^{3/2}}. \tag{G20}$$

The entire result (G17) can then be written as (see, for example, Equations (46)–(47) of Hinton 1983)

$$\boldsymbol{R}_{ab} = \rho_a \nu_{ab}(\boldsymbol{u}_b - \boldsymbol{u}_a), \tag{G21}$$

where the collisional frequency

$$\nu_{ab} = \tau_{ab}^{-1} = \frac{16}{3}\sqrt{\pi}\frac{n_b e^4 Z_a^2 Z_b^2 \ln\Lambda}{m_a^2(v_{\rm tha}^2 + v_{\rm thb}^2)^{3/2}}\left(1 + \frac{m_a}{m_b}\right), \tag{G22}$$

and the thermal speeds $v_{\rm tha}^2 = 2T_a/m_a$. Note that $m_a n_a \nu_{ab} = m_b n_b \nu_{ba}$ holds. The collisional frequency (G22) is identical to Equation (C2) of Schunk (1977); see Equation (179).

It is useful to clarify the physical meaning of the collisional frequencies. Considering momentum equations for two species where all of the spatial gradients are neglected, so that $\partial\boldsymbol{u}_a/\partial t - (eZ_a/m_a)\boldsymbol{E} = \boldsymbol{R}_{ab}/\rho_a$ and $\partial\boldsymbol{u}_b/\partial t - (eZ_b/m_b)\boldsymbol{E} = \boldsymbol{R}_{ba}/\rho_b$, then subtracting

them and defining the difference $\delta\boldsymbol{u} = \boldsymbol{u}_b - \boldsymbol{u}_a$, yields an evolution equation

$$\frac{\partial \delta \boldsymbol{u}}{\partial t} + \nu \delta \boldsymbol{u} = e\boldsymbol{E}\left(\frac{Z_b}{m_b} - \frac{Z_a}{m_a}\right); \qquad \nu = \nu_{ab} + \nu_{ba}. \tag{G23}$$

With no use of Maxwell's equations, and instead assuming an applied (external) constant electric field and also constant collisional frequencies, an initial velocity difference $\delta\boldsymbol{u}(0)$ evolves according to

$$\delta \boldsymbol{u}(t) = \delta \boldsymbol{u}(0) e^{-\nu t} + (1 - e^{-\nu t}) \frac{e\boldsymbol{E}}{\nu}\left(\frac{Z_b}{m_b} - \frac{Z_a}{m_a}\right). \tag{G24}$$

Approximately after time $\tau = 1/\nu$ (which represents many small-angle collisions), the dependence on the initial condition disappears and the difference between the velocities reaches a constant value:

$$\boldsymbol{u}_b - \boldsymbol{u}_a = \frac{e\boldsymbol{E}}{\nu_{ab} + \nu_{ba}}\left(\frac{Z_b}{m_b} - \frac{Z_a}{m_a}\right) = \text{const.} \tag{G25}$$

Provided that $Z_a/m_a \neq Z_b/m_b$, the collisional time $\tau = 1/(\nu_{ab} + \nu_{ba})$ can then be interpreted as an average time that is required for particles "a" and "b" to experience (many small-angle) collisions, so that the difference between their average fluid velocities reaches a constant value proportional to the value of the applied (external) electric field $\boldsymbol{E}$. For the particular case of $Z_a/m_a = Z_b/m_b$, the velocities become equal regardless of the value of applied $\boldsymbol{E}$.

For a particular case of a one ion–electron plasma, $\boldsymbol{u}_e - \boldsymbol{u}_i = -e\boldsymbol{E}/(\nu_{ei} m_e)$, which can also be directly obtained from the quasistatic electron or ion momentum equations. Prescribing the charge neutrality, $n_e = Z_i n_i$, so that the current $\boldsymbol{j} = -en_e(\boldsymbol{u}_e - \boldsymbol{u}_i)$ then yields the relation $\boldsymbol{j} = \sigma\boldsymbol{E}$ with the usual electrical conductivity $\sigma = 1/\eta = e^2 n_e/(\nu_{ei} m_e)$, where σ does not depend on the value of current j (because j is assumed to be small).

G.2. Energy Exchange Rates $\mathrm{Q_{ab}}$

Similar calculations are used to obtain the energy exchange rates Q_{ab}, according to (F8). It is beneficial to notice that $\mathrm{Tr}\,\bar{\boldsymbol{D}}_{ab} = (4c_{ab}/m_a^2)H_b$, and so

$$Q_{ab} = \frac{2c_{ab}}{m_a}\left(1 + \frac{m_a}{m_b}\right)\int f_a \frac{\partial H_b}{\partial \boldsymbol{v}} \cdot \boldsymbol{c}_a d^3v + \frac{2c_{ab}}{m_a}\int f_a H_b d^3v; \tag{G26}$$

$$\frac{\partial H_b}{\partial \boldsymbol{v}} = \frac{n_b}{v_{\mathrm{thb}}^2}\boldsymbol{y}\left(\frac{1}{y^2}\frac{2}{\sqrt{\pi}}e^{-y^2} - \frac{1}{y^3}\,\mathrm{erf}(y)\right), \tag{G27}$$

and because $\boldsymbol{c}_a = \boldsymbol{y}v_{\mathrm{thb}} + \boldsymbol{u}v_{\mathrm{tha}}$, then

$$\frac{\partial H_b}{\partial \boldsymbol{v}} \cdot \boldsymbol{c}_a = \frac{n_b}{v_{\mathrm{thb}}^2}(y^2 v_{\mathrm{thb}} + (\boldsymbol{u}\cdot\boldsymbol{y})v_{\mathrm{tha}})\left(\frac{1}{y^2}\frac{2}{\sqrt{\pi}}e^{-y^2} - \frac{1}{y^3}\,\mathrm{erf}(y)\right). \tag{G28}$$

Importantly, to correctly account for the $|\boldsymbol{u}|^2$ contributions, the f_a has to be expanded further:

$$f_a = \frac{n_a}{\pi^{3/2} v_{\mathrm{tha}}^3} e^{-|\boldsymbol{y}\alpha + \boldsymbol{u}|^2} \simeq \frac{n_a}{\pi^{3/2} v_{\mathrm{tha}}^3} e^{-y^2\alpha^2}(1 - (2\alpha\boldsymbol{y}\cdot\boldsymbol{u} + |\boldsymbol{u}|^2) + 2\alpha^2(\boldsymbol{y}\cdot\boldsymbol{u})^2), \tag{G29}$$

where $\alpha = v_{\mathrm{thb}}/v_{\mathrm{tha}}$. This distribution function yields

$$\int f_a H_b d^3v = \frac{2n_a n_b}{\sqrt{\pi}\, v_{\mathrm{tha}}}\left[\frac{1}{\sqrt{1+\alpha^2}} - \frac{|\boldsymbol{u}|^2}{3(1+\alpha^2)^{3/2}}\right];$$
$$\int f_a \frac{\partial H_b}{\partial \boldsymbol{v}} \cdot \boldsymbol{c}_a d^3v = \frac{2n_a n_b}{\sqrt{\pi}\, v_{\mathrm{tha}}}\left[-\frac{1}{(1+\alpha^2)^{3/2}} + \frac{|\boldsymbol{u}^2|}{(1+\alpha^2)^{5/2}}\right], \tag{G30}$$

and the final result reads

$$Q_{ab} = 3\rho_a \nu_{ab}\frac{T_b - T_a}{m_a + m_b} + \rho_a \nu_{ab}\frac{3}{2}\left(\frac{m_b T_a}{m_b T_a + m_a T_b} - \frac{1}{3}\frac{m_b}{m_b + m_a}\right)|\boldsymbol{u}_b - \boldsymbol{u}_a|^2, \tag{G31}$$

or equivalently,

$$Q_{ab} = 3\rho_a \nu_{ab}\frac{T_b - T_a}{m_a + m_b} + \rho_a \nu_{ab}\frac{m_b(3T_a m_a + 2T_a m_b - T_b m_a)}{2(T_b m_a + T_a m_b)(m_b + m_a)}|\boldsymbol{u}_b - \boldsymbol{u}_a|^2. \tag{G32}$$

Hinton (1983) calculates only the first term, the thermal exchange rate (his Equation (52); see also Landau 1936 for an ion–electron plasma). Calculating $Q_{ab} + Q_{ba} = \rho_a \nu_{ab}|\boldsymbol{u}_b - \boldsymbol{u}_a|^2 = (\boldsymbol{u}_b - \boldsymbol{u}_a)\cdot\boldsymbol{R}_{ab}$ yields the energy conservation, and the result (G31) is well-

defined. (Recalculating $\boldsymbol{R}_{ab}$ with the further expanded f_0 (G29) yields the unchanged result $\boldsymbol{R}_{ab} = \rho_a \nu_{ab}(\boldsymbol{u}_b - \boldsymbol{u}_a)$). As a double check, expanding the more general expression for unrestricted drifts (G64) (by expansion $\Psi_{ab} = 1 - \epsilon^2$) yields

$$Q_{ab} = 3\rho_a \nu_{ab} \frac{T_b - T_a}{m_a + m_b}\left(1 - \frac{|\boldsymbol{u}_b - \boldsymbol{u}_a|^2}{\frac{2T_a}{m_a} + \frac{2T_b}{m_b}}\right) + \rho_a \nu_{ab} \frac{m_b}{m_b + m_a}|\boldsymbol{u}_b - \boldsymbol{u}_a|^2. \tag{G33}$$

Results (G33) and (G31) are equivalent, and valid for an unrestricted difference in temperature. Prescribing that the difference in temperatures is small simplifies the frictional part into

$$Q_{ab} = 3\rho_a \nu_{ab} \frac{T_b - T_a}{m_a + m_b} + \rho_a \nu_{ab} \frac{m_b}{m_a + m_b}|\boldsymbol{u}_b - \boldsymbol{u}_a|^2. \tag{G34}$$

This frictional part is derived elegantly in the Appendix of Braginskii (1965).

G.3. $\mathrm{R_{ab}}$ *and* $\mathrm{Q_{ab}}$ *for Unrestricted Drifts* $\boldsymbol{u}_\mathrm{b} - \boldsymbol{u}_\mathrm{a}$ *(Runaway Effect)*

Here we want to calculate $\boldsymbol{R}_{ab}$ for the general Maxwellian distributions f_a, f_b, with no restriction on the value of the difference $\boldsymbol{u}_b - \boldsymbol{u}_a$. We follow Burgers (1969) and Tanenbaum (1967). Instead of using the Rosenbluth potential H_b and calculating (G14), it is easier to consider

$$\boldsymbol{R}_{ab} = 2\frac{c_{ab}}{m_a}\left(1 + \frac{m_a}{m_b}\right)\int\int f_a(\boldsymbol{v}) f_b(\boldsymbol{v}') \frac{\boldsymbol{v}' - \boldsymbol{v}}{|\boldsymbol{v}' - \boldsymbol{v}|^3} d^3v d^3v'. \tag{G35}$$

Additionally, instead of $\boldsymbol{v}$ and $\boldsymbol{v}'$, it feels more natural to use $\boldsymbol{v}_a = \boldsymbol{v}$ and $\boldsymbol{v}_b = \boldsymbol{v}'$. It is useful to introduce the vectors $\boldsymbol{x} = \boldsymbol{v}_b - \boldsymbol{v}_a$ and $\boldsymbol{u} = \boldsymbol{u}_b - \boldsymbol{u}_a$. The integral is then calculated by introducing the "center-of-mass" velocity,

$$\boldsymbol{C} = \frac{m_a \boldsymbol{v}_a + m_b \boldsymbol{v}_b}{m_a + m_b} - \frac{m_a \boldsymbol{u}_a + m_b \boldsymbol{u}_b}{m_a + m_b} + \frac{m_a m_b}{(m_a + m_b)} \frac{T_b - T_a}{(m_b T_a + m_a T_b)}(\boldsymbol{u} - \boldsymbol{x}), \tag{G36}$$

which transforms

$$f_a f_b = \frac{n_a n_b}{\pi^3 v_{\mathrm{tha}}^3 v_{\mathrm{thb}}^3} \exp\left(-\frac{|\boldsymbol{v}_a - \boldsymbol{u}_a|^2}{v_{\mathrm{tha}}^2} - \frac{|\boldsymbol{v}_b - \boldsymbol{u}_b|^2}{v_{\mathrm{thb}}^2}\right), \tag{G37}$$

into

$$f_a f_b = \frac{n_a n_b}{\pi^3 \tilde{\alpha}^3 \beta^3} \exp\left(-\frac{|\boldsymbol{C}|^2}{\tilde{\alpha}^2} - \frac{|\boldsymbol{x} - \boldsymbol{u}|^2}{\beta^2}\right), \tag{G38}$$

with new thermal speeds

$$\tilde{\alpha}^2 = \frac{2T_a T_b}{m_b T_a + m_a T_b}; \qquad \beta^2 = v_{\mathrm{tha}}^2 + v_{\mathrm{thb}}^2. \tag{G39}$$

Importantly, $d^3v_a d^3v_b = d^3C d^3x$ (by calculating Jacobian). For later calculations of more complicated integrals than (G35), the useful transformations are

$$\begin{aligned} \boldsymbol{c}_a &= \boldsymbol{C} - \frac{m_b T_a}{m_b T_a + m_a T_b}(\boldsymbol{x} - \boldsymbol{u}); \\ \boldsymbol{c}_b &= \boldsymbol{C} + \frac{m_a T_b}{m_b T_a + m_a T_b}(\boldsymbol{x} - \boldsymbol{u}). \end{aligned} \tag{G40}$$

The integral (G35) thus transforms into

$$\boldsymbol{R}_{ab} = 2\frac{c_{ab}}{m_a}\left(1 + \frac{m_a}{m_b}\right)\frac{n_a n_b}{\pi^{3/2}\beta^3}\int \frac{\boldsymbol{x}}{x^3} e^{-\frac{|\boldsymbol{x}-\boldsymbol{u}|^2}{\beta^2}} d^3x, \tag{G41}$$

where we have already integrated over d^3C. One introduces a reference frame in the $\boldsymbol{x}$-space with unit vectors $\hat{\boldsymbol{e}}_1$, $\hat{\boldsymbol{e}}_2$, $\hat{\boldsymbol{e}}_3$, where the direction of vector $\boldsymbol{u}$ defines the axis $\hat{\boldsymbol{e}}_3 = \boldsymbol{u}/u$, so that

$$\boldsymbol{x} = x\sin\theta\cos\phi\hat{\boldsymbol{e}}_1 + x\sin\theta\sin\phi\hat{\boldsymbol{e}}_2 + x\cos\theta\hat{\boldsymbol{e}}_3. \tag{G42}$$

For example, the integration of (G42) over ϕ yields $\int_0^{2\pi} \boldsymbol{x} d\phi = 2\pi x\cos\theta\hat{\boldsymbol{e}}_3$, i.e., the result is in the direction of $\boldsymbol{u}$. Furthermore, because $|\boldsymbol{x} - \boldsymbol{u}|^2 = x^2 + u^2 - 2xu\cos\theta$, the integration of (G41) over ϕ can be carried out, yielding

$$\int \frac{\boldsymbol{x}}{x^3} e^{-\frac{|\boldsymbol{x}-\boldsymbol{u}|^2}{\beta^2}} d^3x = \frac{\boldsymbol{u}}{u} 2\pi \int_0^\infty \int_0^\pi e^{-\frac{|\boldsymbol{x}-\boldsymbol{u}|^2}{\beta^2}} \cos\theta\sin\theta dx d\theta. \tag{G43}$$

To calculate that integral, it is useful to introduce (constant) $\epsilon = u/\beta$, and change the integration into the variables

$$z = \frac{x}{\beta} - s; \qquad s = \epsilon \cos\theta, \tag{G44}$$

so that $|\boldsymbol{x} - \boldsymbol{u}|^2/\beta^2 = z^2 - s^2 + \epsilon^2$, yielding

$$\int \frac{\boldsymbol{x}}{x^3} e^{-\frac{|\boldsymbol{x}-\boldsymbol{u}|^2}{\beta^2}} d^3x = \boldsymbol{u} 2\pi \frac{e^{-\epsilon^2}}{\epsilon^3} \int_{-s}^{\infty} \int_{-\epsilon}^{\epsilon} s e^{-z^2+s^2} dz ds$$
$$= \boldsymbol{u}\pi^{3/2}\left(\frac{\mathrm{erf}(\epsilon)}{\epsilon^3} - \frac{2}{\sqrt{\pi}}\frac{e^{-\epsilon^2}}{\epsilon^2}\right). \tag{G45}$$

In the last integral, it is necessary to first integrate over dz and then over ds, by using

$$\int_{-s}^{\infty} e^{-z^2} dz = \frac{\sqrt{\pi}}{2}(1 + \mathrm{erf}(s));$$
$$\int_{-\epsilon}^{\epsilon} s e^{s^2} \mathrm{erf}(s) ds = e^{\epsilon^2} \mathrm{erf}(\epsilon) - \frac{2}{\sqrt{\pi}}\epsilon. \tag{G46}$$

The final result then reads

$$\boldsymbol{R}_{ab} = \rho_a \nu_{ab} (\boldsymbol{u}_b - \boldsymbol{u}_a) \Phi_{ab}; \tag{G47}$$

$$\Phi_{ab} = \left(\frac{3}{4}\sqrt{\pi}\frac{\mathrm{erf}(\epsilon)}{\epsilon^3} - \frac{3}{2}\frac{e^{-\epsilon^2}}{\epsilon^2}\right); \qquad \epsilon = \frac{|\boldsymbol{u}_b - \boldsymbol{u}_a|}{\sqrt{v_{\mathrm{tha}}^2 + v_{\mathrm{thb}}^2}}, \tag{G48}$$

recovering Equation (26.4) of Burgers (1969) and Equation (25b) of Schunk (1977). For small values $\epsilon \to 0$, the contribution $\Phi \to 1$ (more precisely, $\Phi_{ab} = 1 - (3/5)\epsilon^2$) recovers the previous result (G21) with small drifts. However, for large values $\epsilon \gg 1$, the contribution Φ_{ab} decreases to zero as $\Phi_{ab} = 3\sqrt{\pi}/(4\epsilon^3)$, and thus for large differences the in drifts $|\boldsymbol{u}_b - \boldsymbol{u}_a|$, the momentum exchange rates $\boldsymbol{R}_{ab}$ disappear for Coulomb collisions. This phenomenon is known as the "runaway effect" (Dreicer 1959). It is also possible to write

$$\Phi_{ab} = \frac{3\sqrt{\pi}}{2\epsilon}\widetilde{G}_{ab}(\epsilon); \quad \text{where} \quad \widetilde{G}_{ab}(\epsilon) = \frac{\mathrm{erf}(\epsilon)}{2\epsilon^2} - \frac{e^{-\epsilon^2}}{\sqrt{\pi}\,\epsilon} = \frac{\mathrm{erf}(\epsilon) - \epsilon\,\mathrm{erf}'(\epsilon)}{2\epsilon^2}, \tag{G49}$$

where $\widetilde{G}_{ab}(\epsilon)$ is called the Chandrasekhar function (we use tilde to differentiate it from the Rosenbluth potential G_b), and (G47) then becomes

$$\boldsymbol{R}_{ab} = \frac{3}{2}\sqrt{\pi}\rho_a \nu_{ab}(v_{\mathrm{tha}}^2 + v_{\mathrm{thb}}^2)^{\frac{1}{2}} \frac{\boldsymbol{u}_b - \boldsymbol{u}_a}{|\boldsymbol{u}_b - \boldsymbol{u}_a|}\widetilde{G}_{ab}(\epsilon). \tag{G50}$$

In plasma books (e.g., Helander & Sigmar 2002), the Chandrasekhar function is typically introduced in velocity space as $\widetilde{G}(v/v_{\mathrm{thb}})$, i.e., without drifts and before the integration over d^3v. The runaway effect is then explained on a population of electron species, which gets accelerated by an applied external electric field. Because for large velocities v frictional forces (collisions) decrease as $\widetilde{G} \sim v_{\mathrm{thb}}^2/(2v^2)$, the tail of the distribution function might depart and run away. In this sense, the runaway effect could be viewed as a purely kinetic effect. Nevertheless, an obviously analogous runaway effect exists in the fluid description (i.e., after the integration over d^3v), it is just represented through the difference in the drifts $\boldsymbol{u}_b - \boldsymbol{u}_a$ (which form a current $\boldsymbol{j}$). For example, considering a one ion–electron plasma with an electric current $\boldsymbol{j} = -en_e(\boldsymbol{u}_e - \boldsymbol{u}_i)$, then taking the electron momentum equation and neglecting, for simplicity, all of the terms except for the external $\boldsymbol{E}$ and $\boldsymbol{R}_{ei}$ (including $\partial \boldsymbol{u}_e/\partial t$, which neglects acceleration) yields the relation

$$\boldsymbol{E} = \frac{\boldsymbol{R}_{ei}}{en_e} = \eta \boldsymbol{j}; \qquad \eta = \frac{1}{\sigma} = \frac{\rho_e \nu_{ei}}{e^2 n_e^2}\Phi_{ei}, \tag{G51}$$

which agrees with Equation (33.6) of Burgers (1969). The electrical resistivity η now contains Φ_{ei}, given by (G48) with $\epsilon = j/(en_e v_{\mathrm{the}})$. For small values of current j, the η is independent of j. The runaway effect means that with increasing current j, the electrical resistivity η decreases, and for large current j, it becomes $\eta = (3\sqrt{\pi}/4)en_e\rho_e\nu_{ei}v_{\mathrm{the}}^3/j^3$. In reality, the problem is much more complex when the acceleration is considered, because, subtracting the two momentum equations, the general difference in the velocities $\delta\boldsymbol{u} = \boldsymbol{u}_b - \boldsymbol{u}_a$ now evolves according to a nonlinear differential equation,

$$\frac{\partial \delta \boldsymbol{u}}{\partial t} + \nu \Phi_{ab}(\epsilon)\delta\boldsymbol{u} = e\boldsymbol{E}\left(\frac{Z_b}{m_b} - \frac{Z_a}{m_a}\right); \qquad \nu = \nu_{ab} + \nu_{ba}, \tag{G52}$$

which does not seem to be solvable analytically. Nevertheless (after studying the solutions for some time), it is possible to conclude that there exist two distinct classes of solutions, which are typically separated by the value of the applied constant electric field E with respect to a critical value E_{crit}, where the maximal frictional forces balance the electric forces. For $E < E_{\mathrm{crit}}$, the solutions converge in

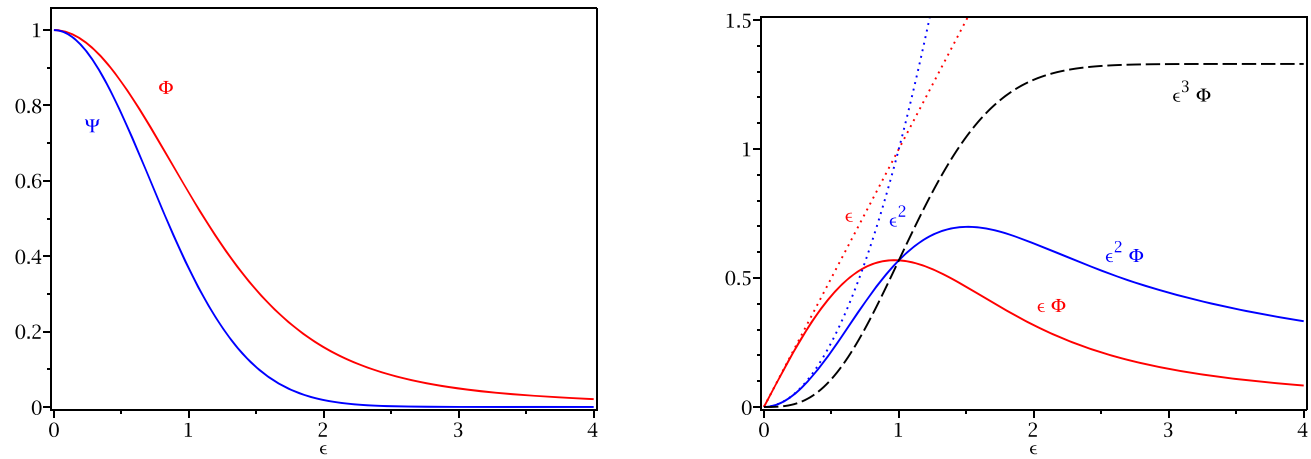

Figure 6. Left: functions Φ_{ab} (red line) and Ψ_{ab} (blue line), with respect to ϵ defined in Equation (G64). Right: functions $\epsilon\Phi_{ab} \sim R_{ab}$ (red line) and $\epsilon^2\Phi_{ab} \sim Q_{ab}$ (blue line), where the temperature is fixed. Corresponding approximations for small drifts with $\Phi_{ab} = 1$ are also plotted (dotted lines). Function $\epsilon\Phi_{ab}$ reaches maximum 0.57 at $\epsilon = 0.97$, and function $\epsilon^2\Phi_{ab}$ reaches maximum 0.70 at $\epsilon = 1.51$. It is possible to conclude that the small drift approximation is reasonably accurate up to $\epsilon = 0.5$, and that very small values $\epsilon \ll 1$ are actually not required. Even though we did not calculate the runaway effect for higher-order moments, out of curiosity we include a function $\epsilon^3\Phi_{ab}$ (black dashed line) that does not decrease to zero for large drifts, but instead converges to a constant value of 1.33.

time toward a situation where $\Phi_{ab} = 1$, and one recovers evolution Equation (G23) with static solution (G25). In contrast, for $E > E_{\rm crit}$, the solutions evolve in time toward a situation with $\Phi_{ab} = 0$, which can be shown, for example, by considering solutions where $\Phi_{ab}(\epsilon)$ is approximated with its asymptotic expansion. For very large values of E, one can straightforwardly prescribe $\Phi_{ab} = 0$, yielding a (collisionless) solution:

$$\boldsymbol{u}_b - \boldsymbol{u}_a = e\boldsymbol{E}\left(\frac{Z_b}{m_b} - \frac{Z_a}{m_a}\right)t. \tag{G53}$$

Thus, provided that $Z_a/m_a \neq Z_b/m_b$ is true, a stationary solution does not exist, and the difference in the velocities grows in time without bounds, before the beam/stream plasma instabilities with the associated development of turbulence (and, in extreme cases, eventually relativistic effects) restrict its further growth. For the particular case $Z_a/m_a = Z_b/m_b$, the runaway effect does not exist, and the difference in the velocities will converge to zero according to (G52). The frictional forces $\epsilon\Phi_{ab}(\epsilon)$ are plotted as a red curve in the right-hand panel of Figure 6. They reach its maximum value $[\epsilon\Phi_{ab}(\epsilon)]_{\rm max} = 0.57$ at $\epsilon = 0.97$ (often rounded as $\epsilon = 1$). The critical electric field $\boldsymbol{E}_{\rm crit}$ is determined by making the maximum frictional forces equal to the electric forces, so that (G52) becomes $\partial\delta\boldsymbol{u}/\partial t = 0$, yielding

$$\boldsymbol{E}_{\rm crit} = \underbrace{[\epsilon\Phi_{ab}(\epsilon)]_{\rm max}}_{0.57}\sqrt{v_{\rm tha}^2 + v_{\rm thb}^2}\,\frac{(\nu_{ab} + \nu_{ba})}{e}\frac{m_a m_b}{(Z_b m_a - Z_a m_b)}\frac{\boldsymbol{u}_b - \boldsymbol{u}_u}{|\boldsymbol{u}_b - \boldsymbol{u}_a|}. \tag{G54}$$

Alternatively, one might use the Chandrasekhar function, where $[\epsilon\Phi_{ab}]_{\rm max} = (3/2)\sqrt{\pi}\,[\widetilde{G}_{ab}]_{\rm max}$, and $[\widetilde{G}_{ab}]_{\rm max} = 0.214$. The runaway effect thus exists for

$$E > E_{\rm crit} = \underbrace{[\widetilde{G}_{ab}(\epsilon)]_{\rm max}}_{0.214}\hat{E}_D; \tag{G55}$$

$$\hat{E}_D = \frac{3\sqrt{\pi}}{2}\sqrt{v_{\rm tha}^2 + v_{\rm thb}^2}\,\frac{(\nu_{ab} + \nu_{ba})}{e}\frac{m_a m_b}{|Z_b m_a - Z_a m_b|}, \tag{G56}$$

where $\hat{E}_D$ can be viewed as a generalized Dreicer electric field for two species with arbitrary masses, charges, and temperatures. By further substituting for the collisional frequencies (we take $\ln\lambda$ to be constant),

$$\hat{E}_D = 8\pi\frac{(m_a + m_b)}{m_a m_b}\frac{(\rho_a + \rho_b)}{|Z_b m_a - Z_a m_b|}\frac{e^3 Z_a^2 Z_b^2 \ln\lambda}{(v_{\rm tha}^2 + v_{\rm thb}^2)}, \tag{G57}$$

which for an ion–electron plasma yields the usual Dreicer electric field

$$E_D = \frac{4\pi n_i e^3 Z_i^2 \ln\lambda}{T_e}. \tag{G58}$$

In the paper of Dreicer (1959), his reference field is defined as $E_c = E_D/2$, so in his notation the runaway effect exists for $E > 0.43E_c$ instead of $E > 0.214E_D$. In most of the recent literature, definition (G58) is used. It is sometimes incorrectly stated that the runaway effect exists for E exceeding E_D, whereas the correct value, as calculated by Dreicer, is almost five times smaller. Note the

dependence of (G58) on T_e, meaning that for any given value of electric field, the runaway effect will appear if the temperatures are sufficiently high. For $Z_a/m_a = Z_b/m_b$, the $\hat{E}_D$ becomes infinitely large, and the runaway effect between these species is not present. For an ion–electron plasma, the Dreicer electric field is also discussed, for example by Tanenbaum (1967, p. 258) and Balescu (1988, p. 775). We found it useful to consider the situation for two arbitrary (charged) species.

Similar to $\boldsymbol{R}_{ab}$, the Q_{ab} is obtained by calculating two integrals in (G26), and the first integral yields

$$\begin{aligned}\int f_a \frac{\partial H_b}{\partial \boldsymbol{v}_a} \cdot \boldsymbol{c}_a d^3 v_a &= \int\int f_a f_b \frac{\boldsymbol{v}_b - \boldsymbol{v}_a}{|\boldsymbol{v}_b - \boldsymbol{v}_a|^3} \cdot \boldsymbol{c}_a d^3 v_a d^3 v_b \\ &= -\frac{n_a n_b}{\pi^{3/2}\beta^3} \frac{m_b T_a}{m_b T_a + m_a T_b} \int \frac{\boldsymbol{x}}{x^3} \cdot (\boldsymbol{x} - \boldsymbol{u}) e^{-\frac{|\boldsymbol{x}-\boldsymbol{u}|^2}{\beta^2}} d^3 x \\ &= -\frac{2 n_a n_b}{\sqrt{\pi}\beta^3} v_{\mathrm{tha}}^2 e^{-\epsilon^2},\end{aligned} \tag{G59}$$

where we have used

$$\int \frac{1}{x} e^{-\frac{|\boldsymbol{x}-\boldsymbol{u}|^2}{\beta^2}} d^3 x = \pi^{3/2}\beta^2 \frac{\mathrm{erf}(\epsilon)}{\epsilon}; \tag{G60}$$

$$\int \frac{\boldsymbol{x}}{x} \cdot (\boldsymbol{x} - \boldsymbol{u}) e^{-\frac{|\boldsymbol{x}-\boldsymbol{u}|^2}{\beta^2}} d^3 x = 2\pi\beta^2 e^{-\epsilon^2}. \tag{G61}$$

The second integral in (G26) yields

$$\int f_a H_b d^3 v_a = \int\int f_a f_b \frac{1}{|\boldsymbol{v}_b - \boldsymbol{v}_a|} d^3 v_a d^3 v_b = \frac{n_a n_b}{\beta} \frac{\mathrm{erf}(\epsilon)}{\epsilon} = \frac{n_a n_b}{\beta^3} \frac{\mathrm{erf}(\epsilon)}{\epsilon^3} |\boldsymbol{u}|^2. \tag{G62}$$

The entire Equation (G26) then becomes

$$Q_{ab} = \rho_a \nu_{ab} \left[-\frac{3T_a}{m_a} e^{-\epsilon^2} + \frac{3}{4}\sqrt{\pi} \frac{\mathrm{erf}(\epsilon)}{\epsilon^3} \frac{m_b}{m_a + m_b} |\boldsymbol{u}_b - \boldsymbol{u}_a|^2 \right], \tag{G63}$$

and the difference in the temperatures $T_b - T_a$ is not directly visible. Nevertheless, the solution can be rewritten into

$$\begin{aligned} &Q_{ab} = \rho_a \nu_{ab} \left[3 \frac{T_b - T_a}{m_a + m_b} \Psi_{ab} + \frac{m_b}{m_a + m_b} |\boldsymbol{u}_b - \boldsymbol{u}_a|^2 \Phi_{ab} \right]; \\ &\Psi_{ab} = e^{-\epsilon^2}; \qquad \Phi_{ab} = \left(\frac{3}{4}\sqrt{\pi} \frac{\mathrm{erf}(\epsilon)}{\epsilon^3} - \frac{3}{2} \frac{e^{-\epsilon^2}}{\epsilon^2} \right); \qquad \epsilon = \frac{|\boldsymbol{u}_b - \boldsymbol{u}_a|}{\sqrt{v_{\mathrm{tha}}^2 + v_{\mathrm{thb}}^2}}, \end{aligned} \tag{G64}$$

recovering Equation (26.8) of Burgers (1969) and Equation (25c) of Schunk (1977). Similar to R_{ab}, for large differences in drifts, the Q_{ab} disappears.

It is of interest to explore the validity of the results with small drifts, obtained in Appendices G.1 and G.2. The functions Φ_{ab} and Ψ_{ab} are plotted in the left-hand panel of Figure 6. Both functions are decreasing, and thus in fluid models with the small drift approximation, the effects of the collisions are overestimated. We fix the temperature (so that ν_{ab} = const.), and in the right-hand panel of Figure 6 we plot the function $\epsilon\Phi_{ab}$, which corresponds to R_{ab} (red line), and function $\epsilon^2\Phi_{ab}$, which corresponds to Q_{ab} (blue line). For large drifts $\epsilon \gg 1$, functions $\epsilon\Phi_{ab} \sim 3\sqrt{\pi}/(4\epsilon^2)$ and $\epsilon^2\Phi_{ab} \sim 3\sqrt{\pi}/(4\epsilon)$.

G.4. Difficulties with Rosenbluth Potentials

It is interesting to analyze why it seems impossible to calculate the runaway effect for $\boldsymbol{R}_{ab}$ through the Rosenbluth potentials, and why one needs to use the "center-of-mass" transformation instead. An attempt to calculate the runaway effect yields

$$\begin{aligned}\boldsymbol{R}_{ab} &= m_a \int f_a \boldsymbol{A}_{ab} d^3 v \\ &= -4 \frac{c_{ab}}{m_a} \left(1 + \frac{m_a}{m_b}\right) \frac{n_a n_b v_{\mathrm{thb}}}{\pi^{3/2} v_{\mathrm{tha}}^3} \int e^{-|\alpha \boldsymbol{y} + \boldsymbol{u}|^2} \frac{\boldsymbol{y}}{y} \underbrace{\left(\frac{\mathrm{erf}(y)}{2y^2} - \frac{1}{\sqrt{\pi}} \frac{e^{-y^2}}{y} \right)}_{\widetilde{G}_{ab}(y)} d^3 y,\end{aligned} \tag{G65}$$

where $\alpha = v_{\rm thb}/v_{\rm tha}$ and $\boldsymbol{u} = (\boldsymbol{u}_b - \boldsymbol{u}_a)/v_{\rm tha}$, and we have also identified the Chandrasekhar function. First, integrating over $d\phi$, where the direction of $\boldsymbol{u}$ forms the axis $\hat{\boldsymbol{e}}_3 = \boldsymbol{u}/u$, yields

$$\int e^{-|\alpha \boldsymbol{y}+\boldsymbol{u}|^2}\frac{\boldsymbol{y}}{y}\left(\frac{\mathrm{erf}(y)}{2y^2} - \frac{1}{\sqrt{\pi}}\frac{e^{-y^2}}{y}\right)d^3y$$
$$= 2\pi\frac{\boldsymbol{u}}{u}e^{-u^2}\int_0^\infty\int_0^\pi e^{-\alpha^2y^2}e^{-2\alpha yu\cos\theta}\cos\theta\sin\theta\left(\frac{\mathrm{erf}(y)}{2} - \frac{y}{\sqrt{\pi}}e^{-y^2}\right)dyd\theta. \tag{G66}$$

Then one can perform the integration over $d\theta$; however, the subsequent integration over dy does not seem possible. Or, one can first attempt the integration over dy, using the substitutions $s = u\cos\theta$, $z = \alpha y + s$, so that $|\alpha\boldsymbol{y} + \boldsymbol{u}|^2 = z^2 - s^2 + u^2$ yields

$$\text{(G66)} = 2\pi\frac{\boldsymbol{u}}{u^3}e^{-u^2}\int_s^\infty\int_{-u}^u se^{+s^2}e^{-z^2}\left[\frac{1}{2}\mathrm{erf}\left(\frac{z-s}{\alpha}\right) - \frac{z-s}{\alpha\sqrt{\pi}}e^{-\frac{(z-s)^2}{\alpha^2}}\right]dzds, \tag{G67}$$

but the one-dimensional integrals over dz again appear impossible to calculate. The problem is the "drift" "s," and also the constants α. For example, the following indefinite integral is easily calculated by parts:

$$\int e^{-(az+b)^2}\mathrm{erf}(az+b)dz = \frac{\sqrt{\pi}}{4a}\mathrm{erf}^2(az+b), \tag{G68}$$

but the result is not useful. Obviously, a different approach has to be used to integrate over the Chandrasekhar function if $f_a^{(0)}$ is a Maxwellian with unrestricted drifts.

Importantly, from Appendix G.3, where the "center-of-mass" transformation is used, we know that the correct answer has to be

$$\int f_a^{(0)}\frac{\boldsymbol{y}}{y}\widetilde{G}_{ab}(y)d^3v \overset{!}{=} -n_a\frac{v_{\rm thb}^2}{v_{\rm tha}^2 + v_{\rm thb}^2}\frac{\boldsymbol{u}_b - \boldsymbol{u}_a}{|\boldsymbol{u}_b - \boldsymbol{u}_a|}\widetilde{G}_{ab}(\epsilon), \tag{G69}$$

where $\boldsymbol{y} = (\boldsymbol{v} - \boldsymbol{u}_b)/v_{\rm thb}$, $\epsilon = |\boldsymbol{u}_b - \boldsymbol{u}_a|\big/\sqrt{v_{\rm tha}^2 + v_{\rm thb}^2}$, and $d^3v = v_{\rm thb}^3 d^3y$; or, written in a full form,

$$\frac{n_a}{\pi^{3/2}v_{\rm tha}^3}\int e^{-\frac{|\boldsymbol{v}-\boldsymbol{u}_a|^2}{v_{\rm tha}^2}}\frac{\boldsymbol{y}}{y}\left(\frac{\mathrm{erf}(y)}{2y^2} - \frac{e^{-y^2}}{\sqrt{\pi}\,y}\right)d^3v$$
$$\overset{!}{=} -n_a\frac{v_{\rm thb}^2}{v_{\rm tha}^2 + v_{\rm thb}^2}\frac{\boldsymbol{u}_b - \boldsymbol{u}_a}{|\boldsymbol{u}_b - \boldsymbol{u}_a|}\left(\frac{\mathrm{erf}(\epsilon)}{2\epsilon^2} - \frac{e^{-\epsilon^2}}{\sqrt{\pi}\,\epsilon}\right). \tag{G70}$$

Finally, written in perhaps the prettiest form, when not referring to any physical quantities (i.e., a form suitable for integral tables),

$$\int_{-\infty}^\infty e^{-|\alpha\boldsymbol{y}+\boldsymbol{u}|^2}\frac{\boldsymbol{y}}{y}\left(\frac{\mathrm{erf}(y)}{2y^2} - \frac{e^{-y^2}}{\sqrt{\pi}\,y}\right)d^3y$$
$$\overset{!}{=} -\frac{\pi^{3/2}}{\alpha(1+\alpha^2)}\frac{\boldsymbol{u}}{u}\left(\frac{\mathrm{erf}(\epsilon)}{2\epsilon^2} - \frac{e^{-\epsilon^2}}{\sqrt{\pi}\,\epsilon}\right); \quad \text{where} \quad \epsilon = \frac{u}{\sqrt{1+\alpha^2}}; \quad \alpha > 0. \tag{G71}$$

It is remarkable that the integral has such a striking symmetry, even though the integral seems impossible to calculate directly, i.e., the integral "transfers" a Chandrasekar function in y-variable to a Chandrasekar function in ϵ-variable. The result seems well-defined, even for $\alpha < 0$, so the restriction is $\alpha \neq 0$ and real (the integral is divergent for $\alpha = 0$). The limit $u \to 0$ yields zero. The "proof" of (G71) can be viewed as analogous when evaluating the one-dimensional Gaussian integral $\int_{-\infty}^\infty e^{-x^2}dx$ through $\iint e^{-(x^2+y^2)}dxdy$ in polar coordinates, where, instead of integrating over d^3v, a trick is used to integrate over d^3vd^3v'.

Appendix H
8-moment Model (Heat Flux and Thermal Force)

To obtain the collisional contributions with the heat flux, one uses the following 8-moment distribution function of Grad:

$$f_b(\boldsymbol{v}') = \frac{n_b}{\pi^{3/2}v_{\rm thb}^3}e^{-\frac{|\boldsymbol{c}_b|^2}{v_{\rm thb}^2}}\left[1 - \frac{m_b}{T_bp_b}\left(1 - \frac{m_b|\boldsymbol{c}_b|^2}{5T_b}\right)\boldsymbol{q}_b\cdot\boldsymbol{c}_b\right]. \tag{H1}$$

The calculations done by Burgers (1969), Schunk (1977), and Killie et al. (2004) were performed using the "center-of-mass" transformation, described in Appendix G.3. Here, to do something slightly different, we verify the calculations by using the Rosenbluth potentials. The route through the Rosenbluth potentials has a great disadvantage, as error functions are encountered even if we are interested only in expressions with small drift velocities (with respect to thermal velocities). This is because the Rosenbluth potentials have to be derived with the exact (H1), and not expanded for small drifts from the beginning. Nevertheless, the route has an

advantage, as it is possible to do a double check in the middle of the calculations, because there are identities that the Rosenbluth potentials must satisfy.

H.1. Rosenbluth Potentials

Using the same variables $\boldsymbol{x} = (\boldsymbol{v}' - \boldsymbol{v})/v_{\rm thb}$ and $\boldsymbol{y} = (\boldsymbol{v} - \boldsymbol{u}_b)/v_{\rm thb}$ as before, so that $\boldsymbol{c}_b = (\boldsymbol{x} + \boldsymbol{y})v_{\rm thb}$, we need to obtain the Rosenbluth potentials

$$H_b(\boldsymbol{v}) = \int \frac{f_b(\boldsymbol{v}')}{|\boldsymbol{v}' - \boldsymbol{v}|} d^3v' = \frac{n_b}{\pi^{3/2} v_{\rm thb}} \int \frac{e^{-|\boldsymbol{x}+\boldsymbol{y}|^2}}{x} \left[1 - \frac{m_b v_{\rm thb}}{T_b p_b} \boldsymbol{q}_b \cdot (\boldsymbol{x} + \boldsymbol{y}) \left(1 - \frac{2}{5} |\boldsymbol{x} + \boldsymbol{y}|^2 \right) \right] d^3x; \tag{H2}$$

$$G_b(\boldsymbol{v}) = \int |\boldsymbol{v}' - \boldsymbol{v}| f_b(\boldsymbol{v}') d^3v' = \frac{n_b v_{\rm thb}}{\pi^{3/2}} \int x e^{-|\boldsymbol{x}+\boldsymbol{y}|^2} \left[1 - \frac{m_b v_{\rm thb}}{T_b p_b} \boldsymbol{q}_b \cdot (\boldsymbol{x} + \boldsymbol{y}) \left(1 - \frac{2}{5} |\boldsymbol{x} + \boldsymbol{y}|^2 \right) \right] d^3x. \tag{H3}$$

It is possible to calculate the following integrals (directly obtainable with Maple in spherical geometry, after the vector integrals containing $\boldsymbol{x}$ are first integrated by hand over $d\phi$):

$$\int \frac{1}{x} e^{-|\boldsymbol{x}+\boldsymbol{y}|^2} d^3x = \pi^{3/2} \frac{\mathrm{erf}(y)}{y}; \tag{H4}$$

$$\int \frac{1}{x} e^{-|\boldsymbol{x}+\boldsymbol{y}|^2} \left(1 - \frac{2}{5} |\boldsymbol{x} + \boldsymbol{y}|^2 \right) d^3x = \frac{2}{5} \pi^{3/2} \frac{\mathrm{erf}(y)}{y} + \frac{2}{5} \pi e^{-y^2}; \tag{H5}$$

$$\int \frac{\boldsymbol{x}}{x} e^{-|\boldsymbol{x}+\boldsymbol{y}|^2} \left(1 - \frac{2}{5} |\boldsymbol{x} + \boldsymbol{y}|^2 \right) d^3x = - \frac{2}{5} \pi^{3/2} \boldsymbol{y} \frac{\mathrm{erf}(y)}{y}, \tag{H6}$$

and similarly:

$$\int x e^{-|\boldsymbol{x}+\boldsymbol{y}|^2} d^3x = \pi^{3/2} \left(y + \frac{1}{2y} \right) \mathrm{erf}(y) + \pi e^{-y^2}; \tag{H7}$$

$$\int x e^{-|\boldsymbol{x}+\boldsymbol{y}|^2} \left(1 - \frac{2}{5} |\boldsymbol{x} + \boldsymbol{y}|^2 \right) d^3x = \frac{2}{5} \pi^{3/2} y \, \mathrm{erf}(y) + \frac{2}{5} \pi e^{-y^2}; \tag{H8}$$

$$\int x \boldsymbol{x} e^{-|\boldsymbol{x}+\boldsymbol{y}|^2} \left(1 - \frac{2}{5} |\boldsymbol{x} + \boldsymbol{y}|^2 \right) d^3x = - \frac{2}{5} \boldsymbol{y} \left[\pi^{3/2} \left(y + \frac{1}{4y^3} \right) \mathrm{erf}(y) + \pi \left(1 - \frac{1}{2y^2} \right) e^{-y^2} \right]. \tag{H9}$$

This yields the final Rosenbluth potentials for the 8-moment model, in the following form:

$$H_b(\boldsymbol{v}) = \frac{n_b}{v_{\rm thb}} \left[\frac{\mathrm{erf}(y)}{y} - \frac{2}{5} \frac{m_b v_{\rm thb}}{T_b p_b} (\boldsymbol{q}_b \cdot \boldsymbol{y}) \frac{1}{\sqrt{\pi}} e^{-y^2} \right]; \tag{H10}$$

$$G_b(\boldsymbol{v}) = n_b v_{\rm thb} \left[\left(y + \frac{1}{2y} \right) \mathrm{erf}(y) + \frac{1}{\sqrt{\pi}} e^{-y^2} \right] + \frac{2}{5} \frac{n_b}{p_b} (\boldsymbol{q}_b \cdot \boldsymbol{y}) \left[\frac{\mathrm{erf}(y)}{2y^3} - \frac{1}{\sqrt{\pi}} \frac{e^{-y^2}}{y^2} \right]. \tag{H11}$$

We will need a vector

$$\frac{\partial H_b}{\partial \boldsymbol{v}} = \frac{n_b}{v_{\rm thb}^2} \left[\boldsymbol{y} \left(\frac{2}{\sqrt{\pi}} \frac{e^{-y^2}}{y^2} - \frac{\mathrm{erf}(y)}{y^3} \right) - \frac{2}{5} \frac{m_b v_{\rm thb}}{T_b p_b} (\boldsymbol{q}_b - 2\boldsymbol{y}(\boldsymbol{q}_b \cdot \boldsymbol{y})) \frac{1}{\sqrt{\pi}} e^{-y^2} \right], \tag{H12}$$

and a matrix

$$\frac{\partial^2 G_b}{\partial \boldsymbol{v}\partial \boldsymbol{v}} = \frac{n_b}{v_{\rm thb}}\left(\bar{\bar{\boldsymbol{I}}} - \frac{\boldsymbol{yy}}{y^2}\right)\left[\frac{1}{\sqrt{\pi}}\frac{e^{-y^2}}{y^2} + \left(\frac{1}{y} - \frac{1}{2y^3}\right)\mathrm{erf}(y)\right] + \frac{n_b}{v_{\rm thb}}\frac{\boldsymbol{yy}}{y^2}\left[\frac{\mathrm{erf}(y)}{y^3} - \frac{2}{\sqrt{\pi}}\frac{e^{-y^2}}{y^2}\right]$$
$$+\frac{n_b m_b}{5T_b p_b}\left\{\left[\boldsymbol{q}_b\boldsymbol{y} + \boldsymbol{y}\boldsymbol{q}_b + (\boldsymbol{q}_b\cdot\boldsymbol{y})\left(\bar{\bar{\boldsymbol{I}}} - \frac{\boldsymbol{yy}}{y^2}\right)\right]\left[-\frac{3}{2}\frac{\mathrm{erf}(y)}{y^5} + \frac{1}{\sqrt{\pi}}\left(\frac{2}{y^2} + \frac{3}{y^4}\right)e^{-y^2}\right]\right.$$
$$\left.+(\boldsymbol{q}_b\cdot\boldsymbol{y})\frac{\boldsymbol{yy}}{y^2}\left[\frac{6}{y^5}\mathrm{erf}(y) - \frac{4}{\sqrt{\pi}}\left(1 + \frac{2}{y^2} + \frac{3}{y^4}\right)e^{-y^2}\right]\right\}. \tag{H13}$$

As a double check, applying $(\partial/\partial\boldsymbol{v})\cdot$ on (H12) recovers $-4\pi f_b$, and applying $(1/2)\mathrm{Tr}$ on (H13) recovers H_b. The dynamical friction vector then reads

$$\boldsymbol{A}_{ab} = 2\frac{c_{ab}}{m_a^2}\left(1 + \frac{m_a}{m_b}\right)\frac{n_b}{v_{\rm thb}^2}\left[\boldsymbol{y}\left(\frac{2}{\sqrt{\pi}}\frac{e^{-y^2}}{y^2} - \frac{\mathrm{erf}(y)}{y^3}\right) - \frac{2}{5}\frac{m_b v_{\rm thb}}{T_b p_b}(\boldsymbol{q}_b - 2\boldsymbol{y}(\boldsymbol{q}_b\cdot\boldsymbol{y}))\frac{1}{\sqrt{\pi}}e^{-y^2}\right], \tag{H14}$$

and after slight rearrangement, the diffusion tensor becomes

$$\bar{\bar{\boldsymbol{D}}}_{ab} = 2\frac{c_{ab}}{m_a^2}\left\{\frac{n_b}{v_{\rm thb}}\bar{\bar{\boldsymbol{I}}}\left[\frac{1}{\sqrt{\pi}}\frac{e^{-y^2}}{y^2} + \left(\frac{1}{y} - \frac{1}{2y^3}\right)\mathrm{erf}(y)\right] + \frac{n_b}{v_{\rm thb}}\frac{\boldsymbol{yy}}{y^2}\left[\left(\frac{3}{2y^3} - \frac{1}{y}\right)\mathrm{erf}(y) - \frac{3}{\sqrt{\pi}}\frac{e^{-y^2}}{y^2}\right]\right.$$
$$+\frac{n_b m_b}{5T_b p_b}[\boldsymbol{q}_b\boldsymbol{y} + \boldsymbol{y}\boldsymbol{q}_b + (\boldsymbol{q}_b\cdot\boldsymbol{y})\bar{\bar{\boldsymbol{I}}}]\left[-\frac{3}{2}\frac{\mathrm{erf}(y)}{y^5} + \frac{1}{\sqrt{\pi}}\left(\frac{2}{y^2} + \frac{3}{y^4}\right)e^{-y^2}\right]$$
$$\left.+\frac{n_b m_b}{5T_b p_b}(\boldsymbol{q}_b\cdot\boldsymbol{y})\frac{\boldsymbol{yy}}{y^2}\left[\frac{15}{2}\frac{\mathrm{erf}(y)}{y^5} - \frac{1}{\sqrt{\pi}}\left(4 + \frac{10}{y^2} + \frac{15}{y^4}\right)e^{-y^2}\right]\right\}. \tag{H15}$$

H.2. Momentum Exchange Rates $\boldsymbol{R}_{\rm ab}$

Then, similar to f_b according to (H1), one prescribes for species "a":

$$f_a(\boldsymbol{v}) = \frac{n_a}{\pi^{3/2}v_{\rm tha}^3}e^{-\frac{|\boldsymbol{c}_a|^2}{v_{\rm tha}^2}}\left[1 - \frac{m_a}{T_a p_a}\left(1 - \frac{m_a|\boldsymbol{c}_a|^2}{5T_a}\right)\boldsymbol{q}_a\cdot\boldsymbol{c}_a\right], \tag{H16}$$

and introduces the variable $\boldsymbol{u} = (\boldsymbol{u}_b - \boldsymbol{u}_a)/v_{\rm tha}$, so that $\boldsymbol{c}_a = \boldsymbol{y}v_{\rm thb} + \boldsymbol{u}v_{\rm tha}$. However, the resulting integrals would yield the runaway effect, and were never evaluated. It is necessary to get rid of the runaway effect, and approximate the f_a with small drifts $u \ll 1$, and in the first step

$$f_a(\boldsymbol{v}) \simeq \frac{n_a}{\pi^{3/2}v_{\rm tha}^3}e^{-\alpha^2 y^2}[1 - 2\alpha(\boldsymbol{y}\cdot\boldsymbol{u}) - u^2 + 2\alpha^2(\boldsymbol{y}\cdot\boldsymbol{u})^2]\left[1 - \frac{m_a}{T_a p_a}\boldsymbol{q}_a\cdot(\boldsymbol{y}v_{\rm thb} + \boldsymbol{u}v_{\rm tha})\right.$$
$$\left.+\frac{m_a^2}{5T_a^2 p_a}\boldsymbol{q}_a\cdot(\boldsymbol{y}v_{\rm thb} + \boldsymbol{u}v_{\rm tha})(y^2 v_{\rm thb}^2 + 2\boldsymbol{y}\cdot\boldsymbol{u}v_{\rm tha}v_{\rm thb} + u^2 v_{\rm tha}^2)\right], \tag{H17}$$

where $\alpha = v_{\rm thb}/v_{\rm tha}$. The distribution function (H17) needs to be further reduced to the "semilinear approximation," where the difference in the temperatures is not restricted, but one keeps only the precision $o(\boldsymbol{u})$ and also neglects all of the cross terms such as $\boldsymbol{q}_a\cdot\boldsymbol{u}$, keeping only

$$f_a(\boldsymbol{v}) \simeq \frac{n_a}{\pi^{3/2}v_{\rm tha}^3}e^{-\alpha^2 y^2}\left[1 - 2\alpha(\boldsymbol{y}\cdot\boldsymbol{u}) - \frac{m_a}{T_a p_a}(\boldsymbol{q}_a\cdot\boldsymbol{y})v_{\rm thb}\left(1 - \frac{2}{5}\alpha^2 y^2\right)\right]. \tag{H18}$$

We want to obtain

$$\boldsymbol{R}_{ab} = 2\frac{c_{ab}}{m_a}\left(1 + \frac{m_a}{m_b}\right)\int f_a\frac{\partial H_b}{\partial\boldsymbol{v}}d^3v, \tag{H19}$$

and we split the calculation into two integrals of (H12). The first integral $\sim \boldsymbol{y}$ calculates

$$\int \boldsymbol{y}\left(\frac{2}{\sqrt{\pi}}\frac{e^{-y^2}}{y^2} - \frac{\mathrm{erf}(y)}{y^3}\right) f_a\, d^3v$$
$$= \frac{n_a v_{\mathrm{thb}}^3}{\pi^{3/2} v_{\mathrm{tha}}^3} 4\pi \left[\frac{\alpha}{3\alpha^2(1+\alpha^2)^{3/2}}\boldsymbol{u} + \frac{m_a}{T_a p_a}\boldsymbol{q}_a v_{\mathrm{thb}} \frac{1}{10\alpha^2(1+\alpha^2)^{5/2}}\right], \tag{H20}$$

where we have used

$$\int_0^\infty e^{-\alpha^2 y^2} y^4 \left(\frac{2}{\sqrt{\pi}}\frac{e^{-y^2}}{y^2} - \frac{\mathrm{erf}(y)}{y^3}\right) dy = -\frac{1}{2\alpha^2(1+\alpha^2)^{3/2}}; \tag{H21}$$

$$\int_0^\infty e^{-\alpha^2 y^2} y^4 \left(1 + \frac{2}{5}\alpha^2 y^2\right)\left(\frac{2}{\sqrt{\pi}}\frac{e^{-y^2}}{y^2} - \frac{\mathrm{erf}(y)}{y^3}\right) dy = -\frac{3}{10\alpha^2(1+\alpha^2)^{5/2}}, \tag{H22}$$

and the second part of (H12) calculates

$$\frac{2}{\sqrt{\pi}}\int e^{-y^2}(\boldsymbol{q}_b - 2\boldsymbol{y}(\boldsymbol{q}_b\cdot\boldsymbol{y}))f_a\, d^3v = \frac{n_a v_{\mathrm{thb}}^3}{\pi^{3/2} v_{\mathrm{tha}}^3}\boldsymbol{q}_b 2\pi \frac{\alpha^2}{(1+\alpha^2)^{5/2}}. \tag{H23}$$

For a quick conversion to the collisional frequencies, it is useful to write

$$\nu_{ab} = \frac{8}{3\sqrt{\pi}}\frac{n_b}{v_{\mathrm{tha}}^3(1+\alpha^2)^{3/2}}\frac{c_{ab}}{m_a^2}\left(1 + \frac{m_a}{m_b}\right). \tag{H24}$$

Putting the results together yields the final result:

$$\boldsymbol{R}_{ab} = \rho_a \nu_{ab}(\boldsymbol{u}_b - \boldsymbol{u}_a) + \nu_{ab}\frac{3}{5}\frac{\mu_{ab}}{T_{ab}}\left(\boldsymbol{q}_a - \frac{\rho_a}{\rho_b}\boldsymbol{q}_b\right), \tag{H25}$$

recovering Equation (41b) of Schunk (1977; derived before by Burgers 1969). Alternatively, $\mu_{ab}/T_{ab} = 2/(v_{\mathrm{tha}}^2 + v_{\mathrm{thb}}^2)$. As a double check, $\boldsymbol{R}_{ab} = -\boldsymbol{R}_{ba}$, and for self-collisions, $\boldsymbol{R}_{aa} = 0$, as it should be. The contribution coming from the heat flux is known as the *thermal force*.

H.3. Heat Flux Exchange Rates

To calculate the heat flux contributions, one needs to calculate

$$\boldsymbol{Q}_{ab}^{(3)\,\prime} = \frac{\delta \boldsymbol{q}_{ab}{}'}{\delta t} = \frac{1}{2}\mathrm{Tr}\,\bar{\bar{\boldsymbol{Q}}}_{ab}^{(3)} - \frac{5}{2}\frac{p_a}{\rho_a}\boldsymbol{R}_{ab} - \frac{1}{\rho_a}\boldsymbol{R}_{ab}\cdot\bar{\bar{\boldsymbol{\Pi}}}_a^{(2)}, \tag{H26}$$

where $\bar{\bar{\boldsymbol{\Pi}}}_a^{(2)} = 0$ for the 8-moment model (the cross term $\boldsymbol{R}_{ab}\cdot\bar{\bar{\boldsymbol{\Pi}}}_a^{(2)}$ would be neglected anyway) and where

$$\frac{1}{2}\mathrm{Tr}\,\bar{\bar{\boldsymbol{Q}}}_{ab}^{(3)} = m_a\int f_a\left[(\boldsymbol{A}_{ab}\cdot\boldsymbol{c}_a)\boldsymbol{c}_a + \frac{1}{2}\boldsymbol{A}_{ab}|\boldsymbol{c}_a|^2\right]d^3v$$
$$+ m_a\int f_a\left[\frac{1}{2}(\mathrm{Tr}\,\bar{\bar{\boldsymbol{D}}}_{ab})\boldsymbol{c}_a + \bar{\bar{\boldsymbol{D}}}_{ab}\cdot\boldsymbol{c}_a\right]d^3v. \tag{H27}$$

We have used $\mathrm{Tr}[\boldsymbol{Acc}]^S = 2(\boldsymbol{A}\cdot\boldsymbol{c})\boldsymbol{c} + \boldsymbol{A}|\boldsymbol{c}|^2$, and because the diffusion tensor is symmetric, $\bar{\bar{\boldsymbol{D}}}^S = 2\bar{\bar{\boldsymbol{D}}}$ and $\mathrm{Tr}[\bar{\bar{\boldsymbol{D}}}^S\boldsymbol{c}]^S = 2(\mathrm{Tr}\,\bar{\bar{\boldsymbol{D}}})\boldsymbol{c} + 4\bar{\bar{\boldsymbol{D}}}\cdot\boldsymbol{c}$. By assuming no restriction on the temperature difference, we have verified (with the great help of Maple) that "semilinear" heat flux contributions (45)–(49) of Schunk (1977; derived before by Burgers 1969) are indeed correct for Coulomb collisions (with $z_{\mathrm{st}} = 3/5$, $z_{\mathrm{st}}{}' = 13/10$, $z_{\mathrm{st}}{}'' = 2$, and also $z_{\mathrm{st}}{}''' = 4$). For Coulomb collisions, the final result (after the subtraction of $\frac{5}{2}\frac{p_a}{\rho_a}\boldsymbol{R}_a$) is written in a compact form in Section 2.3; see Equation (32).

In the "linear approximation," where the temperature differences are small, the result simplifies into

$$\frac{1}{2}\mathrm{Tr}\,\bar{\bar{\boldsymbol{Q}}}_{ab}^{(3)} = \frac{\delta \boldsymbol{q}_{ab}}{\delta t} = \nu_{ab}\left[-\boldsymbol{q}_a D_{ab(1)} + \boldsymbol{q}_b\frac{\rho_a}{\rho_b}D_{ab(4)} + p_a(\boldsymbol{u}_b - \boldsymbol{u}_a)\frac{m_b + \frac{5}{2}m_a}{m_a + m_b}\right], \tag{H28}$$

where the introduced constants are defined in (H30), (H31). Alternatively, by summing over all of the "b" species and separating the self-collisions,

$$\frac{1}{2}\mathrm{Tr}\,\bar{\bar{\boldsymbol{Q}}}_a^{(3)} = \frac{\delta \boldsymbol{q}_a}{\delta t} = -\frac{4}{5}\nu_{aa}\boldsymbol{q}_a - \sum_{b\neq a}\nu_{ab}\left[D_{ab(1)}\boldsymbol{q}_a - D_{ab(4)}\frac{\rho_a}{\rho_b}\boldsymbol{q}_b - p_a(\boldsymbol{u}_b - \boldsymbol{u}_a)\frac{m_b + \frac{5}{2}m_a}{m_a + m_b}\right]; \tag{H29}$$

$$D_{ab(1)} = \frac{1}{(m_a + m_b)^2}\left(3m_a^2 + \frac{1}{10}m_a m_b - \frac{1}{5}m_b^2\right); \tag{H30}$$

$$D_{ab(4)} = \frac{1}{(m_a + m_b)^2}\left(\frac{6}{5}m_b^2 - \frac{3}{2}m_a m_b\right), \tag{H31}$$

recovering Equations (41e)–(43) of Schunk (1977); see also Equations (34)–(36) of Killie et al. (2004). The entire heat flux contributions are thus

$$\begin{aligned}\boldsymbol{Q}_a^{(3)\,\prime} = \frac{\delta \boldsymbol{q}_a{}'}{\delta t} &= \frac{1}{2}\mathrm{Tr}\,\bar{\bar{\boldsymbol{Q}}}_a^{(3)} - \frac{5}{2}\frac{p_a}{\rho_a}\boldsymbol{R}_a \\ &= -\boldsymbol{q}_a\left[\frac{4}{5}\nu_{aa} + \sum_{b\neq a}\nu_{ab}\left(D_{ab(1)} + \frac{3}{2}\frac{p_a}{\rho_a}\frac{\mu_{ab}}{T_{ab}}\right)\right] + \sum_{b\neq a}\boldsymbol{q}_b\nu_{ab}\frac{\rho_a}{\rho_b}\left(D_{ab(4)} + \frac{3}{2}\frac{p_a}{\rho_a}\frac{\mu_{ab}}{T_{ab}}\right) \\ &\quad -\frac{3}{2}p_a\sum_{b\neq a}\nu_{ab}\frac{m_b}{m_a + m_b}(\boldsymbol{u}_b - \boldsymbol{u}_a),\end{aligned} \tag{H32}$$

and enter the right-hand side of the evolution equation for the heat flux vector, for example, in its simplest form:

$$\frac{d_a\boldsymbol{q}_a}{dt} + \Omega_a\hat{\boldsymbol{b}}\times\boldsymbol{q}_a + \frac{5}{2}\frac{p_a}{m_a}\nabla T_a = \boldsymbol{Q}_a^{(3)\,\prime}. \tag{H33}$$

Importantly, in comparison to the BGK operator, the right-hand side also contains all of the heat fluxes $\boldsymbol{q}_b$. Formally, it is still possible to obtain a result for $\boldsymbol{q}_a$ in a quasistatic approximation, as a solution of the equation

$$\hat{\boldsymbol{b}}\times\boldsymbol{q}_a + \frac{\bar{\nu}_a}{\Omega_a}\boldsymbol{q}_a = -\frac{\boldsymbol{a}_a}{\Omega_a}, \tag{H34}$$

where we define

$$\bar{\nu}_a = \frac{4}{5}\nu_{aa} + \sum_{b\neq a}\nu_{ab}\left(D_{ab(1)} + \frac{3}{2}\frac{p_a}{\rho_a}\frac{\mu_{ab}}{T_{ab}}\right); \tag{H35}$$

$$\begin{aligned}\boldsymbol{a}_a &= \frac{5}{2}\frac{p_a}{m_a}\nabla T_a - \sum_{b\neq a}\boldsymbol{q}_b\nu_{ab}\frac{\rho_a}{\rho_b}\left(D_{ab(4)} + \frac{3}{2}\frac{p_a}{\rho_a}\frac{\mu_{ab}}{T_{ab}}\right) \\ &\quad +\frac{3}{2}p_a\sum_{b\neq a}\nu_{ab}\frac{m_b}{m_a + m_b}(\boldsymbol{u}_b - \boldsymbol{u}_a),\end{aligned} \tag{H36}$$

which has the following exact solution:

$$\boldsymbol{q}_a = -\frac{1}{\bar{\nu}_a}(\boldsymbol{a}_a\cdot\hat{\boldsymbol{b}})\hat{\boldsymbol{b}} - \frac{\bar{\nu}_a}{\Omega_a^2 + \bar{\nu}_a^2}\boldsymbol{a}_{a\perp} + \frac{\Omega_a}{\Omega_a^2 + \bar{\nu}_a^2}\hat{\boldsymbol{b}}\times\boldsymbol{a}_a. \tag{H37}$$

Nevertheless, the heat fluxes of various species are coupled.

H.4. One Ion–Electron Plasma

Considering a one ion–electron plasma (so $n_e = Z_i n_i$) with small differences in temperature, and neglecting the ratios m_e/m_i, the ion and electron heat fluxes decouple. For the electron species $D_{ei(1)} = -1/5$, $D_{ei(4)} = 6/5$, and $\mu_{ei} = m_e$, by using abbreviation $\delta\boldsymbol{u} = \boldsymbol{u}_e - \boldsymbol{u}_i$,

$$\boldsymbol{R}_e = -\rho_e\nu_{ei}\delta\boldsymbol{u} + \nu_{ei}\frac{\rho_e}{p_e}\frac{3}{5}\boldsymbol{q}_e; \tag{H38}$$

$$\frac{\delta\boldsymbol{q}_e}{\delta t} = -\boldsymbol{q}_e\left(\frac{4}{5}\nu_{ee} - \frac{1}{5}\nu_{ei}\right) - \nu_{ei}p_e\delta\boldsymbol{u}. \tag{H39}$$

The entire heat flux contributions are

$$\boldsymbol{Q}_e^{(3)\,\prime} = -\,\bar{\nu}_e \boldsymbol{q}_e + \frac{3}{2}\nu_{ei} p_e \delta \boldsymbol{u}; \tag{H40}$$

$$\bar{\nu}_e = \frac{4}{5}\nu_{ee} + \frac{13}{10}\nu_{ei}; \tag{H41}$$

$$\boldsymbol{a}_e = \frac{5}{2}\frac{p_e}{m_e}\nabla T_e - \frac{3}{2}\nu_{ei} p_e \delta \boldsymbol{u}, \tag{H42}$$

yielding a solution for the electron heat flux (split into a thermal part and a frictional part):

$$\boldsymbol{q}_e^T = -\,\kappa_\parallel^e \nabla_\parallel T_e - \kappa_\perp^e \nabla_\perp T_e + \kappa_\times^e \hat{\boldsymbol{b}} \times \nabla T_e; \tag{H43}$$

$$\boldsymbol{q}_e^u = +\,\frac{3}{2}\frac{\nu_{ei}}{\bar{\nu}_e} p_e \delta \boldsymbol{u}_\parallel + \frac{3}{2}\frac{\bar{\nu}_e \nu_{ei}}{\Omega_e^2 + \bar{\nu}_e^2} p_e \delta \boldsymbol{u}_\perp - \frac{3}{2}\frac{\Omega_e \nu_{ei}}{\Omega_e^2 + \bar{\nu}_e^2} p_e \hat{\boldsymbol{b}} \times \delta \boldsymbol{u}, \tag{H44}$$

with the thermal conductivities

$$\kappa_\parallel^e = \frac{5}{2}\frac{p_e}{\bar{\nu}_e m_e}; \qquad \kappa_\perp^e = \frac{5}{2}\frac{p_e}{m_e}\frac{\bar{\nu}_e}{(\Omega_e^2 + \bar{\nu}_e^2)}; \qquad \kappa_\times^e = \frac{5}{2}\frac{p_e}{m_e}\frac{\Omega_e}{(\Omega_e^2 + \bar{\nu}_e^2)}. \tag{H45}$$

The thermal conductivities have the same form as the BGK conductivities. The only difference is that while $\bar{\nu}_e = \nu_{ee} + \nu_{ei}$ for the BGK operator, now we have to use (H41). By using $\nu_{ee} = \nu_{ei}/(Z_i\sqrt{2})$ from Equation (182),

$$\bar{\nu}_e = \left(\frac{1}{Z_i\sqrt{2}}\frac{4}{5} + \frac{13}{10}\right)\nu_{ei}; \quad \text{for} \quad Z_i = 1: \quad \bar{\nu}_e = 1.866\nu_{ei}. \tag{H46}$$

The momentum exchange rates are also split into a frictional part and a thermal part:

$$\boldsymbol{R}_e^u = -\,\rho_e \nu_{ei}\left[\left(1 - \frac{9}{10}\frac{\nu_{ei}}{\bar{\nu}_e}\right)\delta \boldsymbol{u}_\parallel + \left(1 - \frac{9}{10}\frac{\bar{\nu}_e \nu_{ei}}{\Omega_e^2 + \bar{\nu}_e^2}\right)\delta \boldsymbol{u}_\perp + \frac{9}{10}\frac{\Omega_e \nu_{ei}}{\Omega_e^2 + \bar{\nu}_e^2}\hat{\boldsymbol{b}} \times \delta \boldsymbol{u}\right]; \tag{H47}$$

$$\boldsymbol{R}_e^T = -\,\frac{3}{2}\frac{\nu_{ei}}{\bar{\nu}_e} n_e \nabla_\parallel T_e - \frac{3}{2}\frac{\bar{\nu}_e \nu_{ei}}{\Omega_e^2 + \bar{\nu}_e^2} n_e \nabla_\perp T_e + \frac{3}{2}\frac{\Omega_e \nu_{ei}}{\Omega_e^2 + \bar{\nu}_e^2} n_e \hat{\boldsymbol{b}} \times \nabla T_e. \tag{H48}$$

In comparison, the Braginskii (1965) result for $Z_i = 1$ reads

$$\begin{aligned} \boldsymbol{R}_e^u &= -\rho_e \nu_{ei}\left[0.51\delta \boldsymbol{u}_\parallel + \left(1 - \frac{6.42x^2 + 1.84}{x^4 + 14.79x^2 + 3.77}\right)\delta \boldsymbol{u}_\perp + \frac{x(1.70x^2 + 0.78)}{x^4 + 14.79x^2 + 3.77}\hat{\boldsymbol{b}} \times \delta \boldsymbol{u}\right]; \\ \boldsymbol{R}_e^T &= -0.71 n_e \nabla_\parallel T_e - \frac{5.10x^2 + 2.68}{x^4 + 14.79x^2 + 3.77} n_e \nabla_\perp T_e + \frac{x((3/2)x^2 + 3.05)}{x^4 + 14.79x^2 + 3.77} n_e \hat{\boldsymbol{b}} \times \nabla T_e, \end{aligned} \tag{H49}$$

where $x = \Omega_e/\nu_{ei}$. The heat flux and associated thermal force of Burgers and Schunk therefore finally explains the entire mathematical structure of the Braginskii equations, i.e., all of the terms are finally present, only the numerical values are different.

Examining the obtained numerical values in the limit of a strong magnetic field with $Z_i = 1$ (where, for simplicity, we neglect all of the ratios ν_{ei}/Ω_e), yields

$$\begin{aligned} \boldsymbol{R}_e &= -\rho_e \nu_{ei}(0.518\delta \boldsymbol{u}_\parallel + \delta \boldsymbol{u}_\perp) - 0.80 n_e \nabla_\parallel T_e; \\ \boldsymbol{q}_e^u &= +0.80 p_e \delta \boldsymbol{u}_\parallel, \end{aligned} \tag{H50}$$

which is very close to the Braginskii values

$$\begin{aligned} \boldsymbol{R}_e &= -\rho_e \nu_{ei}(0.513\delta \boldsymbol{u}_\parallel + \delta \boldsymbol{u}_\perp) - 0.71 n_e \nabla_\parallel T_e; \\ \boldsymbol{q}_e^u &= +0.71 p_e \delta \boldsymbol{u}_\parallel. \end{aligned} \tag{H51}$$

Note that both results (H50), (H51) contain the same symmetrical constants 0.8 and 0.71 in the frictional heat flux $\boldsymbol{q}_e^u$ and the thermal force $\boldsymbol{R}_e^T$. This is known as the Onsager symmetry, and it is also valid for a general magnetic field strength and a general charge, as can be seen by comparing (H44) and (H48).

Continuing with the strong magnetic field and examining the perpendicular heat conductivities yields ($Z_i = 1$ for $\kappa_\perp^e$)

$$\kappa_\perp^e = 4.66\frac{p_e \nu_{ei}}{m_e \Omega_e^2}; \quad \kappa_\times^e = \frac{5}{2}\frac{p_e}{m_e \Omega_e}, \tag{H52}$$

and both match Braginskii exactly. Nevertheless, the parallel heat conductivity (which is independent of magnetic field strength; $Z_i = 1$)

$$\kappa_{\parallel}^{e} = 1.34\frac{p_e}{\nu_{ei} m_e}, \tag{H53}$$

which is quite low in comparison to the Braginskii value of 3.16.

H.5. Ion Species

For ion species $D_{ie(1)} = 3$, $D_{ie(4)} = -3m_e/(2m_i)$, and identical proton and electron temperatures, the momentum exchange rates (H25) yield

$$\boldsymbol{R}_i = \rho_i \nu_{ie} \delta \boldsymbol{u} - \nu_{ie}\frac{\rho_i}{p_e}\frac{3}{5}\boldsymbol{q}_e = -\boldsymbol{R}_e, \tag{H54}$$

and $\boldsymbol{R}_e$ has already been calculated. Furthermore, the collisional heat flux contributions (H32)–(H37) simplify into

$$\boldsymbol{Q}_i^{(3)\,\prime} = -\bar{\nu}_i \boldsymbol{q}_i; \tag{H55}$$

$$\bar{\nu}_i = \frac{4}{5}\nu_{ii} + 3\nu_{ie}; \tag{H56}$$

$$\boldsymbol{a}_i = \frac{5}{2}\frac{p_i}{m_i}\nabla T_i, \tag{H57}$$

where the electron heat flux $\boldsymbol{q}_e$ notably cancels out exactly for equal temperatures. Ion frequencies should thus be added according to

$$\begin{aligned}\bar{\nu}_i &= \left(\frac{4}{5} + 3\frac{\sqrt{2}}{Z_i}\sqrt{\frac{m_e}{m_i}}\right)\nu_{ii}; \quad \text{for} \quad Z_i = 1: \quad \bar{\nu}_i = 0.899\nu_{ii};\\ &= \frac{4}{5}\left(1 + \frac{15}{2Z_i}\sqrt{\frac{m_e}{2m_i}}\right)\nu_{ii}.\end{aligned} \tag{H58}$$

The model of Burgers–Schunk yields the ion heat flux

$$\boldsymbol{q}_i = -\kappa_{\parallel}^{i}\nabla_{\parallel}T_i - \kappa_{\perp}^{i}\nabla_{\perp}T_i + \kappa_{\times}^{i}\hat{\boldsymbol{b}} \times \nabla T_i, \tag{H59}$$

with the ion thermal conductivities

$$\kappa_{\parallel}^{i} = \frac{5}{2}\frac{p_i}{\bar{\nu}_i m_i}; \qquad \kappa_{\perp}^{i} = \frac{5}{2}\frac{p_i}{m_i}\frac{\bar{\nu}_i}{(\Omega_i^2 + \bar{\nu}_i^2)}; \qquad \kappa_{\times}^{i} = \frac{5}{2}\frac{p_i}{m_i}\frac{\Omega_i}{(\Omega_i^2 + \bar{\nu}_i^2)}, \tag{H60}$$

where frequencies are added according to (H58). Importantly, the ion–electron contributions are not completely negligible, and without them $\bar{\nu}_i = (4/5)\nu_{ii} = 0.8\nu_{ii}$.

However, in the work of Braginskii (1965), the ion–electron collisions are neglected for the ion heat fluxes and viscosities, and only ion self-collisions are accounted for. This can be seen from his ion coefficients that do not depend on Z_i. Neglecting the ion–electron collisions, the model of Burgers–Schunk yields

$$\kappa_{\parallel}^{i} = \frac{25}{8}\frac{p_i}{\nu_{ii} m_i}; \qquad \kappa_{\perp}^{i} = 2\frac{p_i}{m_i}\frac{\nu_{ii}}{\Omega_i^2 + (4/5)^2\nu_{ii}^2}; \qquad \kappa_{\times}^{i} = \frac{5}{2}\frac{p_i}{m_i}\frac{\Omega_i}{\Omega_i^2 + (4/5)^2\nu_{ii}^2}. \tag{H61}$$

For the parallel conductivity, $\kappa_{\parallel}^{i} \sim 25/8 = 3.125$, in comparison to Braginskii's 3.906. In the strong magnetic field limit,

$$\kappa_{\perp}^{i} = 2\frac{p_i}{m_i}\frac{\nu_{ii}}{\Omega_i^2}; \qquad \kappa_{\times}^{i} = \frac{5}{2}\frac{p_i}{m_i\Omega_i}, \tag{H62}$$

and both match Braginskii exactly (!). If ion–electron collisions are taken into account, these Burger–Schunk coefficients change into (for $Z_i = 1$) $\kappa_{\parallel}^{i} \sim 2.78$, $\kappa_{\perp}^{i} \sim 2.24$, and $\kappa_{\times}^{i} \sim 5/2$, and the perpendicular $\kappa_{\perp}^{i}$ would suddenly not match Braginskii. It would not make sense for the electron $\kappa_{\perp}^{e}$ to match Braginskii exactly (for a strong B-field) and the ion $\kappa_{\perp}^{i}$ not to, which is a definitive indication that ion–electron collisions are neglected in Braginskii.

Including the ion–electron collisions, the $\kappa_{\perp}^{i}$ in the strong B-limit reads

$$\kappa_{\perp}^{i} = \frac{p_i\nu_{ii}}{m_i\Omega_i^2}\left(2 + \frac{15}{Z_i}\sqrt{\frac{m_e}{2m_i}}\right). \tag{H63}$$

Neglecting ion–electron collisions with respect to ion–ion (self) collisions is analogous to neglecting 0.1 with respect to 0.8—the contribution is not tiny.

Table 8
Parallel Friction Force $\boldsymbol{R}_e^u = -\alpha_0 \rho_e \nu_{ei} \delta \boldsymbol{u}_\parallel$, Coefficient α_0 is Plotted, or Parallel Electrical Resistivity $\eta_\parallel = 1/\sigma_\parallel = \alpha_0 m_e \nu_{ei}/(e^2 n_e)$

$\parallel$ Friction Force $\boldsymbol{R}_e^u$	$Z_i = 1$	$Z_i = 2$	$Z_i = 3$	$Z_i = 4$	$Z_i = 16$	$Z_i = \infty$
Burgers–Schunk ($N = 1$)	0.518	0.431	0.395	0.376	0.326	0.308
Killie et al.	0.597	0.460	0.391	0.349	0.231	0.182
Braginskii ($N = 2$)	0.513	0.4**31**	0.39**5**	0.375	0.319	0.2949
Landshoff ($N = 4$)	0.508	0.430	0.395			0.29455
Spitzer–Härm ($N = \infty$)	0.506	0.431		0.375	0.319	0.2945

Note. The model of Burgers–Schunk is more precise than that of Killie et al. The model of Landshoff for $N = 1$ matches Burgers–Schunk, and for $N = 2$ it matches Braginskii. For $Z_i = 1$, the value of Landshoff ($N = 4$) is slightly corrected ($0.509 \rightarrow 0.508$, emphasized with bold font) from the more precise work of Kaneko (1960), and the values of Landshoff for other Z_i might be slightly incorrect. The values of Braginskii for $Z_i = 2$, 3 in his Table II are slightly incorrect, and we have used the values from analytic expression (56), which now also match Landshoff ($N = 2$). The Braginskii value for $Z_i = 16$ is also from (56). From Kaneko & Taguchi (1978), Kaneko & Yamao (1980), and Ji & Held (2013), the "final" value for $Z_i = 1$ is $\alpha_0 = 0.50612$, and the result of Spitzer–Härm is correct. Note that by keeping n_e and T_e constant in the definition of ν_{ei}, the friction force $\sim \alpha_0 \nu_{ei}$ actually increases with increasing Z_i (and the electrical conductivity decreases).

Appendix I
Comparison of Various Models with Braginskii (Electrons)

Focusing on the parallel direction, the momentum exchange rates $\boldsymbol{R}_{e\parallel}$ and electron heat flux $\boldsymbol{q}_{e\parallel}$ can be written in a general form:

$$\boldsymbol{R}_{e\parallel} = -\alpha_0 \rho_e \nu_{ei} \delta \boldsymbol{u}_\parallel - \beta_0 n_e \nabla_\parallel T_e;$$
$$\boldsymbol{q}_{e\parallel} = +\beta_0^* p_e \delta \boldsymbol{u}_\parallel - \gamma_0 \frac{p_e}{m_e \nu_{ei}} \nabla_\parallel T_e. \tag{I1}$$

The Braginskii (1965) values of α_0; $\beta_0 = \beta_0^*$ and γ_0 are given in his Table 2 (p. 25). The model of Burgers (1969)–Schunk (1977) is given by

$$\alpha_0 = 1 - \frac{9}{10}\frac{\nu_{ei}}{\bar{\nu}_e}; \quad \beta_0 = \beta_0^* = \frac{3}{2}\frac{\nu_{ei}}{\bar{\nu}_e}; \quad \gamma_0 = \frac{5}{2}\frac{\nu_{ei}}{\bar{\nu}_e}; \quad \bar{\nu}_e = \left(\frac{1}{Z_i\sqrt{2}}\frac{4}{5} + \frac{13}{10}\right)\nu_{ei}, \tag{I2}$$

or equivalently,

$$\alpha_0 = \frac{\sqrt{2} + Z_i}{\sqrt{2} + (13/4)Z_i}; \quad \beta_0 = \beta_0^* = \frac{15 Z_i}{4\sqrt{2} + 13 Z_i}; \quad \gamma_0 = \frac{25 Z_i}{4\sqrt{2} + 13 Z_i}. \tag{I3}$$

The model of Killie et al. (2004), discussed in Appendix I.2, yields

$$\alpha_0 = 1 - \frac{9}{35}\frac{\nu_{ei}}{\bar{\nu}_e}; \quad \beta_0 = \frac{3}{7}\frac{\nu_{ei}}{\bar{\nu}_e}; \quad \beta_0^* = \frac{3}{2}\frac{\nu_{ei}}{\bar{\nu}_e}; \quad \gamma_0 = \frac{5}{2}\frac{\nu_{ei}}{\bar{\nu}_e}; \quad \bar{\nu}_e = \left(\frac{1}{Z_i\sqrt{2}}\frac{16}{35} + \frac{11}{35}\right)\nu_{ei}. \tag{I4}$$

The other included models are described below.

In Table 8, we compare the parallel friction force; in Table 9, the parallel thermal force; in Table 10, the parallel thermal heat flux (thermal conductivity $\kappa_\parallel^e$); and in Table 11, the parallel frictional heat flux. Furthermore, in Table 12, we compare $\kappa_\perp^e$ in the strong magnetic field limit.

We include the numerical model of Spitzer & Härm (1953; see also Spitzer 1962), with their notation being discussed in Appendix I.1, which reads:

$$\alpha_0 = \frac{3\pi}{32\gamma_E}; \quad \beta_0 = \frac{3}{2}\frac{\gamma_T}{\gamma_E}; \quad \beta_0^* = 4\frac{\delta_E}{\gamma_E} - \frac{5}{2}; \quad \gamma_0 = \epsilon\delta_T\frac{320}{3\pi}, \tag{I5}$$

with the numerical values of γ_E, γ_T, δ_E, δ_T, and ϵ given by Table III in Spitzer & Härm (1953). For the Lorentzian plasma ($Z_i = \infty$), the coefficients are $\gamma_E = \gamma_T = \delta_E = \delta_T = 1$ and $\epsilon = 2/5$. We also include the model of Landshoff (1949, 1951), who calculated several transport coefficients (with the inclusion of a magnetic field) before Spitzer and Braginskii, and studied convergence with increasing Laguerre polynomials from $N = 1$ to $N = 4$ (in his work, $i = N + 1$). The model is interesting because for $N = 1$, it matches the values of Burgers–Schunk, and for $N = 2$, it matches Braginskii. His model can be figured out to be

$$\alpha_0 = \frac{1}{Z_i}(\triangle_{00}/\triangle)^{-1}; \quad \beta_0 = \beta_0^* = \frac{5}{2}\frac{\triangle_{01}/\triangle}{\triangle_{00}/\triangle}; \quad \gamma_0 = \frac{25}{4}Z_i\left(\frac{\triangle_{11}}{\triangle} - \frac{(\triangle_{01}/\triangle)^2}{\triangle_{00}/\triangle}\right), \tag{I6}$$

Table 9
Parallel Thermal Force $\boldsymbol{R}_e^T = -\beta_0 n_e \nabla_\parallel T_e$, Coefficient β_0 is Plotted

$\parallel$ Thermal Force $\boldsymbol{R}_e^T$	$Z_i = 1$	$Z_i = 2$	$Z_i = 3$	$Z_i = 4$	$Z_i = 16$	$Z_i = \infty$
Burgers–Schunk	0.804	0.948	1.008	1.041	1.123	1.154
Killie et al.	0.672	0.901	1.015	1.085	1.281	1.364
Braginskii	0.711	0.905	1.016	1.090	1.362	1.521
Landshoff ($N = 4$)	0.7**09**	0.904	1.016			1.5005
Spitzer–Härm	0.703	0.908		1.092	1.346	3/2

Note. The model of Killie et al. is more precise than that of Burgers–Schunk. The model of Landshoff for $N = 1$ matches Burgers–Schunk, and for $N = 2$ it matches Braginskii. For $Z_i = 1$, the Landshoff ($N = 4$) value is slightly corrected ($0.710 \rightarrow 0.709$) from Kaneko. The final value for $Z_i = 1$ from Kaneko et al. and Ji & Held reads $\beta_0 = 0.70287$, and the Spitzer–Härm result is correct.

Table 10
Parallel Electron Heat Conductivity $\kappa_\parallel^e = \gamma_0 p_e/(m_e \nu_{ei})$ (Thermal Heat Flux $\boldsymbol{q}_e^T = -\kappa_\parallel^e \nabla_\parallel T_e$), Coefficient γ_0 is Plotted

$\parallel$ Heat Conductivity $\kappa_\parallel^e$	$Z_i = 1$	$Z_i = 2$	$Z_i = 3$	$Z_i = 4$	$Z_i = 16$	$Z_i = \infty$
Burgers–Schunk	1.34	1.58	1.68	1.73	1.87	1.92
Killie et al.	3.92	5.25	5.92	6.33	7.47	7.95
Braginskii	3.1616	4.890	6.064	6.920	10.334	12.471
Landshoff ($N = 4$)	3.17**8**	4.902	6.069			13.572
Spitzer–Härm	3.203	4.960		6.983	10.629	13.581

Note. The model of Killie et al. is a significant improvement over that of Burgers–Schunk. The model of Landshoff for $N = 1$ matches Burgers–Schunk, and for $N = 2$ it approximately matches Braginskii. For $Z_i = 1$, the Landshoff ($N = 4$) value is slightly corrected ($3.175 \rightarrow 3.178$) from Kaneko. The final value for $Z_i = 1$ from Kaneko et al. and Ji & Held reads $\gamma_0 = 3.2031$, and the Spitzer–Härm result is correct. Note that by keeping n_e and T_e constant in the definition of ν_{ei}, the heat conductivity γ_0/ν_{ei} actually decreases with increasing Z_i.

Table 11
Parallel Electron Frictional Heat Flux $\boldsymbol{q}_e^u = \beta_0^* p_e \delta \boldsymbol{u}_\parallel$

$\parallel$ Frictional Heat Flux $\boldsymbol{q}_e^u$	$Z_i = 1$	$Z_i = 2$	$Z_i = 3$	$Z_i = 4$	$Z_i = 16$	$Z_i = \infty$
Killie et al.	2.35	3.15	3.55	3.80	4.48	4.77
Spitzer–Härm	0.699	0.888		1.089	1.346	3/2

Note. For the models of Burgers–Schunk, Braginskii, and Landshoff, the Onsager symmetry $\beta_0^* = \beta_0$ holds exactly with the values given in Table 9. For the model of Spitzer–Harm, the Onsager symmetry is satisfied only approximately, with the largest discrepancy for $Z_i = 2$, of around 2%. For the model of Killie et al., the Onsager symmetry is broken, and the frictional heat flux values are quite large.

Table 12
Perpendicular Electron Heat Conductivity $\kappa_\perp^e = \gamma_1' p_e \nu_{ei}/(m_e \Omega_e^2)$, in the Limit of a Strong Magnetic Field, Coefficient γ_1' is Plotted

$\perp$ Heat Conductivity $\kappa_\perp^e$	$Z_i = 1$	$Z_i = 2$	$Z_i = 3$	$Z_i = 4$	$Z_i = \infty$
Burgers–Schunk	4.664	3.957	3.721	3.604	3.25
Killie et al.	1.59	1.19	1.06	0.99	0.79
Braginskii	4.664	3.957	3.721	3.604	3.25

Note. The Braginskii values are from his Table II. Interestingly, the Burgers–Schunk model matches the Braginskii values exactly. In fact, both models yield the same analytic expression $\gamma_1' = (\sqrt{2}/Z_i) + 13/4$, see (60), so the numerical comparison between Burgers–Schunk and Braginskii is a bit meaningless (and the reason why the $Z_i = 16$ value was omitted from our table). The table shows that the model of Killie et al. is imprecise.

with the coefficients from Table I of Landshoff (1951). We plot his highest-order model for $N = 4$. The models of Landshoff were calculated with higher numerical precision in the work of Kaneko (1960), where the following conversion has to be used:

$$\alpha_0 = \frac{1}{e^{\mathrm{I}(0)}}; \qquad \beta_0 = \beta_0^* = -\frac{5}{2}\frac{b^{\mathrm{I}(0)}}{e^{\mathrm{I}(0)}}; \qquad \gamma_0 = \frac{25}{4}\left[b^{\mathrm{I}(-1)} - \frac{(b^{\mathrm{I}(0)})^2}{e^{\mathrm{I}(0)}}\right], \tag{I7}$$

with the values in his Tables I, II, and III. In his work, $M = N + 1$, and values for the models from $N = 1$ to $N = 5$ are given, although only for $Z_i = 1$. The model is easily comparable with that of Landshoff (1951) because the same coefficients are given. In our comparison tables, we slightly correct these $Z_i = 1$ values of Landshoff ($N = 4$) with the more precise ones of Kaneko. In the later works of Kaneko & Taguchi (1978) and Kaneko & Yamao (1980), calculations with up to $M = 50$ were made, and the notation is changed into $b^{\mathrm{I}(0)} \to b_1^{\mathrm{I}(0)}$, $b^{\mathrm{I}(-1)} \to b_1^{\mathrm{I}(1)}$. From their work and the recent work of Ji & Held (2013), who used up to 160 Laguerre polynomials, the correct values for charge $Z_i = 1$ read $\alpha_0 = 0.50612$, $\beta_0 = 0.70287$, and $\gamma_0 = 3.2031$.

For the work of Balescu (1988), who was the first to recover Braginskii with the moment approach of Grad, the following conversion has to be used:

$$\alpha_0 = \frac{1}{\widetilde{\sigma}_\parallel}; \qquad \beta_0 = \beta_0^* = -\sqrt{\frac{5}{2}}\frac{\widetilde{\alpha}_\parallel}{\widetilde{\sigma}_\parallel}; \qquad \gamma_0 = \frac{5}{2}\left(\widetilde{\kappa}_\parallel^{\,e} - \frac{\widetilde{\alpha}_\parallel^{\,2}}{\widetilde{\sigma}_\parallel}\right), \tag{I8}$$

with the numerical values for $Z_i = 1$ given in his Table 4.1 (p. 239). For his 13-moment model ($N = 1$), the results are equal to Burgers–Schunk, and for his 21-moment model ($N = 2$), the results are equal to Braginskii. However, for his 29-moment model ($N = 3$), the coefficients of Balescu were shown to be imprecise by Ji & Held (2013), see their Table I, who were able to pinpoint exactly the analytic errors in the collisional matrices of Balescu. That the Balescu $N = 3$ values are indeed incorrect can be quickly double-checked by comparison with the $M = 4$ model of Kaneko (1960), from where the Balescu parameters should be $\widetilde{\sigma}_\parallel = e^{\mathrm{I}(0)} = 1.964$, $\widetilde{\alpha}_\parallel = \sqrt{5/2}\, b^{\mathrm{I}(0)} = -0.887$, and $\widetilde{\kappa}_\parallel^{\,e} = (5/2) b^{\mathrm{I}(-1)} = 1.666$, agreeing with the modern calculations of Ji & Held (2013).

I.1. Notation of Spitzer–Härm (1953)

The exact values of the parallel transport coefficients (with the exception of parallel viscosity) were first numerically obtained by Spitzer & Härm (1953). Essentially, the perturbation ϕ_e (or $f_e^{(1)}$) around a Maxwellian $f_e = f_e^{(0)}(1 - \phi_e)$ that satisfies the Fokker–Planck equation was found numerically, and the obtained result was used to calculate the transport coefficients. No magnetic field is present in their work, and the results can be interpreted as applying to unmagnetized plasmas, or to magnetized plasmas in the direction parallel to magnetic field lines. Similar to Braginskii (Chapters 2 and 4), the paper treats a one ion–electron plasma (with $n_e = Z_i n_i$).

The notation of Spitzer & Härm (1953) can be very confusing. The results are given in a form

$$\boldsymbol{j} = \sigma \boldsymbol{E} + \alpha \nabla T_e; \tag{I9}$$

$$\boldsymbol{q}_e^{\mathrm{Spitzer}} = -\beta \boldsymbol{E} - K \nabla T_e, \tag{I10}$$

with the coefficients σ, α, β, and K given by their Equations (33)–(36). These coefficients contain a quantity C^2. This quantity is only defined by a sentence following Equation (16) in their previous paper by Cohen et al. (1950), which reads "C^2 is the mean square electron velocity," meaning $C = \sqrt{3T_e/m_e}$ with the important factor of 3 present (we use the same notation as Braginskii, with the Boltzmann constant equal to one). Rewriting their coefficients in (I9), (I10) to our notation yields

$$\sigma = \frac{32}{3\pi}\frac{e^2 n_e}{m_e \nu_{ei}}\gamma_E; \qquad \alpha = \frac{16}{\pi}\frac{e n_e}{m_e \nu_{ei}}\gamma_T;$$
$$\beta = \frac{128}{3\pi}\frac{e p_e}{m_e \nu_{ei}}\delta_E; \qquad K = \frac{320}{3\pi}\frac{p_e}{m_e \nu_{ei}}\delta_T, \tag{I11}$$

where the numerical values of γ_E, γ_T, δ_E, and δ_T are given in Table III of Spitzer & Härm (1953). The coefficients (I11) are essentially normalized with respect to a Lorentzian plasma $Z_i = \infty$ (meaning when electron–electron collisions are negligible), in which case $\gamma_E = \gamma_T = \delta_E = \delta_T = 1$.

Unfortunately, Spitzer & Härm (1953) do not define their $\boldsymbol{q}_e^{\mathrm{Spitzer}}$, and only describe it as a "the rate of flow of heat." The heat flux is also not defined in the book of Spitzer (1962), but he notes (Equation (5.45)) that, from the thermodynamics of irreversible processes, the model closely satisfies

$$\beta = \alpha T_e + \frac{5}{2}\frac{T_e}{e}\sigma. \tag{I12}$$

Equation (I12) should be the Onsager symmetry. In the historical literature, there are three other major possibilities regarding how to define the heat flux. The first two choices are:

$$\boldsymbol{q}_a^{***} = \frac{m_a}{2}\int \boldsymbol{v}|\boldsymbol{v}|^2 f_a\, d^3v = \boldsymbol{q}_a + \frac{5}{2}p_a \boldsymbol{u}_a + \boldsymbol{u}_a \cdot \bar{\bar{\boldsymbol{\Pi}}}_a^{(2)} + \frac{\rho_a}{2}|\boldsymbol{u}_a|^2 \boldsymbol{u}_a; \tag{I13}$$

$$\boldsymbol{q}_a^{**} = \int \boldsymbol{v}\left(\frac{m_a v^2}{2} - \frac{5}{2}T_a\right) f_a\, d^3v = \boldsymbol{q}_a + \boldsymbol{u}_a \cdot \bar{\bar{\boldsymbol{\Pi}}}_a^{(2)} + \frac{\rho_a}{2}|\boldsymbol{u}_a|^2 \boldsymbol{u}_a. \tag{I14}$$

The nonlinear terms can be neglected. Spitzer is not using the second choice, and the first choice is almost correct, except that for the electron heat flux, only $(5/2)p_e\boldsymbol{u}_e$ would be created, and not the whole current $\boldsymbol{u}_e - \boldsymbol{u}_i$. The third choice is the definition of Chapman & Cowling (1939), where the heat flux is defined with respect to the *average* velocity of all of the species $\langle \boldsymbol{u}\rangle \equiv (\sum_a \rho_a \boldsymbol{u}_a)/\sum_a \rho_a$, according to

$$\boldsymbol{q}_a{}^* = \frac{m_a}{2}\int (\boldsymbol{v} - \langle \boldsymbol{u}\rangle)|\boldsymbol{v} - \langle \boldsymbol{u}\rangle|^2 f_a d^3v = \boldsymbol{q}_a + \frac{5}{2}p_a \boldsymbol{w}_a + \frac{\rho_a}{2}|\boldsymbol{w}_a|^2 \boldsymbol{w}_a + \boldsymbol{w}_a \cdot \bar{\bar{\boldsymbol{\Pi}}}_a^{(2)}, \tag{I15}$$

where $\boldsymbol{w}_a = \boldsymbol{u}_a - \langle \boldsymbol{u}\rangle$. For an ion–electron plasma $\langle \boldsymbol{u}\rangle = \boldsymbol{u}_i$ and $\boldsymbol{w}_e = \boldsymbol{u}_e - \boldsymbol{u}_i$. Thus, to satisfy (I12), the correct interpretation seems to be

$$\boldsymbol{q}_e^{\text{Spitzer}} = \boldsymbol{q}_e{}^* = \boldsymbol{q}_e + \frac{5}{2}p_e \delta \boldsymbol{u} = \boldsymbol{q}_e - \frac{5}{2}\frac{T_e}{e}\boldsymbol{j}, \tag{I16}$$

where $\boldsymbol{j} = -en_e\delta\boldsymbol{u}$ and $\delta\boldsymbol{u} = \boldsymbol{u}_e - \boldsymbol{u}_i$.

Result (I9) should be viewed as part of the evolution equation for $\partial \boldsymbol{u}_e/\partial t$ (here written in a steady state with all other terms neglected), and substituting the electric field into (I10) then yields

$$\begin{aligned} en_e\boldsymbol{E} = \boldsymbol{R}_e &= \frac{en_e}{\sigma}\boldsymbol{j} - en_e\frac{\alpha}{\sigma}\nabla T_e; \\ \boldsymbol{q}_e &= -\left(\frac{\beta}{\sigma} - \frac{5}{2}\frac{T_e}{e}\right)\boldsymbol{j} - \epsilon K \nabla T_e; \quad \text{where} \quad \epsilon = 1 - \frac{\alpha\beta}{\sigma K} = 1 - \frac{3}{5}\frac{\delta_E\gamma_T}{\delta_T\gamma_E}. \end{aligned} \tag{I17}$$

The numerical coefficient ϵ is given in Table III of Spitzer & Härm (1953) as well. Or, equivalently, by using (I11),

$$\begin{aligned} \boldsymbol{R}_e &= -\frac{3\pi}{32\gamma_E}\rho_e\nu_{ei}\delta\boldsymbol{u} - \frac{3}{2}\frac{\gamma_T}{\gamma_E}n_e\nabla T_e; \\ \boldsymbol{q}_e &= +\left(4\frac{\delta_E}{\gamma_E} - \frac{5}{2}\right)p_e\delta\boldsymbol{u} - \epsilon\delta_T\frac{320}{3\pi}\frac{p_e}{m_e\nu_{ei}}\nabla T_e. \end{aligned} \tag{I18}$$

In this form, the results can be directly compared to Braginskii, with the relations

$$\alpha_0 = \frac{3\pi}{32\gamma_E}; \quad \beta_0 = \frac{3}{2}\frac{\gamma_T}{\gamma_E}; \quad \beta_0^* = 4\frac{\delta_E}{\gamma_E} - \frac{5}{2}; \quad \gamma_0 = \epsilon\delta_T\frac{320}{3\pi}.$$

The Onsager symmetry then reads

$$\frac{3}{2}\gamma_T = 4\delta_E - \frac{5}{2}\gamma_E, \tag{I19}$$

which the model satisfies approximately, and for the Lorentz case exactly. The largest difference appears for $Z_i = 2$, where the left-hand side of (I19) is 0.621 and the right-hand side is 0.607, so Spitzer's claim that Equation (I12) is satisfied to about one part in a thousand seems a bit exaggerated, or we are interpreting his results incorrectly. The model of Spitzer & Härm (1953) and Spitzer (1962) is criticized in the monograph of Balescu (1988, Part 1, p. 266). Nevertheless, the coefficients α_0, β_0, and γ_0 in the model of Spitzer & Härm (1953) are the correct answer, and in comparison with Kaneko & Taguchi (1978), Kaneko & Yamao (1980), or Ji & Held (2013), these coefficients are valid for three decimal digits. For numerical simulations that employ the heat flux of Spitzer & Härm (1953), it seems logical to simply ignore the imprecise β_0^* values, and enforce the Onsager symmetry $\beta_0^* = \beta_0$ in their model by hand.

I.2. Model of Killie et al. (2004)

Instead of the 8-moment distribution function of Grad (H1) used in the model of Burgers–Schunk, Killie et al. (2004) argued that it is better to use

$$f_a = f_a^{(0)}\left[1 - \frac{m_a^2|\boldsymbol{c}_a|^2}{5T_a^2 p_a}\left(1 - \frac{m_a|\boldsymbol{c}_a|^2}{7T_a}\right)\boldsymbol{q}_a \cdot \boldsymbol{c}_a\right], \tag{I20}$$

yielding the collisional contributions (which we did not verify) for small temperature differences

$$\boldsymbol{R}_a = \rho_a\sum_b \nu_{ab}(\boldsymbol{u}_b - \boldsymbol{u}_a) + \sum_b \nu_{ab}\frac{3}{5}\frac{\mu_{ab}}{T_{ab}}\left[\boldsymbol{q}_a\left(1 - \frac{5}{7}\frac{m_b}{m_a + m_b}\right) - \boldsymbol{q}_b\frac{\rho_a}{\rho_b}\left(1 - \frac{5}{7}\frac{m_a}{m_a + m_b}\right)\right], \tag{I21}$$

and

$$\frac{1}{2}\mathrm{Tr}\,\bar{\bar{\boldsymbol{Q}}}_a^{(3)} = \frac{\delta \boldsymbol{q}_a}{\delta t} = -\frac{16}{35}\nu_{aa}\boldsymbol{q}_a - \sum_{b\neq a}\nu_{ab}\left[D_{ab}^{(1)}\boldsymbol{q}_a - D_{ab}^{(4)}\frac{\rho_a}{\rho_b}\boldsymbol{q}_b - p_a(\boldsymbol{u}_b - \boldsymbol{u}_a)\frac{m_b + \frac{5}{2}m_a}{m_a + m_b}\right]; \tag{I22}$$

$$D_{ab}^{(1)} = \frac{1}{(m_a + m_b)^3}\left(3m_a^3 - \frac{1}{2}m_a^2 m_b - \frac{2}{5}m_a m_b^2 - \frac{4}{35}m_b^3\right); \tag{I23}$$

$$D_{ab}^{(4)} = \frac{1}{(m_a + m_b)^3}\left(\frac{6}{5}m_b^3 - \frac{171}{70}m_b^2 m_a - \frac{3}{7}m_b m_a^2\right). \tag{I24}$$

Similar to Burgers–Schunk, they also provide equations for unrestricted temperature differences. Considering an ion–electron plasma yields $D_{ei}^{(1)} = -4/35$, $D_{ei}^{(4)} = 6/5$, and

$$\boldsymbol{R}_e = -\rho_e\nu_{ei}\delta\boldsymbol{u} + \nu_{ei}\frac{\rho_e}{p_e}\frac{6}{35}\boldsymbol{q}_e; \tag{I25}$$

$$\frac{1}{2}\mathrm{Tr}\,\bar{\bar{\boldsymbol{Q}}}_e^{(3)} = \frac{\delta \boldsymbol{q}_e}{\delta t} = -\boldsymbol{q}_e\left(\frac{16}{35}\nu_{ee} - \frac{4}{35}\nu_{ei}\right) - \nu_{ei}p_e\delta\boldsymbol{u}, \tag{I26}$$

with total collisional contributions

$$\boldsymbol{Q}_e^{(3)\,\prime} = -\bar{\nu}_e\boldsymbol{q}_e + \frac{3}{2}\nu_{ei}p_e\delta\boldsymbol{u}; \tag{I27}$$

$$\bar{\nu}_e = \frac{16}{35}\nu_{ee} + \frac{11}{35}\nu_{ei}; \tag{I28}$$

$$\boldsymbol{a}_e = \frac{5}{2}\frac{p_e}{m_e}\nabla T_e - \frac{3}{2}\nu_{ei}p_e\delta\boldsymbol{u}. \tag{I29}$$

This yields the heat flux solution equivalent to Equations (H43)–(H45), with the only difference being that the frequencies are now added according to

$$\bar{\nu}_e = \left(\frac{1}{Z_i\sqrt{2}}\frac{16}{35} + \frac{11}{35}\right)\nu_{ei}; \quad \text{for} \quad Z_i = 1: \quad \bar{\nu}_e = 0.6375\nu_{ei}. \tag{I30}$$

The momentum exchange rates then read

$$\boldsymbol{R}_e^u = -\rho_e\nu_{ei}\left[\left(1 - \frac{9}{35}\frac{\nu_{ei}}{\bar{\nu}_e}\right)\delta\boldsymbol{u}_\parallel + \left(1 - \frac{9}{35}\frac{\bar{\nu}_e\nu_{ei}}{\Omega_e^2 + \bar{\nu}_e^2}\right)\delta\boldsymbol{u}_\perp + \frac{9}{35}\frac{\Omega_e\nu_{ei}}{\Omega_e^2 + \bar{\nu}_e^2}\hat{\boldsymbol{b}}\times\delta\boldsymbol{u}\right]; \tag{I31}$$

$$\boldsymbol{R}_e^T = -\frac{3}{7}\frac{\nu_{ei}}{\bar{\nu}_e}n_e\nabla_\parallel T_e - \frac{3}{7}\frac{\bar{\nu}_e\nu_{ei}}{\Omega_e^2 + \bar{\nu}_e^2}n_e\nabla_\perp T_e + \frac{3}{7}\frac{\Omega_e\nu_{ei}}{\Omega_e^2 + \bar{\nu}_e^2}n_e\hat{\boldsymbol{b}}\times\nabla T_e, \tag{I32}$$

and a direct comparison with Braginskii is done according to

$$\alpha_0 = 1 - \frac{9}{35}\frac{\nu_{ei}}{\bar{\nu}_e}; \quad \beta_0 = \frac{3}{7}\frac{\nu_{ei}}{\bar{\nu}_e}; \quad \beta_0^* = \frac{3}{2}\frac{\nu_{ei}}{\bar{\nu}_e}; \quad \gamma_0 = \frac{5}{2}\frac{\nu_{ei}}{\bar{\nu}_e}; \quad \bar{\nu}_e = \left(\frac{1}{Z_i\sqrt{2}}\frac{16}{35} + \frac{11}{35}\right)\nu_{ei}. \tag{I33}$$

Examining the numerical values for $Z_i = 1$, for example, the parallel heat conductivity reads $\kappa_\parallel^e = 3.92p_e/(\nu_{ei}m_e)$. This is a big improvement in the model of Killie et al. (2004): the conductivity is almost three times larger than the 1.34 value of Burgers–Schunk, and is much closer to the correct value of 3.20. The other results are (strong B-field, $Z_i = 1$)

$$\begin{aligned}\boldsymbol{R}_e &= -\rho_e\nu_{ei}(0.60\delta\boldsymbol{u}_\parallel + \delta\boldsymbol{u}_\perp) - 0.67n_e\nabla_\parallel T_e;\\ \boldsymbol{q}_e^u &= 2.35p_e\delta\boldsymbol{u}_\parallel,\end{aligned} \tag{I34}$$

and the thermal force value of 0.67 is now closer to the correct value of 0.70 as well. However, the frictional heat flux $\boldsymbol{q}_e^u$ is quite large (over three times larger than it should be, 2.35 versus 0.70). Importantly, the Onsager symmetry between $\boldsymbol{q}_e^u$ and $\boldsymbol{R}_e^T$ is broken, which can also be seen from the general results (I32), (H48). Nevertheless, the model indeed improves the parallel thermal heat flux and the parallel thermal force of Burgers–Schunk.

Appendix J
10-moment Model (Viscosity)

To calculate the collisional contributions for the stress tensor with the Landau operator, one uses the following 10-moment distribution function of Grad:

$$f_b(\boldsymbol{v}') = \frac{n_b}{\pi^{3/2} v_{\rm thb}^3} e^{-\frac{|\boldsymbol{c}_b|^2}{v_{\rm thb}^2}} \left[1 + \frac{m_b}{2T_b p_b} \bar{\bar{\boldsymbol{\Pi}}}_b^{(2)} : \boldsymbol{c}_b \boldsymbol{c}_b \right]. \tag{J1}$$

As a reminder, $\bar{\bar{\boldsymbol{\Pi}}}_b^{(2)} : \bar{\bar{\boldsymbol{I}}} = 0$. By using symmetries and a Gaussian integration, it is possible to show that

$$\int \boldsymbol{c}_b \boldsymbol{c}_b e^{-\frac{|\boldsymbol{c}_b|^2}{v_{\rm thb}^2}} d^3v' = \frac{\pi^{3/2}}{2} v_{\rm thb}^5 \bar{\bar{\boldsymbol{I}}}; \qquad \bar{\bar{\boldsymbol{\Pi}}}_b^{(2)} : \int \boldsymbol{c}_b \boldsymbol{c}_b \boldsymbol{v}' e^{-\frac{|\boldsymbol{c}_b|^2}{v_{\rm thb}^2}} d^3v' = 0;$$
$$\bar{\bar{\boldsymbol{\Pi}}}_b^{(2)} : \int \boldsymbol{c}_b \boldsymbol{c}_b \boldsymbol{c}_b \boldsymbol{c}_b e^{-\frac{|\boldsymbol{c}_b|^2}{v_{\rm thb}^2}} d^3v' = \frac{\pi^{3/2}}{2} v_{\rm thb}^7 \bar{\bar{\boldsymbol{\Pi}}}_b^{(2)}. \tag{J2}$$

The last integral is a special case of (J48). Thus, the distribution function (J1) correctly reproduces the density, fluid velocity, and full pressure tensor $m_b \int \boldsymbol{c}_b \boldsymbol{c}_b f_b d^3c_b = p_b \bar{\bar{\boldsymbol{I}}} + \bar{\bar{\boldsymbol{\Pi}}}_b^{(2)}$, so the distribution function is well defined.

J.1. Rosenbluth Potentials

Using the variables $\boldsymbol{x} = (\boldsymbol{v}' - \boldsymbol{v})/v_{\rm thb}$ and $\boldsymbol{y} = (\boldsymbol{v} - \boldsymbol{u}_b)/v_{\rm thb}$ with $\boldsymbol{c}_b = (\boldsymbol{x} + \boldsymbol{y}) v_{\rm thb}$, we need to calculate the Rosenbluth potentials

$$\begin{aligned} H_b(\boldsymbol{v}) &= \int \frac{f_b(\boldsymbol{v}')}{|\boldsymbol{v}' - \boldsymbol{v}|} d^3v' \\ &= \frac{n_b}{\pi^{3/2} v_{\rm thb}} \int \frac{e^{-|\boldsymbol{x}+\boldsymbol{y}|^2}}{x} \left[1 + \frac{\bar{\bar{\boldsymbol{\Pi}}}_b^{(2)}}{p_b} : (\boldsymbol{x} + \boldsymbol{y})(\boldsymbol{x} + \boldsymbol{y}) \right] d^3x; \end{aligned} \tag{J3}$$

$$\begin{aligned} G_b(\boldsymbol{v}) &= \int |\boldsymbol{v}' - \boldsymbol{v}| f_b(\boldsymbol{v}') d^3v' \\ &= \frac{n_b v_{\rm thb}}{\pi^{3/2}} \int x e^{-|\boldsymbol{x}+\boldsymbol{y}|^2} \left[1 + \frac{\bar{\bar{\boldsymbol{\Pi}}}_b^{(2)}}{p_b} : (\boldsymbol{x} + \boldsymbol{y})(\boldsymbol{x} + \boldsymbol{y}) \right] d^3x. \end{aligned} \tag{J4}$$

Using the integrals (J40) and (J44), the final results for the Rosenbluth potentials are

$$H_b = \frac{n_b}{v_{\rm thb}} \left\{ \frac{\mathrm{erf}(y)}{y} + \frac{\bar{\bar{\boldsymbol{\Pi}}}_b^{(2)}}{p_b} : \boldsymbol{y}\boldsymbol{y} \left[\mathrm{erf}(y) \frac{3}{4y^5} - \frac{e^{-y^2}}{\sqrt{\pi}} \left(\frac{1}{y^2} + \frac{3}{2y^4} \right) \right] \right\};$$
$$G_b = n_b v_{\rm thb} \left\{ \frac{e^{-y^2}}{\sqrt{\pi}} + \left(y + \frac{1}{2y} \right) \mathrm{erf}(y) + \frac{\bar{\bar{\boldsymbol{\Pi}}}_b^{(2)}}{p_b} : \boldsymbol{y}\boldsymbol{y} \left[-\frac{3}{4\sqrt{\pi}} \frac{e^{-y^2}}{y^4} + \left(-\frac{1}{4y^3} + \frac{3}{8y^5} \right) \mathrm{erf}(y) \right] \right\}. \tag{J5}$$

We will need the derivative

$$\begin{aligned} \frac{\partial H_b}{\partial \boldsymbol{v}} = {} & \frac{n_b}{v_{\rm thb}^2} \boldsymbol{y} \left(\frac{2}{\sqrt{\pi}} \frac{e^{-y^2}}{y^2} - \frac{\mathrm{erf}(y)}{y^3} \right) \\ & + \frac{n_b}{v_{\rm thb}^2} \frac{2}{p_b} (\bar{\bar{\boldsymbol{\Pi}}}_b^{(2)} \cdot \boldsymbol{y}) \left[\mathrm{erf}(y) \frac{3}{4y^5} - \frac{e^{-y^2}}{\sqrt{\pi}} \left(\frac{1}{y^2} + \frac{3}{2y^4} \right) \right] \\ & + \frac{n_b}{v_{\rm thb}^2 p_b} (\bar{\bar{\boldsymbol{\Pi}}}_b^{(2)} : \boldsymbol{y}\boldsymbol{y}) \boldsymbol{y} \left[\frac{2}{\sqrt{\pi}} \left(\frac{1}{y^2} + \frac{5}{2y^4} + \frac{15}{4y^6} \right) e^{-y^2} - \frac{15}{4} \frac{\mathrm{erf}(y)}{y^7} \right]. \end{aligned} \tag{J6}$$

As a double check, applying $\partial/\partial\, \boldsymbol{v}\cdot$ at the last expression recovers $-4\pi f_b(\boldsymbol{v})$, where, for example,

$$\frac{\partial}{\partial \boldsymbol{v}} \cdot (\bar{\bar{\boldsymbol{\Pi}}}_b^{(2)} \cdot \boldsymbol{y}) = 0; \qquad \frac{\partial}{\partial \boldsymbol{v}} \cdot [(\bar{\bar{\boldsymbol{\Pi}}}_b^{(2)} : \boldsymbol{y}\boldsymbol{y})\boldsymbol{y}] = \frac{5}{v_{\rm thb}} \bar{\bar{\boldsymbol{\Pi}}}_b^{(2)} : \boldsymbol{y}\boldsymbol{y}. \tag{J7}$$

The entire dynamical friction vector for the 10-moment model then becomes

$$\begin{aligned}\boldsymbol{A}_{ab} = 2\frac{c_{ab}}{m_a^2}\left(1 + \frac{m_a}{m_b}\right)\frac{n_b}{v_{\rm thb}^2}\Bigg\{&\boldsymbol{y}\left(\frac{2}{\sqrt{\pi}}\frac{e^{-y^2}}{y^2} - \frac{\mathrm{erf}(y)}{y^3}\right)\\ &+\frac{2}{p_b}(\bar{\bar{\boldsymbol{\Pi}}}_b^{(2)} \cdot \boldsymbol{y})\left[\mathrm{erf}(y)\frac{3}{4y^5} - \frac{e^{-y^2}}{\sqrt{\pi}}\left(\frac{1}{y^2} + \frac{3}{2y^4}\right)\right]\\ &+\frac{1}{p_b}(\bar{\bar{\boldsymbol{\Pi}}}_b^{(2)} : \boldsymbol{y}\boldsymbol{y})\boldsymbol{y}\left[\frac{2}{\sqrt{\pi}}\left(\frac{1}{y^2} + \frac{5}{2y^4} + \frac{15}{4y^6}\right)e^{-y^2} - \frac{15}{4}\frac{\mathrm{erf}(y)}{y^7}\right]\Bigg\}.\end{aligned} \tag{J8}$$

For the diffusion tensor, to perform the subsequent analytic calculations in a clear way, it is useful to write the second Rosenbluth potential G_b by introducing A_1, A_2:

$$G_b = n_b v_{\rm thb}\left[A_1 + \frac{1}{p_b}(\bar{\bar{\boldsymbol{\Pi}}}_b^{(2)} : \boldsymbol{y}\boldsymbol{y})A_2\right], \tag{J9}$$

where

$$\begin{aligned}A_1 &= \frac{e^{-y^2}}{\sqrt{\pi}} + \left(y + \frac{1}{2y}\right)\mathrm{erf}(y);\\ A_2 &= -\frac{3}{4\sqrt{\pi}}\frac{e^{-y^2}}{y^4} + \left(-\frac{1}{4y^3} + \frac{3}{8y^5}\right)\mathrm{erf}(y).\end{aligned} \tag{J10}$$

The required derivatives are then

$$\frac{\partial G_b}{\partial \boldsymbol{v}} = n_b\left[\frac{\boldsymbol{y}}{y}A_1' + \frac{2}{p_b}(\bar{\bar{\boldsymbol{\Pi}}}_b^{(2)} \cdot \boldsymbol{y})A_2 + \left(\frac{\bar{\bar{\boldsymbol{\Pi}}}_b^{(2)}}{p_b} : \boldsymbol{y}\boldsymbol{y}\right)\frac{\boldsymbol{y}}{y}A_2'\right], \tag{J11}$$

and

$$\begin{aligned}\frac{\partial G_b}{\partial \boldsymbol{v}\partial \boldsymbol{v}} = \frac{n_b}{v_{\rm thb}}\Bigg\{&\left(\frac{\bar{\bar{\boldsymbol{I}}}}{y} - \frac{\boldsymbol{y}\boldsymbol{y}}{y^3}\right)A_1' + \frac{\boldsymbol{y}\boldsymbol{y}}{y^2}A_1''\\ &+\frac{2}{p_b}\left[\frac{\boldsymbol{y}}{y}(\bar{\bar{\boldsymbol{\Pi}}}_b^{(2)} \cdot \boldsymbol{y}) + (\bar{\bar{\boldsymbol{\Pi}}}_b^{(2)} \cdot \boldsymbol{y})\frac{\boldsymbol{y}}{y}\right]A_2' + \frac{2}{p_b}\bar{\bar{\boldsymbol{\Pi}}}_b^{(2)}A_2\\ &+\left(\frac{\bar{\bar{\boldsymbol{\Pi}}}_b^{(2)}}{p_b} : \boldsymbol{y}\boldsymbol{y}\right)\left[\left(\frac{\bar{\bar{\boldsymbol{I}}}}{y} - \frac{\boldsymbol{y}\boldsymbol{y}}{y^3}\right)A_2' + \frac{\boldsymbol{y}\boldsymbol{y}}{y^2}A_2''\right]\Bigg\}.\end{aligned} \tag{J12}$$

As a double check, applying $(1/2)\mathrm{Tr}$ at the last expression recovers H_b.

After a slight rearrangement suitable for the calculations, the entire diffusion tensor then becomes

$$\begin{aligned}\boldsymbol{D}_{ab} = 2\frac{c_{ab}}{m_a^2}\frac{n_b}{v_{\rm thb}}\Bigg\{&\bar{\bar{\boldsymbol{I}}}\frac{A_1'}{y} + \frac{\boldsymbol{y}\boldsymbol{y}}{y^2}\left(A_1'' - \frac{A_1'}{y}\right)\\ &+\frac{1}{p_b}[2\boldsymbol{y}(\bar{\bar{\boldsymbol{\Pi}}}_b^{(2)} \cdot \boldsymbol{y}) + 2(\bar{\bar{\boldsymbol{\Pi}}}_b^{(2)} \cdot \boldsymbol{y})\boldsymbol{y} + (\bar{\bar{\boldsymbol{\Pi}}}_b^{(2)} : \boldsymbol{y}\boldsymbol{y})\bar{\bar{\boldsymbol{I}}}]\frac{A_2'}{y}\\ &+\frac{2}{p_b}\bar{\bar{\boldsymbol{\Pi}}}_b^{(2)}A_2 + \frac{1}{p_b}(\bar{\bar{\boldsymbol{\Pi}}}_b^{(2)} : \boldsymbol{y}\boldsymbol{y})\frac{\boldsymbol{y}\boldsymbol{y}}{y^2}\left(A_2'' - \frac{A_2'}{y}\right)\Bigg\},\end{aligned} \tag{J13}$$

with the "coefficients"

$$\frac{A_1'}{y} = \left(\frac{1}{y} - \frac{1}{2y^3}\right)\mathrm{erf}(y) + \frac{1}{\sqrt{\pi}}\frac{e^{-y^2}}{y^2};$$
$$A_1'' - \frac{A_1'}{y} = \left(-\frac{1}{y} + \frac{3}{2y^3}\right)\mathrm{erf}(y) - \frac{3}{\sqrt{\pi}}\frac{e^{-y^2}}{y^2};$$
$$A_2' = \left(\frac{3}{4y^4} - \frac{15}{8y^6}\right)\mathrm{erf}(y) + \frac{e^{-y^2}}{\sqrt{\pi}}\left(\frac{1}{y^3} + \frac{15}{4y^5}\right);$$
$$\frac{A_2'}{y} = \left(\frac{3}{4y^5} - \frac{15}{8y^7}\right)\mathrm{erf}(y) + \frac{e^{-y^2}}{\sqrt{\pi}}\left(\frac{1}{y^4} + \frac{15}{4y^6}\right);$$
$$A_2'' - \frac{A_2'}{y} = \left(-\frac{15}{4y^5} + \frac{105}{8y^7}\right)\mathrm{erf}(y) - \frac{e^{-y^2}}{\sqrt{\pi}}\left(\frac{2}{y^2} + \frac{10}{y^4} + \frac{105}{4y^6}\right). \tag{J14}$$

Or, explicitly, in its entire form:

$$\begin{aligned}\boldsymbol{D}_{ab} = 2\frac{c_{ab}}{m_a^2}\frac{n_b}{v_{\mathrm{thb}}}\Bigg\{&\bar{\bar{\boldsymbol{I}}}\left[\left(\frac{1}{y} - \frac{1}{2y^3}\right)\mathrm{erf}(y) + \frac{1}{\sqrt{\pi}}\frac{e^{-y^2}}{y^2}\right] + \frac{\boldsymbol{yy}}{y^2}\left[\left(-\frac{1}{y} + \frac{3}{2y^3}\right)\mathrm{erf}(y) - \frac{3}{\sqrt{\pi}}\frac{e^{-y^2}}{y^2}\right]\\
&+\frac{1}{p_b}[2\boldsymbol{y}(\bar{\bar{\boldsymbol{\Pi}}}_b^{(2)}\cdot\boldsymbol{y}) + 2(\bar{\bar{\boldsymbol{\Pi}}}_b^{(2)}\cdot\boldsymbol{y})\boldsymbol{y} + (\bar{\bar{\boldsymbol{\Pi}}}_b^{(2)}:\boldsymbol{yy})\bar{\bar{\boldsymbol{I}}}]\left[\left(\frac{3}{4y^5} - \frac{15}{8y^7}\right)\mathrm{erf}(y) + \frac{e^{-y^2}}{\sqrt{\pi}}\left(\frac{1}{y^4} + \frac{15}{4y^6}\right)\right]\\
&+\frac{2}{p_b}\bar{\bar{\boldsymbol{\Pi}}}_b^{(2)}\left[-\frac{3}{4\sqrt{\pi}}\frac{e^{-y^2}}{y^4} + \left(-\frac{1}{4y^3} + \frac{3}{8y^5}\right)\mathrm{erf}(y)\right]\\
&+\left(\frac{\bar{\bar{\boldsymbol{\Pi}}}_b^{(2)}}{p_b}:\boldsymbol{yy}\right)\frac{\boldsymbol{yy}}{y^2}\left[\left(-\frac{15}{4y^5} + \frac{105}{8y^7}\right)\mathrm{erf}(y) - \frac{e^{-y^2}}{\sqrt{\pi}}\left(\frac{2}{y^2} + \frac{10}{y^4} + \frac{105}{4y^6}\right)\right]\Bigg\}.\end{aligned} \tag{J15}$$

J.2. Viscosity Calculation

For species "a," the distribution function in a semilinear approximation reads

$$f_a(\boldsymbol{v}) = \frac{n_a}{\pi^{3/2}v_{\mathrm{tha}}^3}e^{-\alpha^2y^2}\left[1 - 2\alpha(\boldsymbol{y}\cdot\boldsymbol{u}) + \frac{\alpha^2}{p_a}\bar{\bar{\boldsymbol{\Pi}}}_a^{(2)}:\boldsymbol{yy}\right]. \tag{J16}$$

It can be seen that, at the semilinear level, there is no new contribution to the momentum equation. For the pressure tensor equation, we need to calculate the following collisional contributions:

$$\bar{\bar{\boldsymbol{Q}}}_{ab}^{(2)} = m_a\int f_a[\boldsymbol{A}_{ab}\boldsymbol{c}_a]^S d^3v + m_a\int f_a\bar{\bar{\boldsymbol{D}}}_{ab}d^3v, \tag{J17}$$

where the diffusion tensor is symmetric. Starting with the second term, and using the derived formulas (J45)–(J48), the integration over the diffusion tensor then yields

$$\begin{aligned}m_a\int f_a\bar{\bar{\boldsymbol{D}}}_{ab}d^3v = 2\frac{c_{ab}}{m_a^2}\frac{n_b}{v_{\mathrm{thb}}}\frac{\rho_a}{\pi^{3/2}}\alpha^3\Bigg\{&+\bar{\bar{\boldsymbol{I}}}\frac{4\pi}{3}\int_0^\infty(2A_1'y + A_1''y^2)e^{-\alpha^2y^2}dy\\
&+\frac{\bar{\bar{\boldsymbol{\Pi}}}_b^{(2)}}{p_b}8\pi\int_0^\infty\left[\frac{3}{5}y^3A_2' + y^2A_2 + \frac{1}{15}y^4A_2''\right]e^{-\alpha^2y^2}dy\\
&+\frac{\bar{\bar{\boldsymbol{\Pi}}}_a^{(2)}}{p_a}\frac{8\pi}{15}\alpha^2\int_0^\infty y^4\left(A_1'' - \frac{A_1'}{y}\right)e^{-\alpha^2y^2}dy\Bigg\},\end{aligned} \tag{J18}$$

and the further one-dimensional integration brings the following result:

$$m_a \int f_a \bar{\bar{\boldsymbol{D}}}_{ab} d^3v = 2\frac{c_{ab}}{m_a^2}\frac{n_b}{v_{\rm thb}}\frac{\rho_a}{\pi^{3/2}}\alpha^3 \left\{ +\bar{\bar{\boldsymbol{I}}}\frac{4\pi}{3}\frac{1}{\alpha^2\sqrt{1+\alpha^2}} - \frac{\bar{\bar{\boldsymbol{\Pi}}}_b^{(2)}}{p_b}\frac{4\pi}{15}\frac{1}{(1+\alpha^2)^{3/2}} - \frac{\bar{\bar{\boldsymbol{\Pi}}}_a^{(2)}}{p_a}\frac{4\pi}{15}\frac{1}{\alpha^2(1+\alpha^2)^{3/2}} \right\}$$
$$= \rho_a \nu_{ab}\frac{m_b}{m_a+m_b}\left[\bar{\bar{\boldsymbol{I}}}(v_{\rm tha}^2 + v_{\rm thb}^2) - \frac{\bar{\bar{\boldsymbol{\Pi}}}_b^{(2)}}{p_b}\frac{v_{\rm thb}^2}{5} - \frac{\bar{\bar{\boldsymbol{\Pi}}}_a^{(2)}}{p_a}\frac{v_{\rm tha}^2}{5} \right]. \tag{J19}$$

Similarly, the first term in (J17) calculates

$$m_a \int f_a [\boldsymbol{A}_{ab}\boldsymbol{c}_a]^S d^3v = \rho_a \nu_{ab}\left[-\bar{\bar{\boldsymbol{I}}} v_{\rm tha}^2 + \frac{\bar{\bar{\boldsymbol{\Pi}}}_b^{(2)}}{p_b}\frac{3}{5}\frac{v_{\rm thb}^2 v_{\rm tha}^2}{(v_{\rm tha}^2 + v_{\rm thb}^2)} - \frac{\bar{\bar{\boldsymbol{\Pi}}}_a^{(2)}}{p_a}\frac{5v_{\rm thb}^2 + 2v_{\rm tha}^2}{5(v_{\rm tha}^2 + v_{\rm thb}^2)} v_{\rm tha}^2 \right]. \tag{J20}$$

Adding (J19)+(J20) yields the final collisional contributions for the right-hand side of the pressure tensor equation, which can be written in the convenient following form:

$$\bar{\bar{\boldsymbol{Q}}}_{ab}^{(2)} = 2\frac{\rho_a \nu_{ab}}{m_a+m_b}(T_b - T_a)\bar{\bar{\boldsymbol{I}}} - 2\frac{m_a \nu_{ab}}{m_a+m_b}\frac{T_b}{T_{ab}}\left(\bar{\bar{\boldsymbol{\Pi}}}_a^{(2)} - \frac{T_a n_a}{T_b n_b}\bar{\bar{\boldsymbol{\Pi}}}_b^{(2)} \right)$$
$$- \frac{\nu_{ab}}{m_a+m_b}\left[\frac{6}{5}m_b - \frac{4}{5}\mu_{ab}\frac{T_b - T_a}{T_{ab}} \right]\left(\bar{\bar{\boldsymbol{\Pi}}}_a^{(2)} + \frac{\rho_a}{\rho_b}\bar{\bar{\boldsymbol{\Pi}}}_b^{(2)} \right), \tag{J21}$$

with reduced mass and reduced temperature

$$\mu_{ab} = \frac{m_a m_b}{m_a+m_b}; \qquad T_{ab} = \frac{m_a T_b + m_b T_a}{m_a+m_b}.$$

Introducing $\sum_b$ over all of the species, result (J21) identifies with Equation (44) of Schunk (1977; derived before by Burgers). It is valid in the semilinear approximation, for unrestricted temperature differences. For Coulomb collisions, the viscosity calculated through the Rosenbluth potentials (for the Landau collisional operator) thus yields the same result as the Boltzmann collisional operator. By explicitly separating the self-collisions,

$$\bar{\bar{\boldsymbol{Q}}}_a^{(2)} = \sum_b \bar{\bar{\boldsymbol{Q}}}_{ab}^{(2)} = \frac{\delta \bar{\bar{\boldsymbol{p}}}_a}{\delta t}$$
$$= -\frac{6}{5}\nu_{aa}\bar{\bar{\boldsymbol{\Pi}}}_a^{(2)} + \sum_{b\neq a}\left[2\frac{\rho_a \nu_{ab}}{m_a+m_b}(T_b - T_a)\bar{\bar{\boldsymbol{I}}} - 2\frac{m_a \nu_{ab}}{m_a+m_b}\frac{T_b}{T_{ab}}\left(\bar{\bar{\boldsymbol{\Pi}}}_a^{(2)} - \frac{T_a n_a}{T_b n_b}\bar{\bar{\boldsymbol{\Pi}}}_b^{(2)} \right) \right]$$
$$- \sum_{b\neq a}\left[\frac{\nu_{ab}}{m_a+m_b}\left(\frac{6}{5}m_b - \frac{4}{5}\mu_{ab}\frac{T_b - T_a}{T_{ab}} \right)\left(\bar{\bar{\boldsymbol{\Pi}}}_a^{(2)} + \frac{\rho_a}{\rho_b}\bar{\bar{\boldsymbol{\Pi}}}_b^{(2)} \right) \right], \tag{J22}$$

where the "famous" 6/5 constant is present. As a double check, calculating the energy exchange rates yields

$$Q_{ab} = \frac{1}{2}\mathrm{Tr}\,\bar{\bar{\boldsymbol{Q}}}_{ab}^{(2)} = 3\frac{\rho_a \nu_{ab}}{m_a+m_b}(T_b - T_a), \tag{J23}$$

as it should be.

The collisional contributions for the stress tensor are thus

$$\bar{\bar{\boldsymbol{Q}}}_a^{(2)\prime} = \frac{\delta \bar{\bar{\boldsymbol{\Pi}}}_a^{(2)}}{\delta t} = \bar{\bar{\boldsymbol{Q}}}_a^{(2)} - \frac{\bar{\bar{\boldsymbol{I}}}}{3}\mathrm{Tr}\,\bar{\bar{\boldsymbol{Q}}}_a^{(2)}$$
$$= -\frac{6}{5}\nu_{aa}\bar{\bar{\boldsymbol{\Pi}}}_a^{(2)} - \sum_{b\neq a}\left[2\frac{m_a \nu_{ab}}{m_a+m_b}\frac{T_b}{T_{ab}}\left(\bar{\bar{\boldsymbol{\Pi}}}_a^{(2)} - \frac{T_a n_a}{T_b n_b}\bar{\bar{\boldsymbol{\Pi}}}_b^{(2)} \right) \right]$$
$$- \sum_{b\neq a}\left[\frac{\nu_{ab}}{m_a+m_b}\left(\frac{6}{5}m_b - \frac{4}{5}\mu_{ab}\frac{T_b - T_a}{T_{ab}} \right)\left(\bar{\bar{\boldsymbol{\Pi}}}_a^{(2)} + \frac{\rho_a}{\rho_b}\bar{\bar{\boldsymbol{\Pi}}}_b^{(2)} \right) \right], \tag{J24}$$

and enter the right-hand side of its evolution equation, for example, written in its simplest form:

$$\frac{d_a \bar{\bar{\boldsymbol{\Pi}}}_a^{(2)}}{dt} + \Omega_a (\hat{\boldsymbol{b}} \times \bar{\bar{\boldsymbol{\Pi}}}_a^{(2)})^S + p_a \bar{\bar{\boldsymbol{W}}}_a = \frac{\delta \bar{\bar{\boldsymbol{\Pi}}}_a^{(2)}}{\delta t}. \tag{J25}$$

Importantly, in the collisionless regime, the right-hand side of (J25) simply goes to zero. It is possible to write a general solution in a quasistatic approximation, but the stress tensors of various species are coupled.

J.3. Small Temperature Differences

For a particular case of small temperature differences between species,

$$\bar{\bar{\boldsymbol{Q}}}_a^{(2)} = \frac{\delta \bar{\bar{\boldsymbol{p}}}_a}{\delta t} = -\frac{6}{5}\nu_{aa} \bar{\bar{\boldsymbol{\Pi}}}_a^{(2)} - 2\sum_{b \neq a} \frac{m_a \nu_{ab}}{m_a + m_b}\left[\bar{\bar{\boldsymbol{p}}}_a - \frac{n_a}{n_b}\bar{\bar{\boldsymbol{p}}}_b + \frac{3}{5}\frac{m_b}{m_a}\left(\bar{\bar{\boldsymbol{\Pi}}}_a^{(2)} + \frac{\rho_a}{\rho_b}\bar{\bar{\boldsymbol{\Pi}}}_b^{(2)}\right)\right], \tag{J26}$$

where one uses $\bar{\bar{\boldsymbol{p}}} = p\bar{\bar{\boldsymbol{I}}} + \bar{\bar{\boldsymbol{\Pi}}}^{(2)}$, recovering Equation (41d) of Schunk (1977). Finally, for the stress tensor,

$$\bar{\bar{\boldsymbol{Q}}}_a^{(2)\prime} = \frac{\delta \bar{\bar{\boldsymbol{\Pi}}}_a^{(2)}}{\delta t} = -\frac{6}{5}\nu_{aa} \bar{\bar{\boldsymbol{\Pi}}}_a^{(2)} - 2\sum_{b \neq a} \frac{m_a \nu_{ab}}{m_a + m_b}\left[\left(1 + \frac{3}{5}\frac{m_b}{m_a}\right)\bar{\bar{\boldsymbol{\Pi}}}_a^{(2)} - \frac{2}{5}\frac{n_a}{n_b}\bar{\bar{\boldsymbol{\Pi}}}_b^{(2)}\right]. \tag{J27}$$

J.4. One Ion–Electron Plasma

For a plasma consisting of one ion species and electrons, in the first step

$$\bar{\bar{\boldsymbol{Q}}}_i^{(2)\prime} = \frac{\delta \bar{\bar{\boldsymbol{\Pi}}}_i^{(2)}}{\delta t} = -\left(\frac{6}{5}\nu_{ii} + 2\nu_{ie}\right)\bar{\bar{\boldsymbol{\Pi}}}_i^{(2)} + \frac{4}{5}\nu_{ie}\frac{n_i}{n_e}\bar{\bar{\boldsymbol{\Pi}}}_e^{(2)}; \tag{J28}$$

$$\bar{\bar{\boldsymbol{Q}}}_e^{(2)\prime} = \frac{\delta \bar{\bar{\boldsymbol{\Pi}}}_e^{(2)}}{\delta t} = -\frac{6}{5}(\nu_{ee} + \nu_{ei})\bar{\bar{\boldsymbol{\Pi}}}_e^{(2)} + \frac{4}{5}\nu_{ei}\frac{\rho_e}{\rho_i}\bar{\bar{\boldsymbol{\Pi}}}_i^{(2)}. \tag{J29}$$

Nevertheless, because for example for the parallel viscosity the ion $\bar{\bar{\boldsymbol{\Pi}}}_i^{(2)}$ is larger than the electron $\bar{\bar{\boldsymbol{\Pi}}}_e^{(2)}$ by a factor of $\sqrt{m_i/m_e}$, the coupling is only weak and the last terms in the above expressions can be neglected for simplicity. Then,

$$\bar{\bar{\boldsymbol{Q}}}_i^{(2)\prime} = \frac{\delta \bar{\bar{\boldsymbol{\Pi}}}_i^{(2)}}{\delta t} = -\bar{\nu}_i \bar{\bar{\boldsymbol{\Pi}}}_i^{(2)}; \qquad \bar{\nu}_i = \frac{6}{5}\nu_{ii} + 2\nu_{ie} = \frac{6}{5}\left(1 + \frac{5}{3}\frac{\sqrt{2}}{Z_i}\sqrt{\frac{m_e}{m_i}}\right)\nu_{ii}; \tag{J30}$$

$$\bar{\bar{\boldsymbol{Q}}}_e^{(2)\prime} = \frac{\delta \bar{\bar{\boldsymbol{\Pi}}}_e^{(2)}}{\delta t} = -\bar{\nu}_e \bar{\bar{\boldsymbol{\Pi}}}_e^{(2)}; \qquad \bar{\nu}_e = \frac{6}{5}(\nu_{ee} + \nu_{ei}) = \frac{6}{5}\left(1 + \frac{1}{Z_i\sqrt{2}}\right)\nu_{ei}. \tag{J31}$$

In a quasistatic approximation, one derives the following viscosity coefficients:

$$\eta_0^a = \frac{p_a}{\bar{\nu}_a}; \quad \eta_1^a = \frac{p_a \bar{\nu}_a}{4\Omega_a^2 + \bar{\nu}_a^2}; \quad \eta_2^a = \frac{p_a \bar{\nu}_a}{\Omega_a^2 + \bar{\nu}_a^2}; \quad \eta_3^a = \frac{2p_a \Omega_a}{4\Omega_a^2 + \bar{\nu}_a^2}; \quad \eta_4^a = \frac{p_a \Omega_a}{\Omega_a^2 + \bar{\nu}_a^2}, \tag{J32}$$

which have the same form as the BGK viscosities. The difference is that while $\bar{\nu}_i = \nu_{ii} + \nu_{ie}$ and $\bar{\nu}_e = \nu_{ee} + \nu_{ei}$ for the BGK operator, here the frequencies have to be added according to (J30), (J31).

Importantly, because Braginskii (1965) neglected the ion–electron collisions for ion viscosities, direct comparison with Braginskii has to done with $\bar{\nu}_i = (6/5)\nu_{ii}$. Using this approximation, the parallel viscosities of the Burger–Schunk model are

$$\eta_0^i = \frac{5}{6}\frac{p_i}{\nu_{ii}}; \qquad \eta_0^e = \frac{5}{6}\frac{Z_i\sqrt{2}}{(1 + Z_i\sqrt{2})}\frac{p_e}{\nu_{ei}}, \tag{J33}$$

where $5/6 = 0.83$, contrasting with the Braginskii ion value of 0.96. Considering a specific case $Z_i = 1$, the electron viscosity $\eta_0^e = 0.49 p_e/\nu_{ei}$, contrasting with Braginskii's value of 0.73.

J.5. Strong Magnetic Field Limit

Examining the strong magnetic field limit, the viscosities for ions become

$$\eta_1^i = \frac{3}{10}\frac{p_i \nu_{ii}}{\Omega_i^2}; \qquad \eta_2^i = \frac{6}{5}\frac{p_i \nu_{ii}}{\Omega_i^2}; \qquad \eta_3^i = \frac{1}{2}\frac{p_i}{\Omega_i}; \qquad \eta_4^i = \frac{p_i}{\Omega_i}, \tag{J34}$$

(with relations $\eta_2^a = 4\eta_1^a$, $\eta_4^a = 2\eta_3^a$ valid for both electrons and ions). All four viscosities match Braginskii exactly! Similarly, for electrons in the strong magnetic field limit, the Burgers–Schunk model yields

$$\eta_1^e = \frac{3}{10}\left(1 + \frac{1}{Z_i\sqrt{2}}\right)\frac{p_e\nu_{ei}}{\Omega_e^2}; \qquad \eta_2^e = \frac{6}{5}\left(1 + \frac{1}{Z_i\sqrt{2}}\right)\frac{p_e\nu_{ei}}{\Omega_e^2}; \qquad \eta_3^e = \frac{1}{2}\frac{p_e}{\Omega_e}; \qquad \eta_4^e = \frac{p_e}{\Omega_e}. \tag{J35}$$

Evaluation for $Z_i = 1$ yields $\eta_1^e = 0.51 p_e\nu_{ei}/\Omega_e^2$, and again all match Braginskii exactly. If Braginskii had provided electron viscosities for different Z_i values, all four viscosity coefficients (except for parallel η_0) would match his results exactly.

If ion–electron collisions are considered, the gyroviscosities η_3^i, η_4^i given by (J34) remain unchanged, and the perpendicular viscosities become

$$\eta_1^i = \frac{p_i\nu_{ii}}{\Omega_i^2}\frac{3}{10}\left(1 + \frac{5}{3}\frac{\sqrt{2}}{Z_i}\sqrt{\frac{m_e}{m_i}}\right); \qquad \eta_2^i = \frac{p_i\nu_{ii}}{\Omega_i^2}\frac{6}{5}\left(1 + \frac{5}{3}\frac{\sqrt{2}}{Z_i}\sqrt{\frac{m_e}{m_i}}\right), \tag{J36}$$

where again $\eta_2^i = 4\eta_1^i$ holds. That the result (J36) is indeed correct, and can be checked against the 2-Laguerre Equation (89b) of Ji & Held (2013) when written in a strong B-limit. (Use $\zeta = (1/Z_i)\sqrt{m_e/m_i}$, $r_i = \Omega_i\hat{\tau}_{ii}$, and $\eta_2^i = \hat{\eta}_2^i p_i\hat{\tau}_{ii}$, with conversion $\hat{\tau}_{ii} = \tau_{ii}/\sqrt{2}$, because we use Braginskii's definition of τ_{ii}; see Section 8.2). Interestingly, the result does not change in their 3-Laguerre model (or higher-order models). The same is true for the perpendicular heat conductivities $\kappa_\perp^a$.

J.6. Table of Integrals

To calculate the first Rosenbluth potential H_b, we use the following integrals:

$$\boldsymbol{yy}\int\frac{1}{x}e^{-|\boldsymbol{x}+\boldsymbol{y}|^2}d^3x = \boldsymbol{yy}\pi^{3/2}\frac{\mathrm{erf}(y)}{y}; \tag{J37}$$

$$\int\frac{\boldsymbol{x}}{x}e^{-|\boldsymbol{x}+\boldsymbol{y}|^2}d^3x = -\boldsymbol{y}\pi\left[\frac{e^{-y^2}}{y^2} + \sqrt{\pi}\left(\frac{1}{y} - \frac{1}{2y^3}\right)\mathrm{erf}(y)\right]; \tag{J38}$$

$$\begin{aligned}\int\frac{\boldsymbol{xx}}{x}e^{-|\boldsymbol{x}+\boldsymbol{y}|^2}d^3x = {}& \bar{\bar{\boldsymbol{I}}}\pi\left[\frac{e^{-y^2}}{2y^2} + \frac{\sqrt{\pi}}{2}\mathrm{erf}(y)\left(\frac{1}{y} - \frac{1}{2y^3}\right)\right]\\ &+\boldsymbol{yy}\pi\left[e^{-y^2}\left(\frac{1}{y^2} - \frac{3}{2y^4}\right) + \sqrt{\pi}\,\mathrm{erf}(y)\left(\frac{1}{y} - \frac{1}{y^3} + \frac{3}{4y^5}\right)\right],\end{aligned} \tag{J39}$$

and so

$$\begin{aligned}\int\frac{(\boldsymbol{x}+\boldsymbol{y})(\boldsymbol{x}+\boldsymbol{y})}{x}e^{-|\boldsymbol{x}+\boldsymbol{y}|^2}d^3x = {}& \bar{\bar{\boldsymbol{I}}}\pi\left[\frac{e^{-y^2}}{2y^2} + \frac{\sqrt{\pi}}{2}\mathrm{erf}(y)\left(\frac{1}{y} - \frac{1}{2y^3}\right)\right]\\ &+\boldsymbol{yy}\pi\left[\sqrt{\pi}\,\mathrm{erf}(y)\frac{3}{4y^5} - e^{-y^2}\left(\frac{1}{y^2} + \frac{3}{2y^4}\right)\right].\end{aligned} \tag{J40}$$

To calculate the second Rosenbluth G_b, we use

$$\boldsymbol{yy}\int xe^{-|\boldsymbol{x}+\boldsymbol{y}|^2}d^3x = \boldsymbol{yy}\pi\left[e^{-y^2} + \sqrt{\pi}\left(y + \frac{1}{2y}\right)\mathrm{erf}(y)\right]; \tag{J41}$$

$$\int x\boldsymbol{x}e^{-|\boldsymbol{x}+\boldsymbol{y}|^2}d^3x = -\boldsymbol{y}\pi\left[\left(1 + \frac{1}{2y^2}\right)e^{-y^2} + \sqrt{\pi}\left(y + \frac{1}{y} - \frac{1}{4y^3}\right)\mathrm{erf}(y)\right]; \tag{J42}$$

$$\begin{aligned}\int x\boldsymbol{xx}e^{-|\boldsymbol{x}+\boldsymbol{y}|^2}d^3x = {}& \bar{\bar{\boldsymbol{I}}}\pi\left[\left(\frac{1}{2} + \frac{1}{4y^2}\right)e^{-y^2} + \sqrt{\pi}\left(\frac{y}{2} - \frac{1}{8y^3} + \frac{1}{2y}\right)\mathrm{erf}(y)\right]\\ &+\boldsymbol{yy}\pi\left[\left(1 + \frac{1}{y^2} - \frac{3}{4y^4}\right)e^{-y^2} + \sqrt{\pi}\left(y + \frac{3}{2y} - \frac{3}{4y^3} + \frac{3}{8y^5}\right)\mathrm{erf}(y)\right],\end{aligned} \tag{J43}$$

and so

$$\int x(\boldsymbol{x}+\boldsymbol{y})(\boldsymbol{x}+\boldsymbol{y})e^{-|\boldsymbol{x}+\boldsymbol{y}|^2}d^3x = \bar{\bar{\boldsymbol{I}}}\pi\left[\left(\frac{1}{2}+\frac{1}{4y^2}\right)e^{-y^2}+\sqrt{\pi}\left(\frac{y}{2}-\frac{1}{8y^3}+\frac{1}{2y}\right)\mathrm{erf}(y)\right]$$
$$+\boldsymbol{y}\boldsymbol{y}\pi\left[-\frac{3}{4y^4}e^{-y^2}+\sqrt{\pi}\left(-\frac{1}{4y^3}+\frac{3}{8y^5}\right)\mathrm{erf}(y)\right]. \tag{J44}$$

To calculate the viscosity, the Rosenbluth potentials are integrated by the following scheme:

$$\int \boldsymbol{y}\boldsymbol{y}f(y)e^{-\alpha^2y^2}d^3y = \frac{\bar{\bar{\boldsymbol{I}}}}{3}\int y^2f(y)e^{-\alpha^2y^2}d^3y = \bar{\bar{\boldsymbol{I}}}\frac{4\pi}{3}\int_0^\infty y^4f(y)e^{-\alpha^2y^2}dy; \tag{J45}$$

$$\int \boldsymbol{y}(\bar{\bar{\boldsymbol{\Pi}}}_b^{(2)}\cdot\boldsymbol{y})f(y)e^{-\alpha^2y^2}d^3y = \bar{\bar{\boldsymbol{\Pi}}}_b^{(2)}\frac{4\pi}{3}\int_0^\infty y^4f(y)e^{-\alpha^2y^2}dy; \tag{J46}$$

$$\bar{\bar{\boldsymbol{\Pi}}}_b^{(2)}\colon \int \boldsymbol{y}\boldsymbol{y}f(y)e^{-\alpha^2y^2}d^3y = 0, \tag{J47}$$

where, in our case, functions $f(y)$ are well behaved, so these integrals hold. Additionally, for any symmetric (3×3) matrix $\bar{\bar{\boldsymbol{A}}}$,

$$\bar{\bar{\boldsymbol{A}}}\colon \int \boldsymbol{y}\boldsymbol{y}\boldsymbol{y}\boldsymbol{y}f(y)e^{-\alpha^2y^2}d^3y = \left[\bar{\bar{\boldsymbol{A}}}+(\mathrm{Tr}\bar{\bar{\boldsymbol{A}}})\frac{\bar{\bar{\boldsymbol{I}}}}{2}\right]\frac{8\pi}{15}\int_0^\infty y^6f(y)e^{-\alpha^2y^2}dy, \tag{J48}$$

and for the stress tensor, $\mathrm{Tr}\,\bar{\bar{\boldsymbol{\Pi}}}_b^{(2)} = 0$ (the integral can be calculated by splitting $\bar{\bar{\boldsymbol{A}}}\colon \boldsymbol{y}\boldsymbol{y}$ explicitly into components, and then by using symmetries, for example).

J0.6.1. Spherical Integration

To obtain the integrals (J39), for example, one introduces an orthogonal reference frame in the x-space with unit vectors $\hat{\boldsymbol{e}}_1$, $\hat{\boldsymbol{e}}_2$, $\hat{\boldsymbol{e}}_3$, where the direction of $\boldsymbol{y}$ forms axis $\hat{\boldsymbol{e}}_3 = \boldsymbol{y}/y$, so that

$$\boldsymbol{x} = x\sin\theta\cos\phi\hat{\boldsymbol{e}}_1 + x\sin\theta\sin\phi\hat{\boldsymbol{e}}_2 + x\cos\theta\hat{\boldsymbol{e}}_3, \tag{J49}$$

which then allows one to first perform the integral over $d\phi$,

$$\int_0^{2\pi}\boldsymbol{x}d\phi = 2\pi x\cos\theta\hat{\boldsymbol{e}}_3; \tag{J50}$$

$$\int_0^{2\pi}\boldsymbol{x}\boldsymbol{x}d\phi = \pi x^2\sin^2\theta\bar{\bar{\boldsymbol{I}}} + \pi x^2(3\cos^2\theta-1)\hat{\boldsymbol{e}}_3\hat{\boldsymbol{e}}_3, \tag{J51}$$

and then over $d\theta dx$.

Appendix K
Braginskii Heat Flux (11-moment Model)

We use the usual *reducible* Hermite polynomials with a perturbation of the distribution function $f_b = f_b^{(0)}(1+\chi_b)$ (see the details in Appendix B):

$$\chi_b = \frac{1}{10}\tilde{h}_i^{b(3)}\tilde{H}_i^{b(3)} + \frac{1}{280}\tilde{h}_i^{b(5)}\tilde{H}_i^{b(5)}, \tag{K1}$$

where

$$\tilde{H}_i^{b(3)} = \delta_{jk}\tilde{H}_{ijk}^{b(3)} = \tilde{c}_i^b(\tilde{c}_b^2-5);$$
$$\tilde{H}_i^{b(5)} = \delta_{jk}\delta_{lm}\tilde{H}_{ijklm}^{b(5)} = \tilde{c}_i^b(\tilde{c}_b^4-14\tilde{c}_b^2+35). \tag{K2}$$

For the clarity of the calculations, here we only consider the heat flux part of χ_b (i.e., the 11-moment model), but the full 21-moment model can be implicitly assumed for the final collisional contributions at the semilinear level. The orthogonality relations are (species indices are dropped)

$$\int \tilde{H}_i^{(3)}\tilde{H}_j^{(3)}\phi^{(0)}d^3\tilde{c} = 10\delta_{ij}; \qquad \int \tilde{H}_i^{(5)}\tilde{H}_j^{(5)}\phi^{(0)}d^3\tilde{c} = 280\delta_{ij}, \tag{K3}$$

yielding (K1). By using this perturbation χ_b, one can directly calculate the heat flux vector and the fifth-order moment vector

$$\vec{q}_i^{\,b} = \frac{m_b}{2}\int f_b c_i c^2 d^3c = \frac{p_b}{2}\sqrt{\frac{T_b}{m_b}}\,\tilde{h}_i^{\,b(3)};$$
$$X_i^{b(5)} = m_b\int f_b c_i c^4 d^3c = p_b\frac{T_b}{m_b}\sqrt{\frac{T_b}{m_b}}\,(\tilde{h}_i^{\,b(5)} + 14\tilde{h}^{b(3)}), \tag{K4}$$

or one can directly calculate the Hermite moments

$$\tilde{h}_i^{\,b(3)} = \frac{2}{p_b}\sqrt{\frac{m_b}{T_b}}\,\vec{q}_i^{\,b};$$
$$\tilde{h}_i^{\,b(5)} = \frac{1}{p_b}\sqrt{\frac{m_b}{T_b}}\left(\frac{m_b}{T_b}X_i^{b(5)} - 28\vec{q}_i^{\,b}\right). \tag{K5}$$

Note that we have chosen to define all of the vectors and tensors (including $X_i^{b(5)}$, $\tilde{H}_i^{(3)}$, $\tilde{H}_i^{(5)}$, etc.) without any additional normalization factors, so they are directly obtained from higher-order tensors by just applying contractions. The sole exception is the heat flux vector, which contains a factor of $1/2$, to match its usual definition. As also noted after Equation (B41), the reminder of this exception in the index notation is the arrow on the heat flux vector components $\boldsymbol{q}_i$. We will again use the Rosenbluth potentials, and not the center-of-mass transformation. However, this time we will keep working with the Hermite fluid moments, which has a nice advantage in that the expressions can be kept in a partially dimensionless form.

K.1. Rosenbluth Potentials

By introducing

$$\tilde{\boldsymbol{c}}_b = \sqrt{\frac{m_b}{T_b}}(\boldsymbol{v}' - \boldsymbol{u}_b); \qquad |\boldsymbol{v}' - \boldsymbol{v}| = \sqrt{\frac{T_b}{m_b}}|\tilde{\boldsymbol{c}}_b - \tilde{\boldsymbol{y}}|; \qquad \tilde{\boldsymbol{y}} = \sqrt{\frac{m_b}{T_b}}(\boldsymbol{v} - \boldsymbol{u}_b), \tag{K6}$$

so that our previously used $\boldsymbol{y} = \tilde{\boldsymbol{y}}/\sqrt{2}$, the Rosenbluth potentials read

$$H_b(\boldsymbol{v}) = \int \frac{f_b(\boldsymbol{v}')}{|\boldsymbol{v}' - \boldsymbol{v}|}d^3v' = n_b\sqrt{\frac{m_b}{T_b}}\int\frac{\phi_b^{(0)}}{|\tilde{\boldsymbol{c}}_b - \tilde{\boldsymbol{y}}|}(1 + \chi_b)d^3\tilde{c}_b;$$
$$G_b(\boldsymbol{v}) = \int |\boldsymbol{v}' - \boldsymbol{v}|f_b(\boldsymbol{v}')d^3v' = n_b\sqrt{\frac{T_b}{m_b}}\int|\tilde{\boldsymbol{c}}_b - \tilde{\boldsymbol{y}}|\phi_b^{(0)}(1 + \chi_b)d^3\tilde{c}_b, \tag{K7}$$

and calculate

$$H_b(\boldsymbol{v}) = n_b\sqrt{\frac{m_b}{T_b}}\left[\frac{1}{\tilde{y}}\,\mathrm{erf}\left(\frac{\tilde{y}}{\sqrt{2}}\right) - \sqrt{\frac{2}{\pi}}\frac{e^{-\tilde{y}^2/2}}{10}\left(\tilde{\boldsymbol{y}}\cdot\tilde{\boldsymbol{h}}^{b(3)} + (\tilde{y}^2 - 5)\frac{\tilde{\boldsymbol{y}}\cdot\tilde{\boldsymbol{h}}^{b(5)}}{28}\right)\right];$$
$$G_b(\boldsymbol{v}) = n_b\sqrt{\frac{T_b}{m_b}}\left[\sqrt{\frac{2}{\pi}}e^{-\tilde{y}^2/2} + \left(\tilde{y} + \frac{1}{\tilde{y}}\right)\mathrm{erf}\left(\frac{\tilde{y}}{\sqrt{2}}\right)\right.$$
$$\left. + \left(\frac{\mathrm{erf}(\tilde{y}/\sqrt{2})}{5\tilde{y}^3} - \sqrt{\frac{2}{\pi}}\frac{e^{-\tilde{y}^2/2}}{5\tilde{y}^2}\right)\tilde{\boldsymbol{y}}\cdot\tilde{\boldsymbol{h}}^{b(3)} - \sqrt{\frac{2}{\pi}}\frac{e^{-\tilde{y}^2/2}}{140}\tilde{\boldsymbol{y}}\cdot\tilde{\boldsymbol{h}}^{b(5)}\right]. \tag{K8}$$

The derivatives calculate using $\partial/\partial v_i = \sqrt{m_b/T_b}\,\partial/\partial\tilde{y}_i$ and

$$\frac{\partial H_b}{\partial\boldsymbol{v}} = \frac{n_b m_b}{T_b}\left[\tilde{\boldsymbol{y}}\left(\sqrt{\frac{2}{\pi}}\frac{e^{-\tilde{y}^2/2}}{\tilde{y}^2} - \frac{\mathrm{erf}(\tilde{y}/\sqrt{2})}{\tilde{y}^3}\right)\right.$$
$$\left. - \sqrt{\frac{2}{\pi}}\frac{e^{-\tilde{y}^2/2}}{10}\left(\tilde{\boldsymbol{h}}^{b(3)} - \tilde{\boldsymbol{y}}(\tilde{\boldsymbol{y}}\cdot\tilde{\boldsymbol{h}}^{b(3)}) + (\tilde{y}^2 - 5)\frac{\tilde{\boldsymbol{h}}^{b(5)}}{28} - (\tilde{y}^2 - 7)\frac{\tilde{\boldsymbol{y}}(\tilde{\boldsymbol{y}}\cdot\tilde{\boldsymbol{h}}^{b(5)})}{28}\right)\right], \tag{K9}$$

and further applying $(\partial/\partial\boldsymbol{v})\cdot$ recovers $-4\pi f_b$. It is useful to write the second Rosenbluth potential as

$$G_b(\boldsymbol{v}) = n_b\sqrt{\frac{T_b}{m_b}}\,[\tilde{A}_1 + \tilde{A}_3\tilde{\boldsymbol{y}}\cdot\tilde{\boldsymbol{h}}^{b(3)} + \tilde{A}_5\tilde{\boldsymbol{y}}\cdot\tilde{\boldsymbol{h}}^{b(5)}], \tag{K10}$$

where

$$\tilde{A}_1 = \sqrt{\frac{2}{\pi}}\, e^{-\tilde{y}^2/2} + \left(\tilde{y} + \frac{1}{\tilde{y}}\right)\mathrm{erf}\left(\frac{\tilde{y}}{\sqrt{2}}\right);$$
$$\tilde{A}_3 = \frac{\mathrm{erf}(\tilde{y}/\sqrt{2})}{5\tilde{y}^3} - \sqrt{\frac{2}{\pi}}\,\frac{e^{-\tilde{y}^2/2}}{5\tilde{y}^2};$$
$$\tilde{A}_5 = -\sqrt{\frac{2}{\pi}}\,\frac{e^{-\tilde{y}^2/2}}{140}, \tag{K11}$$

so that the second derivative calculates easily:

$$\frac{\partial}{\partial \boldsymbol{v}}\frac{\partial G_b}{\partial \boldsymbol{v}} = n_b\sqrt{\frac{m_b}{T_b}}\left\{\bar{\bar{\boldsymbol{I}}}\frac{\tilde{A}_1{}'}{\tilde{y}} + \frac{\tilde{\boldsymbol{y}}\tilde{\boldsymbol{y}}}{\tilde{y}^2}\left(\tilde{A}_1{}'' - \frac{\tilde{A}_1{}'}{\tilde{y}}\right)\right.$$
$$+(\tilde{\boldsymbol{y}}\tilde{\boldsymbol{h}}^{b(3)} + \tilde{\boldsymbol{h}}^{b(3)}\tilde{\boldsymbol{y}} + \bar{\bar{\boldsymbol{I}}}(\tilde{\boldsymbol{y}}\cdot\tilde{\boldsymbol{h}}^{b(3)}))\frac{\tilde{A}_3{}'}{\tilde{y}} + \frac{\tilde{\boldsymbol{y}}\tilde{\boldsymbol{y}}}{\tilde{y}^2}(\tilde{\boldsymbol{y}}\cdot\tilde{\boldsymbol{h}}^{b(3)})\left(\tilde{A}_3{}'' - \frac{\tilde{A}_3{}'}{\tilde{y}}\right)$$
$$\left.+(\tilde{\boldsymbol{y}}\tilde{\boldsymbol{h}}^{b(5)} + \tilde{\boldsymbol{h}}^{b(5)}\tilde{\boldsymbol{y}} + \bar{\bar{\boldsymbol{I}}}(\tilde{\boldsymbol{y}}\cdot\tilde{\boldsymbol{h}}^{b(5)}))\frac{\tilde{A}_5{}'}{\tilde{y}} + \frac{\tilde{\boldsymbol{y}}\tilde{\boldsymbol{y}}}{\tilde{y}^2}(\tilde{\boldsymbol{y}}\cdot\tilde{\boldsymbol{h}}^{b(5)})\left(\tilde{A}_5{}'' - \frac{\tilde{A}_5{}'}{\tilde{y}}\right)\right\}, \tag{K12}$$

and applying $(1/2)\mathrm{Tr}$ recovers H_b. The coefficients are

$$\tilde{A}_1{}' = \sqrt{\frac{2}{\pi}}\,\frac{e^{-\tilde{y}^2/2}}{\tilde{y}} + \left(1 - \frac{1}{\tilde{y}^2}\right)\mathrm{erf}\left(\frac{\tilde{y}}{\sqrt{2}}\right);$$
$$\tilde{A}_3{}' = \sqrt{\frac{2}{\pi}}\left(\frac{1}{\tilde{y}} + \frac{3}{\tilde{y}^3}\right)\frac{e^{-\tilde{y}^2/2}}{5} - \frac{3}{5\tilde{y}^4}\,\mathrm{erf}\left(\frac{\tilde{y}}{\sqrt{2}}\right);$$
$$\tilde{A}_5{}' = \sqrt{\frac{2}{\pi}}\,\frac{\tilde{y}e^{-\tilde{y}^2/2}}{140};$$
$$\tilde{A}_1{}'' = -\sqrt{\frac{2}{\pi}}\,\frac{2}{\tilde{y}^2}e^{-\tilde{y}^2/2} + \frac{2}{\tilde{y}^3}\,\mathrm{erf}\left(\frac{\tilde{y}}{\sqrt{2}}\right);$$
$$\tilde{A}_3{}'' = -\sqrt{\frac{2}{\pi}}\left(1 + \frac{4}{\tilde{y}^2} + \frac{12}{\tilde{y}^4}\right)\frac{e^{-\tilde{y}^2/2}}{5} + \frac{12}{5\tilde{y}^5}\,\mathrm{erf}\left(\frac{\tilde{y}}{\sqrt{2}}\right);$$
$$\tilde{A}_5{}'' = -\sqrt{\frac{2}{\pi}}\,(\tilde{y}^2 - 1)\frac{e^{-\tilde{y}^2/2}}{140}, \tag{K13}$$

and so

$$\tilde{A}_1{}'' - \frac{\tilde{A}_1{}'}{\tilde{y}} = -\sqrt{\frac{2}{\pi}}\,\frac{3}{\tilde{y}^2}e^{-\tilde{y}^2/2} - \left(\frac{1}{\tilde{y}} - \frac{3}{\tilde{y}^3}\right)\mathrm{erf}\left(\frac{\tilde{y}}{\sqrt{2}}\right);$$
$$\tilde{A}_3{}'' - \frac{\tilde{A}_3{}'}{\tilde{y}} = -\sqrt{\frac{2}{\pi}}\left(1 + \frac{5}{\tilde{y}^2} + \frac{15}{\tilde{y}^4}\right)\frac{e^{-\tilde{y}^2/2}}{5} + \frac{3}{\tilde{y}^5}\,\mathrm{erf}\left(\frac{\tilde{y}}{\sqrt{2}}\right);$$
$$\tilde{A}_5{}'' - \frac{\tilde{A}_5{}'}{\tilde{y}} = -\sqrt{\frac{2}{\pi}}\,\frac{\tilde{y}^2e^{-\tilde{y}^2/2}}{140}. \tag{K14}$$

K.2. Dynamical Friction Vector and Diffusion Tensor

The dynamical friction vector thus reads

$$\boldsymbol{A}^{ab} = 2\frac{c_{ab}}{m_a^2}\left(1 + \frac{m_a}{m_b}\right)\frac{n_b m_b}{T_b}\left[\tilde{\boldsymbol{y}}\left(\sqrt{\frac{2}{\pi}}\,\frac{e^{-\tilde{y}^2/2}}{\tilde{y}^2} - \frac{\mathrm{erf}(\tilde{y}/\sqrt{2})}{\tilde{y}^3}\right)\right.$$
$$\left.-\sqrt{\frac{2}{\pi}}\,\frac{e^{-\tilde{y}^2/2}}{10}\left(\tilde{\boldsymbol{h}}^{b(3)} - \tilde{\boldsymbol{y}}(\tilde{\boldsymbol{y}}\cdot\tilde{\boldsymbol{h}}^{b(3)}) + (\tilde{y}^2 - 5)\frac{\tilde{\boldsymbol{h}}^{b(5)}}{28} - (\tilde{y}^2 - 7)\frac{\tilde{\boldsymbol{y}}(\tilde{\boldsymbol{y}}\cdot\tilde{\boldsymbol{h}}^{b(5)})}{28}\right)\right], \tag{K15}$$

and the diffusion tensor

$$\bar{\bar{\boldsymbol{D}}}^{ab} = 2\frac{c_{ab}}{m_a^2} n_b \sqrt{\frac{m_b}{T_b}} \left\{ \bar{\bar{\boldsymbol{I}}} \frac{\tilde{A}_1'}{\tilde{y}} + \frac{\tilde{\boldsymbol{y}}\tilde{\boldsymbol{y}}}{\tilde{y}^2}\left(\tilde{A}_1'' - \frac{\tilde{A}_1'}{\tilde{y}}\right) \right.$$
$$+ (\tilde{\boldsymbol{y}}\tilde{\boldsymbol{h}}^{b(3)} + \tilde{\boldsymbol{h}}^{b(3)}\tilde{\boldsymbol{y}} + \bar{\bar{\boldsymbol{I}}}(\tilde{\boldsymbol{y}} \cdot \tilde{\boldsymbol{h}}^{b(3)}))\frac{\tilde{A}_3'}{\tilde{y}} + \frac{\tilde{\boldsymbol{y}}\tilde{\boldsymbol{y}}}{\tilde{y}^2}(\tilde{\boldsymbol{y}} \cdot \tilde{\boldsymbol{h}}^{b(3)})\left(\tilde{A}_3'' - \frac{\tilde{A}_3'}{\tilde{y}}\right)$$
$$\left. + (\tilde{\boldsymbol{y}}\tilde{\boldsymbol{h}}^{b(5)} + \tilde{\boldsymbol{h}}^{b(5)}\tilde{\boldsymbol{y}} + \bar{\bar{\boldsymbol{I}}}(\tilde{\boldsymbol{y}} \cdot \tilde{\boldsymbol{h}}^{b(5)}))\frac{\tilde{A}_5'}{\tilde{y}} + \frac{\tilde{\boldsymbol{y}}\tilde{\boldsymbol{y}}}{\tilde{y}^2}(\tilde{\boldsymbol{y}} \cdot \tilde{\boldsymbol{h}}^{b(5)})\left(\tilde{A}_5'' - \frac{\tilde{A}_5'}{\tilde{y}}\right) \right\}, \tag{K16}$$

or in its entire beauty:

$$\bar{\bar{\boldsymbol{D}}}^{ab} = 2\frac{c_{ab}}{m_a^2} n_b \sqrt{\frac{m_b}{T_b}} \left\{ \bar{\bar{\boldsymbol{I}}} \left[\sqrt{\frac{2}{\pi}} \frac{e^{-\tilde{y}^2/2}}{\tilde{y}^2} + \left(\frac{1}{\tilde{y}} - \frac{1}{\tilde{y}^3}\right)\mathrm{erf}\left(\frac{\tilde{y}}{\sqrt{2}}\right) \right] \right.$$
$$+ \frac{\tilde{\boldsymbol{y}}\tilde{\boldsymbol{y}}}{\tilde{y}^2}\left[-\sqrt{\frac{2}{\pi}}\frac{3}{\tilde{y}^2}e^{-\tilde{y}^2/2} - \left(\frac{1}{\tilde{y}} - \frac{3}{\tilde{y}^3}\right)\mathrm{erf}\left(\frac{\tilde{y}}{\sqrt{2}}\right) \right]$$
$$+ (\tilde{\boldsymbol{y}}\tilde{\boldsymbol{h}}^{b(3)} + \tilde{\boldsymbol{h}}^{b(3)}\tilde{\boldsymbol{y}} + \bar{\bar{\boldsymbol{I}}}(\tilde{\boldsymbol{y}} \cdot \tilde{\boldsymbol{h}}^{b(3)}))\left[\sqrt{\frac{2}{\pi}}\left(\frac{1}{\tilde{y}^2} + \frac{3}{\tilde{y}^4}\right)\frac{e^{-\tilde{y}^2/2}}{5} - \frac{3}{5\tilde{y}^5}\mathrm{erf}\left(\frac{\tilde{y}}{\sqrt{2}}\right) \right]$$
$$+ \frac{\tilde{\boldsymbol{y}}\tilde{\boldsymbol{y}}}{\tilde{y}^2}(\tilde{\boldsymbol{y}} \cdot \tilde{\boldsymbol{h}}^{b(3)})\left[-\sqrt{\frac{2}{\pi}}\left(1 + \frac{5}{\tilde{y}^2} + \frac{15}{\tilde{y}^4}\right)\frac{e^{-\tilde{y}^2/2}}{5} + \frac{3}{\tilde{y}^5}\mathrm{erf}\left(\frac{\tilde{y}}{\sqrt{2}}\right) \right]$$
$$+ (\tilde{\boldsymbol{y}}\tilde{\boldsymbol{h}}^{b(5)} + \tilde{\boldsymbol{h}}^{b(5)}\tilde{\boldsymbol{y}} + \bar{\bar{\boldsymbol{I}}}(\tilde{\boldsymbol{y}} \cdot \tilde{\boldsymbol{h}}^{b(5)}))\left[\sqrt{\frac{2}{\pi}}\frac{e^{-\tilde{y}^2/2}}{140} \right]$$
$$\left. + \frac{\tilde{\boldsymbol{y}}\tilde{\boldsymbol{y}}}{\tilde{y}^2}(\tilde{\boldsymbol{y}} \cdot \tilde{\boldsymbol{h}}^{b(5)})\left[-\sqrt{\frac{2}{\pi}}\frac{\tilde{y}^2 e^{-\tilde{y}^2/2}}{140} \right] \right\}. \tag{K17}$$

As a reminder,

$$\tilde{\boldsymbol{y}} = \sqrt{\frac{m_b}{T_b}}(\boldsymbol{v} - \boldsymbol{u}_b); \qquad c_{ab} = 2\pi e^4 Z_a^2 Z_b^2 \ln\Lambda. \tag{K18}$$

K.3. Distribution Function for Species "a"

The general distribution function for species "*a*" reads

$$f_a = f_a^{(0)}(1 + \chi_a) = n_a\left(\frac{m_a}{T_a}\right)^{3/2}\phi_a^{(0)}(1 + \chi_a); \qquad \phi_a^{(0)} = \frac{e^{-\tilde{c}_a^2/2}}{(2\pi)^{3/2}}; \qquad \tilde{c}_a = \sqrt{\frac{m_a}{T_a}}(\boldsymbol{v} - \boldsymbol{u}_a), \tag{K19}$$

where the perturbation

$$\chi_a = \frac{1}{10}\tilde{h}_i^{a(3)}\tilde{H}_i^{a(3)}(\tilde{\boldsymbol{c}}_a) + \frac{1}{280}\tilde{h}_i^{a(5)}\tilde{H}_i^{a(5)}(\tilde{\boldsymbol{c}}_a). \tag{K20}$$

To avoid the complicated runaway effect, the weight has to be expanded with small drifts, for example, by defining

$$\tilde{\boldsymbol{u}} = (\boldsymbol{u}_b - \boldsymbol{u}_a)\sqrt{\frac{m_a}{T_a}}; \qquad \alpha = \frac{\sqrt{T_b/m_b}}{\sqrt{T_a/m_a}}; \qquad \tilde{\boldsymbol{c}}_a = \alpha\tilde{\boldsymbol{y}} + \tilde{\boldsymbol{u}}, \tag{K21}$$

so that the expansion for small drifts

$$e^{-\tilde{c}_a^2/2} = e^{-|\alpha\tilde{\boldsymbol{y}} + \tilde{\boldsymbol{u}}|^2/2} \simeq e^{-\alpha^2\tilde{y}^2/2}(1 - \alpha\tilde{\boldsymbol{y}} \cdot \tilde{\boldsymbol{u}}). \tag{K22}$$

In comparison to our previously used normalization, $\tilde{\boldsymbol{y}} = \boldsymbol{y}\sqrt{2}$ and $\tilde{\boldsymbol{u}} = \boldsymbol{u}\sqrt{2}$ and $\tilde{\boldsymbol{c}}_a = \boldsymbol{c}_a\sqrt{2}/v_{\mathrm{tha}}$. The perturbation χ_a contains Hermite polynomials, and these also have to be expanded in the semilinear approximation. Importantly, after contraction with the

Hermite (fluid) moments,

$$\tilde{h}_i^{a(3)}\tilde{H}_i^{a(3)}(\tilde{\boldsymbol{c}}_a) \simeq \tilde{h}_i^{a(3)}\alpha\tilde{y}_i(\alpha^2\tilde{y}^2 - 5) = \tilde{h}_i^{a(3)}\tilde{H}_i^{a(3)}(\alpha\tilde{\boldsymbol{y}});$$
$$\tilde{h}_i^{a(5)}\tilde{H}_i^{a(5)}(\tilde{\boldsymbol{c}}_a) \simeq \tilde{h}_i^{a(5)}\alpha\tilde{y}_i(\alpha^4\tilde{y}^4 - 14\alpha^2\tilde{y}^2 + 35) = \tilde{h}_i^{a(5)}\tilde{H}_i^{a(5)}(\alpha\tilde{\boldsymbol{y}}), \tag{K23}$$

where all of the drift $\tilde{\boldsymbol{u}}$ contributions such as $\tilde{h}_i^{a(3)}\tilde{u}_i$ are neglected in the semilinear approximation. The expanded distribution function thus reads

$$f_a = n_a\left(\frac{m_a}{T_a}\right)^{3/2}\frac{e^{-\alpha^2\tilde{y}^2/2}}{(2\pi)^{3/2}}(1 - \alpha\tilde{\boldsymbol{y}}\cdot\tilde{\boldsymbol{u}} + \chi_a), \tag{K24}$$

with the perturbation

$$\chi_a = \frac{1}{10}\tilde{h}_i^{a(3)}\tilde{H}_i^{a(3)}(\alpha\tilde{\boldsymbol{y}}) + \frac{1}{280}\tilde{h}_i^{a(5)}\tilde{H}_i^{a(5)}(\alpha\tilde{\boldsymbol{y}}). \tag{K25}$$

The integrals are evaluated with $d^3v = (T_b/m_b)^{3/2}d^3\tilde{y}$, so a useful shortcut is

$$\int f_a d^3v = n_a\alpha^3\int\frac{e^{-\alpha^2\tilde{y}^2/2}}{(2\pi)^{3/2}}(1 - \alpha\tilde{\boldsymbol{y}}\cdot\tilde{\boldsymbol{u}} + \chi_a)d^3\tilde{y}. \tag{K26}$$

Also, it is useful to express c_{ab} directly through the collisional frequencies ν_{ab}, according to

$$2\frac{c_{ab}n_b}{m_a^2}\left(1 + \frac{m_a}{m_b}\right) = 3\nu_{ab}\sqrt{\frac{\pi}{2}}(1 + \alpha^2)^{3/2}\left(\frac{T_a}{m_a}\right)^{3/2}. \tag{K27}$$

K.4. Momentum Exchange Rates $\mathrm{R_{ab}}$

The momentum exchange rates calculate

$$\begin{aligned}\boldsymbol{R}_{ab} &= m_a\int f_a\boldsymbol{A}^{ab}d^3v\\ &= \nu_{ab}\rho_a\sqrt{\frac{T_a}{m_a}}\tilde{\boldsymbol{u}} + \frac{3}{5}\nu_{ab}\frac{\mu_{ab}}{T_{ab}}\left[\frac{p_a}{2}\sqrt{\frac{T_a}{m_a}}\tilde{\boldsymbol{h}}^{a(3)} - \frac{\rho_a}{\rho_b}\frac{p_b}{2}\sqrt{\frac{T_b}{m_b}}\tilde{\boldsymbol{h}}^{b(3)}\right]\\ &\quad -\frac{3}{56}\nu_{ab}\left(\frac{\mu_{ab}}{T_{ab}}\right)^2\left[p_a\left(\frac{T_a}{m_a}\right)^{3/2}\tilde{\boldsymbol{h}}^{a(5)} - \frac{\rho_a}{\rho_b}p_b\left(\frac{T_b}{m_b}\right)^{3/2}\tilde{\boldsymbol{h}}^{b(5)}\right],\end{aligned} \tag{K28}$$

or expressed through the usual fluid variables,

$$\begin{aligned}\boldsymbol{R}_{ab} &= \nu_{ab}\rho_a(\boldsymbol{u}_b - \boldsymbol{u}_a) + \frac{3}{5}\nu_{ab}\frac{\mu_{ab}}{T_{ab}}\left[\boldsymbol{q}^a - \frac{\rho_a}{\rho_b}\boldsymbol{q}^b\right]\\ &\quad -\frac{3}{56}\nu_{ab}\left(\frac{\mu_{ab}}{T_{ab}}\right)^2\left[\left(\boldsymbol{X}^{a(5)} - 28\frac{T_a}{m_a}\boldsymbol{q}^a\right) - \frac{\rho_a}{\rho_b}\left(\boldsymbol{X}^{b(5)} - 28\frac{T_b}{m_b}\boldsymbol{q}^b\right)\right].\end{aligned} \tag{K29}$$

Note that $\boldsymbol{R}_{ab} = -\boldsymbol{R}_{ba}$. An alternative form reads

$$\begin{aligned}\boldsymbol{R}_{ab} &= \nu_{ab}\rho_a(\boldsymbol{u}_b - \boldsymbol{u}_a) + \nu_{ab}\frac{\mu_{ab}}{T_{ab}}\left[\boldsymbol{q}^a\left(\frac{3}{5} + \frac{3}{2}\frac{\mu_{ab}}{m_a}\frac{T_a}{T_{ab}}\right) - \frac{\rho_a}{\rho_b}\boldsymbol{q}^b\left(\frac{3}{5} + \frac{3}{2}\frac{\mu_{ab}}{m_b}\frac{T_b}{T_{ab}}\right)\right]\\ &\quad -\frac{3}{56}\nu_{ab}\left(\frac{\mu_{ab}}{T_{ab}}\right)^2\left[\boldsymbol{X}^{a(5)} - \frac{\rho_a}{\rho_b}\boldsymbol{X}^{b(5)}\right],\end{aligned} \tag{K30}$$

or yet another one:

$$\begin{aligned}\boldsymbol{R}_{ab} &= \nu_{ab}\rho_a(\boldsymbol{u}_b - \boldsymbol{u}_a) + \nu_{ab}\frac{\mu_{ab}}{T_{ab}}\left[\boldsymbol{q}^a\frac{\frac{21}{10}T_am_b + \frac{3}{5}T_bm_a}{T_am_b + T_bm_a} - \frac{\rho_a}{\rho_b}\boldsymbol{q}^b\frac{\frac{3}{5}T_am_b + \frac{21}{10}T_bm_a}{T_am_b + T_bm_a}\right]\\ &\quad -\frac{3}{56}\nu_{ab}\left(\frac{\mu_{ab}}{T_{ab}}\right)^2\left[\boldsymbol{X}^{a(5)} - \frac{\rho_a}{\rho_b}\boldsymbol{X}^{b(5)}\right].\end{aligned} \tag{K31}$$

K.5. Heat Flux Exchange Rates

We need to calculate the collisional contributions for the heat flux

$$\frac{1}{2}\mathrm{Tr}\,\bar{\bar{\boldsymbol{Q}}}_{ab}^{(3)} = \frac{\delta \boldsymbol{q}_{ab}}{\delta t} = m_a \int f_a \left[(\boldsymbol{A}_{ab} \cdot \boldsymbol{c}_a)\boldsymbol{c}_a + \frac{1}{2}\boldsymbol{A}_{ab}|\boldsymbol{c}_a|^2 \right] d^3v + m_a \int f_a \left[\frac{1}{2}(\mathrm{Tr}\,\bar{\bar{\boldsymbol{D}}}_{ab})\boldsymbol{c}_a + \bar{\bar{\boldsymbol{D}}}_{ab} \cdot \boldsymbol{c}_a \right] d^3v, \tag{K32}$$

where the velocity

$$\boldsymbol{c}_a = \sqrt{\frac{T_a}{m_a}}\tilde{\boldsymbol{c}}_a = \sqrt{\frac{T_a}{m_a}}(\alpha\tilde{\boldsymbol{y}} + \tilde{\boldsymbol{u}}). \tag{K33}$$

Before attempting the integration of (K32), it is useful to apply the semilinear approximation, which yields step by step

$$\boldsymbol{A}^{ab} \cdot \boldsymbol{c}_a \simeq 2\frac{c_{ab}}{m_a^2}\left(1 + \frac{m_a}{m_b}\right)\frac{n_b m_b}{T_b}\sqrt{\frac{T_a}{m_a}}\left[(\alpha\tilde{y}^2 + \tilde{\boldsymbol{y}} \cdot \tilde{\boldsymbol{u}})\left(\sqrt{\frac{2}{\pi}}\frac{e^{-\tilde{y}^2/2}}{\tilde{y}^2} - \frac{\mathrm{erf}(\tilde{y}/\sqrt{2})}{\tilde{y}^3}\right) - \sqrt{\frac{2}{\pi}}\frac{e^{-\tilde{y}^2/2}}{10}\alpha\left((\tilde{\boldsymbol{y}} \cdot \tilde{\boldsymbol{h}}^{b(3)})(1 - \tilde{y}^2) + \frac{(\tilde{\boldsymbol{y}} \cdot \tilde{\boldsymbol{h}}^{b(5)})}{28}(8\tilde{y}^2 - \tilde{y}^4 - 5)\right)\right]; \tag{K34}$$

$$(\boldsymbol{A}^{ab} \cdot \boldsymbol{c}_a)\boldsymbol{c}_a \simeq 2\frac{c_{ab}}{m_a^2}\left(1 + \frac{m_a}{m_b}\right)\frac{n_b m_b}{T_b}\frac{T_a}{m_a}\left[+ \alpha(\alpha\tilde{y}^2\tilde{\boldsymbol{y}} + \tilde{\boldsymbol{y}}(\tilde{\boldsymbol{y}} \cdot \tilde{\boldsymbol{u}}) + \tilde{y}^2\tilde{\boldsymbol{u}})\left(\sqrt{\frac{2}{\pi}}\frac{e^{-\tilde{y}^2/2}}{\tilde{y}^2} - \frac{\mathrm{erf}(\tilde{y}/\sqrt{2})}{\tilde{y}^3}\right) - \sqrt{\frac{2}{\pi}}\frac{e^{-\tilde{y}^2/2}}{10}\alpha^2\left(\tilde{\boldsymbol{y}}(\tilde{\boldsymbol{y}} \cdot \tilde{\boldsymbol{h}}^{b(3)})(1 - \tilde{y}^2) + \frac{\tilde{\boldsymbol{y}}(\tilde{\boldsymbol{y}} \cdot \tilde{\boldsymbol{h}}^{b(5)})}{28}(8\tilde{y}^2 - \tilde{y}^4 - 5)\right)\right]. \tag{K35}$$

Furthermore, in the semilinear approximation,

$$|\boldsymbol{c}_a|^2 \simeq \frac{T_a}{m_a}(\alpha^2\tilde{y}^2 + 2\alpha\tilde{\boldsymbol{y}} \cdot \tilde{\boldsymbol{u}}), \tag{K36}$$

and thus

$$\boldsymbol{A}^{ab}|\boldsymbol{c}_a|^2 \simeq 2\frac{c_{ab}}{m_a^2}\left(1 + \frac{m_a}{m_b}\right)\frac{n_b m_b}{T_b}\frac{T_a}{m_a}\left[+ \alpha(\alpha\tilde{y}^2\tilde{\boldsymbol{y}} + 2\tilde{\boldsymbol{y}}(\tilde{\boldsymbol{y}} \cdot \tilde{\boldsymbol{u}}))\left(\sqrt{\frac{2}{\pi}}\frac{e^{-\tilde{y}^2/2}}{\tilde{y}^2} - \frac{\mathrm{erf}(\tilde{y}/\sqrt{2})}{\tilde{y}^3}\right) - \sqrt{\frac{2}{\pi}}\frac{e^{-\tilde{y}^2/2}}{10}\alpha^2\tilde{y}^2\left(\tilde{\boldsymbol{h}}^{b(3)} - \tilde{\boldsymbol{y}}(\tilde{\boldsymbol{y}} \cdot \tilde{\boldsymbol{h}}^{b(3)}) + (\tilde{y}^2 - 5)\frac{\tilde{\boldsymbol{h}}^{b(5)}}{28} - (\tilde{y}^2 - 7)\frac{\tilde{\boldsymbol{y}}(\tilde{\boldsymbol{y}} \cdot \tilde{\boldsymbol{h}}^{b(5)})}{28}\right)\right]. \tag{K37}$$

For the diffusion tensor,

$$\mathrm{Tr}\,\bar{\bar{\boldsymbol{D}}}^{ab} = 2\frac{c_{ab}}{m_a^2}n_b\sqrt{\frac{m_b}{T_b}}\left\{\left(2\frac{\tilde{A}_1'}{\tilde{y}} + \tilde{A}_1''\right) + (\tilde{\boldsymbol{y}} \cdot \tilde{\boldsymbol{h}}^{b(3)})\left(4\frac{\tilde{A}_3'}{\tilde{y}} + \tilde{A}_3''\right) + (\tilde{\boldsymbol{y}} \cdot \tilde{\boldsymbol{h}}^{b(5)})\left(4\frac{\tilde{A}_5'}{\tilde{y}} + \tilde{A}_5''\right)\right\}, \tag{K38}$$

and in the semilinear approximation:

$$\frac{1}{2}(\mathrm{Tr}\,\bar{\bar{\boldsymbol{D}}}^{ab})\boldsymbol{c}_a \simeq 2\frac{c_{ab}}{m_a^2}\frac{n_b}{\alpha}\left\{(\alpha\tilde{\boldsymbol{y}}+\tilde{\boldsymbol{u}})\left(\frac{\tilde{A}_1'}{\tilde{y}}+\frac{\tilde{A}_1''}{2}\right)\right.$$
$$\left.+\alpha\tilde{\boldsymbol{y}}(\tilde{\boldsymbol{y}}\cdot\tilde{\boldsymbol{h}}^{b(3)})\left(2\frac{\tilde{A}_3'}{\tilde{y}}+\frac{\tilde{A}_3''}{2}\right)+\alpha\tilde{\boldsymbol{y}}(\tilde{\boldsymbol{y}}\cdot\tilde{\boldsymbol{h}}^{b(5)})\left(2\frac{\tilde{A}_5'}{\tilde{y}}+\frac{\tilde{A}_5''}{2}\right)\right\}; \tag{K39}$$

$$\bar{\bar{\boldsymbol{D}}}^{ab}\cdot\boldsymbol{c}_a \simeq 2\frac{c_{ab}}{m_a^2}\frac{n_b}{\alpha}\left\{\alpha\tilde{\boldsymbol{y}}\tilde{A}_1''+\tilde{\boldsymbol{u}}\frac{\tilde{A}_1'}{\tilde{y}}+\frac{\tilde{\boldsymbol{y}}(\tilde{\boldsymbol{y}}\cdot\tilde{\boldsymbol{u}})}{\tilde{y}^2}\left(\tilde{A}_1''-\frac{\tilde{A}_1'}{\tilde{y}}\right)\right.$$
$$+\alpha\tilde{\boldsymbol{h}}^{b(3)}\tilde{y}\tilde{A}_3'+\alpha\tilde{\boldsymbol{y}}(\tilde{\boldsymbol{y}}\cdot\tilde{\boldsymbol{h}}^{b(3)})\left(\frac{\tilde{A}_3'}{\tilde{y}}+\tilde{A}_3''\right)$$
$$\left.+\alpha\tilde{\boldsymbol{h}}^{b(5)}\tilde{y}\tilde{A}_5'+\alpha\tilde{\boldsymbol{y}}(\tilde{\boldsymbol{y}}\cdot\tilde{\boldsymbol{h}}^{b(5)})\left(\frac{\tilde{A}_5'}{\tilde{y}}+\tilde{A}_5''\right)\right\}. \tag{K40}$$

Collecting all of the results together, the first part of (K32) becomes

$$(\boldsymbol{A}^{ab}\cdot\boldsymbol{c}_a)\boldsymbol{c}_a+\frac{1}{2}\boldsymbol{A}^{ab}|\boldsymbol{c}_a|^2 \simeq 2\frac{c_{ab}}{m_a^2}\left(1+\frac{m_a}{m_b}\right)\frac{n_b}{\alpha^2}\left\{+\alpha\left(\frac{3}{2}\alpha\tilde{y}^2\tilde{\boldsymbol{y}}+2\tilde{\boldsymbol{y}}(\tilde{\boldsymbol{y}}\cdot\tilde{\boldsymbol{u}})+\tilde{y}^2\tilde{\boldsymbol{u}}\right)\left(\sqrt{\frac{2}{\pi}}\frac{e^{-\tilde{y}^2/2}}{\tilde{y}^2}-\frac{\mathrm{erf}(\tilde{y}/\sqrt{2})}{\tilde{y}^3}\right)\right.$$
$$-\sqrt{\frac{2}{\pi}}\frac{e^{-\tilde{y}^2/2}}{10}\alpha^2\left(\frac{1}{2}\tilde{y}^2\tilde{\boldsymbol{h}}^{b(3)}+\tilde{\boldsymbol{y}}(\tilde{\boldsymbol{y}}\cdot\tilde{\boldsymbol{h}}^{b(3)})(1-\frac{3}{2}\tilde{y}^2)\right.$$
$$\left.\left.+\frac{1}{2}\tilde{y}^2(\tilde{y}^2-5)\frac{\tilde{\boldsymbol{h}}^{b(5)}}{28}+\frac{\tilde{\boldsymbol{y}}(\tilde{\boldsymbol{y}}\cdot\tilde{\boldsymbol{h}}^{b(5)})}{28}\left(\frac{23}{2}\tilde{y}^2-\frac{3}{2}\tilde{y}^4-5\right)\right)\right\}; \tag{K41}$$

and the second part of (K32) becomes

$$\frac{1}{2}(\mathrm{Tr}\,\bar{\bar{\boldsymbol{D}}}^{ab})\boldsymbol{c}_a+\bar{\bar{\boldsymbol{D}}}^{ab}\cdot\boldsymbol{c}_a \simeq 2\frac{c_{ab}}{m_a^2}\frac{n_b}{\alpha}\left\{\alpha\tilde{\boldsymbol{y}}\left(\frac{\tilde{A}_1'}{\tilde{y}}+\frac{3\tilde{A}_1''}{2}\right)+\tilde{\boldsymbol{u}}\left(2\frac{\tilde{A}_1'}{\tilde{y}}+\frac{\tilde{A}_1''}{2}\right)+\frac{\tilde{\boldsymbol{y}}(\tilde{\boldsymbol{y}}\cdot\tilde{\boldsymbol{u}})}{\tilde{y}^2}\left(\tilde{A}_1''-\frac{\tilde{A}_1'}{\tilde{y}}\right)\right.$$
$$+\alpha\tilde{\boldsymbol{h}}^{b(3)}\tilde{y}\tilde{A}_3'+\alpha\tilde{\boldsymbol{y}}(\tilde{\boldsymbol{y}}\cdot\tilde{\boldsymbol{h}}^{b(3)})\left(3\frac{\tilde{A}_3'}{\tilde{y}}+\frac{3}{2}\tilde{A}_3''\right)$$
$$\left.+\alpha\tilde{\boldsymbol{h}}^{b(5)}\tilde{y}\tilde{A}_5'+\alpha\tilde{\boldsymbol{y}}(\tilde{\boldsymbol{y}}\cdot\tilde{\boldsymbol{h}}^{b(5)})\left(3\frac{\tilde{A}_5'}{\tilde{y}}+\frac{3}{2}\tilde{A}_5''\right)\right\}. \tag{K42}$$

Now (K32) can be directly integrated, again by applying a semilinear approximation during the integration. By using (K26) and (K27), the entire collisional integral (K32) can be written in a symbolic form:

$$\frac{1}{2}\mathrm{Tr}\,\bar{\bar{\boldsymbol{Q}}}_{ab}^{(3)} = m_a n_a 3\alpha^3\nu_{ab}\sqrt{\frac{\pi}{2}}(1+\alpha^2)^{3/2}\left(\frac{T_a}{m_a}\right)^{3/2}$$
$$\times\int\frac{e^{-\alpha^2\tilde{y}^2/2}}{(2\pi)^{3/2}}(1-\alpha\tilde{\boldsymbol{y}}\cdot\tilde{\boldsymbol{u}}+\chi_a)\left[\frac{1}{\alpha^2}\{\mathrm{K41}\}+\frac{1}{(1+\frac{m_a}{m_b})\alpha}\{\mathrm{K42}\}\right]d^3\tilde{y}, \tag{K43}$$

where {K41} and {K42} represent only parts of the corresponding equations that are inside the curly brackets. The final result of the integration reads

$$\frac{1}{2}\mathrm{Tr}\,\bar{\bar{\boldsymbol{Q}}}_{ab}^{(3)} = \frac{\delta\boldsymbol{q}_{ab}}{\delta t} = -\nu_{ab}p_a(\boldsymbol{u}_b-\boldsymbol{u}_a)U_{ab(1)}$$
$$-\nu_{ab}D_{ab(1)}\frac{p_a}{2}\sqrt{\frac{T_a}{m_a}}\tilde{\boldsymbol{h}}^{a(3)}+\nu_{ab}D_{ab(2)}\frac{\rho_a}{\rho_b}\frac{p_b}{2}\sqrt{\frac{T_b}{m_b}}\tilde{\boldsymbol{h}}^{b(3)}$$
$$+\nu_{ab}E_{ab(1)}p_a\sqrt{\frac{T_a}{m_a}}\tilde{\boldsymbol{h}}^{a(5)}+\nu_{ab}E_{ab(2)}\frac{\rho_a}{\rho_b}p_b\sqrt{\frac{T_b}{m_b}}\tilde{\boldsymbol{h}}^{b(5)}, \tag{K44}$$

with the mass-ratio coefficients

$$
\begin{aligned}
U_{ab(1)} &= \frac{(4T_a - 11T_b)m_a m_b - 2T_a m_b^2 - 5T_b m_a^2}{2(T_a m_b + T_b m_a)(m_b + m_a)};\\
D_{ab(1)} &= -\frac{6T_a^2 m_a m_b^2 + 2T_a^2 m_b^3 + 21T_a T_b m_a^2 m_b - 5T_a T_b m_a m_b^2 - 30T_b^2 m_a^3 - 52T_b^2 m_a^2 m_b}{10(T_a m_b + T_b m_a)^2(m_b + m_a)};\\
D_{ab(2)} &= \frac{3m_b T_a[(10T_a - 11T_b)m_a m_b + 4T_a m_b^2 - 5T_b m_a^2]}{10(T_a m_b + T_b m_a)^2(m_b + m_a)};\\
E_{ab(1)} &= -\frac{3T_a m_b[6T_a^2 m_a m_b^2 + 2T_a^2 m_b^3 + 27T_a T_b m_a^2 m_b - 11T_a T_b m_a m_b^2 - 84T_b^2 m_a^3 - 118T_b^2 m_a^2 m_b]}{560(T_a m_b + T_b m_a)^3(m_b + m_a)};\\
E_{ab(2)} &= -\frac{3m_a m_b T_a T_b[16T_a m_a m_b + 10T_a m_b^2 - 5T_b m_a^2 - 11T_b m_a m_b]}{112(T_a m_b + T_b m_a)^3(m_b + m_a)}.
\end{aligned}
\tag{K45}
$$

As a double check, we have verified that neglecting the fifth-order Hermite moments $\tilde{\boldsymbol{h}}^{(5)}$ in (K44) yields a model that matches Burgers–Schunk; see Equations (45)–(49) in Schunk (1977; after there prescribing Coulomb collisions). For small temperature differences, the mass-ratio coefficients simplify into

$$
\begin{aligned}
U_{ab(1)} &= -\frac{(5/2)m_a + m_b}{m_a + m_b};\\
D_{ab(1)} &= \frac{3m_a^2 + \frac{1}{10}m_a m_b - \frac{1}{5}m_b^2}{(m_a + m_b)^2}; \qquad D_{ab(2)} = \frac{\frac{6}{5}m_b^2 - \frac{3}{2}m_a m_b}{(m_a + m_b)^2};\\
E_{ab(1)} &= \frac{3}{560}\frac{m_b(84m_a^2 + 7m_a m_b - 2m_b^2)}{(m_a + m_b)^3}; \qquad E_{ab(2)} = \frac{15}{112}\frac{m_a m_b(m_a - 2m_b)}{(m_a + m_b)^3}.
\end{aligned}
\tag{K46}
$$

The model is easily changed from Hermite moments to fluid moments by

$$
\begin{aligned}
\boldsymbol{q}_a &= \frac{p_a}{2}\sqrt{\frac{T_a}{m_a}}\tilde{\boldsymbol{h}}^{a(3)}; \qquad p_a\sqrt{\frac{T_a}{m_a}}\tilde{\boldsymbol{h}}^{a(5)} = \frac{m_a}{T_a}\boldsymbol{X}_a^{(5)} - 28\boldsymbol{q}_a;\\
\boldsymbol{q}_b &= \frac{p_b}{2}\sqrt{\frac{T_b}{m_b}}\tilde{\boldsymbol{h}}^{b(3)}; \qquad p_b\sqrt{\frac{T_b}{m_b}}\tilde{\boldsymbol{h}}^{b(5)} = \frac{m_b}{T_b}\boldsymbol{X}_b^{(5)} - 28\boldsymbol{q}_b.
\end{aligned}
\tag{K47}
$$

The heat flux exchange rates become

$$
\begin{aligned}
\boldsymbol{Q}_{ab}^{(3)\,\prime} &= \frac{\delta \boldsymbol{q}_{ab}{}'}{\delta t} = \frac{1}{2}\mathrm{Tr}\,\bar{\bar{\boldsymbol{Q}}}_{ab}^{(3)} - \frac{5}{2}\frac{p_a}{\rho_a}\boldsymbol{R}_{ab}\\
&= -\nu_{ab}p_a(\boldsymbol{u}_b - \boldsymbol{u}_a)\hat{U}_{ab(1)} - \nu_{ab}\hat{D}_{ab(1)}\boldsymbol{q}_a + \nu_{ab}\hat{D}_{ab(2)}\frac{\rho_a}{\rho_b}\boldsymbol{q}_b\\
&\quad + \nu_{ab}\hat{E}_{ab(1)}\frac{\rho_a}{p_a}\boldsymbol{X}_a^{(5)} - \nu_{ab}\hat{E}_{ab(2)}\frac{\rho_a}{\rho_b}\frac{\rho_b}{p_b}\boldsymbol{X}_b^{(5)},
\end{aligned}
\tag{K48}
$$

with mass-ratio coefficients (introducing hat)

$$
\begin{aligned}
\hat{U}_{ab(1)} &= U_{ab(1)} + \frac{5}{2};\\
\hat{D}_{ab(1)} &= D_{ab(1)} + 28E_{ab(1)} + \frac{3}{2}\frac{T_a}{m_a}\frac{\mu_{ab}}{T_{ab}} + \frac{15}{4}\frac{T_a^2}{m_a^2}\frac{\mu_{ab}^2}{T_{ab}^2};\\
\hat{D}_{ab(2)} &= D_{ab(2)} - 28E_{ab(2)} + \frac{3}{2}\frac{T_a}{m_a}\frac{\mu_{ab}}{T_{ab}} + \frac{15}{4}\frac{T_a T_b}{m_a m_b}\frac{\mu_{ab}^2}{T_{ab}^2};\\
\hat{E}_{ab(1)} &= E_{ab(1)} + \frac{15}{112}\frac{T_a^2}{m_a^2}\frac{\mu_{ab}^2}{T_{ab}^2};\\
\hat{E}_{ab(2)} &= -\left(E_{ab(2)} - \frac{15}{112}\frac{T_a T_b}{m_a m_b}\frac{\mu_{ab}^2}{T_{ab}^2}\right).
\end{aligned}
\tag{K49}
$$

By introducing summation over all of the "b" species and separating the self-collisions, the final results are given by (18), (19).

K.6. Fifth-order Moment Exchange Rates

We need to calculate the collisional contributions for the right-hand side of the evolution equation for vector $X_i^{a(5)}$, which is obtained by calculating

$$\begin{aligned}\boldsymbol{Q}_{ab}^{(5)} &= \mathrm{Tr}\mathrm{Tr}\bar{\bar{\boldsymbol{Q}}}_{ab}^{(5)} = \frac{\delta \boldsymbol{X}_{ab}^{(5)}}{\delta \mathrm{t}} = m_a \int \boldsymbol{c}_a |\boldsymbol{c}_a|^4 C_{ab}(f_a) d^3v \\ &= m_a \int f_a (\boldsymbol{A}^{ab} |\boldsymbol{c}_a|^4 + 4(\boldsymbol{A}^{ab} \cdot \boldsymbol{c}_a)|\boldsymbol{c}_a|^2 \boldsymbol{c}_a) d^3v \\ &\quad + m_a \int f_a (4(\bar{\bar{\boldsymbol{D}}}^{ab} \cdot \boldsymbol{c}_a)|\boldsymbol{c}_a|^2 + 4(\bar{\bar{\boldsymbol{D}}}^{ab} : \boldsymbol{c}_a \boldsymbol{c}_a)\boldsymbol{c}_a + 2(\mathrm{Tr}\bar{\bar{\boldsymbol{D}}}^{ab})|\boldsymbol{c}_a|^2 \boldsymbol{c}_a) d^3v. \end{aligned} \tag{K50}$$

Again, before the integration of (K50), it is useful to apply the semilinear approximation, which calculates step by step

$$\begin{aligned}\boldsymbol{A}^{ab}|\boldsymbol{c}_a|^4 \simeq 2\frac{c_{ab}}{m_a^2}\left(1 + \frac{m_a}{m_b}\right)\frac{n_b m_b}{T_b}\left(\frac{T_a}{m_a}\right)^2 \Bigg[&+ \alpha(\alpha^3 \tilde{y}^4 \tilde{\boldsymbol{y}} + 4\alpha^2 \tilde{y}^2 \tilde{\boldsymbol{y}}(\tilde{\boldsymbol{y}} \cdot \tilde{\boldsymbol{u}}))\left(\sqrt{\frac{2}{\pi}}\frac{e^{-\tilde{y}^2/2}}{\tilde{y}^2} - \frac{\mathrm{erf}(\tilde{y}/\sqrt{2})}{\tilde{y}^3}\right) \\ &- \sqrt{\frac{2}{\pi}}\frac{e^{-\tilde{y}^2/2}}{10}\alpha^4 \tilde{y}^4 \left(\tilde{\boldsymbol{h}}^{b(3)} - \tilde{\boldsymbol{y}}(\tilde{\boldsymbol{y}} \cdot \tilde{\boldsymbol{h}}^{b(3)}) + (\tilde{y}^2 - 5)\frac{\tilde{\boldsymbol{h}}^{b(5)}}{28} - (\tilde{y}^2 - 7)\frac{\tilde{\boldsymbol{y}}(\tilde{\boldsymbol{y}} \cdot \tilde{\boldsymbol{h}}^{b(5)})}{28}\right)\Bigg]; \end{aligned} \tag{K51}$$

$$\begin{aligned}(\boldsymbol{A}^{ab} \cdot \boldsymbol{c}_a)\boldsymbol{c}_a|\boldsymbol{c}_a|^2 \simeq 2\frac{c_{ab}}{m_a^2}\left(1 + \frac{m_a}{m_b}\right)\frac{n_b m_b}{T_b}\left(\frac{T_a}{m_a}\right)^2 \Bigg[&+ \alpha(\alpha^3 \tilde{y}^4 \tilde{\boldsymbol{y}} + \alpha^2 \tilde{y}^4 \tilde{\boldsymbol{u}} + 3\alpha^2 \tilde{y}^2 \tilde{\boldsymbol{y}}(\tilde{\boldsymbol{y}} \cdot \tilde{\boldsymbol{u}}))\left(\sqrt{\frac{2}{\pi}}\frac{e^{-\tilde{y}^2/2}}{\tilde{y}^2} - \frac{\mathrm{erf}(\tilde{y}/\sqrt{2})}{\tilde{y}^3}\right) \\ &- \sqrt{\frac{2}{\pi}}\frac{e^{-\tilde{y}^2/2}}{10}\alpha^4 \tilde{y}^2 \left(\tilde{\boldsymbol{y}}(\tilde{\boldsymbol{y}} \cdot \tilde{\boldsymbol{h}}^{b(3)})(1 - \tilde{y}^2) + \frac{\tilde{\boldsymbol{y}}(\tilde{\boldsymbol{y}} \cdot \tilde{\boldsymbol{h}}^{b(5)})}{28}(8\tilde{y}^2 - \tilde{y}^4 - 5)\right)\Bigg]; \end{aligned} \tag{K52}$$

$$\begin{aligned}\bar{\bar{\boldsymbol{D}}}^{ab} : \boldsymbol{c}_a \boldsymbol{c}_a \simeq 2\frac{c_{ab}}{m_a^2} n_b \sqrt{\frac{m_b}{T_b}}\frac{T_a}{m_a}\Bigg\{&(\alpha^2 \tilde{y}^2 + 2\alpha(\tilde{\boldsymbol{y}} \cdot \tilde{\boldsymbol{u}}))A_1'' \\ &+ \alpha^2 \tilde{y}^2 (\tilde{\boldsymbol{y}} \cdot \tilde{\boldsymbol{h}}^{b(3)})\left(\tilde{A}_3'' + 2\frac{\tilde{A}_3'}{\tilde{y}}\right) + \alpha^2 \tilde{y}^2 (\tilde{\boldsymbol{y}} \cdot \tilde{\boldsymbol{h}}^{b(5)})\left(\tilde{A}_5'' + 2\frac{\tilde{A}_5'}{\tilde{y}}\right)\Bigg\}; \end{aligned} \tag{K53}$$

$$\begin{aligned}\bar{\bar{\boldsymbol{D}}}^{ab} \cdot \boldsymbol{c}_a|\boldsymbol{c}_a|^2 \simeq 2\frac{c_{ab}}{m_a^2}\frac{n_b}{\alpha}\frac{T_a}{m_a}\Bigg\{&\alpha^3 \tilde{y}^2 \tilde{\boldsymbol{y}} \tilde{A}_1'' + \alpha^2 \tilde{\boldsymbol{u}} \tilde{y} \tilde{A}_1' + \alpha^2 \tilde{\boldsymbol{y}}(\tilde{\boldsymbol{y}} \cdot \tilde{\boldsymbol{u}})\left(3\tilde{A}_1'' - \frac{\tilde{A}_1'}{\tilde{y}}\right) \\ &+ \alpha^3 \tilde{y}^2 \left[\tilde{\boldsymbol{h}}^{b(3)} \tilde{y} \tilde{A}_3' + \tilde{\boldsymbol{y}}(\tilde{\boldsymbol{y}} \cdot \tilde{\boldsymbol{h}}^{b(3)})\left(\frac{\tilde{A}_3'}{\tilde{y}} + \tilde{A}_3''\right)\right] \\ &+ \alpha^3 \tilde{y}^2 \left[\tilde{\boldsymbol{h}}^{b(5)} \tilde{y} \tilde{A}_5' + \tilde{\boldsymbol{y}}(\tilde{\boldsymbol{y}} \cdot \tilde{\boldsymbol{h}}^{b(5)})\left(\frac{\tilde{A}_5'}{\tilde{y}} + \tilde{A}_5''\right)\right]\Bigg\}; \end{aligned} \tag{K54}$$

$$\begin{aligned}(\bar{\bar{\boldsymbol{D}}}^{ab} : \boldsymbol{c}_a \boldsymbol{c}_a)\boldsymbol{c}_a \simeq 2\frac{c_{ab}}{m_a^2}\frac{n_b}{\alpha}\frac{T_a}{m_a}\Bigg\{&(\alpha^3 \tilde{y}^2 \tilde{\boldsymbol{y}} + \alpha^2 \tilde{y}^2 \tilde{\boldsymbol{u}} + 2\alpha^2 \tilde{\boldsymbol{y}}(\tilde{\boldsymbol{y}} \cdot \tilde{\boldsymbol{u}}))A_1'' \\ &+ \alpha^3 \tilde{y}^2 \tilde{\boldsymbol{y}}(\tilde{\boldsymbol{y}} \cdot \tilde{\boldsymbol{h}}^{b(3)})\left(2\frac{\tilde{A}_3'}{\tilde{y}} + \tilde{A}_3''\right) + \alpha^3 \tilde{y}^2 \tilde{\boldsymbol{y}}(\tilde{\boldsymbol{y}} \cdot \tilde{\boldsymbol{h}}^{b(5)})\left(2\frac{\tilde{A}_5'}{\tilde{y}} + \tilde{A}_5''\right)\Bigg\}; \end{aligned} \tag{K55}$$

$$\begin{aligned}2(\mathrm{Tr}\bar{\bar{\boldsymbol{D}}}^{ab})\boldsymbol{c}_a|\boldsymbol{c}_a|^2 \simeq 2\frac{c_{ab}}{m_a^2}\frac{n_b}{\alpha}\frac{T_a}{m_a}\Bigg\{&(\alpha^3 \tilde{y}^2 \tilde{\boldsymbol{y}} + \alpha^2 \tilde{y}^2 \tilde{\boldsymbol{u}} + 2\alpha^2 \tilde{\boldsymbol{y}}(\tilde{\boldsymbol{y}} \cdot \tilde{\boldsymbol{u}}))\left(4\frac{\tilde{A}_1'}{\tilde{y}} + 2\tilde{A}_1''\right) \\ &+ \alpha^3 \tilde{y}^2 \tilde{\boldsymbol{y}}(\tilde{\boldsymbol{y}} \cdot \tilde{\boldsymbol{h}}^{b(3)})\left(8\frac{\tilde{A}_3'}{\tilde{y}} + 2\tilde{A}_3''\right) + \alpha^3 \tilde{y}^2 \tilde{\boldsymbol{y}}(\tilde{\boldsymbol{y}} \cdot \tilde{\boldsymbol{h}}^{b(5)})\left(8\frac{\tilde{A}_5'}{\tilde{y}} + 2\tilde{A}_5''\right)\Bigg\}. \end{aligned} \tag{K56}$$

Collecting the results together, the first part of (K50) becomes

$$\boldsymbol{A}^{ab}|\boldsymbol{c}_a|^4 + 4(\boldsymbol{A}^{ab}\cdot\boldsymbol{c}_a)\boldsymbol{c}_a|\boldsymbol{c}_a|^2 \simeq 2\frac{c_{ab}}{m_a^2}\left(1+\frac{m_a}{m_b}\right)\frac{n_b}{\alpha^2}\frac{T_a}{m_a}\Bigg\{ + \alpha(5\alpha^3\tilde{y}^4\tilde{\boldsymbol{y}} + 4\alpha^2\tilde{y}^4\tilde{\boldsymbol{u}} + 16\alpha^2\tilde{y}^2\tilde{\boldsymbol{y}}(\tilde{\boldsymbol{y}}\cdot\tilde{\boldsymbol{u}}))\left(\sqrt{\frac{2}{\pi}}\frac{e^{-\tilde{y}^2/2}}{\tilde{y}^2} - \frac{\mathrm{erf}(\tilde{y}/\sqrt{2})}{\tilde{y}^3}\right)$$
$$-\sqrt{\frac{2}{\pi}}\frac{e^{-\tilde{y}^2/2}}{10}\alpha^4\tilde{y}^2\Bigg(\tilde{y}^2\tilde{\boldsymbol{h}}^{b(3)} + \tilde{\boldsymbol{y}}(\tilde{\boldsymbol{y}}\cdot\tilde{\boldsymbol{h}}^{b(3)})(4-5\tilde{y}^2) + \tilde{y}^2(\tilde{y}^2-5)\frac{\tilde{\boldsymbol{h}}^{b(5)}}{28}$$
$$+\frac{\tilde{\boldsymbol{y}}(\tilde{\boldsymbol{y}}\cdot\tilde{\boldsymbol{h}}^{b(5)})}{28}(39\tilde{y}^2-5\tilde{y}^4-20)\Bigg)\Bigg\}, \tag{K57}$$

and the second part of (K50) reads

$$4(\bar{\bar{\boldsymbol{D}}}^{ab}\cdot\boldsymbol{c}_a)|\boldsymbol{c}_a|^2 + 4(\bar{\bar{\boldsymbol{D}}}^{ab}:\boldsymbol{c}_a\boldsymbol{c}_a)\boldsymbol{c}_a + 2(\mathrm{Tr}\bar{\bar{\boldsymbol{D}}}^{ab})|\boldsymbol{c}_a|^2\boldsymbol{c}_a \simeq 2\frac{c_{ab}}{m_a^2}\frac{n_b}{\alpha}\frac{T_a}{m_a}$$
$$\times\Bigg\{\alpha^3\tilde{y}^2\tilde{\boldsymbol{y}}\left(4\frac{\tilde{A}_1'}{\tilde{y}} + 10\tilde{A}_1''\right) + \alpha^2\tilde{y}^2\tilde{\boldsymbol{u}}\left(8\frac{\tilde{A}_1'}{\tilde{y}} + 6\tilde{A}_1''\right) + \alpha^2\tilde{\boldsymbol{y}}(\tilde{\boldsymbol{y}}\cdot\tilde{\boldsymbol{u}})\left(4\frac{\tilde{A}_1'}{\tilde{y}} + 24\tilde{A}_1''\right)$$
$$+4\alpha^3\tilde{y}^3\tilde{\boldsymbol{h}}^{b(3)}\tilde{A}_3' + \alpha^3\tilde{y}^2\tilde{\boldsymbol{y}}(\tilde{\boldsymbol{y}}\cdot\tilde{\boldsymbol{h}}^{b(3)})\left(20\frac{\tilde{A}_3'}{\tilde{y}} + 10\tilde{A}_3''\right)$$
$$+4\alpha^3\tilde{y}^3\tilde{\boldsymbol{h}}^{b(5)}\tilde{A}_5' + \alpha^3\tilde{y}^2\tilde{\boldsymbol{y}}(\tilde{\boldsymbol{y}}\cdot\tilde{\boldsymbol{h}}^{b(5)})\left(20\frac{\tilde{A}_5'}{\tilde{y}} + 10\tilde{A}_5''\right)\Bigg\}. \tag{K58}$$

Now (K50) can be integrated, and the entire collisional integral can be written in a symbolic form:

$$\boldsymbol{Q}_{ab}^{(5)} = m_a n_a 3\alpha^3\nu_{ab}\sqrt{\frac{\pi}{2}}(1+\alpha^2)^{3/2}\left(\frac{T_a}{m_a}\right)^{5/2}$$
$$\times\int\frac{e^{-\alpha^2\tilde{y}^2/2}}{(2\pi)^{3/2}}(1-\alpha\tilde{\boldsymbol{y}}\cdot\tilde{\boldsymbol{u}}+\chi_a)\left[\frac{1}{\alpha^2}\{\mathrm{K57}\} + \frac{1}{(1+\frac{m_a}{m_b})\alpha}\{\mathrm{K58}\}\right]d^3\tilde{y}, \tag{K59}$$

where {K57} and {K58} represent only parts of the corresponding equations that are inside the curly brackets. The integration yields

$$\boldsymbol{Q}_{ab}^{(5)} = \mathrm{Tr}\mathrm{Tr}\bar{\bar{\boldsymbol{Q}}}_{ab}^{(5)} = \frac{\delta\boldsymbol{X}_{ab}^{(5)}}{\delta t} = \nu_{ab}\frac{T_a}{m_a}\Bigg\{+p_a(\boldsymbol{u}_b-\boldsymbol{u}_a)U_{ab(2)}$$
$$-F_{ab(1)}\frac{p_a}{2}\sqrt{\frac{T_a}{m_a}}\tilde{\boldsymbol{h}}^{a(3)} - F_{ab(2)}\frac{\rho_a}{\rho_b}\frac{p_b}{2}\sqrt{\frac{T_b}{m_b}}\tilde{\boldsymbol{h}}^{b(3)}$$
$$-G_{ab(1)}p_a\sqrt{\frac{T_a}{m_a}}\tilde{\boldsymbol{h}}^{a(5)} + G_{ab(2)}\frac{\rho_a}{\rho_b}p_b\sqrt{\frac{T_b}{m_b}}\tilde{\boldsymbol{h}}^{b(5)}\Bigg\}, \tag{K60}$$

with mass-ratio coefficients

$$U_{ab(2)} = -\frac{16T_a^2m_am_b^2 - 8T_a^2m_b^3 + 56T_aT_bm_a^2m_b - 52T_aT_bm_am_b^2 - 35T_b^2m_a^3 - 119T_b^2m_a^2m_b}{(T_am_b+T_bm_a)^2(m_b+m_a)};$$
$$F_{ab(1)} = \{40T_a^4m_am_b^3 + 8T_a^4m_b^4 + 180T_a^3T_bm_a^2m_b^2 + 68T_a^3T_bm_am_b^3 + 315T_a^2T_b^2m_a^3m_b + 207T_a^2T_b^2m_a^2m_b^2$$
$$+700T_aT_b^3m_a^4 + 392T_aT_b^3m_a^3m_b - 280T_b^4m_a^4\}[5(T_am_b+T_bm_a)^3(m_b+m_a)T_a]^{-1};$$
$$F_{ab(2)} = -\frac{3T_am_b[16T_a^2m_b^3 + 140T_aT_bm_a^2m_b + 72T_aT_bm_am_b^2 - 35T_b^2m_a^3 - 119T_b^2m_a^2m_b]}{5(T_am_b+T_bm_a)^3(m_b+m_a)};$$
$$G_{ab(1)} = -\{40T_a^4m_am_b^4 + 8T_a^4m_b^5 + 220T_a^3T_bm_a^2m_b^3 + 140T_a^3T_bm_am_b^4 + 495T_a^2T_b^2m_a^3m_b^2$$
$$+627T_a^2T_b^2m_a^2m_b^3 + 3640T_aT_b^3m_a^4m_b + 1916T_aT_b^3m_a^3m_b^2 - 1400T_b^4m_a^5$$
$$-3304T_b^4m_a^4m_b\}[280(T_am_b+T_bm_a)^4(m_a+m_b)]^{-1};$$
$$G_{ab(2)} = \frac{3T_aT_bm_a^2m_b[8T_a^2m_b^2 - 32T_aT_bm_am_b - 28T_aT_bm_b^2 + 5T_b^2m_a^2 + 17T_b^2m_am_b]}{8(T_am_b+T_bm_a)^4(m_a+m_b)}. \tag{K61}$$

For small temperature differences, the mass-ratio coefficients simplify into

$$U_{ab(2)} = \frac{35m_a^2 + 28m_a m_b + 8m_b^2}{(m_a + m_b)^2};$$
$$F_{ab(1)} = \frac{420m_a^3 + 287m_a^2 m_b + 100m_a m_b^2 + 8m_b^3}{5(m_a + m_b)^3};$$
$$F_{ab(2)} = \frac{3}{5}\frac{m_b(35m_a^2 - 56m_a m_b - 16m_b^2)}{(m_a + m_b)^3};$$
$$G_{ab(1)} = \frac{1400m_a^4 - 1736m_a^3 m_b - 675m_a^2 m_b^2 - 172m_a m_b^3 - 8m_b^4}{280(m_a + m_b)^4};$$
$$G_{ab(2)} = \frac{15}{8}\frac{m_a^2 m_b(m_a - 4m_b)}{(m_a + m_b)^4}. \tag{K62}$$

Rewritten with fluid moments, the exchange rates for the fifth-order moment become

$$\boldsymbol{Q}_{ab}^{(5)\,\prime} = \boldsymbol{Q}_{ab}^{(5)} - 35\frac{p_a^2}{\rho_a^2}\boldsymbol{R}_{ab} = \frac{\delta \boldsymbol{X}_{ab}^{(5)\,\prime}}{\delta t} = \nu_{ab}\left\{-\frac{p_a^2}{\rho_a}(\boldsymbol{u}_b - \boldsymbol{u}_a)\hat{U}_{ab(2)}\right.$$
$$\left. -\hat{F}_{ab(1)}\frac{p_a}{\rho_a}\boldsymbol{q}_a + \hat{F}_{ab(2)}\frac{p_a}{\rho_a}\frac{\rho_a}{\rho_b}\boldsymbol{q}_b - \hat{G}_{ab(1)}\boldsymbol{X}_a^{(5)} - \hat{G}_{ab(2)}\frac{p_a}{p_b}\boldsymbol{X}_b^{(5)}\right\}, \tag{K63}$$

with mass-ratio coefficients (introducing hat)

$$\hat{U}_{ab(2)} = -(U_{ab(2)} - 35);$$
$$\hat{F}_{ab(1)} = F_{ab(1)} - 28G_{ab(1)} + 35\frac{T_a}{m_a}\frac{\mu_{ab}}{T_{ab}}V_{ab(1)};$$
$$\hat{F}_{ab(2)} = -\left(F_{ab(2)} + 28G_{ab(2)} - 35\frac{T_a}{m_a}\frac{\mu_{ab}}{T_{ab}}V_{ab(2)}\right);$$
$$\hat{G}_{ab(1)} = G_{ab(1)} - \frac{15}{8}\frac{T_a^2}{m_a^2}\frac{\mu_{ab}^2}{T_{ab}^2};$$
$$\hat{G}_{ab(2)} = -\left(G_{ab(2)} - \frac{15}{8}\frac{T_a T_b}{m_a m_b}\frac{\mu_{ab}^2}{T_{ab}^2}\right). \tag{K64}$$

The final results are given by (20), (21).

Appendix L
Braginskii Viscosity (15-moment Model)

We use polynomials derived from the *reducible* Hermite polynomials (see the details in Appendix B), with the perturbation of the distribution function $f_b(\boldsymbol{v}') = f_b^{(0)}(1 + \chi_b)$

$$\chi_b = \frac{1}{2}\tilde{h}_{ij}^{b(2)}\tilde{H}_{ij}^{b(2)} + \frac{1}{28}\hat{h}_{ij}^{b(4)}\hat{H}_{ij}^{b(4)}. \tag{L1}$$

For the clarity of the calculations, we only consider the viscous part of χ_b (i.e., the 15-moment model) here, but the full 22-moment model can be implicitly assumed for the final collisional contributions at the semilinear level. The Hermite polynomials are (dropping species index "b" for the polynomials and velocities $\tilde{\boldsymbol{c}}$)

$$\tilde{H}_{ij}^{(2)} = \tilde{c}_i\tilde{c}_j - \delta_{ij};$$
$$\tilde{H}_{ij}^{(4)} \equiv \tilde{H}_{ijkk}^{(4)} = \left(\tilde{c}_i\tilde{c}_j - \frac{\delta_{ij}}{3}\tilde{c}^2\right)(\tilde{c}^2 - 7) + \frac{\delta_{ij}}{3}\tilde{H}^{(4)};$$
$$\tilde{H}^{(4)} \equiv \tilde{H}_{iikk}^{(4)} = \tilde{c}^4 - 10\tilde{c}^2 + 15;$$
$$\hat{H}_{ij}^{(4)} \equiv \tilde{H}_{ij}^{(4)} - \frac{\delta_{ij}}{3}\tilde{H}^{(4)} = \left(\tilde{c}_i\tilde{c}_j - \frac{\delta_{ij}}{3}\tilde{c}^2\right)(\tilde{c}^2 - 7). \tag{L2}$$

The irreducible polynomials yield the same perturbation χ_b. By using the perturbation (L1), one can calculate the fluid moments $\Pi_{ij}^{b(2)}$, $\Pi_{ij}^{b(4)}$, or one can directly calculate the Hermite moments

$$\tilde{h}_{ij}^{b(2)} = \frac{1}{p_b}\Pi_{ij}^{b(2)}; \qquad \hat{h}_{ij}^{b(4)} = \frac{\rho_b}{p_b^2}\Pi_{ij}^{b(4)} - \frac{7}{p_b}\Pi_{ij}^{b(2)}, \tag{L3}$$

yielding the same relations. Both $\tilde{h}_{ij}^{(2)}$ and $\hat{h}_{ij}^{(4)}$ are traceless (and $\tilde{h}_{ij}^{(2)} = \hat{h}_{ij}^{(2)}$).

L.1. Rosenbluth Potentials

The notation reads

$$\tilde{\boldsymbol{c}}_b = \sqrt{\frac{m_b}{T_b}}(\boldsymbol{v}' - \boldsymbol{u}_b); \qquad |\boldsymbol{v}' - \boldsymbol{v}| = \sqrt{\frac{T_b}{m_b}}|\tilde{\boldsymbol{c}}_b - \tilde{\boldsymbol{y}}|; \qquad \tilde{\boldsymbol{y}} = \sqrt{\frac{m_b}{T_b}}(\boldsymbol{v} - \boldsymbol{u}_b),$$

the Rosenbluth potentials are

$$H_b(\boldsymbol{v}) = \int \frac{f_b(\boldsymbol{v}')}{|\boldsymbol{v}' - \boldsymbol{v}|}d^3v' = n_b\sqrt{\frac{m_b}{T_b}}\int \frac{\phi_b^{(0)}}{|\tilde{\boldsymbol{c}}_b - \tilde{\boldsymbol{y}}|}(1 + \chi_b)d^3\tilde{c}_b;$$
$$G_b(\boldsymbol{v}) = \int |\boldsymbol{v}' - \boldsymbol{v}|f_b(\boldsymbol{v}')d^3v' = n_b\sqrt{\frac{T_b}{m_b}}\int |\tilde{\boldsymbol{c}}_b - \tilde{\boldsymbol{y}}|\phi_b^{(0)}(1 + \chi_b)d^3\tilde{c}_b,$$

and further calculate

$$H_b(\boldsymbol{v}) = n_b\sqrt{\frac{m_b}{T_b}}\left\{\frac{1}{\tilde{y}}\operatorname{erf}\left(\frac{\tilde{y}}{\sqrt{2}}\right) + \frac{1}{2}(\tilde{\tilde{\boldsymbol{h}}}^{b(2)}:\tilde{\boldsymbol{y}}\tilde{\boldsymbol{y}})\left[\frac{3}{\tilde{y}^5}\operatorname{erf}\left(\frac{\tilde{y}}{\sqrt{2}}\right) - \sqrt{\frac{2}{\pi}}\left(\frac{1}{\tilde{y}^2} + \frac{3}{\tilde{y}^4}\right)e^{-\tilde{y}^2/2}\right]\right.$$
$$\left. -\frac{1}{28}(\hat{\tilde{\boldsymbol{h}}}^{b(4)}:\tilde{\boldsymbol{y}}\tilde{\boldsymbol{y}})\sqrt{\frac{2}{\pi}}e^{-\tilde{y}^2/2}\right\}; \tag{L4}$$

$$G_b(\boldsymbol{v}) = n_b\sqrt{\frac{T_b}{m_b}}\left\{\sqrt{\frac{2}{\pi}}e^{-\tilde{y}^2/2} + \left(\tilde{y} + \frac{1}{\tilde{y}}\right)\operatorname{erf}\left(\frac{\tilde{y}}{\sqrt{2}}\right)\right.$$
$$-\frac{1}{2}(\tilde{\tilde{\boldsymbol{h}}}^{b(2)}:\tilde{\boldsymbol{y}}\tilde{\boldsymbol{y}})\left[\frac{3}{\tilde{y}^4}\sqrt{\frac{2}{\pi}}e^{-\tilde{y}^2/2} + \left(\frac{1}{\tilde{y}^3} - \frac{3}{\tilde{y}^5}\right)\operatorname{erf}\left(\frac{\tilde{y}}{\sqrt{2}}\right)\right]$$
$$\left. -\frac{1}{14}(\hat{\tilde{\boldsymbol{h}}}^{b(4)}:\tilde{\boldsymbol{y}}\tilde{\boldsymbol{y}})\left[\sqrt{\frac{2}{\pi}}\left(\frac{1}{\tilde{y}^2} + \frac{3}{\tilde{y}^4}\right)e^{-\tilde{y}^2/2} - \frac{3}{\tilde{y}^5}\operatorname{erf}\left(\frac{\tilde{y}}{\sqrt{2}}\right)\right]\right\}. \tag{L5}$$

The derivative of the first Rosenbluth potential becomes

$$\frac{\partial H_b}{\partial \boldsymbol{v}} = \frac{n_b m_b}{T_b}\left\{\tilde{\boldsymbol{y}}\left(\sqrt{\frac{2}{\pi}}\frac{e^{-\tilde{y}^2/2}}{\tilde{y}^2} - \frac{\operatorname{erf}(\tilde{y}/\sqrt{2})}{\tilde{y}^3}\right)\right.$$
$$+(\tilde{\tilde{\boldsymbol{h}}}^{b(2)}\cdot\tilde{\boldsymbol{y}})\left[\frac{3}{\tilde{y}^5}\operatorname{erf}\left(\frac{\tilde{y}}{\sqrt{2}}\right) - \sqrt{\frac{2}{\pi}}\left(\frac{1}{\tilde{y}^2} + \frac{3}{\tilde{y}^4}\right)e^{-\tilde{y}^2/2}\right]$$
$$+\frac{1}{2}(\tilde{\tilde{\boldsymbol{h}}}^{b(2)}:\tilde{\boldsymbol{y}}\tilde{\boldsymbol{y}})\tilde{\boldsymbol{y}}\left[-\frac{15}{\tilde{y}^7}\operatorname{erf}\left(\frac{\tilde{y}}{\sqrt{2}}\right) + \sqrt{\frac{2}{\pi}}\left(\frac{1}{\tilde{y}^2} + \frac{5}{\tilde{y}^4} + \frac{15}{\tilde{y}^6}\right)e^{-\tilde{y}^2/2}\right]$$
$$\left. -\frac{1}{14}(\hat{\tilde{\boldsymbol{h}}}^{b(4)}\cdot\tilde{\boldsymbol{y}})\sqrt{\frac{2}{\pi}}e^{-\tilde{y}^2/2} + \frac{1}{28}(\hat{\tilde{\boldsymbol{h}}}^{b(4)}:\tilde{\boldsymbol{y}}\tilde{\boldsymbol{y}})\tilde{\boldsymbol{y}}\sqrt{\frac{2}{\pi}}e^{-\tilde{y}^2/2}\right\}. \tag{L6}$$

For the second Rosenbluth potential, it is useful to use the form

$$G_b(\boldsymbol{v}) = n_b\sqrt{\frac{T_b}{m_b}}[\tilde{A}_1 + \tilde{A}_2(\tilde{\tilde{\boldsymbol{h}}}^{b(2)}:\tilde{\boldsymbol{y}}\tilde{\boldsymbol{y}}) + \tilde{A}_4(\hat{\tilde{\boldsymbol{h}}}^{b(4)}:\tilde{\boldsymbol{y}}\tilde{\boldsymbol{y}})], \tag{L7}$$

where

$$\tilde{A}_1 = \sqrt{\frac{2}{\pi}}\, e^{-\tilde{y}^2/2} + \left(\tilde{y} + \frac{1}{\tilde{y}}\right)\mathrm{erf}\left(\frac{\tilde{y}}{\sqrt{2}}\right);$$
$$\tilde{A}_2 = -\frac{1}{2}\left[\frac{3}{\tilde{y}^4}\sqrt{\frac{2}{\pi}}\, e^{-\tilde{y}^2/2} + \left(\frac{1}{\tilde{y}^3} - \frac{3}{\tilde{y}^5}\right)\mathrm{erf}\left(\frac{\tilde{y}}{\sqrt{2}}\right)\right];$$
$$\tilde{A}_4 = -\frac{1}{14}\left[\sqrt{\frac{2}{\pi}}\left(\frac{1}{\tilde{y}^2} + \frac{3}{\tilde{y}^4}\right)e^{-\tilde{y}^2/2} - \frac{3}{\tilde{y}^5}\,\mathrm{erf}\left(\frac{\tilde{y}}{\sqrt{2}}\right)\right]. \tag{L8}$$

Its second derivative then calculates

$$\begin{aligned}\frac{\partial}{\partial \boldsymbol{v}}\frac{\partial G_b}{\partial \boldsymbol{v}} = n_b\sqrt{\frac{m_b}{T_b}}\Bigg\{&\bar{\bar{\boldsymbol{I}}}\frac{\tilde{A}_1{}'}{\tilde{y}} + \frac{\tilde{\boldsymbol{y}}\tilde{\boldsymbol{y}}}{\tilde{y}^2}\left(\tilde{A}_1{}'' - \frac{\tilde{A}_1{}'}{\tilde{y}}\right)\\
&+[2\tilde{\boldsymbol{y}}\,(\tilde{\bar{\bar{\boldsymbol{h}}}}^{b(2)}\cdot\tilde{\boldsymbol{y}}) + 2(\tilde{\bar{\bar{\boldsymbol{h}}}}^{b(2)}\cdot\tilde{\boldsymbol{y}})\tilde{\boldsymbol{y}} + \bar{\bar{\boldsymbol{I}}}\,(\tilde{\bar{\bar{\boldsymbol{h}}}}^{b(2)}:\tilde{\boldsymbol{y}}\tilde{\boldsymbol{y}})]\frac{\tilde{A}_2{}'}{\tilde{y}}\\
&+2\tilde{A}_2\tilde{\bar{\bar{\boldsymbol{h}}}}^{b(2)} + \frac{\tilde{\boldsymbol{y}}\tilde{\boldsymbol{y}}}{\tilde{y}^2}(\tilde{\bar{\bar{\boldsymbol{h}}}}^{b(2)}:\tilde{\boldsymbol{y}}\tilde{\boldsymbol{y}})\left(\tilde{A}_2{}'' - \frac{\tilde{A}_2{}'}{\tilde{y}}\right)\\
&+[2\tilde{\boldsymbol{y}}\,(\hat{\bar{\bar{\boldsymbol{h}}}}^{b(4)}\cdot\tilde{\boldsymbol{y}}) + 2(\hat{\bar{\bar{\boldsymbol{h}}}}^{b(4)}\cdot\tilde{\boldsymbol{y}})\tilde{\boldsymbol{y}} + \bar{\bar{\boldsymbol{I}}}\,(\hat{\bar{\bar{\boldsymbol{h}}}}^{b(4)}:\tilde{\boldsymbol{y}}\tilde{\boldsymbol{y}})]\frac{\tilde{A}_4{}'}{\tilde{y}}\\
&+2\tilde{A}_4\hat{\bar{\bar{\boldsymbol{h}}}}^{b(4)} + \frac{\tilde{\boldsymbol{y}}\tilde{\boldsymbol{y}}}{\tilde{y}^2}(\hat{\bar{\bar{\boldsymbol{h}}}}^{b(4)}:\tilde{\boldsymbol{y}}\tilde{\boldsymbol{y}})\left(\tilde{A}_4{}'' - \frac{\tilde{A}_4{}'}{\tilde{y}}\right)\Bigg\},\end{aligned} \tag{L9}$$

with coefficients

$$\begin{aligned}\tilde{A}_1{}' &= \sqrt{\frac{2}{\pi}}\frac{e^{-\tilde{y}^2/2}}{\tilde{y}} + \left(1 - \frac{1}{\tilde{y}^2}\right)\mathrm{erf}\left(\frac{\tilde{y}}{\sqrt{2}}\right);\\
\tilde{A}_2{}' &= \left(\frac{1}{\tilde{y}^3} + \frac{15}{2\tilde{y}^5}\right)\sqrt{\frac{2}{\pi}}\, e^{-\tilde{y}^2/2} + \frac{3}{2}\left(\frac{1}{\tilde{y}^4} - \frac{5}{\tilde{y}^6}\right)\mathrm{erf}\left(\frac{\tilde{y}}{\sqrt{2}}\right);\\
\tilde{A}_4{}' &= \frac{1}{14}\left(\frac{1}{\tilde{y}} + \frac{5}{\tilde{y}^3} + \frac{15}{\tilde{y}^5}\right)\sqrt{\frac{2}{\pi}}\, e^{-\tilde{y}^2/2} - \frac{15}{14\tilde{y}^6}\,\mathrm{erf}\left(\frac{\tilde{y}}{\sqrt{2}}\right);\\
\tilde{A}_1{}'' &= -\frac{2}{\tilde{y}^2}\sqrt{\frac{2}{\pi}}\, e^{-\tilde{y}^2/2} + \frac{2}{\tilde{y}^3}\,\mathrm{erf}\left(\frac{\tilde{y}}{\sqrt{2}}\right);\\
\tilde{A}_2{}'' &= -\left(\frac{1}{\tilde{y}^2} + \frac{9}{\tilde{y}^4} + \frac{45}{\tilde{y}^6}\right)\sqrt{\frac{2}{\pi}}\, e^{-\tilde{y}^2/2} + \left(-\frac{6}{\tilde{y}^5} + \frac{45}{\tilde{y}^7}\right)\mathrm{erf}\left(\frac{\tilde{y}}{\sqrt{2}}\right);\\
\tilde{A}_4{}'' &= -\frac{1}{14}\left(1 + \frac{6}{\tilde{y}^2} + \frac{30}{\tilde{y}^4} + \frac{90}{\tilde{y}^6}\right)\sqrt{\frac{2}{\pi}}\, e^{-\tilde{y}^2/2} + \frac{45}{7\tilde{y}^7}\,\mathrm{erf}\left(\frac{\tilde{y}}{\sqrt{2}}\right),\end{aligned} \tag{L10}$$

and

$$\begin{aligned}\tilde{A}_1{}'' - \frac{\tilde{A}_1{}'}{\tilde{y}} &= -\frac{3}{\tilde{y}^2}\sqrt{\frac{2}{\pi}}\, e^{-\tilde{y}^2/2} - \left(\frac{1}{\tilde{y}} - \frac{3}{\tilde{y}^3}\right)\mathrm{erf}\left(\frac{\tilde{y}}{\sqrt{2}}\right);\\
\tilde{A}_2{}'' - \frac{\tilde{A}_2{}'}{\tilde{y}} &= -\left(\frac{1}{\tilde{y}^2} + \frac{10}{\tilde{y}^4} + \frac{105}{2\tilde{y}^6}\right)\sqrt{\frac{2}{\pi}}\, e^{-\tilde{y}^2/2} - \frac{15}{2}\left(\frac{1}{\tilde{y}^5} - \frac{7}{\tilde{y}^7}\right)\mathrm{erf}\left(\frac{\tilde{y}}{\sqrt{2}}\right);\\
\tilde{A}_4{}'' - \frac{\tilde{A}_4{}'}{\tilde{y}} &= -\frac{1}{14}\left(1 + \frac{7}{\tilde{y}^2} + \frac{35}{\tilde{y}^4} + \frac{105}{\tilde{y}^6}\right)\sqrt{\frac{2}{\pi}}\, e^{-\tilde{y}^2/2} + \frac{15}{2\tilde{y}^7}\,\mathrm{erf}\left(\frac{\tilde{y}}{\sqrt{2}}\right).\end{aligned} \tag{L11}$$

As a double check, applying $(1/2)\mathrm{Tr}$ on (L9) yields

$$\frac{1}{2}\mathrm{Tr}\frac{\partial}{\partial \boldsymbol{v}}\frac{\partial \mathrm{G}_b}{\partial \boldsymbol{v}} = n_b\sqrt{\frac{m_b}{T_b}}\frac{1}{2}\left\{\tilde{A}_1'' + 2\frac{\tilde{A}_1'}{\tilde{y}} + (\bar{\bar{\tilde{\boldsymbol{h}}}}^{b(2)}:\tilde{\boldsymbol{y}}\tilde{\boldsymbol{y}})\left(\tilde{A}_2'' + 6\frac{\tilde{A}_2'}{\tilde{y}}\right)\right.$$
$$\left. + (\hat{\bar{\tilde{\boldsymbol{h}}}}^{b(4)}:\tilde{\boldsymbol{y}}\tilde{\boldsymbol{y}})\left(\tilde{A}_4'' + 6\frac{\tilde{A}_4'}{\tilde{y}}\right)\right\} = H_b, \tag{L12}$$

recovering the first Rosenbluth potential (L4). Similarly, applying $(\partial/\partial \boldsymbol{v})\cdot$ on (L6) recovers $-4\pi f_b(\boldsymbol{v})$. Both Rosenbluth potentials seem to be calculated correctly.

L.2. Dynamical Friction Vector and Diffusion Tensor

The dynamical friction vector becomes

$$\begin{aligned}\boldsymbol{A}^{ab} = 2\frac{c_{ab}}{m_a^2}\left(1 + \frac{m_a}{m_b}\right)\frac{n_b m_b}{T_b}\Bigg\{&\tilde{\boldsymbol{y}}\left(\sqrt{\frac{2}{\pi}}\frac{e^{-\tilde{y}^2/2}}{\tilde{y}^2} - \frac{\mathrm{erf}(\tilde{y}/\sqrt{2})}{\tilde{y}^3}\right)\\ &+(\bar{\bar{\tilde{\boldsymbol{h}}}}^{b(2)}\cdot\tilde{\boldsymbol{y}})\left[\frac{3}{\tilde{y}^5}\mathrm{erf}\left(\frac{\tilde{y}}{\sqrt{2}}\right) - \sqrt{\frac{2}{\pi}}\left(\frac{1}{\tilde{y}^2} + \frac{3}{\tilde{y}^4}\right)e^{-\tilde{y}^2/2}\right]\\ &+\frac{1}{2}(\bar{\bar{\tilde{\boldsymbol{h}}}}^{b(2)}:\tilde{\boldsymbol{y}}\tilde{\boldsymbol{y}})\tilde{\boldsymbol{y}}\left[-\frac{15}{\tilde{y}^7}\mathrm{erf}\left(\frac{\tilde{y}}{\sqrt{2}}\right) + \sqrt{\frac{2}{\pi}}\left(\frac{1}{\tilde{y}^2} + \frac{5}{\tilde{y}^4} + \frac{15}{\tilde{y}^6}\right)e^{-\tilde{y}^2/2}\right]\\ &-\frac{1}{14}(\hat{\bar{\tilde{\boldsymbol{h}}}}^{b(4)}\cdot\tilde{\boldsymbol{y}})\sqrt{\frac{2}{\pi}}e^{-\tilde{y}^2/2} + \frac{1}{28}(\hat{\bar{\tilde{\boldsymbol{h}}}}^{b(4)}:\tilde{\boldsymbol{y}}\tilde{\boldsymbol{y}})\tilde{\boldsymbol{y}}\sqrt{\frac{2}{\pi}}e^{-\tilde{y}^2/2}\Bigg\},\end{aligned} \tag{L13}$$

and the diffusion tensor

$$\begin{aligned}\bar{\bar{\boldsymbol{D}}}^{ab} = 2\frac{c_{ab}}{m_a^2}n_b\sqrt{\frac{m_b}{T_b}}\Bigg\{&\bar{\bar{\boldsymbol{I}}}\frac{\tilde{A}_1'}{\tilde{y}} + \frac{\tilde{\boldsymbol{y}}\tilde{\boldsymbol{y}}}{\tilde{y}^2}\left(\tilde{A}_1'' - \frac{\tilde{A}_1'}{\tilde{y}}\right)\\ &+[2\tilde{\boldsymbol{y}}(\bar{\bar{\tilde{\boldsymbol{h}}}}^{b(2)}\cdot\tilde{\boldsymbol{y}}) + 2(\bar{\bar{\tilde{\boldsymbol{h}}}}^{b(2)}\cdot\tilde{\boldsymbol{y}})\tilde{\boldsymbol{y}} + \bar{\bar{\boldsymbol{I}}}(\bar{\bar{\tilde{\boldsymbol{h}}}}^{b(2)}:\tilde{\boldsymbol{y}}\tilde{\boldsymbol{y}})]\frac{\tilde{A}_2'}{\tilde{y}}\\ &+2\tilde{A}_2\bar{\bar{\tilde{\boldsymbol{h}}}}^{b(2)} + \frac{\tilde{\boldsymbol{y}}\tilde{\boldsymbol{y}}}{\tilde{y}^2}(\bar{\bar{\tilde{\boldsymbol{h}}}}^{b(2)}:\tilde{\boldsymbol{y}}\tilde{\boldsymbol{y}})\left(\tilde{A}_2'' - \frac{\tilde{A}_2'}{\tilde{y}}\right)\\ &+[2\tilde{\boldsymbol{y}}(\hat{\bar{\tilde{\boldsymbol{h}}}}^{b(4)}\cdot\tilde{\boldsymbol{y}}) + 2(\hat{\bar{\tilde{\boldsymbol{h}}}}^{b(4)}\cdot\tilde{\boldsymbol{y}})\tilde{\boldsymbol{y}} + \bar{\bar{\boldsymbol{I}}}(\hat{\bar{\tilde{\boldsymbol{h}}}}^{b(4)}:\tilde{\boldsymbol{y}}\tilde{\boldsymbol{y}})]\frac{\tilde{A}_4'}{\tilde{y}}\\ &+2\tilde{A}_4\hat{\bar{\tilde{\boldsymbol{h}}}}^{b(4)} + \frac{\tilde{\boldsymbol{y}}\tilde{\boldsymbol{y}}}{\tilde{y}^2}(\hat{\bar{\tilde{\boldsymbol{h}}}}^{b(4)}:\tilde{\boldsymbol{y}}\tilde{\boldsymbol{y}})\left(\tilde{A}_4'' - \frac{\tilde{A}_4'}{\tilde{y}}\right)\Bigg\},\end{aligned} \tag{L14}$$

where $c_{ab} = 2\pi e^4 Z_a^2 Z_b^2 \ln\Lambda$.

L.3. Distribution Function for Species "a"

To avoid the complicated runaway effect, the distribution function $f_a(\boldsymbol{v}) = f_a^{(0)}(1 + \chi_a)$ has to be expanded for small drifts, in the semilinear approximation. Following the derivation and notation introduced in Appendix C.3, the expanded distribution function becomes

$$f_a = n_a\left(\frac{m_a}{T_a}\right)^{3/2}\frac{e^{-\alpha^2\tilde{y}^2/2}}{(2\pi)^{3/2}}(1 - \alpha\tilde{\boldsymbol{y}}\cdot\tilde{\boldsymbol{u}} + \chi_a), \tag{L15}$$

now with the perturbation

$$\chi_a = \frac{1}{2}\tilde{h}_{ij}^{a(2)}\tilde{H}_{ij}^{a(2)}(\alpha\tilde{\boldsymbol{y}}) + \frac{1}{28}\hat{h}_{ij}^{a(4)}\hat{H}_{ij}^{a(4)}(\alpha\tilde{\boldsymbol{y}}), \tag{L16}$$

where

$$\tilde{h}_{ij}^{a(2)}\tilde{H}_{ij}^{a(2)}(\alpha\tilde{\boldsymbol{y}}) = \tilde{h}_{ij}^{a(2)}\alpha^2\tilde{y}_i\tilde{y}_j;$$
$$\hat{h}_{ij}^{a(4)}\hat{H}_{ij}^{a(4)}(\alpha\tilde{\boldsymbol{y}}) = \hat{h}_{ij}^{a(4)}\alpha^2\tilde{y}_i\tilde{y}_j(\alpha^2\tilde{y}^2 - 7), \tag{L17}$$

so the perturbation reads

$$\chi_a = \frac{\alpha^2}{2}(\tilde{\bar{\bar{\boldsymbol{h}}}}^{a(2)} : \tilde{\boldsymbol{y}}\tilde{\boldsymbol{y}}) + \frac{\alpha^2}{28}(\hat{\bar{\bar{\boldsymbol{h}}}}^{a(4)} : \tilde{\boldsymbol{y}}\tilde{\boldsymbol{y}})(\alpha^2\tilde{y}^2 - 7). \tag{L18}$$

As a reminder,

$$\tilde{\boldsymbol{u}} = (\boldsymbol{u}_b - \boldsymbol{u}_a)\sqrt{\frac{m_a}{T_a}}; \qquad \alpha = \frac{\sqrt{T_b/m_b}}{\sqrt{T_a/m_a}}.$$

L.4. Pressure Tensor Exchange Rates

We need to calculate the collisional contributions for the right-hand side of the pressure tensor equation, and these contributions read

$$\bar{\bar{\boldsymbol{Q}}}_{ab}^{(2)} = m_a \int f_a [\boldsymbol{A}_{ab}\boldsymbol{c}_a]^S d^3v + m_a \int f_a \bar{\bar{\boldsymbol{D}}}_{ab} d^3v. \tag{L19}$$

By implying

$$\boldsymbol{c}_a = \sqrt{\frac{T_a}{m_a}}(\alpha\tilde{\boldsymbol{y}} + \tilde{\boldsymbol{u}}),$$

in the semilinear approximation,

$$\begin{aligned}\boldsymbol{A}^{ab}\boldsymbol{c}_a \simeq 2\frac{c_{ab}}{m_a^2}\left(1 + \frac{m_a}{m_b}\right)\frac{n_b m_b}{T_b}\sqrt{\frac{T_a}{m_a}}\Bigg\{&(\alpha\tilde{\boldsymbol{y}}\tilde{\boldsymbol{y}} + \tilde{\boldsymbol{y}}\tilde{\boldsymbol{u}})\left(\sqrt{\frac{2}{\pi}}\frac{e^{-\tilde{y}^2/2}}{\tilde{y}^2} - \frac{\mathrm{erf}(\tilde{y}/\sqrt{2})}{\tilde{y}^3}\right)\\
&+\alpha(\tilde{\bar{\bar{\boldsymbol{h}}}}^{b(2)} \cdot \tilde{\boldsymbol{y}})\tilde{\boldsymbol{y}}\left[\frac{3}{\tilde{y}^5}\mathrm{erf}\left(\frac{\tilde{y}}{\sqrt{2}}\right) - \sqrt{\frac{2}{\pi}}\left(\frac{1}{\tilde{y}^2} + \frac{3}{\tilde{y}^4}\right)e^{-\tilde{y}^2/2}\right]\\
&+\frac{\alpha}{2}(\tilde{\bar{\bar{\boldsymbol{h}}}}^{b(2)} : \tilde{\boldsymbol{y}}\tilde{\boldsymbol{y}})\tilde{\boldsymbol{y}}\tilde{\boldsymbol{y}}\left[-\frac{15}{\tilde{y}^7}\mathrm{erf}\left(\frac{\tilde{y}}{\sqrt{2}}\right) + \sqrt{\frac{2}{\pi}}\left(\frac{1}{\tilde{y}^2} + \frac{5}{\tilde{y}^4} + \frac{15}{\tilde{y}^6}\right)e^{-\tilde{y}^2/2}\right]\\
&-\frac{\alpha}{14}(\hat{\bar{\bar{\boldsymbol{h}}}}^{b(4)} \cdot \tilde{\boldsymbol{y}})\tilde{\boldsymbol{y}}\sqrt{\frac{2}{\pi}}e^{-\tilde{y}^2/2} + \frac{\alpha}{28}(\hat{\bar{\bar{\boldsymbol{h}}}}^{b(4)} : \tilde{\boldsymbol{y}}\tilde{\boldsymbol{y}})\tilde{\boldsymbol{y}}\tilde{\boldsymbol{y}}\sqrt{\frac{2}{\pi}}e^{-\tilde{y}^2/2}\Bigg\},\end{aligned} \tag{L20}$$

and

$$\begin{aligned}[\boldsymbol{A}^{ab}\boldsymbol{c}_a]^S \simeq 2\frac{c_{ab}}{m_a^2}\left(1 + \frac{m_a}{m_b}\right)\frac{n_b m_b}{T_b}\sqrt{\frac{T_a}{m_a}}\Bigg\{&(2\alpha\tilde{\boldsymbol{y}}\tilde{\boldsymbol{y}} + \tilde{\boldsymbol{y}}\tilde{\boldsymbol{u}} + \tilde{\boldsymbol{u}}\tilde{\boldsymbol{y}})\left(\sqrt{\frac{2}{\pi}}\frac{e^{-\tilde{y}^2/2}}{\tilde{y}^2} - \frac{\mathrm{erf}(\tilde{y}/\sqrt{2})}{\tilde{y}^3}\right)\\
&+\alpha((\tilde{\bar{\bar{\boldsymbol{h}}}}^{b(2)} \cdot \tilde{\boldsymbol{y}})\tilde{\boldsymbol{y}} + \tilde{\boldsymbol{y}}(\tilde{\bar{\bar{\boldsymbol{h}}}}^{b(2)} \cdot \tilde{\boldsymbol{y}}))\left[\frac{3}{\tilde{y}^5}\mathrm{erf}\left(\frac{\tilde{y}}{\sqrt{2}}\right) - \sqrt{\frac{2}{\pi}}\left(\frac{1}{\tilde{y}^2} + \frac{3}{\tilde{y}^4}\right)e^{-\tilde{y}^2/2}\right]\\
&+\alpha(\tilde{\bar{\bar{\boldsymbol{h}}}}^{b(2)} : \tilde{\boldsymbol{y}}\tilde{\boldsymbol{y}})\tilde{\boldsymbol{y}}\tilde{\boldsymbol{y}}\left[-\frac{15}{\tilde{y}^7}\mathrm{erf}\left(\frac{\tilde{y}}{\sqrt{2}}\right) + \sqrt{\frac{2}{\pi}}\left(\frac{1}{\tilde{y}^2} + \frac{5}{\tilde{y}^4} + \frac{15}{\tilde{y}^6}\right)e^{-\tilde{y}^2/2}\right]\\
&-\frac{\alpha}{14}((\hat{\bar{\bar{\boldsymbol{h}}}}^{b(4)} \cdot \tilde{\boldsymbol{y}})\tilde{\boldsymbol{y}} + \tilde{\boldsymbol{y}}(\hat{\bar{\bar{\boldsymbol{h}}}}^{b(4)} \cdot \tilde{\boldsymbol{y}}))\sqrt{\frac{2}{\pi}}e^{-\tilde{y}^2/2} + \frac{\alpha}{14}(\hat{\bar{\bar{\boldsymbol{h}}}}^{b(4)} : \tilde{\boldsymbol{y}}\tilde{\boldsymbol{y}})\tilde{\boldsymbol{y}}\tilde{\boldsymbol{y}}\sqrt{\frac{2}{\pi}}e^{-\tilde{y}^2/2}\Bigg\}.\end{aligned} \tag{L21}$$

The first term of (L19) is rewritten as

$$m_a \int f_a [\boldsymbol{A}_{ab}\boldsymbol{c}_a]^S d^3v = m_a n_a \alpha^3 \int \frac{e^{-\alpha^2\tilde{y}^2/2}}{(2\pi)^{3/2}}(1 - \alpha\tilde{\boldsymbol{y}} \cdot \tilde{\boldsymbol{u}} + \chi_a)[\boldsymbol{A}_{ab}\boldsymbol{c}_a]^S d^3\tilde{y}, \tag{L22}$$

and by using the following integrals:

$$\begin{aligned}
\int \tilde{\boldsymbol{y}}\tilde{\boldsymbol{y}} f(\tilde{y}) e^{-\alpha^2\tilde{y}^2/2} d^3y &= \bar{\bar{\boldsymbol{I}}} \frac{4\pi}{3} \int_0^\infty \tilde{y}^4 f(\tilde{y}) e^{-\alpha^2\tilde{y}^2/2} d\tilde{y};\\
\int \tilde{\boldsymbol{y}} (\tilde{\bar{\bar{\boldsymbol{h}}}}^{b(2)} \cdot \tilde{\boldsymbol{y}}) f(\tilde{y}) e^{-\alpha^2\tilde{y}^2/2} d^3\tilde{y} &= \tilde{\bar{\bar{\boldsymbol{h}}}}^{b(2)} \frac{4\pi}{3} \int_0^\infty \tilde{y}^4 f(\tilde{y}) e^{-\alpha^2\tilde{y}^2/2} d\tilde{y};\\
\tilde{\bar{\bar{\boldsymbol{h}}}}^{b(2)}: \int \tilde{\boldsymbol{y}}\tilde{\boldsymbol{y}} f(\tilde{y}) e^{-\alpha^2\tilde{y}^2/2} d^3\tilde{y} &= 0;\\
\tilde{\bar{\bar{\boldsymbol{h}}}}^{b(2)}: \int \tilde{\boldsymbol{y}}\tilde{\boldsymbol{y}}\tilde{\boldsymbol{y}}\tilde{\boldsymbol{y}} f(\tilde{y}) e^{-\alpha^2\tilde{y}^2/2} d^3\tilde{y} &= \tilde{\bar{\bar{\boldsymbol{h}}}}^{b(2)} \frac{8\pi}{15} \int_0^\infty \tilde{y}^6 f(\tilde{y}) e^{-\alpha^2\tilde{y}^2/2} d\tilde{y},
\end{aligned} \tag{L23}$$

and by further applying the semilinear approximation, it integrates

$$\begin{aligned}
m_a \int f_a [\boldsymbol{A}_{ab}\boldsymbol{c}_a]^S d^3v = \rho_a \nu_{ab} \Bigg[&-2\frac{T_a}{m_a}\bar{\bar{\boldsymbol{I}}} + \frac{6}{5}\tilde{\bar{\bar{\boldsymbol{h}}}}^{b(2)} \frac{T_a T_b}{T_a m_b + T_b m_a} - \frac{3}{7}\hat{\bar{\bar{\boldsymbol{h}}}}^{b(4)} \frac{m_a T_a T_b^2}{(T_a m_b + T_b m_a)^2}\\
&- \frac{2}{5}\frac{T_a}{m_a}\tilde{\bar{\bar{\boldsymbol{h}}}}^{a(2)} \frac{2T_a m_b + 5T_b m_a}{T_a m_b + T_b m_a} + \frac{3}{35}\frac{T_a}{m_a}\hat{\bar{\bar{\boldsymbol{h}}}}^{a(4)} \frac{T_a m_b (2T_a m_b + 7T_b m_a)}{(T_a m_b + T_b m_a)^2} \Bigg].
\end{aligned} \tag{L24}$$

Similarly, the second term of (L19) integrates

$$\begin{aligned}
m_a \int f_a \bar{\bar{\boldsymbol{D}}}_{ab} d^3v = \frac{\rho_a \nu_{ab}}{m_a + m_b} \Bigg[&\bar{\bar{\boldsymbol{I}}} \frac{2}{m_a}(T_a m_b + T_b m_a) - \frac{2}{5} T_b \tilde{\bar{\bar{\boldsymbol{h}}}}^{b(2)} + \frac{3}{35}\frac{m_a T_b^2}{T_a m_b + T_b m_a}\hat{\bar{\bar{\boldsymbol{h}}}}^{b(4)}\\
&- \frac{2}{5}\frac{T_a m_b}{m_a}\tilde{\bar{\bar{\boldsymbol{h}}}}^{a(2)} + \frac{3}{35}\frac{m_b^2 T_a^2}{m_a(T_a m_b + T_b m_a)}\hat{\bar{\bar{\boldsymbol{h}}}}^{a(4)} \Bigg].
\end{aligned} \tag{L25}$$

Adding the last two equations together finally yields

$$\begin{aligned}
\bar{\bar{\boldsymbol{Q}}}_{ab}^{(2)} = \frac{\rho_a \nu_{ab}}{m_a + m_b} [&+2(T_b - T_a)\bar{\bar{\boldsymbol{I}}} - K_{ab(1)} T_a \tilde{\bar{\bar{\boldsymbol{h}}}}^{a(2)} + K_{ab(2)} T_b \tilde{\bar{\bar{\boldsymbol{h}}}}^{b(2)}\\
&+ L_{ab(1)} T_a \hat{\bar{\bar{\boldsymbol{h}}}}^{a(4)} - L_{ab(2)} T_b \hat{\bar{\bar{\boldsymbol{h}}}}^{b(4)}],
\end{aligned} \tag{L26}$$

with mass-ratio coefficients

$$\begin{aligned}
K_{ab(1)} &= \frac{2(2T_a m_a m_b + 3T_a m_b^2 + 5T_b m_a^2 + 6T_b m_a m_b)}{5(T_a m_b + T_b m_a) m_a};\\
K_{ab(2)} &= \frac{2(3T_a m_a + 2T_a m_b - T_b m_a)}{5(T_a m_b + T_b m_a)};\\
L_{ab(1)} &= \frac{3T_a m_b (2T_a m_a m_b + 3T_a m_b^2 + 7T_b m_a^2 + 8T_b m_a m_b)}{35(T_a m_b + T_b m_a)^2 m_a};\\
L_{ab(2)} &= \frac{3m_a T_b (5T_a m_a + 4T_a m_b - T_b m_a)}{35(T_a m_b + T_b m_a)^2}.
\end{aligned} \tag{L27}$$

As a partial double check of the entire formulation, by neglecting the fourth-order Hermite moments $\hat{\bar{\bar{\boldsymbol{h}}}}^{(4)}$ in (L26), it can be verified that the model is then equivalent to Burgers–Schunk; see Equation (44) in Schunk (1977), or our previous Equation (J21). For a

particular case of small temperature differences, the mass-ratio coefficients simplify into

$$K_{ab(1)} = \frac{2(5m_a + 3m_b)}{5m_a}; \qquad K_{ab(2)} = \frac{4}{5};$$
$$L_{ab(1)} = \frac{3(7m_a + 3m_b)m_b}{35m_a(m_b + m_a)}; \qquad L_{ab(2)} = \frac{12m_a}{35(m_a + m_b)}, \tag{L28}$$

and for self-collisions, $K_{aa(1)} = 16/5$, $K_{aa(2)} = 4/5$, $L_{aa(1)} = 3/7$, and $L_{aa(2)} = 6/35$.

L.5. Viscosity Tensor Exchange Rates

The collisional contributions for the viscosity tensor $\bar{\bar{\mathbf{\Pi}}}_a^{(2)}$ become

$$\begin{aligned}\bar{\bar{\boldsymbol{Q}}}_{ab}^{(2)\prime} &= \frac{\delta \bar{\bar{\mathbf{\Pi}}}_{ab}^{(2)}}{\delta t} = \bar{\bar{\boldsymbol{Q}}}_{ab}^{(2)} - \frac{\bar{\bar{\boldsymbol{I}}}}{3}\,\mathrm{Tr}\,\bar{\bar{\boldsymbol{Q}}}_{ab}^{(2)} \\ &= \frac{\rho_a \nu_{ab}}{m_a + m_b}[-K_{ab(1)} T_a \tilde{\bar{\bar{\boldsymbol{h}}}}^{a(2)} + K_{ab(2)} T_b \tilde{\bar{\bar{\boldsymbol{h}}}}^{b(2)} \\ &\quad + L_{ab(1)} T_a \hat{\bar{\bar{\boldsymbol{h}}}}^{a(4)} - L_{ab(2)} T_b \hat{\bar{\bar{\boldsymbol{h}}}}^{b(4)}],\end{aligned} \tag{L29}$$

and introducing summation over all of the "b" species, and rewritten with fluid moments,

$$\begin{aligned}\bar{\bar{\boldsymbol{Q}}}_{a}^{(2)\prime} &= -\frac{21}{10}\nu_{aa}\bar{\bar{\mathbf{\Pi}}}_a^{(2)} + \frac{9}{70}\nu_{aa}\frac{\rho_a}{p_a}\bar{\bar{\mathbf{\Pi}}}_a^{(4)} \\ &\quad + \sum_{b\neq a}\frac{\rho_a \nu_{ab}}{m_a + m_b}\left[-(K_{ab(1)} + 7L_{ab(1)})\frac{1}{n_a}\bar{\bar{\mathbf{\Pi}}}_a^{(2)} + (K_{ab(2)} + 7L_{ab(2)})\frac{1}{n_b}\bar{\bar{\mathbf{\Pi}}}_b^{(2)}\right. \\ &\quad \left. + L_{ab(1)}\frac{\rho_a}{n_a p_a}\bar{\bar{\mathbf{\Pi}}}_a^{(4)} - L_{ab(2)}\frac{\rho_b}{n_b p_b}\bar{\bar{\mathbf{\Pi}}}_b^{(4)}\right].\end{aligned} \tag{L30}$$

It is useful to define (introducing hat)

$$\hat{K}_{ab(1)} = K_{ab(1)} + 7L_{ab(1)}; \qquad \hat{K}_{ab(2)} = K_{ab(2)} + 7L_{ab(2)}, \tag{L31}$$

and the final mass-ratio coefficients are given by (23).

L.6. Fourth-order Moment Exchange Rates

We need to calculate the collisional contributions

$$\begin{aligned}\mathrm{Tr}\,\bar{\bar{\boldsymbol{Q}}}_{ab}^{(4)} &= \frac{\delta\,\mathrm{Tr}\,\bar{\bar{\boldsymbol{r}}}_{ab}}{\delta t} = m_a \int \boldsymbol{c}_a \boldsymbol{c}_a |\boldsymbol{c}_a|^2 C_{ab}(f_a) d^3v \\ &= m_a \int f_a [(\boldsymbol{A}^{ab}\boldsymbol{c}_a)^S |\boldsymbol{c}_a|^2 + 2(\boldsymbol{A}^{ab}\cdot\boldsymbol{c}_a)\boldsymbol{c}_a\boldsymbol{c}_a] d^3v \\ &\quad + m_a \int f_a [(\mathrm{Tr}\,\bar{\bar{\boldsymbol{D}}}^{ab})\boldsymbol{c}_a\boldsymbol{c}_a + \bar{\bar{\boldsymbol{D}}}^{ab}|\boldsymbol{c}_a|^2 + 2((\bar{\bar{\boldsymbol{D}}}^{ab}\cdot\boldsymbol{c}_a)\boldsymbol{c}_a)^S] d^3v.\end{aligned} \tag{L32}$$

There will be no $\tilde{\boldsymbol{u}}$ contributions at the end, and it is simpler to suppress these from the beginning ($\tilde{\boldsymbol{u}} = 0$), and just use $\boldsymbol{c}_a = \sqrt{T_a/m_a}\,\alpha\tilde{\boldsymbol{y}}$. Then one evaluates step by step:

$$\begin{aligned}\boldsymbol{A}^{ab}\cdot\boldsymbol{c}_a = 2\frac{c_{ab}}{m_a^2}\left(1+\frac{m_a}{m_b}\right)\frac{n_b m_b}{T_b}\sqrt{\frac{T_a}{m_a}}\,\alpha\Bigg\{&\left(\sqrt{\frac{2}{\pi}}\,e^{-\tilde{y}^2/2}-\frac{\mathrm{erf}(\tilde{y}/\sqrt{2})}{\tilde{y}}\right)\\ &+(\tilde{\bar{\bar{\boldsymbol{h}}}}^{b(2)}:\tilde{\boldsymbol{y}}\tilde{\boldsymbol{y}})\left[-\frac{9}{2\tilde{y}^5}\,\mathrm{erf}\left(\frac{\tilde{y}}{\sqrt{2}}\right)+\frac{1}{2}\left(1+\frac{3}{\tilde{y}^2}+\frac{9}{\tilde{y}^4}\right)\sqrt{\frac{2}{\pi}}\,e^{-\tilde{y}^2/2}\right]\\ &+\frac{1}{28}(\hat{\bar{\bar{\boldsymbol{h}}}}^{b(4)}:\tilde{\boldsymbol{y}}\tilde{\boldsymbol{y}})(-2+\tilde{y}^2)\sqrt{\frac{2}{\pi}}\,e^{-\tilde{y}^2/2}\Bigg\};\end{aligned} \tag{L33}$$

$$\begin{aligned}2(\boldsymbol{A}^{ab}\cdot\boldsymbol{c}_a)\boldsymbol{c}_a\boldsymbol{c}_a = 2\frac{c_{ab}}{m_a^2}\left(1+\frac{m_a}{m_b}\right)\frac{n_b m_b}{T_b}\sqrt{\frac{T_a}{m_a}}\,\frac{T_a}{m_a}\alpha^3\Bigg\{&2\tilde{\boldsymbol{y}}\tilde{\boldsymbol{y}}\left(\sqrt{\frac{2}{\pi}}\,e^{-\tilde{y}^2/2}-\frac{\mathrm{erf}(\tilde{y}/\sqrt{2})}{\tilde{y}}\right)\\ &+(\tilde{\bar{\bar{\boldsymbol{h}}}}^{b(2)}:\tilde{\boldsymbol{y}}\tilde{\boldsymbol{y}})\tilde{\boldsymbol{y}}\tilde{\boldsymbol{y}}\left[-\frac{9}{\tilde{y}^5}\,\mathrm{erf}\left(\frac{\tilde{y}}{\sqrt{2}}\right)+\left(1+\frac{3}{\tilde{y}^2}+\frac{9}{\tilde{y}^4}\right)\sqrt{\frac{2}{\pi}}\,e^{-\tilde{y}^2/2}\right]\\ &+\frac{1}{14}(\hat{\bar{\bar{\boldsymbol{h}}}}^{b(4)}:\tilde{\boldsymbol{y}}\tilde{\boldsymbol{y}})\tilde{\boldsymbol{y}}\tilde{\boldsymbol{y}}(-2+\tilde{y}^2)\sqrt{\frac{2}{\pi}}\,e^{-\tilde{y}^2/2}\Bigg\};\end{aligned} \tag{L34}$$

$$\begin{aligned}(\boldsymbol{A}^{ab}\boldsymbol{c}_a)^S|\boldsymbol{c}_a|^2 = 2\frac{c_{ab}}{m_a^2}\left(1+\frac{m_a}{m_b}\right)\frac{n_b m_b}{T_b}\sqrt{\frac{T_a}{m_a}}\,\frac{T_a}{m_a}\alpha^3\Bigg\{&2\tilde{\boldsymbol{y}}\tilde{\boldsymbol{y}}\left(\sqrt{\frac{2}{\pi}}\,e^{-\tilde{y}^2/2}-\frac{\mathrm{erf}(\tilde{y}/\sqrt{2})}{\tilde{y}}\right)\\ &+((\tilde{\bar{\bar{\boldsymbol{h}}}}^{b(2)}\cdot\tilde{\boldsymbol{y}})\tilde{\boldsymbol{y}}+\tilde{\boldsymbol{y}}(\tilde{\bar{\bar{\boldsymbol{h}}}}^{b(2)}\cdot\tilde{\boldsymbol{y}}))\left[\frac{3}{\tilde{y}^3}\,\mathrm{erf}\left(\frac{\tilde{y}}{\sqrt{2}}\right)-\left(1+\frac{3}{\tilde{y}^2}\right)\sqrt{\frac{2}{\pi}}\,e^{-\tilde{y}^2/2}\right]\\ &+(\tilde{\bar{\bar{\boldsymbol{h}}}}^{b(2)}:\tilde{\boldsymbol{y}}\tilde{\boldsymbol{y}})\tilde{\boldsymbol{y}}\tilde{\boldsymbol{y}}\left[-\frac{15}{\tilde{y}^5}\,\mathrm{erf}\left(\frac{\tilde{y}}{\sqrt{2}}\right)+\left(1+\frac{5}{\tilde{y}^2}+\frac{15}{\tilde{y}^4}\right)\sqrt{\frac{2}{\pi}}\,e^{-\tilde{y}^2/2}\right]\\ &-\frac{1}{14}((\hat{\bar{\bar{\boldsymbol{h}}}}^{b(4)}\cdot\tilde{\boldsymbol{y}})\tilde{\boldsymbol{y}}+\tilde{\boldsymbol{y}}(\hat{\bar{\bar{\boldsymbol{h}}}}^{b(4)}\cdot\tilde{\boldsymbol{y}}))\tilde{y}^2\sqrt{\frac{2}{\pi}}\,e^{-\tilde{y}^2/2}+\frac{1}{14}(\hat{\bar{\bar{\boldsymbol{h}}}}^{b(4)}:\tilde{\boldsymbol{y}}\tilde{\boldsymbol{y}})\tilde{\boldsymbol{y}}\tilde{\boldsymbol{y}}\tilde{y}^2\sqrt{\frac{2}{\pi}}\,e^{-\tilde{y}^2/2}\Bigg\},\end{aligned} \tag{L35}$$

and adding the last two results together,

$$\begin{aligned}&(\boldsymbol{A}^{ab}\boldsymbol{c}_a)^S|\boldsymbol{c}_a|^2+2(\boldsymbol{A}^{ab}\cdot\boldsymbol{c}_a)\boldsymbol{c}_a\boldsymbol{c}_a\\ &=2\frac{c_{ab}}{m_a^2}\left(1+\frac{m_a}{m_b}\right)\frac{n_b m_b}{T_b}\sqrt{\frac{T_a}{m_a}}\,\frac{T_a}{m_a}\alpha^3\Bigg\{4\tilde{\boldsymbol{y}}\tilde{\boldsymbol{y}}\left(\sqrt{\frac{2}{\pi}}\,e^{-\tilde{y}^2/2}-\frac{\mathrm{erf}(\tilde{y}/\sqrt{2})}{\tilde{y}}\right)\\ &\quad+((\tilde{\bar{\bar{\boldsymbol{h}}}}^{b(2)}\cdot\tilde{\boldsymbol{y}})\tilde{\boldsymbol{y}}+\tilde{\boldsymbol{y}}(\tilde{\bar{\bar{\boldsymbol{h}}}}^{b(2)}\cdot\tilde{\boldsymbol{y}}))\left[\frac{3}{\tilde{y}^3}\,\mathrm{erf}\left(\frac{\tilde{y}}{\sqrt{2}}\right)-\sqrt{\frac{2}{\pi}}\left(1+\frac{3}{\tilde{y}^2}\right)e^{-\tilde{y}^2/2}\right]\\ &\quad+(\tilde{\bar{\bar{\boldsymbol{h}}}}^{b(2)}:\tilde{\boldsymbol{y}}\tilde{\boldsymbol{y}})\tilde{\boldsymbol{y}}\tilde{\boldsymbol{y}}\left[-\frac{24}{\tilde{y}^5}\,\mathrm{erf}\left(\frac{\tilde{y}}{\sqrt{2}}\right)+\left(2+\frac{8}{\tilde{y}^2}+\frac{24}{\tilde{y}^4}\right)\sqrt{\frac{2}{\pi}}\,e^{-\tilde{y}^2/2}\right]\\ &\quad-\frac{1}{14}((\hat{\bar{\bar{\boldsymbol{h}}}}^{b(4)}\cdot\tilde{\boldsymbol{y}})\tilde{\boldsymbol{y}}+\tilde{\boldsymbol{y}}(\hat{\bar{\bar{\boldsymbol{h}}}}^{b(4)}\cdot\tilde{\boldsymbol{y}}))\tilde{y}^2\sqrt{\frac{2}{\pi}}\,e^{-\tilde{y}^2/2}+\frac{1}{14}(\hat{\bar{\bar{\boldsymbol{h}}}}^{b(4)}:\tilde{\boldsymbol{y}}\tilde{\boldsymbol{y}})\tilde{\boldsymbol{y}}\tilde{\boldsymbol{y}}(-2+2\tilde{y}^2)\sqrt{\frac{2}{\pi}}\,e^{-\tilde{y}^2/2}\Bigg\}.\end{aligned} \tag{L36}$$

Similarly, for the diffusion tensor, calculating step by step,

$$\bar{\bar{\boldsymbol{D}}}^{ab}\cdot\boldsymbol{c}_a = 2\frac{c_{ab}}{m_a^2}n_b\sqrt{\frac{m_b}{T_b}}\sqrt{\frac{T_a}{m_a}}\,\alpha\left\{\tilde{\boldsymbol{y}}\tilde{A}_1'' + (\bar{\bar{\tilde{\boldsymbol{h}}}}^{b(2)}\cdot\tilde{\boldsymbol{y}})(2\tilde{y}\tilde{A}_2' + 2\tilde{A}_2) + \tilde{\boldsymbol{y}}(\bar{\bar{\tilde{\boldsymbol{h}}}}^{b(2)}:\tilde{\boldsymbol{y}}\tilde{\boldsymbol{y}})\left(\tilde{A}_2'' + 2\frac{\tilde{A}_2'}{\tilde{y}}\right)\right.$$
$$\left.+(\hat{\bar{\tilde{\boldsymbol{h}}}}^{b(4)}\cdot\tilde{\boldsymbol{y}})(2\tilde{y}\tilde{A}_4' + 2\tilde{A}_4) + \tilde{\boldsymbol{y}}(\hat{\bar{\tilde{\boldsymbol{h}}}}^{b(4)}:\tilde{\boldsymbol{y}}\tilde{\boldsymbol{y}})\left(\tilde{A}_4'' + 2\frac{\tilde{A}_4'}{\tilde{y}}\right)\right\}; \tag{L37}$$

$$\mathrm{Tr}\,\bar{\bar{\boldsymbol{D}}}^{ab} = 2\frac{c_{ab}}{m_a^2}n_b\sqrt{\frac{m_b}{T_b}}\left\{\tilde{A}_1'' + 2\frac{\tilde{A}_1'}{\tilde{y}}\right.$$
$$\left.+(\bar{\bar{\tilde{\boldsymbol{h}}}}^{b(2)}:\tilde{\boldsymbol{y}}\tilde{\boldsymbol{y}})\left(\tilde{A}_2'' + 6\frac{\tilde{A}_2'}{\tilde{y}}\right) + (\hat{\bar{\tilde{\boldsymbol{h}}}}^{b(4)}:\tilde{\boldsymbol{y}}\tilde{\boldsymbol{y}})\left(\tilde{A}_4'' + 6\frac{\tilde{A}_4'}{\tilde{y}}\right)\right\}; \tag{L38}$$

$$\mathrm{Tr}\,\bar{\bar{\boldsymbol{D}}}^{ab}\boldsymbol{c}_a\boldsymbol{c}_a = 2\frac{c_{ab}}{m_a^2}n_b\sqrt{\frac{m_b}{T_b}}\frac{T_a}{m_a}\alpha^2\left\{\tilde{\boldsymbol{y}}\tilde{\boldsymbol{y}}\left(\tilde{A}_1'' + 2\frac{\tilde{A}_1'}{\tilde{y}}\right)\right.$$
$$\left.+(\bar{\bar{\tilde{\boldsymbol{h}}}}^{b(2)}:\tilde{\boldsymbol{y}}\tilde{\boldsymbol{y}})\tilde{\boldsymbol{y}}\tilde{\boldsymbol{y}}\left(\tilde{A}_2'' + 6\frac{\tilde{A}_2'}{\tilde{y}}\right) + (\hat{\bar{\tilde{\boldsymbol{h}}}}^{b(4)}:\tilde{\boldsymbol{y}}\tilde{\boldsymbol{y}})\tilde{\boldsymbol{y}}\tilde{\boldsymbol{y}}\left(\tilde{A}_4'' + 6\frac{\tilde{A}_4'}{\tilde{y}}\right)\right\}; \tag{L39}$$

$$\bar{\bar{\boldsymbol{D}}}^{ab}|\boldsymbol{c}_a|^2 = 2\frac{c_{ab}}{m_a^2}n_b\sqrt{\frac{m_b}{T_b}}\frac{T_a}{m_a}\alpha^2\left\{\bar{\bar{\boldsymbol{I}}}\tilde{y}\tilde{A}_1' + \tilde{\boldsymbol{y}}\tilde{\boldsymbol{y}}\left(\tilde{A}_1'' - \frac{\tilde{A}_1'}{\tilde{y}}\right)\right.$$
$$+[2\tilde{\boldsymbol{y}}(\bar{\bar{\tilde{\boldsymbol{h}}}}^{b(2)}\cdot\tilde{\boldsymbol{y}}) + 2(\bar{\bar{\tilde{\boldsymbol{h}}}}^{b(2)}\cdot\tilde{\boldsymbol{y}})\tilde{\boldsymbol{y}} + \bar{\bar{\boldsymbol{I}}}(\bar{\bar{\tilde{\boldsymbol{h}}}}^{b(2)}:\tilde{\boldsymbol{y}}\tilde{\boldsymbol{y}})]\tilde{y}\tilde{A}_2'$$
$$+2\tilde{y}^2\tilde{A}_2\bar{\bar{\tilde{\boldsymbol{h}}}}^{b(2)} + \tilde{\boldsymbol{y}}\tilde{\boldsymbol{y}}(\bar{\bar{\tilde{\boldsymbol{h}}}}^{b(2)}:\tilde{\boldsymbol{y}}\tilde{\boldsymbol{y}})\left(\tilde{A}_2'' - \frac{\tilde{A}_2'}{\tilde{y}}\right)$$
$$+[2\tilde{\boldsymbol{y}}(\hat{\bar{\tilde{\boldsymbol{h}}}}^{b(4)}\cdot\tilde{\boldsymbol{y}}) + 2(\hat{\bar{\tilde{\boldsymbol{h}}}}^{b(4)}\cdot\tilde{\boldsymbol{y}})\tilde{\boldsymbol{y}} + \bar{\bar{\boldsymbol{I}}}(\hat{\bar{\tilde{\boldsymbol{h}}}}^{b(4)}:\tilde{\boldsymbol{y}}\tilde{\boldsymbol{y}})]\tilde{y}\tilde{A}_4'$$
$$\left.+2\tilde{y}^2\tilde{A}_4\hat{\bar{\tilde{\boldsymbol{h}}}}^{b(4)} + \tilde{\boldsymbol{y}}\tilde{\boldsymbol{y}}(\hat{\bar{\tilde{\boldsymbol{h}}}}^{b(4)}:\tilde{\boldsymbol{y}}\tilde{\boldsymbol{y}})\left(\tilde{A}_4'' - \frac{\tilde{A}_4'}{\tilde{y}}\right)\right\}; \tag{L40}$$

$$2[(\bar{\bar{\boldsymbol{D}}}^{ab}\cdot\boldsymbol{c}_a)\boldsymbol{c}_a]^S = 2\frac{c_{ab}}{m_a^2}n_b\sqrt{\frac{m_b}{T_b}}\frac{T_a}{m_a}\alpha^2\left\{4\tilde{\boldsymbol{y}}\tilde{\boldsymbol{y}}\tilde{A}_1''\right.$$
$$+2[(\bar{\bar{\tilde{\boldsymbol{h}}}}^{b(2)}\cdot\tilde{\boldsymbol{y}})\tilde{\boldsymbol{y}}]^S(2\tilde{y}\tilde{A}_2' + 2\tilde{A}_2) + 4\tilde{\boldsymbol{y}}\tilde{\boldsymbol{y}}(\bar{\bar{\tilde{\boldsymbol{h}}}}^{b(2)}:\tilde{\boldsymbol{y}}\tilde{\boldsymbol{y}})\left(\tilde{A}_2'' + 2\frac{\tilde{A}_2'}{\tilde{y}}\right)$$
$$\left.+2[(\hat{\bar{\tilde{\boldsymbol{h}}}}^{b(4)}\cdot\tilde{\boldsymbol{y}})\tilde{\boldsymbol{y}}]^S(2\tilde{y}\tilde{A}_4' + 2\tilde{A}_4) + 4\tilde{\boldsymbol{y}}\tilde{\boldsymbol{y}}(\hat{\bar{\tilde{\boldsymbol{h}}}}^{b(4)}:\tilde{\boldsymbol{y}}\tilde{\boldsymbol{y}})\left(\tilde{A}_4'' + 2\frac{\tilde{A}_4'}{\tilde{y}}\right)\right\}, \tag{L41}$$

and adding the last three results together,

$$(\mathrm{Tr}\,\bar{\bar{\boldsymbol{D}}}^{ab})\boldsymbol{c}_a\boldsymbol{c}_a + \bar{\bar{\boldsymbol{D}}}^{ab}|\boldsymbol{c}_a|^2 + 2[(\bar{\bar{\boldsymbol{D}}}^{ab}\cdot\boldsymbol{c}_a)\boldsymbol{c}_a]^S$$
$$= 2\frac{c_{ab}}{m_a^2}n_b\sqrt{\frac{m_b}{T_b}}\frac{T_a}{m_a}\alpha^2\left\{\bar{\bar{\boldsymbol{I}}}\tilde{y}\tilde{A}_1' + \tilde{\boldsymbol{y}}\tilde{\boldsymbol{y}}\left(6\tilde{A}_1'' + \frac{\tilde{A}_1'}{\tilde{y}}\right)\right.$$
$$+2[(\bar{\bar{\tilde{\boldsymbol{h}}}}^{b(2)}\cdot\tilde{\boldsymbol{y}})\tilde{\boldsymbol{y}}]^S(3\tilde{y}\tilde{A}_2' + 2\tilde{A}_2) + \bar{\bar{\boldsymbol{I}}}(\bar{\bar{\tilde{\boldsymbol{h}}}}^{b(2)}:\tilde{\boldsymbol{y}}\tilde{\boldsymbol{y}})\tilde{y}\tilde{A}_2'$$
$$+2\tilde{y}^2\tilde{A}_2\bar{\bar{\tilde{\boldsymbol{h}}}}^{b(2)} + \tilde{\boldsymbol{y}}\tilde{\boldsymbol{y}}(\bar{\bar{\tilde{\boldsymbol{h}}}}^{b(2)}:\tilde{\boldsymbol{y}}\tilde{\boldsymbol{y}})\left(6\tilde{A}_2'' + 13\frac{\tilde{A}_2'}{\tilde{y}}\right)$$
$$+2[(\hat{\bar{\tilde{\boldsymbol{h}}}}^{b(4)}\cdot\tilde{\boldsymbol{y}})\tilde{\boldsymbol{y}}]^S(3\tilde{y}\tilde{A}_4' + 2\tilde{A}_4) + \bar{\bar{\boldsymbol{I}}}(\hat{\bar{\tilde{\boldsymbol{h}}}}^{b(4)}:\tilde{\boldsymbol{y}}\tilde{\boldsymbol{y}})\tilde{y}\tilde{A}_4'$$
$$\left.+2\tilde{y}^2\tilde{A}_4\hat{\bar{\tilde{\boldsymbol{h}}}}^{b(4)} + \tilde{\boldsymbol{y}}\tilde{\boldsymbol{y}}(\hat{\bar{\tilde{\boldsymbol{h}}}}^{b(4)}:\tilde{\boldsymbol{y}}\tilde{\boldsymbol{y}})\left(6\tilde{A}_4'' + 13\frac{\tilde{A}_4'}{\tilde{y}}\right)\right\}. \tag{L42}$$

Now, by using (L36), (L42), we are ready to calculate the collisional integrals (L32). The first integral in (L32) calculates

$$
\begin{aligned}
& m_a \int f_a [(\boldsymbol{A}^{ab}\boldsymbol{c}_a)^S|\boldsymbol{c}_a|^2 + 2(\boldsymbol{A}^{ab}\cdot\boldsymbol{c}_a)\boldsymbol{c}_a\boldsymbol{c}_a]d^3v \\
&= \rho_a\nu_{ab}\frac{p_a^2}{\rho_a^2}\Bigg\{-\bar{\bar{\boldsymbol{I}}}\frac{4(2T_am_b+5T_bm_a)}{(T_am_b+T_bm_a)} - \bar{\bar{\boldsymbol{h}}}^{b(2)}\frac{6(3T_am_b-7T_bm_a)T_bm_a}{5(T_am_b+T_bm_a)^2} \\
&\quad + \hat{\bar{\bar{\boldsymbol{h}}}}^{b(4)}\frac{3(T_am_b-T_bm_a)T_b^2m_a^2}{(T_am_b+T_bm_a)^3} \\
&\quad - \tilde{\bar{\bar{\boldsymbol{h}}}}^{a(2)}\frac{4(8T_a^2m_b^2+28T_aT_bm_am_b+35T_b^2m_a^2)}{5(T_am_b+T_bm_a)^2} \\
&\quad + \hat{\bar{\bar{\boldsymbol{h}}}}^{a(4)}\frac{2(8T_a^3m_b^3+36T_a^2T_bm_am_b^2+63T_aT_b^2m_a^2m_b-70T_b^3m_a^3)}{35(T_am_b+T_bm_a)^3}\Bigg\}.
\end{aligned}
\tag{L43}
$$

The second integral in (L32) calculates

$$
\begin{aligned}
& m_a \int f_a [(\mathrm{Tr}\,\bar{\bar{\boldsymbol{D}}}^{ab})\boldsymbol{c}_a\boldsymbol{c}_a + \bar{\bar{\boldsymbol{D}}}^{ab}|\boldsymbol{c}_a|^2 + 2((\bar{\bar{\boldsymbol{D}}}^{ab}\cdot\boldsymbol{c}_a)\boldsymbol{c}_a)^S]d^3v \\
&= \rho_a\nu_{ab}\frac{p_a^2}{\rho_a^2}\Bigg\{\bar{\bar{\boldsymbol{I}}}\frac{4(2T_am_b+5T_bm_a)}{T_a(m_b+m_a)} + \tilde{\bar{\bar{\boldsymbol{h}}}}^{b(2)}\frac{2(11T_am_b-7T_bm_a)T_bm_a}{5T_a(T_am_b+T_bm_a)(m_b+m_a)} \\
&\quad - \hat{\bar{\bar{\boldsymbol{h}}}}^{b(4)}\frac{3(23T_am_b-7T_bm_a)T_b^2m_a^2}{35T_a(T_am_b+T_bm_a)^2(m_b+m_a)} \\
&\quad + \tilde{\bar{\bar{\boldsymbol{h}}}}^{a(2)}\frac{2(4T_a^2m_b^2+21T_aT_bm_am_b+35T_b^2m_a^2)}{5T_a(T_am_b+T_bm_a)(m_b+m_a)} \\
&\quad - \hat{\bar{\bar{\boldsymbol{h}}}}^{a(4)}\frac{m_b(T_am_b+7T_bm_a)(4T_am_b+19T_bm_a)}{35(T_am_b+T_bm_a)^2(m_b+m_a)}\Bigg\}.
\end{aligned}
\tag{L44}
$$

Adding (L43) and (L44) together then yields the collisional contributions

$$
\begin{aligned}
\mathrm{Tr}\,\bar{\bar{\boldsymbol{Q}}}_{ab}^{(4)} = \rho_a\nu_{ab}\frac{p_a^2}{\rho_a^2}\Bigg\{&+\bar{\bar{\boldsymbol{I}}}\frac{4(2T_am_b+5T_bm_a)m_a}{(T_am_b+T_bm_a)(m_b+m_a)}\frac{(T_b-T_a)}{T_a} \\
&-M_{ab(1)}\tilde{\bar{\bar{\boldsymbol{h}}}}^{a(2)} + M_{ab(2)}\tilde{\bar{\bar{\boldsymbol{h}}}}^{b(2)} - N_{ab(1)}\hat{\bar{\bar{\boldsymbol{h}}}}^{a(4)} - N_{ab(2)}\hat{\bar{\bar{\boldsymbol{h}}}}^{b(4)}\Bigg\},
\end{aligned}
\tag{L45}
$$

with mass-ratio coefficients

$$
\begin{aligned}
M_{ab(1)} &= \{2(16T_a^3m_am_b^2 + 12T_a^3m_b^3 + 56T_a^2T_bm_a^2m_b + 31T_a^2T_bm_am_b^2 + 70T_aT_b^2m_a^3 \\
&\quad +14T_aT_b^2m_a^2m_b - 35T_b^3m_a^3)\}[5T_a(T_am_b+T_bm_a)^2(m_b+m_a)]^{-1}; \\
M_{ab(2)} &= -\frac{2T_bm_a(9T_a^2m_am_b - 2T_a^2m_b^2 - 21T_aT_bm_a^2 - 25T_aT_bm_am_b + 7T_b^2m_a^2)}{5(T_am_b+T_bm_a)^2T_a(m_b+m_a)}; \\
N_{ab(1)} &= -\{16T_a^3m_am_b^3 + 12T_a^3m_b^4 + 72T_a^2T_bm_a^2m_b^2 + 21T_a^2T_bm_am_b^3 + 126T_aT_b^2m_a^3m_b \\
&\quad -54T_aT_b^2m_a^2m_b^2 - 140T_b^3m_a^4 - 273T_b^3m_a^3m_b\}[35(T_am_b+T_bm_a)^3(m_b+m_a)]^{-1}; \\
N_{ab(2)} &= -\frac{3T_b^2m_a^2(35T_a^2m_am_b + 12T_a^2m_b^2 - 35T_aT_bm_a^2 - 51T_aT_bm_am_b + 7T_b^2m_a^2)}{35(T_am_b+T_bm_a)^3T_a(m_b+m_a)}.
\end{aligned}
\tag{L46}
$$

For a particular case of small temperature differences between species, the mass-ratio coefficients simplify into

$$
\begin{aligned}
M_{ab(1)} &= \frac{2(35m_a^2+35m_am_b+12m_b^2)}{5(m_b+m_a)^2}; \qquad M_{ab(2)} = \frac{4m_a(7m_a+m_b)}{5(m_b+m_a)^2}; \\
N_{ab(1)} &= \frac{140m_a^3+7m_a^2m_b-25m_am_b^2-12m_b^3}{35(m_b+m_a)^3}; \qquad N_{ab(2)} = \frac{12m_a^2(7m_a-3m_b)}{35(m_b+m_a)^3},
\end{aligned}
\tag{L47}
$$

and for self-collisions, $M_{aa(1)} = 41/5$, $M_{aa(2)} = 8/5$, $N_{aa(1)} = 11/28$, and $N_{aa(2)} = 6/35$.

L.7. Exchange Rates $\bar{\bar{\boldsymbol{Q}}}_a^{(4)\prime}$

Applying trace at (L45) yields the scalar

$$\mathrm{TrTr}\bar{\bar{\boldsymbol{Q}}}_{ab}^{(4)} = \rho_a \nu_{ab} \frac{p_a^2}{\rho_a^2}\left\{+3\frac{4(2T_a m_b + 5T_b m_a)m_a}{(T_a m_b + T_b m_a)(m_b + m_a)}\frac{(T_b - T_a)}{T_a}\right\}, \tag{L48}$$

and thus

$$\begin{aligned}\bar{\bar{\boldsymbol{Q}}}_{ab}^{(4)\prime} &\equiv \mathrm{Tr}\,\bar{\bar{\boldsymbol{Q}}}_{ab}^{(4)} - \frac{\bar{\bar{\boldsymbol{I}}}}{3}\mathrm{TrTr}\bar{\bar{\boldsymbol{Q}}}_{ab}^{(4)} \\ &= \rho_a \nu_{ab}\frac{p_a^2}{\rho_a^2}[-M_{ab(1)}\tilde{\bar{\bar{\boldsymbol{h}}}}^{a(2)} + M_{ab(2)}\tilde{\bar{\bar{\boldsymbol{h}}}}^{b(2)} - N_{ab(1)}\hat{\bar{\bar{\boldsymbol{h}}}}^{a(4)} - N_{ab(2)}\hat{\bar{\bar{\boldsymbol{h}}}}^{b(4)}].\end{aligned} \tag{L49}$$

Finally, introducing summation over all of the "b" species, and rewritten with fluid moments,

$$\begin{aligned}\bar{\bar{\boldsymbol{Q}}}_a^{(4)\prime} = &-\frac{53}{20}\nu_{aa}\frac{p_a}{\rho_a}\bar{\bar{\boldsymbol{\Pi}}}_a^{(2)} - \frac{79}{140}\nu_{aa}\bar{\bar{\boldsymbol{\Pi}}}_a^{(4)} + \sum_{b\neq a}\nu_{ab}\Bigg[-(M_{ab(1)} - 7N_{ab(1)})\frac{p_a}{\rho_a}\bar{\bar{\boldsymbol{\Pi}}}_a^{(2)} \\ &+(M_{ab(2)} + 7N_{ab(2)})\frac{p_a^2}{\rho_a p_b}\bar{\bar{\boldsymbol{\Pi}}}_b^{(2)} - N_{ab(1)}\bar{\bar{\boldsymbol{\Pi}}}_a^{(4)} - N_{ab(2)}\frac{p_a^2\rho_b}{p_b^2\rho_a}\bar{\bar{\boldsymbol{\Pi}}}_b^{(4)}\Bigg].\end{aligned} \tag{L50}$$

It is useful to define (introducing tilde)

$$\hat{M}_{ab(1)} = M_{ab(1)} - 7N_{ab(1)}; \qquad \hat{M}_{ab(2)} = M_{ab(2)} + 7N_{ab(2)}, \tag{L51}$$

and the final mass-ratio coefficients are given by (25).

Appendix M
Collisional Contributions for Scalar $\widetilde{X}^{(4)}$

Here we consider the perturbation

$$\chi_b = \frac{1}{120}\tilde{h}^{b(4)}\tilde{H}^{b(4)}, \tag{M1}$$

with the Hermite polynomial $\tilde{H}^{(4)} = \tilde{c}^4 - 10\tilde{c}^2 + 15$ and the Hermite moment $\tilde{h}^{b(4)} = \frac{\rho_b}{p_b^2}\widetilde{X}^{b(4)}$. The Rosenbluth potentials become

$$H_b(\boldsymbol{v}) = n_b\sqrt{\frac{m_b}{T_b}}\left\{\frac{1}{\tilde{y}}\mathrm{erf}\left(\frac{\tilde{y}}{\sqrt{2}}\right) + \frac{1}{120}\tilde{h}^{b(4)}(3 - \tilde{y}^2)\sqrt{\frac{2}{\pi}}e^{-\tilde{y}^2/2}\right\}; \tag{M2}$$

$$G_b(\boldsymbol{v}) = n_b\sqrt{\frac{T_b}{m_b}}\left\{\sqrt{\frac{2}{\pi}}e^{-\tilde{y}^2/2} + \left(\tilde{y} + \frac{1}{\tilde{y}}\right)\mathrm{erf}\left(\frac{\tilde{y}}{\sqrt{2}}\right) - \frac{1}{60}\tilde{h}^{b(4)}\sqrt{\frac{2}{\pi}}e^{-\tilde{y}^2/2}\right\}, \tag{M3}$$

and the dynamical friction vector and the diffusion tensor become

$$\begin{aligned}\boldsymbol{A}^{ab} = 2\frac{c_{ab}}{m_a^2}\left(1 + \frac{m_a}{m_b}\right)\frac{n_b m_b}{T_b}\Bigg\{&\tilde{\boldsymbol{y}}\left(\sqrt{\frac{2}{\pi}}\frac{e^{-\tilde{y}^2/2}}{\tilde{y}^2} - \frac{\mathrm{erf}(\tilde{y}/\sqrt{2})}{\tilde{y}^3}\right) \\ &-\tilde{\boldsymbol{y}}\frac{\tilde{h}^{b(4)}}{120}\sqrt{\frac{2}{\pi}}(5 - y^2)e^{-\tilde{y}^2/2}\Bigg\},\end{aligned} \tag{M4}$$

$$\begin{aligned}\bar{\bar{\boldsymbol{D}}}^{ab} = 2\frac{c_{ab}}{m_a^2}n_b\sqrt{\frac{m_b}{T_b}}\Bigg\{&\bar{\bar{\boldsymbol{I}}}\frac{\tilde{A}_1'}{\tilde{y}} + \frac{\tilde{\boldsymbol{y}}\tilde{\boldsymbol{y}}}{\tilde{y}^2}\left(\tilde{A}_1'' - \frac{\tilde{A}_1'}{\tilde{y}}\right) \\ &+(\bar{\bar{\boldsymbol{I}}} - \tilde{\boldsymbol{y}}\tilde{\boldsymbol{y}})\frac{\tilde{h}^{b(4)}}{60}\sqrt{\frac{2}{\pi}}e^{-\tilde{y}^2/2}\Bigg\}.\end{aligned} \tag{M5}$$

The perturbation $\chi_a = (\tilde{h}^{a(4)}/120)(\alpha^4\tilde{y}^4 - 10\alpha^2\tilde{y}^2 + 15)$.

M.1. Pressure Tensor Exchange Rates

It is sufficient to consider $\boldsymbol{c}_a = \sqrt{T_a/m_a}\,\alpha\tilde{\boldsymbol{y}}$, and so

$$[\boldsymbol{A}^{ab}\boldsymbol{c}_a]^S = 2\frac{c_{ab}}{m_a^2}\left(1+\frac{m_a}{m_b}\right)\frac{n_b m_b}{T_b}\sqrt{\frac{T_a}{m_a}}\left\{2\alpha\tilde{\boldsymbol{y}}\tilde{\boldsymbol{y}}\left(\sqrt{\frac{2}{\pi}}\frac{e^{-\tilde{y}^2/2}}{\tilde{y}^2}-\frac{\mathrm{erf}(\tilde{y}/\sqrt{2})}{\tilde{y}^3}\right)\right.$$
$$\left.-2\alpha\tilde{\boldsymbol{y}}\tilde{\boldsymbol{y}}\frac{\tilde{h}^{b(4)}}{120}\sqrt{\frac{2}{\pi}}(5-y^2)e^{-\tilde{y}^2/2}\right\}, \tag{M6}$$

which further integrates

$$m_a\int f_a[\boldsymbol{A}^{ab}\boldsymbol{c}_a]^S d^3v = \rho_a\nu_{ab}\bar{\bar{\boldsymbol{I}}}\left[-2\frac{T_a}{m_a}-\tilde{h}^{b(4)}\frac{T_aT_b^2m_a}{4(T_am_b+T_bm_a)^2}\right.$$
$$\left.-\tilde{h}^{a(4)}\frac{m_bT_a^2(T_am_b-4T_bm_a)}{20m_a(T_am_b+T_bm_a)^2}\right], \tag{M7}$$

together with

$$m_a\int f_a\bar{\bar{\boldsymbol{D}}}_{ab}d^3v = \frac{\rho_a\nu_{ab}}{m_a+m_b}\bar{\bar{\boldsymbol{I}}}\left[\frac{2}{m_a}(T_am_b+T_bm_a)+\tilde{h}^{b(4)}\frac{T_b^2m_a}{20(T_am_b+T_bm_a)}\right.$$
$$\left.+\tilde{h}^{a(4)}\frac{m_b^2T_a^2}{20m_a(T_am_b+T_bm_a)}\right]. \tag{M8}$$

Adding the last two results together yields the collisional contributions

$$\bar{\bar{\boldsymbol{Q}}}_{ab}^{(2)} = \frac{\rho_a\nu_{ab}}{m_a+m_b}\bar{\bar{\boldsymbol{I}}}\left[+2(T_b-T_a)-T_b\tilde{h}^{b(4)}\frac{T_bm_a(5T_am_a+4T_am_b-T_bm_a)}{20(T_am_b+T_bm_a)^2}\right.$$
$$\left.+T_a\tilde{h}^{a(4)}\frac{T_am_b(5T_bm_b+4T_bm_a-T_am_b)}{20(T_am_b+T_bm_a)^2}\right], \tag{M9}$$

which can be written as

$$\bar{\bar{\boldsymbol{Q}}}_{ab}^{(2)} = \frac{\rho_a\nu_{ab}}{m_a+m_b}\bar{\bar{\boldsymbol{I}}}[+2(T_b-T_a)+P_{ab(1)}T_a\tilde{h}^{a(4)}-P_{ab(2)}T_b\tilde{h}^{b(4)}], \tag{M10}$$

with mass-ratio coefficients

$$P_{ab(1)} = \frac{T_am_b(5T_bm_b+4T_bm_a-T_am_b)}{20(T_am_b+T_bm_a)^2};\qquad P_{ab(2)} = \frac{T_bm_a(5T_am_a+4T_am_b-T_bm_a)}{20(T_am_b+T_bm_a)^2}, \tag{M11}$$

or for the particular case of small temperature differences,

$$P_{ab(1)} = \frac{m_b}{5(m_b+m_a)};\qquad P_{ab(2)} = \frac{m_a}{5(m_b+m_a)}. \tag{M12}$$

The pressure tensor exchange rates (M10) are rewritten to fluid variables, according to

$$\bar{\bar{\boldsymbol{Q}}}_{ab}^{(2)} = \frac{\rho_a\nu_{ab}}{m_a+m_b}\bar{\bar{\boldsymbol{I}}}\left[+2(T_b-T_a)+P_{ab(1)}\frac{\rho_a}{n_ap_a}\widetilde{X}_a^{(4)}-P_{ab(2)}\frac{\rho_b}{n_bp_b}\widetilde{X}_b^{(4)}\right]. \tag{M13}$$

The energy exchange rates then become

$$Q_{ab} = \frac{1}{2}\mathrm{Tr}\,\bar{\bar{\boldsymbol{Q}}}_{ab}^{(2)} = \frac{\rho_a\nu_{ab}}{(m_a+m_b)}\left[+3(T_b-T_a)+\frac{3}{2}P_{ab(1)}\frac{\rho_a}{n_ap_a}\widetilde{X}_a^{(4)}-\frac{3}{2}P_{ab(2)}\frac{\rho_b}{n_bp_b}\widetilde{X}_b^{(4)}\right], \tag{M14}$$

and the collisional contributions for the stress tensor are

$$\bar{\bar{\boldsymbol{Q}}}_{ab}^{(2)\prime} = \bar{\bar{\boldsymbol{Q}}}_{ab}^{(2)}-\frac{\bar{\bar{\boldsymbol{I}}}}{3}\mathrm{Tr}\,\bar{\bar{\boldsymbol{Q}}}_{ab}^{(2)} = 0. \tag{M15}$$

The scalar perturbations $\widetilde{X}_a^{(4)}$ and $\widetilde{X}_b^{(4)}$ thus do not modify the $\bar{\bar{\boldsymbol{Q}}}_{ab}^{(2)\prime}$, but they enter the conservation of energy. The final model uses $\hat{P}_{ab(1)} = (3/2)P_{ab(1)}$ and $\hat{P}_{ab(2)} = (3/2)P_{ab(2)}$, and the result is written in Section 7.1, Equation (140). The result is also shown in the discussion, Equation (177).

M.2. Fourth-order Moment Exchange Rates

It is straightforward to calculate

$$\begin{aligned}&(\boldsymbol{A}^{ab}\boldsymbol{c}_a)^S|\boldsymbol{c}_a|^2 + 2(\boldsymbol{A}^{ab}\cdot\boldsymbol{c}_a)\boldsymbol{c}_a\boldsymbol{c}_a\\ &=2\frac{c_{ab}}{m_a^2}\left(1+\frac{m_a}{m_b}\right)\frac{n_b m_b}{T_b}\left(\frac{T_a}{m_a}\right)^{3/2}\alpha^3\left\{4\tilde{\boldsymbol{y}}\tilde{\boldsymbol{y}}\left(\sqrt{\frac{2}{\pi}}\,e^{-\tilde{y}^2/2}-\frac{\mathrm{erf}(\tilde{y}/\sqrt{2})}{\tilde{y}}\right)\right.\\ &\quad\left.-4\tilde{\boldsymbol{y}}\tilde{\boldsymbol{y}}\tilde{y}^2(5-\tilde{y}^2)\frac{\tilde{h}^{b(4)}}{120}\sqrt{\frac{2}{\pi}}\,e^{-\tilde{y}^2/2}\right\},\end{aligned}\tag{M16}$$

together with

$$\begin{aligned}&(\mathrm{Tr}\,\bar{\bar{\boldsymbol{D}}}^{ab})\boldsymbol{c}_a\boldsymbol{c}_a + \bar{\bar{\boldsymbol{D}}}^{ab}|\boldsymbol{c}_a|^2 + 2[(\bar{\bar{\boldsymbol{D}}}^{ab}\cdot\boldsymbol{c}_a)\boldsymbol{c}_a]^S\\ &=2\frac{c_{ab}}{m_a^2}n_b\sqrt{\frac{m_b}{T_b}}\frac{T_a}{m_a}\alpha^2\left\{\bar{\bar{\boldsymbol{I}}}\tilde{y}\tilde{A}_1{}' + \tilde{\boldsymbol{y}}\tilde{\boldsymbol{y}}\left(6\tilde{A}_1{}'' + \frac{\tilde{A}_1{}'}{\tilde{y}}\right)\right.\\ &\quad\left.+[\bar{\bar{\boldsymbol{I}}}\tilde{y}^2 + \tilde{\boldsymbol{y}}\tilde{\boldsymbol{y}}(7-6\tilde{y}^2)]\frac{\tilde{h}^{b(4)}}{60}\sqrt{\frac{2}{\pi}}\,e^{-\tilde{y}^2/2}\right\},\end{aligned}\tag{M17}$$

and to integrate

$$\begin{aligned}&m_a\int f_a[(\boldsymbol{A}^{ab}\boldsymbol{c}_a)^S|\boldsymbol{c}_a|^2 + 2(\boldsymbol{A}^{ab}\cdot\boldsymbol{c}_a)\boldsymbol{c}_a\boldsymbol{c}_a]d^3v\\ &=\rho_a\nu_{ab}\frac{p_a^2}{\rho_a^2}\bar{\bar{\boldsymbol{I}}}\left\{-\frac{4(2T_am_b+5T_bm_a)}{(T_am_b+T_bm_a)} + \tilde{h}^{b(4)}\frac{m_a^2T_b^2(2T_am_b-5T_bm_a)}{2(T_am_b+T_bm_a)^3}\right.\\ &\quad\left.+\tilde{h}^{a(4)}\frac{2T_a^3m_b^3+9T_a^2T_bm_am_b^2+72T_aT_b^2m_a^2m_b-40T_b^3m_a^3}{30(T_am_b+T_bm_a)^3}\right\},\end{aligned}\tag{M18}$$

together with

$$\begin{aligned}&m_a\int f_a[(\mathrm{Tr}\,\bar{\bar{\boldsymbol{D}}}^{ab})\boldsymbol{c}_a\boldsymbol{c}_a + \bar{\bar{\boldsymbol{D}}}^{ab}|\boldsymbol{c}_a|^2 + 2((\bar{\bar{\boldsymbol{D}}}^{ab}\cdot\boldsymbol{c}_a)\boldsymbol{c}_a)^S]d^3v\\ &=\rho_a\nu_{ab}\frac{p_a^2}{\rho_a^2}\bar{\bar{\boldsymbol{I}}}\left\{\frac{4(2T_am_b+5T_bm_a)}{T_a(m_b+m_a)} - \tilde{h}^{b(4)}\frac{T_b^2m_a^2(2T_am_b-T_bm_a)}{2T_a(T_am_b+T_bm_a)^2(m_b+m_a)}\right.\\ &\quad\left.-\tilde{h}^{a(4)}\frac{m_b(2T_a^2m_b^2+T_aT_bm_am_b+44T_b^2m_a^2)}{30(T_am_b+T_bm_a)^2(m_b+m_a)}\right\}.\end{aligned}\tag{M19}$$

Adding the last two results together then yields the collisional contributions

$$\mathrm{Tr}\,\bar{\bar{\boldsymbol{Q}}}_{ab}^{(4)} = \rho_a\nu_{ab}\frac{p_a^2}{\rho_a^2}\bar{\bar{\boldsymbol{I}}}\left\{+S_{ab(0)}\frac{(T_b-T_a)}{T_a} - S_{ab(1)}\tilde{h}^{a(4)} - S_{ab(2)}\tilde{h}^{b(4)}\right\},\tag{M20}$$

with mass-ratio coefficients

$$\begin{aligned}S_{ab(0)} &= \frac{4m_a(2T_am_b+5T_bm_a)}{(T_am_b+T_bm_a)(m_b+m_a)};\\ S_{ab(1)} &= -\{m_a(2T_a^3m_b^3+9T_a^2T_bm_am_b^2+6T_a^2T_bm_b^3+72T_aT_b^2m_a^2m_b+27T_aT_b^2m_am_b^2\\ &\quad -40T_b^3m_a^3-84T_b^3m_a^2m_b)\}[30(T_am_b+T_bm_a)^3(m_b+m_a)]^{-1};\\ S_{ab(2)} &= -\frac{T_b^2m_a^3(2T_a^2m_b-5T_aT_bm_a-6T_aT_bm_b+T_b^2m_a)}{2T_a(T_am_b+T_bm_a)^3(m_b+m_a)}.\end{aligned}\tag{M21}$$

For the particular case of small temperature differences,

$$\begin{aligned}S_{ab(0)} &= \frac{4m_a(5m_a+2m_b)}{(m_b+m_a)^2};\\ S_{ab(1)} &= \frac{2m_a(10m_a^2-7m_am_b-2m_b^2)}{15(m_b+m_a)^3};\qquad S_{ab(2)} = \frac{2m_a^3}{(m_b+m_a)^3},\end{aligned}\tag{M22}$$

and for self-collisions, $S_{aa(1)} = 1/60$ and $S_{aa(2)} = 1/4$. Applying a trace at (M20) and changing to fluid moments yields

$$\mathrm{TrTr}\bar{\bar{\boldsymbol{Q}}}_{ab}^{(4)} = 3\nu_{ab}\frac{p_a^2}{\rho_a}\left\{+S_{ab(0)}\frac{(T_b - T_a)}{T_a} - S_{ab(1)}\frac{\rho_a}{p_a^2}\widetilde{X}_a^{(4)} - S_{ab(2)}\frac{\rho_b}{p_b^2}\widetilde{X}_b^{(4)}\right\}, \tag{M23}$$

and the collisional contributions for the stress tensor $\bar{\bar{\boldsymbol{\Pi}}}_a^{(4)}$ are

$$\bar{\bar{\boldsymbol{Q}}}_{ab}^{(4)\,\prime} \equiv \mathrm{Tr}\,\bar{\bar{\boldsymbol{Q}}}_{ab}^{(4)} - \frac{\bar{\bar{\boldsymbol{I}}}}{3}\mathrm{TrTr}\bar{\bar{\boldsymbol{Q}}}_{ab}^{(4)} = 0. \tag{M24}$$

M.3. Collisional Contributions $\widetilde{Q}_a^{(4)\,\prime}$

The collisional contributions for the evolution equation $\widetilde{X}_a^{(4)}$, Equation (C33), then become

$$\begin{aligned}\widetilde{Q}_{ab}^{(4)\,\prime} &= \mathrm{TrTr}\bar{\bar{\boldsymbol{Q}}}_{ab}^{(4)} - 20\frac{p_a}{\rho_a}Q_{ab}\\ &= \nu_{ab}\left\{+\frac{p_a^2}{\rho_a}\frac{(T_b - T_a)}{T_a}\left(3S_{ab(0)} - \frac{60m_a}{m_a + m_b}\right) - \widetilde{X}_a^{(4)}\left(3S_{ab(1)} + \frac{30m_a}{m_a + m_b}P_{ab(1)}\right)\right.\\ &\quad\left. - \frac{p_a^2\rho_b}{p_b^2\rho_a}\widetilde{X}_b^{(4)}\left(3S_{ab(2)} - \frac{30m_a}{(m_a + m_b)}\frac{T_b}{T_a}P_{ab(2)}\right)\right\}.\end{aligned} \tag{M25}$$

It is useful to define

$$\begin{aligned}\hat{S}_{ab(0)} &= -\left(3S_{ab(0)} - \frac{60m_a}{m_a + m_b}\right);\\ \hat{S}_{ab(1)} &= 3S_{ab(1)} + \frac{30m_a}{m_a + m_b}P_{ab(1)};\\ \hat{S}_{ab(2)} &= -\left(3S_{ab(2)} - \frac{30m_a}{(m_a + m_b)}\frac{T_b}{T_a}P_{ab(2)}\right),\end{aligned} \tag{M26}$$

and the final model then reads

$$\begin{aligned}\widetilde{Q}_{ab}^{(4)\,\prime} &= \mathrm{TrTr}\bar{\bar{\boldsymbol{Q}}}_{ab}^{(4)} - 20\frac{p_a}{\rho_a}Q_{ab}\\ &= \nu_{ab}\left\{-\frac{p_a^2}{\rho_a}\frac{(T_b - T_a)}{T_a}\hat{S}_{ab(0)} - \widetilde{X}_a^{(4)}\hat{S}_{ab(1)} + \frac{p_a^2\rho_b}{p_b^2\rho_a}\widetilde{X}_b^{(4)}\hat{S}_{ab(2)}\right\},\end{aligned} \tag{M27}$$

with mass-ratio coefficients given by (143).

Appendix N
Coupling of Two Species

Here we would like to emphasize the usefulness of the multifluid formulation, which makes the calculation of transport coefficients straightforward. We consider two species with indices "a" and "b." The evolution equations for the heat fluxes "a" become

$$\begin{aligned}\frac{d_a}{dt}\boldsymbol{q}_a + \Omega_a\hat{\boldsymbol{b}}\times\boldsymbol{q}_a + \frac{5}{2}p_a\nabla\left(\frac{p_a}{\rho_a}\right) &= -\,[2\nu_{aa} + \nu_{ab}\hat{D}_{ab(1)}]\boldsymbol{q}_a + \nu_{ab}\hat{D}_{ab(2)}\frac{\rho_a}{\rho_b}\boldsymbol{q}_b\\ &\quad + \left[\frac{3}{70}\nu_{aa} + \nu_{ab}\hat{E}_{ab(1)}\right]\frac{\rho_a}{p_a}\boldsymbol{X}_a^{(5)} - \nu_{ab}\hat{E}_{ab(2)}\frac{\rho_a}{p_b}\boldsymbol{X}_b^{(5)} - p_a\nu_{ab}(\boldsymbol{u}_b - \boldsymbol{u}_a)\hat{U}_{ab(1)};\end{aligned} \tag{N1}$$

$$\begin{aligned}\frac{d_a}{dt}\boldsymbol{X}_a^{(5)} + \Omega_a\hat{\boldsymbol{b}}\times\boldsymbol{X}_a^{(5)} + 70\frac{p_a^2}{\rho_a}\nabla\left(\frac{p_a}{\rho_a}\right) &= -\left[\frac{76}{5}\nu_{aa} + \nu_{ab}\hat{F}_{ab(1)}\right]\frac{p_a}{\rho_a}\boldsymbol{q}_a + \nu_{ab}\hat{F}_{ab(2)}\frac{p_a}{\rho_b}\boldsymbol{q}_b\\ &\quad - \left[\frac{3}{35}\nu_{aa} + \nu_{ab}\hat{G}_{ab(1)}\right]\boldsymbol{X}_a^{(5)} - \nu_{ab}\hat{G}_{ab(2)}\frac{p_a}{p_b}\boldsymbol{X}_b^{(5)} - \frac{p_a^2}{\rho_a}\nu_{ab}(\boldsymbol{u}_b - \boldsymbol{u}_a)\hat{U}_{ab(2)},\end{aligned} \tag{N2}$$

together with the evolution equations for the heat fluxes "b":

$$\frac{d_b}{dt}\boldsymbol{q}_b + \Omega_b\hat{\boldsymbol{b}}\times\boldsymbol{q}_b + \frac{5}{2}p_b\nabla\left(\frac{p_b}{\rho_b}\right) = -\,[2\nu_{bb} + \nu_{ba}\hat{D}_{ba(1)}]\boldsymbol{q}_b + \nu_{ba}\hat{D}_{ba(2)}\frac{\rho_b}{\rho_a}\boldsymbol{q}_a + \left[\frac{3}{70}\nu_{bb} + \nu_{ba}\hat{E}_{ba(1)}\right]\frac{\rho_b}{p_b}\boldsymbol{X}_b^{(5)} - \nu_{ba}\hat{E}_{ba(2)}\frac{\rho_b}{p_a}\boldsymbol{X}_a^{(5)} + p_b\nu_{ba}(\boldsymbol{u}_b - \boldsymbol{u}_a)\hat{U}_{ba(1)}; \tag{N3}$$

$$\frac{d_b}{dt}\boldsymbol{X}_b^{(5)} + \Omega_b\hat{\boldsymbol{b}}\times\boldsymbol{X}_b^{(5)} + 70\frac{p_b^2}{\rho_b}\nabla\left(\frac{p_b}{\rho_b}\right) = -\left[\frac{76}{5}\nu_{bb} + \nu_{ba}\hat{F}_{ba(1)}\right]\frac{p_b}{\rho_b}\boldsymbol{q}_b + \nu_{ba}\hat{F}_{ba(2)}\frac{p_b}{\rho_a}\boldsymbol{q}_a - \left[\frac{3}{35}\nu_{bb} + \nu_{ba}\hat{G}_{ba(1)}\right]\boldsymbol{X}_b^{(5)} - \nu_{ba}\hat{G}_{ba(2)}\frac{p_b}{p_a}\boldsymbol{X}_a^{(5)} + \frac{p_b^2}{\rho_b}\nu_{ba}(\boldsymbol{u}_b - \boldsymbol{u}_a)\hat{U}_{ba(2)}, \tag{N4}$$

where, for similar temperatures, the mass-ratio coefficients are given by (27), (28), and for arbitrary temperatures by (19), (21). The system is fully specified and after prescribing a quasistatic approximation it can be solved. Unfortunately, the general analytic solution is too long to write, even for the unmagnetized case. It is beneficial to consider a specific example. Nevertheless, the above system is a very powerful tool, which allows one to obtain the transport coefficients between two different species, it being a two ion plasma, or precise solutions for a specific one ion–electron plasma, without neglecting m_e/m_i (see Section 8.8).

Similarly, the viscosity between two species is described by the evolution equations for the viscosity tensors of species "a":

$$\frac{d_a}{dt}\bar{\bar{\boldsymbol{\Pi}}}_a^{(2)} + \Omega_a(\hat{\boldsymbol{b}}\times\bar{\bar{\boldsymbol{\Pi}}}_a^{(2)})^S + p_a\bar{\bar{\boldsymbol{W}}}_a = -\,\frac{21}{10}\nu_{aa}\bar{\bar{\boldsymbol{\Pi}}}_a^{(2)} + \frac{9}{70}\nu_{aa}\frac{\rho_a}{p_a}\bar{\bar{\boldsymbol{\Pi}}}_a^{(4)} + \frac{\rho_a\nu_{ab}}{m_a + m_b}\left[-\hat{K}_{ab(1)}\frac{1}{n_a}\bar{\bar{\boldsymbol{\Pi}}}_a^{(2)} + \hat{K}_{ab(2)}\frac{1}{n_b}\bar{\bar{\boldsymbol{\Pi}}}_b^{(2)} + L_{ab(1)}\frac{\rho_a}{n_a p_a}\bar{\bar{\boldsymbol{\Pi}}}_a^{(4)} - L_{ab(2)}\frac{\rho_b}{n_b p_b}\bar{\bar{\boldsymbol{\Pi}}}_b^{(4)}\right]; \tag{N5}$$

$$\frac{d_a}{dt}\bar{\bar{\boldsymbol{\Pi}}}_a^{(4)} + \Omega_a(\hat{\boldsymbol{b}}\times\bar{\bar{\boldsymbol{\Pi}}}_a^{(4)})^S + 7\frac{p_a^2}{\rho_a}\bar{\bar{\boldsymbol{W}}}_a = -\,\frac{53}{20}\nu_{aa}\frac{p_a}{\rho_a}\bar{\bar{\boldsymbol{\Pi}}}_a^{(2)} - \frac{79}{140}\nu_{aa}\bar{\bar{\boldsymbol{\Pi}}}_a^{(4)} + \nu_{ab}\left[-\hat{M}_{ab(1)}\frac{p_a}{\rho_a}\bar{\bar{\boldsymbol{\Pi}}}_a^{(2)} + \hat{M}_{ab(2)}\frac{p_a^2}{\rho_a p_b}\bar{\bar{\boldsymbol{\Pi}}}_b^{(2)} - N_{ab(1)}\bar{\bar{\boldsymbol{\Pi}}}_a^{(4)} - N_{ab(2)}\frac{p_a^2\rho_b}{p_b^2\rho_a}\bar{\bar{\boldsymbol{\Pi}}}_b^{(4)}\right], \tag{N6}$$

together with the evolution equations for the viscosity tensors of species "b":

$$\frac{d_b}{dt}\bar{\bar{\boldsymbol{\Pi}}}_b^{(2)} + \Omega_b(\hat{\boldsymbol{b}}\times\bar{\bar{\boldsymbol{\Pi}}}_b^{(2)})^S + p_b\bar{\bar{\boldsymbol{W}}}_b = -\,\frac{21}{10}\nu_{bb}\bar{\bar{\boldsymbol{\Pi}}}_b^{(2)} + \frac{9}{70}\nu_{bb}\frac{\rho_b}{p_b}\bar{\bar{\boldsymbol{\Pi}}}_b^{(4)} + \frac{\rho_b\nu_{ba}}{m_a + m_b}\left[-\hat{K}_{ba(1)}\frac{1}{n_b}\bar{\bar{\boldsymbol{\Pi}}}_b^{(2)} + \hat{K}_{ba(2)}\frac{1}{n_a}\bar{\bar{\boldsymbol{\Pi}}}_a^{(2)} + L_{ba(1)}\frac{\rho_b}{n_b p_b}\bar{\bar{\boldsymbol{\Pi}}}_b^{(4)} - L_{ba(2)}\frac{\rho_a}{n_a p_a}\bar{\bar{\boldsymbol{\Pi}}}_a^{(4)}\right]; \tag{N7}$$

$$\frac{d_b}{dt}\bar{\bar{\boldsymbol{\Pi}}}_b^{(4)} + \Omega_b(\hat{\boldsymbol{b}}\times\bar{\bar{\boldsymbol{\Pi}}}_b^{(4)})^S + 7\frac{p_b^2}{\rho_b}\bar{\bar{\boldsymbol{W}}}_b = -\,\frac{53}{20}\nu_{bb}\frac{p_b}{\rho_b}\bar{\bar{\boldsymbol{\Pi}}}_b^{(2)} - \frac{79}{140}\nu_{bb}\bar{\bar{\boldsymbol{\Pi}}}_b^{(4)} + \nu_{ba}\left[-\hat{M}_{ba(1)}\frac{p_b}{\rho_b}\bar{\bar{\boldsymbol{\Pi}}}_b^{(2)} + \hat{M}_{ba(2)}\frac{p_b^2}{\rho_b p_a}\bar{\bar{\boldsymbol{\Pi}}}_a^{(2)} - N_{ba(1)}\bar{\bar{\boldsymbol{\Pi}}}_b^{(4)} - N_{ba(2)}\frac{p_b^2\rho_a}{p_a^2\rho_b}\bar{\bar{\boldsymbol{\Pi}}}_a^{(4)}\right]. \tag{N8}$$

Here the heat fluxes (N1)–(N4) and viscosities (N5)–(N8) are decoupled, but one can consider more precise solutions with coupling between heat fluxes and viscosities, similar to Section 6.

N.1. Protons and Alpha Particles (Unmagnetized)

As an example, we consider collisions between protons and alpha particles (fully ionized Helium with proton mass 4). The protons will be the "a" species and the alpha particles will be "b" species. For the ion coefficients, the collisions with electrons are neglected in an analogous fashion to Braginskii (1965). By prescribing mass $m_b = 4m_a$, the mass-ratio coefficients with equal temperatures

$T_a = T_b$ become

$$\hat{D}_{ab(1)} = \frac{499}{125}; \qquad \hat{D}_{ab(2)} = \frac{396}{125}; \qquad \hat{E}_{ab(1)} = \frac{87}{875}; \qquad \hat{E}_{ab(2)} = \frac{9}{175}; \qquad \hat{U}_{ab(1)} = \frac{6}{5};$$
$$\hat{F}_{ab(1)} = \frac{7624}{125}; \qquad \hat{F}_{ab(2)} = \frac{4848}{125}; \qquad \hat{G}_{ab(1)} = -\frac{171}{125}; \qquad \hat{G}_{ab(2)} = \frac{12}{25}; \qquad \hat{U}_{ab(2)} = 24,$$
$$\hat{D}_{ba(1)} = \frac{2011}{500}; \qquad \hat{D}_{ba(2)} = \frac{117}{250}; \qquad \hat{E}_{ba(1)} = \frac{897}{14000}; \qquad \hat{E}_{ba(2)} = \frac{9}{700}; \qquad \hat{U}_{ba(1)} = \frac{3}{10};$$
$$\hat{F}_{ba(1)} = \frac{979}{50}; \qquad \hat{F}_{ba(2)} = \frac{1383}{125}; \qquad \hat{G}_{ba(1)} = \frac{8907}{7000}; \qquad \hat{G}_{ba(2)} = \frac{3}{10}; \qquad \hat{U}_{ba(2)} = \frac{39}{5}. \tag{N9}$$

By specifying the charges $Z_a = 1$, $Z_b = 2$, the four different collisional frequencies are related by

$$\nu_{ba} = \frac{\rho_a}{\rho_b}\nu_{ab}; \qquad \nu_{ab} = 8\frac{n_b}{n_a}\sqrt{\frac{2}{5}}\nu_{aa}; \qquad \nu_{bb} = 8\frac{n_b}{n_a}\nu_{aa}, \tag{N10}$$

and we choose ν_{aa} as the reference frequency. Furthermore, applying the charge neutrality $n_a + 2n_b = n_e$, we choose as a reference the normalized density $N_a \equiv n_a/n_e$ and express $n_b/n_e = (1 - N_a)/2$. We also prescribe $\nabla T_a = \nabla T_b$.

Solving the system then yields the (parallel) thermal heat fluxes $\boldsymbol{q}_a^T = -\kappa_a \nabla T_a$, $\boldsymbol{q}_b^T = -\kappa_b \nabla T_a$, with thermal conductivities

$$\kappa_a = \frac{T_a n_a}{m_a \nu_{aa}}\hat{\kappa}_a; \qquad \kappa_b = \frac{T_a n_b}{m_b \nu_{bb}}\hat{\kappa}_b, \tag{N11}$$

and with normalized fully analytic values

$$\hat{\kappa}_a = N_a\left\{\left(-\frac{17989001}{10557600}\sqrt{10} + \frac{292708195}{54054912}\right)N_a^3 + \left(\frac{2129490299}{675686400}\sqrt{10} - \frac{1032644005}{108109824}\right)N_a^2 + \left(-\frac{98252949}{45045760}\sqrt{10} + \frac{8035835}{1689216}\right)N_a + \frac{51625}{70384}\sqrt{10} + \frac{3425}{140768}\right\} \Big/ \triangle_1\,; \tag{N12}$$

$$\hat{\kappa}_b = 32(1 - N_a)\left\{\frac{125}{1024} + \left(\frac{128513167}{2162196480}\sqrt{10} - \frac{166007075}{864878592}\right)N_a^3 + \left(-\frac{67953383}{540549120}\sqrt{10} + \frac{386788475}{864878592}\right)N_a^2 + \left(\frac{15671599}{216219648}\sqrt{10} - \frac{1540025}{4504576}\right)N_a\right\} \Big/ \triangle_1\,; \tag{N13}$$

$$\triangle_1 = \left[1 + \left(-\frac{722521001}{563072000}\sqrt{10} + \frac{14274588957}{3519200000}\right)N_a^4 + \left(\frac{1043512703}{337843200}\sqrt{10} - \frac{8606493541}{879800000}\right)N_a^3 + \left(-\frac{23828129}{8798000}\sqrt{10} + \frac{15644893541}{1759600000}\right)N_a^2 + \left(\frac{23828129}{26394000}\sqrt{10} - 4\right)N_a\right], \tag{N14}$$

or with numerical values

$$\hat{\kappa}_a = N_a[2.3438 + 0.02684N_a^3 + 0.4144N_a^2 - 2.1404N_a]/\triangle_1\,; \tag{N15}$$

$$\hat{\kappa}_b = 32(1 - N_a)[0.1221 - 0.003988N_a^3 + 0.04968N_a^2 - 0.1127N_a]/\triangle_1\,; \tag{N16}$$

$$\triangle_1 = 1 - 0.001559N_a^4 - 0.01485N_a^3 + 0.3266N_a^2 - 1.1451N_a. \tag{N17}$$

Note that n_a/ν_{aa} is independent of n_a, and that is why the definitions (N11) were chosen. For the "b" species (the alpha particles), the results are written in a form so that it is easy to use $32n_b/(\nu_{bb}m_b) = n_a/(\nu_{aa}m_a)$. As a double check, prescribing

$$N_a = 1; \quad \Rightarrow \quad \kappa_a = \frac{T_a n_a}{\nu_{aa} m_a}\frac{125}{32}; \qquad \kappa_b = 0;$$
$$N_a = 0; \quad \Rightarrow \quad \kappa_a = 0; \qquad \kappa_b = \frac{T_a n_b}{\nu_{bb} m_b}\frac{125}{32}, \tag{N18}$$

as it should be. In general, the thermal conductivities of single-ion plasmas compare as $\kappa_a/\kappa_b = \sqrt{m_b/m_a}\,(Z_b/Z_a)^4$. In our case, the thermal conductivity of pure alpha particles is 32 times smaller than that of pure protons. The thermal conductivities $\hat{\kappa}_a$, $\hat{\kappa}_b$ are plotted in the left panel of Figure 7.

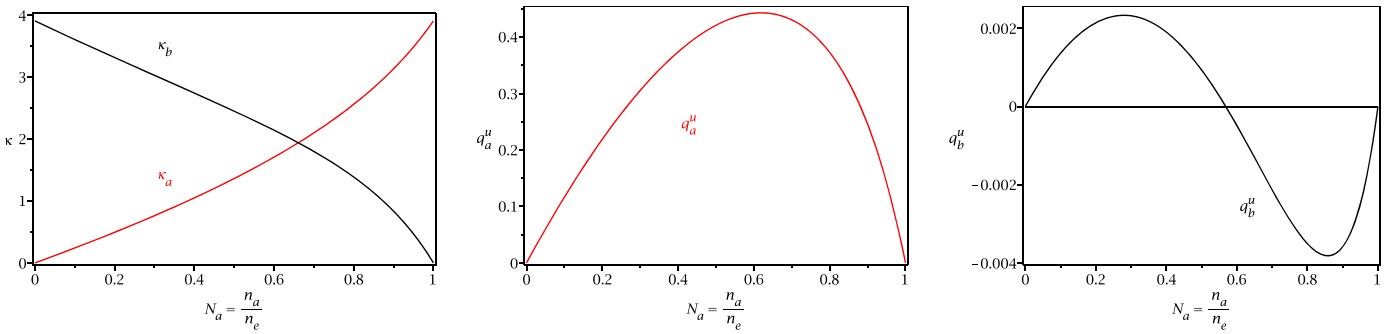

Figure 7. Left: proton thermal conductivity $\hat{\kappa}_a$ (red), given by (N15), and alpha particle thermal conductivity $\hat{\kappa}_b$ (black), given by (N16). Middle: proton frictional heat flux given by β_{0a} (N22). Right: alpha particle frictional heat flux given by β_{0b} (N23). Note the surprising change of sign of β_{0b} for $N_a > 0.57$. We have verified that the same effect is present in the simplified 13-moment model of Burgers (1969)–Schunk (1977).

The frictional heat fluxes read

$$\boldsymbol{q}_a^u = -T_a n_e(\boldsymbol{u}_b - \boldsymbol{u}_a)\beta_{0a}; \qquad \boldsymbol{q}_b^u = -T_a n_e(\boldsymbol{u}_b - \boldsymbol{u}_a)\beta_{0b}; \tag{N19}$$

$$\beta_{0a} = N_a(1-N_a)\left\{\left(-\frac{150058601}{43990000} + \frac{1522393}{1407680}\sqrt{10}\right)N_a^3 + \left(+\frac{258658601}{43990000} - \frac{199422}{109975}\sqrt{10}\right)N_a^2 + \left(-\frac{16290}{4399} + \frac{99711}{109975}\sqrt{10}\right)N_a + \frac{5430}{4399}\right\} \Big/ \triangle_1 ; \tag{N20}$$

$$\beta_{0b} = N_a(1-N_a)\left\{\frac{7351}{1407680}\sqrt{10} + \left(-\frac{54551}{22522880}\sqrt{10} + \frac{264247}{35192000}\right)N_a^3 + \left(\frac{289783}{22522880}\sqrt{10} - \frac{2663863}{70384000}\right)N_a^2 + \left(-\frac{22053}{1407680}\sqrt{10} + \frac{2663863}{140768000}\right)N_a\right\} \Big/ \triangle_1 , \tag{N21}$$

where the denominator $\triangle_1$ is identical to (N14), and with numerical values

$$\beta_{0a} = N_a(1-N_a)[1.2344 + 0.008776N_a^3 + 0.1457N_a^2 - 0.8360N_a] / \triangle_1 ; \tag{N22}$$

$$\beta_{0b} = N_a(1-N_a)[0.01651 - 0.0001504N_a^3 + 0.002839N_a^2 - 0.03062N_a] / \triangle_1 . \tag{N23}$$

In both limits $N_a = 0$, 1, the frictional heat fluxes disappear. The frictional heat fluxes are plotted in the middle and right panels of Figure 7.

N.2. Viscosities

One first calculates the required viscosity mass-ratio coefficients, which for the protons ("a") and alpha particles ("b") become

$$\begin{aligned}
&\hat{K}_{ab(1)} = \frac{398}{25}; \quad \hat{K}_{ab(2)} = \frac{32}{25}; \quad L_{ab(1)} = \frac{228}{175}; \quad L_{ab(2)} = \frac{12}{175};\\
&\hat{M}_{ab(1)} = \frac{934}{125}; \quad \hat{M}_{ab(2)} = \frac{32}{125}; \quad N_{ab(1)} = -\frac{8}{35}; \quad N_{ab(2)} = -\frac{12}{875};\\
&\hat{K}_{ba(1)} = \frac{323}{100}; \quad \hat{K}_{ba(2)} = \frac{68}{25}; \quad L_{ba(1)} = \frac{93}{700}; \quad L_{ba(2)} = \frac{48}{175};\\
&\hat{M}_{ba(1)} = -\frac{368}{125}; \quad \hat{M}_{ba(2)} = \frac{1424}{125}; \quad N_{ba(1)} = \frac{256}{125}; \quad N_{ba(2)} = \frac{192}{175},
\end{aligned} \tag{N24}$$

and which enter evolution Equations (N5)–(N8). For an unmagnetized plasma, a quasistatic solution of these equations then yields the viscosity tensors

$$\begin{aligned}
\bar{\bar{\boldsymbol{\Pi}}}_a^{(2)} &= -\frac{p_a}{\nu_{aa}}[\hat{\eta}_{aa}\bar{\bar{\boldsymbol{W}}}_a + \hat{\eta}_{ab}\bar{\bar{\boldsymbol{W}}}_b];\\
\bar{\bar{\boldsymbol{\Pi}}}_b^{(2)} &= -\frac{p_b}{\nu_{bb}}[8\hat{\eta}_{ab}\bar{\bar{\boldsymbol{W}}}_a + \hat{\eta}_{bb}\bar{\bar{\boldsymbol{W}}}_b],
\end{aligned} \tag{N25}$$

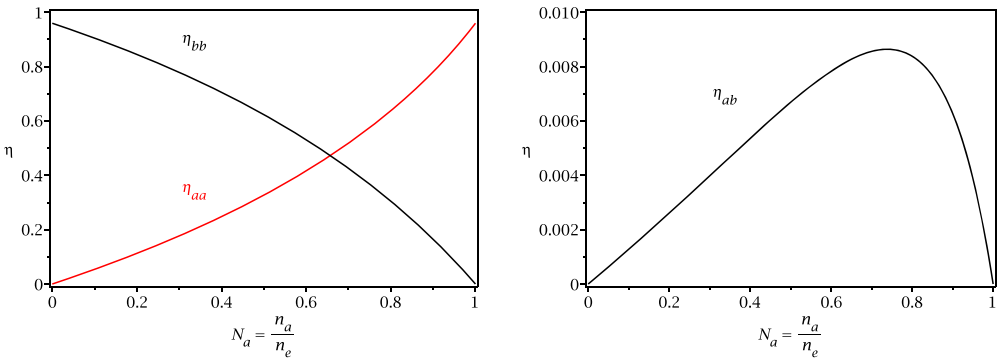

Figure 8. Normalized viscosities of the proton and alpha particle plasma, according to (N26). Collisions with electrons are neglected, in an analogous fashion to Braginskii. Left: proton viscosity $\hat{\eta}_{aa}$ (red) and alpha particle viscosity $\hat{\eta}_{bb}$ (black). Right: "cross-viscosity" $\hat{\eta}_{ab}$.

with numerical values

$$\begin{aligned}
\hat{\eta}_{aa} &= N_a(-0.05464N_a^3 + 0.3704N_a^2 - 0.7717N_a + 0.5173)/\triangle\,;\\
\hat{\eta}_{ab} &= N_a(1-N_a)(0.001874N_a^2 - 0.008142N_a + 0.01248)/\triangle\,;\\
\hat{\eta}_{bb} &= 8(1-N_a)(-0.01150N_a^3 + 0.07862N_a^2 - 0.1729N_a + 0.11997)/\triangle\,;\\
\triangle &= 1 + 0.03923N_a^4 - 0.3759N_a^3 + 1.2959N_a^2 - 1.8953N_a.
\end{aligned} \tag{N26}$$

Note that $p_a/\nu_{aa} = 8p_b/\nu_{bb}$, and the chosen form (N25) emphasizes that the "cross-viscosities" $\hat{\eta}_{ab}$ are directly related. In general, the viscosities of a pure single ion species compare as $\eta_a/\eta_b = \sqrt{m_a/m_b}\,(Z_b/Z_a)^4$, so in our case the viscosity of the pure alpha particles is eight times smaller than that of the pure protons. We provide only numerical values for the solutions (N26), nevertheless it can be shown that for $N_a = 1$, the proton viscosity $\hat{\eta}_{aa} = 1025/1068$, and the same result is obtained for the alpha particle viscosity $\hat{\eta}_{bb}$ if $N_a = 0$. The "cross-viscosity" $\hat{\eta}_{ab}$ becomes zero for both $N_a = 1$ and $N_a = 0$. The results are plotted in Figure 8.

N.3. Deuterium and Tritium Plasma (Unmagnetized)

Here we calculate another example of deuterium–tritium plasma, also considered by Simakov & Molvig (2016b). Plasma consisting of deuterium–tritium is probably the most efficient way of achieving plasma fusion. It is, for example, being used in the JET machine (see e.g., Joffrin et al. 2019), and it will be used in ITER.[9] Of course, we do not consider the peculiar complications associated with the neoclassical toroidal geometry, as our calculation is classical. The deuterium core consists of one proton and one neutron. The tritium core consists of one proton and two neutrons. Deuterium will be the "a" species, and tritium will be the "b" species. The collisions with electrons are neglected. By prescribing $m_b = (3/2)m_a$, the mass-ratio coefficients with equal temperatures $T_b = T_a$ become

$$\begin{aligned}
&\hat{D}_{ab(1)} = \frac{1989}{500};\quad \hat{D}_{ab(2)} = \frac{324}{125};\quad \hat{E}_{ab(1)} = \frac{189}{2000};\quad \hat{E}_{ab(2)} = \frac{81}{1400};\quad \hat{U}_{ab(1)} = \frac{9}{10};\\
&\hat{F}_{ab(1)} = \frac{13543}{250};\quad \hat{F}_{ab(2)} = \frac{5022}{125};\quad \hat{G}_{ab(1)} = -\frac{1373}{1400};\quad \hat{G}_{ab(2)} = \frac{81}{100};\quad \hat{U}_{ab(2)} = \frac{99}{5},\\
&\hat{D}_{ba(1)} = \frac{521}{125};\quad \hat{D}_{ba(2)} = \frac{189}{125};\quad \hat{E}_{ba(1)} = \frac{78}{875};\quad \hat{E}_{ba(2)} = \frac{27}{700};\quad \hat{U}_{ba(1)} = \frac{3}{5};\\
&\hat{F}_{ba(1)} = \frac{5832}{125};\quad \hat{F}_{ba(2)} = \frac{3672}{125};\quad \hat{G}_{ba(1)} = -\frac{307}{875};\quad \hat{G}_{ba(2)} = \frac{18}{25};\quad \hat{U}_{ba(2)} = \frac{72}{5}.
\end{aligned} \tag{N27}$$

Further specifying $Z_a = Z_b = 1$, the collisional frequencies are related by

$$\nu_{ab} = \frac{n_b}{n_a}\sqrt{\frac{6}{5}}\,\nu_{aa};\qquad \nu_{bb} = \frac{n_b}{n_a}\sqrt{\frac{2}{3}}\,\nu_{aa}, \tag{N28}$$

and the charge neutrality $n_a + n_b = n_e$ implies $n_b/n_e = 1 - N_a$, where $N_a = n_a/n_e$. These mass-ratio coefficients and collisional frequencies are used in the system (N1)–(N4). We present quasistatic solutions only for the unmagnetized case, and we assume $\nabla T_a = \nabla T_b$. The thermal heat fluxes $\boldsymbol{q}_a^T = -\kappa_a \nabla T_a$; $\boldsymbol{q}_b^T = -\kappa_b \nabla T_a$ are given by

$$\kappa_a = \frac{T_a n_a}{m_a \nu_{aa}}\hat{\kappa}_a;\qquad \kappa_b = \frac{T_a n_b}{m_b \nu_{bb}}\hat{\kappa}_b, \tag{N29}$$

[9] www.iter.org/sci/FusionFuels

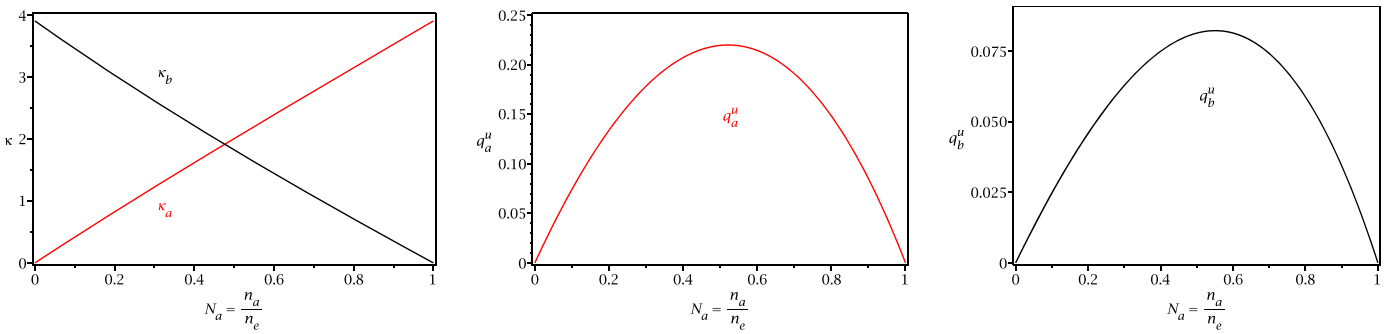

Figure 9. Left: deuterium thermal conductivity $\hat{\kappa}_a$ (red) and tritium thermal conductivity $\hat{\kappa}_b$ (black), given by (N30). Middle: deuterium frictional heat flux, given by β_{0a} (N32). Right: tritium frictional heat flux given by β_{0b} (N33). Note that the frictional heat fluxes $\boldsymbol{q}_b^u$ are defined with opposite signs in (N31) and (N19).

and with numerical values

$$\begin{aligned}
\hat{\kappa}_a &= N_a(4.2135 - 0.009780N_a^3 + 0.06292N_a^2 + 1.4992N_a)/\triangle\,;\\
\hat{\kappa}_b &= \sqrt{3/2}\,(1 - N_a)(3.1894 - 0.001385N_a^3 + 0.04936N_a^2 + 0.9845N_a)/\triangle\,;\\
\triangle &= 1 - 0.0021475N_a^4 - 0.01543N_a^3 + 0.01753N_a^2 + 0.4761N_a,
\end{aligned} \tag{N30}$$

where one can also use $\sqrt{3/2}\,n_b/(m_b\nu_{bb}) = n_a/(\nu_{aa}m_a)$. The frictional heat fluxes are given by

$$\boldsymbol{q}_a^u = -T_a n_e(\boldsymbol{u}_b - \boldsymbol{u}_a)\beta_{0a}; \qquad \boldsymbol{q}_b^u = +T_a n_e(\boldsymbol{u}_b - \boldsymbol{u}_a)\beta_{0b}; \tag{N31}$$

$$\beta_{0a} = N_a(1 - N_a)[0.81156 + 0.010099N_a^3 + 0.098815N_a^2 + 0.50235N_a]/\triangle\,; \tag{N32}$$

$$\beta_{0b} = N_a(1 - N_a)[0.26178 + 0.0088461N_a^3 + 0.069351N_a^2 + 0.24742N_a]/\triangle\,. \tag{N33}$$

N.4. Viscosities

The required viscosity mass-ratio coefficients for deuterium ("*a*") and tritium ("*b*") become

$$\begin{aligned}
&\hat{K}_{ab(1)} = \frac{397}{50}; \quad \hat{K}_{ab(2)} = \frac{44}{25}; \quad L_{ab(1)} = \frac{207}{350}; \quad L_{ab(2)} = \frac{24}{175};\\
&\hat{M}_{ab(1)} = \frac{166}{25}; \quad \hat{M}_{ab(2)} = \frac{184}{125}; \quad N_{ab(1)} = \frac{86}{875}; \quad N_{ab(2)} = \frac{48}{875};\\
&\hat{K}_{ba(1)} = \frac{124}{25}; \quad \hat{K}_{ba(2)} = \frac{56}{25}; \quad L_{ba(1)} = \frac{54}{175}; \quad L_{ba(2)} = \frac{36}{175};\\
&\hat{M}_{ba(1)} = \frac{444}{125}; \quad \hat{M}_{ba(2)} = \frac{24}{5}; \quad N_{ba(1)} = \frac{702}{875}; \quad N_{ba(2)} = \frac{324}{875},
\end{aligned} \tag{N34}$$

and enter evolution Equations (N5)–(N8). For an unmagnetized plasma, the solutions read

$$\begin{aligned}
\bar{\bar{\boldsymbol{\Pi}}}_a^{(2)} &= -\frac{p_a}{\nu_{aa}}[\hat{\eta}_{aa}\bar{\bar{\boldsymbol{W}}}_a + \hat{\eta}_{ab}\bar{\bar{\boldsymbol{W}}}_b];\\
\bar{\bar{\boldsymbol{\Pi}}}_b^{(2)} &= -\frac{p_b}{\nu_{bb}}\left[\sqrt{\frac{2}{3}}\,\hat{\eta}_{ab}\bar{\bar{\boldsymbol{W}}}_a + \hat{\eta}_{bb}\bar{\bar{\boldsymbol{W}}}_b\right],
\end{aligned} \tag{N35}$$

with numerical values

$$\begin{aligned}
\hat{\eta}_{aa} &= N_a(0.0046589N_a^3 + 0.0064481N_a^2 + 0.17316N_a + 0.85048)/\triangle\,;\\
\hat{\eta}_{ab} &= N_a(1 - N_a)(0.0049729N_a^2 + 0.028578N_a + 0.16621)/\triangle\,;\\
\hat{\eta}_{bb} &= \sqrt{2/3}\,(1 - N_a)(-0.0057061N_a^3 - 0.047294N_a^2 - 0.10519N_a + 1.17543)/\triangle\,;\\
\triangle &= 1 + 0.00017711N_a^4 - 0.00044516N_a^3 - 0.020987N_a^2 + 0.099409N_a.
\end{aligned} \tag{N36}$$

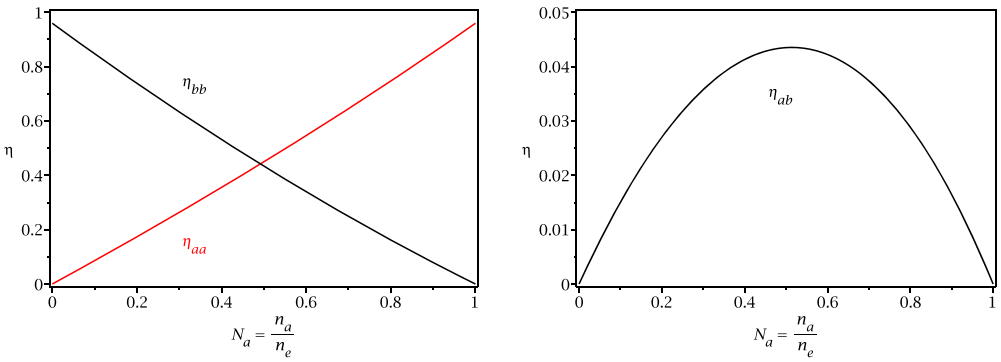

Figure 10. Viscosities of deuterium and tritium plasma, according to (N36). Left: deuterium viscosity $\hat{\eta}_{aa}$ (red) and tritium viscosity $\hat{\eta}_{bb}$ (black). Right: "cross-viscosity" $\hat{\eta}_{ab}$.

The solutions are written in a form so that one can directly use $\sqrt{2/3}\,p_b/\nu_{bb} = p_a/\nu_{aa}$, and are plotted in Figure 10. To obtain more precise solutions, one should include the collisions with electrons (i.e., consider coupling between three species). Nevertheless, the self-collisional values $1025/1068 = 0.96$ will only change to roughly 0.89 (see, for example, Equation (217)), and the plotted viscosity profiles will not change much.

ORCID iDs

P. Hunana https://orcid.org/0000-0002-9860-9759
T. Passot https://orcid.org/0000-0002-6845-9729
E. Khomenko https://orcid.org/0000-0003-3812-620X
D. Martínez-Gómez https://orcid.org/0000-0002-2653-7020
M. Collados https://orcid.org/0000-0002-6210-9648
A. Tenerani https://orcid.org/0000-0003-2880-6084
G. P. Zank https://orcid.org/0000-0002-4642-6192
Y. Maneva https://orcid.org/0000-0002-2422-6050
M. L. Goldstein https://orcid.org/0000-0002-5317-988X
G. M. Webb https://orcid.org/0000-0002-0617-9502

References

Bale, S. D., Pulupa, M., Salem, C., Chen, C. H. K., & Quataert, E. 2013, ApJL, 769, L22
Balescu, R. 1988, Transport Processes in Plasmas, Vol. 1 and 2 (Amsterdam: North-Holland)
Barakat, A. R., & Schunk, R. W. 1981, JPhD, 14, 421
Barakat, A. R., & Schunk, R. W. 1982, PlPh, 24, 389
Bhatnagar, P. L., Gross, E. P., & Krook, M. 1954, PhRv, 94, 511
Braginskii, S. I. 1958, JETP, 6, 358
Braginskii, S. I. 1965, RvPP, 1, 205
Burgers, J. M. 1969, Flow Equations for Composite Gases (New York: Academic)
Canullo, M. V., Costa, A., & Ferro-Fontan, C. 1996, ApJ, 462, 1005
Chapman, S., & Cowling, T. G. 1939, The Mathematical Theory of Non-Uniform Gases (Cambridge: Cambridge Univ. Press)
Chen, J. G., Xu, X. Q., & Lei, Y. A. 2019, CoPhC, 236, 128
Chew, G. F., Goldberger, M. L., & Low, F. E. 1956, RSPSA, 236, 112
Chodura, R., & Pohl, F. 1971, PlPh, 13, 645
Cohen, R. S., Spitzer, L., & Routly, P. M. 1950, PhRv, 80, 230
Cranmer, S. R., & Schiff, A. J. 2021, JGRA, 126, e29666
Cuperman, S., & Dryer, M. 1985, ApJ, 298, 414
Cuperman, S., Weiss, I., & Dryer, M. 1980, ApJ, 239, 345
Cuperman, S., Weiss, I., & Dryer, M. 1981, ApJ, 251, 297
Demars, H. G., & Schunk, R. W. 1979, JPhD, 12, 1051
Dreicer, H. 1959, PhRv, 115, 238
Epperlein, E. M., & Haines, M. G. 1986, PhFl, 29, 1029
Fitzpatrick, R. 2015, Plasma Physics. An Introduction (London, Boca Raton, FL: Taylor and Francis, CRC Press)
Gary, S. P. 1993, Theory of Space Plasma Microinstabilities (New York: Cambridge Univ. Press)
Goswami, P., Passot, T., & Sulem, P. L. 2005, PhPl, 12, 102109
Grad, H. 1949a, CPAM, 2, 325
Grad, H. 1949b, CPAM, 2, 331
Grad, H. 1958, HDP, 3, 205
Gross, E. P., & Krook, M. 1956, PhRv, 102, 593
Gurnett, D. A., & Bhattacharjee, A. 2005, Introduction to Plasma Physics: With Space and Laboratory Applications (Cambridge: Cambridge Univ. Press)
Haack, J. R., Hauck, C. D., & Murillo, M. S. 2017, JSP, 168, 826
Halekas, J. S., Whittlesey, P. L., Larson, D. E., et al. 2021, A&A, 650, A15
Hammett, G., Dorland, W., & Perkins, F. 1992, PhFlB, 4, 2052
Hammett, G. W., & Perkins, W. F. 1990, PhRvL, 64, 3019
Helander, P., & Sigmar, D. J. 2002, Collisional Transport in Magnetized Plasmas (Cambridge: Cambridge Univ. Press)
Hellinger, P., & Trávníček, P. M. 2009, PhPl, 16, 054501
Hinton, F. L. 1983, in Handbook of Plasma Physics, Vol. 1: Basic Plasma Physics 1, ed. M. N. Rosenbluth & R. Z. Sagdeev (Amsterdam: North-Holland), 147
Hirshman, S., & Sigmar, D. 1981, NucFu, 21, 1079
Hirshman, S. P., & Sigmar, D. J. 1977, PhFl, 20, 418
Hollweg, J. V. 1974, JGR, 79, 3845
Hollweg, J. V. 1976, JGR, 81, 1649
Hunana, P., Tenerani, A., Zank, G. P., et al. 2019a, JPlPh, 85, 205850603
Hunana, P., Tenerani, A., Zank, G. P., et al. 2019b, JPlPh, 85, 205850602
Hunana, P., & Zank, G. P. 2017, ApJ, 839, 13
Hunana, P., Zank, G. P., Laurenza, M., et al. 2018, PhRvL, 121, 135101
Ji, J.-Y., & Held, E. D. 2006, PhPl, 13, 102103
Ji, J.-Y., & Held, E. D. 2013, PhPl, 20, 042114
Ji, J.-Y., & Held, E. D. 2015, PhPl, 22, 062114
Ji, J.-Y., & Joseph, I. 2018, PhPl, 25, 032117
Joffrin, E., Abduallev, S., Abhangi, M., et al. 2019, NucFu, 59, 112021
Joseph, I., & Dimits, A. M. 2016, CoPP, 56, 504
Kaneko, B. S. 1960, JPSJ, 15, 1685
Kaneko, S., & Taguchi, M. 1978, JPSJ, 45, 1380
Kaneko, S., & Yamao, A. 1980, JPSJ, 48, 2098
Kaufman, A. N. 1960, PhFl, 3, 610
Khomenko, E., & Collados, M. 2012, ApJ, 747, 87
Khomenko, E., Collados, M., Díaz, A., & Vitas, N. 2014, PhPl, 21, 092901
Killie, M. A., Janse, A. M., Lie-Svendsen, O., & Leer, E. 2004, ApJ, 604, 842
Krommes, J. A. 2018a, JPlPh, 84, 925840401
Krommes, J. A. 2018b, JPlPh, 84, 905840601
Kunz, M. W. 2021, Lecture Notes on Irreversible Processes in Plasmas, www.astro.princeton.edu/~kunz/Site/AST554/AST554_lecture_notes_Kunz.pdf
Lancia, L., Albertazzi, B., Boniface, C., et al. 2014, PhRvL, 113, 235001
Landau, L. 1936, Phys. Z. Sowjetunion, 10, 154
Landau, L. 1937, J. Exptl. Theoret. Phys. U.S.S.R., 7, 203
Landi, S., Matteini, L., & Pantellini, F. 2014, ApJL, 790, L12
Landshoff, R. 1949, PhRv, 76, 904
Landshoff, R. 1951, PhRv, 82, 442

Luciani, J. F., Mora, P., & Virmont, J. 1983, PhRvL, 51, 1664
Macmahon, A. 1965, PhFl, 8, 1840
Meyer, E., & Sessler, G. 1957, ZPhy, 149, 15
Meyrand, R., Kanekar, A., Dorland, W., & Schekochihin, A. A. 2019, PNAS, 116, 1185
Mikhailovskii, A. B., & Smolyakov, A. I. 1985, Sov. Phys. JETP, 61, 109
Oraevskii, V., Chodura, R., & Feneberg, W. 1968, PlPh, 10, 819
Passot, T., & Sulem, P. L. 2007, PhPl, 14, 082502
Passot, T., Sulem, P. L., & Hunana, P. 2012, PhPl, 19, 082113
Perrone, D., Passot, T., Laveder, D., et al. 2018, PhPl, 25, 052302
Ramos, J. J. 2005, PhPl, 12, 052102
Salem, C., Hubert, D., Lacombe, C., et al. 2003, ApJ, 585, 1147
Schunk, R. W. 1975, P&SS, 23, 437
Schunk, R. W. 1977, RvGSP, 15, 429
Schurtz, G. P., Nicolaï, P. D., & Busquet, M. 2000, PhPl, 7, 4238
Scudder, J. D. 2021, ApJ, 907, 90
Simakov, A. N., & Molvig, K. 2014, PhPl, 21, 024503
Simakov, A. N., & Molvig, K. 2016a, PhPl, 23, 032115
Simakov, A. N., & Molvig, K. 2016b, PhPl, 23, 032116
Snyder, P. B., & Hammett, G. W. 2001, PhPl, 8, 3199
Snyder, P. B., Hammett, G. W., & Dorland, W. 1997, PhPl, 4, 3974
Spitzer, L. 1962, Physics of Fully Ionized Gases (2nd ed.; New York: Wiley)
Spitzer, L., & Härm, R. 1953, PhRv, 89, 977
Stubbe, P. 1994, PhFl, 6, 3164
Stubbe, P., & Sukhorukov, A. I. 1999, PhPl, 6, 2976
Sulem, P. L., & Passot, T. 2015, JPlPh, 81, 325810103
Tanenbaum, B. S. 1967, Plasma Physics (New York: McGraw-Hill)
Verscharen, D., Klein, K. G., & Maruca, B. A. 2019, LRSP, 16, 5
Wang, L., Zhu, B., Xu, X.-q., & Li, B. 2019, AIPA, 9, 015217
Zank, G. P. 2014, Transport Processes in Space Physics and Astrophysics (Berlin: Springer)
Zaqarashvili, T. V., Carbonell, M., Ballester, J. L., & Khodachenko, M. L. 2012, A&A, 544, A143
Zaqarashvili, T. V., Khodachenko, M. L., & Rucker, H. O. 2011, A&A, 529, A82
Zhdanov, V. M. 2002, PPCF, 44, 2283